Telecommunications Series 54

Standard Codecs

Image compression to advanced video coding

3rd Edition

Mohammed Ghanbari

IET TELECOMMUNICATIONS SERIES 54

Standard Codecs

Standard Codecs

Image compression to advanced video coding

3rd Edition

Mohammed Ghanbari

The Institution of Engineering and Technology

Published by The Institution of Engineering and Technology, London, United Kingdom

The Institution of Engineering and Technology is registered as a Charity in England & Wales (no. 211014) and Scotland (no. SC038698).

First published 1999 as *Video Coding: An introduction to standard codecs* (0 85296 762 4)
Second edition published 2003 as *Standard Codecs: Image compression to advanced video coding* (0 85296 710 1)
Third edition 2011

British Library Cataloguing in Publication Data
A catalogue record for this product is available from the British Library

ISBN 978-0-86341-964-5 (paperback)
ISBN 978-1-84919-113-5 (PDF)

Typeset in India by MPS Ltd, a Macmillan Company
Printed in the UK by CPI Antony Rowe, Chippenham

To Sorour, Shirin and Soroush

Contents

Preface to first edition

Television is an important part of our lives. In developing countries, where the TV sets can outnumber telephones by more than 50, its impact can be even greater. Advances in the multimedia industry and advent of digital TV and other services will only increase its influence in global terms.

There is a considerable and growing will to support these developments through global standards. As an example, the call for videoconferencing proposals in the 1980s, which led to the H.261 audiovisual codec, attracted 15 proposals; in February 1999, 650 research proposals on MPEG-7 were submitted to the MPEG committee meeting in Lancaster, UK.

This book aims to address some of these exciting developments by looking at the fundamentals behind them. The intention is to provide material that is useful to a wide range of readers, from researchers in video coding to managers in the multimedia industry.

In writing this book, I have made use of invaluable documents prepared by the working parties of the ISO/IEC and ITU. I am also in debt to the work of my former and current research students and assistants. In particular, I would like to acknowledge the work by Pedro Assuancao, Soroush Ghanbari, Ebroul Izquierdo, Fernando Lopes, Antonio Pinheiro, Eva Rosdiana, Vassilis Seferidis, Tamer Shanableh, Eduardo da Silva, Kuan Hui Tan, Kwee Teck Tan, Qi Wang, David Wilson and John Woods, who have directly or indirectly contributed to the realisation of this book.

Finally, I would like to express my deepest gratitude to my mentor Professor Charles Hughes, who with his great vision and tireless effort taught me how to be a competitive researcher. He encouraged me to write this book and very patiently read every chapter of it and made numerous valuable comments. Charles, thanks for everything.

Mohammed Ghanbari
June 1999

Author (left) receiving the Rayleigh prize for the first edition of this book that was awarded by IEE as the best book of the year 2000.

Preface to second edition

The first edition of the book was published in August 1999. It was received with an overwhelming worldwide support, such that it had to be reprinted in less than 18 months. The book was reviewed by distinguished video coding experts across the globe, from the United States to Australia, and the comments were published in numerous prestigious international journals, such as *IEEE Signal Processing, IEE Review* and *EBU Review*. Because of these successes, the book was recognised as the best book of the year 2000 by IEE and was awarded the Rayleigh prize.

Video coding is a dynamic field, and many changes have happened since the first edition. At that time, JPEG2000 was under development, but now it is mature enough to be reported. In 1999, work on MPEG-7 had just started, but today we have more information on how video databases can be searched, and the work has progressed into MPEG-21. At the turn of the millennium, particular emphasis was put on mobile communications and video streaming over IP networks. Consequently, the joint work of ISO/IEC and ITU on very low bit rate video coding has lead to the development of the H.26L standard. In the second edition, the important and fundamental aspects of all these new and exciting events are explained. Of course, the remaining parts of the book have also undergone some amendments, either to clarify certain subjects or to explain new ideas in video coding. On the basis of the comments of my colleagues at various universities round the world (who have used the book as a textbook), I have designed a few problems at the end of each chapter. The model answers are given at the end of the book.

In addition to the material used in the first edition, I would like to acknowledge the work of several of my research associates, assistants and students, in particular Randa Atta, Soroush Ghanbari, Mislav Grgic, Hiroshi Gunji, Ekram Khan, Fernando Lopes, Mike Nilsson, Antonio Pinheiro, Kai Sun and C.K. Tan.

Finally, my deepest gratitude goes to Professor Charles Hughes, who has very passionately read all parts of the manuscript and has made numerous valuable comments. Charles, once more, thank you very much.

Mohammed Ghanbari
February 2003

Preface to third edition

It is more than seven years since the revised version of the book was published in 2003. At that time, advanced video coding (AVC), now known as H.264/AVC, was under development. Information about this codec was, at that time, very limited, and what was available then was reported under H.26L. Now the standard is complete, and the codec is one of the most successful joint products of the ITU and ISO/IEC. Numerous variants of this codec by several manufacturers have already been marketed. These codecs can serve a variety of applications, ranging from digital HDTV broadcasting, IPTV, video storage, videoconferencing, video streaming, etc. Today, interested readers of video coding technology are more eager to find out about H.264/AVC than any other codecs. In fact, no book on video coding is complete without H.264.

As is the speciality of this book, each standard codec is described in a chapter, but design and explanations of material in chapters are evolutionary. Description of standards is made dependent on each other, and where necessary, similarities and dissimilarities between them are explained. It is not the intention of the book to explain in details how a specific coding tool is implemented, since interested readers can always refer to the draft recommendation of the standard. Rather, it is aimed to explain the philosophy behind the introduction of a specific coding tool and how it can improve the compression gain. I believe, this not only helps the readers to better understand the specification manual of a standard codec but also helps them to open up their imagination to improve the codec's performance. It should not be forgotten that standards are all about the semantics for decoders and encoders are flexible to generate the required bitstream syntax the best way they can.

In the new edition, in addition to adding a complete description of H.264/AVC in Chapter 11, other chapters have also been refined. In particular, Chapter 9 on H.263, which is the nuclei of H.264, has been revised, and all its optional tools, which have been imported into H.264, are highlighted.

In revising the book, as before, I owe much of the credits to my current and former students, particularly to Ismail Ali, Mohammad Altaf, Randa Atta, Shirin Ghanbari, Mahdi Ghandi, Ekram Khan. Sandro Moiron and Hoang Nguyen, who assisted in running tests, checking my arguments against the source codes and the manuals of the H.264/AVC standard and, of course, drawing several diagrams. I am also grateful to Mike Nilsson for his critical comments on the new chapter on H.264. Many thanks to all.

Mohammed Ghanbari
November 2010

Chapter 1
History of video coding

Digital video compression techniques have played an important role in the world of telecommunication and multimedia systems where bandwidth is still a valuable commodity. Hence, video coding techniques are of prime importance for reducing the amount of information needed for a picture sequence without losing much of its quality, judged by the human viewers. Modern compression techniques involve very complex electronic circuits, and the cost of these can only be kept to an acceptable level by high-volume production of large-scale integration (LSI) chips. Standardisation of the video compression techniques is therefore essential.

Straightforward pulse code modulation (PCM) coding of TV signals at 140 Mbit/s was introduced in the 1970s. It conformed to the digital hierarchy used mainly for multichannel telephony, but the high bit rate restricted its application to TV programme distribution and studio editing. Digital TV operation for satellites became attractive since the signals were compatible with the time-division multiple access systems then coming into use. Experimental systems in 1980 used bit rates of about 45 Mbit/s for National Television System Committee (NTSC) signals and 60 Mbit/s for the phase alternate line (PAL) standard.

An analogue videophone system tried out in the 1960s had not proved viable, but by the 1970s it was realised that visual speaker identification could substantially improve a multiparty discussion, and videoconference services were considered. This provided the impetus for the development of low bit rate video coding. With the available technology in the 1980s, COST211 video codec, based on differential pulse code modulation (DPCM), was standardised by International Telegraph and Telephone Consultative Committee, from the French name ‘‘Comité Consultatif International Téléphonique et Télégraphique’’ (CCITT), under the H.120 standard. The codecs target bit rate was at 2 Mbit/s for Europe and 1.544 Mbit/s for North America, suitable for their respective first levels of digital hierarchy. However, the image quality, although having very good spatial resolution (due to the nature of DPCM working on pixel-by-pixel bases), had a very poor temporal quality. It was soon realised that in order to improve the image quality, without exceeding the target bit rate, less than 1 bit should be used to code each pixel. This was only possible if a group of pixels were coded together, such that the bit per pixel is fractional. This led to the design of so-called block-based codecs.

During the late 1980s study period, of the 15 block-based videoconferencing proposals submitted to the telecommunication standardisation sector of the

International Telecommunication Union (ITU-T formerly CCITT), 14 were based on the discrete cosine transform (DCT) and only one on vector quantisation (VQ). The subjective quality of video sequences presented to the panel showed hardly any significant differences between the two coding techniques. In parallel to ITU-T's investigation during 1984–88, the Joint Photographic Experts Group (JPEG) was also interested in compression of static images. They chose the DCT as the main unit of compression, mainly because of the possibility of progressive image transmission. JPEG's decision undoubtedly influenced the ITU-T in favouring DCT over VQ. By now there was worldwide activity in implementing the DCT in chips and on digital signal processors (DSPs).

By the late 1980s, it was clear that the recommended ITU-T videoconferencing codec would use a combination of interframe DPCM for minimum coding delay and the DCT. The codec showed greatly improved picture quality over H.120. In fact, the image quality for videoconferencing applications was found reasonable at 384 kbit/s or higher, and good quality was possible at significantly higher bit rates of around 1 Mbit/s. This effort, although originally directed at video coding at 384 kbit/s, was later extended to systems based on multiples of 64 kbit/s ($p \times 64$ kbits, where p can take values from 1 to 30). The standard definition was completed in late 1989 and is officially called the H.261 standard (the coding method is often referred to as '$p \times 64$').

The success of H.261 was a milestone for low bit rate coding of video at reasonable quality. In the early 1990s, the Motion Picture Experts Group (MPEG) started investigating coding techniques for storage of video, such as CD-ROMs. The aim was to develop a video codec capable of compressing highly active video such as movies, on hard discs, with a performance comparable to that of video home systems (VHS) and video cassette recorders (VCRs). In fact, the basic framework of the H.261 standard was used as a starting point in the design of the codec. The first generation of MPEG, called the MPEG-1 standard, was capable of accomplishing this task at 1.5 Mbit/s. Since for storage of video, encoding and decoding delays are not a major constraint, one can trade delay for compression efficiency. For example, in the temporal domain, a DCT might be used rather than a DPCM, or DPCM used but with much improved motion estimation, such that the motion compensation removes temporal correlation. This latter option was adopted within MPEG-1.

It is ironic that in the development of H.261, motion compensation was thought to be optional, since it was believed that after motion compensation little was left to be decorrelated by the DCT. However, later research showed that efficient motion compensation can reduce the bit rate. For example, it is difficult to compensate for the uncovered background, unless one looks ahead at the movement of the objects. This was the main principle in MPEG-1, where the motion in most picture frames is looked at from past and future, and this proved to be very effective.

Soon after the development of MPEG-1 in 1991, MPEG-1 decoders/players became commonplace for multimedia on computers. MPEG-1 decoder plug-in hardware boards (e.g. MPEG magic cards) became very popular, and software MPEG-1 decoders were available with the release of new operating systems or multimedia extensions for PC and Mac platforms. Because in all standard video codecs only the decoders have to comply with proper syntax, software-based encoding has added extra flexibility that improved the performance of MPEG-1 later.

Although MPEG-1 was optimised for typical applications using noninterlaced video of 25 frames/s (in European format) or 30 frames/s (in North America) at bit rates in the range of 1.2–1.5 Mbit/s (for image quality comparable to home VCRs), it can certainly be used at higher bit rates and resolutions. Early versions of MPEG-1 for interlaced video, such as those used in broadcast, were called MPEG-1+. Broadcasters, who were initially reluctant to use any compression on video, fairly soon adopted a new generation of MPEG, called MPEG-2, for coding of interlaced video at bit rates of 4–9 Mbit/s. MPEG-2 has made a significant impact in a range of applications such as digital terrestrial broadcasting, digital satellite TV, digital cable TV, digital versatile disc (DVD) and many others. In November 1998, OnDigital of the United Kingdom started terrestrial broadcasting of BBC and ITV programmes in MPEG-2, and almost at the same time several satellite operators such as Sky-Digital launched MPEG-2-coded television pictures direct to homes. In fact, digital video owes much of its success to MPEG-2.

Since in MPEG-2 the number of bidirectionally predicted pictures is at the discretion of the encoder, this number may be chosen for an acceptable coding delay. This technique may then be used for telecommunication systems. For this reason, the ITU-T has also adopted MPEG-2 under the generic name of H.262 for telecommunications. H.262/MPEG-2 apart from coding high-resolution and higher bit rate video also has the interesting property of scalability, such that from a single MPEG-2 bitstream two or more videos at various spatial, temporal or quality resolutions can be extracted. This scalability is very important for video networking applications. For example, in applications such as video on demand and multicasting the client may wish to receive videos of their own quality choice, or in networking applications during network congestion, less essential parts of the bitstream can be discarded without significantly impairing the received video pictures.

Following the MPEG-2 standard, coding of high definition television (HDTV) was seen to be the next requirement. This became known as MPEG-3. However, the versatility of MPEG-2, being able to code video of any resolution, left no place for MPEG-3, and hence it was abandoned. Although Europe was slow in deciding whether to use HDTV, broadcast of HDTV with the MPEG-2 compression in the United States started at the beginning of new millennium. It is foreseen that in the United States by the year 2014, the existing transmission of analogue NTSC video will cease to exist, and HDTV/MPEG-2 will be the only terrestrial broadcasting format. A few years later, Europe chose H.264/AVC for its terrestrial and satellite broadcast of HDTV.

After so much development on MPEG-1 and -2, one might wonder what is next. Certainly we have not yet addressed the question of sending video at very low bit rates, such as of 64 kbit/s or less. This of course depends on the demand for such services. However, there are signs that in the very near future such demands may arise. For example, currently, owing to a new generation of modems allowing bit rates of 56 kbit/s or so over public switched telephone networks (PSTN), videophones at such low bit rates are needed. Currently, there are demands for sending video over mobile networks, where the channel capacity is very scarce. In fact, the wireless industry is the main driving force behind the low bit rate image/video compression. For instance, during the two months of June and July, in 2002, about two millions of picture-phone sets were sold in Japan alone. A picture-phone is a digital photo camera that grabs still pictures, compresses and sends them as a text file over the mobile network. On the video front, in October 2002, the Japanese company NTT DoCoMo announced the launch of its first hand-held mobile video codec. The codec had the size of mobile phones, at the price of almost US$350.

To fulfil this goal, MPEG group started working on a very low bit rate video codec, under the name of MPEG-4. Before achieving acceptable image quality at such bit rates, new demands arose. These were mainly caused by the requirements of multimedia, where there was a considerable demand for coding of multi-viewpoint scenes, graphics and synthetic, as well as natural scenes. Applications such as virtual studio and interactive video were the main driving forces. Ironically, critics say that since MPEG-4 could not deliver the very low bit rate codec that it had promised, the goal posts have been moved.

Work on very low bit rate systems, because of the requirement of PSTN and mobile applications, was carried out by the ITU-T and a new video codec named H.263 was devised to fulfil the goal of MPEG-4. This codec, which is an extension of H.261, but uses lessons learned from MPEG developments, is sophisticated enough to code small dimensioned video pictures at low frame rates within 10–64 kbit/s. Over the years, the compression efficiency of this codec has been improved steadily through several iterations and amendments. Throughout its evolution, the codec has then been renamed H.263+ and H.263++ to indicate the improvements. Because of a very effective coding strategy used in this codec, the recommendation even defines the application of this codec to very high resolution images such as HDTV, albeit at higher bit rates.

Before leaving the subject of MPEG-4, I should add that the main effort on MPEG-4 was on functionality, since this is what makes MPEG-4 distinct from other coders. In MPEG-4, images are coded as objects, and the generated bitstream is scalable. This provides the possibility of interacting with video, choosing the parts that are of interest. Moreover, natural images can be mixed with synthetic video, in what is called virtual studio. MPEG-4 defines a new coding method based on models of objects for coding synthetic objects. It also uses the wavelet transform for coding of still images. However, MPEG-4, as part of its functionality for coding of natural images, uses a technique similar to H.263; hence, it is equally capable of coding video at very low bit rates.

The fruitful outcome of the MPEG-2/H.262 video codec product under the joint effort of the MPEG and ITU encouraged the two standard bodies to further collaboration. In 1997, the video coding experts group of the ITU-T started the advanced video coding (AVC) project, under the name of H.26L, with L standing for the long-term objectives. In 2001, the ISO/IEC MPEG joined the project and formed a joint video team (JVT). The objective of JVT was to create a single video coding standard to outperform the most optimised H.263 and MPEG-4 video codecs. The first version of H.26L standard was technically finalised in year 2002, and was officially ratified at the end of year 2003. In the end, the H.26L codec was called H.264 by the ITU-U community and MPEG-4 part 10 by the ISO/IEC MPEG group.

Now, in 2010, H.264/MPEG-4 v10 has become a de facto video codec for all applications. Both terrestrial and satellite HDTV are mainly broadcasted in H.264. New storage devices such as high-capacity Blu-ray for increased quality and storage efficiency use H.264 family codecs. New video services launched by telcos, such as Internet Protocol television (IPTV), video over Internet, catch up TV and video streaming in general use H.264 family. A variant of this codec has been manufactured under various brand names, like Microsoft VC1, Chinese ASV, DivX+, Sorenson, etc., which are based on H.264. Now, in 2010, we can only say H.264 is a codec for all video communication, distribution, storage and networking applications.

As we see, the video coding standards have evolved under two brand names, H.26*x* and MPEG-*x*. The H.26*x* codecs are recommended by the telecommunication standardisation sector of the ITU-T. The ITU-T recommendations have been designed for telecommunications applications, such as video conferencing and video telephony. The MPEG-*x* products are the work of International Standardisation Organisation and the International Electrotechnical Commission, Joint Technical Committee number 1 (ISO/IEC JTC1). The MPEG standards have been designed mostly to address the needs of video storage (e.g. CD-ROM, DVD), broadcast TV and video streaming (e.g. video over Internet). For the most parts, the two standardisation committees have worked independently on different standards. However, there were exceptions, where their joint work resulted in standards such as H.262/MPEG-2 and H.264/MPEG-4 part 10 (v10). Figure 1.1 summarises the evolution of video coding standards by the two organisations and their joint effort from the beginning in 1984 till now (2010). The Figure also shows the evolution of still image coding under the joint work of ITU and ISO/IEC, which is best known as the JPEG group.

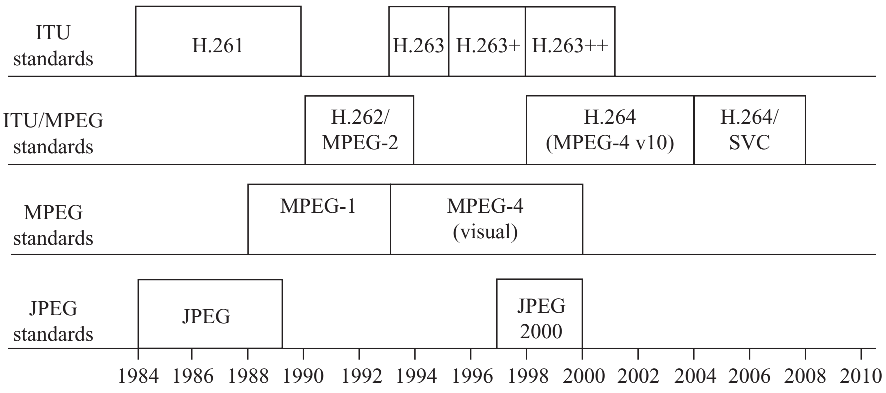

Figure 1.1 Evolution of video coding standards by the ITU-T and ISO/IEC committees

It should be noted that video coding is an ongoing worldwide activity, and new standards now and then are introduced. This of course is in response to the market demand. For instance, in July 2009, ISO/IEC has initiated a new project for coding of super high quality video, which is known as 4K video (4000 $\times$ 2000) pixels. The main application for such a very high resolution video is digital cinema, and work is also ongoing for 8K video (8000 $\times$ 4000) in film industry. Unfortunately, at the time of revising the book not much new information is known about these new directions to be reported, but surely as we will see in this book, all the codecs have evolved from each other. No doubt, the future video codecs will have their roots in these codecs, especially on H.264. It appears ITU and MPEG will be working jointly again, and the new activity is currently called Joint Collaborative Team on Video Coding (JCT-VC).

It should be noted that MPEG activity is not just confined to the compression of audio-visual contents. The MPEG committee has also been active in the other aspects of audio-visual information. For example, work on object- or content-based coding of MPEG-4 has brought new requirements, in particular searching for content in image databases. In early 2000, a working group under MPEG-7 undertook to study these requirements. The MPEG-7 standard builds on the other standards, such as MPEG-1, -2 and -4. Its main function is to define a set of descriptors for multimedia databases to look for specific image/video clips, using image characteristics such as colour, texture and information about the shape of objects. These pictures may be coded by either of the standard video codecs, or even in analogue forms.

The advances made on content description in MPEG-7 and coding and compression of contents under MPEG-4 provided the customers with an efficient access to these contents. There was a need to produce specifications of standardised interfaces and protocols that allow customers to access the wide variety of content providers. This is the task undertaken by the MPEG-21, under the name of multimedia framework.

In this book, we start by reviewing briefly the basics of video, including scanning, formation of colour components at various video formats and quality evaluation of video. At the end of each chapter, a few problems have been designed, either to cover some specific parts of the book in greater depth or for a better appreciation of those parts. Principles of video compression techniques used in the standard codecs are given in Chapter 3. These include the three fundamental elements of compression: spatial, temporal and intersymbol redundancy reductions. The DCT, as the core element of all the standard codecs, and its fast implementation is presented. Quantisation of the DCT coefficients for bit rate reduction is given. The most important element of temporal redundancy reduction, namely motion compensation, is discussed in this chapter. Two variable length coding techniques for reduction of the entropy of the symbols, namely, Huffman and arithmetic coding, are described. Special attention is paid on the arithmetic coding, because of its role and importance in recent video codecs. The chapter ends with an overview of a generic interframe video codec, which is used as a generic codec in the following chapters to describe various standard codecs.

Because of the importance of wavelet coding in the new generation of standard codecs, Chapter 4 is specifically devoted to the description of the basic principles of wavelet-based image coding. The three well-known techniques for compression of wavelet-based image coding (embedded zero-tree wavelet, EZW; set partitioning in hierarchical trees, SPIHT and embedded block coding with optimised truncation, EBCOT) are presented. Their relative compression efficiencies are compared with each other.

Coding of still pictures, under the Joint Photographic Experts Group (JPEG), is presented in Chapter 5. Lossless and lossy compression versions of JPEG, as well as baseline JPEG and its extension with sequential and progressive modes, are described. The chapter also includes a new standard for still image coding under JPEG2000. Potential for improving the picture quality under this new codec and its new functionalities are described.

Chapter 6 describes the H.261 video codec for teleconferencing applications. The structure of picture blocks and the concept of the macroblock as the basic unit of coding are defined. Selection of the best macroblock type for efficient coding is presented. The chapter examines the efficiency of zigzag scanning of the DCT coefficients for coding. The efficiency of two-dimensional variable length coding of zigzag-scanned DCT coefficients is compared with one-dimensional variable length codes.

Chapter 7 explains MPEG-1 video coding technique for storage applications. The concept of group of pictures (GOP) for flexible access to compressed video is explained. Differences between MPEG-1 and H.261, as well as the similarities, are highlighted. These include the nature of motion compensation and various forms of coding of picture types used in this codec. Editing, pause, fast forward and fast reverse picture tricks are discussed.

Chapter 8 is devoted to coding of high-quality moving pictures with the MPEG-2 standard. The concepts of profile and level with their applications are defined. The two main concepts of interlacing and scalability, which discriminate this codec from MPEG-1, are given. The best predictions for the non-scalable codecs from the fields, frames and/or their combinations are discussed. On the scalability, the three fundamental scalable codecs, spatial, signal-to-noise ratio and temporal scalable codecs are analysed, and the quality of some coded pictures with these methods is contrasted. Layered coding is contrasted against scalability and the additional overhead due to scalability/layering is also compared with the nonscalable encoder. The chapter ends with transmission of MPEG-2-coded video for broadcast applications and video over ATM networks, as well as its storage on the DVD.

Chapter 9 discusses H.263 video coding for very low bit rate applications. The fundamental differences and similarities between this codec and H.261 and MPEG-1/2 are highlighted. Special interest is paid to the importance of motion compensation in this codec. Methods of improving the compression efficiency of this codec under various optional modes are discussed. Rather than describing all the annexes (optional modes) one by one, the important optional tools that had the potential to be extended to other codecs are described. Most of these optional modes became the core elements of H.264. Where necessary, how and in what form they have been implemented in H.264 are also indicated. In fact Chapter 9 is feeding into H.264 in Chapter 11, and it is recommended to be read before moving into Chapter 11. Since H.263 is an attractive video coding tool for mobile applications, special interest is paid on the transmission of H.263 coded video over unreliable channels. In this regard, error correction for transmission of video over mobile networks is discussed. Methods of improving the robustness of the codecs against channel errors are given, as well as postprocessing and concealment of erroneous video are explained. The chapter ends with introduction of scalable coding of H.263 video.

In Chapter 10, a new method of video coding based on the image content is presented. The profile and level set out for this codec are outlined. The concept of image plane that enables users to interact with the individual objects and change their characteristics is introduced. Methods for segmenting video frames into objects and their extractions are explained. Coding of arbitrary shaped objects with a particular emphasis on coding of their shapes is studied. The shape-adaptive DCT as a natural coding scheme for these objects is analysed.

Coding of synthetic objects with model-based coding and still images with the wavelet transform is introduced. It is shown how video can be coded with the wavelet transform, and its quality is compared with that of H.263. Performance of frame-based MPEG-4 is also compared with that of H.263 for some channel error rates using mobile and fixed network environments. The chapter ends with the scalability defined for content-based coding.

Chapter 11 deals with the H.264 standard. Most of the optional modes of H.263 in Chapter 9 have been implemented in a more efficient way in H.264. These include deblocking filter, data partitioning, multiple reference frame, etc. However, some new features unique to H.264, like intra prediction, hierarchical B-pictures, switching pictures, as well as some new error resiliency like flexible macroblock ordering and redundant slices, are explained. H.264 also uses two sets of context-adaptive Huffman and arithmetic coding, which are explained in great details. Extension of H.264 towards scalable video coding is also studied. Finally, a unique feature of this standard in isolating the video coding layer from its transport over the network, under the name of network abstraction layer (NAL), is studied. Various packetisation strategies and external signalling for robust video transmission are discussed too.

The book ends with a chapter on content description, search and video browsing under the name MPEG-7. Various content search methods exploiting the visual information such as colour, texture, shape and motion are described. Some practical examples for video search by textures and shapes are given. The chapter ends with a brief look at the multimedia framework under MPEG-21 to define standards for easy and efficient use of contents by the customers.

Chapter 2
Video basics

Before discussing the fundamentals of video compression, let us look at how video signals are generated. Their characteristics will help us to understand how they can be exploited for bandwidth reduction without actually introducing perceptual distortions. In this regard, we first look at image formation and colour video. Interlaced/progressive video is explained, and its impact on the signal bandwidth and display units is discussed. Representation of video in digital form and the need for bit rate reductions are addressed. Finally, the image formats to be coded for various applications and their quality assessments are analysed.

2.1 Analogue video

2.1.1 Scanning

Video signals are normally generated at the output of a camera by scanning a two-dimensional moving scene and converting it into a one-dimensional electric signal. A moving scene is a collection of individual pictures or images, where each scanned picture generates a frame of the picture. Scanning starts at the top left corner of the picture and ends at the bottom right.

The choice of number of scanned lines per picture is a trade-off between the bandwidth, flicker and resolution. Increasing the number of scanning lines per picture increases the spatial resolution. Similarly, increasing the number of pictures per second will increase the temporal resolution. There is a lower limit to the number of pictures per second, below which flicker becomes perceptible. Hence, flicker-free, high-resolution video requires larger bandwidth.

If a frame is formed by the single scanning of a picture, it is called progressive scanning. Alternatively, two pictures may be scanned at two different times, with the lines interleaved, such that two consecutive lines of a frame belong to alternate fields to form a frame. In this case, each scanned picture is called a field, and the scanning is called interlaced. Figure 2.1 shows progressive and interlaced frames.

The concept behind interlaced scanning is to trade-off vertical–spatial resolution with that of the temporal. For instance, slow-moving objects can be perceived with higher vertical resolution, since there are not many changes between the successive fields. At the same time, the human eye does not perceive flicker since the objects are displayed at field rates. For fast-moving objects, although vertical resolution is reduced, the human eye is not sensitive to spatial resolutions at high display rates.

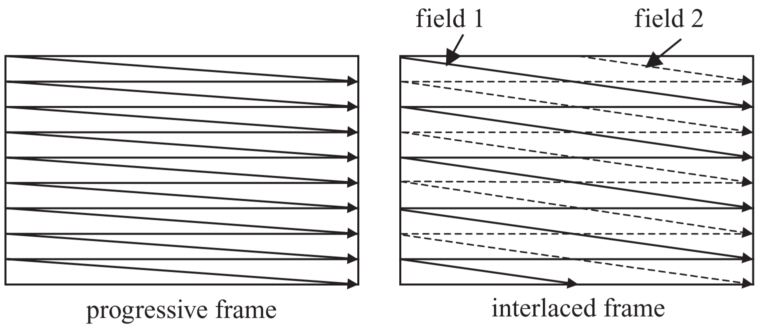

Figure 2.1 Progressive and interlaced frames

Therefore, the bandwidth of television signals is halved without significant loss of picture resolution. Usually, in interlaced video, the number of lines per field is half the number of lines per frame, or the number of fields per second is twice the number of frames per second. Hence, the number of lines per second remains fixed.

It should be noted that if high spatio-temporal video is required, for example, in high definition television (HDTV), then the progressive mode should be used. Although interlaced video is a good trade-off in television, it may not be suitable for computer displays, owing to the closeness of the screen to the viewer and the type of material normally displayed, such as text and graphs. If television pictures were to be used with computers, the result would be an annoying interlines flicker, line crawling, etc. To avoid these problems, computers use noninterlaced (also called progressive or sequential) displays with refresh rates higher than 50/60 frames/s, typically 72 frames/s.

2.1.2 Colour components

During the scanning, a camera generates three primary colour signals called red, green and blue, the so-called RGB signals. These signals may be further processed for transmission and storage. For compatibility with the black and white video and because the three colour signals are highly correlated, a new set of signals at different colour space are generated. These are called colour systems, and the three standards are National Television System Committee (NTSC), phase alternate line (PAL) and sequential couleur avec memoire (SECAM) [1]. We will concentrate on the PAL system as an example, although the basic principles involved in the other systems are very similar.

The colour space in PAL is represented by *YUV*, where *Y* represents the luminance and *U* and *V* represent the two colour components. The basis *YUV* colour space can be generated from gamma-corrected RGB (referred to in equations as $R'G'B'$) components as follows:

$$\begin{aligned}
Y &= 0.299R' + 0.587G' + 0.114B' \\
U &= -0.147R' - 0.289G' + 0.436B' = 0.492(B' - Y) \\
V &= 0.615R' - 0.515G' - 0.100B' = 0.877(R' - Y)
\end{aligned} \tag{2.1}$$

In the PAL system, the luminance bandwidth is normally 5 MHz, though in PAL system-I, used in the United Kingdom, it is 5.5 MHz. The bandwidth of each colour component is only 1.5 MHz, because the human eye is less sensitive to colour resolution. For this reason, in most image processing applications, such as motion estimation, decisions on the type of blocks to be coded or not coded (see Chapter 6) are made on the luminance component only. The decision is then extended to the corresponding colour components. Note that for higher-quality video, such as HDTV, the luminance and chrominance components may have the same bandwidth, but nevertheless all the decisions are made on the luminance components. In some applications, the chrominance bandwidth may be reduced much further than the ratio of 1.5 MHz/5 MHz.

2.2 Digital video

The process of digitising analogue video involves the three basic operations of filtering, sampling and quantisation. The filtering operation is employed to avoid the aliasing artefacts of the follow-up sampling process. The filtering applied to the luminance can be different from those of chrominance, owing to different bandwidth requirements.

Filtered luminance and chrominance signals are sampled to generate a discrete time signal. The minimum rate at which each component can be sampled is its Nyquist rate and corresponds to twice the signal bandwidth. For a PAL system, this is in the range of 10–11 MHz. However, due to the requirement to make the sampling frequency a harmonic of the analogue signal line frequency, the sampling rate for broadcast quality signals has been recommended by CCIR (International Radio Consultative Committee; now called International Telecommunication Union, ITU) to be 13.5 MHz, under CCIR-601 recommendation [2]. This is close to three times the PAL subcarrier frequency. The chrominance sampling frequency has also been defined to be half the luminance sampling frequency. Finally, sampled signals are quantised to 8-bit resolution, suitable for video broadcasting applications.

It should be noted that colour space recommended by CCIR-601 is very close to the PAL system. The precise luminance and chrominance equations under this recommendation are as follows:

$$\begin{aligned} Y &= 0.257R' + 0.504G' + 0.098B' + 16 \\ C_b &= -0.148R' - 0.291G' + 0.439B' + 128 \\ C_r &= 0.439R' - 0.368G' - 0.071B' + 128 \end{aligned} \tag{2.2}$$

The slight departure from the PAL parameters is due to the requirement that in the digital range, Y should take values in the range of 16–235 quantum levels. Also, the normally AC chrominance components of U and V are centred on the grey level 128, and the range is defined from 16 to 240. The reasons for these modifications are

- to reduce the granular noise of all three signals in later stages of processing and
- to make chrominance values positive to ease processing operations (e.g. storage).

Note that despite a unique definition for Y, C_b and C_r, the CCIR-601 standard for European broadcasting is different from that for North America and the Far East. In the former, the number of lines per frame is 625 and the number of frames per second is 25. In the latter, these values are 525 and 30, respectively. The number of samples per active line, called picture elements (pixels), is 720 for both systems. In the 625-line system, the total number of pixels per line, including the horizontal blanking, is 13.5 MHz times 64μs, equal to 864 pixels. Note also that despite the differences in the number of lines and frames rates, the number of pixels generated per second under both CCIR-601/625 and CCIR-601/525 is the same. This is because in digital television we are interested in the active parts of the picture, and the number of active television lines per frame in CCIR-601/625 is 576 and the total number of pixels per second becomes equal to $720 \times 576 \times 25 = 10\,368\,000$. In CCIR-601/525, the number of active lines is 480, and the total number of pixels per second is $720 \times 480 \times 30 = 10\,368\,000$.

The total bit rate is then calculated by considering that there are half the luminance pixels for each of the chrominance pixels, and with 8 bit/pixel, the total bit rate becomes $10\,368\,000 \times 2 \times 8 = 165\,888\,000$ bit/s. Had we included all the horizontal and vertical blanking, then the total bandwidth would be $13.5 \times 10^6 \times 2 \times 8 = 216$ Mbit/s. Either of these values is much greater than the equivalent analogue bandwidth; hence, the video compression to reduce the digital bit rate is very demanding. In the following chapters, we will show how such a huge bit rate can be compressed down to less than 10 Mbit/s, without noticeable effect on picture quality.

2.3 Image format

CCIR-601 is based on an image format for studio quality. For broadcast applications, this is mostly known as standard television (SDTV). For other applications, images with various degrees of resolutions and dimensions might be preferred. For example, in video conferencing or video telephony, small image sizes with lower resolutions require much less bandwidth than the studio or broadcast video, and at the same time the resultant image quality is quite acceptable for the application. On the other hand, for HDTV, larger image sizes with improved luminance and chrominance resolutions are preferred.

2.3.1 SIF images

In most cases, the video sources to be coded by standard video codecs are produced by CCIR-601 digitised video signals direct from the camera. It is then logical to relate picture resolutions and dimensions of various applications to those of

CCIR-601. The first sets of images related to CCIR-601 are the lower resolution images for storage applications.

A lower resolution to CCIR-601 would be an image sequence with half the CCIR-601 resolutions in each direction. That is, in each CCIR-601 standard, active parts of the image in the horizontal, vertical and temporal dimensions are halved. For this reason, it is called source input format (SIF) [3]. The resultant picture is noninterlaced (progressive). The positions of the chrominance samples share the same block boundaries with those of the luminance samples, as shown in Figure 2.2. For every four luminance samples, Y, there will be one pair of chrominance components, C_b and C_r.

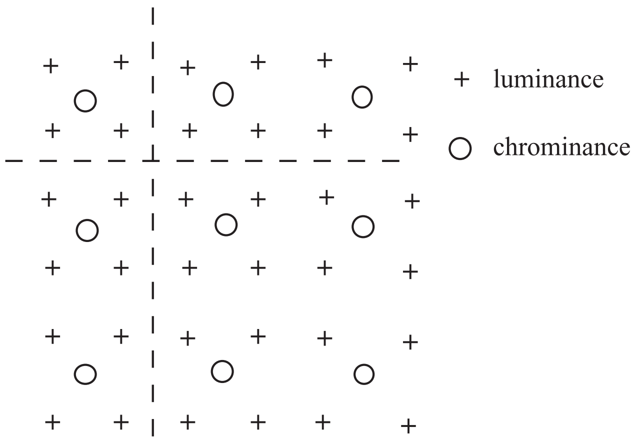

Figure 2.2 Positioning of luminance and chrominance samples (dashed lines indicate macroblock boundaries)

Thus, for the European standard, the SIF picture resolution becomes 360 pixels/line, 288 lines/picture and 25 pictures/s. For North America and the Far East, these values are 360, 240 and 30, respectively.

One way of converting the source video rate (temporal resolution) is to use only odd or even fields. Another method is to take the average values of the two fields. Discarding one field normally introduces aliasing artefacts, but simple averaging blurs the picture. For better SIF picture quality more sophisticated methods of rate conversion are required, which inevitably demand more processing power. The horizontal and vertical resolutions are halved after filtering and subsampling of the video source.

Considering that in CCIR-601 the chrominance bandwidth is half of the luminance, then the number of each chrominance pixel per line is half of the luminance pixels, but their frame rates and the number of lines per frame are equal. This is normally referred to as 4:2:2 image format. Figure 2.3 shows the luminance and chrominance components for the 4:2:2 image format. As the figure shows, in the scanning direction (horizontal), there is a pair of chrominance samples for every

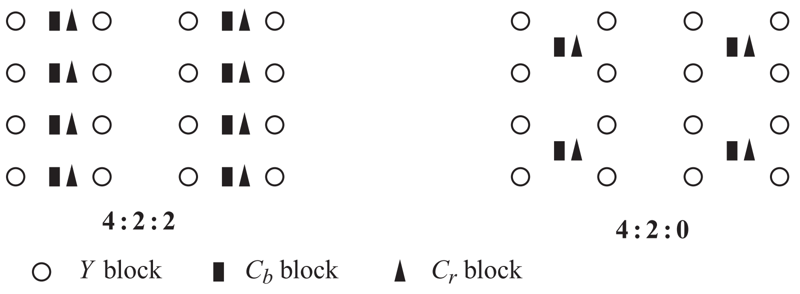

Figure 2.3 Sampling pattern for 4:2:2 (CCIR-601) and 4:2:0 SIF

alternate luminance sample, but the chrominance components are present in every line. For SIF pictures, there is a pair of chrominance samples for every four luminance pixels as shown in the figure.

Thus, in SIF, the horizontal and vertical resolutions of luminance will be half of the source resolutions, but for the chrominance, while horizontal resolution is halved, the vertical resolution has to be one quarter. This is called 4:2:0 format.

The low-pass filters used for filtering the source video are different for luminance and chrominance coefficients. The luminance filter coefficient is a seven-tap filter with the following characteristics:

$$[-29 \quad 0 \quad 88 \quad 138 \quad 88 \quad 0 \quad -29]//256 \tag{2.3}$$

Use of a power of two for the devisor allows a simple hardware implementation.

For the chrominance, the filter characteristic is a four-tap filter of the type

$$[1 \quad 3 \quad 3 \quad 1]//8 \tag{2.4}$$

Hence, the chrominance samples have to be placed at a horizontal position in the middle of the luminance samples, with a phase shift of half a sample. These filters are not part of the international standard, and other filters may be used. Figure 2.4 illustrates the subsampling and low-pass filtering of the CCIR-601 format video into SIF format.

Note that the number of luminance pixels per line of CCIR-601 is 720. Hence, the horizontal resolutions of SIF luminance and chrominance should be 360 and 180, respectively. Since in the standard codecs the coding unit is based on macroblocks of 16×16 pixels, 360 is not divisible by 16. Therefore, from each of the leftmost and rightmost sides of SIF, four pixels are removed.

The preprocessing into SIF format is not normative. Other preprocessing steps and other resolutions may be used. The picture size need not even be a multiple of 16. In this case, a video coder adds padding pixels to the right or bottom edges of the picture. For example, a horizontal resolution of 360 pixels could be coded by adding eight pixels to the right edge of each horizontal row, bringing the total to 368.

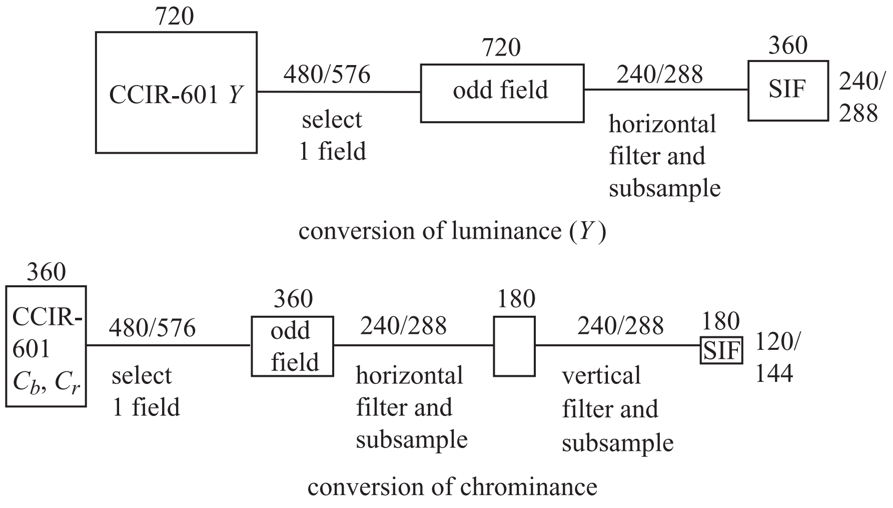

Figure 2.4 Conversion of CCIR-601 to SIF

Now 23 macroblocks would be coded in each row. The decoder would discard the extra padding pixels after decoding, giving the final decoded resolution of 360 pixels.

The sampling format of 4:2:0 should not be confused with that of the 4:1:1 format used in some digital VCRs. In this format, chrominance has the same vertical resolution as luminance, but horizontal resolution is one quarter. This can be represented with a sampling pattern shown in Figure 2.5. Note that 4:1:1 has the same number of pixels as 4:2:0!

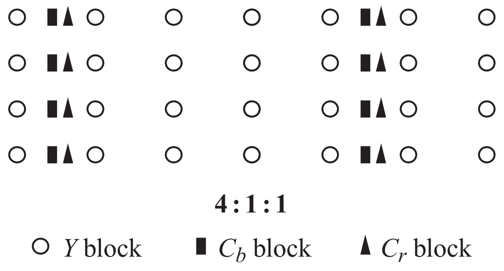

Figure 2.5 Sampling pattern of 4:1:1 image format

2.3.2 *Conversion from SIF to CCIR-601 format*

An SIF is converted to its corresponding CCIR-601 format by spatial upsampling as shown in Figure 2.6. A linear-phase finite impulse response (FIR) is applied after the insertion of zeros between samples [3]. A filter that can be used for upsampling the luminance is a seven-tap FIR filter with the impulse response of

$$[-12 \quad 0 \quad 140 \quad 256 \quad 140 \quad 0 \quad -12]//256 \tag{2.5}$$

At the end of the lines, some special techniques such as replicating the last pixel must be used. Note that the DC response of this filter has a gain of 2. This is due to the inserted alternate zeros in the upsampled samples, such that the upsampled values retain their maximum nominal value of 255.

According to CCIR recommendation 601, the chrominance samples need to be co-sited with the luminance samples 1, 3, 5 ... To achieve the proper location, the upsampling filter should have an even number of taps, as given by

$$[1 \quad 3 \quad 3 \quad 1]//4 \tag{2.6}$$

Note again, the filter has a gain of 2.

The SIF may be reconstructed by inserting four black pixels to each end of the horizontal luminance line in the decoded bitmap, and two grey pixels (value of 128) to each of the horizontal chrominance lines. The luminance SIF may then be upsampled horizontally and vertically. The chrominance SIF should be upsampled once horizontally and twice vertically, as shown in Figure 2.6*b*.

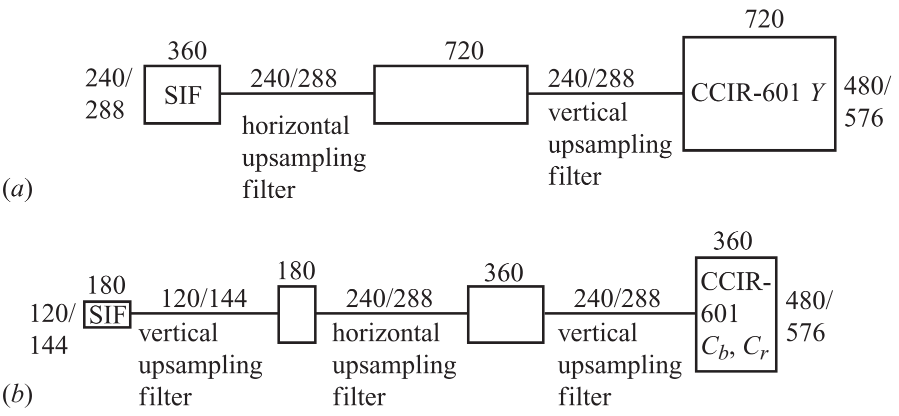

Figure 2.6 Upsampling and filtering of (a) luminance and (b) chrominance signals from SIF to CCIR-601 format

2.3.3 CIF image format

For a worldwide videoconferencing, a video codec has to cope with the CCIR-601 of both European (625 line, 50 Hz) and North America and Far East (525 line, 60 Hz) video formats. Hence, CCIR-601 video sources from these two different formats had to be converted to a common format. The picture resolutions also needed to be reduced to be able to code them at lower bit rates.

Considering that in CCIR-601 the number of pixels per line in both 625/50 and 525/60 standards is 720 pixels/line, half of this value, 360 pixels/line, was chosen as the horizontal resolution. For the vertical and temporal resolutions, a value intermediate between the two standards was chosen such that the combined vertical × temporal resolutions were one quarter of that of CCIR-601. The 625/50 system has the greater vertical resolution. Since the active picture area is 576 lines, half of this value is 288 lines. On the other hand, the 525/60 system has the greater temporal resolution, so that the half rate is 30 Hz. The combination of 288 lines and 30 Hz gives the required vertical × temporal resolution. This is illustrated in Figure 2.7.

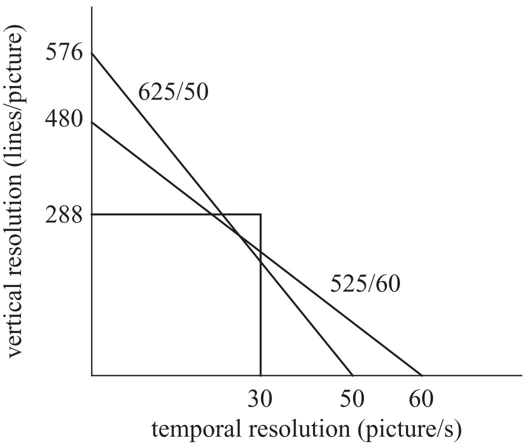

Figure 2.7 Spatio-temporal relation in CIF format

Such an intermediate selection of vertical resolution from one standard and temporal from the other leads to the adopted name common intermediate format (CIF). Therefore, a CIF picture has a luminance with 360 pixels/lines, 288 lines/picture and 30 (precisely 29.97) pictures/s [4]. The colour components are at half the spatial resolution of luminance, with 180 pixels/line and 144 lines/picture. Temporal resolutions of colour components are the same as for the luminance at 29.97 Hz.

In CIF format, like SIF, pictures are progressive (noninterlaced), and the positions of the chrominance samples share the same block boundaries with that of the luminance samples, as shown in Figure 2.2. Also like SIF, the image format is also 4:2:0 and similar down-conversion and up-conversion filters to those shown in Figures 2.4 and 2.6 can also be applied to CIF images. Note the difference between SIF-625 and CIF and SIF-525 and CIF. In the former, the only difference is in the number of pictures per second, while in the latter they differ in the number of lines per picture.

2.3.4 Sub-QCIF, QSIF, QCIF

For certain applications such as video over mobile networks or video telephony it is possible to reduce the frame rate. Known reduced frame rates for CIF and SIF-525 are 15, 10 and 7.5 frames/s. These rates for SIF-625 are 12.5 and 8.3 frames/s. To balance the spatio-temporal resolutions, the spatial resolutions of the images are normally reduced, nominally by halving in each direction. These are called quarter-SIF (QSIF) and quarter-CIF (QCIF) for SIF and CIF formats, respectively. Conversion of SIF or CIF to QSIF and QCIF (or vice versa) can be carried out with a similar method of converting CCIR-601 to SIF and CIF, respectively, using the same filter banks shown in Figures 2.4 and 2.6. Lower frame rate QSIF and QCIF images are normally used for very low bit rate video.

Certain applications, such as video over mobile networks, even demand smaller image sizes. Sub-QCIF is the smallest standard image size, with the horizontal and vertical picture resolutions of 128 pixels by 96 pixels, respectively. The frame rate can be very low (e.g. 5 frames/s) to suit the channel rate. The image format in this case is 4:2:0, and hence the chrominance resolution is half the luminance resolution in each direction.

2.3.5 HDTV

Currently HDTV has a nominal resolution of twice the 525 line CCIR-601 format. Hence, the filter banks of Figures 2.4 and 2.6 can also be used for the image size conversion. Also, since in HDTV higher chrominance bandwidth is desired, 4:2:2 format is a favourite format but still 4:2:0 format is used at the distribution (broadcast and transmission). However, for higher-quality video the chrominance bandwidth can even be made equal to the luminance. Hence, there will be a pair of chrominance pixels for every luminance pixel, and the image format is called 4:4:4. In some cases, HDTV is progressive to improve vertical resolution.

It is common practice to define image format in terms of relations between 8×8 pixel blocks and a macroblock of 16×16 pixels. The concept of macroblock and block is explained in Chapter 6. Figure 2.8 shows how blocks of luminance and chrominance in various 4:2:0, 4:2:2 and 4:4:4 image formats are defined.

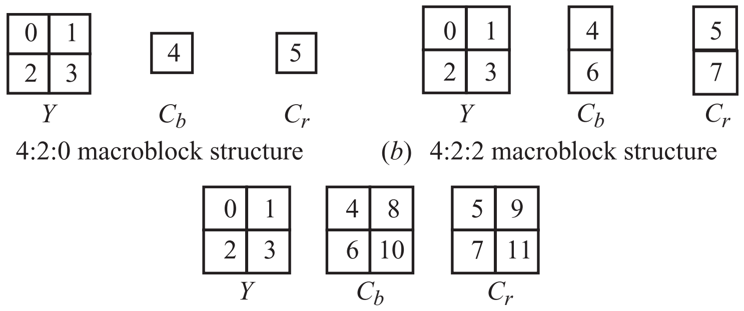
0 1 2 3
4
5
Y
C_b
C_r
(*a*) 4:2:0 macroblock structure
0 1 2 3
4 6
5 7
Y
C_b
C_r
(*b*) 4:2:2 macroblock structure
0 1 2 3
4 8 6 10
5 9 7 11
Y
C_b
C_r
(*c*) 4:4:4 macroblock structure

Figure 2.8 Macroblock structures in 4:2:0, 4:2:2 and 4:4:4 image formats

For a more detail representation of image formats, especially discriminating 4:2:0 from 4:1:1, one can relate the horizontal and vertical resolutions of the chrominance components to those of luminance as shown in Table 2.1. Note that the luminance resolution is the same as the number of pixels in each scanning direction.

Table 2.1 Percentage of each chrominance component resolution with respect to luminance in the horizontal and vertical directions

Image format	**Horizontal (%)**	**Vertical (%)**
4:4:4	100	100
4:2:2	50	100
4:2:0	50	50
4:1:1	25	100

2.3.6 Conversion from film

Sometimes sources available for compression consist of film material, which has a nominal frame rate of 24 pictures/s. This rate can be converted to 30 pictures/s by the pull-down technique [3]. In this mode, digitised pictures are displayed alternately for 3 and 2 television field times, generating 60 fields/s. This alteration may not be exact, since the actual frame rate in the 525/60 system is 29.97 frames/s. Editing and splicing of compressed video after the conversion might also have changed the pull-down timing. A sophisticated encoder might detect the duplicated fields, average them to reduce digitisation noise and code the result at the original 24 pictures/s rate. This should give a significant improvement in quality over coding at 30 pictures/s. This is because, first of all, when coding at 24 pictures/s, the bit rate budget per frame is larger than that for 30 pictures/s. Second, direct coding of 30 pictures/s destroys the 3:2 pull-down timing and gives a jerky appearance to the final decoded video.

2.3.7 Temporal resampling

Since the picture rates are limited to those commonly used in the television industry, the same techniques may be applied. For example, conversion from 24 pictures/s to 60 fields can be achieved by the technique of 3:2 pull-down. Video coded at 25 pictures/s can be converted to 50 fields/s by displaying the original decoded lines in the odd CCIR-601 fields, and the interpolated lines in the even fields. Video coded at 29.97 or 30 pictures/s may be converted to a field rate twice as large as using the same method.

2.4 Picture quality assessment

Conversion of digital pictures from one format to another, as well as their compression for bit rate reduction, introduces some distortions. It is of great importance to know whether the introduced distortion is acceptable to the viewers. Traditionally, this has been done by subjective assessments, where the degraded pictures are shown to a group of subjects, and their views on the perceived quality or distortions are sought.

Over the years, many subjective assessment methodologies have been developed and validated. Among them are the double-stimulus impairment scale (DSIS), where the subjects are asked to rate the impairment of the processed picture with respect to the reference unimpaired picture, and the double-stimulus continuous quality scale (DSCQS), where the order of the presentation of the reference and processed pictures is unknown to the subjects. The subjects will then give a score between 1 and 100 containing adjectival guidelines placed at 20-point intervals (1–20 = bad, 21–40 = poor, 41–60 = fair, 61–80 = good and 81–100 = excellent) for each picture, and their difference is an indication of the quality [5]. Pictures are presented to the viewers for about 10 s, and the average of the viewers' scores, defined as the mean opinion score (MOS), is a measure of video quality. At least 20–25 nonexpert viewers are required to give a reliable MOS, excluding the outliers.

These methods are usually used in assessment of still images. For video evaluation, single-stimulus continuous quality evaluation (SSCQE) is preferred, where the time-varying picture quality of the processed video without reference is evaluated by the subjects [5]. In this method, subjects are asked to continuously evaluate the video quality of a set of video scenes. The judgement criteria are the five scales used in the DSCQS above. Since video sequences are long, they are segmented into 10 s shots, and for each video segment an MOS is calculated.

Although these methods give reliable indications of the perceived image quality, they are unfortunately time consuming and expensive. An alternative is the objective measurements, or video quality metrics, which employ some mathematical models to mimic the human visual systems behaviour.

In 1997, the Video Quality Experts Group (VQEG) formed from experts of ITU-T study group 6 and ITU-T study group 9 undertook this task [6]. They are considering three methods for the development of the video quality metric. In the first method, called the full reference (FR-TV) model, both the processed and the reference video segments are fed to the model and the outcome is a quantitative indicator of the video quality. In the second method, called reduced reference (RR-TV) model, some features extracted from the spatio-temporal regions of the reference picture (e.g. mean and variance of pixels, colour histograms) are made available to the model. The processed video is then required to generate a similar statistics in those regions. In the third model, called no reference (NR-TV), or single ended, the processed video without any information from the reference picture excites the model. All these models should be validated with the SSCQE methods for various video segments. Early results indicate that these methods compared with the SSCQE perform satisfactorily, with a correlation coefficient between 0.8 and 0.9 [7].

Until any of these quality metrics become standards, it is customary to use the simplest form of objective measurement, which is the ratio of the peak-to-peak signal to the root mean squared processing noise. This is referred to as peak-to-peak signal-to-noise ratio (PSNR) and defined as

$$\mathrm{PSNR} = 10\log_{10}\left[\frac{255^2}{\frac{1}{N}\sum_i\sum_j (Y_{ref}(i,j) - Y_{prc}(i,j))^2}\right] \tag{2.7}$$

where $Y_{ref}(i, j)$ and $Y_{prc}(i, j)$ are the pixel values of the reference and processed images, respectively, and N is the total number of pixels in the image. In this equation, the peak signal with an 8-bit resolution is 255, and the noise is the square of the pixel-to-pixel difference (error) between the reference image and the image under study. Although it has been claimed that in some cases PSNR's accuracy is doubtful, its relative simplicity makes it a very popular choice.

Perhaps the main criticism against the PSNR is that the human interpretation of the distortions at different parts of the video can be different. Although it is hoped that the variety of interpretations can be included in the objective models, there are still some issues that not only the simple PSNR but also more sophisticated objective models may fail to address. For example, if a small part of a picture in a video is severely degraded, this hardly affects the PSNR or any objective model parameters (depending on the area of distortion), but this distortion attracts the observers attention, and the video looks as bad as if a larger part of the picture was distorted. This type of distortion is very common in video, where due to a single bit error, blocks of 16×16 pixels might be erroneously decoded. This has almost no significant effect on PSNR but can be viewed as an annoying artefact. In this case, there will be a large discrepancy between the objective and subjective test results.

On the other hand, one may argue that under similar conditions if one system has a better PSNR than the other, then the subjective quality can be better but not worse. This is the main reason that PSNR is still used in comparing the performance of various video codecs. However, in comparing codecs, PSNR or any objective measure should be used with great care to ensure that the types of coding distortions are not significantly different from each other. For instance, objective results from the blockiness distortion produced by the block-based video codecs can be different from the picture smearing distortion introduced by the filter-based codecs. The fact is that even the subjects may interpret these distortions differently. It appears that expert viewers prefer blockiness distortion to the smearing, and nonexperts' views are opposite!

In addition to the above-mentioned problems of subjective and objective measurements of video quality, the impact of people's expectation from video quality cannot be ignored. As technology progresses and viewers' become more familiar with digital video, their level of expectation from video quality can grow. Hence, a quality that today might be regarded 'good' may be rated as 'fair' or 'poor' tomorrow. For instance, watching a head-and-shoulders video coded at 64 kbit/s by the early prototypes of the video codecs in the mid-1980s was very fascinating. This was despite the fact that pictures were coded at 1 or 2 frames/s, and waiving the hands in front of the camera would freeze the picture for a few seconds, or cause a complete picture break-up. But today, even 64-kbit/s coded video at 4–5 frames/s, without picture freeze, does not look attractive. As another example, most people might be quite satisfied with the quality of the broadcast TV at home, both analogue and digital, but if they watch football spectators on a broadcast TV side by side to an HDTV video, they then realise how much information they are missing. These are all indications that people's expectation from video quality in the future will be higher. Thus, video codecs either have to be more sophisticated or be assigned with more channel bandwidth. Fortunately, with the advances in digital technology and growth in networks bandwidth, both are feasible, and in the future we will witness better-quality video services.

2.5 Problems

1. In a PAL system, determine the values of the three colour primaries R, G and B for the following colours: red, green, blue, yellow, cyan, magenta and white.
2. Calculate the luminance and chrominance values of the colours in problem 1, if they are digitised into 8 bits, according to CCIR-601 specification.
3. Calculate the horizontal scanning line frequency for CCIR-601/625 and CCIR-601/525 line systems and hence their periods.
4. CCIR-601/625 video is normally digitised at 13.5 MHz sampling rate. Find the number of pixels per scanning line. If there are 720 pixels in the active part of the horizontal scanning, find the duration of horizontal scanning fly-back (i.e. horizontal blanking interval).
5. Repeat problem 4 for CCIR-601/525.
6. Find the bit rate per second of the following video formats (only active pixels are considered):
   a. CCIR-601/625; 4:2:2
   b. CCIR-601/525; 4:2:2
   c. SIF/625; 4:2:0
   d. SIF/525; 4:2:0
   e. CIF
   f. SIF/625; 4:1:1
   g. SIF/525; 4:1:1
   h. QCIF (15 Hz)
   i. Sub-QCIF (10 Hz)
7. The luminance values of a set of pixels in a CCIR-601 video are as follows: 128; 128; 128; 120; 60; 50; 180; 154; 198; 205; 105; 61; 93; 208; 250; 190; 128; 128; 128.

   They are filtered and downsampled by 2:1 into SIF format. Find the luminance values of seven SIF samples, starting from the fourth pixel of CCIR-601.

8. The luminance values of the SIF pixels in problem 7 are upsampled and filtered into CCIR-601 format. Find the reconstructed CCIR-601 format pixel values. Calculate the PSNR of the reconstructed samples.

9. A pure sinusoid is linearly quantised into n bits.
   a. Show that the signal-to-quantisation noise ratio (SNR) in dB is given by $\mathrm{SNR} = 6n + 1.78$.
   b. Find such an expression for PSNR.
   c. Calculate the minimum bit per pixel required for quantising video, such that PSNR is better than 58 dB.

(Hint: the mean-squared quantisation error of a uniformly quantised waveform with step size Δ is $\Delta^2/12$)

References

1. NETRAVALI, A.N. and HASKELL, B.G.: *Digital Pictures, Representation and Compression and Standards*, 2nd edn, Plenum Press, New York, 1995
2. CCIR Recommendation 601: 'Digital methods of transmitting television information', Recommendation 601, encoding parameters of digital television for studios
3. MPEG-1: 'Coding of moving pictures and associated audio for digital storage media at up to about 1.5 Mbit/s', ISO/IEC 11172-2: video, November 1991
4. OKUBO, S.: Video codec standardisation in CCITT study group XV. *Signal Process. Image Commun.*, 1989, **1**, pp. 45–54
5. Recommendation ITU-R BT.500 (revised): 'Methodology for the subjective assessment of the quality of television pictures'
6. VQEG: The video quality Experts Group, RRNR-TV Group Test Plan, draft version 1.4, 2000
7. TAN, K.T., GHANBARI, M. and PEARSON D.E.: 'An objective measurement tool for MPEG video quality'. *Signal Process.*, 1998, **7**, pp. 279–294

Chapter 3
Principles of video compression

The statistical analysis of video signals indicates that there is a strong correlation both between successive picture frames and within the picture elements themselves. Theoretically, decorrelation of these signals can lead to bandwidth compression without significantly affecting image resolution. Moreover, the insensitivity of the human visual system to loss of certain spatio-temporal visual information can be exploited for further reduction. Hence, subjectively lossy compression techniques can be used to reduce video bit rates while maintaining an acceptable image quality.

For coding still images, only the spatial correlation is exploited. Such a coding technique is called intraframe coding and is the basis for Joint Photographic Experts Group (JPEG) coding. If temporal correlation is exploited as well, then it is called interframe coding. Interframe predictive coding is the main coding principle that is used in all standard video codecs, such as H.261, H.263, H.264 and Motion Picture Experts Group (MPEG)-1, -2 and -4. It is based on the following three fundamental redundancy reduction principles:

1. Spatial redundancy reduction: to reduce spatial redundancy among the pixels within a picture (similarity of pixels, within the frames) by employing some data compressors, such as transform coding.
2. Temporal redundancy reduction: to remove similarities between the successive pictures by coding their differences.
3. Entropy coding: to reduce the redundancy between the compressed data symbols, using variable length coding (VLC) techniques.

A detailed description of these redundancy reduction techniques is given in the following sections.

3.1 Spatial redundancy reduction

3.1.1 Predictive coding

In the early days of image compression, both signal processing tools and storage devices were scarce resources. At the time, a simple method for redundancy reduction was to predict the value of pixels based on the values previously coded, and code the prediction error. This method is called differential pulse code modulation (DPCM). Figure 3.1 shows a block diagram of a DPCM codec, where the differences between the incoming pixels from the predictions in the predictor are quantised and

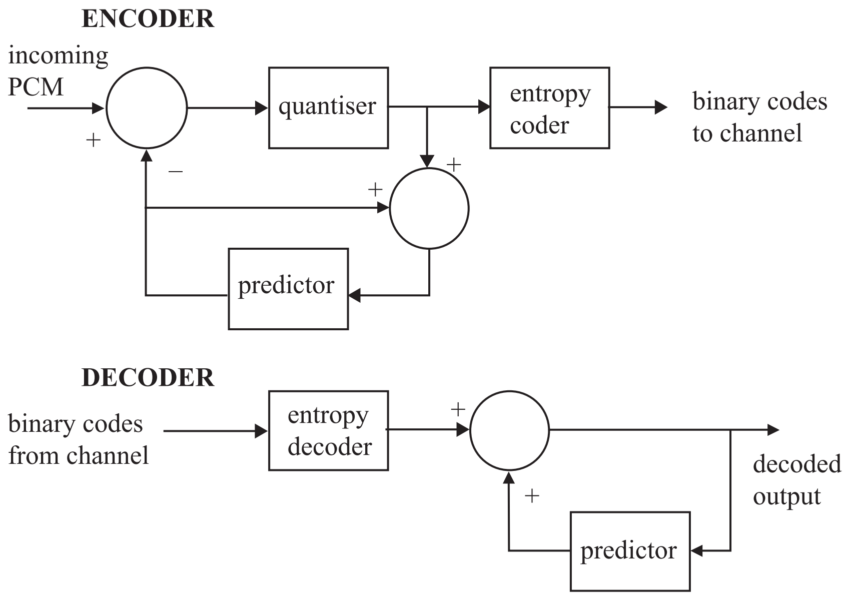

Figure 3.1 Block diagram of a DPCM codec

coded for transmission. At the decoder, the received error signal is added to the prediction to reconstruct the signal. If the quantiser is not used, it is called lossless coding, and the compression relies on the entropy coder, which is explained later.

Best predictions are those from the neighbouring pixels, either from the same frame or pixels from the previous frame, or their combinations. The former is called intraframe predictive coding and the latter interframe predictive coding. Their combination is called hybrid predictive coding.

It should be noted that no matter what prediction is used, every pixel is predictively coded. The minimum number of bits that can be assigned to each prediction error is 1 bit. Hence, this type of coding is not suitable for low bit rate video coding. Lower bit rates can be achieved if a group of pixels is coded together, such that the average bit per pixel can be less than 1 bit. Block transform coding is most suitable for this purpose. Despite this, DPCM is still used in video compression. For example, interframe DPCM has lower coding latency than interframe block coding. Also, DPCM might be used in coding of motion vectors or block addresses. If motion vectors in a moving object move in the same direction, coding of their differences will reduce the motion vector information. Of course, the coding would be lossless.

3.1.2 Transform coding

Transform domain coding is mainly used to remove the spatial redundancies in images by mapping the pixels into a transform domain prior to data reduction.

The strength of transform coding in achieving data compression is that the image energy of most natural scenes is mainly concentrated in the low-frequency region, and hence into a few transform coefficients. These coefficients can then be quantised with the aim of discarding insignificant coefficients, without significantly affecting the reconstructed image quality. This quantisation process is, however, lossy in that the original values cannot be retained.

To see how transform coding can lead to data compression, consider joint occurrences of 2 pixels as shown in Figure 3.2.

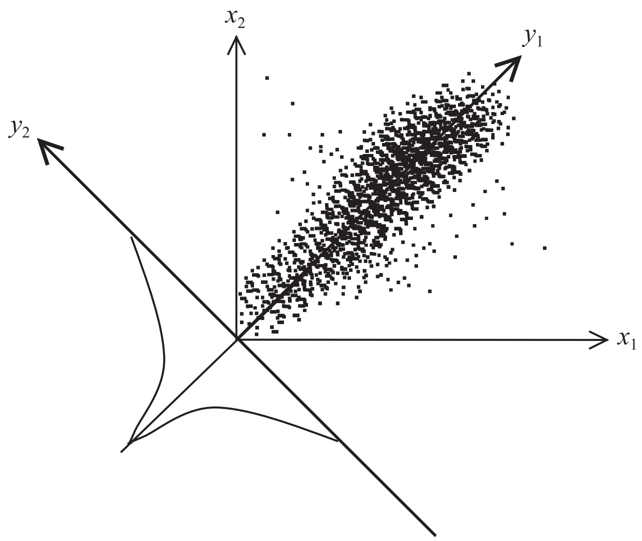

Figure 3.2 Joint occurrences of a pair of pixels

Although each pixel x_1 or x_2 may take any value uniformly between 0 (black) and its maximum value 255 (white), since there is a high correlation (similarity) between them, then it is most likely that their joint occurrences lie mainly on a 45-degree line, as shown in the figure. Now if we rotate the x_1x_2 coordinates by 45 degrees, to a new position y_1y_2, then the joint occurrences on the new coordinates have a uniform distribution along the y_1 axis, but are highly peaked around zero on the y_2 axis. Certainly, the bits required to represent the new parameter y_1 can be as large as any of x_1 or x_2, but those for the other parameter y_2 are much less. Hence, on average, y_1 and y_2 can be represented at a lower bit rate than x_1 and x_2.

Rotation of x_1x_2 coordinates by 45 degrees is a transformation of vector $[x_1, x_2]$ by a transformation matrix T, shown as follows:

$$T = \begin{bmatrix} \cos 45 & \sin 45 \\ \sin 45 & -\cos 45 \end{bmatrix} = \frac{1}{\sqrt{2}} \begin{bmatrix} 1 & 1 \\ 1 & -1 \end{bmatrix} \tag{3.1}$$

Thus, in this example, the transform coefficients $[y_1, y_2]$ become

$$[y_1, y_2] = \frac{1}{\sqrt{2}} \begin{bmatrix} 1 & 1 \\ 1 & -1 \end{bmatrix} \begin{bmatrix} x_1 \\ x_2 \end{bmatrix}$$

or (3.2)

$$y_1 = \frac{1}{\sqrt{2}}(x_1 + x_2) \quad \text{and} \quad y_2 = \frac{1}{\sqrt{2}}(x_1 - x_2)$$

where y_1 is called the average or DC value of x_1 and x_2, and y_2 represents their residual differences. The normalisation factor of $1/\sqrt{2}$ makes sure that the signal energy due to transformation is not changed (Parseval theorem). This means that the signal energy in the pixel domain, $x_1^2 + x_2^2$, is equal to the signal energy in the transform domain, $y_1^2 + y_2^2$. Hence, the transformation matrix is orthonormal.

Now if instead of 2 pixels, we take N correlated pixels, and then transform the coordinates such that y_1 lies on the main diagonal of the sphere, then only y_1 coefficient becomes significant, and the remaining $N - 1$ coefficients, $y_2, y_3, \ldots, y_N$, only carry the residual information. Thus, compared to 2-pixel case, larger dimensions of transformation can lead to higher compression. Exactly how large the dimensions should be depends on how far pixels can still be correlated to each other. Also, the elements of the transformation matrix, called the basis vectors, have an important role in the compression efficiency. They should be such that only one of the transform coefficients, or at most a few of them, becomes significant, and the remaining ones are small.

An ideal choice for the transformation matrix is the one that completely decorrelates the transform coefficients. Thus, if R_{xx} is the covariance matrix of the input source (pixels), x, then the elements of the transformation matrix T are calculated such that the covariance of the coefficients $R_{yy} = TR_{xx}T^T$ is a diagonal matrix (zero off-diagonal elements). A transform that is derived on this basis is the well-known Karhunen–Loève transform (KLT) [1]. However, although this transform is optimum, and hence it can give the maximum compression efficiency, it is not suitable for image compression. This is because, as the image statistics change, the elements of the transform need to be recalculated. Thus, in addition to extra computational complexity, these elements need to be transmitted to the decoder. The extra overhead involved in the transmission significantly restricts the overall compression efficiency. Despite this, KLT is still useful and can be used as a benchmark for evaluating the compression efficiency of other transforms.

A better choice for the transformation matrix is that of the discrete cosine transform (DCT). The reason for this is that it has well-defined (fixed) and smoothly varying basis vectors that resemble the intensity variations of most natural images, such that image energy is matched to a few coefficients. For this reason, its rate distortion performance closely follows that of the KLT, and results in almost identical compression gain [1]. Equally important is the availability of efficient fast DCT transformation algorithms that can be used, especially in software-based image coding applications [2].

Since in natural image sequences, pixels are correlated in the horizontal and vertical directions as well as in the temporal direction of the image sequence, a natural choice for DCT is a three-dimensional one. However, any transformation in the temporal domain requires storage of several picture frames, introducing a long delay, which restricts application of transform coding in telecommunications. Hence, transformation is confined to two dimensions.

A two-dimensional DCT is a separable process that is implemented using two one-dimensional DCTs: one in the horizontal direction followed by one in the vertical. For a block of *MN* pixels, the forward one-dimensional transform of *N* pixels is given by

$$F(u) = \sqrt{\frac{2}{N}}C(u)\sum_{x=0}^{N-1} f(x)\cos\left(\frac{\pi(2x+1)u}{2N}\right), \quad u = 0, 1, \ldots, N-1 \qquad (3.3)$$

where

$$\begin{aligned} C(u) &= \sqrt{\frac{1}{2}}, && \text{for } u = 0 \\ C(u) &= 1, && \text{otherwise} \end{aligned}$$

f(*x*) represents the intensity of the *x*th pixel, and *F*(*u*) represents the *N* one-dimensional transform coefficients. The inverse one-dimensional transform is thus defined as

$$f(x) = \sqrt{\frac{2}{N}}\sum_{u=0}^{N-1} C(u)F(u)\cos\left(\frac{\pi(2x+1)u}{2N}\right), \quad x = 0, 1, \ldots, N-1 \qquad (3.4)$$

Note that the $\sqrt{1/N}$ normalisation factor is used to make transformation orthonormal. That is, the energy in both pixel and transform domains is to be equal. In the standard codecs, the normalisation factor for the two-dimensional DCT is defined as 1/2. This gives the DCT coefficients in the range of -2047 to $+2047$. The normalisation factor in the pixel domain is then adjusted accordingly (e.g. it becomes 2/*N*).

To derive the final two-dimensional transform coefficients, *N* sets of one-dimensional transforms of length *M* are taken over the one-dimensional transform coefficients of similar frequency in the vertical direction:

$$F(u,v) = \sqrt{\frac{2}{M}}C(v)\sum_{y=0}^{M-1} F(u,y)\cos\left(\frac{\pi(2y+1)v}{2M}\right), \quad v = 0, 1, \ldots, M-1 \qquad (3.5)$$

where *C*(*v*) is defined similarly to *C*(*u*).

Thus, a block of *MN* pixels is transformed into *MN* coefficients. The *F*(0, 0) coefficient represents the DC value of the block. Coefficient *F*(0, 1), which is the DC value of all the first one-dimensional AC coefficients, represents the first

AC coefficient in the horizontal direction of the block. Similarly, $F(1, 0)$, which is the first AC coefficient of all one-dimensional DC values, represents the first AC coefficient in the vertical direction, and so on.

In practice, $M = N = 8$, such that a two-dimensional transform of $8 \times 8 = 64$ pixels results in 64 transform coefficients. The choice of such a block size is a compromise between the compression efficiency and the blocking artefacts of coarsely quantised coefficients. Although larger block sizes have good compression efficiency, the blocking artefacts are subjectively very annoying. At the early stage of standardisation of video codecs, the block sizes were made optional at 4×4, 8×8 and 16×16. Now the block size in all standard codecs is 8×8, except in H.264, in which it is 4×4.

3.1.3 Mismatch control

Implementation of both forward and inverse transforms (e.g. eqns 3.3 and 3.4) requires the *cos* elements to be approximated with finite numbers. Because of this approximation, the reconstructed signal, even without any quantisation, cannot be an exact replica of the input signal to the forward transform. For image and video coding applications, this mismatch needs to be controlled; otherwise, the accumulated error due to approximation can grow out of control resulting in an annoying picture artefact.

One way of preventing error accumulation is to let the error to oscillate between two small levels. This guarantees that the accumulated error never exceeds its limit. The approach taken in the standard codecs is to say (e.g. MPEG-2) that the sum of all the values of the $8 \times 8 = 64$ transform coefficients should be an odd number (no matter whether they are quantised or not), at the decoder. In case the sum is an even number, the value of the highest frequency coefficient, $F(7, 7)$, is either incremented or decremented by 1, depending on whether its value itself is odd or even, respectively. This, of course, introduces a very small error, but it cannot be noticed on images, for two reasons. First, at the inverse transform, the reconstructed pixels are divided by a large value in the order of N^2. Second, since error is introduced by the highest frequency coefficient, it appears as a very high frequency, small amplitude dither-like noise, which is not perceivable at all (the human eye is very tolerant to high-frequency noise).

3.1.4 Fast DCT transform

To calculate transform coefficients, every one-dimensional forward or inverse transformation requires eight multiplications and seven additions. This process is repeated for 64 coefficients in both the horizontal and vertical directions. Since software-based video compression is highly desirable, methods of reducing such a huge computational burden are highly desirable.

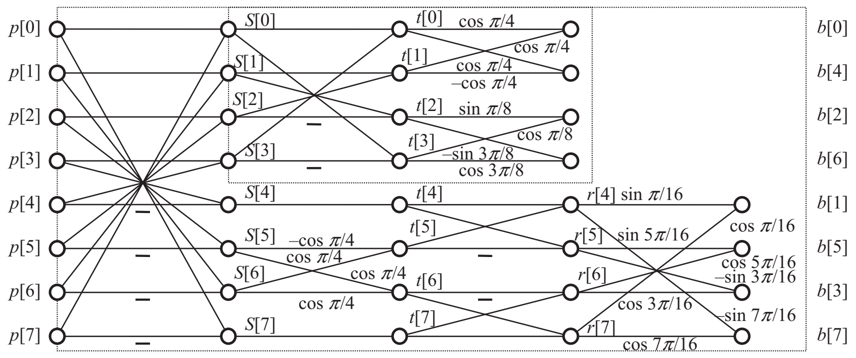

Figure 3.3 A fast DCT flow chart

The fact that DCT is a type of discrete Fourier transform, with the advantage of all real coefficients, enables one to use a fast transform, similar to the fast Fourier transform, to calculate transform coefficients with complexity proportional to $N\log_2 N$, rather than N^2. Figure 3.3 shows a butterfly representation of the fast DCT [2]. Intermediate nodes share some of the computational burden, hence reducing the overall complexity. In the figure, $p[0]$–$p[7]$ are the inputs to the forward DCT, and $b[0]$–$b[7]$ are the transform coefficients. The inputs can be either the 8 pixels for the source image or eight transform coefficients of the first stage of the one-dimensional transform. Similarly, for inverse transformation, $b[0]$–$b[7]$ are the inputs to the inverse DCT (IDCT), and $p[0]$–$p[7]$ are the outputs. A C language program for fast forward DCT is given in Appendix A. In this program, some modifications to the butterfly matrices are made to trade off the number of additions for multiplications, since multiplications are more computationally intensive than additions. A similar program can be written for the inverse transform.

3.2 Quantisation of DCT coefficients

The domain transformation of the pixels does not actually yield any compression. A block of 64 pixels is transformed into 64 coefficients. Because of the orthonormality of transformation, the energies in both the pixel and the transform domains are equal; hence, no compression is achieved. However, transformation causes the significant part of the image energy to be concentrated at the lower frequency components, with the majority of the coefficients having little energy. It is the quantisation and VLC of the DCT coefficients that lead to bit rate reduction. Moreover, by exploiting the human eye's characteristics, which are less sensitive to picture distortions at higher frequencies, one can apply even coarser quantisation at these frequencies, to give greater compression. Coarser quantisation step sizes force more coefficients to zero, and as a result, more compression is gained, but, of course, the picture quality deteriorates accordingly.

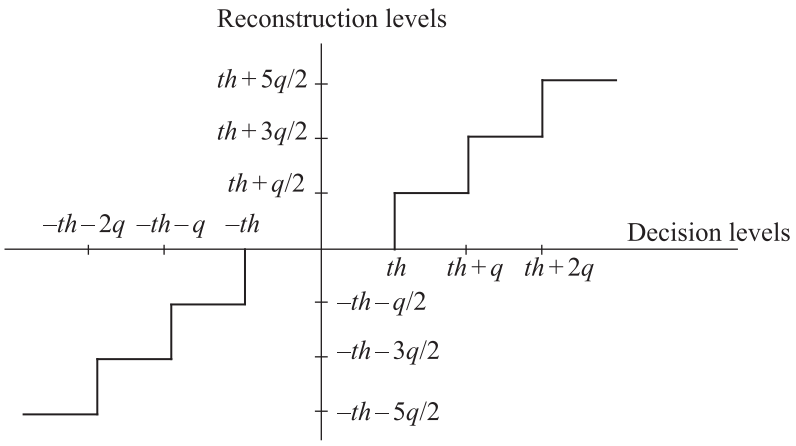

Figure 3.4 Quantisation characteristics

The class of quantiser that has been used in all standard video codecs is based around the so-called uniform threshold quantiser (UTQ). It has equal step sizes with reconstruction values pegged to the centroid of the steps. This is illustrated in Figure 3.4.

The two key parameters that define a UTQ are the threshold value, *th*, and the step size, *q*. The centroid value is typically defined midway between quantisation intervals. Note that although AC transform coefficients have nonuniform characteristics, and hence can be better quantised with nonuniform quantiser step sizes (the DC coefficient has a fairly uniform distribution), bit rate control would be easier if they were quantised linearly. Hence, a key property of UTQ is that the step sizes can be easily adapted to facilitate rate control.

A further two subclasses of UTQ can be identified within the standard codecs, namely those with and without a dead zone. They are illustrated in Figure 3.5 and are hereafter abbreviated as UTQ-DZ and UTQ, respectively. The term dead zone commonly refers to the central region of the quantiser, whereby the coefficients are quantised to zero.

Typically, UTQ is used for quantising intraframe DC, $F(0, 0)$, coefficients, while UTQ-DZ is used for the AC and the DC coefficients of interframe prediction error. This is intended primarily to cause more nonsignificant AC coefficients to become zero, thus increasing the compression. Both quantisers are derived from the generic quantiser of Figure 3.4, where in UTQ, *th* is set to zero, but in UTQ-DZ, it is set to $q/2$, and in the most inner region it is allowed to vary between $q/2$ to q, just to increase the number of zero-valued outputs, as shown in Figure 3.5. Thus, the dead zone length can be from q to $2q$. In some implementations (e.g. H.263 or MPEG-4), the decision and/or the reconstruction levels of the UTQ-DZ quantiser might be shifted by $q/4$ or $q/2$.

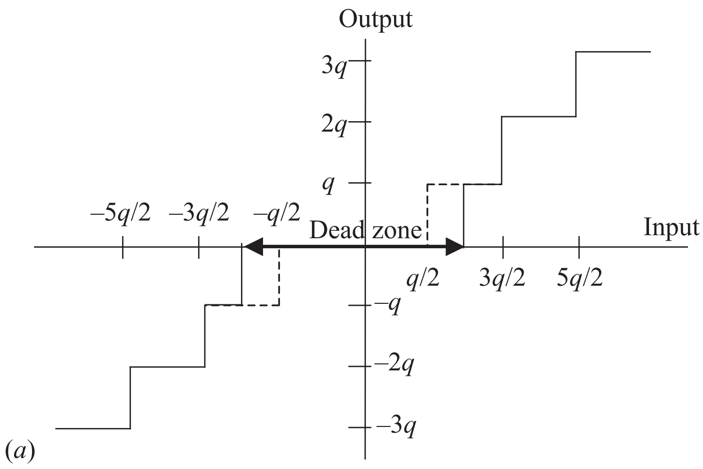

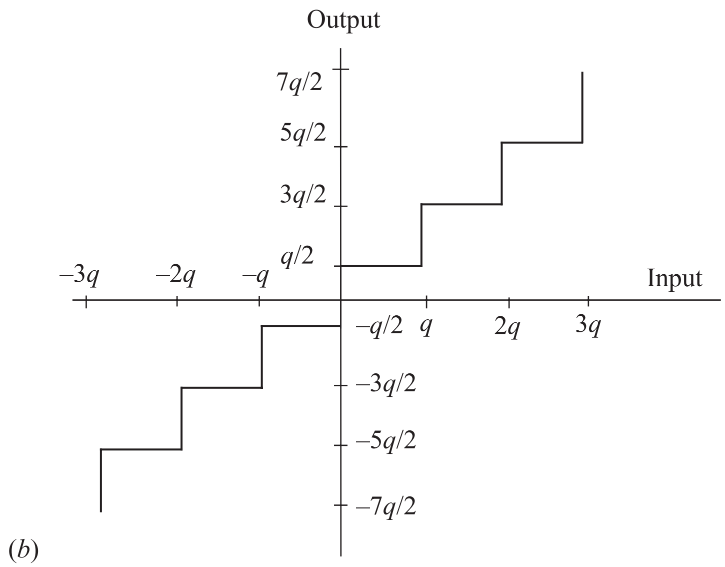

Figure 3.5 Uniform quantisers (a) with and (b) without dead zone

In practice, rather than transmitting a quantised coefficient to the decoder, its ratio to the quantiser step size, called quantisation index, *I*, is transmitted:

$$I(u,v) = \left\lfloor \frac{F(u,v)}{q} \right\rfloor \tag{3.6}$$

(In eqn. 3.6 the symbol $\lfloor \cdot \rfloor$ stands for rounding to the nearest integer.) The reason for defining the quantisation index is that it has a much smaller entropy than the quantised coefficient. At the decoder, the reconstructed coefficients, $F^q(u, v)$, after inverse quantisation, are given by

$$F^q(u,v) = \left\{ I(u,v) \pm \frac{1}{2} \right\} \times q \tag{3.7}$$

If required, depending on the polarity of the index, an addition or subtraction of half the quantisation step is required to deliver the centroid representation, reflecting the quantisation characteristics of Figure 3.5.

It is worth noting that for the standard codecs, the quantiser step size q is fixed at 8 for UTQ, but varies from 2 to 62, in even step sizes, for the UTQ-DZ. Hence, the entire quantiser range, or the quantiser parameter Q_p (half the quantiser step size), can be defined with 5 bits (1–31).

Uniform quantisers with and without dead zone can also be used in DPCM coding of pixels (section 3.1). Here, threshold is set to zero, $th = 0$, and the quantisers are usually identified with even and odd number of levels, respectively.

One of the main problems of linear quantisers in DPCM is that for lower bit rates, the number of quantisation levels is limited and hence the quantiser step size is large. In coding of plain areas of the picture, if a quantiser with even number of levels is used, then the reconstructed pixels oscillate between $-q/2$ and $q/2$. This type of noise at these areas, in particular at low luminance levels, is visible and is called granular noise.

Larger quantiser step sizes with the odd number of levels (dead zone) reduce the granular noise, but cause loss of pixel resolution at the plain areas. This type of noise when the quantiser step size is relatively large is annoying and is called the contouring noise.

To reduce granular and contouring noises, the quantiser step size should be reduced. This, of course, for a limited number of quantisation levels (low bit rate) reduces the outmost reconstruction level. In this case, large pixel transitions such as sharp edges cannot be coded with good fidelity. It might take several cycles for the encoder to code one large sharp edge. Hence, edges appear smeared, and this type of noise is known as slope overload noise.

To reduce the slope overload noise without increasing the granular or contouring noises, the quantiser step size can change adaptively. For example, a lower step size quantiser is used at the plain areas, and a larger step size is employed at the edges and high-texture areas. Note that the overhead of adaptation can be very costly (e.g. 1 bit/pixel).

The other method is to use a nonlinear quantiser with small step sizes at the inner levels and larger step sizes at the outer levels. This suits DPCM video better than the linear quantiser. Nonlinear quantisers reduce the entropy of the data more than linear quantisers. Hence, data are less dependent on the VLC, increasing the robustness of the DPCM video to channel errors.

3.3 Temporal redundancy reduction

By using the differences between successive images, temporal redundancy is reduced. This is called *interframe* coding. For static parts of the image sequence, temporal differences will be close to zero, and hence are not coded. Those parts that change between the frames, due to either illumination variation or motion of the objects, result in significant image error, which needs to be coded. Image changes due to motion can be significantly reduced if the motion of the object can be estimated, and the difference is taken on the motion-compensated image.

Figure 3.6 shows the interframe error between successive frames of the Claire test image sequence and its motion-compensated counterpart. It is clear that motion compensation can substantially reduce the interframe error.

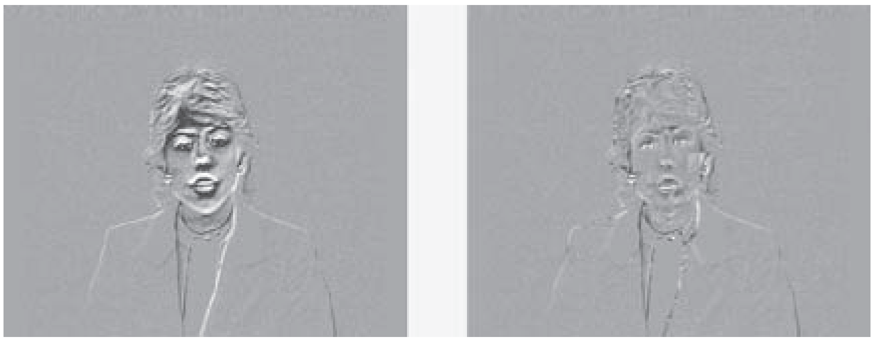

Figure 3.6 (a) Interframe and (b) motion-compensated interframe pictures

3.3.1 Motion estimation

To carry out motion compensation, the motion of the moving objects has to be estimated first. This is called *motion estimation* (ME). The commonly used ME technique in all the standard video codecs is the block matching algorithm (BMA). In a typical BMA, a frame is divided into blocks of MN pixels or, more usually, square blocks of N^2 pixels [3]. Then, for a maximum motion displacement of w pixels/frame, the current block of pixels is matched against a corresponding block at the same coordinates but in the previous frame, within the square window of width $N + 2w$ (Figure 3.7). The best match on the basis of a matching criterion yields the displacement.

Various measures such as the cross-correlation function (CCF), mean-squared error (MSE) and mean absolute error (MAE) can be used in the matching criterion [4–6]. For the best match, in the CCF the correlation has to be maximised, whereas in the latter two the distortion must be minimised. In practical coders, both MSE and MAE are used, since it is believed that CCF would not give good motion tracking, especially when the displacement is not large [6]. The matching functions of the type MSE and MAE are defined as, for MSE:

$$M(i,j) = \frac{1}{N^2}\sum_{m=1}^{N}\sum_{n=1}^{N}(f(m,n) - g(m+i,n+j))^2, \quad -w \le i,\ j \le w \tag{3.8}$$

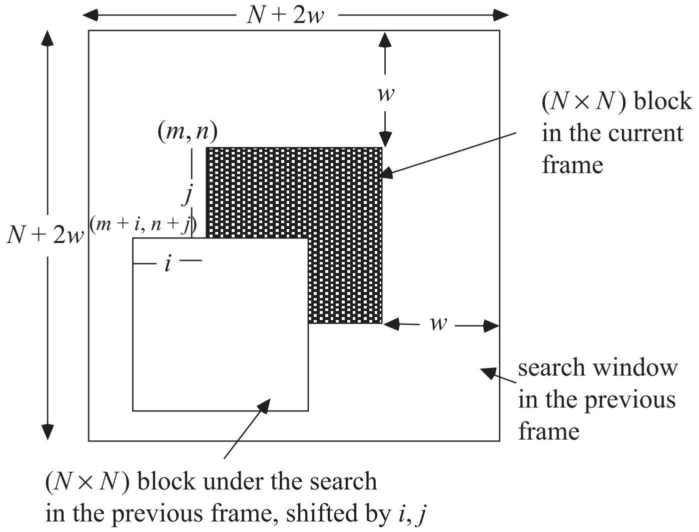

$N+2w$
$N+2w$
w
(m, n)
j
$(m+i, n+j)$
i
w
$(N \times N)$ block in the current frame
search window in the previous frame
$(N \times N)$ block under the search in the previous frame, shifted by i, j

Figure 3.7 The current and previous frames in a search window

and for MAE:

$$M(i,j) = \frac{1}{N^2}\sum_{m=1}^{N}\sum_{n=1}^{N}|f(m,n) - g(m+i, n+j)|, \quad -w \le i, j \le w \tag{3.9}$$

where $f(m, n)$ represents the current block of N^2 pixels at coordinates (m, n) and $g(m + i, n + j)$ represents the corresponding block in the previous frame at new coordinates $(m + i, n + j)$. At the best-matched position of $i = a$ and $j = b$, the motion vector, $MV(a, b)$, represents the displacement of all the pixels within the block.

To locate the best match by full search, $(2w + 1)^2$ evaluations of the matching criterion are required. To reduce processing cost, MAE is preferred to MSE, and hence is used in all the video codecs. However, for each block of N^2 pixels, we still need to carry out $(2w + 1)^2$ tests, each with almost $2N^2$ additions and subtractions. This is still far from being suitable for implementation of BMA in software-based codecs. Measurements of the video encoders' complexity show that ME comprises almost 50–70 per cent of the overall encoder's complexity [7]. This, of course, depends on the motion activity in the scene and whether a fast DCT is used in deriving the transform coefficients. For example, the percentage of the processing time required to calculate the motion vectors of Mobile and Claire test image sequences in an MPEG-1 software-based encoder is given in Table 3.1. Note that although more processing time is required for ME in B-pictures than P-pictures, since the search range in P-pictures is much larger than that for B-pictures, the overall processing time for ME in P-pictures can be larger than that of the B-pictures, as shown in the table. The reason for these is dealt with in Chapter 7,

Table 3.1 Percentage of processing time required to carry out motion estimation in an MPEG-1 encoder

Category	**Fast DCT**		**Brute force DCT**	
Picture type	**Mobile**	**Claire**	**Mobile**	**Claire**
P-frame ME	66.1%	68.4%	53.3%	56.1%
B-frame ME	58.2%	60.9%	46.2%	48.7%

when we talk about different picture types in the MPEG-1 encoder. In any case, as ME is a costly process, fast ME techniques are highly desirable.

3.3.2 Fast motion estimation

In the past two decades, a number of fast search methods for ME have been introduced to reduce the computational complexity of BMA. The basic principle of these methods is that the number of search points can be reduced by selectively checking only a small number of specific points, assuming that the distortion measure monotonically decreases towards the best-matched point. Jain and Jain [6] were the first to use a two-dimensional logarithmic (TDL) search method to track the direction of a minimum MSE distortion measure. In their method, the distortion for the five initial positions, one at the centre of the coordinate and four at coordinates ($\pm w/2$, $\pm w/2$) of the search window, is computed first. In the next step, three more positions with the same step size in the direction of the previous minimum position are searched. The step size is then halved, and the above procedure is continued until the step size becomes unity. Finally, all the nine positions are searched. With this method, for $w = 5$ pixels/frame, 21 positions are searched as opposed to 121 positions required in the full search method (FSM).

Koga *et al.* [8] use a three-step search (TSS) method to compute motion displacements up to 6 pixels/frame. In their method, all eight positions surrounding the coordinate with a step size of $w/2$ are searched first. At each minimum position, the search step size is halved, and the next eight new positions are searched. This method, for $w = 6$ pixels/frame, searches 25 positions to locate the best match. The technique is the recommended method for the test of software-based H.261 [9] for videophone applications.

In Kappagantula and Rao's [4] modified motion estimation algorithm (MMEA), prior to halving the step sizes, two more positions are also searched. With this method, for $w = 7$ pixels/frame, only 19 MAE computations are required. In Srinivasan and Rao's [10] conjugate direction search (CDS) method, at every iteration of the direction search, two conjugate directions with a step size of 1 pixel, centred at the minimum position, are searched. Thus, for $w = 5$ pixels/frame, there will be only 13 searches at most.

Another method of fast BMA is the cross-search algorithm (CSA) [11]. In this method, the basic idea is still a logarithmic step search, which has also been exploited in [4], [6] and [8], but with some differences, which lead to fewer computational search points. The main difference is that at each iteration there are four search locations, which are the end points of a cross ($\times$) rather than ($+$). Also, at the final stage, the search points can be either the end points of ($\times$) or ($+$) crosses, as shown in Figure 3.8. For a maximum motion displacement of w pixels/frame, the total number of computations becomes $5 + 4\log_2 w$.

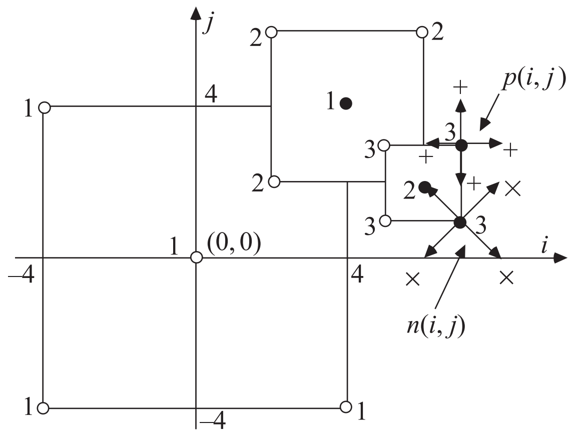

Figure 3.8 An example of the CSA search for w = 8 pixels/frame

Puri *et al.* [12] have introduced the orthogonal search algorithm (OSA) in which, with a logarithmic step size, at each iteration four new locations are searched. This is the fastest method of all known fast MBAs. In this method, at every step, two positions are searched alternately in the vertical and horizontal directions. The total number of test points is $1 + 4\log_2 w$.

Table 3.2 shows the computational complexity of various fast search methods, for a range of motion speed from 4 to 16 pixels/frame. The motion compensation efficiencies of these algorithms for a motion speed of $w = 8$ pixels/frame for two test image sequences are tabulated in Table 3.3.

Table 3.2 Computational complexity

Algorithm	**Maximum number of search points**	***w***		
		4	**8**	**16**
FSM	$(2w + 1)^2$	81	289	1089
TDL	$2 + 7 \log_2 w$	16	23	30
TSS	$1 + 8 \log_2 w$	17	25	33
MMEA	$1 + 6 \log_2 w$	13	19	25
CDS	$3 + 2w$	11	19	35
OSA	$1 + 4 \log_2 w$	9	13	17
CSA	$5 + 4 \log_2 w$	13	17	21

Table 3.3 Compensation efficiency

Algorithm	**Split screen**		**Trevor white**	
	Entropy (bits/pel)	**Standard deviation**	**Entropy (bits/pel)**	**Standard deviation**
FSM	4.57	7.39	4.41	6.07
TDL	4.74	8.23	4.60	6.92
TSS	4.74	8.19	4.58	6.86
MMEA	4.81	8.56	4.69	7.46
CDS	4.84	8.86	4.74	7.54
OSA	4.85	8.81	4.72	7.51
CSA	4.82	8.65	4.68	7.42

It can be seen that although fast search methods reduce the computational complexity of the FSM significantly, their ME accuracy (compensation efficiency) has not been degraded noticeably.

3.3.3 Hierarchical motion estimation

The assumption of monotonic variation of image intensity employed in the fast BMAs often causes false estimations, especially for larger picture displacements. These methods perform well for slow moving objects, such as those in video conferencing. However, for higher motion speeds, due to the intrinsic selective nature of these methods, they often converge to a local minimum of distortion.

One method of alleviating this problem is to subsample the image to smaller sizes, such that the motion speed is reduced by the sampling ratio. The process is done on a multilevel image pyramid, known as the hierarchical block matching algorithm (HBMA) [13]. In this technique, pyramids of the image frames are reconstructed by successive two-dimensional filtering and subsampling of the current and past image frames. Figure 3.9 shows a three-level pyramid, where for simplicity each level of the upper level of the pyramid is taken as the average of 4 adjacent pixels of one level below. Effectively this is a form of low-pass filtering.

Conventional block matching with a block size of 16 pixels, either full search or any fast method, is first applied to the highest level of the pyramid (level 2 in Figure 3.9). This motion vector is then doubled in size, and further refinement within 1-pixel search is carried out in the following level. The process is repeated to the lowest level. Therefore, with an n-level pyramid, the maximum motion speed of w at the highest level is reduced to $w/2^{n-1}$.

For example, a maximum motion speed of 32 pixels/frame with a three-level pyramid is reduced to 8 pixels/frame, which is quite manageable by any fast search method. Note that this method can also be regarded as another type of fast search, with a performance very close to the full search, irrespective of the motion speed, but the computational complexity can be very close to the fast logarithmic methods.

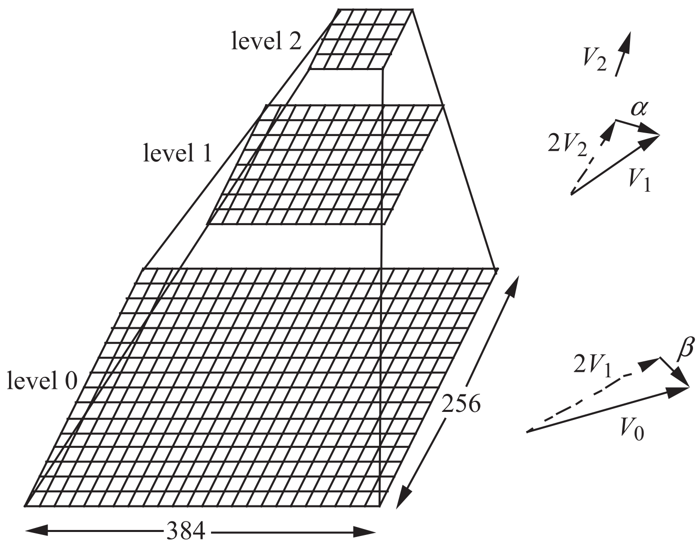

Figure 3.9 A three-level image pyramid

As an example, for a maximum motion speed of 32 pixels/frame, which is very common in high-definition video or most TV sports programmes (particularly in the P-pictures of the standard codecs, which can be several frames apart from each other), although the nonhierarchical full-search BMA requires $(2 \times 32 + 1)^2 = 4225$ operations, a four-level hierarchy, where the motion speed at the top level is $32/2^{4-1} = 4$ pixels/frame, only requires $(2 \times 4 + 1)^2 + 3 \times 9 = 108$ operations. Here with the FSM, 81 operations are carried out at the top level, and at each lower level nine new positions are searched.

3.4 Variable length coding

For further bit rate reduction, the transform coefficients and the coordinates of the motion vectors are variable length coded. In VLC, short code words are assigned to the highly probable values and long code words to the less probable ones. The lengths of the codes should vary inversely with the probability of occurrences of the various symbols in VLC. The bit rate required to code these symbols is the inverse of the logarithm of probability, p, at base 2 (bits), that is, $\log_2 p$. Hence, the entropy of the symbols, which is the minimum average bits required to code the symbols, can be calculated as

$$H(x) = -\sum_{i=1}^{n} p_i \log_2 p_i \tag{3.10}$$

There are two types of VLC, which are employed in the standard video codecs. They are Huffman coding and arithmetic coding. It is noted that Huffman coding is a simple VLC, but its compression can never reach as low as the entropy due to the constraint that the assigned symbols must have an integral number of bits. However, the arithmetic coding can approach the entropy since the symbols are not coded individually [14]. Huffman coding is employed in all standard codecs to encode the quantised DCT coefficients as well as motion vectors. Arithmetic coding is used, for example, in JPEG, JPEG2000, H.263, H.264 and shape and still image coding of MPEG-4 [15–17], where extra compression is demanded.

3.4.1 Huffman coding

Huffman coding is the most commonly known VLC method based on probability statistics. It assigns an output code to each symbol with the output codes being as short as 1 bit, or considerably longer than the input symbols, depending on their probability. The optimal number of bits to be used for each symbol is $-\log_2 p$, where p is the probability of a given symbol.

However, since the assigned code words have to consist of an integral number of bits, this makes Huffman coding suboptimum. For example, if the probability of a symbol is 0.33, the optimum number of bits to code that symbol is around 1.6 bits, but the Huffman coding scheme has to assign either 1 or 2 bits to the code. In either case, on average, it will lead to more bits compared to its entropy. As the probability of a symbol becomes very high, Huffman coding becomes very nonoptimal. For example, for a symbol with a probability of 0.9, the optimal code size should be 0.15 bits, but Huffman coding assigns a minimum value of 1 bit code to the symbol, which is six times larger than necessary. Hence, it can be seen that resources are wasted.

To generate the Huffman code for symbols with a known probability of occurrence, the following steps are carried out:

- Rank all the symbols in the order of their probability of occurrence.
- Successively merge every two symbols with the least probability to form a new composite symbol, and rerank order them: this will generate a tree, where each node is the probability of all nodes beneath it.
- Trace a path to each leaf, noting the direction at each node.

Figure 3.10 shows an example of Huffman coding of seven symbols, A–G. Their probabilities in descending order are shown in the third column. In the next column, the two smallest probabilities are added, and the combined probability is included in the new order. The procedure continues to the last column, where a single probability of 1 is reached. Starting from the last column, for every branch of probability a 0 is assigned on the top and 1 in the bottom, shown in bold digits in the figure. The corresponding code word (shown in the first column) is read off by following the sequence from right to left. Although with fixed word length each sample is represented by 3 bits, it is represented in VLC from 2 to 4 bits.

The average bit per symbol is then

$$\begin{aligned}&0.25 \times 2 + 0.20 \times 2 + 0.18 \times 3 + 0.15 \times 3 + 0.12 \times 3 + 0.06 \times 4 + 0.04 \times 4\\&\quad = 2.65\,\text{bits}\end{aligned}$$

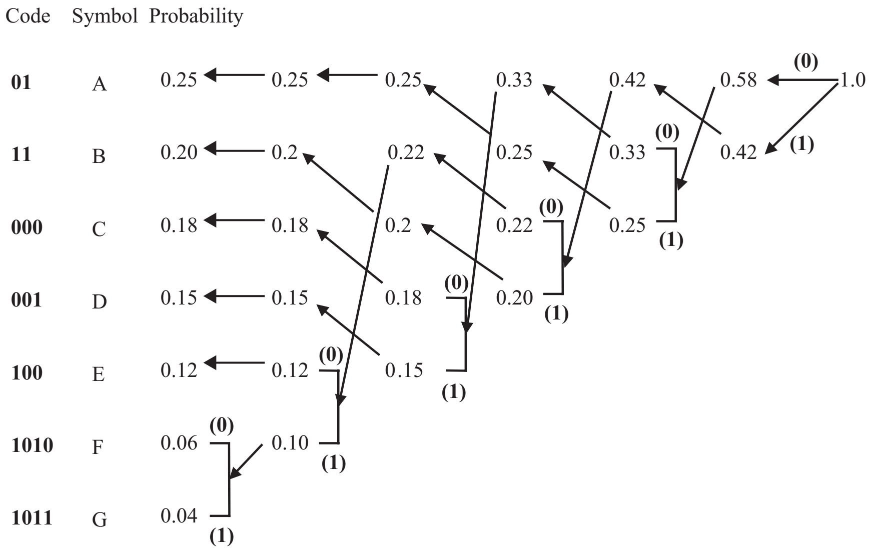

Figure 3.10 An example of Huffman code for seven symbols

which is very close to the entropy, given by

$$-(0.25\log_2 0.25 + 0.2\log_2 0.2 + 0.18\log_2 0.18 + 0.15\log_2 0.15 + 0.12\log_2 0.12 + 0.06\log_2 0.06 + 0.04\log_2 0.04) = 2.62\ \text{bits}$$

It should be noted that for a large number of symbols, such as the values of DCT coefficients, such a method can lead to a long string of bits for the very rarely occurring values, and is impractical. In such cases, normally a group of symbols is represented by the symbols' aggregate probabilities, and the combined probabilities are Huffman coded, the so-called modified Huffman code. This method is used in JPEG. Another method, which is used in H.261 and MPEG, is two-dimensional Huffman, or three-dimensional Huffman in H.263 [9,16].

3.4.2 Arithmetic coding

Huffman coding can be optimum if the symbol probability is an integer power of 1/2, which is usually not the case. Arithmetic coding is a data compression technique that encodes data by creating a code string, which represents a fractional value on the number line between 0 and 1 [14]. It encourages clear separation between the model for representing data and the encoding of information with respect to that model. Another advantage of arithmetic coding is that it dispenses with the restriction that each symbol must translate into an integral number of bits, thereby coding more efficiently. It actually achieves the theoretical entropy bound to compression efficiency for any source. In other words, arithmetic coding is a practical way of implementing entropy coding.

There are two types of modelling used in arithmetic coding: the fixed model and adaptive model. Modelling is a way of calculating, in any given context, the distribution of probabilities for the next symbol to be coded. It must be possible for the decoder to produce exactly the same probability distribution in the same context. Note that probabilities in the model are represented as integer frequency counts. Unlike the Huffman type, arithmetic coding accommodates adaptive models easily and is computationally efficient. The reason why data compression requires adaptive coding is that the input data source may change during encoding, due to motion and texture.

In the fixed model, both encoder and decoder know the assigned probability to each symbol. These probabilities can be determined by measuring frequencies in representative samples to be coded, and the symbol frequencies remain fixed. Fixed models are effective when the characteristics of the data source are close to the model and have little fluctuation.

In the adaptive model, the assigned probabilities may change as each symbol is coded, based on the symbol frequencies seen so far. Each symbol is treated as an individual unit, and hence there is no need for a representative sample of text. Initially all the counts might be the same, but they update, as each symbol is seen, to approximate the observed frequencies. The model updates the inherent distribution, so the prediction of the next symbol should be close to the real distribution mean, making the path from the symbol to the root shorter.

Because of the important role of arithmetic coding in the advanced video coding techniques, a more detailed description of this coding technique is given in the following sections.

3.4.2.1 Principles of arithmetic coding

The fundamental idea of arithmetic coding is to use a scale in which the coding intervals of real numbers between 0 and 1 are represented. This is in fact the cumulative probability density function of all the symbols that add up to 1. The interval needed to represent the message becomes smaller as the message becomes longer, and the number of bits needed to specify that interval is increased. According to the symbol probabilities generated by the model, the size of the interval is reduced by successive symbols of the message. The more likely symbols reduce the range less than the less likely ones, and hence they contribute fewer bits to the message.

To explain how arithmetic coding works, a fixed-model arithmetic code is used in the example for easy illustration. Suppose the alphabet is {**a, e, i, o, u, !**}, and the fixed model is used with the probabilities shown in Table 3.4.

Once the symbol probability is known, each individual symbol needs to be assigned a portion of the [0, 1) range that corresponds to its probability of appearance in the cumulative density function. Note also that the character with a range of [lower, upper) owns everything from lower value up to, but not including, the upper value. So, the alphabet **u** with probability 0.1, defined in the cumulative range of [0.8, 0.9), can take any value from 0.8 to 0.8999....

The most significant portion of an arithmetic coded message is the first symbol to be encoded. Using an example that a message **eaii!** is to be coded, the first

*Table 3.4 Example: fixed model for alphabet {**a, e, i, o, u, !**}*

Symbol	Probability	Range
a	0.2	[0.0, 0.2)
e	0.3	[0.2, 0.5)
i	0.1	[0.5, 0.6)
o	0.2	[0.6, 0.8)
u	0.1	[0.8, 0.9)
!	0.1	[0.9, 1.0)

symbol to be coded is **e**. Hence, the final coded message has to be a number greater than or equal to 0.2 and less than 0.5. After the first character is encoded, we know that the lower number and the upper number now bind our range for the output. Each new symbol to be encoded will further restrict the possible range of the output number during the rest of the encoding process.

The next character to be encoded, **a**, is in the range of 0–0.2 in the new interval. It is not the first number to be encoded, so it belongs to the range corresponding to 0–0.2, but in the new subrange of [0.2, 0.5). This means that the number is now restricted to the range of [0.2, 0.26), since the previous range was 0.3 ($0.5 - 0.2 = 0.3$) units long and one-fifth of that is 0.06. The next symbol to be encoded, **i**, is in the range of [0.5, 0.6), which corresponds to 0.5–0.6 in the new subrange of [0.2, 0.26) and gives the smaller range [0.23, 0.236). Applying this rule for coding of successive characters, Table 3.5 shows the successive build-up of the range of the message coded so far.

Figure 3.11 shows another representation of the encoding process. The range is expanded to fill the whole range at every stage and marked with a scale that gives the end points as a number. The final range, [0.23354, 0.2336), represents the message **eaii!**. This means that if we transmit any number in the range of $0.23354 \geq x < 0.2336$, that number represents the whole message of eaii!.

Given this encoding scheme, it is relatively easy to see how during the decoding the individual elements of the **eaii!** message are decoded. To verify this, suppose a number $x = 0.23355$ in the range of $0.23354 \geq x < 0.2336$ is transmitted. The decoder, using the same probability intervals as the encoder, performs a similar procedure. Starting with the initial interval [0, 1), only the interval [0.2, 0.5) of **e**

Table 3.5 Representation of arithmetic coding process

	New character	Range
Initially		[0, 1)
After seeing a symbol	**e**	[0.2, 0.5)
	a	[0.2, 0.26)
	i	[0.23, 0.236)
	i	[0.233, 0.2336)
	!	[0.23354, 0.2336)

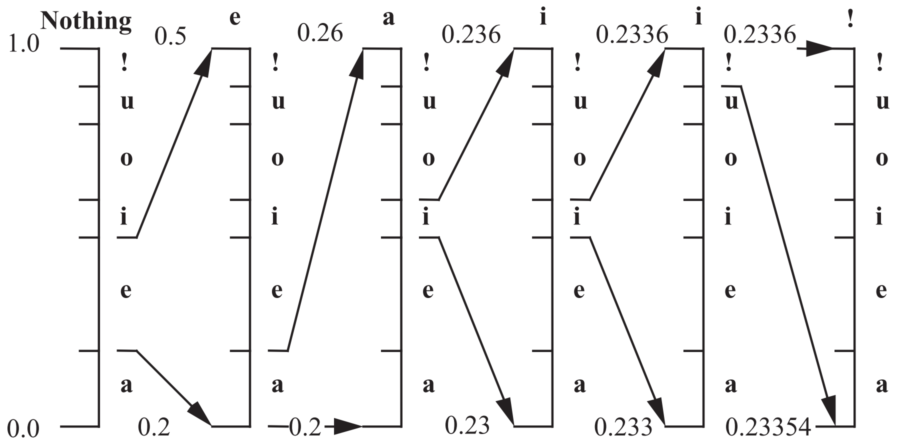

Figure 3.11 Representation of arithmetic coding process with the interval scaled up at each stage for the message ***eaii!***

envelops the transmitted code of 0.23355. So the first symbol can only be **e**. Similar to the encoding process, the symbol intervals are then defined in the new interval [0.2, 0.5). This is equivalent to defining the code within the initial range [0, 1), but offsetting the code by the lower value and then scaling up within its original range. That is, the new code will be (0.23355 − 0.2)/(0.5 − 0.2) = 0.11185, which is enveloped by the interval [0.0, 0.2) of symbol **a**. Thus, the second decoded symbol is **a**. To find the third symbol, a new code within the range of **a** should be found, that is, (0.11185 − 0.0)/(0.2 − 0.0) = 0.55925. This code is enveloped by the range of [0.5, 0.6) of symbol **i**, and the resulting new code after decoding the third symbol will be (0.55925 − 0.5)/(0.6 − 0.5) = 0.5925, which is again enveloped by [0.5, 0.6). Hence, the fourth symbol will be **i**. Repeating this procedure will yield a new code of (0.5925 − 0.5)/(0.6 − 0.5) = 0.925. This code is enveloped by [0.9, 1), which decodes symbol **!**, the end of decoding symbol, and the decoding process is terminated. Table 3.6 shows the whole decoding process of the message **eaii!**. In general, the decoding process can be formulated as

$$R_{n+1} = \frac{R_n - L_n}{U_n - L_n} \tag{3.11}$$

Table 3.6 Representation of decoding process of arithmetic coding

Encoded number	Output symbol	Range
0.23354	**e**	[0.2, 0.5)
0.233	**a**	[0.0, 0.2)
0.23	**i**	[0.5, 0.6)
0.23	**i**	[0.5, 0.6)
0.2	**!**	[0.9, 1.0)

where R_n is a code within the range of lower value L_n and upper value U_n of the nth symbol and R_{n+1} is the code for the next symbol.

3.4.2.2 Binary arithmetic coding

In the preceding section, we saw that as the number of symbols in the message increases, the range of the message becomes smaller. If we continue coding more symbols, then the final range may even become smaller than the precision of any computer to define such a range. To resolve this problem, we can work with binary arithmetic coding.

In Figure 3.11, we see that after each stage of coding, if we expand the range to its full range of [0, 1), the apparent range is increased. However, the values of the lower and upper numbers are still small. Therefore, if the initial range of [0, 1) is replaced by a larger range of [0, *MAX_VAL*), where *MAX_VAL* is the largest integer number that a computer can handle, then the precision problem is resolved. If we use 16-bit integer numbers, then $MAX\_VAL = 2^{16}-1$. Hence, rather than defining the cumulative probability in the range of [0, 1), we define their cumulative frequencies scaled up within the range of $[0, 2^{16}-1)$.

At the start, the coding interval [lower, upper) is initialised to the whole scale [0, *MAX_VAL*). The model's frequencies, representing the probability of each symbol in this range, are also set to their initial values in the range. To encode a new symbol element e_k assuming that symbols $e_1 \cdots e_{k-1}$ have already been coded, we project the model scale to interval resulting from the sequence of events. The new interval [*lower′*, *upper′*) for the sequence $e_1 \cdots e_k$ is calculated from the old interval [*lower, upper*) of the sequence $e_1 \cdots e_{k-1}$ as follows:

$$\begin{aligned}
lower' &= lower + width\ ^*\ low/maxfreq \\
width' &= width\ ^*\ symb\_width/maxfreq \\
upper' &= lower' + width' \\
&= lower + width\ ^*\ (low + symb\_width)/maxfreq \\
&= lower + width\ ^*\ up/maxfreq
\end{aligned}$$

where

$$\begin{aligned}
width &= upper - lower\ (old\ \ interval) \\
width' &= upper' - lower'(new\ \ interval) \\
symb\_width &= up - low\ \ (model's\ frequency)
\end{aligned}$$

At this stage of the coding process, we do not need to keep the previous interval [*lower, upper*) in the memory, so we allocate the new values [*lower′*, *upper′*). We then compare the new interval with the scale [0, *MAX_VAL*) to determine whether there is any bit for transmission down the channel. These bits are due to the redundancy in the binary representation of lower and upper values. For example, if values of both lower and upper levels are less than half the [0, *MAX_VAL*) range, then their most significant number in binary form is 0. Similarly, if both belong to the upper half range, their most significant number is 1. Hence, we can make a general rule:

- If lower and upper levels belong to the first half of the scale, the most significant bit for both will be 0.
- If lower and upper levels belong to the second half of the scale, their most significant bit will be 1.
- Otherwise, when lower and upper levels belong to the different halves of the scale, their most significant bits will be different (0 and 1).

Thus, for the cases where lower and upper values have the same most significant bit, we send this bit down the channel and calculate the new interval as follows:

- Sending a 0 corresponds to removal of the second half of the scale and keeping its first half only; the new scale is expanded by a factor 2 to obtain its representation in the whole scale of [0, *MAX_VAL*) again, as shown in Figure 3.12.
- Sending a 1 corresponds to the shift of the second half of the scale to its first half, that is, subtracting half of the scale value and multiplying the result by a factor 2 to obtain its representation in the whole scale again, as shown in Figure 3.13.

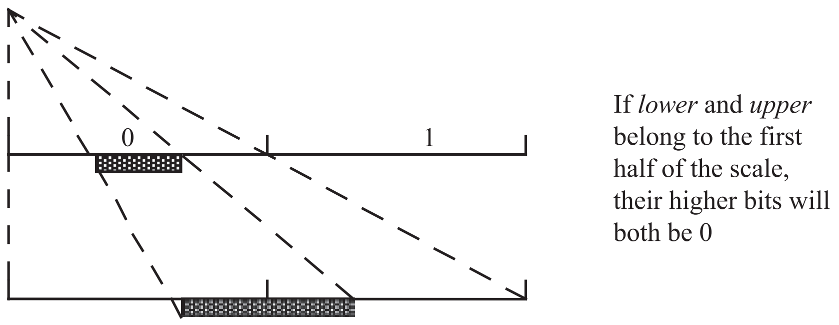
0
1
If *lower* and *upper* belong to the first half of the scale, their higher bits will both be 0

Figure 3.12 Both lower and upper values in the first half

If the interval always remains in either half of the scale after a bit has been sent, the operation is repeated as many times as necessary to obtain an interval occupying both halves of the scale. The complete procedure is called the interval testing loop.

Now we go back to the case where both of the lower and upper values are not in either of the half intervals. Here we identify two cases: first, the lower value is in the second quarter of the scale and the upper value is in the third quarter. Hence, the range of frequency is less than 0.5. In this case, in the binary representation, the two most significant bits are different, 01 for lower and 10 for the upper, but we can deduce some information from them. That is, in both cases, the second bit is the complementary bit to the first. Hence, if we can find out the second bit, the previous bit is its complement. Therefore, if the second bit is 1, then the previous value

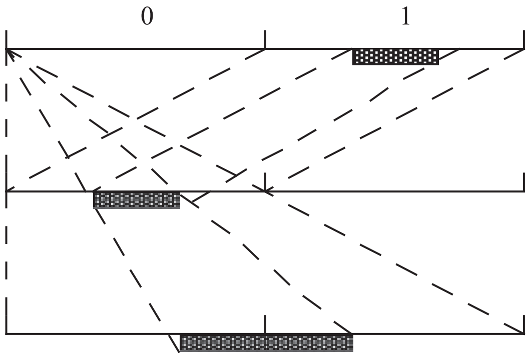

If *lower* and *upper* belong to the second half of the scale, their higher bits will both be 1

Figure 3.13 Both lower and upper values in the second half

should be 0, and we are in the second quarter, meaning the lower value. Similar conclusions can be drawn for the upper value.

Thus, we need to divide the interval within the scale of [0, *MAX_VAL*) into four segments instead of two. Then the scaling and shifting for this case will be done only on the portion of the scale containing second and third quarters, as shown in Figure 3.14.

Thus, the general rule for this case is as follows:

- If the interval belongs to the second and third quarters of the scale: an unknown bit **?** is sent to a waiting buffer for later definition and the interval transformed as shown in Figure 3.14.

  Finally,
- If the interval belongs to more than two different quarters of the scale (the interval occupies parts of three or four different quarters), there is no need to transform the coding interval. The process exits from this loop and goes to the next step in the execution of the program; this means that if the probability in that interval is greater than 0.5, no bits are transmitted; this is the most important part of arithmetic coding that leads to low bit rate.

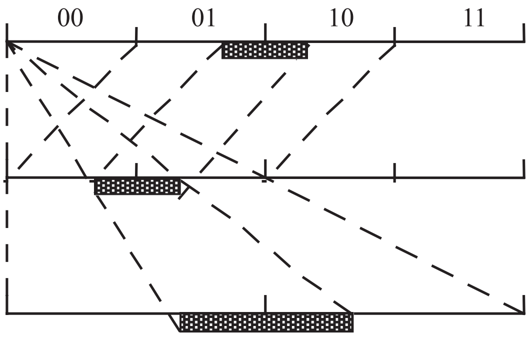

If lower and upper belong to the second and third quarters of the scale, an unknown bit is sent to a waiting buffer for later transmission, and the interval shifted by quarter

Figure 3.14 Lower and upper levels in the second and third quarters, respectively

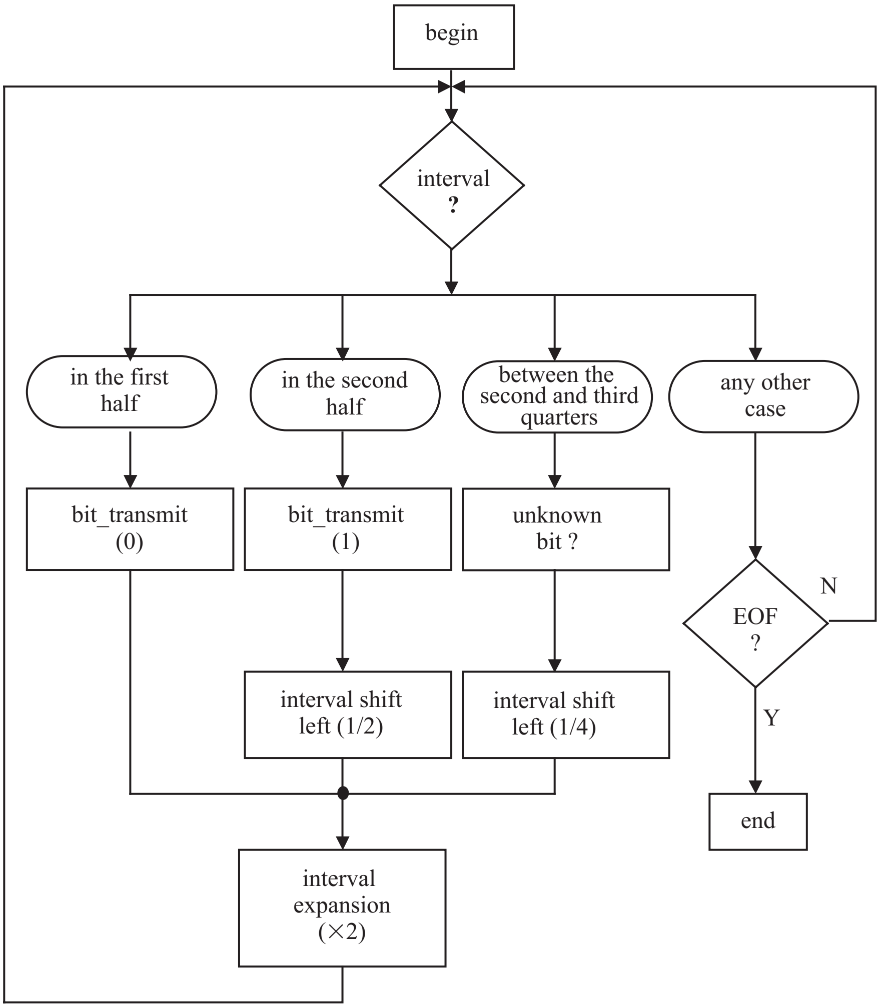

Figure 3.15 A flow chart for binary arithmetic coding

A flow chart of the interval testing loop is shown in Figure 3.15, and a detailed example of coding a message is given in Figure 3.16. For every symbol to be coded, we invoke the flow chart of Figure 3.15, except where the symbol is the end of file symbol, where the program stops. After each testing loop, the model can be updated (frequencies modified if the adaptive option has been chosen).

A C program of binary arithmetic coding is given in Figure 3.16.

The values of `low` and `high` are initialised to 0 and `top`, respectively. PSC_FIFO is a first-in, first-out (FIFO) for buffering the output bits from the arithmetic encoder. The model is specified through `cumul_freq[]`, and the symbol is specified using its index in the model.

```
#define q1 16384
#define q2 32768
#define q3 49152
#define top 65535

static long low, high, opposite_bits, length;
void encode_a_symbol (int index, int cumul_freq[])
{
      length = high - low +1;
      high = low -1 + (length * cumul_freq[index]) / cumul_freq[0];
      low += (length * cumul_freq[index+1])/ cumul_freq[0];
      for( ; ; ){
        if(high <q2){
         send out a bit "0" to PSC_FIFO;
         while (opposite_bits > 0) {
           send out a bit "1" to PSC_FIFO;
           opposite_bits--;

         }
      }
      else if (low >= q2) {
        send out a bit "1" to PSC_FIFO;
        while (opposite_bits > 0) {
        send out a bit "0" to PSC_FIFO;
        opposite_bits--;
      }
      low -= q2;
             high -= q2;
   }
   else if (low >= q1 && high < q3) {
     opposite_bits += 1;
     low -= q1;
     high -= q1;
   }
   else break;
   low *= 2;
   high = 2 * high + 1;
   }
 }
```

Figure 3.16 A C program of binary arithmetic coding

3.4.2.3 An example of binary arithmetic coding

Because of the complexity of the arithmetic algorithm, a simple example is given in this section. To simplify the operations further, we use a fixed model with four symbols **a, b**, **c** and **d**, where their fixed probabilities and cumulative probabilities are given in Table 3.7, and the message sequence of events to be encoded is **bbacd**.

Considering what we saw earlier, we start by initialising the whole range to [0, 1). In sending **b**, which has a range of [0.3, 0.8), since lower $= 0.3$ is in the second quarter and upper $= 0.8$ in the fourth quarter (occupying more than two quarters), nothing is sent, and no scaling is required, as shown in Table 3.8.

To send the next **b**, that is, **bb**, since the previous width $= 0.8 - 0.3 = 0.5$, the new interval becomes $[0.3 + 0.3 \times 0.5, 0.3 + 0.8 \times 0.5) = [0.45, 0.7)$. This time lower $= 0.45$ is in the second quarter but upper $= 0.7$ is in the third quarter, so the unknown bit **?** is sent to the buffer, such that its value is to be determined later.

Table 3.7 Probability and cumulative probability of four symbols as an example

Symbol	pdf	cdf
a	0.3	[0.0, 0.3)
b	0.5	[0.3, 0.8)
c	0.1	[0.8, 0.9)
d	0.1	[0.9, 1.0)

*Table 3.8 Generated binary bits of coding **bbacd** message*

Encoding	Coding interval	Width	Bit
Initialisation	[0, 1)	1	
After b	[0.3, 0.8)	0.5	
After bb	[0.45, 0.7)	0.25	
After interval test	[0.4, 0.9)	0.5	**?**
After bba	[0.40, 0.55)	0.15	
After interval test	[0.3, 0.6)	0.3	**?**
After interval test	[0.1, 0.7)	0.6	**?**
After bbac	[0.58, 0.64)	0.06	
After interval test	[0.16, 0.28)	0.12	**1000**
After interval test	[0.32, 0.56)	0.24	**0**
After interval test	[0.14, 0.62)	0.48	**?**
After bbacd	[0.572, 0.620)	0.048	
After interval test	[0.144, 0.240)	0.096	**10**
After interval test	[0.288, 0.480)	0.192	**0**
After interval test	[0.576, 0.960)	0.384	**0**
After interval test	[0.152, 0.920)	0.768	**1**

Note that since range [0.45, 0.7) covers second and third quarters, according to Figure 3.14, we have to shift both of them by a quarter (0.25) and then magnify by a factor of 2, that is, the new interval is $[(0.45 - 0.25) \times 2, (0.7 - 0.25) \times 2) = [0.4, 0.9)$, which has a width of 0.5. To code the next symbol **a**, the range becomes $[0.4 + 0 \times 0.5, 0.4 + 0.3 \times 0.5) = [0.4, 0.55)$. Again since lower and upper levels are at the second and third quarters, the unknown **?** is stored. According to Figure 3.14, both quarters are shifted by 0.25 and magnified by 2, $[(0.4 - 0.25) \times 2, (0.55 - 0.25) \times 2) = [0.3, 0.6)$.

Again [0.3, 0.6) is in the second and third intervals, so another **?** is stored. If we shift and magnify again $[(0.3 - 0.25) \times 2, (0.6 - 0.25) \times 2) = [0.1, 0.7)$, which now lies in the first and third quarters, nothing is sent and not scaled. Now if we code **c**, that is, **bbac**, the interval becomes $[0.1 + 0.8 \times 0.6, 0.1 + 0.9 \times 0.6) = [0.58, 0.64)$.

Now since [0.58, 0.64) is in the second half, we send 1. We now go back and convert all **?** to 000 complementary to 1. Thus, we have sent 1000 so far. Note that bits belonging to **?** are transmitted after finding a 1 or 0. Similarly, the subsequent symbols are coded, and the final generated bit sequence becomes 1000010001. Table 3.8 shows this example in a tabular representation. A graphical representation is given in Figure 3.17.

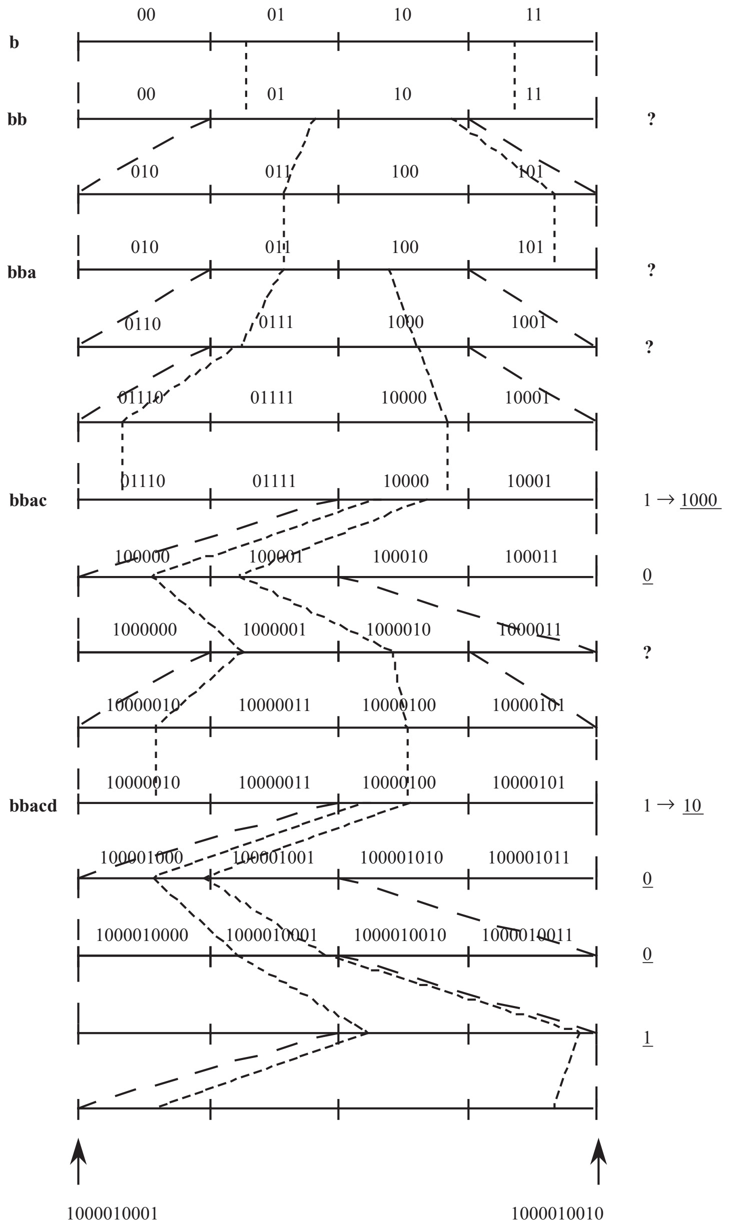

Figure 3.17 Derivation of the binary bits for the given example

3.4.2.4 Adaptive arithmetic coding

In adaptive arithmetic coding, the assigned probability to the symbols changes as each symbol is coded [18]. For binary (integer) coding, this is accomplished by assigning a frequency of 1 to each symbol at the start of the coding (initialisation). As a symbol is coded, the frequency of that symbol is incremented by one. Hence, the frequencies of symbols are adapted to their number of appearances so far. The decoder follows a similar procedure. At every stage of coding, a test is done to see if the cumulative frequency (sum of the frequencies of all symbols) exceeds the *MAX_VAL*. If this is the case, all frequencies are halved (minimum 1), and encoding continues. For a better adaptation, the frequencies of the symbols may be initialised to a predefined distribution that matches the overall statistics of the symbols better. For better results, the frequencies are updated from only N most recently coded symbols. It has been shown that this method of adaptation with a limited past history can reduce the bit rate by more than 30 per cent below the first-order entropy of the symbols [19]. The reason for this is that if some rare events that normally have high entropy could occur in clusters, then, within the only N most recent events, they now become the more frequent events, and hence require lower bit rates.

3.4.2.5 Context-based arithmetic coding

A popular method for adaptive arithmetic coding is to adapt the assigned probability to a symbol, according to the context of its neighbours. This is called context-based arithmetic coding, and forms an essential element of some image/video coding standards, such as JPEG2000, H.264/AVc and MPEG-4. It is more efficient when it is applied to binary data, like the bit plane or the sign bits in JPEG2000 or binary shapes in MPEG-4. We now explain this method with a simple example. Assume binary symbols of *a, b* and *c*, which may take values of 0 or 1, are the three immediate neighbours of a binary symbol *x*, as shown in Figure 3.18.

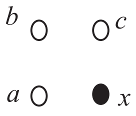

Figure 3.18 Three immediate neighbouring symbols to x

Because of high correlation between the symbols in the image data, if the neighbouring symbols of *a, b* and *c* are mainly 1, then it is logical to assign a high probability for coding symbol x when its value is 1. Conversely, if the neighbouring symbols are mainly 0, the assigned probability of $x = 1$ should be reduced. Thus, we can define the context for coding a 1 symbol as

$$\text{Context} = 2^2c + 2^1b + 2^0a = 4c + 2b + a \tag{3.12}$$

For the binary values of *a, b* and *c*, the context has a value between 0 and 7. Higher values of the context indicate that a higher probability should be assigned for coding of 1, and a complementary probability when the value of x is 0.

3.5 A generic interframe video codec

Figure 3.19 shows a generic interframe encoder that is used in all the standard video codecs, such as H.261, H.263, H.264, MPEG-1, MPEG-2 and MPEG-4 [16,17, 20–22]. In the following sections, each element of this codec is described in a general sense. The specific aspects of these codecs are addressed in more detail in the relevant chapters.

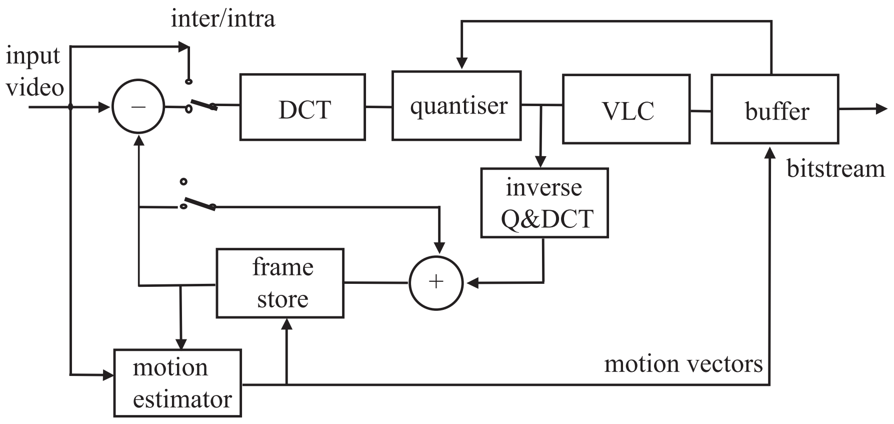

Figure 3.19 A generic interframe predictive coder

3.5.1 *Interframe loop*

In interframe predictive coding, the difference between pixels in the current frame and their prediction values from the previous frame is coded and transmitted. At the receiver, after decoding the error signal of each pixel, it is added to a similar prediction value to reconstruct the picture. The better the predictor, the smaller the error signal, and hence the transmission bit rate. If the scene is still, a good prediction for the current pixel is the same pixel in the previous frame. However, when there is a motion, assuming that movement in the picture is only a shift of object position, then a pixel in the previous frame, displaced by a motion vector, is used.

3.5.2 *Motion estimator*

Assigning a motion vector to each pixel is very costly. Instead, a group of pixels is motion compensated, such that the motion vector overhead per pixel can be very small. In standard codecs, a block of 16×16 pixels, known as a macroblock (MB) (to be differentiated from 8×8 DCT blocks), is motion estimated and compensated. It should be noted that ME is only carried out on the luminance parts of the pictures. A scaled version of the same motion vector is used for compensation of chrominance blocks, depending on the picture format.

3.5.3 Inter/intra switch

Every MB is either interframe or intraframe coded, called inter/intra MBs. The decision on the type of MB depends on the coding technique, which is explained in greater detail in the relevant chapters. For example, in JPEG, all MBs are intraframe coded, as JPEG is mainly used for coding of still pictures.

3.5.4 DCT

Every MB is divided into 8×8 luminance and chrominance pixel blocks. Each block is then transformed via the DCT. There are four luminance blocks in each MB, but the number of chrominance blocks depends on the colour resolutions (image format).

3.5.5 Quantiser

As mentioned in section 3.2, there are two types of quantisers. One with a dead zone for the AC coefficients and the DC coefficient of inter MB, the other without the dead zone is used for the DC coefficient of intra MB. The range of quantised coefficients can be from -2047 to $+2047$. With a dead zone quantiser, if the modulus (absolute value) of a coefficient is less than the quantiser step size q, it is set to zero; otherwise, it is quantised according to eqn. 3.6, to generate quantiser indices.

3.5.6 Variable length coding

The quantiser indices are variable length coded, according to the type of VLC used. Motion vectors, as well as the address of coded MBs, are also variable length coded.

3.5.7 IQ and IDCT

To generate a prediction for interframe coding, the quantised DCT coefficients are first inverse quantised and inverse DCT coded. These are added to their previous picture values (after a frame delay by the frame store) to generate a replica of decoded picture. The picture is then used as a prediction for coding of the next picture in the sequence.

3.5.8 Buffer

The bit rate generated by an interframe coder is variable. This is because the bit rate is primarily a function of picture activity (motion of objects and their details). Therefore, to transmit coded video into fixed rate channels (e.g. 2 Mbit/s links), the bit rate has to be regulated. Storing the coded data in a buffer and then emptying the buffer at the channel rate does this. However, if the picture activity is such that the buffer may overflow (violent motion), then a feedback from the buffer to the quantiser can regulate the bit rate. Here, as the buffer occupancy increases, the feedback forces the quantiser step size to be increased to reduce the bit rate.

Similarly, if the picture activity is less (coding mainly slow motion parts of frames), then the quantiser step size is reduced to improve the picture quality.

3.5.9 Decoder

The compressed bitstream, after demultiplexing and variable length decoding (VLD), separates the motion vectors and the DCT coefficients. Motion vectors are used by motion compensation and the DCT coefficients after the inverse quantisation and IDCT are converted to error data. They are then added to the motion-compensated previous frame to reconstruct the decoded picture, as shown in Figure 3.20.

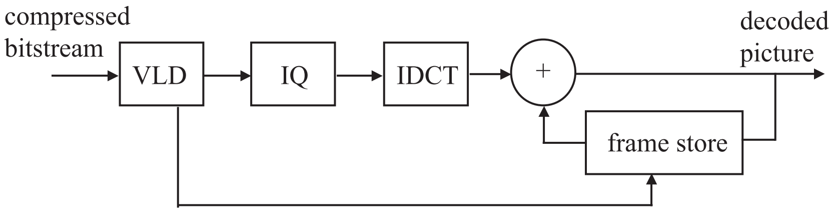

Figure 3.20 Block diagram of a decoder

3.6 Constant and variable bit rates

The bit rate generated by the encoder of Figure 3.19 is called constant bit rate (CBR), requiring a fixed channel bandwidth. An alternative solution is to use a transmission system that can adapt to the variable bit rate (VBR). For VBR coding, the feedback and the smoothing buffer are no longer needed. The quantiser step size in this case is fixed.

In an asynchronous transfer mode (ATM) system [23], the information is transmitted in the form of fixed-length packets or cells, and when a cell is full, it is transmitted. This can happen at any time, so that the transmission system has a bit rate capability that matches the encoder. The advantage is realised only when several video channels are multiplexed together. When one channel is generating cells in rapid succession, corresponding to high picture activity, it is probable that the other channels will generate cells at a lower rate. Only rarely will the total bit rate of the multiplex be exceeded and freeze-out occur.

3.7 Problems

1. In the linear quantiser of Figure 3.4, derive the quantisation characteristics in terms of inputs and outputs, for each of the following conditions:
   a. $th = q = 16$
   b. $th = 0, q = 16$

2. The following 8-bit resolution luminance samples are DPCM encoded with the prediction of previous sample:

   10, 14, 25, 240, 195, 32

   If the quantisation is uniform with $th = 0$ and $q = 8$,
   a. find the reconstructed samples (assume predictor is initialised to zero);
   b. calculate the PSNR of the decoded samples.

3. A 3-bit nonuniform quantiser is defined as:

Input	**Output**
if $\lvert x\rvert \geq 4$	$y = \pm 2$
$4 < \lvert x\rvert \geq 10$	$y = \pm 6$
$10 < \lvert x\rvert \geq 25$	$y = \pm 15$
else	$y = \pm 50$

   If the DPCM data of problem 2 are quantised with this quantiser, find the reconstructed samples and the resulting PSNR value.

4. A step function signal with the following 8-bit digitised values:

   20; 20; 20; 20; 20; 231; 231; 231; 231; 231; 231; 231; 231; 231

   is DPCM coded with the nonuniform quantiser of problem 3. Plot the reconstructed samples, and identify the positions where slope overload and granular noise occur.

5. Determine the elements of the 8×8 orthonormal forward and IDCT transformation matrices.

6. Use the DCT matrix of problem 5 to code the following 8 pixels:

   35; 81; 190; 250; 200; 150; 100; 21

   a. Find the transform coefficients.
   b. Why is only one AC coefficient significant?
   c. Reconstruct the pixels without any quantisation; comment on the reconstructed pixel values.

7. The DCT coefficients of problem 6 are linearly quantised with a linear and dead zone quantiser with a step size of $th = q = 16$. Find the PSNR of the reconstructed pixels.

8. Find the PSNR of the reconstructed pixels if in problem 7 the following coefficients are retained for quantisation and the remaining coefficients are set to zero:
   a. DC coefficient
   b. DC and the second AC coefficient

9. A 2×2 block of pixels in the current frame is matched against a similar size block in the previous frame, as shown in Figure 3.21, within a search window

18	24	31	15	16	18
11	20	23	41	11	9
23	21	18	17	4	18
15	31	24	21	13	9

previous frame

25	32
11	19

current frame

Figure 3.21 A block of 2 × 2 pixels in the current frame and its corresponding block in the previous frame shown in the shaded area

of ±2 pixels horizontally and ±1 pixel vertically. Find the best-matched motion vector of the block, if distortion criterion is based on:

a. MSE

b. MAE

10. For a maximum motion speed of 6 pixels/frame:
    a. Calculate the number of operations required by the FSM.
    b. If each block contains 16 × 16 pixels, calculate the number of multiplications and additions, if the cost function was:
       i. MSE
       ii. MAE

11. Repeat problem 10 for the following fast search methods:
    a. TDL
    b. TSS
    c. CSA
    d. OSA

12. Four symbols of **a, b, c** and **d** with probabilities $p(\mathbf{a}) = 0.2$, $p(\mathbf{b}) = 0.45$, $p(\mathbf{c}) = 0.3$ and $p(\mathbf{d}) = 0.05$ are Huffman coded. Derive the Huffman codes for these symbols, and compare the average bit rate with that of the entropy.

13. In problem 12, a message comprising of five symbols **cbdad** is Huffman coded.
    a. Write down the generated bitstream for this message.
    b. If there is a single error in:
       (i) first bit
       (ii) third bit
       (iii) fifth bit

    what is the decoded message in each case?

14. If the intervals of [0.0, 0.2), [0.2, 0.7), [0.7, 0.95) and [0.95, 1) are assigned for arithmetic coding of strings of **a, b, c** and **d**, respectively, find the lower and upper values of the arithmetic coded string of **cbcab**.

15. With the interval of strings of **a, b** and **c** defined in problem 14, suppose the arithmetic decoder receives 0.83955:
    a. Decode the first three symbols of the message.
    b. Decode the first five symbols of the message.

16. In arithmetic coding, symbols can be decoded using the following equation:

$$R_{n+1} = \frac{R_n - L_n}{U_n - L_n}$$

where R_0 is the received number and $[L_n, U_n)$ is the interval of nth symbol in the stream. Use this equation to decode symbols in problem 15.

17. Find the binary arithmetic coding of string **cbcab** of problem 14.

18. Decimal numbers can be represented in binary form by their expansions in powers of 2^{-1}. Derive the first 11 binary digits of the decimal number 0.83955. Compare your results with that of problem 17.

19. The binary digits of arithmetic coded string **cbcab** are corrupted at:
    a. first bit
    b. third bit
    c. fifth bit

    Decode the first five symbols of the string in each case.

References

1. JAIN, A.K.: *Fundamentals of Digital Image Processing*, Prentice Hall, Upper Saddle River, 1989
2. CHEN, W., SMITH, C. and FRALICK, S.: 'A fast computational algorithm for the discrete cosine transform', *IEEE Trans. Commun.*, 1979, **COM-25**, pp. 1004–1009
3. ISHIGURO, T. and IINUMA, K.: 'Television bandwidth compression transmission by motion-compensated interframe coding', *IEEE Commun. Mag.*, 1982, **10**, pp. 24–30
4. KAPPAGANTULA, S. and RAO, K.R.: 'Motion compensated predictive coding', Proceedings of International Technical Symposium, SPIE, San Diego, CA, August 1983
5. BERGMANN, H.C.: 'Displacement estimation based on the correlation of image segments', IRE Conference on the Electronic Image Processing, York, UK, July 1982
6. JAIN, J.R. and JAIN, A.K.: 'Displacement measurement and its application in interframe image coding', *IEEE Trans. Commun.*, 1981, **COM-29**, pp. 1799–1808
7. SHANABLEH, T. and GHANBARI, M.: 'Heterogeneous video transcoding to lower spatio-temporal resolutions and different encoding formats', *IEEE Trans. Multimedia*, 2002, **2:2**, pp. 101–110
8. KOGA, T., IINUMA, K., HIRANO, A., IIJIMA, Y. and ISHIGURO, T.: 'Motion compensated interframe coding for video conferencing', Proceedings of National Telecommunication Conference, New Orleans, LA, 29 November–3 December 1981, pp. G5.3.1–G5.3.5
9. CCITT Working Party XV/4: 'Description of reference model 8 (RM8)', Specialists Group on Coding for Visual Telephony, doc. 525, June 1989

10. SRINIVASAN, R. and RAO, K.R.: ‘Predictive coding based on efficient motion estimation’, IEEE International Conference on Communications, Amsterdam, 14–17 May, 1984, pp. 521–526
11. GHANBARI, M.: ‘The cross search algorithm for motion estimation’, *IEEE Trans. Commun.*, 1990, **38:7**, pp. 950–953
12. PURI, A., HANG, H.M. and SCHILLING, D.L.: ‘An efficient block-matching algorithm for motion compensated coding’, Proceedings of IEEE ICASSP’87, 1987, pp. 25.4.1–25.4.4
13. BIERLING, M.: ‘Displacement estimation by hierarchical block matching’, *Proc. SPIE Vis. Commun. Image Process.*, 1988, **1001**, pp. 942–951
14. LANGDON, G.G.: ‘An introduction to arithmetic coding’, *IBM J. Res. Dev.*, 1984, **28:2**, pp. 135–149
15. PENNEBAKER, W.B. and MITCHELL, J.L.: *JPEG: Still Image Compression Standard*, Van Nostrand Reinhold, New York, 1993
16. H.263: ‘Draft ITU-T Recommendation H.263, video coding for low bit rate communication’, September 1997
17. MPEG-4: ‘Testing and evaluation procedures document’, ISO/IEC JTC1/SC29/WG11, N999, July 1995
18. WITTEN, I.H., NEAL, R.M. and CLEARY, J.G.: ‘Arithmetic coding for data compression’, *Commun. ACM*, 1987, **30:6**, pp. 520–540
19. GHANBARI, M.: ‘Arithmetic coding with limited past history’, *Electron. Lett.*, 1991, **27:13**, pp. 1157–1159
20. H.261: ‘ITU-T Recommendation H.261, video codec for audiovisual services at p$\times$64 kbit/s’, Geneva, 1990
21. MPEG-1: ‘Coding of moving pictures and associated audio for digital storage media at up to about 1.5 Mbit/s’, ISO/IEC 1117-2: video, November 1991
22. MPEG-2: ‘Generic coding of moving pictures and associated audio information’, ISO/IEC 13818-2: video, Draft International Standard, November 1994
23. CUTHBURT, A.C. and SAPANEL, J.C.: *ATM: The Broadband Telecommunications Solution*, IEE Publishing, London, 1993

Chapter 4 Subband and wavelet

Coding of still images under MPEG-4 [1] and the decision by the JPEG committee to recommend a new standard under JPEG2000 [2] have brought up a new image compression technique. The committee have decided to recommend a new way of coding of still images based on the wavelet transform, in sharp contrast to the discrete cosine transform (DCT) used in the other standard codecs, as well as the original JPEG. In this chapter, we introduce this wavelet transform and show how it can be used for image compression.

4.1 Why wavelet transform?

Before describing the wavelet transform and its usage in image compression, it is essential to answer two fundamental questions:

1. What is wrong with the DCT and why should we use wavelet?
2. If wavelet is superior to DCT, why did not original JPEG use it?

The answer to the first part is as follows. The DCT and the other block-based transforms partition an image into nonoverlapping blocks and process each block separately. At very low bit rates, the transform coefficients need to be coarsely quantised and so there will be a significant reconstruction error after the decoding. This error is more visible at the block boundaries by causing a discontinuity in the image and is best known as the blocking artefact. One way of reducing this artefact is to allow the basis functions to decay towards zero at these points or to overlap over the adjacent blocks. The latter technique is called the lapped orthogonal transform [3]. The wavelet transform is a special type of such transform and hence it is expected to eliminate blocking artefacts.

The answer to the second part relates to the state of the art in image coding in the mid-1980s, the time when the original JPEG was under development. At that time although wavelet transform and its predecessor, subband coding, were known, there was no efficient method of coding the wavelet transform coefficients to be comparable with the DCT. In fact, the proposals submitted to the JPEG committee were all DCT-based codecs, none on the wavelet. Also almost at the same time, out of the 15 proposals to the H.61 committee, there were 14 DCT-based codecs and 1 vector quantisation method and none on the wavelet. Thus, in the mid-1980s, the compression performance coupled with the considerable momentum already behind the DCT led the JPEG committee to adopt DCT-based coding as the foundation of JPEG.

However, the state of the wavelet transform–based image compression techniques has significantly improved since the introduction of the original JPEG. Much of the credit should go to Jussef Shapiro who by the introduction of the embedded zero tree wavelet (EZW) made a significant breakthrough in coding of the wavelet coefficients [4]. At the end of this chapter, this method, and the other similar methods that exploit the multiresolution properties of the wavelet transform to give a computationally simple but efficient compression algorithm, is introduced.

4.2 Subband coding

Before describing the wavelet transform, let us look at its predecessor, subband coding, which sometimes is called the early wavelet transform [5]. As we will see later, in terms of image coding they are similar. However, subband coding is a product designed by engineers [6], while wavelet transform was introduced by mathematicians [7]. Therefore, before proceeding to mathematics, which sometimes is cumbersome to follow, an engineering view to the multiresolution signal processing may help to understand it better.

Subband coding was first introduced by Crochiere *et al.* in 1976 [6], and has since proved to be a simple and powerful technique for speech and image compression. The basic principle is the partitioning of the signal spectrum into several frequency bands, then coding and transmitting each band separately. This is particularly suited to image coding. First, natural images tend to have a nonuniform frequency spectrum, with most of the energy being concentrated in the lower-frequency band. Second, the human perception of noise tends to fall off at both high and low frequencies, and this enables the designer to adjust the compression distortion according to perceptual criteria. Third, since images are processed in their entirety, and not in artificial blocks, there is no block structure distortion in the coded picture, as occurs in the block transform–based image encoders, such as DCT.

Thus, subband, like the Fourier transform, is based on the frequency domain analysis of the image, but its filter banks have a better decorrelation property that suits natural images better. This can be explained as follows: Fourier basis functions are very exact in frequency, but are spatially not precise. In other words, the signal energy of the Fourier basis functions is not concentrated at one frequency, but spread over all space. This would not be a problem if image pixels were always correlated. However, in reality, pixels in images of interest generally have low correlation, especially across the image discontinuities such as edges. In contrast to Fourier basis functions, the subband bases not only have fairly good frequency concentration but also are spatially compact. If image edges are not too closely packed, most of the subband basis elements will not intersect with them, thus performing a better decorrelation on average.

In subband coding, the band splitting is done by passing the image data through a bank of band-pass analysis filters, as shown in Figure 4.1. To adapt the

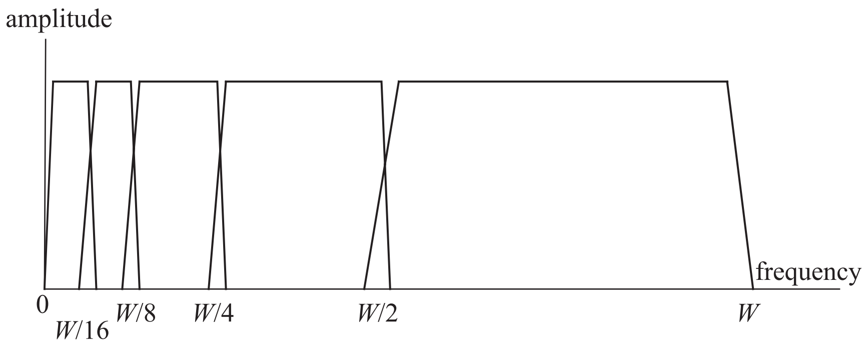

Figure 4.1 A bank of band-pass filters

frequency response of the decomposed pictures to the characteristics of the human visual system, filters are arranged into octave bands.

Since the bandwidth of each filtered version of the image is reduced, they can now in theory be downsampled at a lower rate, according to the Nyquist criteria, giving a series of reduced size subimages. The subimages are then quantised, coded and transmitted. The received subimages are restored to their original sizes and passed through a bank of synthesis filters, where they are interpolated and added to reconstruct the image.

In the absence of quantisation error, it is required that the reconstructed picture be an exact replica of the input picture. This can only be achieved if the spatial frequency response of the analysis filters tiles the spectrum without overlapping, which requires infinitely sharp transition regions and cannot be realised practically. Instead, the analysis filter responses have finite transition regions and do overlap, as shown in Figure 4.1, which means that the downsampling/upsampling processes introduce aliasing distortion into the reconstructed picture.

To eliminate the aliasing distortion, the synthesis and analysis filters have to have certain relationships such that the aliased components in the transition regions cancel each other out. To see how such a relation can make alias-free subband coding possible, consider a two-band subband, as shown in Figure 4.2.

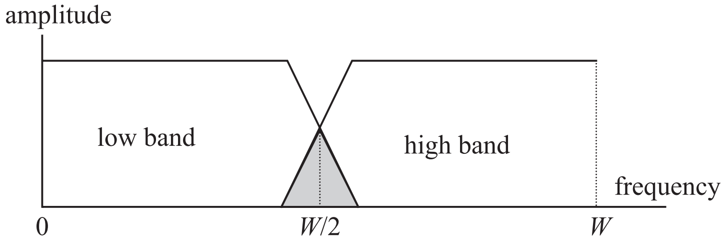

Figure 4.2 A two-band analysis filter

The corresponding two-band subband encoder/decoder is shown in Figure 4.3. In this diagram, filters $H_0(z)$ and $H_1(z)$ represent the z-transform transfer functions of the respective low-pass and high-pass analysis filters. Filters $G_0(z)$ and $G_1(z)$ are the corresponding synthesis filters. The downsampling and upsampling factors are 2.

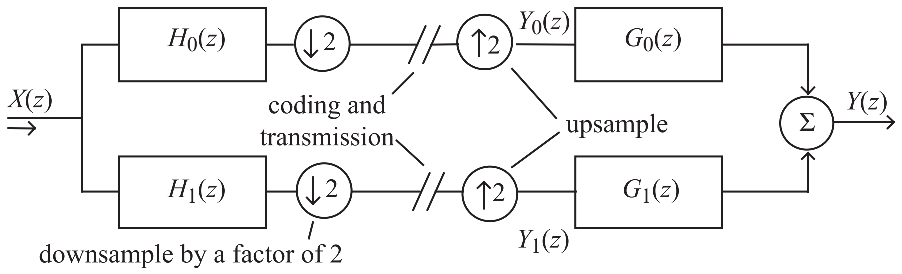

Figure 4.3 A two-band subband encoder/decoder

At the encoder, downsampling by 2 is carried out by discarding alternate samples, the remainder being compressed into half the distance occupied by the original sequence. This is equivalent to compressing the source image by a factor of 2, which doubles all the frequency components present. The frequency domain effect of this downsampling/compression is thus to double the width of all components in the sampled spectrum.

At the decoder, the upsampling is a complementary procedure: it is achieved by inserting a zero-valued sample between each input sample and is equivalent to a spatial expansion of the input sequence. In the frequency domain, the effect is as usual the reverse and all components are compressed towards zero frequency.

The problem with these operations is the impossibility of constructing ideal, sharp-cut analysis filters. This is illustrated in Figure 4.4*a*. Spectrum A shows the original sampled signal that has been low-pass filtered so that some energy remains above $F_s/4$, the cut-off of the ideal filter for the task. Downsampling compresses the signal and expands to give B, and C is the picture after expansion or upsampling. As well as those at multiples of F_s, this process generates additional spectrum components at odd multiples of $F_s/2$. These cause aliasing when the final subband recovery takes place as at D.

In the high-pass case, Figure 4.4*b*, the same phenomena occur, so that on recovery there is aliased energy in the region of $F_s/4$. The final output image is generated by adding the low-pass and high-pass subbands regenerated by the upsamplers and associated filters. The aliased energy would normally be expected to cause interference. However, if the phases of the aliased components from the high- and low-pass subbands can be made to differ by π, then cancellation occurs and the recovered signal is alias free.

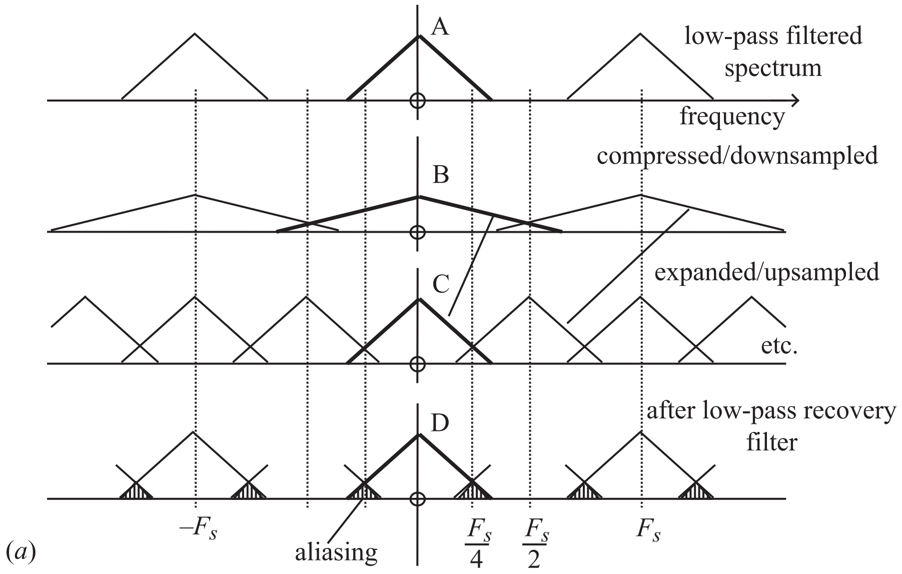

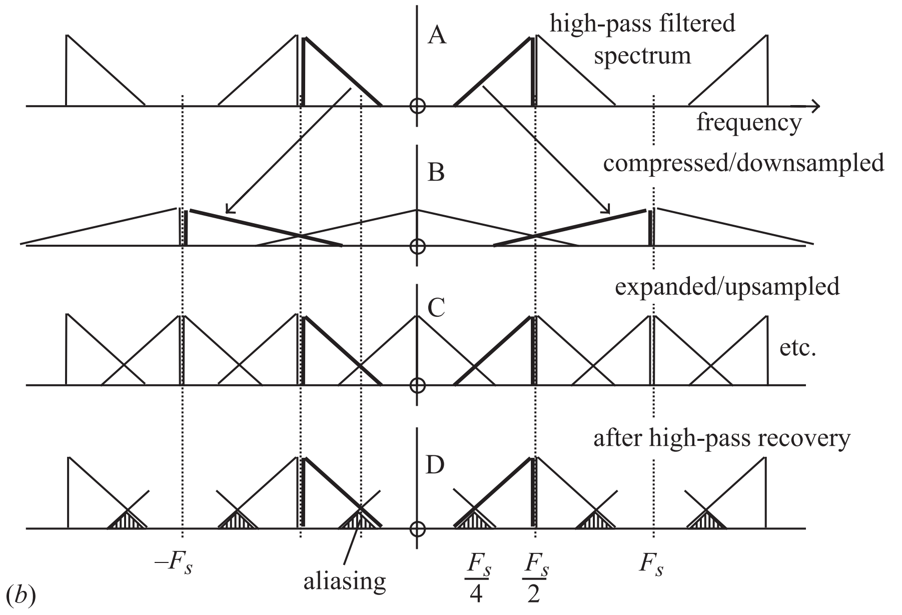

Figure 4.4 (a) Low-pass subband generation and recovery; (b) high-pass subband generation and recovery

How this can be arranged is best analysed by reference to z-transforms. Referring to Figure 4.3, after the synthesis filters, the reconstructed output in z-transform notation can be written as

$$Y(z) = G_0(z) \cdot Y_0(z) + G_1(z) \cdot Y_1(z) \tag{4.1}$$

where $Y_0(z)$ and $Y_1(z)$ are inputs to the synthesis filters after upsampling. Assuming there are no quantisation and transmission errors, the reconstructed samples are given by

$$\begin{aligned} Y_0(z) &= \frac{1}{2}[H_0(z) \cdot X(z) + H_0(-z) \cdot X(-z)] \\ Y_1(z) &= \frac{1}{2}[H_1(z) \cdot X(z) + H_1(-z) \cdot X(-z)] \end{aligned} \tag{4.2}$$

where the aliasing components from the downsampling of the lower and higher bands are given by $H_0(-z)X(-z)$ and $H_1(-z)X(-z)$, respectively. By substituting these two equations in the previous one, we get

$$\begin{aligned} Y(z) = &\frac{1}{2}[H_0(z) \cdot G_0(z) + H_1(z) \cdot G_1(z)]X(z) \\ &+\frac{1}{2}[H_0(-z) \cdot G_0(z) + H_1(-z) \cdot G_1(z)]X(-z) \end{aligned} \tag{4.3}$$

The first term is the desired reconstructed signal, while the second term is aliased components. The aliased components can be eliminated regardless of the amount of overlap in the analysis filters by defining the synthesis filters as

$$G_0(z) = H_1(-z) \quad \text{and} \quad G_1(z) = -H_0(-z) \tag{4.4}$$

With such a relation between the synthesis and analysis filters, the reconstructed signal now becomes

$$Y(z) = \frac{1}{2}[H_0(z) \cdot H_1(-z) - H_0(-z) \cdot H_1(z)]X(z) \tag{4.5}$$

If we define $P(z) = H_0(z)H_1(-z)$, then the reconstructed signal can be written as

$$Y(z) = \frac{1}{2}[P(z) - P(-z)]X(z) \tag{4.6}$$

Now the reconstructed signal can be a perfect but an m-sample delayed replica of the input signal, if

$$P(z) - P(-z) = 2z^{-m} \tag{4.7}$$

Thus, the z-transform input/output signals are given by

$$Y(z) = z^{-m}X(z) \tag{4.8}$$

This relation in the pixel domain implies that the reconstructed pixel sequence $\{y(n)\}$ is an exact replica of the input sequence but delayed by m pixels, that is, $\{x(n-m)\}$.

In these equations, $P(z)$ is called the product filter and m the delay introduced by the filter banks. The design of analysis/synthesis filters is based on factorisation of the product filter $P(z)$ into linear phase components $H_0(z)$ and $H_1(-z)$, with the constraint that the difference between the product filter and its image should be a simple delay, then the product filter must have an odd number of coefficients. LeGall and Tabatabai [8] have used a product filter $P(z)$ of the kind:

$$P(z) = \frac{1}{16}(-1 + 9z^{-2} + 16z^{-3} + 9z^{-4} - z^{-6}) \tag{4.9}$$

and by factorising have obtained several solutions for each pair of the analysis and synthesis filters:

$$\begin{aligned}
&H_0(z) = \frac{1}{4}(-1 + 3z^{-1} + 3z^{-2} - z^{-3}), \quad H_1(-z) = \frac{1}{4}(1 + 3z^{-1} + 3z^{-2} + z^{-3})\\
&\text{or}\\
&H_0(z) = \frac{1}{4}(1 + 3z^{-1} + 3z^{-2} + z^{-3}), \quad H_1(-z) = \frac{1}{4}(-1 + 3z^{-1} + 3z^{-2} - z^{-3})\\
&\text{or}\\
&H_0(z) = \frac{1}{8}(-1 + 2z^{-1} + 6z^{-2} + 2z^{-3} - z^{-4}), \quad H_1(-z) = \frac{1}{2}(1 + 2z^{-1} + z^{-2})
\end{aligned} \tag{4.10}$$

The synthesis filters $G_0(z)$ and $G_1(z)$ are then derived using their relations with the analysis filters, according to eqn. 4.4. Each of the above equation pairs gives the results $P(z) - P(-z) = 2z^{-3}$, which implies that the reconstruction is perfect with a delay of three samples.

4.3 Wavelet transform

The wavelet transform is a special case of subband coding and is becoming very popular for image and video coding. While subband coding of images is based on frequency analysis, the wavelet transform is based on the approximation theory. However, for natural images that are locally smooth and can be modelled as piecewise polynomials, a properly chosen polynomial function can lead to frequency domain analysis, like that of subband. In fact, wavelets provide an efficient means for approximating such functions with a small number of basis elements. Mathematically, a wavelet transform of a square-integrable function $x(t)$ is its decomposition into a set of basis functions, such as

$$X_w(a,b) = \int_{-\infty}^{\infty} x(t)\Psi_{a,b}(t)dt \tag{4.11}$$

where $\Psi_{a,b}(t)$ is known as the basis function, which is a time dilation and translation version of a band-pass signal $\Psi(t)$, called the mother wavelet and defined as

$$\Psi_{a,b} = \frac{1}{\sqrt{a}}\Psi\left(\frac{t-b}{a}\right) \tag{4.12}$$

where a and b are time dilation and translation parameters, respectively. The effects of these parameters are shown in Figure 4.5.

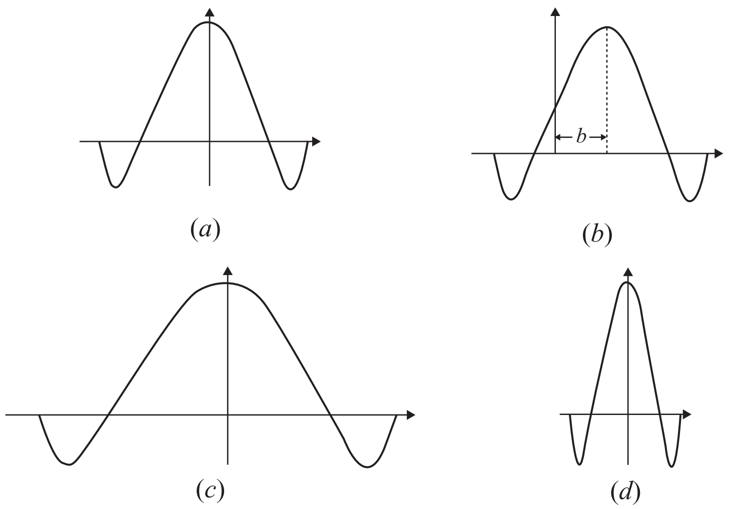

Figure 4.5 Effect of time dilation and translation on the mother wavelet (a) mother wavelet $\Psi(t) = \Psi_{1,0}(t)$, $a = 1$, $b = 0$; (b) wavelet $\Psi_{1,b}(t)$ $a = 1$, $b \neq 0$; (c) wavelet $\Psi_{2,0}(t)$ at scale $a = 2$, $b = 0$; and (d) wavelet $\Psi_{0.5,0}(t)$ at scale $a = 1/2$, $b = 0$

The width of the basis function varies with the dilation factor (or scale) a. The larger is a, the wider becomes the basis function in the time domain and hence narrower in the frequency domain. Thus, it allows varying time and frequency resolutions (with trade-off between both) in the wavelet transform. It is this property of the wavelet transform that makes it suitable for analysing signals having features of different sizes as present in the natural images. For each feature size, there is a basis function $\Psi_{a,b}(t)$ in which it will be best analysed. For example, in a picture of a house with a person looking through a window, the basis function with larger a will analyse conveniently the house as a whole. The person by the window will be best analysed at a smaller scale and the eyes of the person at even smaller scale. So the wavelet transform is analogous to the analysis of a signal in the frequency domain using band-pass filters of variable central frequency (which depends on parameter a) but with a constant quality factor. Note that in filters the quality factor is the ratio of the centre frequency to the bandwidth of the filter.

4.3.1 Discrete wavelet transform

As wavelet transform defined in eqn. 4.11 maps a one-dimensional signal $x(t)$ into a two-dimensional function $X_w(a, b)$, this increase in dimensionality makes it extremely redundant, and the original signal can be recovered from the wavelet transform computed on the discrete values of a and b [9]. The a can be made discrete by choosing $a = a_0^m$, with $a_0 > 1$ and m an integer. As a increases, the bandwidth of the basis function (or frequency resolution) decreases, and hence more resolution cells are needed to cover the region. Similarly, making b discrete corresponds to sampling in time (sampling frequency depends on the bandwidth of the signal to be sampled, which in turn is inversely proportional to a), it can be chosen as $b = nb_0a_0^m$. For $a_0 = 2$ and $b_0 = 1$ there are choices of $\Psi(t)$ such that the function $\Psi_{m,n}(t)$ forms an orthonormal basis of space of square-integrable functions. This implies that any square-integrable function $x(t)$ can be represented as linear combination of basis functions as

$$x(t) = \sum_{m=-\infty}^{\infty} \sum_{n=-\infty}^{\infty} \alpha_{m,n}\Psi_{m,n}(t) \tag{4.13}$$

where $\alpha_{m,n}$ are known as the wavelet transform coefficients of $x(t)$ and are obtained from eqn. 4.11 by

$$\alpha_{m,n} = \int_{-\infty}^{\infty} x(t)\Psi_{m,n}(t) \tag{4.14}$$

It is interesting to note that for every increment in m, the value of a doubles. This implies doubling the width in the time domain and halving the width in the frequency domain. This is equivalent to signal analysis with octave band decomposition and corresponds to dyadic wavelet transform similar to that shown in Figure 4.1, used to describe the basic principles of subband coding, and hence the wavelet transform is a type of subband coding.

4.3.2 Multiresolution representation

Application of the wavelet transform to image coding can be better understood with the notion of multiresolution signal analysis. Suppose there is a function $\Phi(t)$ such that the set $\Phi(t - n)$, $n \in Z$ is orthonormal. Also suppose $\Phi(t)$ is the solution of a two-scale difference equation

$$\Phi(t) = \sum_{n=-\infty}^{\infty} c_n\sqrt{2}\Phi(2t - n) \tag{4.15}$$

$$\text{where } c_n = \int_{-\infty}^{\infty} \Phi(t)\sqrt{2}\Phi(2t-n)dt \tag{4.16}$$

Let $x(t)$ be a square-integrable function, which can be represented as a linear combination of $\Phi(t - n)$ as

$$x(t) = \sum_{n=-\infty}^{\infty} c_n \Phi(t-n) \tag{4.17}$$

where c_n is the expansion coefficient and is the projection of $x(t)$ onto $\Phi(t - n)$. Since dilation of a function varies its resolution, it is possible to represent $x(t)$ at various resolutions by dilating and contracting the function $\Phi(t)$. Thus, $x(t)$ at any resolution m can be represented as

$$x_m(t) = 2^{-m/2} \sum_n c_n{}^m \Phi(2^{-m}t - n) \tag{4.18}$$

If V_m is the space generated by $2^{-m/2}\Phi(2^{-m}t - n)$, then from eqn. 4.15, $\Phi(t)$ is such that for any $i > j$, the function that generates space V_i is also in V_j, that is, $V_i \subset V_j$ $(i > j)$. Thus, spaces at successive scales can be nested such that V_m for increasing m can be viewed as the space of decreasing resolution. Therefore, a space at a coarser resolution V_{j-1} can be decomposed into two subspaces: a space at a finer resolution V_j and an orthogonal complement of V_j, represented by W_j such that $V_j + W_j = V_{j-1}$, where $W_j \perp V_j$. The space W_j is the space of differences between the coarser and the finer scale resolutions, which can be seen as the amount of detail added when going from smaller resolution V_j to a larger resolution V_{j-1}. The hierarchy of spaces is depicted in Figure 4.6.

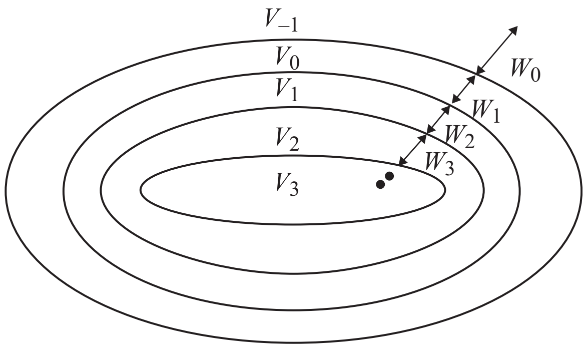

Figure 4.6 Multiresolution spaces

Mallat [10] has shown that, in general, the basis for W_j consists in translations and dilations of a single prototype function $\Psi(t)$, called a wavelet. Thus, W_m is the space generated by $\Psi_{m,n}(t) = 2^{-m/2}\Psi(2^{-m}t - n)$. The wavelet $\Psi(t) \in V_{-1}$ can be obtained from $\Phi(t)$ as

$$\Psi(t) = \sum_{n=-\infty}^{\infty} (-1)^n c_{1-n}\sqrt{2}\Phi(2t - n) \tag{4.19}$$

The function $\Phi(t)$ is called the scaling function of the multiresolution representation. Thus, the wavelet transform coefficients of eqn. 4.14 correspond to the projection of $x(t)$ onto a detail space of resolution m, W_m. Hence, a wavelet transform basically decomposes a signal into spaces of different resolutions. In the literature, these kinds of decomposition are, in general, referred to as multiresolution decomposition. Here is an example of calculating the Haar wavelet through this technique.

Example (Haar wavelet)
The scaling function of the Haar wavelet is the well-known rectangular (rect) function:

$$\Phi(t) = \begin{cases} 1 & 0 \le t \le 1 \\ 0 & \text{otherwise} \end{cases}$$

As the rect function satisfies eqn. 4.15 with c_n calculated from eqn. 4.16 as

$$c_n = \begin{cases} \dfrac{1}{\sqrt{2}} & n = 0,1 \\ 0 & \text{otherwise} \end{cases}$$

Thus, using eqn. 4.19, the Haar wavelet can be found as

$$\Psi(t) = \Phi(2t) - \Phi(2t - 1)$$

$$\Psi(t) = \begin{cases} 1 & 0 \le t < \dfrac{1}{2} \\ -1 & \dfrac{1}{2} \le t < 1 \end{cases}$$

The scaling function $\Phi(t)$ (a rect function) and the corresponding Haar wavelet $\Psi(t)$ for this example are shown in Figure 4.7*a* and *b*, respectively. In terms of approximation perspective, the multiresolution decomposition can be explained as follows. Let $x(t)$ be approximated at resolution j by function $A_j x(t)$ through the expansion series of the orthogonal basis functions. While W_j represents the space of

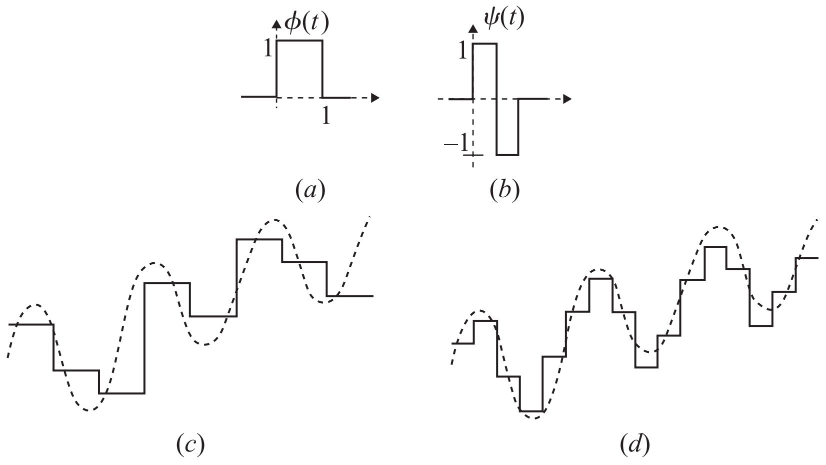

Figure 4.7 (a) Haar scaling function; (b) Haar wavelet; (c) approximation of a continuous function, x(t), at coarser resolution $A_0x(t)$ and (d) higher resolution approximation $A_1x(t)$

difference between a coarser scale V_{j-1} and a finer scale V_j, $D_jx(t) \in W_j$ represents the difference of approximation of $x(t)$ at $(j - 1)$th and jth resolution (i.e. $D_jx(t) = A_{j-1}x(t) - A_jx(t)$).

Thus, signal $x(t)$ can be split as $x(t) = A_{-1}x(t) = A_0x(t) + D_0x(t)$.

Figure 4.7*c* and *d* show the approximations of a continuous function at the two successive resolutions using rectangular scaling function. The coarser approximation $A_0x(t)$ is shown in Figure 4.7*c*, and at higher resolution, approximation $A_1x(t)$ in Figure 4.7*d*, where scaling function is a dilated version of the rectangular function. For a smooth function $x(t)$, most of the variation (signal energy) is contained in $A_0x(t)$, and $D_0x(t)$ is nearly zero. By repeating this splitting procedure and partitioning $A_0x(t) = A_1x(t) + D_1x(t)$, the wavelet transform of signal $x(t)$ can be obtained, and hence the original function $x(t)$ can be represented in terms of its wavelets as

$$x(t) = D_0x(t) + D_1x(t) + D_2x(t) + \cdots + D_nx(t) + A_nx(t) \tag{4.20}$$

where n represents the number of decompositions. Since the dynamic ranges of the detail signals $D_jx(t)$ are much smaller than the original function $x(t)$, they are easier to code than the coefficients in the series expansion of eqn. 4.13.

4.3.3 Wavelet transform and filter banks

For the repeated splitting procedure described above to be practical, there should be an efficient algorithm for obtaining $D_jx(t)$ from the original expansion coefficient of $x(t)$. One of the consequences of multiresolution space partitioning is that the scaling function $\Phi(t)$ possesses self-similarity property. If $\Phi(t)$ and $\overline{\Phi}(t)$ are the analysis and synthesis scaling functions, and $\Psi(t)$ and $\overline{\Psi}(t)$ are analysis and synthesis wavelets, then, since $V_j \subset V_{j-1}$, these functions can be recursively defined as

$$\begin{aligned}
\Phi(t) &= \sum_{n=-\infty}^{\infty} c_n \sqrt{2}\Phi(2t-n) \\
\overline{\Phi}(t) &= \sum_{n=-\infty}^{\infty} \overline{c}_n \sqrt{2}\overline{\Phi}(2t-n) \\
\Psi(t) &= \sum_{n=-\infty}^{\infty} d_n \sqrt{2}\Phi(2t-n) \\
\text{and} \quad \overline{\Psi}(t) &= \sum_{n=-\infty}^{\infty} \overline{d}_n \sqrt{2}\overline{\Phi}(2t-n)
\end{aligned} \tag{4.21}$$

These recurrence relations provide the ways to calculate the coefficients of approximation of $x(t)$ at resolution j, $A_jx(t)$ and coefficients of detail signal $D_jx(t)$ from the coefficients of approximation of $x(t)$ at a higher resolution $A_{j-1}x(t)$. In fact, simple mathematical manipulations can reveal that both the coefficients of approximation at a finer resolution and detail coefficients can be obtained by convolving the coefficient of approximation at a coarser resolution with a filter and downsampling it by a factor of 2. For a lower resolution approximation coefficient, the filter is a low-pass filter with taps $h_k = c_{-k}$ and for the details the filter is a high-pass filter with taps $g_k = d_{-k}$. Inversely, the signal at a higher resolution can be recovered from its approximation at a lower resolution and coefficients of the corresponding detail signal. It can be accomplished by upsampling the coefficients of approximation at a lower resolution and detail coefficients by a factor of 2, convolving them with the synthesis filters of taps $\overline{h}_k = \overline{c}_k$ and $\overline{g}_k = \overline{d}_k$, respectively, and adding them together. One step of splitting and inverse process is shown in Figure 4.8, which is in fact the same as Figure 4.3 for subband. Thus, the filtering process splits the signals into low-pass and high-pass frequency components and hence increases frequency resolution by a factor of 2, but by downsampling reduces the temporal resolution by the same factor. Hence, at each successive step, better frequency resolution at the expense of temporal resolution is achieved.

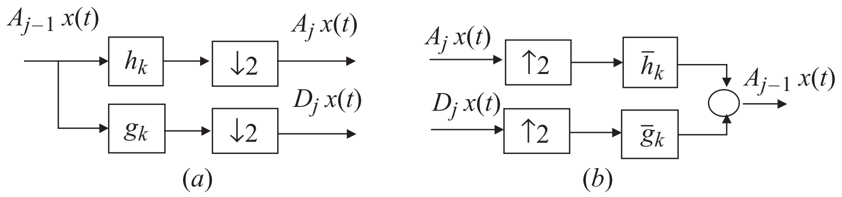

Figure 4.8 One-stage wavelet transform (a) analysis and (b) synthesis

4.3.4 Higher-order systems

The multidimensional wavelet transform can be obtained by extending the concept of the two-band filter structure of Figure 4.8 in each dimension. For example, decomposition of a two-dimensional image can be performed by carrying out one-dimensional decomposition in the horizontal and then in the vertical directions.

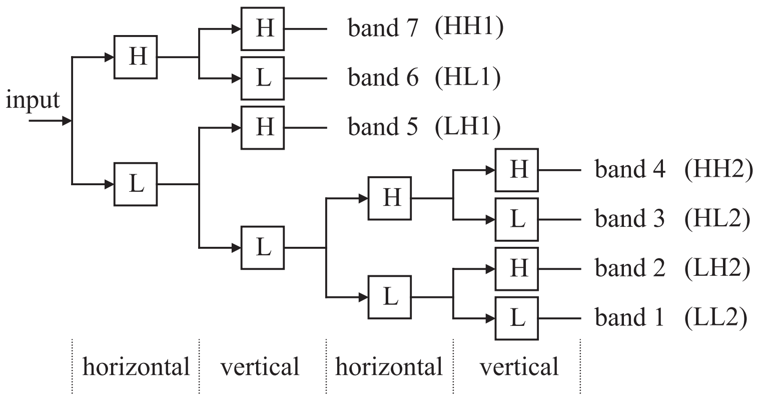

Figure 4.9 Multiband wavelet transform coding using repeated two-band splits

A seven-band wavelet transform coding of this type is illustrated in Figure 4.9, where band splitting is carried out alternately in the horizontal and vertical directions. In the figure, L and H represent the low-pass and high-pass analysis filters, respectively, with a 2:1 downsampling. At the first stage of dyadic decomposition, three subimages with high-frequency contents are generated. The subimage LH1 has mainly low horizontal but high vertical frequency image details. This is reversed in the HL1 subimage. The HH1 subimage has high horizontal and high vertical image details. These image details at a lower frequency are represented by the LH2, HL2 and HH2 bands, respectively. The LL2 band is a low-pass subsampled image, which is a replica of the original image, but at a smaller size.

4.3.5 Wavelet filter design

As we saw in section 4.3.3, in practice, wavelet transform can be realised by a set of filter banks, similar to those of subband. Relations between the analysis and synthesis of the scaling and wavelet functions also follow those of the synthesis and analysis filters of the subband. Hence, we can use the concept of the product filter, defined in eqn. 4.7, to design wavelet filters. However, if we use the product filter as was used for subband, we do not achieve anything new. But if we add some constraints on the product filter, such that the property of the wavelet transform is maintained, then a set of wavelet filters can be designed.

One of the constraints required to be imposed on the product filter $P(z)$ is that the resultant filters $H_0(z)$ and $H_1(z)$ be continuous, as required by the wavelet definition. Moreover, it is sometimes desirable to have wavelets with the largest possible number of continuous derivatives. This property in terms of z-transform means that the wavelet filters and consequently the product filter should have zeros at $z = -1$. A measure of the number of derivatives or number of zeros at $z = -1$ is given by the regularity of the wavelets and also called the number of vanishing moments [11]. This means in order to have regular filters, filters must have sufficient number of zeros at $z = -1$, the larger the number of zeros, the more regular the filter is.

Also, since in images, phase carries important information, it is necessary that filters must have linear phase responses. On the other hand, although the orthogonal filters have energy preserving property but most of the orthogonal filters do not have phase linearity. A particular class of filters that have linear phase in their both analysis and synthesis, and are very close to orthogonal are known as the biorthogonal filters. In biorthogonal filters, the low-pass analysis and the high-pass synthesis filters are orthogonal to each other, and similarly the high-pass analysis and the low-pass synthesis are orthogonal to each other, hence the name biorthogonal. Note that, in the biorthogonal filters, since the low pass and the high pass of either analysis or synthesis filter can be of different lengths, they are not themselves orthogonal to each other.

Thus, for a wavelet filter to have at least n zeros at $z = -1$, we chose the product filter to be [12]

$$P(z) = (1 + z^{-1})^{2n} Q(z) \tag{4.22}$$

where $Q(z)$ has n unknown coefficients. Depending on the choice of $Q(z)$ and the regularity of the desired wavelets, one can design a set of wavelets as desired. For example, with

$$n = 2 \quad \text{and} \quad Q(z) = -1 + 4z^{-1} - z^{-2}$$

the product filter becomes

$$P(z) = (1 + z^{-1})^4 (-1 + 4z^{-1} - z^{-2}) \tag{4.23}$$

and with a proper weighting for orthonormality and then factorisation, it leads to two sets of (5,3) and (4,4) filter banks of eqn. 4.10. The weighting factor is determined from eqn. 4.7. These filters were originally derived for subbands, but as we see they can also be used for wavelets. Filter pair (5,3) is the recommended filter for the lossless image coding in JPEG2000 [13]. The coefficients of its analysis filters are tabulated in Table 4.1.

As another example with

$$\begin{gathered} n = 3 \quad \text{and} \quad Q(z) = 1 - 6z^{-1} + \frac{38}{3} z^{-2} - 6z^{-3} + z^{-4} \\ P(z) = (1 + z^{-1})^6 \, (1 - 6z^{-1} + \frac{38}{3} z^{-2} - 6z^{-3} + z^{-4}) \end{gathered} \tag{4.24}$$

Table 4.1 Low-pass and high-pass analysis filters of integer (5,3) biorthogonal filter

n	**Low pass**	**High pass**
0	6/8	+1
±1	2/8	−1/2
±2	−1/8	

Table 4.2 Low-pass and high-pass analysis filters of Daubechies (9,3) biorthogonal filter

n	**Low pass**	**High pass**
0	0.99436891104360	0.70710678118655
±1	0.41984465132952	−0.35355339059327
±2	−0.17677669529665	
±3	−0.06629126073624	
±4	0.03314563036812	

Table 4.3 Low-pass and high-pass analysis filters of Daubechies (9,7) biorthogonal filter

n	**Low pass**	**High pass**
0	0.85269865321930	−0.7884848720618
±1	0.37740268810913	0.41809244072573
±2	−0.11062402748951	0.04068975261660
±3	−0.02384929751586	−0.06453905013246
±4	0.03782879857992	

the (9,3) pair of Daubechies filters [9] can be derived, which are given in Table 4.2. These filter banks are recommended for still image coding in MPEG-4 [14].

Another popular biorthogonal filter is the Daubechies (9,7) filter bank, recommended for lossy image coding in the JPEG2000 standard [13]. The coefficients of its low-pass and high-pass analysis filters are tabulated in Table 4.3. These filters are known to have the highest compression efficiency.

The corresponding low-pass and high-pass synthesis filters can be derived from the above analysis filters, using the relationship between the synthesis and analysis filters given by eqn. 4.4. That is, $G_0(z) = H_1(-z)$ and $G_1(z) = -H_0(-z)$.

Example

As an example of wavelet transform, Figure 4.10 shows all the seven subimages generated by the encoder of Figure 4.9 for a single frame of the flower garden test

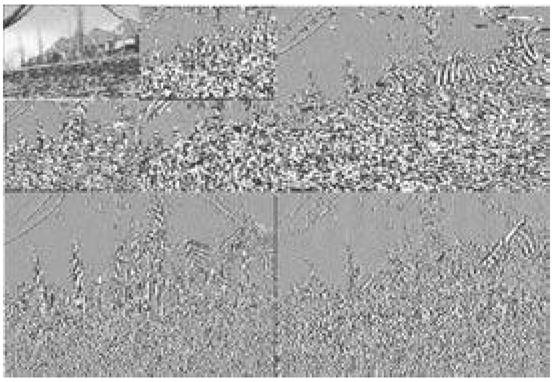

(*a*)

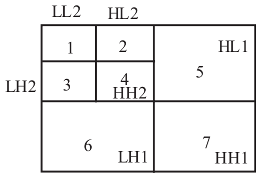

(*b*)

Figure 4.10 (a) The seven subimages generated by the encoder of Figure 4.9 and (b) layout of individual bands

sequence, with a nine-tap low-pass and three-tap high-pass analysis Daubechies filter pairs, (9,3), given in Table 4.2. These filters have been recommended for coding of still images in MPEG-4 [14], which has been shown to achieve good compression efficiency.

The original image (not shown) dimensions were 352 pixels by 240 lines. Bands 1–4, at two levels of subdivision, are 88 by 60, while bands 5–7 are 176 by 120 pixels. All bands but band 1 (LL2) have been amplified by a factor of 4 and an offset of +128 to enhance visibility of the low level details they contain. The scope for bandwidth compression arises mainly from the low-energy levels that appear in the high-pass subimages.

Since at image borders all the input pixels are not available, a symmetric extension of the input texture is performed before applying the wavelet transform at each level [14]. The type of symmetric extension can vary. For example, in MPEG-4, to satisfy the perfect reconstruction conditions with the Daubechies (9,3) tap analysis filter pairs, two types of symmetric extensions are used.

Type A is only used at the synthesis stage. It is used at the trailing edge of low-pass filtering and the leading edge of high-pass filtering stages. If the pixels at the boundary of the objects are represented by **abcde**, then the type A extension becomes edcba|**abcde**, where the letters in bold type are the original pixels and those in plain are the extended pixels. Note that for a (9,3) analysis filter pair of Table 4.2, the synthesis filter pair will be (3,9) with $G_0(z) = H_1(-z)$ and $G_1(z) = -H_0(-z)$, as was shown in eqn. 4.4.

Type B extension is used for both leading and trailing edges of the low- and high-pass analysis filters. For the synthesis filters, it is used at the leading edge of the low pass but at the trailing edge of the high pass. With this type of extension, the extended pixels at the leading and trailing edges become edcb|**abcde** and **abcde**|dcba, respectively.

4.4 Coding of the wavelet subimages

The lowest band of the wavelet subimages is a replica of the original image, but at much reduced size, depending on the number of decomposition levels, as can be seen from Figure 4.10. For example, if the number of wavelet decomposition levels is too high, then there is not much correlation between the pixels of the lowest band. In this case, pixel-by-pixel coding, as used in the JPEG2000 standard, is good enough. On the other hand, for MPEG-4, where not as many decomposition levels as JPEG2000 are used, there are some residual correlations between them. These can be reduced by differential pulse code modulation (DPCM) coding. Also, depending on whether wavelet transform is applied to still images or video, this band can be coded accordingly. However, in the relevant chapters, coding of this band for appropriate application is described.

For efficient compression of higher bands as well as for a wide range of scalability, the higher-order wavelet coefficients are coded with a zero tree (ZT) structure like the EZW algorithm first introduced by Shapiro [4]. This method and its variants are based on two concepts: quantisation by successive approximation and exploitation of the similarities of the bands of the same orientation.

4.4.1 Quantisation by successive approximation

Quantisation by successive approximation is the representation of a wavelet coefficient value in terms of progressively smaller quantisation step sizes. The number of passes of the approximation depends on the desired quantisation distortions. To see how successive approximation can lead to quantisation, consider Figure 4.11, where a coefficient of length L is successively refined to its final quantised value of $\hat{L}$.

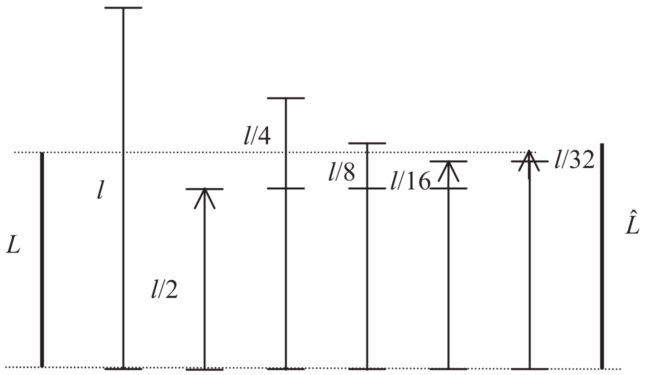

Figure 4.11 Principles of successive approximation

The process begins by choosing an initial yardstick length l. The value of l is set to half the largest coefficient in the image. If the coefficient is larger than the yardstick, it is represented with the yardstick value; otherwise, its value is set to zero. After each pass, the yardstick length is halved and the error magnitude, which is the difference between the original value of the coefficient and its reconstructed value, is compared with the new yardstick. The process is continued, such that the final error is acceptable. Hence, increasing the number of passes, the error in the representation of L by $\hat{L}$ can be made arbitrarily small.

With regard to Figure 4.11, the quantised length L can be expressed as

$$\hat{L} = 0 \times l + 1 \times \frac{l}{2} + 0 \times \frac{l}{4} + 0 \times \frac{l}{8} + 1 \times \frac{l}{16} + 1 \times \frac{l}{32} \cdots = \frac{l}{2} + \frac{l}{16} + \frac{l}{32} \qquad (4.25)$$

where only yardstick lengths smaller than quantisation error are considered. Therefore, given an initial yardstick length l, a length L can be represented as a string of 1 and 0 symbols. As each symbol 1 or 0 is added, the precision in the representation of L increases, and thus the distortion level decreases. This process is in fact equivalent to the binary representation of real numbers, called bit plane representation, where each number is represented by a string of 0s and 1s. By increasing the number of digits, the error in the representation can be made arbitrarily small.

Bit plane quantisation is another form of successive approximation that has been used in some standard codecs such as the JPEG2000. Here, the wavelet coefficients are first represented by their maximum possible precision. This depends on the input pixel resolution (e.g. 8 bits) and the dynamic range of the wavelet filters coefficients. The symbols that represent the quantised coefficients are encoded 1 bit at a time, starting with the most significant bit (MSB) and preceding to the least significant bit (LSB). Thus, for an M-bit plane quantisation with the finest quantiser step size of Δ, the yardstick is $\Delta 2^{M-1}$, where Δ is the basic quantiser step size.

4.4.2 Similarities among the bands

A two-stage wavelet transform (seven bands) of the flower garden image sequence with the position of the bands was shown in Figure 4.10. It can be seen that the vertical bands look like scaled versions of each other, as do the horizontal and diagonal bands. Of particular interest in these subimages is that the nonsignificant coefficients from bands of the same orientation tend to be in the same corresponding locations. Also, the edges are approximately at the same corresponding positions. Considering that subimages of lower bands (higher stages of decomposition) have half the dimensions of their higher bands, one can make a quad tree representation of the bands of the same orientation, as shown in Figure 4.12 for a ten band (three-stage wavelet transform).

In this figure, a coefficient in the lowest vertical band, LH_3, corresponds to four coefficients of its immediately higher band LH_2, which relates to 16 coefficients in LH_1. Thus, if a coefficient in LH_3 is zero, it is likely that its children in the higher bands of LH_2 and LH_1 are zero. The same is true for the other horizontal and diagonal bands. This tree of zeros, called ZT, is an efficient way of representing a large group of zeros of the wavelet coefficients. Here, the root of the ZT is required

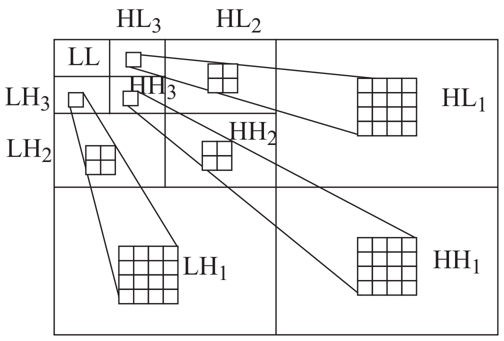

Figure 4.12 Quad tree representation of the bands of the same orientation

to be identified and then the descendant children in the higher bands can be ignored.

4.5 EZW algorithm

The combination of the ZT roots with successive approximation has opened up a very interesting coding tool for not only efficient compression of wavelet coefficients but also as a means for spatial and signal-to-noise ratio (SNR) scalability [4].

The encoding algorithm with slight modification on the successive approximation, for efficient coding, according to EZW [4] is described as follows:

1. The image mean is computed and extracted from the image. This depends on how the lowest band LL is coded. If it is coded independently of other bands, such as with DPCM in MPEG-4, then this stage can be ignored.
2. An R-stage (3R + 1 band) wavelet transform is applied to the (zero mean) image.
3. The initial yardstick length l is set to half of the maximum absolute value of the wavelet coefficients.
4. A list of the coordinates of the coefficients, called the dominant list, is generated. This list determines the order in which the coefficients are scanned. It must be such that coefficients from a lower-frequency band (higher scale) are always scanned before the ones from a higher-frequency band. Two empty lists of coefficient coordinates, called the subordinate list and the temporary list, are also created.
5. The wavelet transform of the image is scanned, and if a wavelet coefficient is smaller than the current yardstick length l, it is reconstructed to zero. Otherwise, it is reconstructed as $\pm 3l/2$, according to its sign.
6. *Dominant pass*: the reconstructed coefficients are scanned again, according to the order in the dominant list, generating a string of symbols as follows: if a reconstructed coefficient is positive or negative, a + or − symbol is added to

the string and the coordinates of this coefficient are appended to the subordinate list. If a reconstructed coefficient is zero, its coordinates are appended to the temporary list. In the case of a zero-valued reconstructed coefficient, two different symbols can be appended to the string; if all its corresponding coefficients in bands of the same orientation and higher frequencies are zero, a ZT root is added to the string, and its corresponding coefficients are removed from the dominant list and added to the temporary list (since they are already known to be zero, they do not need to be scanned again). Otherwise, an isolated zero (Z) is added to the string. The strings generated from the four-symbol alphabet of +, –, ZT and Z are encoded with an adaptive arithmetic encoder [15], whose model is updated to four symbols at the beginning of this pass. However, during the scanning of the highest horizontal, vertical and diagonal frequency bands (HL_1, LH_1 and HH_1 of Figure 4.12), no ZT roots can be generated. Therefore, just before the scanning of the first coefficient of these bands, the model of the arithmetic coder is updated to three symbols of +, – and Z.

7. The yardstick length l is halved.
8. *Subordinate pass*: the coefficients that previously have not been reconstructed as zero are scanned again according to their order in the subordinate list, and each one has added to it either $+l/2$ or $-l/2$ in order to minimise the magnitude of its reconstruction error. If $l/2$ is added, a + symbol is appended to the string, and if $l/2$ is subtracted, a – symbol is appended. At the end of the subordinate pass, the subordinate list is reordered so that the coefficients whose reconstructed values have higher magnitudes come first. The + and – symbols of this pass are encoded with the arithmetic coder, which had its model updated to two symbols (+ and –) at the beginning of this pass.
9. The dominant list is replaced by the temporary list, and the temporary list is emptied.
10. The whole process is repeated from step 5. It stops at any point when the size of the bitstream exceeds the desired bit rate budget.

An observation has to be made on the dominant pass (step 6). In this pass, only the reconstructed values of the coefficients that are still in the dominant list can be affected. Therefore, in order to increase the number of ZT roots, the coefficients not in the dominant list can be considered zero for determining if a zero-valued coefficient is either a ZT root or an isolated zero.

The bitstream includes a header giving extra information to the decoder. The header contains the number of wavelet transform stages, the image dimensions, the initial value of the yardstick length and the image mean. Both the encoder and decoder initially have identical dominant lists. As the bitstream is decoded, the decoder updates the reconstructed image, as well as its subordinate and temporary lists. In this way, it can exactly track the stages of the encoder and can therefore properly decode the bitstream. It is important to observe that the ordering of the subordinate list in step 8 is carried out based only on the reconstructed coefficient values, which are available to the decoder. If it was not so, the decoder would not be able to track the encoder, and thus the bitstream would not be properly decoded.

4.5.1 Analysis of the algorithm

The above algorithm has many interesting features, which make it especially significant to note. Among them are the following:

a. The use of ZTs, which exploits similarities among the bands of the same orientation and reduces the number of symbols to be coded.
b. The use of a very small alphabet to represent an image (maximum number of four symbols) makes adaptive arithmetic coding very efficient, because it adapts itself very quickly to any changes in the statistics of the symbols.
c. Since the maximum distortion level of a coefficient at any stage is bounded by the current yardstick length, the average distortion level in each pass is also given by the current yardstick, being the same for all bands.
d. At any given pass, only the coefficients with magnitudes larger than the current yardstick length are encoded nonzero. Therefore, the coefficients with higher magnitudes tend to be encoded before the ones with smaller magnitudes. This implies that the EZW algorithm tends to give priority to the most important information in the encoding process. This is aided by the ordering of the subordinate in step 8. Thus, for the given bit rate, the bits are spent where they are needed most.
e. Since the EZW algorithm employs a successive approximation process, the addition of a new symbol (+, –, ZT and Z) to the string just further refines the reconstructed image. Furthermore, while each symbol is being added to the string, it is encoded into the bitstream; hence, the encoding and decoding can stop at any point, and an image with a level of refinement corresponding to the symbols encoded/decoded so far can be recovered. Therefore, the encoding and decoding of an image can stop when the bit rate budget is exhausted, which makes possible an extremely precise bit rate control. In addition, because of the prioritisation of the more important information mentioned in item (d), no matter where in the bitstream the decoding is stopped, the best possible image quality for that bit rate is achieved.
f. *Spatial/SNR scalability*: to achieve spatial or SNR scalability, two different scanning methods are employed in this scheme. For spatial scalability, the wavelet coefficients are scanned in the subband-by-subband fashion, from the lowest to the highest frequency subbands. For SNR scalability, the wavelet coefficients are scanned in each tree from the top to the bottom. The scanning method is defined in the bitstream.

4.6 Set partitioning in hierarchical trees (SPIHT)

The compression efficiency of EZW is, to some extent, due to the use of arithmetic coding. Said and Pearlman [16] have introduced a variant of coding of wavelet coefficients by successive approximation, which even without arithmetic coding outperforms EZW (see Figure 4.20). They call it set partitioning in hierarchical trees (SPIHT). Both EZW and SPIHT are spatial tree-based encoding techniques that exploit magnitude correlation across bands of the decomposition. Each generates a fidelity progressive bitstream by encoding, in turn, each bit plane of a quantised dyadic subband decomposition. Both use significance test on sets of coefficients to efficiently isolate and encode high-magnitude coefficients. However, the crucial parts in the SPIHT coding process are the way the subsets of the wavelet coefficients are partitioned and the significant information is conveyed.

One of the main features of this scheme in transmitting the ordering data is that it is based on the fact that the execution path of an algorithm is defined by the results of the comparisons of its branching points. So, if the encoder and decoder have the same sorting algorithm, then the decoder can duplicate the encoder's execution path if it receives the results of the magnitude comparisons. The ordering information can be recovered from the execution path.

The sorting algorithm divides the set of wavelet coefficients, $\{C_{i,j}\}$, into partitioning subsets T_m and performs the magnitude test:

$$\max_{\substack{(i,j)\\(i,j)\in T_m}} \{|C_{i,j}|\} \geq 2^n? \tag{4.26}$$

If the decoder receives a no to that answer (the subset is insignificant), then it knows that all coefficients in T_m are insignificant. If the answer is yes (the subset is significant), then a certain rule shared by the encoder and decoder is used to partition T_m into new subset $T_{m,l}$ and the significant test is then applied to the new subsets. This set division process continues until the magnitude test is done to all single-coordinate significant subsets in order to identify each significant coefficient.

To reduce the number of magnitude comparisons (message bits), a set partitioning rule that uses an expected ordering in the hierarchy defined by the subband pyramid is defined (similar to Figure 4.12, used in ZT coding). In section 4.4.2, we saw how the similarities among the subimages of the same orientation can be exploited to create a spatial orientation tree (SOT). The objective is to create new partitions such that subsets expected to be insignificant contain a huge number of elements and subsets expected to be significant contain only one element.

To make clear the relationship between magnitude comparisons and message bits, the following function is used:

$$\begin{aligned} S_n(T) &= 1, \quad \text{if} \max_{\substack{(i,j)\\(i,j)\in T}} \{|C_{i,j}|\} \geq 2^n \\ &= 0, \quad \text{otherwise} \end{aligned} \tag{4.27}$$

to indicate the significance of a set of coordinates T. To simplify the notation of single pixel sets, $S_n(\{(i,j)\})$ is represented by $S_n(i,j)$.

To see how SPHIT can be implemented, let us assume $O(i,j)$ to represent a set of coordinates of all offsprings of node (i,j). For instance, except the highest and lowest pyramid levels, $O(i,j)$ is defined in terms of its offsprings as

$$O(i,j) = \{(2i,2j), (2i, 2j+1), (2i+1, 2j), (2i+1, 2j+1)\} \tag{4.28}$$

We also define $D(i,j)$ as a set of coordinates of all descendants of the node (i,j), and H, a set of coordinates of all SOT roots (nodes in the highest pyramid level). Finally, $L(i,j)$ is defined as

$$L(i,j) = D(i,j) - O(i,j) \tag{4.29}$$

The $O(i,j)$, $D(i,j)$ and $L(i,j)$ in an SOT are shown in Figure 4.13.

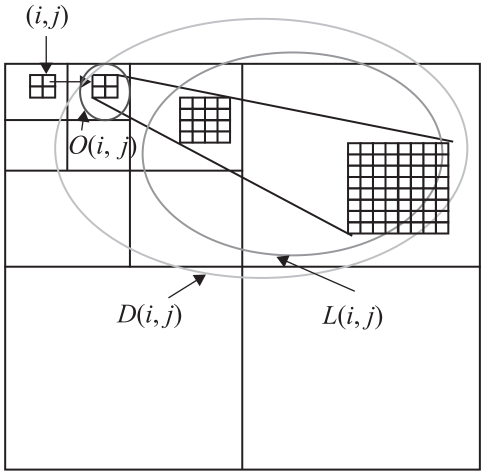

Figure 4.13 SOT and set partitioning in SPIHT

With the use of parts of the SOTs as the partitioning subsets in the sorting algorithm, the set partitioning rules are defined as follows:

- The initial partition is formed with the sets $\{(i,j)\}$ and $D(i,j)$, for all $(i,j) \in H$.
- If $D(i,j)$ is significant, then it is partitioned into $L(i,j)$ plus the four single-element sets with $(k,l) \in O(i,j)$.
- If $L(i,j)$ is significant, then it is partitioned into the four sets $D(k,l)$, with $(k,l) \in O(i,j)$.
- Each of the four sets now has the format of the original set, and the same partitioning can be used recursively.

4.6.1 Coding algorithm

Since the order in which the subsets are tested for significance is important, the significance information in a practical implementation is stored in three ordered lists, called the list of insignificant sets (LIS), list of insignificant pixels (LIP) and list of significant pixels (LSP). In all lists, each entry is identified by a coordinate (i, j), which in the LIP and LSP represents individual pixels, and in the LIS represents either the set $D(i, j)$ or $L(i, j)$. To differentiate between them, it is said that an LIS entry is of type A if it represents $D(i, j)$ and of type B if it represents $L(i, j)$ [16].

During the sorting pass, the pixels in the LIP, which were insignificant in the previous pass, are tested, and those that become significant are moved to the LSP. Similarly, sets are sequentially evaluated following the LIS order, and when a set is found to be significant, it is removed from the list and partitioned. The new subsets with more than one element are added back to the LIS, while the single-coordinate sets are added to the end of the LIP or the LSP depending on whether they are insignificant or significant, respectively. The LSP contain the coordinates of the pixels that are visited in the refinement pass.

Thus, the algorithm can be summarised as follows:

```
1. Initialisation: let the initial yardstick, n, be $n = \lfloor \log_2(\max_{(i,j)}\{|C_{i,j}|\}) \rfloor$. Set the
   LSP as an empty set list, and add the coordinates $(i, j) \in H$ to the LIP, and only
   those with descendants also to the LIS, as the type A entries.
2. Sorting pass:
   2.1. for each entry $(i, j)$ in the LIP do:
        2.1.1. output $S_n(i, j)$
        2.1.2. if $S_n(i, j) = 1$, then move $(i, j)$ to the LSP and output the sign
               of $C_{i,j}$
   2.2. for each entry $(i, j)$ in the LIS do:
        2.2.1. if the entry is of type A then
               2.2.1.1. output $S_n(D(i, j))$
               2.2.1.2. if $S_n(D(i, j)) = 1$ then
                        2.2.1.2.1. for each $(k, l) \in O(i, j)$ do:
                                   2.2.1.2.1.1. output $S_n(k, l)$
                                   2.2.1.2.1.2. if $S_n(k, l) = 1$, then add $(k, l)$
                                                to the LSP and output the
                                                sign of $C_{k,l}$
                                   2.2.1.2.1.3. if $S_n(k, l) = 0$, then add $(k, l)$
                                                to the end of the LIP
                        2.2.1.2.2. if $L(i, j) \neq \Phi$, then move $(i, j)$ to the end of
                                   the LIS as an entry of type B, and go to step
                                   2.2.2; otherwise, remove entry $(i, j)$ from
                                   the LIS
        2.2.2. if the entry is of type B then
               2.2.2.1. output $S_n(L(i, j))$
               2.2.2.2. if $S_n(L(i, j)) = 1$ then
```

```
                    2.2.2.2.1. add each $(k, l) \in O(i, j)$ to the end of the
                               LIS as an entry of type A
                    2.2.2.2.2. remove $(i, j)$ from the LIS.
```

3. *Refinement pass*: for each entry (i, j) in the LSP, except those included in the last sorting pass (i.e. with same n), output the nth MSB of $|C_{i,j}|$.
4. *Quantisation step update*: decrement n by 1 and go to step 2.

One important characteristics of the algorithm is that the entries added to the end of the LIS above are evaluated before the same sorting pass ends. So, when it is said for each entry in the LIS, it is meant those that are being added to its end. Also similar to EZW, the rate can be precisely controlled because the transmitted information is formed of single bits. The encoder can estimate the progressive distortion reduction and stop at a desired distortion value.

Note that, in this algorithm, the encoder outputs all branching conditions based on the outcome of the wavelet coefficients. Thus, to obtain the desired decoder's algorithm, which duplicates the encoder's execution path as it sorts the significant coefficients, we simply replace the words output with input. The ordering information is recovered when the coordinate of the significant coefficients is added to the end of the LSP. But note that whenever the decoder inputs data, its three control lists (LIS, LIP and LSP) are identical to the ones used by the encoder at the moment it outputs that data, which means that the decoder indeed recovers the ordering from the execution path.

An additional task done by the decoder is to update the reconstructed image. For the value of n, when a coordinate is moved to the LSP, it is known that $2^n \leq |C_{i,j}| < 2^{n+1}$. So, the decoder uses this information, plus the sign bit that is input just after the insertion in the LSP, to set the reconstructed coefficients $\hat{C}_{i,j} = \pm 1.5 \times 2^n$. Similarly, during the refinement pass, the decoder adds or subtracts 2^{n-1} to $\hat{C}_{i,j}$ when it inputs the bits of the binary representation of $|C_{i,j}|$. In this manner, the distortion gradually decreases during both the sorting and refinement passes.

At the end, it is worth mentioning some of the differences between EZW and SPIHT. The first difference is that they use slightly different SOT. In EZW, each root node in the top LL band has three offsprings, one in each high-frequency subband at the same decomposition level, and all other coefficients have four children in the lower decomposition subband of the same orientation. However, in SPIHT, in a group of 2×2 root nodes in the top LL band, top left node has no descendant and the other three have four offsprings each in the high-frequency band of the corresponding orientation. Thus, SPIHT uses less number of trees with more elements per tree than in EZW. Another important difference is in their set partitioning rules. SPIHT has an additional partitioning step in which a descendant (type A) set is split into four individual child coefficients and a grand descendant (type B) set. EZW explicitly performs a breadth first search of the hierarchical trees, moving from coarser to finer subbands. Though it is not explicit, SPIHT does a roughly breadth first search as well. After partitioning a grand descendant set, SPIHT places the four new descendant sets at the end of the LIS. Appending to the LIS results in the approximate breadth first traversal.

4.7 Embedded block coding with optimised truncation (EBCOT)

Embedded block coding with optimised truncation (EBCOT) [17] is another wavelet-based coding algorithm that has the capability of embedding many advanced features in a single bitstream while exhibiting a state-of-the-art compression performance. Because of its rich set of features, modest implementation complexity and excellent compression performance, the EBCOT algorithm has been adopted in the evolving new still image coding standard, under the name of JPEG2000. Thus, because of the important role of EBCOT in the JPEG2000, we describe this coding technique in some detail. Before describing this new method of wavelet coding, let us investigate the problem with EZW and SPIHT that caused their rejection for JPEG2000.

As seen in Chapter 5, spatial and SNR scalability of images are among the many requirements from the JPEG2000 standard. Spatial scalability means to be able to decode pictures of various spatial resolutions from the compressed bitstream. This is, in fact, an inherent property of the wavelet transform, irrespective of how the wavelet coefficients are coded, since at any level of the decomposition, the lowest band of that level gives a smaller replica of the original picture. The SNR scalability means to be able to decode pictures of various qualities from the compressed bitstream. In both EZW and SPIHT, this is achieved by successive approximation or bit plane encoding of the wavelet coefficients. Thus, it appears that EZW and SPIHT coding of the wavelet-coded images can meet these two scalability requirements. However, the bitstreams of both EZW and SPIHT inherently offer only SNR scalability. If spatial scalability is required, then the bitstream should be modified accordingly, which is then not SNR scalable. This is because the ZT-based structure used in these methods involves downward dependencies between the subbands produced by the successive wavelet decompositions. These dependencies interfere with the resolution scalability. Moreover, the interband dependency by the use of ZT structure causes the error to propagate through the bands. This again does not meet the error resilience requirement of JPEG2000.

These shortfalls can be overcome, if each subband was coded independently. Even to make coding more flexible, subband samples can be partitioned into small blocks and to code each block independently. The dependencies may exist within a block but not between different blocks. The size of the blocks determines the degree to which one is prepared to sacrifice coding efficiency in exchange of flexibility in the ordering of information within the final compressed bitstream. The independent block coding paradigm is the heart of EBCOT. This independent coding allows local processing of the samples in each block, which is advantageous for hardware implementation. It also makes highly parallel implementation possible where multiple blocks are encoded and decoded simultaneously. More importantly, because of flexibility in the rearrangement of bits in the EBCOT, simultaneous SNR and spatial scalability is possible. Obviously, the error encountered in any block's bitstream will clearly have no influence on other blocks and hence improves the robustness. Finally, since, unlike EZW and SPHIT, similarities between the bands are not exploited, there is small deficiency in the compression performance. This is compensated by the use of more efficient context-based arithmetic coding and the postcompression rate distortion (PCRD) optimisation.

In EBCOT, each subband is partitioned into relatively small block of samples, called code blocks. Typical code block size is either 32 × 32 or 64 × 64, and each code block is coded independently. The actual coding algorithm in EBCOT can be divided into three stages:

1. bit plane quantisation
2. binary arithmetic coding (tier 1 coding)
3. bitstream organisation (tier 2 coding)

Each of these steps is described briefly in the following subsections.

4.7.1 Bit plane quantisation

All code blocks of a subband use the same quantiser. The basic quantiser step size Δ_b of a subband b is selected on the basis of either perceptual importance of the subband or rate control. The quantiser maps the magnitude of a wavelet coefficient to a quantised index, as shown in Figure 4.14, keeping its sign. It has uniform characteristics (equal step size) with a dead zone of twice the step size.

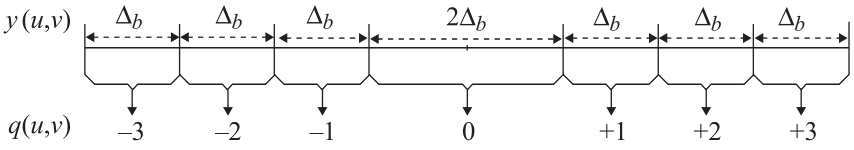

Figure 4.14 Uniform dead zone quantiser with step size Δ_b

In bit plane coding, the quantiser index is encoded one bit at a time, starting from the MSB and preceding to the LSB. If K is the sufficient number of bits to represent any quantisation index in a code block, then the maximum coefficient magnitude will be $\Delta_b(2^K - 1)$. An embedded bitstream for each code block is formed by first coding the MSB, that is, $(K - 1)$th bit together with the sign of any significant sample for all the samples in the code block. Then the next MSB, that is, $(K - 2)$th bit, is coded until all the bit planes are encoded. If the bitstream is truncated then some or all the samples in the block may be missing one or more least significant bits. This is equivalent to having used a coarser dead zone quantiser with step size $\Delta_b 2^p$, where p is the index of the last available bit plane for the relevant sample or p least significant bits of quantiser index still remain to be encoded.

4.7.2 Conditional arithmetic coding of bit planes (tier 1 coding)

During progressive bit plane coding, substantial redundancies exist between the successive bit planes. The EBCOT algorithm has exploited these redundancies in two ways. The first is to identify whether a coefficient should be coded, and the second, how best the entropy coding can be adapted to the statistics of the neighbouring coefficients. Both of these goals are achieved through the introduction of the binary significance state σ. It is defined to signify the importance of each coefficient in a code block. At the beginning of the coding process, the significant states of all the samples in the code block are initialised to 0 and then changed to 1 immediately after coding the first nonzero magnitude bit for the sample. Since the neighbouring coefficients generally have similar significance resulting in clusters of similar binary symbols in a plane, then the significance state, σ, is a good indicator for a bit plane of a coefficient to be a candidate for coding.

Also, in EBCOT, adaptive binary arithmetic is used for entropy coding of each symbol. Again, the clustering of significance of neighbours can be exploited to adapt the probability model, based on the significance states of its immediate neighbours. This is called context-based binary arithmetic coding, where the probability assigned to code a binary symbol of 0 or 1 or the positive/negative sign of a coefficient is derived from the context of its eight immediate neighbours, shown in Figure 4.15.

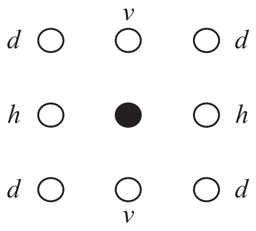

Figure 4.15 Eight immediate neighbouring symbols

In general, the eight immediate neighbours can have 256 different contextual states, or as many contextual states for the positive and negative signs. In EBCOT, the probability models used by the arithmetic coder are limited within 18 different contexts: 9 for the significance propagation, 1 for run length and 5 for sign coding and 3 for refinement. These contexts are explained in the relevant parts.

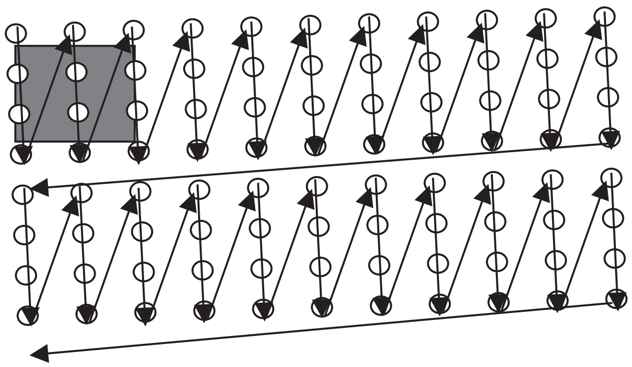

Figure 4.16 Stripe scanned order in a code block

Since the status of the eight immediate neighbours affects the formation of the probability model, the way coefficients in a code block are scanned should be defined. In the JPEG2000 standard, in every bit plane of a code block, the coefficients are visited in a stripe scan order with height of four pixels as shown in Figure 4.16.

Starting from the top left, the first 4 bits of the first column are scanned. Then the 4 bits of the second column, until the width of the code block is covered. Then the second 4 bits of the first column of the next stripe are scanned and so on. The stripe height of four has been chosen to facilitate hardware and software implementations.

4.7.3 Fractional bit plane coding

The quantised coefficients in a code block are bit plane encoded independent of other code blocks in the subbands. Instead of encoding the entire bit plane in one pass, each bit plane is encoded in three subbit planes passes, called fractional bit plane coding. The reason for this is to be able to truncate the bitstream at the end of each pass to create a near-optimum bitstream. This is also known as PCRD optimisation [18]. Here, the pass that results in a largest reduction in distortion for the smallest increase in bit rate is encoded first.

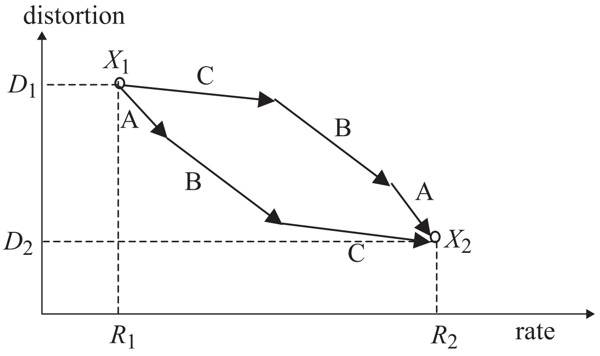

Figure 4.17 The impact of order of fractional bit plane coding in distortion reduction

The goal and benefits of fractional bit plane coding can be understood with the help of Figure 4.17. Suppose (R_1, D_1) and (R_2, D_2) are the rate distortion pairs corresponding to two adjacent bit planes p_1 and p_2. Also, assume during the encoding of each pass, the increase in bit rate and reduction in distortion follow the characteristics identified by labels A, B and C. As we see, in coding the whole bit plane, that is, going from point X_1 to point X_2, no matter which route is followed, the ultimate bit rate is increased from R_1 to R_2, and the distortion is reduced from D_1 to D_2. But if due to the limit in the bit rate budget, the bit rate has to be truncated between R_1 and R_2, $R_1 \leq R \leq R_2$, then it is better to follow the passes in sequence of ABC rather than CBA.

This sort of fractional bit plane coding is in fact a method of optimising the rate distortion curve, with the aim of generating finely embedded bitstream, which is known as the PCRD optimisation in EBCOT [18]. Figure 4.18 compares the optimised rate distortion associated with the fractional bit plane encoding versus that of the conventional bit plane encoding. The solid dots represent the rate distortion pairs at the end of each bit plane, and the solid line is the rate distortion curve that one could expect to obtain by truncating the bitstream produced by this method to an arbitrary bit rate. On the other hand, the end points associated with each pass of the fractional bit plane coding are shown with blank circles, and the broken line illustrates its rate distortion curve. Since initial coding passes generally have steeper rate distortion slopes, the end point for each coding pass lies below the convex interpolation of the bit plane termination point. Thus, fractional bit plane encoding results in a near-optimum coding performance compared with simple bit plane coding.

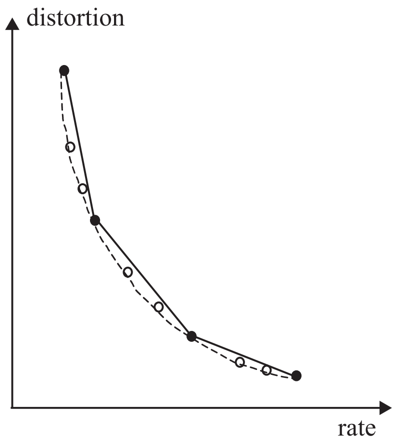

Figure 4.18 Rate distortion with optimum truncation

Generally, in coding a coefficient, the largest reduction in distortion occurs when the coefficient is insignificant, but it is more likely to become significant during the coding. Moderate reduction in distortion is when the coefficient is already significant and the coding refines it. Finally, the least reduction in distortion is when the insignificant coefficient after the encoding is likely to remain insignificant. These are, in fact, the remaining coefficients that are not coded in the two previous cases. Thus, it is reasonable to divide the bit plane encoding into three passes and encode each pass in the above encoding order. In JPEG2000, the fractional bit plane is carried out in three passes. The roles played by each encoding pass and their order of significance in generating optimum bitstream is given below.

4.7.3.1 Significance propagation pass

This is the first pass of the fractional bit plane encoding that gives the largest reduction in the encoding distortion. In this pass, the bit of a coefficient in a given bit plane is encoded, if and only if, prior to this pass, the state of the coefficient was insignificant but at least one of its eight immediate neighbours has significant states. If the coefficient is to be coded, the magnitude of its bit, 0 or 1, is arithmetic coded with a derived probability model from the context of its eight immediate neighbours, shown in Figure 4.15. The probability assigned to bit 0 is complementary to the probability assigned to bit 1. The context selection is based upon the significance of sample's eight immediate neighbours, which are grouped in three categories:

$$\begin{aligned}&\text{Horizontal: } h_i(u,v) = \sigma_i(u-1,v) + \sigma_i(u+1,v)\\&\text{Vertical: } v_i(u,v) = \sigma_i(u,v-1) + \sigma_i(u,v+1)\\&\text{Diagonal: } d_i(u,v) = \sum_{m=\pm 1}\sum_{n=\pm 1}\sigma_i(u+m,v+n)\end{aligned} \tag{4.30}$$

where $h_i(u, v)$, $v_i(u, v)$ and $d_i(u, v)$ are the horizontal, vertical and diagonal neighbours for the ith coefficient at coordinates (u, v), and $\sigma_i(u, v)$ is the significance state of a coefficient at that coordinate. Neighbours that lie outside the code block are interpreted as insignificant for the purpose of constructing these three quantities. To optimise both model adaptations cost and implementation complexity, 256 possible neighbourhood configurations are mapped to nine distinct coding contexts based on eqn. 4.30, as shown in Table 4.4.

To make identical context assignment for LH and HL bands, the code blocks of HL subbands are transposed before the coding. The LH subband responds most strongly to horizontal edges in the original image, so the context mapping gives more emphasis on the horizontal neighbours.

Note that the significance propagation pass includes only those bits of coefficients that were insignificant before this pass and have a nonzero context. If the bit of the coefficient is 1 (the coefficient becomes significant for the first time), then its

Table 4.4 Assignment of the nine contexts based on neighbourhood significance

LL, LH and HL bands				**HH band**		
$h_i(u, v)$	$v_i(u, v)$	$d_i(u, v)$	**Context**	$d_i(u, v)$	$h_i(u, v) + v_i(u, v)$	**Context**
0	0	0	0	0	0	0
0	0	1	1	0	1	1
0	0	>1	2	0	>1	2
0	1	X	3	1	0	3
0	2	X	4	1	1	4
1	0	0	5	1	>1	5
1	0	>0	6	2	0	6
1	>0	X	7	2	>0	7
2	X	X	8	>2	X	8

state of significance, σ, is changed to 1 to affect the context of its following neighbours. Thus, the significance of states of coefficients propagates throughout the coding, and hence the name given to this pass is significance propagation pass. Note also that if a sample is located at the boundary of a block, then only the available immediate neighbours are considered and the significance state of the missing neighbours is assumed to be zero.

Finally, if a coefficient is found to be significant, its sign is also arithmetic coded. Since the sign bits from the adjacent samples exhibit substantial statistical dependencies, they can be effectively exploited to improve the arithmetic coding efficiency. For example, the wavelet coefficients of horizontal and vertical edges are likely to be of the same polarity. Those after and before the edge are of mainly opposite polarity. In EBCOT algorithm, the arithmetic coding of sign bit employs five contexts. Context design is based upon the relevant sample's immediate horizontal and vertical neighbours, each of which may be in one of the three states: significant and positive, significant and negative, and insignificant. There are thus $3^4 = 81$ unique neighbourhood configurations. The details of the symmetry configurations and approximations to map these 81 configurations to one of the five context levels can be found in [18].

4.7.3.2 Magnitude refinement pass

The magnitude refinement pass is the second most efficient encoding pass. During this pass, the magnitude bit of a coefficient that has already become significant in a previous bit plane is arithmetic coded. The magnitude refinement pass includes the bits from the coefficients that are already significant, except those that have just become significant in the immediately preceding significance propagation pass. There are three contexts for the arithmetic coder, which are derived from the summation of the significance states of the horizontal, vertical and diagonal neighbours. These are the states currently known to the decoder and not the states used before the significance decoding pass. Further, it is dependent on whether this is the first refinement bit (the bit immediately after the significance and sign bits).

In general, the refinement bits have an even distribution, unless the coefficient has just become significant in the previous bit plane (i.e. the magnitude bit to be encoded is the first refinement bit). This condition is first tested and if it is satisfied, the magnitude bit is encoded using two contexts, based on the significance of the eight immediate neighbours (see Figure 4.15). Otherwise, it is coded with a single context regardless of the neighbouring values.

4.7.3.3 Clean-up pass

All the bits not encoded during the previous two passes of significance propagation and refinement passes are encoded in the clean-up pass. That is, the coefficients that are insignificant and had the context value of zero (none of the eight immediate neighbours were significant) during the significance propagation pass. Generally, the coefficients coded in this pass have a very small probability of being significant and hence are expected to remain insignificant. Therefore, a special mode, called the run mode, is used to aggregate the coefficients of remaining significant. A run mode is entered if all the four samples in a vertical column of the stripe of Figure 4.16 have insignificant neighbours. Specifically, run mode is executed if each of the following conditions holds:

- four consecutive samples must all be insignificant, that is, $\sigma_i(u + m, v) = 0$, for $0 \leq m \leq 3$;
- the samples must have insignificant neighbours, that is, $h_i(u + m, v) = v_i(u + m, v) = d_i(u + m, v) = 0$, for $0 \leq m \leq 3$;
- samples must reside within the same subblock;
- the horizontal index of the first sample, u, must be even.

In the run mode, a binary symbol is arithmetic coded with a single context to specify whether all the four samples in the vertical column remain insignificant. Symbol 0 implies all the four samples are insignificant, and symbol 1 implies at least one of four samples becomes significant in the current bit plane. If the symbol is 1, then two additional arithmetic coded bits are used to specify the location of the first nonzero coefficient in the vertical column.

Since it is equally likely that any of the four samples in the column to be the first nonzero sample, the arithmetic coding uses a uniform context. Thus, run mode has a negligible role in the coding efficiency. It is primarily used to improve the throughput of the arithmetic encoder through symbol aggregation.

After specifying the position of the first nonzero symbol in the run, the remaining samples in the vertical column are coded in the same manner as in the significance propagation pass and use the same nine contexts. Similarly, if at least one of four coefficients in the vertical column has a significant neighbour, the run mode is disabled and all the coefficients in that column are again coded with procedure used for the significance propagation pass.

For each code block, the number of MSB planes that are entirely zero is signalled in the bitstream. Since the significance state of all the coefficients in the first nonzero MSB is zero, this plane only uses the clean-up pass, and the other two passes are not used.

Example

To show how the wavelet coefficients in a fractional bit plane are coded, Figure 4.19 illustrates a graphical demonstration of step-by-step encoding from bit plane to bit plane and pass to pass.

The Barbara image of size 256 $\times$ 256 pixels with two levels of wavelet decomposition generates seven subimages, as shown in Figure 4.19. Except for the lowest band, the magnitudes of all the other bands are magnified by a factor of 4, for better illustration of image details. The code block size is assumed to be a square array of 64 $\times$ 64 coefficients. Hence, every high-frequency band of LH1, HL1 and HH1 is coded in four code blocks, and the remaining bands of LL2, LH2, HL2 and HH2 in one code block each, that is, the whole image is coded in 16 code blocks. The bitstreams generated by each pass in every bit plane are also shown in square boxes with different textures.

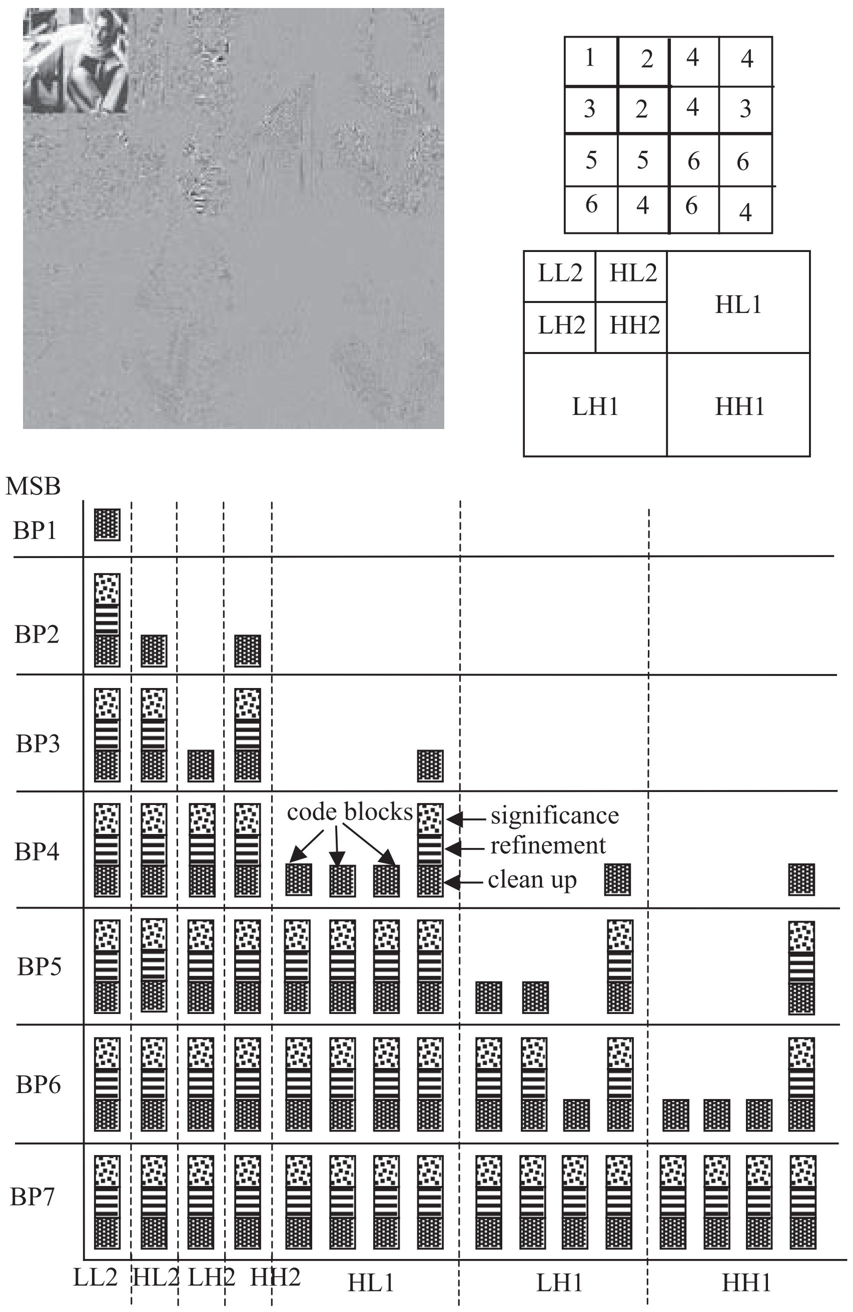

Figure 4.19 An illustration of fractional bit plane encoding

Before the coding starts, the significance states of all the code blocks are initialised to zero. For each code block, the encoding starts from the MSB plane. Since the LL2 band has a higher energy (larger wavelet coefficients) than the other bands, in this example only some of the MSB of the code block of this band are significant at the first scanned bit plane, PB1. In this bit plane, the MSBs of none of the other code blocks are significant (they are entirely zero) and are not coded at all.

Since the code block of LL2 band in BP1 is coded for the first time (the significant states of all the coefficients are initialised to zero), the MSB bit of every coefficient has a nonsignificant neighbour and hence cannot be coded at the significance propagation pass. Also, none of the bits is coded at the refinement pass, because these coefficients had not been coded in the previous bit plane. Therefore, all the bits are left to be coded in the clean-up pass, and they constitute the bitstream of this pass.

At the second bit plane, BP2, some of the coefficients in the HL2 and HH2 code blocks become significant for the first time. Hence, as was explained earlier, they are coded only at the clean-up pass, as shown in the figure. For the code block of LL2, since the coefficients with significant magnitudes of this code block have already been coded at the clean-up pass of BP1, the code block uses all the three passes. Those coefficients of the bit plane BP2 with insignificant states that have at least one state significant immediate neighbour are coded with the significance propagation pass. The state significant coefficients are now refined in the refinement pass. The remaining coefficients are coded at the clean-up pass. Other code blocks in this bit plane are not coded at all.

At the third bit plane, BP3, some of the coefficients of the code block of subband LH2 and those of the one of the code blocks of subband HL1 become significant for the first time; hence, they are coded only in the clean-up pass. The code blocks of LL2, HL2 and HH2 are now coded at the three passes. The remaining code blocks are not coded at all. The bit plane numbers of those code blocks that are coded for the first time are also shown in the figure with numbers from 1 to 6. As we see after bit plane 7, all the code blocks of the bands are coded, in all the three passes.

4.7.4 Layer formation and bitstream organisation (tier 2 coding)

The arithmetic coding of the bit plane data is referred as tier 1 coding. The tier 1 coding generates a collection of bitstreams with one independent embedded bitstream for each code block. The purpose of tier 2 coding is to multiplex the bitstreams for transmission and to signal the ordering of the resulting coded bit plane pass in an efficient manner. The second tier coding process can be best viewed as a somewhat elaborated parser for recovering pointers to code block segments in the bitstream. It is this coding step that enables the bitstream to have SNR, spatial and arbitrary progression and scalability.

The compressed bitstream from each code block is distributed across one or more layers in the final compressed bitstream. Each layer represents a quality increment. The number of passes included in a specific layer may vary from one code block to another and is typically determined by the encoder as a result of PCRD optimisation. The quality layers provide the feature of SNR scalability of the final bitstream such that truncating the bitstream to any whole number of layers yields approximately an optimal rate distortion representation of the image. However, employing a large number of quality layers can minimise the approximation. On the other hand, more quality layer implies a large overhead as auxiliary information to identify the contribution made by each code block to each layer. When the number of layers is large, only a subset of the code blocks will contribute to any given layer, introducing substantial redundancy in this auxiliary information. This redundancy is exploited in tier 2 coding to efficiently code the auxiliary information for each quality layer.

4.7.5 Rate control

Rate control refers to the process of generating an optimal image for a bit rate and is strictly an encoder issue. In section 4.7.3, we introduced the fractional bit plane coding as one of these methods. In [17], Taubman proposes an efficient rate control method for the EBCOT compression algorithm that achieves a desired rate in a single iteration with minimum distortion. This method is known as PCRD optimisation. A JPEG2000 encoder, with several possible variations, can also use this method.

In another form of PCRD, each subband is first quantised using a very fine step size, and the bit planes of the resulting code blocks are entropy coded (tier 1 coding). This typically generates more coding passes for each code block than will be eventually included in the final bitstream. Next, a Lagrangian *R-D* optimisation is performed to determine the number of coding passes from each code block that should be included in the final compressed bitstream to achieve the desired bit rate. If more than single quality layer is desired, this process can be repeated at the end of each layer to determine the additional number of coding passes from each code block that need to be included in the next layer. The details of PCRD optimisation can be found in [18].

At the end of this chapter, it is worth comparing the compression efficiency of the three methods of wavelet coding, namely, EZW, SPIHT and EBCOT. Figure 4.20 shows the quality of Lena image coded with these methods at various bit rates. As the figure shows, EZW has the poorest performance of all. The SPIHT, even without arithmetic coding, outperforms EZW by about 0.3–0.4 dB. Adding arithmetic coding into SPIHT improves the coding efficiency by another 0.3 dB. The EBCOT algorithm, adopted in the JPEG2000 standard, is as good as the best of SPIHT.

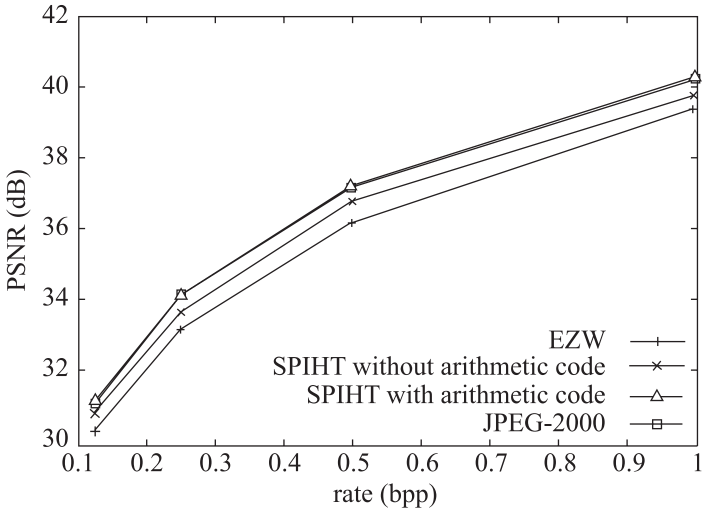

Figure 4.20 Compression performance of various wavelet coding algorithms

4.8 Problems

1. Derive the analysis and synthesis subband filters of the product filter $P(z)$ defined by its z-transform as

$$P(z) = \frac{1}{16}(-1 + 9z^{-2} + 16z^{-3} + 9z^{-4} - z^{-6})$$

2. The z-transform of a pair of low-pass and high-pass analysis filters is given by

$$H_0(z) = \frac{1}{\sqrt{2}}(1 + z^{-1}) \quad \text{and} \quad H_1(z) = \frac{1}{\sqrt{2}}(1 - z^{-1})$$

   a. Calculate the product filter and deduce the amount of end-to-end encoding/decoding delay.
   b. Derive the corresponding pairs of the synthesis filters.

3. The product filter for wavelets with n zeros at $z = 1$ is given by

$$P(z) = (1 + z^{-1})^{2n} Q(z)$$

   Use eqn. 4.7 to calculate the weighting factor of the product filter $P(z)$ and the corresponding end-to-end coding delay, for

   a. $n = 2$ and $Q(z) = -1 + 4z^{-1} - z^{-2}$
   b. $n = 3$ and $Q(z) = 1 - 6z^{-1} + \frac{38}{3}z^{-2} - 6z^{-3} + z^{-4}$

4. Show that the low- and high-pass analysis filters of (a) in problem 3 are, in fact, the (5,3) and (4,4) subband filters of LeGall and Tabatabai.
5. Show that the filters for (b) in problem 3 are the (9,3) Daubechies filter pairs.
6. Derive the corresponding pairs of the synthesis filters of problems 4 and 5.
7. List major similarities and differences between EZW and SPIHT.
8. Consider a three-level wavelet transform coefficients of 8×8 image shown in Figure 4.21. Assume it has been generated by a three-level wavelet transform:
   a. Show different steps in the first dominant pass (MSB plane) of EZW algorithm.
   b. Assuming that EZW uses 2 bits to code symbols in the alphabet {POS, NEG, ZT, Z} and 1 bit to code the sign bit, calculate total number of bits outputted in this pass.

63	–34	49	10	7	13	–12	7
–31	23	14	–13	3	4	6	–1
15	14	3	–12	5	–7	3	9
–9	–7	–14	8	4	–2	3	2
–5	9	–1	47	4	6	–2	2
3	0	–3	2	3	–2	0	4
2	–3	6	–4	3	6	3	6
5	11	5	6	0	3	–4	4

Figure 4.21 A block of three-level 8×8 transform coefficients

9. a. In Figure 4.21, calculate the number of bits outputted in the first significant pass of the SPIHT algorithm.
   b. Comment on the results of 8(b) and 9(a).

References

1. MPEG 4: ‘Video shape coding’, ISO/IEC JTC1/SC29/WG11, N1584, March 1997
2. SKODRAS, A., CHRISTOPOULOS, C. and EBRAHIMI, T.: ‘The JPEG 2000 still image compression standard’, *IEEE Signal Process. Mag.,* September 2001, pp. 36–58

3. MALAVER, H.S., and STAELIN, D.H.: ‘The LOT: transform coding without blocking effects’, *IEEE Trans. Acoust. Speech Signal Process.*, 1989, **37:4**, pp. 553–559
4. SHAPIRO, J.M.: ‘Embedded image coding using zero trees of wavelet coefficients’, *IEEE Trans. Signal Process.*, 1993, **4:12**, pp. 3445–3462
5. USEVITCH, B.E.: ‘A tutorial on modern lossy wavelet image compression: foundation of JPEG 2000’, *IEEE Signal Process.* **18:5**, *Mag.*, 2001, pp. 22–35
6. CROCHIERE, R.E., WEBER, S.A. and FLANAGAN, J.L.: ‘Digital coding of speech in sub bands’, *Bell Syst. Tech. J.*, 1967, **55**, pp. 1069–1085
7. DAUBECHIES, I.: ‘Orthonormal bases of compactly supported wavelets’, *Commun. Pure Appl. Math.*, 1988, **41**, pp. 909–996
8. LE GALL, D. and TABATABAI, A.: ‘Subband coding of images using symmetric short kernel filters and arithmetic coding techniques’, IEEE International Conference on Acoustics, Speech and Signal Processing, ICASSP’98, 1988, pp. 761–764
9. DAUBECHIES, I.: ‘The wavelet transform, time frequency localization and signal analysis’, *IEEE Trans. Inf. Theory*, 1990, **36:5**, pp. 961–1005
10. MALLAT, S.: ‘A theory of multiresolution signal decomposition: the wavelet representation’, *IEEE Trans. Pattern Anal. Mach. Intell.*, 1989, **11:7**, pp. 674–693
11. DAUBECHIES, I.: ‘Orthogonal bases of compactly supported wavelets II, variations on a theme’, *SIAM J. Math. Anal.*, 1993, **24:2**, pp. 499–519
12. DA SILVA, E.A.B.: ‘Wavelet transforms in image coding’, PhD thesis, 1995, University of Essex, UK
13. RABBANI, M. and JOSH, R.: ‘An overview of the JPEG2000 still image compression standard’, *Signal Process. Image Commun.*, 2002, **17:1**, pp. 15–46
14. MPEG 4: ‘Video verification model version 11’, ISO/IEC JTC1/SC29/WG11, N2171, Tokyo, March 1998
15. WITTEN, I.H., NEAL, R.M. and CLEARY, J.G.: ‘Arithmetic coding for data compression’, *Commun. ACM*, 1987, **30:6**, pp. 520–540
16. SAID, A. and PEARLMAN, W.A.: ‘A new, fast and efficient image codec based on set partitioning in hierarchical trees’, *IEEE Trans. Circuits Syst. Video Technol.*, 1996, **6:3**, pp. 243–250
17. TAUBMAN, D.: ‘High performance scalable image compression with EBCOT’, *IEEE Trans. Image Process.*, 2000, **9:7**, pp. 1158–1170
18. TAUBMAN, D., ORDENLICH, E., WEINBERGER, M. and SEROUSSI, G.: ‘Embedded block coding in JPEG2000’, *Signal Process. Image Commun.*, 2002, **17:1**, pp. 1–24

Chapter 5
Coding of still pictures (JPEG and JPEG2000)

In the mid-1980s, joint work by the members of the International Telecommunication Union (Telegraphy section) (ITU-T) and the International Standards Organisation (ISO) led to a standardisation for compression of greyscale and colour still images [1]. This effort was then known as the Joint Photographic Experts Group (JPEG). As it is apparent, the word joint refers to the collaboration between the ITU-T and ISO. The JPEG encoder is capable of coding full colour images at an average compression ratio of 15:1 for subjectively transparent quality [2]. Its design meets special constraints, which make the standard very flexible. For example, the JPEG encoder is parametrisable so that the desired compression/quality trade-offs can be determined based on the application or the wishes of the user [3].

JPEG can also be used in coding of video, on the basis that video is a succession of still images. In this case, the process is called motion JPEG. Currently, motion JPEG has found numerous applications. The most notable one is video coding for transmission over packet networks with unspecified bandwidth or bit rates (UBR). A good example of UBR networks is the Internet where, because of unpredictability of the network load, congestion may last for a significant amount of time. Since in motion JPEG, each frame is independently coded, it is an ideal encoder of video for such a hostile environment.

Another application of motion JPEG is video compression for recording on magnetic tapes, where again the independent coding of pictures increases the flexibility of the encoder for recording requirements, such as editing, pause, fast forward and fast rewind. Also, such an encoder can be very resilient to loss of information, since the channel error will not propagate through the image sequence. However, since the coding of I-pictures in the MPEG-2 standard is similar to motion JPEG, normally video compression for recording purposes is carried out with the I-picture part of the MPEG-2 encoder. The I-pictures are encoded without reference to previous or subsequent pictures. This is explained in Chapter 7.

At the turn of the millennium, the JPEG committee decided to develop another standard for compression of still images, named the JPEG2000 standard [4]. This was in response to growing demands for multimedia, Internet and a variety of digital imagery applications. However, in terms of compression methodology, these two standards are very different. Hence, in order to discriminate between them, throughout the book, the original JPEG is called JPEG and the new one JPEG2000.

5.1 Lossless compression

The JPEG standard specifies two classes of encoding and decoding, namely lossless and lossy compression. Lossless compression is based on a simple predictive DPCM method using neighbouring pixel values, while discrete cosine transform (DCT) is employed for the lossy mode.

Figure 5.1 shows the main elements of a lossless JPEG image encoder.

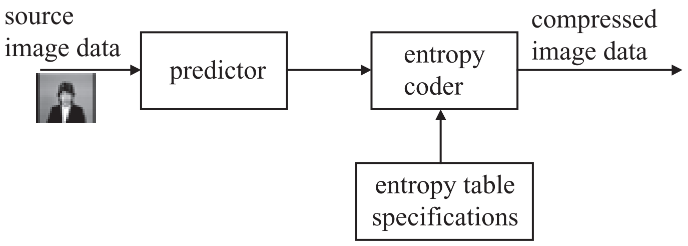

Figure 5.1 Lossless encoder

The digitised source image data in the forms of either RGB or YC_bC_r are fed to the predictor. The image can take any format from 4:4:4 down to 4:1:0, with any size and amplitude precision (e.g. 8 bit/pixel). The predictor is of the simple DPCM type (see Figure 3.1), where every individual pixel of each colour component is differentially encoded. The prediction for an input pixel x is made from combinations of up to three neighbouring pixels at positions a, b and c from the same picture of the same colour component, as shown in Figure 5.2.

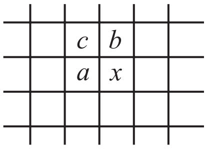

Figure 5.2 Three-sample prediction neighbourhood

The prediction is then subtracted from the actual value of the pixel at position x, and the difference is losslessly entropy coded by either Huffman or arithmetic coding. The entropy table specifications unit determines the characteristics of the variable length codes (VLCs) of either entropy coding methods.

The encoding process might be slightly modified by reducing the precision of input image samples by one or more bits prior to lossless coding. For lossless processes, sample precision is specified to be between 2 and 16 bits. This achieves higher compression than normal lossless coding but has lower compression than DCT-based lossy coding for the same bit rate and image quality. Note that this is in fact a type of lossy compression, since reduction in the precision of input pixels by b bits is equivalent to the quantisation of the difference samples by a quantiser step size of 2^b.

5.2 Lossy compression

In addition to the lossless compression, the JPEG standard defines three lossy compression modes. These are called baseline sequential mode, progressive mode and hierarchical mode. These modes are all based on the DCT to achieve a substantial compression while producing a reconstructed image with high visual fidelity. The main difference between these modes is the way in which the DCT coefficients are transmitted.

The simplest DCT-based coding is referred to as the baseline sequential process, and it provides capability that is sufficient for many applications. The other DCT-based processes that extend the baseline sequential process to a broader range of applications are referred to as extended DCT-based processes. In any extended DCT-based decoding processes, the baseline decoding is required to be present in order to provide a default decoding capability.

5.2.1 Baseline sequential mode compression

Baseline sequential mode compression is usually called baseline coding for short. In this mode, an image is partitioned into 8×8 nonoverlapping pixel blocks from left to right and top to bottom. Each block is DCT coded, and all the 64 transform coefficients are quantised to the desired quality. The quantised coefficients are immediately entropy coded and output as part of the compressed image data, thereby minimising coefficient storage requirements.

Figure 5.3 illustrates the JPEG's baseline compression algorithm. Each 8-bit sample is level shifted by subtracting $2^{8-1=7} = 128$ before being DCT coded. This is known as DC-level shifting. The 64 DCT coefficients are then uniformly quantised according to the step size given in the application-specific quantisation matrix. The use of a quantisation matrix allows different weighting to be applied according to the sensitivity of the human visual system (HVS) to a coefficient of the frequency.

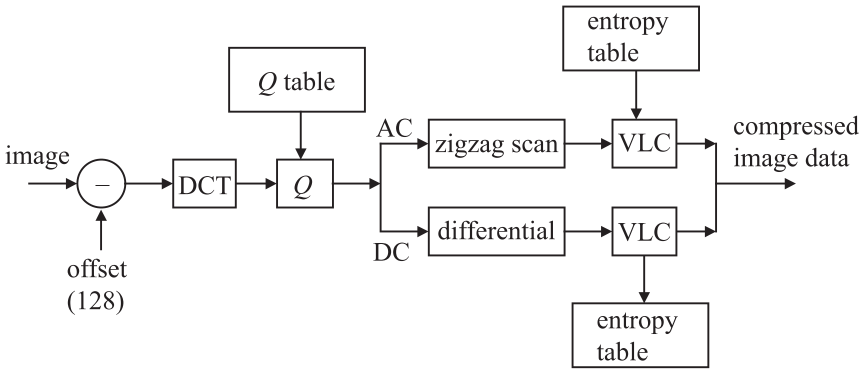

Figure 5.3 Block diagram of a baseline JPEG encoder

Two examples of quantisation tables are given in Tables 5.1 and 5.2 [5]. These tables are based on psychovisual thresholding and are derived empirically using luminance and chrominance with a 2:1 horizontal subsampling. These tables may not be suitable for any particular application, but they give good results for most images with an 8-bit precision.

Table 5.1 Luminance Q table

16	11	10	16	24	40	51	61
12	12	14	19	26	58	60	55
14	13	16	24	40	57	69	56
14	17	22	29	51	87	80	62
18	22	37	56	68	109	103	77
24	35	55	64	81	104	113	92
49	64	78	87	103	121	120	101
72	92	95	98	112	100	103	99

Table 5.2 Chrominance Q table

17	18	24	47	99	99	99	99
18	21	26	66	99	99	99	99
24	26	56	99	99	99	99	99
47	66	99	99	99	99	99	99
99	99	99	99	99	99	99	99
99	99	99	99	99	99	99	99
99	99	99	99	99	99	99	99
99	99	99	99	99	99	99	99

If the elements of the quantisation tables of luminance and chrominance are represented by $Q(u,v)$, then a quantised DCT coefficient with the horizontal and the vertical spatial frequencies of u and v, $F^q(u,v)$, is given by

$$F^q(u,v) = \left\lfloor \frac{F(u,v)}{Q(u,v)} \right\rfloor \tag{5.1}$$

where $F(u,v)$ is the transform coefficient value prior to quantisation and $\lfloor . \rfloor$ means rounding the division to the nearest integer. At the decoder, the quantised coefficients are inverse quantised by

$$F^Q(u,v) = F^q(u,v) \times Q(u,v) \tag{5.2}$$

to reconstruct the quantised coefficients.

A quality factor *q_JPEG* is normally used to control the elements of the quantisation matrix *Q*(*u*,*v*) [3]. The range of *q_JPEG* percentage value is between 1 and 100 per cent. The JPEG quantisation matrices of Tables 5.1 and 5.2 are used for *q_JPEG* = 50, for the luminance and chrominance, respectively. For other quality factors, the elements of the quantisation matrix, *Q*(*u*,*v*), are multiplied by the compression factor α, defined as [3]

$$\begin{aligned} \alpha &= \frac{50}{q\_JPEG} && \text{if} \quad 1 \le q\_JPEG \le 50 \\ \alpha &= 2 - \frac{2 \times q\_JPEG}{100} && \text{if} \quad 50 \le q\_JPEG \le 99 \end{aligned} \tag{5.3}$$

subject to the condition that the minimum value of the modified quantisation matrix elements, $\alpha\ Q(u,v)$, is 1. For a 100 per cent quality, *q_JPEG* = 100, that is, lossless compression; all the elements of $\alpha\ Q(u,v)$ are set to 1.

After quantisation, the DC (commonly referred to as (0,0)) coefficient and the 63 AC coefficients are coded separately as shown in Figure 5.3. The DC coefficients are DPCM coded with prediction of the DC coefficient from the previous block, as shown in Figure 5.4, that is, difference between DC coefficients (DIFF) = $DC_i - DC_{i-1}$. This separate treatment from the AC coefficients is to exploit the correlation between the DC values of adjacent blocks and to code them more efficiently as they typically contain the largest portion of the image energy. The 63 AC coefficients starting from coefficient AC(1,0) are run length coded following a zigzag scan, as shown in Figure 5.4.

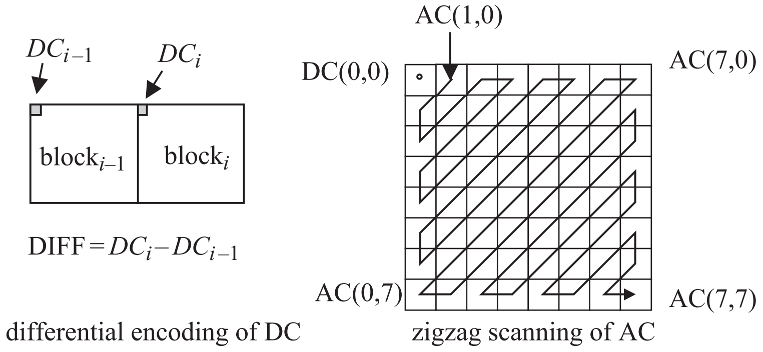

Figure 5.4 Preparing the DCT coefficients for entropy coding

The adoption of a zigzag scanning pattern is to facilitate entropy coding by encountering the most likely nonzero coefficients first. This is due to the fact that for most natural scenes, the image energy is mainly concentrated in a few low-frequency transform coefficients.

5.2.2 Run length coding

Entropy coding of the baseline encoder is accomplished in two stages. The first stage is the translation of the quantised DCT coefficients into an intermediate set of symbols. In the second stage, VLCs are assigned to each symbol. For the JPEG standard, a symbol is structured in two parts: a VLC for the first part, normally referred to as symbol-1, followed by a binary representation of the amplitude for the second part, symbol-2.

5.2.2.1 Coding of DC coefficients

Instead of assigning individual VLC words (e.g. Huffman code) to each DIFF, the DIFF values are categorised based on the magnitude range called CAT. The CAT is then variable length coded. Table 5.3 shows the categories for the range of amplitudes in the baseline JPEG. Since the DCT coefficient values are in the range –2047 to 2047, there are 11 categories for nonzero coefficients. Category zero is not used for symbols but for defining the end of block (EOB) code.

Table 5.3 The category (CAT) of the baseline encoder

CAT	Range
0	–
1	–1; 1
2	–3,–2; 2,3
3	–7,...,–4; 4,...,7
4	–15,...,–8; 8,...,15
5	–31,...,–16; 16,...,31
6	–63,...,–32; 32,...,63
7	–127,...,–64; 64,...,127
8	–255,...,–128; 128,...,255
9	–511,...,–256; 256,...,511
10	–1023,...,–512; 512,...,1023
11	–2047,...,–1024; 1024,...,2047

The CAT after being variable length coded is appended with additional bits to specify the actual DIFF values (amplitude) within the category. Here, CAT is symbol-1 and the appended bits represent symbol-2.

When the DIFF is positive, the appended bits are just the lower-order bits of the DIFF. When it is negative, the appended bits become the lower-order bits of DIFF-1. The lower-order bits start from the point where the most significant bit (MSB) of the appended bit sequence is 1 for positive differences and 0 for negative differences. For example, for DIFF $= 6 = 0000\ldots00\underline{110}$, the appended bits start from 1; hence, it would be 110. This is because DIFF is positive and the MSB of the appended bits should be 1. Also, since 6 is in the range of 4–7 (Table 5.3), the value of CAT is 3. From Table B.1 the code word for CAT $= 3$ is 100. Thus, the overall code word for DIFF $= 6$ is **100110**, where 100 is the VLC of CAT (symbol-1) and 110 is the appended code word (symbol-2).

For a negative DIFF, such as DIFF = –3, first of all, –3 is in the range of –3 to −2; thus, from Table 5.3, CAT = 2, and its VLC from Table B.1 is 011. However, to find the appended bits, DIFF – 1 = –4 = 1111 . . . 1$\underline{00}$, where the lower-order bits are 00. Note that the MSB of the appended bits is 0. Thus, the code word becomes **01100**.

5.2.2.2 Coding of AC coefficients

For each nonzero AC coefficient in zigzag scan order, symbol-1 is described as a two-dimensional *event* of (RUN, CAT), sometimes called (RUN, SIZE). For the baseline encoder, CAT is the category for the amplitude of a nonzero coefficient in the zigzag order and RUN is the number of zeros preceding this nonzero coefficient. The maximum length of run is limited to 15. Encoding of runs greater than 15 is done by a special symbol (15, 0), which is a run length of 15 zero coefficients followed by a coefficient of zero amplitude. Hence, it can be interpreted as the extension symbol with 16 zero coefficients. There can be up to three consecutive (15, 0) symbols before the terminating symbol-1 followed by a single symbol-2. For example, a (RUN = 34, CAT = 5) pair would result in three symbols *a*, *b* and *c*, with *a* = (15, 0), *b* = (15, 0) and *c* = (2, 5).

An EOB is designated to indicate that the rest of the coefficients of the block in the zigzag scanning order are quantised to zero. The EOB symbol is represented by (RUN = 0, CAT = 0).

The AC code table for symbol-1 consists of one Huffman code word (maximum length 16 bits, not including additional bits) for each possible composite event. Table B.2 shows the code words for all possible combinations of RUN and CAT of symbol-1 [4]. The format of the additional bits (symbol-2) is the same as in the coding of DIFF in DC coefficients. For the *k*th AC coefficient in the zigzag scan order, *ZZ*(*k*), the additional bits are either the lower-order bits of *ZZ*(*k*) when *ZZ*(*k*) is positive or the lower-order bits of *ZZ*(*k*) − 1 when *ZZ*(*k*) is negative. To clarify this, let us look at a simple example.

Example: the quantised DCT coefficients of a luminance block are shown in Figure 5.5. If the DC coefficient in the previous luminance block was 29, find the code words for coding of the DC and AC coefficients.

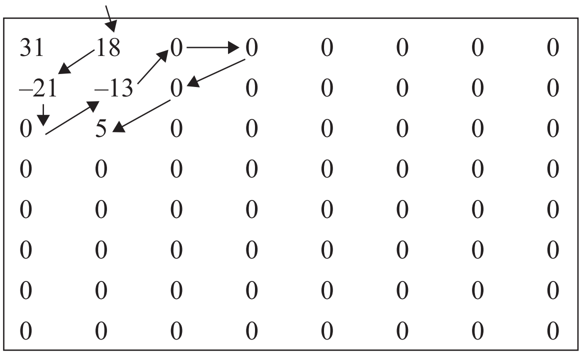

31	18	0	0	0	0	0	0
–21	–13	0	0	0	0	0	0
0	5	0	0	0	0	0	0
0	0	0	0	0	0	0	0
0	0	0	0	0	0	0	0
0	0	0	0	0	0	0	0
0	0	0	0	0	0	0	0
0	0	0	0	0	0	0	0

Figure 5.5 Quantised DCT coefficients of a luminance block

Code word for the DC coefficient: DIFF = 31 – 29 = 2. From Table 5.3, CAT = 2, and according to Table B.1, the Huffman code for this value of CAT is 011. To find the appended bits, since DIFF $= 2 > 0$, $2 = 000\ldots00\underline{10}$. Thus, the appended bits are 10. Hence, the overall code word for coding the DC coefficient is 01110.

Code words for the AC coefficients: Scanning starts from the first nonzero AC coefficient that has a value of 18. From Table 5.3, the CAT value for 18 is 5, and since there is no zero-value AC coefficient before it, RUN = 0. Hence, symbol-1 is (0, 5). From Table B.2, the code word for (0, 5) is 11010. The symbol-2 is the lower-order bits of $ZZ(k) = 18 = 000\ldots0\underline{10010}$, which is 10010. Thus, the first AC code word is 1101010010.

The next nonzero AC coefficient in the zigzag scan order is –21. Since it has no zero coefficient before it and it is in the range of –31 to –16, it has RUN = 0 and CAT = 5. Thus, symbol-1 of this coefficient is (0, 5), which again, from Table B.2 of Appendix B, has a code word of 11010. For symbol-2, since $-21 < 0$, $ZZ(k) - 1 = -21 - 1 = -22 = 111\ldots11\underline{01010}$, and symbol-2 becomes 01010 (note that the appended bits start from where the MSB is 0). Thus, the overall code word for the second nonzero AC coefficient is 1101001010.

The third nonzero AC coefficient in the scan is –13, which has one zero coefficient before it. Then RUN = 1, and from its range, CAT is 4. From Table B.2 of Appendix B, the code word for (RUN = 1, CAT = 4) is 111110110. To find symbol-2, $ZZ(k) - 1 = -13 - 1 = -14 = 111\ldots11\underline{0010}$. Thus, symbol-2 = 0010, and the whole code word becomes 1111101100010.

The fourth and the final nonzero AC coefficient is 5 (CAT = 3), which is preceded by three zeros (RUN = 3). Thus, symbol-1 is (3, 3), which, from Table B.2, has a code word of 111111110101. For symbol-2, since $ZZ(k) = 5 = 000\ldots00\underline{101}$, the lower-order bits are 101, and the whole code word becomes 111111110101101.

Since five is the last nonzero AC coefficient, the encoding terminates here, and the EOB code is transmitted, which is defined as (0,0) symbol with no appended bits. From Table B.2, its code word is 1010.

5.2.2.3 Entropy coding

For coding of the magnitude categories or run length events, the JPEG standard specifies two alternative entropy coding methods, namely Huffman coding and arithmetic coding. Huffman coding procedures use Huffman tables, and the type of table is determined by the entropy table specifications, shown in Figure 5.3. Arithmetic coding methods use arithmetic coding conditioning tables, which may also be determined by the entropy table specification. There can be up to four different Huffman and arithmetic coding tables for each DC and AC coefficient. No default values for Huffman tables are specified, so the applications may choose tables appropriate for their own environment. Default tables are defined for the arithmetic coding conditioning. Baseline sequential coding uses Huffman coding, while the extended DCT-based and lossless processes may use either Huffman or arithmetic coding (see Table 5.4).

Table 5.4 Summary: essential characteristics of coding process

Baseline process (required for all DCT-based decoders)

- DCT-based process
- source image: 8-bit samples within each component
- sequential
- Huffman coding: 2 AC and 2 DC tables
- decoders shall process scans with 1, 2, 3 and 4 components
- interleaved and noninterleaved scans

Extended DCT-based processes

- DCT-based process
- source image: 8- or 12-bit samples
- sequential or progressive
- Huffman or arithmetic coding: 4 AC and 4 DC tables
- decoder shall process scans with 1, 2, 3 and 4 components
- interleaved and noninterleaved scans

Lossless process

- predictive process (not DCT based)
- source image; N-bit samples ($2 \leq N \leq 16$)
- sequential
- Huffman or arithmetic coding: 4 tables
- decoders shall process scans with 1, 2, 3 and 4 components
- interleaved and noninterleaved scans

Hierarchical processes

- multiple layers (nondifferential and differential)
- uses extended DCT-based or lossless processes
- decoders shall process scans with 1, 2, 3 and 4 components
- interleaved and noninterleaved scans

In arithmetic coding of AC coefficients, the length of zero run is no longer limited to 15; it can go up to the end of the block (e.g. 62). Also, arithmetic coding may be made adaptive to increase the coding efficiency. Adaptive means that the probability estimates for each context are developed based on a prior coding decision for that context. The adaptive binary arithmetic coder may use a statistical model to improve encoding efficiency. The statistical model defines the contexts that are used to select the conditional probability estimates used in the encoding and decoding procedures.

5.2.3 Extended DCT-based process

The baseline encoder only supports basic coding tools, which are sufficient for most image compression applications. These include input image with 8-bit/pixel precision, Huffman coding of the run length and sequential transmission. If other modes or any input image precision are required, and in particular, if arithmetic coding is employed to achieve higher compression, then the term extended DCT-based process is applied to the encoder. Table 5.4 summarises all the JPEG-supported coding modes.

Figure 5.6 illustrates the reconstruction of a decoded image in a sequential mode (baseline or extended). As mentioned, as soon as a block of pixels is coded, its 64 coefficients are quantised, coded and transmitted. The receiver, after decoding the coefficients, inverse quantisation and inverse transformation, sequentially adds them to the reconstructed image. Depending on the channel rate, it might take some time to reconstruct the whole image. In Figure 5.6, reconstructed images at 25, 50, 75 and 100 per cent of image are shown.

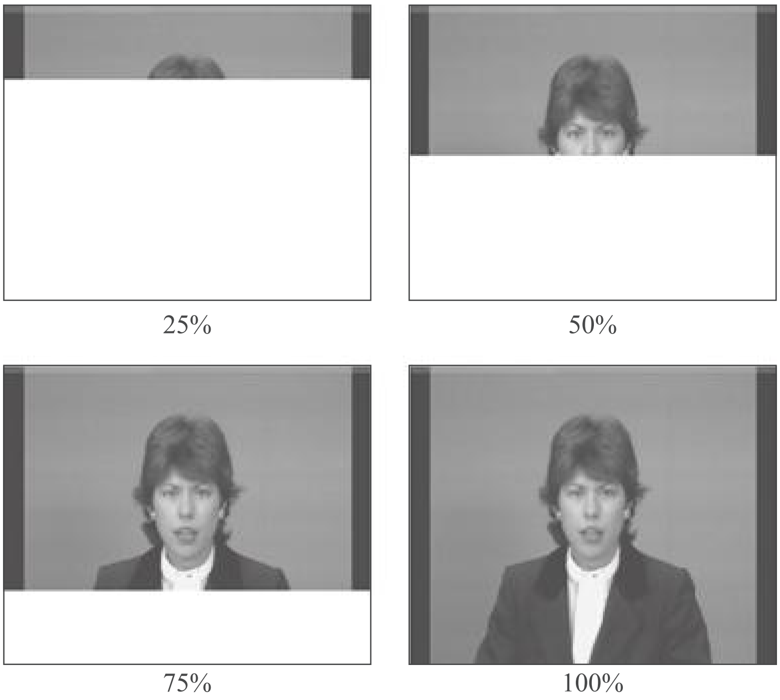

Figure 5.6 Reconstructed images in sequential mode

In the progressive mode, the quantised coefficients are stored in the local buffer and transmitted later. There are two procedures by which the quantised coefficients in the buffer may be partially encoded within a scan. First, for the highest image quality (lowest quantisation step size), only a specified band of coefficients from the zigzag scanned sequence needs to be coded. This procedure is called spectral selection, since each band typically contains coefficients that occupy a lower or higher part of the frequency spectrum for the 8 $\times$ 8 block. Second, the coefficients within the current band need not be encoded to their full accuracy within each scan (coarser quantisation). On a coefficient's first encoding, a specified number of the MSBs are encoded first. In subsequent scans, the less significant bits are then encoded. This procedure is called successive approximation or bit plane encoding. Either procedure may be used separately, or they may be mixed in flexible combinations.

Figure 5.7 shows the reconstructed image quality with the first method. In this figure, the first image is reconstructed from the DC coefficient only, with its full-quantised precision. The second image is made up of DC (coefficient 0) plus the AC coefficients 1 and 8, according to the zigzag scan order. That is, after receiving the two new AC coefficients, a new image is reconstructed from these coefficients and the previously received DC coefficients. The third image is made up of coefficients 0, 1, 8, 16, 9, 2, 3, 10, 17 and 24. In the last image, all the significant coefficients (up to EOB) are included.

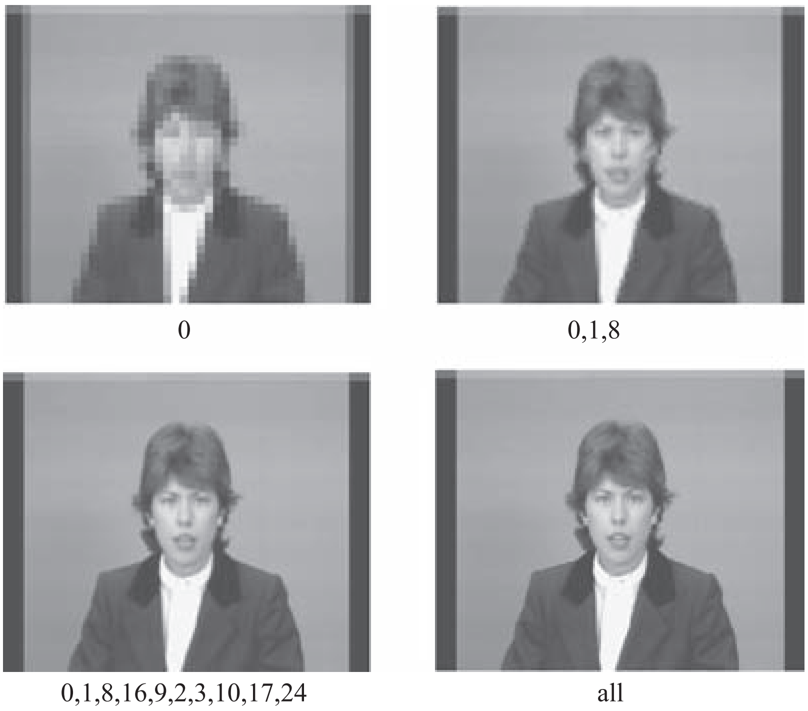

Figure 5.7 Reconstructed reconstruction in sequential mode

5.2.4 Hierarchical mode

In the hierarchical mode, an image is coded as a sequence of layers in a pyramid. Each lower-size image provides prediction for the next upper layer. Except for the top level of the pyramid, for each luminance and colour component at the lower levels, the difference between the source components and the reference reconstructed image is coded. The coding of the differences may be done using only DCT-based processes, only lossless processes or DCT-based processes with a final lossless process for each component.

Downsampling and upsampling filters, similar to those of Figures 2.4 and 2.6, may be used to provide a pyramid of spatial resolution, as shown in Figure 5.8. The hierarchical coder including the downsampling and upsampling filters is shown in Figure 5.9.

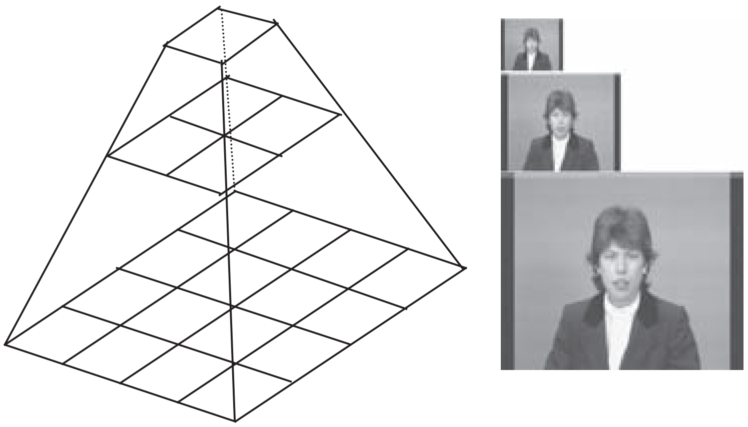

Figure 5.8 Hierarchical multiresolution encoding

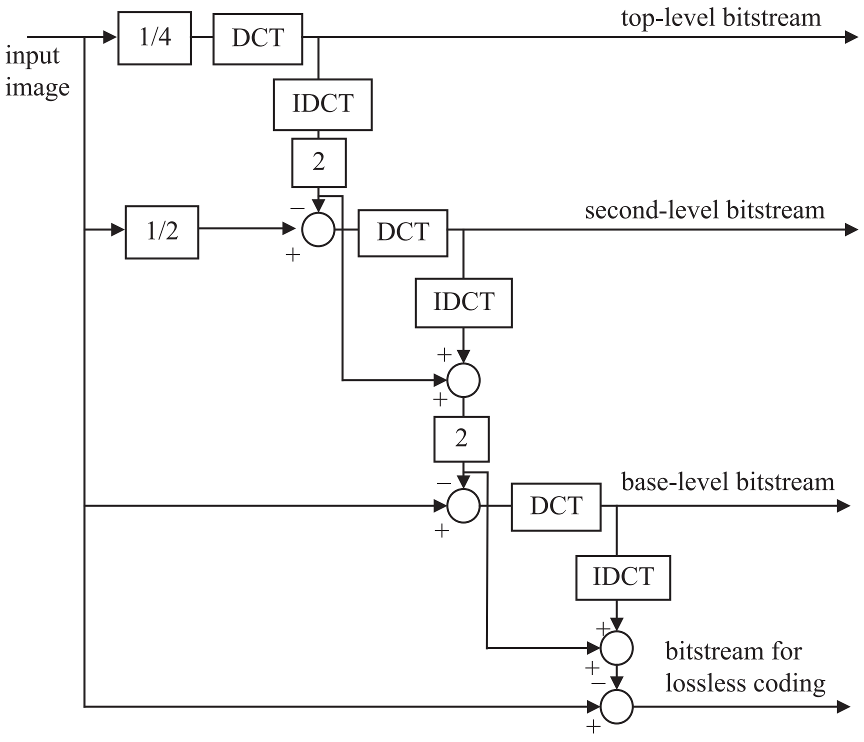

Figure 5.9 A three-level hierarchical encoder

In this figure, the image is low pass filtered and subsampled by 4:1 in both directions to give an image size reduced by 1/16. The baseline encoder then encodes the reduced image. The decoded image at the receiver may be interpolated by 1:4 to give the full size image for display. At the encoder, another baseline encoder encodes the difference between the subsampled input image by 2:1 and the 1:2 upsampled decoded image. By repeating this process, the image is progressively coded, and at the decoder it is progressively built up. The bit rate at each level depends on the quantisation step size at that level. Finally, for lossless reversibility of the coded image, the difference between the input image and the latest decoded image is lossless entropy coded (no quantisation).

As we see, the hierarchical mode offers a progressive representation similar to the progressive DCT-based mode, but it is useful in environments that have multiresolution requirements. The hierarchical mode also offers the capability of progressive transmission to a final lossless stage, as shown in Figure 5.9.

5.2.5 Extra features

In coding of colour pictures, encoding is called noninterleaved if all blocks of a colour component are coded before beginning to code the next component. Encoding is interleaved if the encoder compresses a block of 8 $\times$ 8 pixels from each component in turn, considering the image format. For example, with the 4:4:4 format, one block from each luminance and two chrominance components are coded. In the 4:2:0 format, the encoder codes four luminance blocks before coding one block from each of C_b and C_r.

The encoder is also flexible to allow different blocks within a single component to be compressed using different quantisation tables, resulting in a variation in the reconstructed image quality, based on their perceived relative importance. This method of coding is called region of interest (ROI) coding. Also, the standard can allow different regions within a single image block to be compressed at different rates.

5.3 JPEG2000

Before describing the basic principles of the JPEG2000 standard, it might be useful to understand why we need another standard. Perhaps the most convincing explanation is that since the introduction of JPEG in 1980s, too much has changed in the digital image industry. For example, current demands for compressed still images range from Web logos of sizes less than 10 kbytes to high-quality scanned images of the order of 5 Gbytes [6]. The existing JPEG surely is not optimised to efficiently code such a wide range of images. Moreover, scalability and interoperability requirements of digital imagery in a heterogeneous network of ATM, Internet, mobile, etc. make the matter much more complicated.

The JPEG2000 standard is devised with the aim of providing the best quality or performance and capabilities to market evolution that the current JPEG standard fails to cater for. In the meantime, it is assumed that Internet, colour facsimile, printing, scanning, digital photography, remote sensing, mobile, medical imagery, digital libraries/archives and e-commerce are among the most immediate demands. Each application area imposes a requirement that JPEG2000 should fulfil. Some of the most important features [7] that this standard aims to deliver are as follows:

Superior low bit rate performance: This standard should offer performance superior to the current standards at low bit rates (e.g. below 0.25 bit/pixel for highly detailed greyscale images). This significantly improved low bit rate performance should be achieved without sacrificing performance on the rest of the rate distortion spectrum. Examples of applications that need this feature include image transmission over networks and remote sensing. This is the highest-priority feature.

Continuous tone and bilevel compression: It is desired to have a standard coding system that is capable of compressing both continuous tone and bilevel images [8]. If feasible, the standard should strive to achieve this with similar system resources. The system should compress and decompress images with various dynamic ranges (e.g. 1–16 bits) for each colour component. Examples of applications that can use this feature include compound documents with images and text, medical images with annotation overlays, graphic and computer-generated images with binary and near-to-binary regions, alpha and transparency planes, and facsimile.

Lossless and lossy compression: It is desired to provide lossless compression naturally in the course of progressive decoding (i.e. difference image encoding, or any other technique, which allows for the lossless reconstruction to be valid). Examples of applications that can use this feature include medical images where loss is not always tolerable, image archival pictures where the highest quality is vital for preservation but not necessary for display, network systems that supply devices with different capabilities and resources, and prepress imagery.

Progressive transmission by pixel accuracy and resolution: Progressive transmission that allows images to be reconstructed with increasing pixel accuracy or spatial resolution is essential for many applications. This feature allows the reconstruction of images with different resolutions and pixel accuracy, as needed or desired, for different target devices. Examples of applications include the Web browsing, image archiving and printing.

ROI coding: Often there are parts of an image that are more important than others. This feature allows user-defined ROI in the image to be randomly accessed and/or decompressed with less distortion than the rest of the image.

Robustness to bit errors: It is desirable to consider robustness to bit errors while designing the code stream. One application where this is important is wireless communication channels. Portions of the code stream may be more important than others in determining decoded image quality. Proper design of the code stream can aid subsequent error correction systems in alleviating catastrophic decoding failures. Use of error confinement, error concealment, restart capabilities or source channel coding schemes can help minimise the effects of bit errors.

Open architecture: It is desirable to allow open architecture to optimise the system for different image types and applications. With this feature, the decoder is only required to implement the core tool set and a parser that understands the code stream. If necessary, unknown tools are requested by the decoder and sent from the source.

Protective image security: Protection of a digital image can be achieved by means of methods such as watermarking, labelling, stamping, fingerprinting, encryption and scrambling. Watermarking and fingerprinting are invisible marks set inside the image content to pass a protection message to the user. Labelling is already implemented in some imaging formats such as SPIFF and must be easy to transfer back and forth to the JPEG2000 image file. Stamping is a mark set on top of a displayed image that can only be removed by a specific process. Encryption and scrambling can be applied on the whole image file or limited to part of it (header, directory, image data) to avoid unauthorised use of the image.

5.4 JPEG2000 encoder

The JPEG2000 standard follows the generic structure of the intraframe still image coding introduced for the baseline JPEG, that is, decorrelating the pixels within a frame by means of transformation and then quantising and entropy coding of the quantised transform coefficients for further compression. However, in order to meet the design requirements set forth in section 5.3, in addition to the specific requirements from the transformation and coding, certain preprocessing on the pixels and postprocessing of the compressed data are necessary. Figure 5.10 shows a block diagram of a JPEG2000 encoder.

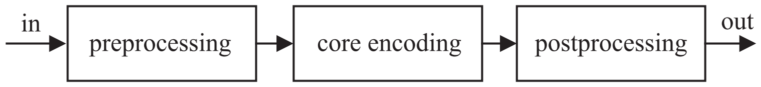

Figure 5.10 A general block diagram of the JPEG2000 encoder

In presenting this coder, we only talk about the fundamentals behind this standard. More details can be found in the ISO standardisation documents and several key papers [7,9,10].

5.4.1 Preprocessor

Image pixels prior to compression are preprocessed to make certain goals easier to achieve. There are three elements in this preprocessor.

5.4.1.1 Tiling

Partitioning the image into rectangular nonoverlapping pixel blocks, known as tiling, is the first stage in preprocessing. The tile size is arbitrary and can be as large as the whole image size down to a single pixel. A tile is the basic unit of coding, where all the encoding operations, from transformation down to bitstream formation, are applied to tiles independent of each other. Tiling is particularly important to reduce memory requirement, and since they are coded independently, any part of the image can be accessed and processed differently from the other parts of the image. However, because of tiling, the correlation between the pixels in adjacent tiles is not exploited, and hence, as the tile size is reduced, the compression gain of the encoder is also reduced.

5.4.1.2 DC-level shifting

Similar to DC-level shifting in the JPEG standard (Figure 5.3), values of the RGB colour components within the tiles are DC shifted by 2^{B-1}, for B bits per colour component. Such an offset makes certain processing, such as numerical overflow, arithmetic coding and context specification, simpler. In particular, this allows the lowest subband, which is a DC signal, to be encoded along with the rest of the AC wavelet coefficients. At the decoder, the offset is added back to the colour component values.

5.4.1.3 Colour transformation

There are significant correlations between the RGB colour components. Hence, prior to compression by the core encoder, they are decorrelated by some form of transformation. In JPEG2000, two types of colour decorrelation transforms are recommended.

In the first type, the decorrelated colour components YC_bC_r, are derived from the three colour primaries RGB according to

$$\begin{bmatrix} Y \\ C_b \\ C_r \end{bmatrix} = \begin{bmatrix} 0.299 & 0.587 & 0.114 \\ -0.16875 & -0.33126 & 0.500 \\ 0.500 & -0.41869 & -0.08131 \end{bmatrix} \begin{bmatrix} \mathrm{R} \\ \mathrm{G} \\ \mathrm{B} \end{bmatrix} \tag{5.4}$$

Note that this transformation is slightly different from the one used for coding colour video (see section 2.2). Also note that since transformation matrix elements are approximated (not exact), the decoded RGB colour components cannot be free from loss even if YC_bC_r are losslessly coded. Hence, this type of colour transformation is irreversible, and it is called irreversible colour transformation (ICT). ICT is used only for lossy compression.

The JPEG2000 standard also defines a colour transformation for lossless compression. Therefore, the transformation matrix elements are required to be integer. In this mode, the transformed colour components are referred to as *YUV*, and are defined as

$$\begin{bmatrix} Y \\ U \\ V \end{bmatrix} = \begin{bmatrix} 0.25 & 0.5 & 0.25 \\ 1 & -1 & 0 \\ 0 & -1 & 1 \end{bmatrix} \begin{bmatrix} \mathrm{R} \\ \mathrm{G} \\ \mathrm{B} \end{bmatrix} \tag{5.5}$$

Here the colour decorrelation is not as good as ICT, but it has the property that if *YUV* are losslessly coded, then the exact values of the original RGB can be retrieved. This type of transformation is called reversible colour transformation (RCT). RCT may also be used for lossy coding, but since ICT has a better decorrelation property than RCT, use of RCT can reduce the overall compression efficiency.

It is worth mentioning that in compression of colour images, colour fidelity may be traded for that of luminance. In the JPEG standard, this is done by subsampling the chrominance components C_b and C_r, or U and V, like the 4:2:2 and 4:2:0 image formats. In JPEG2000, image format is always 4:4:4, and the colour subsampling is done by the wavelet transform of the core encoder. For example, in coding of a 4:4:4 image format, if the highest LH, HL and HH bands of C_b and C_r chrominance components are set to zero, it has the same effect as coding of a 4:2:0 image format.

5.4.2 Core encoder

Each transformed colour component of YC_bC_r/YUV is coded by the core encoder. As in the JPEG encoder, the main elements of the core encoder are transformation, quantisation and entropy coding. Thus, a more detailed block diagram of JPEG2000 is given in Figure 5.11.

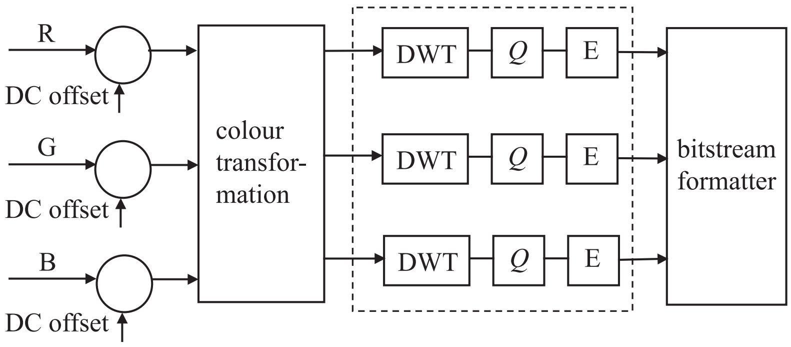

Figure 5.11 The encoding elements of JPEG2000

In the following sections, these elements and their roles in image compression are presented.

5.4.2.1 Discrete wavelet transform

In JPEG2000, transformation of pixels that in the JPEG standard was DCT has been replaced by the discrete wavelet transform (DWT). This has been chosen to fulfil some of the requirements set forth by the JPEG2000 committee:

- Multiresolution image representation is an inherent property of the wavelet transform. This also provides simple signal-to-noise ratio (SNR) and spatial scalability without sacrificing compression efficiency.
- Since wavelet transform is a class of lapped orthogonal transform, it does not create blocking artefacts even for small tile sizes.
- For larger-dimension images, the number of subband decomposition levels can be increased. Hence, by exploiting a larger area of pixel intercorrelation, a higher compression gain can be achieved. Thus, for images coded at low bit rates, DWT is expected to produce better compression gain than the DCT, which only exploits correction with 8×8 pixels.
- DWT with integer coefficients, such as the (5,3) tap wavelet filters, can be used for lossless coding. Note that in DCT, since the cosine elements of the transformation matrix are approximated, lossless coding is not possible.

The JPEG2000 standard recommends two types of filter banks for lossy and lossless coding. The default irreversible transform used in the lossy compression is the Daubechies (9,7)-tap filter [11]. For reversible transform, a requirement for lossless compression is the LeGall and Tabatabai's (5,3)-tap filters, as they have integer coefficients [12]. Table 5.5 shows the normalised coefficients (rounded to six decimal points) of the low- and high-pass analysis filters $H_0(z)/H_1(z)$ of the (9,7) and (5,3) filters. Those of the synthesis $G_0(z)$ and $G_1(z)$ filters can be derived from the usual method of $G_0(z) = H_1(-z)$ and $G_1(z) = -H_0(-z)$.

Table 5.5 Low- and high-pass analysis filter banks

Coefficients	**Lossy compression (9,7)**		**Lossless compression (5,3)**	
	Low pass $H_0(z)$	**High pass $H_1(z)$**	**Low pass $H_0(z)$**	**High pass $H_1(z)$**
0	+0.602949	+1.115087	3/4	1
±1	+0.266864	−0.591272	1/4	−1/2
±2	−0.078223	−0.057544	−1/8	
±3	−0.016864	+0.091272		
±4	+0.026729			

Note that to preserve image energy in the pixel and the wavelet domains, the integer filter coefficients in the lossless compression are normalised for unity gain. Since the low- and high-pass filter lengths are not equal, these types of filters are called biorthogonal. The lossy (9,7) Daubechies filter pairs [11] are also biorthogonal.

5.4.2.2 Quantisation

After the wavelet transform, all the coefficients are quantised linearly with a dead band zone quantiser (Figure 3.5). The quantiser step size can vary from band to band, and since image tiles are coded independently, it can also vary from tile to tile. However, one quantiser step size is allowed per subband of each tile. The choice of the quantiser step size can be driven by the perceptual importance of that band on the HVS, similar to the quantisation weighting matrix used in JPEG (Table 5.1), or by other considerations, such as the bit rate budget.

As mentioned in Chapter 4, wavelet coefficients are most efficiently coded when they are quantised by successive approximation, which is the bit plane representation of the quantised coefficients. In this context, the quantiser step size in each subband, called the basic quantiser step size, Δ, is related to the dynamic range of that subband such that the initial quantiser step size after several passes ends up with the basic quantiser step size Δ. In JPEG2000, the basic quantiser step size for band b, Δ_b, is represented with a total of 2 bytes, an 11-bit mantissa μ_b and a 5-bit exponent ε_b according to the relationship

$$\Delta_b = 2^{R_b-\varepsilon_b}\left(1+\frac{\mu_b}{2^{11}}\right) \tag{5.6}$$

where R_b is the number of bits representing the nominal dynamic range of the subband b. That is, 2^{R_b} is greater than the magnitude of the largest coefficient in subband b. Values of μ_b and ε_b for each subband are explicitly transmitted to the decoder. For lossless coding, used with reversible (5, 3) filter banks, $\mu_b = 0$ and $\varepsilon_b = R_b$, which results in $\Delta_b = 1$. On the other hand, the maximum value of Δ_b is almost twice the dynamic range of the input sample when $\varepsilon_b = 0$ and μ_b has its maximum value, which is sufficient for all practical cases of interest.

5.4.2.3 Entropy coding

The indices of the quantised coefficients in each subband are entropy coded to create the compressed bitstream. In Chapter 4, we introduced three efficient methods of coding these indices, namely embedded zero tree (EZW), set partitioning in hierarchical tree (SPIHT) and embedded block coding with optimised truncation (EBCOT). As mentioned in section 4.7, the JPEG committee chose the EBCOT because of its many interesting features that fulfil the JPEG2000 objectives. Details of EBCOT were given in section 4.7, but here we only summarise its principles and show how it is used in the JPEG2000 standard.

In EBCOT, each subband of an image tile is partitioned into small rectangular blocks called code blocks, and code blocks are encoded independently. The dimensions of the code blocks are specified by the encoder, and although they may be chosen freely, there are some constraints: they must be an integer power of 2, the total number of coefficients in a code block cannot exceed 4096 and the height of the code block cannot be less than 4. Thus, the maximum length of the code block is 1024 coefficients.

The quantiser indices of the wavelet coefficients are bit plane encoded, 1 bit at a time, starting from the MSB and preceding to the least significant bit (LSB). During this progressive bit plane encoding, if the quantiser index is still zero, that coefficient is called insignificant. Once the first nonzero bit is encoded, the coefficient becomes significant and its sign is encoded. For significant coefficients, all subsequent bits are referred to as refinement bits. Since in the wavelet decomposition, the main image energy is concentrated at lower-frequency bands, many quantiser indices of the higher-frequency bands will be insignificant at the earlier bit planes. Clustering of insignificant coefficients in bit planes creates strong redundancies among the neighbouring coefficients that are exploited by JPEG2000 through a context-based adaptive arithmetic coding.

In JPEG2000, instead of encoding the entire bit plane in one pass, each bit plane is encoded in three subbit plane passes. This is called fractional bit plane encoding, and the passes are known as significance propagation pass, refinement pass and clean-up pass. The reason for this is to be able to truncate the bitstream at the end of each pass to create a near optimum bitstream. Here, the pass that results in a largest reduction in distortion for the smallest increase in bit rate is encoded first.

In the significance propagation pass, the bit of a coefficient in a given bit plane is encoded if and only if prior to this pass the coefficient was insignificant and at least one of its eight immediate neighbours was significant. The bit of the coefficient in that bit plane, 0 or 1, is then arithmetic coded with a probability model derived from the context of its eight immediate neighbours. Since neighbouring coefficients are correlated, it is more likely that the coded coefficient becomes significant, resulting in a large reduction in the coding distortion. Hence, this pass is the first to be executed in the fractional bit plane coding.

In the refinement pass, a coefficient is coded if it was significant in the previous bit plane. Refining the magnitude of a coefficient reduces the distortion moderately. Finally, coefficients that were not coded in the two previous passes are coded in the clean-up pass. These are mainly insignificant coefficients (having eight insignificant immediate neighbours) and are likely to remain insignificant. Hence, their contributions in reducing distortions are minimal and are used in the last pass. For more details of coding, refer to EBCOT in section 4.7.

5.4.3 Postprocessing

Once the entire image has been compressed, the bitstream generated by the individual code blocks is postprocessed to facilitate various functionalities of the JPEG2000 standard. This part is similar to the layer formation and bitstream organisation of EBCOT known as tier 2 (see section 4.7).

To form the final bitstream, the bits generated by the three spatially consistent coded blocks (one from each subband at each resolution level) comprise a packet partition location called *precinct* [9]. A collection of packets, one from each precinct, at each resolution level comprises the layer. Figure 5.12 shows the

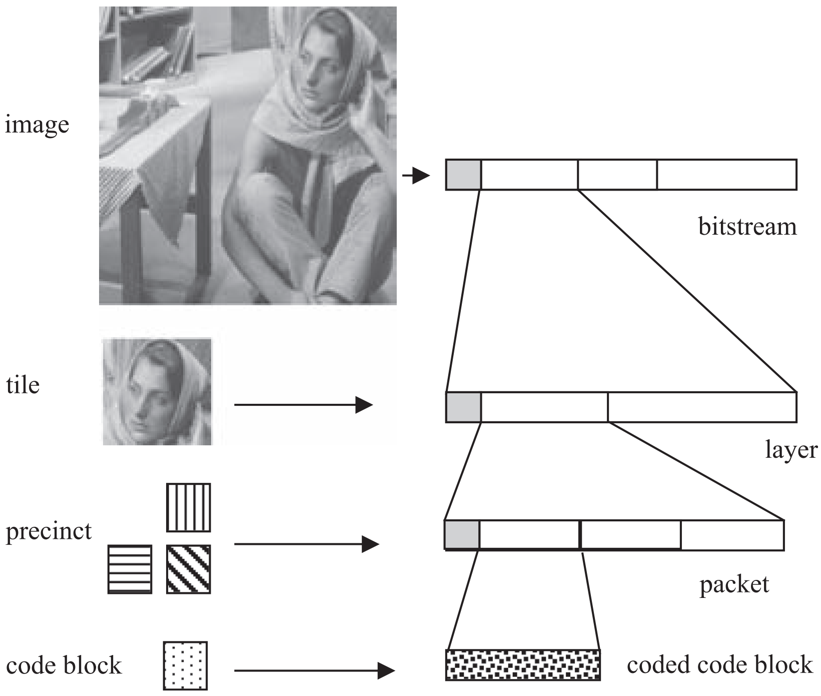

Figure 5.12 Correspondence between the spatial data and bitstream

relationship between the packetised bitstream and the units of image, such as the code block, precinct, tile and the image itself.

Here the smallest unit of compressed data is the coded bits from a code block. Data from three code blocks of a precinct make a packet, with an appropriate header, addressing the precinct position in the image. Packets are then grouped into the layer and finally form the bitstream, all with their relevant headers, to facilitate flexible decoding. Since precincts correspond to spatial locations, a packet could be interpreted as one quality increment for one resolution at one spatial location. Similarly, a layer could be viewed as one quality increment for the entire image. Each layer successively and gradually improves the image quality and resolution, so that the decoder is able to decode the code block contributions contained in the layer in sequence. Since ordering of packets into the layer and hence into the bitstream can be as desired, various forms of progressive image transmission can be realised.

5.5 Some interesting features of JPEG2000

Independent coding of code blocks and flexible multiplexing of quality packets into the bitstream exhibit some interesting phenomena. Some of the most remarkable features of JPEG2000 are outlined in the followings sections.

5.5.1 Region of interest

In certain applications, it might be desired to code parts of a picture at higher quality than the other parts. For example, in Web browsing, one might be interested in a logo of a complex Web page image that needs to be seen first. This part needs to be given higher priority for transmission. Another example is in medical images, where the ROI might be an abnormality in the part of the whole image that requires special attention.

Figure 5.13 shows an example of ROI, where the head and scarf of Barbara are coded at higher quality than the rest of the picture, called background. Loss of image quality outside the ROI (outside the white box), in particular on the tablecloth, trousers and the books, is very clear.

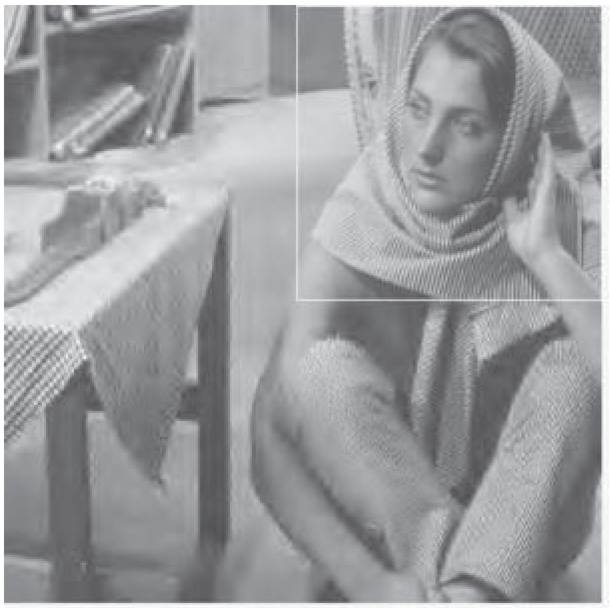

Figure 5.13 Region of interest with better quality

Coding of the ROI in the JPEG2000 standard is implemented through the so-called maxshift method [13]. The basic principle in this method is to scale (shift) up the coefficients such that their bits are placed at a higher level than the bits associated with the background data, as shown in Figure 5.14. Depending on the scale value, *S*, some bits of the ROI coefficients might be encoded together with those of the background, like Figure 5.14*a*, or all the bits of ROI are encoded before any background data are coded, as shown in Figure 5.14*b*. In any case, the ROI at the decoder is decoded or refined before the rest of the image.

It is interesting to note that if the value of scaling, *S*, is computed such that the minimum coefficient belonging to ROI is larger than the maximum coefficient of

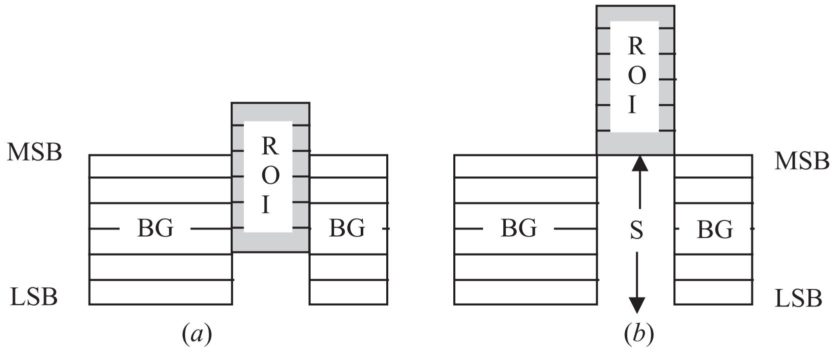

Figure 5.14 Scaling of the ROI coefficients

the background, then it is possible to have arbitrary shaped ROIs, without the need for defining the ROI shape to the decoder. This is because every received coefficient that is smaller than S belongs to the background and can be easily identified.

5.5.2 *Scalability*

Scalability is one of the important parts of all the image/video coding standards. Scalable image coding means being able to decode more than one quality or resolution image from the bitstream. This allows the decoders of various capabilities to decode images according to their processing powers or needs. For example, while low-performance decoders may decode only a small portion of the bitstream, providing basic quality or resolution images, high-performance decoders may decode a larger portion of the bitstream, proving higher-quality images. The most well-known types of scalability in JPEG2000 are the SNR and spatial scalabilities. Since in JPEG2000 code blocks are individually coded, bitstream scalability is easily realised. To have either of the SNR or spatial scalability, the compressed data from the code blocks should be inserted into the bitstream in the proper order.

5.5.2.1 Spatial scalability

In spatial scalability, from a single bitstream, images of various spatial resolutions can be decoded. The smaller-size picture with an acceptable resolution is the base layer, and the parts of the bitstream added to the base layer to create higher-resolution images comprise the next enhancement layer, as shown in Figure 5.15.

In JPEG2000, because of the octave band decomposition of the wavelet transform, spatial scalability is easily realised. In this mode, compressed data of the code blocks have to be packed into the bitstream such that all the bit planes of the lower-level subbands precede those of the higher bands.

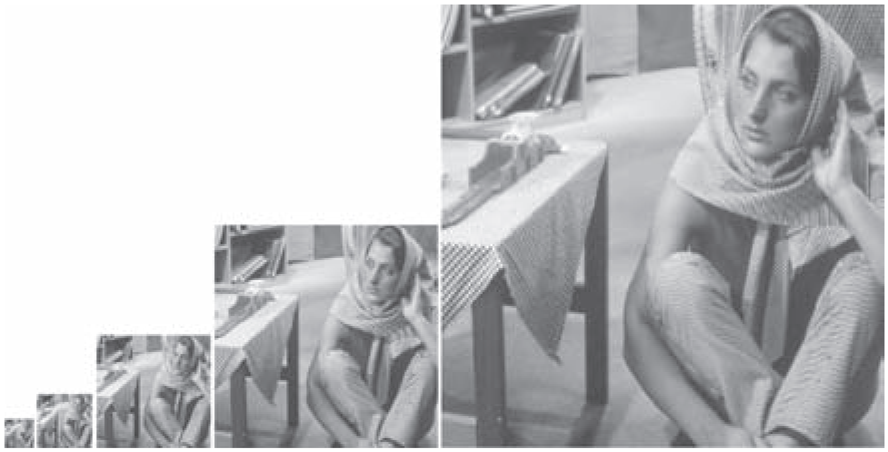

Figure 5.15 Spatial scalable decoding

5.5.2.2 SNR scalability

The SNR scalability involves producing at least two levels of images of the same spatial resolutions, but at different quality, from a single bitstream. The lowest-quality image is called the base layer, and the parts of the bitstream that enhance the image quality are called enhancement layers. In JPEG2000, through bit plane encoding, the lowest significant bit plane that gives an acceptable image quality can be regarded as the base layer image. Added quality from the subsequent bit planes produce a set of enhanced images. Figure 5.16 shows a nine-layer SNR scalable image produced by bit plane coding from a single layer, where the compressed code block data from a bit plane of all the subbands are packed before the data from the next bit plane.

In Figure 5.16, the first picture is made up from coding the MSB of the lowest LL band. As bit plane coding progresses towards lower bits, more bands are coded, improving the image quality. Any of the images shown in the figure can be regarded as the base layer, but for an acceptable quality, picture number 4 or 5 may just meet the criterion. The remaining higher-quality images become its enhanced versions at different quality levels.

5.5.3 Resilience

Compressed bitstreams, especially those using VLCs (e.g. arithmetic coding), are extremely sensitive to channel errors. Even a single bit error may destroy the structure of the following valid code words, corrupting a very large part of the image. Resilience and robustness to channel errors are the most desired features expected from any image/video encoder. Fortunately, in JPEG2000, since the individual quality packets can be independently decoded, the effect of channel errors can be confined to the area covered by these packets. This is not the case with the other wavelet transform encoders such as EZW and SPIHT. Figure 5.17

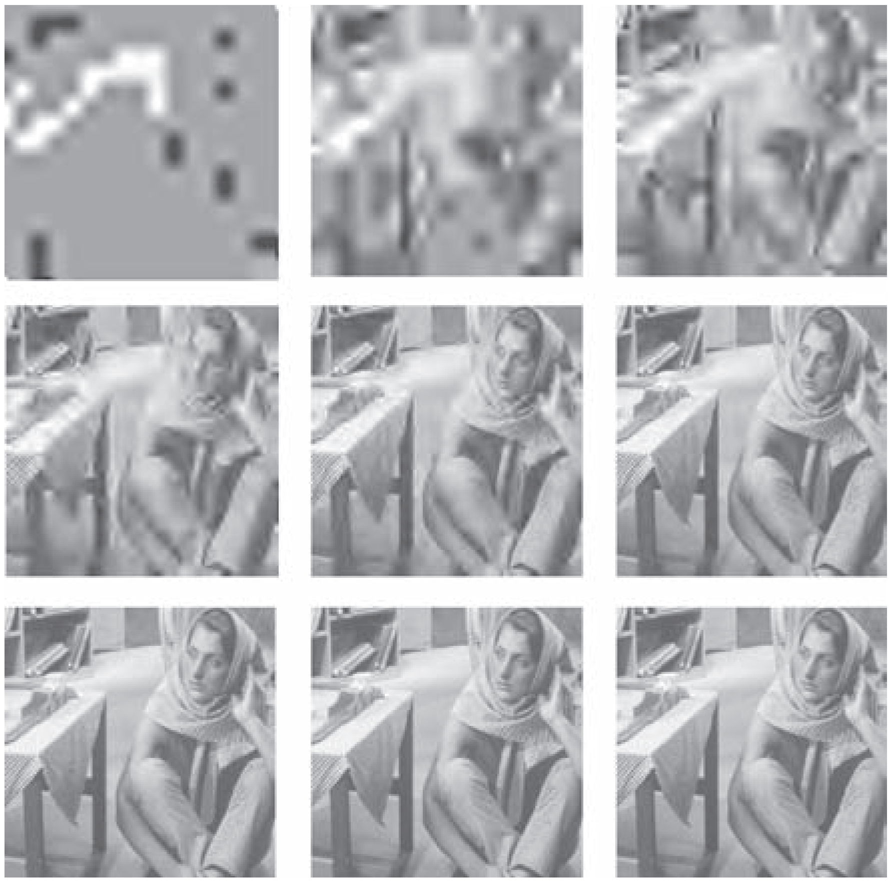
Figure 5.16 SNR scalable decoding

shows the impact of a single bit error on the reconstructed picture, encoded by the SPIHT and JPEG2000. As the figure shows, although a single bit error destroys the whole picture encoded by SPIHT, its effect on JPEG2000 is only limited to a small area around Barbara's elbow.

It is worth noting that the SPIHT encoder, even without arithmetic coding, is very sensitive to channel errors. For example, a single bit error in the early pass of list of insignificant set (LIS) (see section 4.6) can corrupt the whole image, as can be seen from Figure 5.17*a*. In fact, this picture is not arithmetic coded at all, and the single bit error was introduced at the first pass of the LIS data. Of course it is possible to guard EZW and SPIHT compressed data against channel errors. For instance, if the bitstream generated by each tree of EZW/SPIHT can be marked, then propagation of errors into the trees can be prevented. This requires some extra bits to be inserted between the tree's bitstreams as the resynchronisation markers. This inevitably increases the bit rate. Since the resynchronisation marker bits are

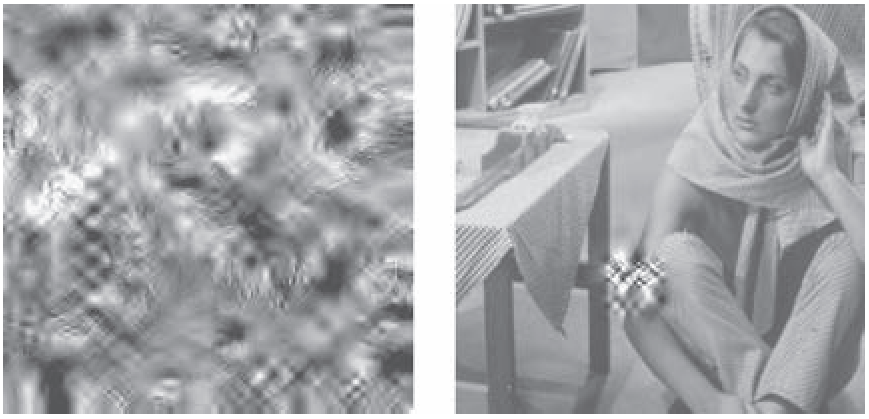
(*a*) SPIHT (*b*) JPEG2000

Figure 5.17 Effect of single bit error on the reconstructed image, encoded by SPIHT and JPEG2000

fixed in rate, irrespective of the encoded bit rate, the increase in bit rate is more significant at lower bit rates than that at higher bit rates. For example, in coding Barbara with SPIHT at 0.1, 0.5 and 1 bit/pixel, the overhead in bits will be 2.7, 0.64 and 0.35 per cent, respectively.

5.6 Problems

1. The luminance quantisation Table 5.1 is used in the baseline JPEG for a quality factor of 50 per cent. Find the quantisation table for the following quality factors:
   a. 25 per cent
   b. 99 per cent
   c. 100 per cent
2. In problem 1, find the corresponding tables for the chrominance.
3. The DCT transform coefficients (luminance) of an 8×8 pixel block prior to quantisation are given by

$$\begin{array}{rrrrrrrr}
1000 & -2 & 35 & 18 & 15 & -8 & 62 & 5 \\
-4 & 15 & -21 & -4 & 51 & 2 & -11 & 1 \\
9 & -8 & 13 & -11 & 43 & -20 & 7 & -3 \\
-17 & 16 & -11 & 3 & -2 & 5 & -13 & 6 \\
-6 & 12 & 42 & -15 & 31 & -2 & 7 & -3 \\
12 & -7 & 2 & -11 & 15 & -5 & 3 & 18 \\
-19 & 52 & 6 & 13 & 4 & -10 & 8 & 10 \\
35 & -11 & -7 & 3 & 5 & 9 & 7 & 382
\end{array}$$

Find the quantisation indices for the baseline JPEG with the quality factors of

a. 50 per cent
b. 25 per cent

4. In problem 3, if the quantised index of the DC coefficient in the previous block was 50, find the pairs of symbol-1 and symbol-2 for the given quality factors.
5. Derive the Huffman code for the 25 per cent quality factor of problem 4, and hence, calculate the number of bits required to code this block.
6. A part of the stripe of the wavelet coefficients of a band is given as

20	30
−16	65
31	11
50	24

Assume that the highest bit plane is 6. Using EBCOT identify which coefficient is coded at bit plane 6 and which one at bit plane 5. In each case identify the type of fractional bit plane used.

References

1. ISO 10918-1 (JPEG): 'Digital compression and coding of continuous-tone still images', 1991
2. FURHT, B.: 'A survey of multimedia compression techniques and standards. Part I: JPEG standard', *Real-time Imaging*, 1995, **1**, pp. 49–67
3. WALLACE, G.K.: 'The JPEG still picture compression standard', *Commun. ACM*, 1991, **34:4**, pp. 30–44
4. JPEG2000: 'JPEG2000 Part 2, Final Committee Draft', ISO/IEC JTC1/SC29/WG1 N2000, December 2000
5. PENNEBAKER, W.B. and MITCHELL, J.L.: *JPEG: Still Image Compression Standard*, Van Nostrand Reinhold, New York, 1993
6. SKODRAS, A., CHRISTOPOULOS, C. and EBRAHIMI, T.: 'The JPEG2000 still image compression standard', *IEEE Signal Process.* **18:5**, *Mag*., 2001, pp. 36–58
7. CHIEN, T. and CHIEN, A.: 'Visual evaluation of JPEG-2000 colour image compression performance', ISO/IECJTC1/SC29/WG1 N1583, March 2000
8. WANG, Q. and GHANBARI, M.: 'Graphics segmentation based coding of multimedia images', *Electronics Lett.*, 1995, **31:6**, pp. 542–544
9. RABBANI, M. and JOSHI, R.: 'An overview of the JPEG2000 image compression standard', *Signal Process. Image Commun.*, 2002, **17:1**, pp. 3–48
10. SANTA-CRUZ, D., GROSBOIS, R. and EBRAHIMI, T.: 'JPEG2000 performance evaluation and assessment', *Signal Process. Image Commun.,* 2002, **17:1**, pp. 113–130

11. DAUBECHIES, I.: ‘The wavelet transform, time frequency localization and signal analysis’, *IEEE Trans Inf. Theory*, 1990, **36:5**, pp. 961–1005
12. LE GALL, D. and TABATABAI, A.: ‘Subband coding of images using symmetric short kernel filters and arithmetic coding techniques’, IEEE International Conference on Acoustics, Speech and Signal Processing, ICASSP’98, 1988, pp. 761–764
13. CHRISTOPOULOS, C.A., ASKELF, J. and LARSSON, M.: ‘Efficient methods for encoding regions of interest in the up-coming JPEG2000 still image coding standard’, *IEEE Signal Process. Let.*, 2000, **7**, pp. 247–249

Chapter 6
Coding for videoconferencing (H.261)

The H.261 standard defines the video coding and decoding methods for digital transmission over Integrated Services Digital Network (ISDN) at rates of $p \times 64$ kbit/s, where p is in the range of 1–30 [1]. The video bit rates will lie between approximately 64 and 1920 kbit/s. The recommendation is aimed at meeting projected customer demand for videophone, videoconferencing and other audio-visual services. It was ratified in December 1990.

The coding structure of H.261 is very similar to that of the generic codec of Chapter 3 (Figure 3.19). That is, it is an interframe discrete cosine transform (DCT)-based coding technique. Interframe prediction is first carried out in the pixel domain. The prediction error is then transformed into the frequency domain, where the quantisation for bandwidth reduction takes place. Motion compensation (MC) can be included in the prediction stage, although it is optional. Thus, the coding technique removes temporal redundancy by interframe prediction and spatial redundancy by transform coding. Techniques have been devised to make the codec more efficient, and at the same time suitable for telecommunications.

It should be noted that any recommendation only specifies what is expected for a decoder; it does not give information on how to design it. Even less information is given about the encoder. Therefore, the design of the encoder and the decoder is at the discretion of the manufacturer, provided they comply with the syntax bitstream. Since the aim of this book is the introduction to the fundamentals of video coding standards, rather than giving instructions on the details of a specific codec, we concentrate on the reference model (RM) codec. The RM is a software-based codec, which is devised to be used in laboratories to study the core elements as a basis for the design of flexible hardware specifications.

During the development of H.261, from May 1988 to May 1989, the RM underwent eight refinement cycles. The last version, known as reference model eight (RM8) [2], is in fact the basis of the current H.261. However, the two may not be exactly identical (though very similar), and the manufacturers may decide on a different approach for better optimisation of their codecs. Herein we interchangeably use RM8 for H.261. Before describing this codec, we will first look at the picture format, and spatio-temporal resolutions of the images to be coded with H.261.

6.1 Video format and structure

Figure 6.1 shows a block diagram of an H.261-based audio-visual system, where a preprocessor converts the International Radio Consultative Committee (CCIR)-601 video (video at the output of a camera) to a new format. The coding parameters of the compressed video signal are multiplexed and then combined with the audio, data and end-to-end signalling for transmission. The transmission buffer controls the bit rate, either by changing the quantiser step size at the encoder or, in more severe cases, by requesting reduction in frame rate to be carried out at the preprocessor.

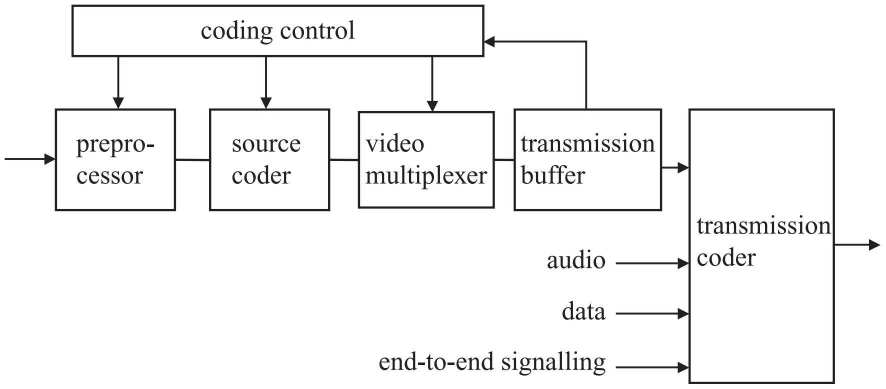

Figure 6.1 A block diagram of an H.261 audio-visual encoder

The H.261 standard also allows up to three pictures to be interpolated between transmitted pictures, thus reducing the frame rate to 15, 10 and 7.5, respectively. The use of quarter–common intermediate format (QCIF) resolution will reduce the sample rate even further to suit low bit rate channels.

In CIF and QCIF, DCT blocks are grouped into macroblocks (MBs) of four luminance and two corresponding C_b and C_r chrominance blocks. The MBs are in turn grouped into layers termed groups of blocks (GOB). A CIF frame has 12 GOBs and QCIF has 3, as illustrated in Figure 6.2.

The objectives of structuring an image into MBs and layers are as follows:

- using similar inter/intra coding mode for luminance and chrominance blocks at the same area;
- using one motion vector for both luminance and chrominance blocks;
- efficient coding of the large number of 8×8 DCT blocks that will be expected to be without coded information in interframe coding; this is implemented via the inclusion of variable length codes (VLC) for coded block pattern (CBP) and MB addressing [1];
- allowing synchronisation to be re-established when bits are corrupted by the insertion of start codes in the GOB headers; note that since DCT coefficients are variable length coded, any error during the transmission renders the remaining variable length coded data undecodable; hence, with a GOB structure, only a portion of the picture is degraded;

- carrying side information appropriate for GOB, MB or higher layers; this includes picture format, temporal references, MB type, quantiser index, etc.

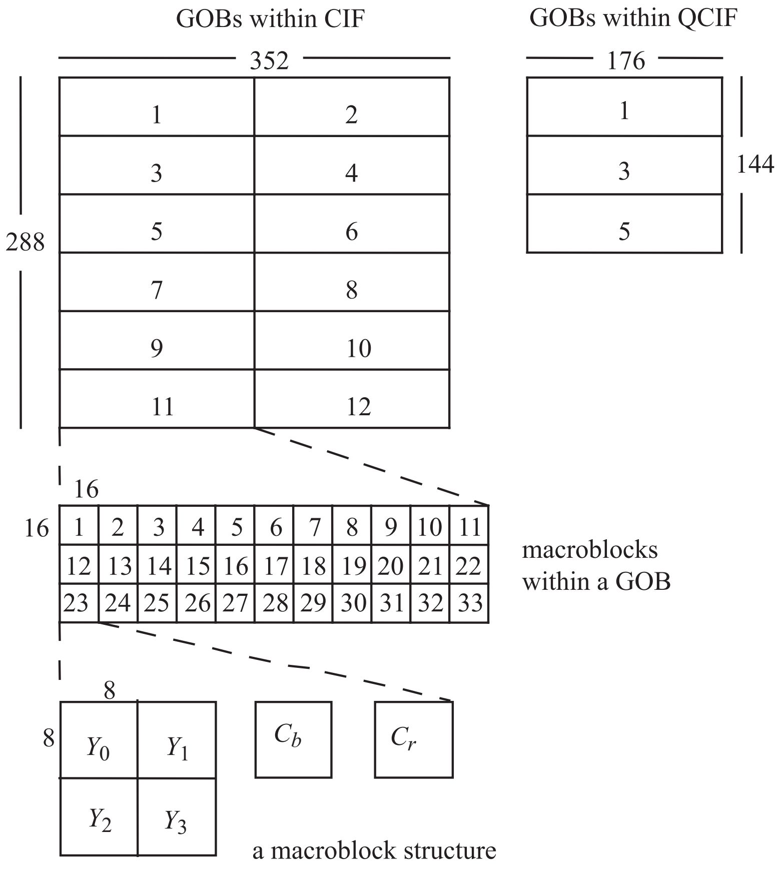

Figure 6.2 Block, macroblock and GOB structure of CIF and QCIF formatted pictures

6.2 Video source coding algorithm

The video coding algorithm is shown in Figure 6.3, which is similar to the generic interframe coder of Figure 3.19. The main elements are the prediction including MC, transform coding, quantisation, VLC and rate control. The prediction error (inter mode) or the input picture (intra mode) is subdivided into 16 × 16 MB pixels, which may or may not be transmitted. MBs that are to be transmitted are divided into 8 × 8 pixel blocks, which are transform coded (DCT), quantised and variable length coded for transmission. As discussed in section 6.1, the atomic coding unit in all standard video codecs is an MB. Hence, in describing the codec we will explain how each MB is coded.

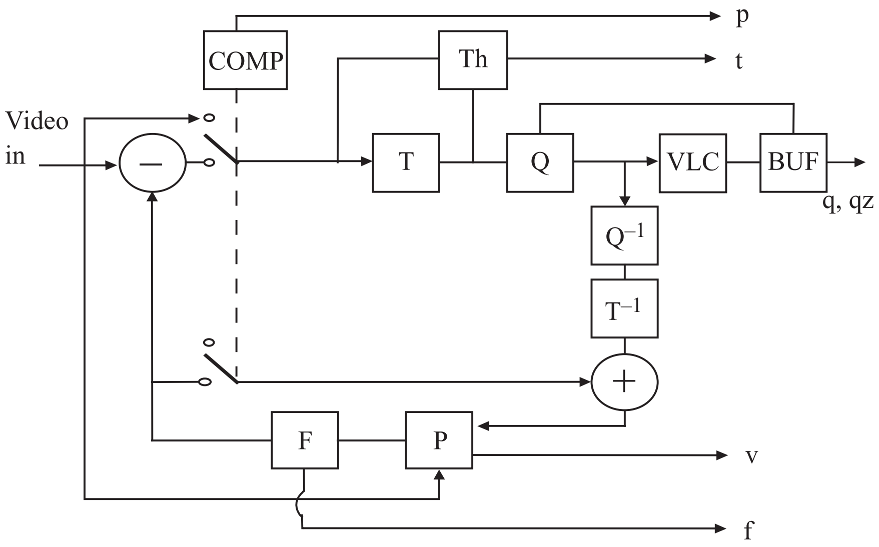

Figure 6.3 A block diagram of H.261 video encoder

In Figure 6.3, the function of each coding element and the messages carried by each flag are as follows:

COMP: a comparator for deciding inter/intra coding mode for an MB
Th: threshold, to extend the quantisation range
T: transform coding blocks of 8 $\times$ 8 pixels
T^{-1}: inverse transform
Q: quantisation of DCT coefficients
Q^{-1}: inverse quantisation
P: picture memory with motion-compensated variable delay
F: loop filter
p: flag for inter/intra
t: flag for transmitted or not
q: quantisation index for transform coefficients
qz: quantiser indication
v: motion vector information
f: switching on/off of the loop filter

Details of the functions of each block are described in the following sections.

6.2.1 Prediction

The prediction is interpicture, which may include MC, since MC in H.261 is optional. The decoder accepts one motion vector per MB. Both horizontal and vertical components of these motion vectors have integer values not exceeding ± 15 pixels/frame. Motion estimation is only based on the luminance pixels, and the vector is used for MC of all four luminance blocks in the MB. Halving the component values of the MB motion vector and truncating them towards zero derives the motion vector for each of the two chrominance blocks. Motion vectors are restricted such that all pixels referenced by them are within the coded picture area.

For the transmission of motion vectors, their differences are variable length coded. The differential technique is based on one-dimensional prediction, that is, the difference between the successive motion vectors in a row of GOBs. For the first MB in the GOB, the initial vector is set to zero.

6.2.2 MC/NO_MC decision

Not all the MBs in a picture are motion compensated. The decision whether an MB should be motion compensated depends on whether motion-compensated prediction can substantially reduce the prediction error. Figure 6.4 shows the region (shaded) where MC is preferred. In this figure, the absolute values of frame difference, *fd*, and those of motion-compensated frame difference, *mfd*, normalised to $16 \times 16 = 256$ pixels inside the MB are compared.

From the figure, we see that if motion-compensated error is slightly, but not significantly, less than the nonmotion-compensated error, we prefer to use nonmotion compensation (NO_MC). This is because MC entails a motion vector overhead (even if it might be zero); hence, if the difference between MC and NO_MC error cannot justify the extra bits, there is no advantage in using MC.

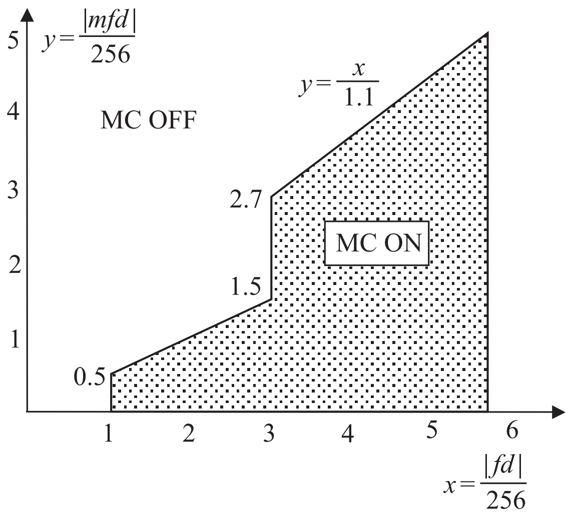

Figure 6.4 MC/NO_MC mode decision

6.2.3 Inter/intra decision

Sometimes it might be advantageous to intraframe code an MB, rather than interframe coding it. There are at least two reasons for intraframe coding:

1. Scene cuts or, in the event of violent motion, interframe prediction errors may not be less than those of the intraframe. Hence, intraframe pictures might be coded at lower bit rates.
2. Intraframe coded pictures have a better error resilience to channel errors. Note that in interframe coding, at the decoder, the received data are added to the previous frame to reconstruct the coded picture. In the event of channel error, the error propagates into the subsequent frames. If that part of the picture is not updated, the error can persist for a long time.

Similar to the MC/NO_MC decision, one can make a decision for coding an MB in inter or intra mode. In this case, the variance of intraframe MB is compared with that of interframe MB (motion compensated or not). The smallest is chosen. Figure 6.5 shows the characteristics of the function for inter/intra decision. Here for large variances, no preference between the two modes is given, but for smaller variances, interframe is preferred. The reason is that, in intra mode, the DC coefficients of the blocks have to be quantised with a quantiser without a dead zone and with 8-bit resolutions. This increases the bit rate compared to that of the interframe mode, and hence interframe is preferred.

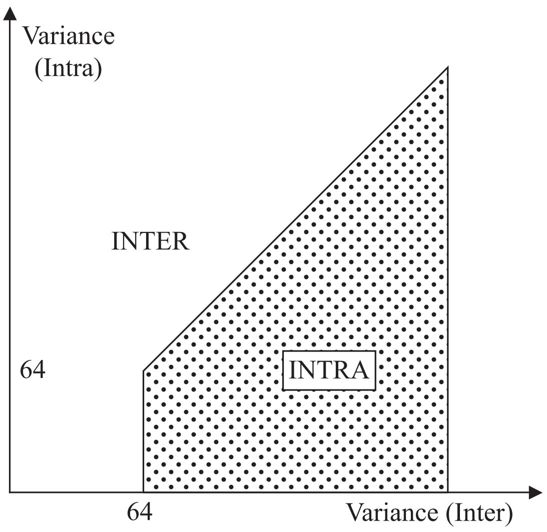

Figure 6.5 Inter/intra mode decision

6.2.4 Forced updating

As mentioned, intraframe coded MB increases the resilience of H.261 codec to channel errors. In case in inter/intra MB decision, no intra mode is chosen, some of the MBs in a frame are forced to be intra coded. The specification recommends that an MB should be updated at least once every 132 frames. This means that for CIF pictures with 396 MBs/frame, on average 3 MBs of every frame are intraframe coded. This has an important impact on the quality of pictures due to errors. For example, in CIF pictures at 10 Hz, the effect of channel errors may corrupt up to 132 frames, and be visible for almost 13 s.

6.3 Other types of macroblocks

In H.261, there are as many as eight different types of MBs:

1. *Inter coded*: interframe coded MBs with no motion vector or with a zero motion vector.
2. *MC coded*: motion-compensated MB, where the MC error is significant and needs to be DCT coded.
3. *MC not coded*: these are motion-compensated error MBs, where the motion-compensated error is insignificant. Hence, there is no need to be DCT coded.
4. *Intra coded*: intraframe coded MBs.
5. *Skipped*: if all the six blocks in an MB without MC have an insignificant energy, they are not coded. These MBs are sometimes called skipped, not-coded or fixed MBs. These types of MBs normally occur at the static parts of the image sequence. Fixed MBs are therefore not transmitted, and at the decoder they are copied from the previous frame.

   Since the quantiser step sizes are determined at the beginning of each GOB or row of GOBs, they have to be transmitted to the receiver. Hence, the first MBs have to be identified with a new quantiser parameter. Therefore, we can have some new MB types:
6. *Inter coded + Q*
7. *MC coded + Q*
8. *Intra+Q*

To summarise the type of MB selection, we can draw a flow chart indicating how each one of the 396 MBs in a picture is coded. Decisions on the types of coding follow Figure 6.6 from left to right.

6.3.1 Addressing of macroblocks

If all the quantised components in one of the six blocks in an MB are zero, the block is declared as not coded. When all six blocks are not coded, the MB is declared not coded (fixed MB or skipped MB). In other cases, the MBs are declared coded, and are variable length coded. The shortest code is assigned to inter code MB and the longest to intra+Q, as they are the most frequent and most rare MB types, respectively.

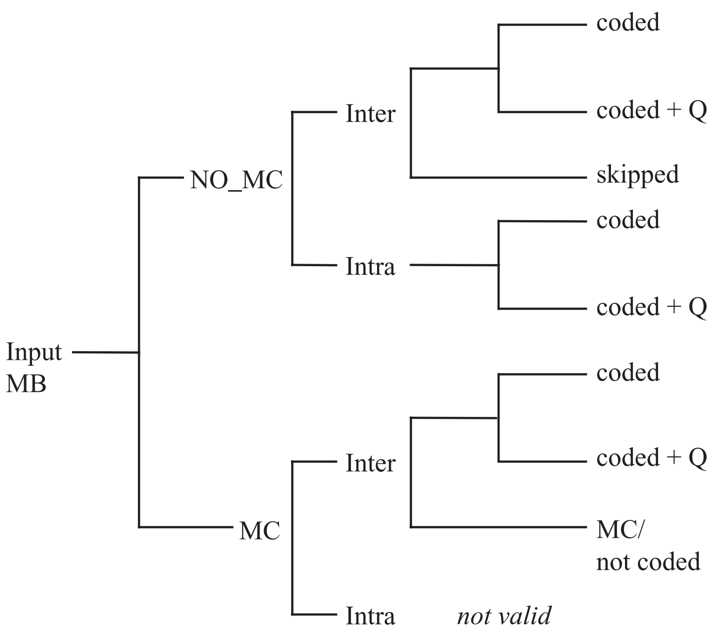

Figure 6.6 Decision tree for macroblock type

Once the type of an MB is identified and variable length coded, its position inside the GOB should also be determined. Considering that H.261 is a video-conferencing codec, normally used for coding head-and-shoulders pictures, it is more likely that coded MBs are in the foreground of the picture. Hence, they are normally clustered in regions. Therefore, the overhead information for addressing of the positions of the coded MB is minimised if they are relatively addressed to each other. The relative addresses are represented by run lengths, which are the number of fixed MBs to the next coded MB. Figure 6.7 shows an example of addressing the coded MBs within a GOB. Numbers represent the relative addressing value of the number of fixed MBs preceding a nonfixed MB. The GOB start code indicates the beginning of the GOB. These relative addressing numbers are finally variable length coded.

6.3.2 Addressing of blocks

Since an MB has six blocks, four luminance and two chrominance, there will be $2^6 = 64$ different combinations of the coded/noncoded blocks. Except the one with all six blocks not coded (fixed MB), the remaining 63 are identified within 63 different patterns. The pattern information consists of a set of 63 coded block pattern (CBP) indicating coded/noncoded blocks within an MB. With a coding order of Y_0, Y_1, Y_2, Y_3, C_b and C_r, the block pattern information or pattern number is defined as

$$\text{Pattern number} = 32Y_0 + 16Y_1 + 8Y_2 + 4Y_3 + 2C_b + C_r \tag{6.1}$$

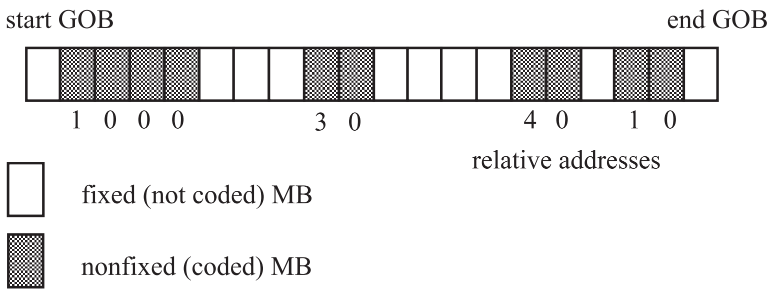

Figure 6.7 Relative addressing of coded MB

where the coded and noncoded blocks are assigned 1 and 0, respectively. Each pattern number is then variable length coded. It should be noted that if an MB is intracoded (or intra+Q), its pattern information is not transmitted. This is because, in intraframe coded MB, all blocks have significant energy and will be definitely coded. In other words, there will not be any noncoded blocks in an intra coded MB. Figure 6.8 illustrates two examples of the CBP, where some of the luminance or chrominance blocks are not coded.

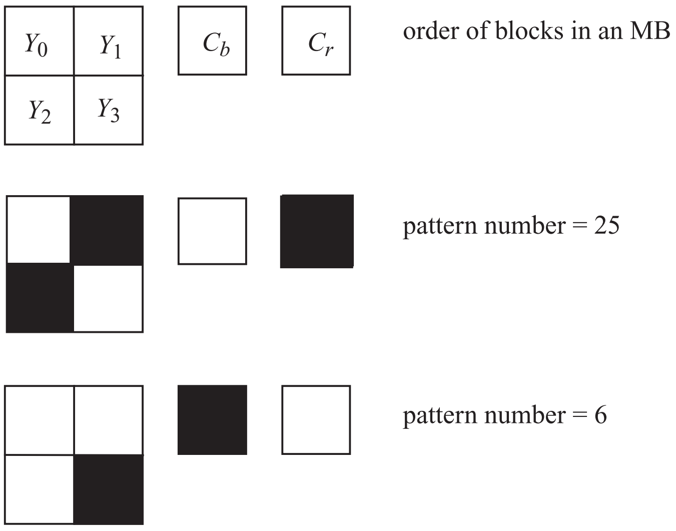

Figure 6.8 Examples of bit pattern for indicating the coded/not-coded blocks in an MB (black, coded; white, not coded)

6.3.3 Addressing of motion vectors

The motion vectors of the motion-compensated MBs are differentially coded with a prediction from their immediate preceding motion vector. The prediction vector is set to zero if either the MB is the first MB of each row of GOB or the previous MB was not coded, coded with zero motion vector or intra coded.

The differential vector is then variable length coded and is known as the motion vector data (MVD). The MVD consists of a pair of VLC, the first component for the differential horizontal value and the second component for the differential vertical displacement. Since most head-and-shoulders type scenes normally move in a rigid fashion, differential encoding of motion vectors can significantly reduce the motion vector overhead. However, this makes motion vectors very sensitive to channel errors, but the extent of the error propagation is limited within the GOB.

6.4 Quantisation and coding

Every one of the six blocks of a selected MB is transform coded with a two-dimensional DCT. The DCT coefficients of each block are then quantised and coded. In section 3.2 we described two types of quantiser. The one without a dead zone is used for quantising the DC coefficient of intra MB. For the H.261 standard, this quantiser uses a fixed step size of eight. The second type is with a dead zone for coding AC coefficients and the DC coefficient of interframe coded MB (MC or NO_MC).

For the latter case, a threshold, *th*, may be added to the quantiser scale, such that the dead zone is increased, causing more zero coefficients for efficient compression. Figure 6.9 shows this quantiser, where a threshold, *th*, is added to every step size. The value of the threshold is sent to the receiver as side information (see Figure 6.3). Ratios of the quantised coefficients to the quantiser step size, called indices, are to be coded.

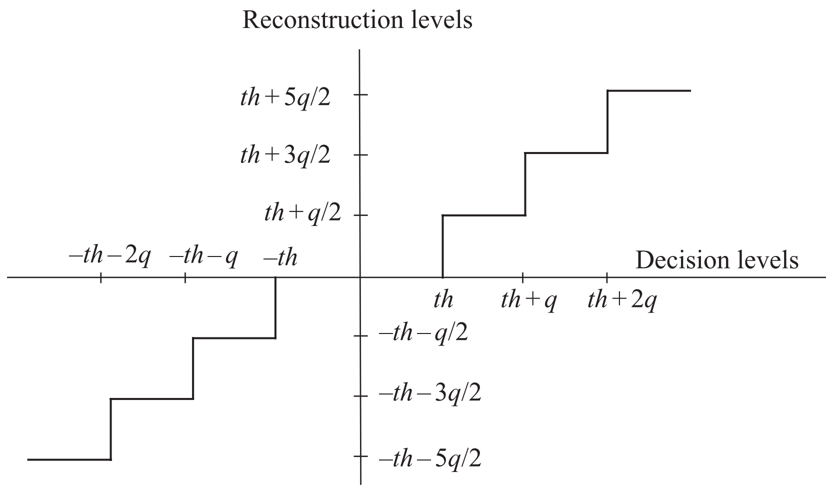

Figure 6.9 A uniform quantiser with threshold

6.4.1 Two-dimensional variable length coding

For transmission of the quantisation parameters, a special order is defined that increases the efficiency of capturing the nonzero components. Starting from the DC coefficient on the top left corner of an 8 × 8 coefficient matrix, the values are scanned in a zigzag sequence as shown in Figure 6.10.

The justification for this is that in natural images, the main energy of the transform coefficients is concentrated in the lower frequencies (top left corner). Hence, the coefficients that normally have the larger values are scanned first. Scanning of the indices terminates when the last nonzero coefficient has been reached.

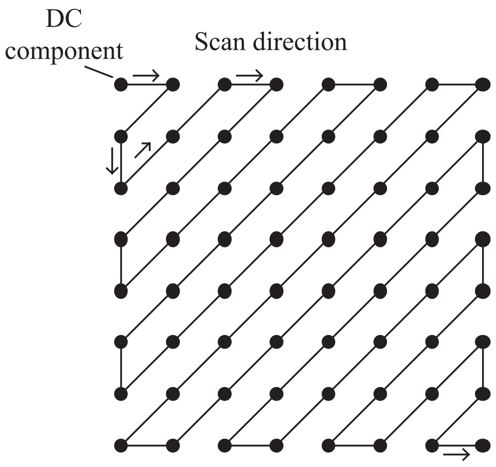

Figure 6.10 Zigzag scanning of 8 × 8 transform coefficients

To increase the coding efficiency, a two-dimensional variable length code (2D-VLC) has been adopted. The 2D-VLC is performed in two stages. In the first stage, an event is produced for every nonzero index. The event is a combination of the index magnitude (index) and the number of zeros preceding that index (run).

To see how a two-dimensional index and run generation makes 2D-VLC coding very efficient, the following example is based on a coder having a quantiser step size of q =16 with equal threshold levels $th = q$. Let us assume a pixel block is DCT coded with coefficient values as shown partly in Figure 6.11.

After zigzag scanning, coefficients are quantised. For a dead zone of $th = 16$, coefficient values less than this threshold are set to zero. Larger values are quantised according to the quantisation characteristics (see Figure 6.9). Here we see that rather than 1D-VLC coding of 17 individual coefficients, we need to code only 5 two-dimensional events, which requires substantially fewer bits.

In this 2D-VLC, since the range of index (possible values of indices) can vary from -127 to $+127$, and the range of run (number of zeros preceding an index) may vary from 0 to 63, there will be $2 \times 128 \times 64 = 16\ 384$ possible events.

Design of a Huffman code for this large number of symbols is impractical. Some code words might be as long as 200 bits! Here we use what might be called a modified Huffman code. In this code, all the symbols with small probabilities are grouped together and are identified with an *ESCAPE* symbol. The *ESCAPE* symbol has a probability equal to the sum of all it represents. Now the most commonly occurring events and the *ESCAPE* symbol are encoded with VLC (Huffman code) in the usual way. Events with low probabilities are identified with a fixed-length *run* and *index*, appended to the *ESCAPE* code. The end of block (*EOB*) code is also one of the symbols to be variable length coded.

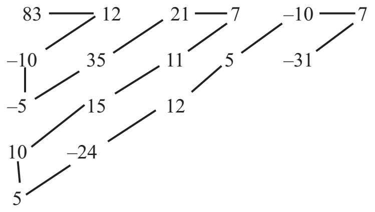

Raw coefficients	83	12	–10	–5	35	21	7	11	15	10	5	–24	12	5	–10	7	–31
New coefficients	83	0	0	0	35	21	0	0	0	0	0	–24	0	0	0	0	–31
Quantised values	88	0	0	0	40	24	0	0	0	0	0	–24	0	0	0	0	–24
Index	5	0	0	0	2	1	0	0	0	0	0	–1	0	0	0	0	–1

Events to be transmitted: (run, index) (0,5) (3,2) (0,1) (5,–1) (4,–1)

Figure 6.11 Zigzag scanning and run–index generation

In H.261, *ESCAPE* is 6 bits long (i.e. 000001); thus, rare events with 6-bit run (0–63) and 8-bit *index* (-127 to $+127$) require 20 bits [1]. The *EOB* code is represented with a 2-bit word. The DC/intra index is linearly quantised with a step size of eight and no dead zone. The resulting value is coded with an 8-bit resolution.

Figure 6.12 shows an example of a 2D-VLC table for positive values of indices, derived from statistics of coding the Claire test image sequence. As we see, most frequent events are registered at low index and low run values. The sum of the rare events, which represents the frequency of the *ESCAPE*, is even less than some frequent events. The corresponding 2D-VLC table is also shown next to the frequency table. Also in this example the sum has the same frequency as the event (run $=4$, index $=1$). They are expected to have the same word length. Other events can be defined as *ESCAPE* + normal run + normal index, with:

ESCAPE code $=6$ bits;
normal run $=6$ bits (1 out of 64 possible values);
normal index $=8$ bits (1 out of 128 values) plus the sign bit;
total bits for the modified Huffman coded events $= 6+6+8=20$.

index (absolute value)

run	1	2	3	4	5	6	7	8 128
0	12187	17055	3189	1403	606	262	125	39 6 1 0
1	6216	3144	1283	446	149	54	31	5 0
2	3233	1558	546	195	44	10	4	4
3	2040	920	333	118	33	6	1	
4	1394	563	161	42	27	2		
5	982	399	144	41	12	4		
6	734	246	65	36	18			
7	601	167	70	16	17			
8	500	134	40	15	15			
9	405	118	30	17	7			
10	305	119	34	18				
11	307	99	27	19				
12	225	45	12	14				
13	138	35	4	17				
14	84	28	5					
15	67	16	0					
·	37	10						
63	39	5						

SUM = 1159

index (absolute value)

run	1	2	3	4	5	6	7	8 128
0	4	4	5	5	8	9	10	
1	5	6	7	8	10	11		
2	5	6	8	9				
3	6	7	9	10				
4	7	8	10					
5	7	8	10					
6	8	9	11					
7	8	9	11					
8	8	10						
9	8	10						
10	9	10						
11	9							
12	9							
13	10							
14	11							
15	11							
·								
63								

normal events (run & index) are linearly coded + VLC of *ESCAPE* code

Figure 6.12 An example of run and index frequency and the resulting 2D-VLC table

6.5 Loop filter

At low bit rates the quantiser step size is normally large. Larger step sizes can force many DCT coefficients to zero. If only the DC and a few AC coefficients remain, then the reconstructed picture appears blocky. When the positions of blocky areas vary from one frame to another, it appears as a high-frequency noise, commonly referred to as mosquito noise. The blockiness degradations at the slant edges of the image appear as staircase noise. Figure 6.13 illustrates single shots of a CIF size Claire test image sequence and its coded version at 256 kbit/s. The sequence is in colour, with 352 pixels by 288 lines at 30 Hz, but only the luminance is shown. The colour components have a quarter resolution of luminance (176 pixels by

144 lines). As can be seen, at this bit rate the coded image quality is very good with no visible distortions.

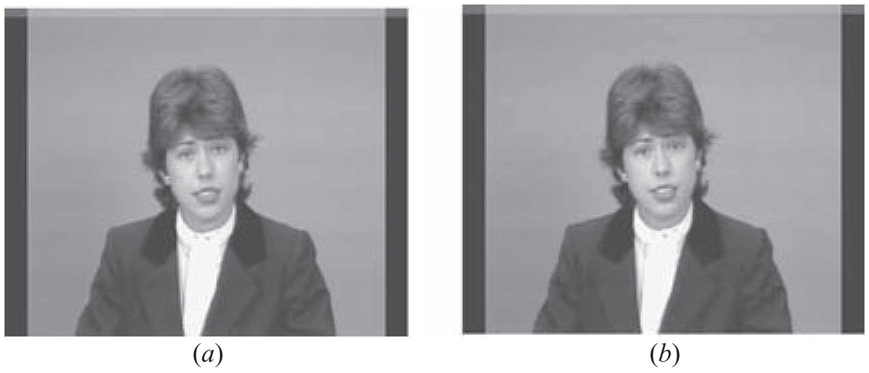

Figure 6.13 Picture of Claire: (a) original and (b) H.261 coded at 256 kbit/s

At lower bit rates, artefacts begin to appear. This is shown in Figure 6.14, where there are more severe distortions at 64 kbit/s than at 128 kbit/s. When the sequence is displayed at its normal rate (30 Hz), the positions of the distortions move at different directions over the picture, and the appearance of mosquito noise is quite visible.

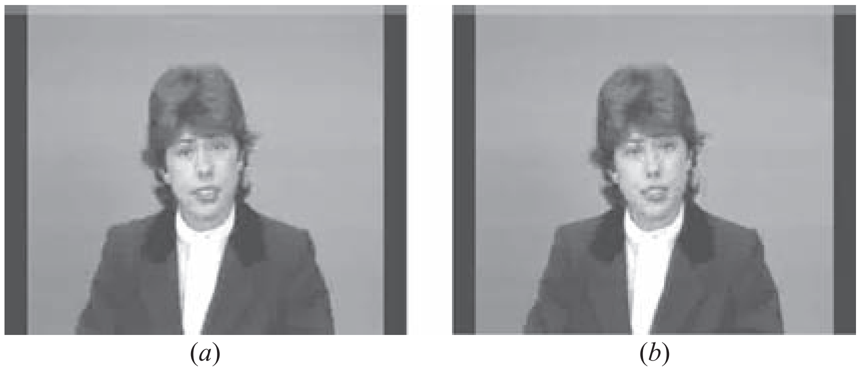

Figure 6.14 H.261 coded at (a) 128 kbit/s and (b) 64 kbit/s

Coarse quantisation of the coefficients that results in the loss of high-frequency components implies that compression can be modelled as a low-pass filtering process [3,4]. These artefacts are to some extent reduced by using the loop filter (see position of the loop filter in Figure 6.3). The low-pass filter removes the high-frequency and block boundary distortions. The same pictures with the use of a loop filter are shown in Figure 6.15.

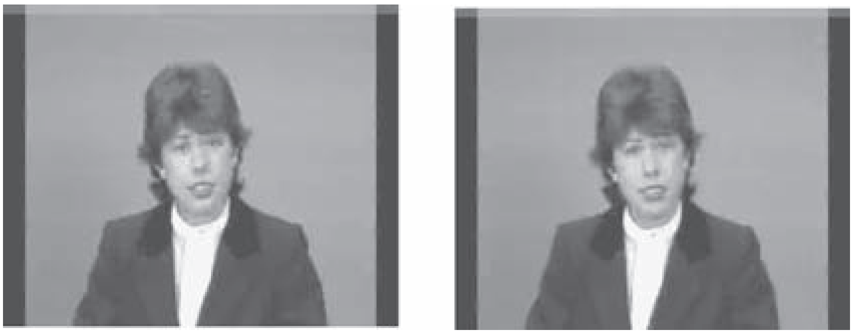

(*a*) (*b*)

Figure 6.15 Coded pictures with loop filter: (a) 128 kbit/s and (b) 64 kbit/s

Loop filtering is introduced after the motion compensator to improve the prediction. It should be noted that the loop filter has a picture blurring effect. It should be activated only for blocks with motion; otherwise, nonmoving parts of the pictures are repeatedly filtered in the following frames, blurring the picture. Since it is motion based, loop filtering is thus carried out on an MB basis, and it has an impulse response given by

$$h(x,y) = \frac{1}{16}\begin{bmatrix} 1 & 2 & 1 \\ 2 & 4 & 2 \\ 1 & 2 & 1 \end{bmatrix} \tag{6.2}$$

for pixels well inside the picture. For pixels at the image border, or corners, another function may be used. Figure 6.16 shows an example of the filter response in these areas.

9	3							
3	1							
			1	2	1			
			2	**4**	2			
			1	2	1			
			1	2	1			
			3	**6**	3			

Figure 6.16 Loop filter impulse response in various parts of the image

The loop filter was first defined for H.261 and its enhanced version was later applied to H.264. In its simplest form in H.261, the loop filter is activated for all six DCT blocks of an MB. The filtering should be applied for coding rates less than 6×64 kbit/s = 386 kbit/s and switched off otherwise. At higher bit rates, the filter does not improve the subjective quality of the picture [3]. MPEG-1 does not specify the requirement of a loop filter because pictures coded with MPEG-1 are at much higher bit rates than 386 kbit/s.

6.6 Rate control

The bit rate resulting from the DCT-based coding algorithm fluctuates according to the nature of the video sequence. Variations in the speed of moving objects, their size and texture are the main cause for bit rate variation. The objective of a rate controller is to achieve a constant bit rate for transmission over a circuit-switched network. A transmission buffer is usually needed to smooth out the bit rate fluctuations, which are inherent in the interframe coding scheme.

The usual method for bit rate control is to monitor the buffer occupancy and vary the quantiser step size according to the buffer fullness [3,5]. In RM8, the quantiser step size is calculated as a linear function of the buffer content and is expressed by

$$q = 2\left\lfloor \frac{\text{buffer content}}{200p} \right\rfloor + 2 \tag{6.3}$$

where p is the multiplier used in specifying the bit rates as in $p \times 64$ kbit/s, and $\lfloor \cdot \rfloor$ stands for integer division with truncation towards zero.

The buffer control system usually has two additional operating states to prevent buffer underflow or buffer overflow from occurring. If the buffer content reaches the trigger point for overflow state, current and subsequent coded data are not sent to allow the buffer to be emptied. Only trivial side information pertaining to the coded GOB or frame is transmitted.

On the other extreme, bit stuffing is invoked when buffer underflow is threatened. It is essential that buffer underflow is avoided so that the decoder can maintain synchronisation.

In practice, to allow maximum freedom of the H.261 standard codec structure, a hypothetical reference decoder (HRD) buffer is defined. All encoders are required to be compliant with this buffer. The HRD is best explained with reference to Figure 6.17.

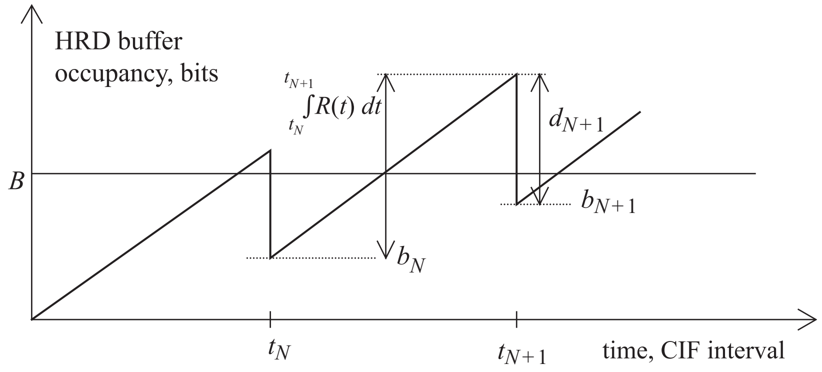

Figure 6.17 Hypothetical reference buffer occupancy

The hypothetical buffer is initially empty. It is examined at CIF intervals (1/29.97 $\cong$ 33 ms), and if at least one complete coded picture is in the buffer, then all the data from the earliest picture are instantly removed (e.g. at t_N in Figure 6.17) [6]. Immediately after removing the above data, the buffer occupancy should be less than B, with $B = 4R_{max}/29.97$ and R_{max} being the maximum video bit rate to be used in the connection. To meet this requirement, the number of bits for $(N + 1)$th coded picture, d_{N+1} must satisfy

$$d_{N+1} > b_N + \int_{t_N}^{t_{N+1}} R(t)dt - B \tag{6.4}$$

where b_N is the buffer occupancy just after time t_N, t_N is the time at which the Nth coded picture is removed from the HRD buffer and $R(t)$ is the video bit rate at time t. Note that the time interval $(t_{N+1}–t_N)$ is an integer number of CIF picture periods (1/29.97, 2/29.97, 3/29.97, ...).

This specification constrains all encoders to restrict the picture start lead jitters to four CIF picture period's worth of channel bits. This prevents decoder buffer overflow at the decoder in a correctly designed H.261 codec. Jitters in the opposite direction (phase lag) are not constrained by the H.261 recommendation. Phase lag corresponds to buffer underflow at the decoder, which is simply dealt with by making the decoder wait for sufficient bits to have arrived to continue decoding.

A major deficiency with the RM8/H.261 model rate controls is that bits might be unfairly distributed across the image. For example, in the active parts of the picture sequences, such as in the middle of the head-and-shoulders pictures, the buffer tends to fill up very quickly, and hence the quantiser step size rises rapidly. This causes the rest of the picture to be coded coarsely. One of the key issues in H.261, as well as any video codec, is the way the quantiser step size or the rate control is managed. In the past decade, numerous manufacturers have produced H.261 codecs, but they may not perform equally. Because of the need for interoperability, the general structure of H.261 must be based on coding elements as shown in Figure 6.3. Therefore, the only part that makes one codec better than the others is the rate control mechanism. This part is kept secret by the manufacturers and is subject to further research.

6.7 Problems

1. In a CIF picture, find the number of MBs and blocks per
   a. GOB
   b. picture

2. Calculate the MB interval in CIF pictures. How large is this value for a QCIF video at 10 Hz?

3. The absolute value of the motion-compensated frame difference per MB, $|mfd|$, is normally smaller than that without MC, $|fd|$. In a search for MC, the

following values for $|mfd|$ and $|fd|$ have been calculated. Using Figure 6.4, determine in which of the following cases MC should be used:

a. $|fd| = 1200$ and $|mfd|$=1000
b. $|fd| = 600$ and $|mfd|$=500
c. $|fd| = 200$ and $|mfd|$=50

4. Why is NO_MC preferred to MC for very small frame difference images?

5. To decide whether an MB should be interframe or intraframe coded, the variances of intraframe and motion-compensated interframe MBs are compared, according to Figure 6.5. Find in each of the following whether an MB should be intraframe or interframe coded:

   a. $\sigma^2_{intra} = 1500$, $\sigma^2_{inter} = 1450$
   b. $\sigma^2_{intra} = 500$, $\sigma^2_{inter} = 600$
   c. $\sigma^2_{intra} = 50$, $\sigma^2_{inter} = 60$

6. In MBs with small energy (inter or intra), why is inter MB preferred to intra MB?

7. Calculate the CBP indices of the following MBs in an H.261 codec if:

   a. all the blocks in the MB are coded
   b. only the luminance blocks are coded
   c. only the chrominance blocks are coded

8. Assume the transform coefficients of the block given in problem 3 of Chapter 5 belong to an H.261 codec. These coefficients are linearly quantised with the quantiser of Figure 6.9, with $th = 16$ and $q = 12$. Using Figure 6.12, calculate the number of bits required to code this block.

9. Pixels on the top left corner of a picture have values of:

200	135	180	210
75	110	134	230
62	89	52	14

   and are filtered with the loop filter of Figure 6.16. Find the filtered values of these pixels.

10. The maximum quantiser step size in H.261 is 62 (quantiser index is 31, defined with 5 bits). A 384-kbit/s H.261 encoder with an RM8 type rate control has a smoothing buffer of 5 kbytes. Find the spare capacity of the buffer when the quantiser step size is at its maximum value.

References

1. H.261: ‘Recommendation H.261, video codec for audiovisual services at p×64 kbit/s’, Geneva, 1990
2. CCITT SG XV WP/1/Q4: ‘Specialist group on coding for visual telephony’, Description of reference Model 8 (RM8), 1989

3. PLOMPEN, R.H.J.M.: 'Motion video coding for visual telephony' (Proefschrift, 1989)
4. NGAN, K.N.: 'Two-dimensional transform domain decimation technique', IEEE International Conference on Acoustics Speech and Signal Processing, ICASSP'86, 1986, pp. 1001–1004
5. CHEN, C.T. and WONG, A.: 'A self-governing rate buffer control strategy for pseudoconstant bit rate video coding', *IEEE Trans. Image Process.*, 1993, **2:1**, pp. 50–59
6. CARR, M.D.: 'Video codec hardware to realise a new world standard', *Br. Telecom. J.*, 1990, **8:3**, pp. 28–35

Chapter 7
Coding of moving pictures for digital storage media (MPEG-1)

MPEG-1 is the first generation of video codecs proposed by the Motion Picture Experts Group (MPEG) as a standard to provide video coding for digital storage media (DSM), such as compact disc (CD), digital audio tape (DAT), Winchester discs and optical drives [1]. This development was in response to industry needs for an efficient way of storing visual information on storage media other than the conventional analogue video cassette recorders (VCRs). At the time the CD-ROMs had the capability of 648 Mbytes, sufficient to accommodate movie programmes at a rate of approximately 1.2 Mbit/s, and the MPEG standard aimed to conform roughly to this target. Although in most applications the MPEG-1 video bit rate is in the range of 1–1.5 Mbit/s, the international standard does not limit the bit rate, and higher bit rates might be used for other applications.

It was also envisaged that the stored data be within both 625 and 525 line television systems and provide flexibility for use with workstations and personal computers. For this reason, the MPEG-1 standard is based on progressively scanned images and does not recognise interlacing. Interlaced sources have to be converted to a noninterlaced format before coding. After decoding, the decoded image may be converted back to provide an interlaced format for display.

Since coding for digital storage can be regarded as a competitor to VCRs, MPEG-1 video quality at the rate of 1–1.5 Mbit/s is expected to be comparable to VCRs. Also, it should provide the viewing conditions associated with VCRs such as forward play, freeze picture, fast forward, fast reverse, slow forward and random access. The ability of the decoder to provide these modes depends, to some extent, on the nature of DSM. However, it should be borne in mind that efficient coding and flexibility in operation are not compatible. Provision of the added functionality of random access necessitates regular intraframe pictures in the coded sequence. Those frames that do not exploit temporal redundancy in the video have poor compression, and as a result the overall bit rate is increased.

Both H.261 [2] and MPEG-1 [1] are standards defined for relatively low bit rate coding of low spatial resolution pictures. Like H.261, MPEG-1 utilises DCT for lossy coding of its intraframe and interframe prediction errors. The MPEG-1 video coding algorithm is largely an extension of H.261, and many of the features are common. Their bitstreams are, however, incompatible, although their encoding units are very similar.

The MPEG-1 standard, like H.261, does not specify the design of the decoder, and even less information is given about the encoder. What is expected from

MPEG-1, like H.261, is to produce a bitstream that is decodable. Manufacturers are free to choose any algorithms they wish and to optimise them for better efficiency and functionality. Therefore, in this chapter, we again look at the fundamentals of MPEG-1 coding rather than the details of the implementation.

7.1 Systems coding outline

The MPEG-1 standard gives the syntax description of how audio, video and data are combined into a single data stream. This sequence is formally termed as the ISO 11172 stream [3]. The structure of this ISO 11172 stream is illustrated in Figure 7.1. It consists of a compression layer and a systems layer. In this book, we study only the video part of the compression layer, but the systems layer is important for the proper delivery of the coded bitstream to the video decoder, and hence we briefly describe it.

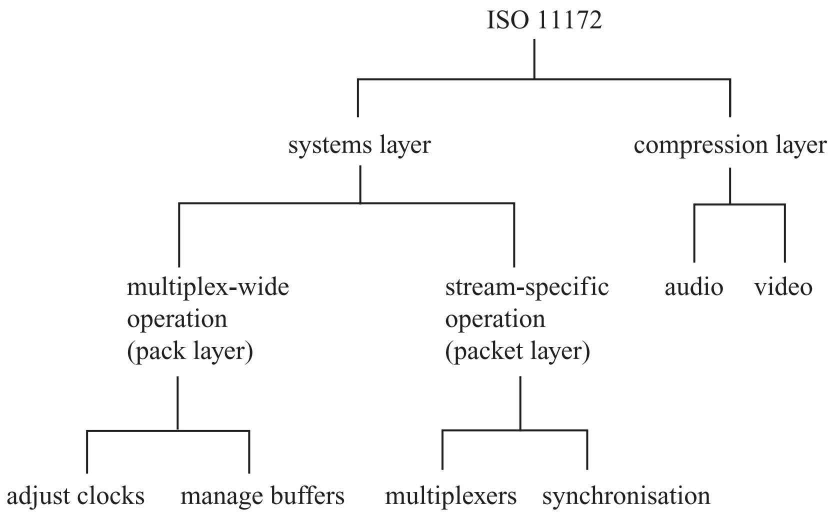

Figure 7.1 Structure of an ISO 11172 stream

The MPEG-1 systems standard defines a packet structure for multiplexing coded audio and video into one stream and keeping it synchronised. The systems layer is organised into two sublayers known as the pack and packet layers. A pack consists of a pack header that gives the systems clock reference (SCR) and the bit rate of the multiplexed stream followed by one or more packets. Each packet has its own header that conveys essential information about the elementary data that it carries. The aim of the systems layer is to support the combination of video and audio elementary streams. The basic functions are as follows:

- synchronised presentation of decoded streams
- construction of the multiplexed stream

- initialisation of buffering for playback start-up
- continuous buffer management
- time identification

In the systems layer, elements of direct interest to the video encoding and decoding processes are mainly those of the stream-specific operations, namely, multiplexing and synchronisation.

7.1.1 Multiplexing elementary streams

The multiplexing of elementary audio, video and data is performed at the packet level. Each packet thus contains only one elementary data type. The systems layer syntax allows up to 32 audio, 16 video and 2 data streams to be multiplexed together. If more than two data streams are needed, substreams may be defined.

7.1.2 Synchronisation

Multiple elementary streams are synchronised by means of presentation time stamps (PTS) in the ISO 11172 bitstream. End-to-end synchronisation is achieved when the encoders record time stamps during capture of raw data. The receivers will then make use of these PTS in each associated decoded stream to schedule their presentations. Playback synchronisation is pegged onto a master time base, which may be extracted from one of the elementary streams, DSM, channel or some external source. This prototypical synchronisation arrangement is illustrated in Figure 7.2. The occurrences of PTS and other information such as SCR and systems headers will also be essential for facilitating random access of the MPEG-1 bitstream. This set of access codes should therefore be located near to the part of the elementary stream where decoding can begin. In the case of video, this site will be near the head of an intraframe.

To ensure guaranteed decoder buffer behaviour, MPEG-1 systems layer employs a systems target decoder (STD) and decoding time stamp (DTS). The DTS differs from PTS only in the case of video pictures that require additional reordering delay during the decoding process.

7.2 Preprocessing

The source material for video coding may exist in a variety of forms such as computer files or live video in CCIR-601 format [4]. If CCIR-601 is the source, since MPEG-1 is for coding of video at VCR resolutions, then source input format (SIF) is normally used. These source pictures must be processed prior to coding. In Chapter 2, we explained how CCIR-601 video was converted to SIF format. If the source is film, we also discussed the conversion methodology in that chapter. However, if computer source files do not have the SIF format, they have to be converted too. In MPEG-1, another preprocessing is required to reorder the input pictures for coding. This is called picture reordering.

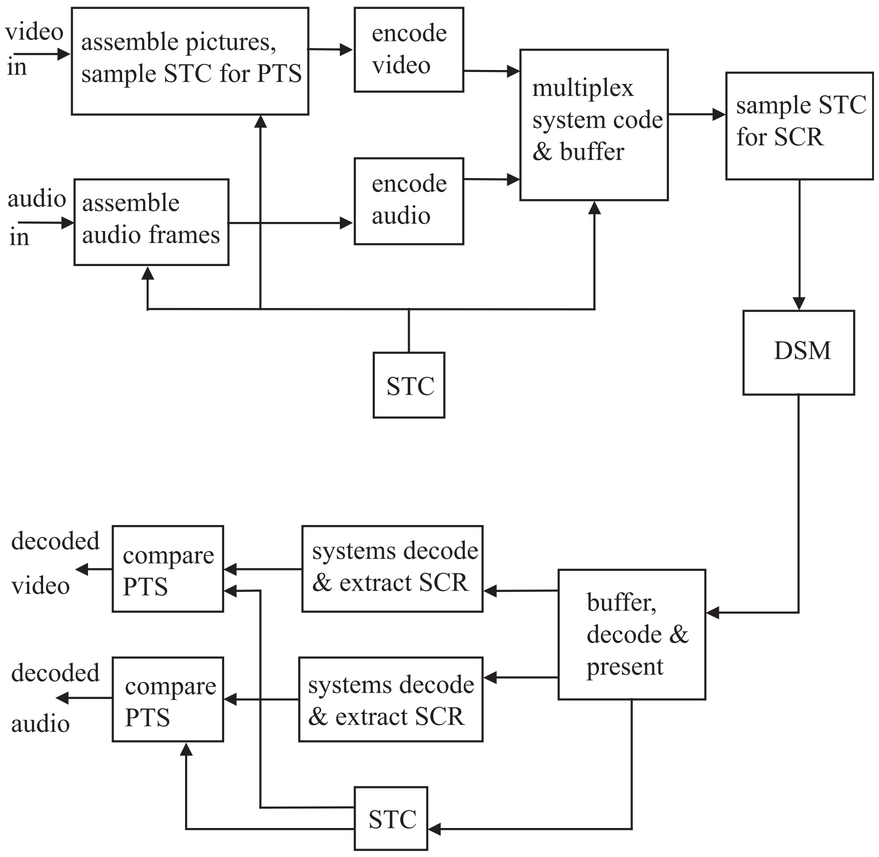

Figure 7.2 Prototypical encoder and decoder of MPEG-1, illustrating end-to-end synchronisation (STC, systems time clock; SCR, systems clock reference; PTS, presentation time stamp; DSM, digital storage media)

7.2.1 Picture reordering

Because of the conflicting requirements of random access and highly efficient coding, the MPEG suggested that all pictures of a video sequence should not be coded in the same way. They identified four types of picture in a video sequence. The first type is called I-pictures, which are coded without reference to the previous picture. They provide access points to the coded sequence for decoding. These pictures are intraframe coded as for JPEG, with a moderate compression. The second type is the P-pictures, which are predictively coded with reference to the previous I- or P-coded pictures. They themselves are used as a reference (anchor) for coding of the future pictures. Coding of these pictures is very similar to H.261. The third type is called B-pictures, or bidirectionally coded pictures, which may use past, future or combinations of both pictures in their predictions. This increases the motion compensation efficiency, since occluded parts of moving objects may be better compensated for from the future frame. B-pictures are never used for predictions. This part, which is unique to MPEG, has two important implications:

1. If B-pictures are not used for predictions of future frames, then they can be coded with the highest possible compression without any side effects. This is because, if one picture is coarsely coded and is used as a prediction, the coding distortions are transferred to the next frame. This frame then needs more bits to clear the previous distortions, and the overall bit rate may increase rather than decrease.
2. In applications such as transmission of video over packet networks, B-pictures may be discarded (e.g. due to buffer overflow) without affecting the next decoded pictures [5]. Note that if any part of the H.261 pictures, or I- and P-pictures in MPEG, is corrupted during the transmission, the effect will propagate until they are refreshed [6].

Figure 7.3 illustrates the relationship between these three types of picture. Since B-pictures use I- and P-pictures as predictions, they have to be coded later. This requires reordering the incoming picture order, which is carried out at the preprocessor.

The fourth picture type is the D-pictures. They are intraframe coded, where only the DC coefficients are retained. Hence, the picture quality is poor and normally used for applications like fast forward. D-pictures are not part of the GOP; hence, they are not present in a sequence containing any other picture types.

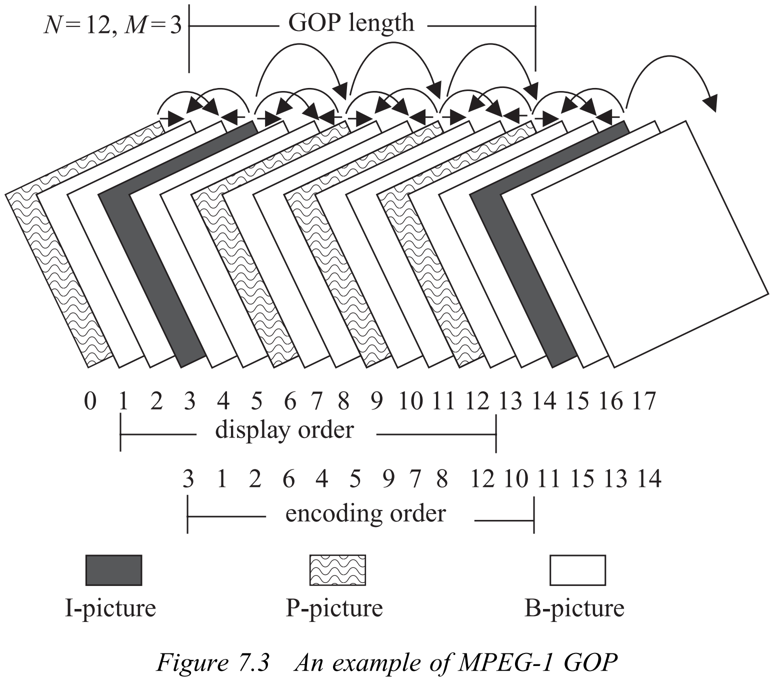

Figure 7.3 An example of MPEG-1 GOP

7.3 Video structure

7.3.1 Group of pictures

Since in the H.261 standard, successive frames are similarly coded, a picture is the top level of the coding hierarchy. In MPEG-1, due to the existence of several picture types, a group of pictures, called GOP, is the highest level of the hierarchy. A GOP is a series of one or more pictures to assist random access into the picture sequence. The first coded picture in the group is an I-picture. It is followed by an arrangement for P- and B-pictures, as shown in Figure 7.3.

The GOP length is normally defined as the distance between I-pictures, which is represented by parameter N in the standard codecs. The distance between the anchor I/P and P-pictures is represented by M. In the above figure, $N = 12$ and $M = 3$. The GOP may be of any length, but it should be at least one I-picture in each GOP. Applications requiring random access, fast forward play or fast and normal reverse play may use short GOPs. GOP may also start at scene cuts or other cases where motion compensation is not effective. The number of consecutive B-pictures varies. Neither a P- nor a B-picture needs to be present. For most applications, GOP in the SIF-625/50 format has $N = 12$ and $M = 3$. In SIF-525/60, the values are 15 and 3, respectively.

The encoding or transmission order of pictures differs from the display or incoming picture order. In the figure, B-pictures 1 and 2 are encoded after P-picture 0 and I-picture 3. Also in this figure, B-pictures 13 and 14 are a part of the next GOP. While their display order is 0, 1, 2, …, 11, their encoding order is 3, 1, 2, 6, 4, 5, …. This reordering introduces delays amounting to several frames at the encoder (equal to the number of B-pictures between the anchor I- and P-pictures). The same amount of delay is introduced at the decoder in putting the transmission/decoding sequence back to its original. This format inevitably limits the application of MPEG-1 for telecommunications.

7.3.2 Picture

All the three main picture types, I, P and B, have the same SIF size with 4:2:0 format. In SIF-625, the luminance part of each picture has 360 pixels, 288 lines and 25 Hz, and those of each chrominance are 180 pixels, 144 lines and 25 Hz. In SIF-525, these values for luminance are 360 pixels, 240 lines and 30 Hz, and for the chrominance are 180, 120 and 30, respectively. For 4:2:0 format images, the luminance and chrominance samples are positioned as shown in Figure 2.3.

7.3.3 Slice

Each picture is divided into a group of macroblocks, called *slices*. In H.261 such a group was called GOB. The reason for defining a slice is the same as that for defining a group of blocks (GOB), namely, resetting the variable length code (VLC) to prevent channel error propagation into the picture. Slices can have different sizes within a picture, and the division in one picture need not be the same as division in any other picture.

The slices can begin and end at any macroblock in a picture, but with some constraints. The first slice must begin at the top left of the picture (the first macroblock), and the end of the last slice must be the bottom right macroblock (the last macroblock) of the picture, as shown in Figure 7.4. Therefore, the minimum number of slices per picture is one, and the maximum number is equal to the number of macroblocks (e.g. 396 in SIF-625).

Each slice starts with a slice start code and is followed by a code that defines its position and a code that sets the quantisation step size. Note that in H.261, the quantisation step sizes were set at each GOB or row of GOBs, but in MPEG-1 they can be set at any macroblock (see section 7.3.4). Therefore, in MPEG-1, the main reason for defining slices is not to reset a new quantiser but to prevent the effects of channel error propagation. If the coded data are corrupted, and the decoder detects it, then it can search for the new slice, and the decoding starts from that point. Part of the picture slice from the start of the error to the next slice can then be degraded. Therefore, in a noisy environment, it is desirable to have as many slices as possible. On the other hand, each slice has a large overhead, called slice start code (minimum of 32 bits). This creates a large overhead in the total bit rate. For example, if we use the slice structure of Figure 7.4, where there is one slice for each row of MBs, then for SIF-625 video there are 18 slices/picture, and with 25 Hz video, the slice overhead can be $32 \times 18 \times 25 = 14\,400$bit/s.

1 begin	end 1
2 begin	end 2
3 begin	end 3
4 begin	end 4
5 begin	end 5
6 begin	end 6
7 begin	end 7
8 begin	end 8
9 begin	end 9
10 begin	end 10
11 begin	end 11
12 begin	end 12
13 begin	end 13
14 begin	end 14
15 begin	end 15
16 begin	end 16
17 begin	end 17
18 begin	end 18

Figure 7.4 An example of slice structure for SIF-625 pictures

To optimise the slice structure, that is, to give a good immunity from channel errors and at the same time to minimise the slice overhead, one might use short slices for macroblocks with significant energy (such as intra MB) and long slices for less significant ones (e.g. macroblocks in B-pictures). Figure 7.5 shows a slice structure, where in some parts the slice length extends beyond several rows of macroblocks and in some cases is less than one row.

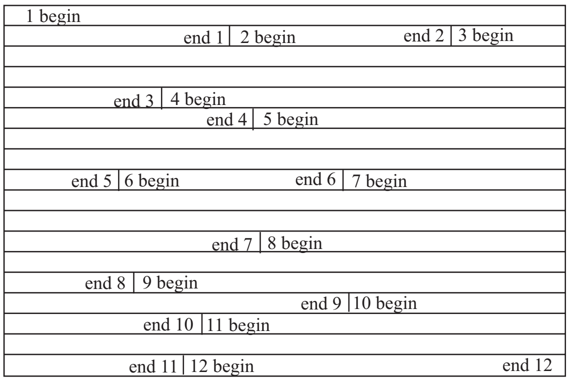

Figure 7.5 Possible arrangement of slices in SIF-625

7.3.4 Macroblock

Slices are divided into macroblocks of 16 × 16 pixels, similar to the division of GOB into macroblocks in H.261. Macroblocks in turn are divided into blocks for coding. In Chapter 6, we gave a detailed description of how a macroblock was coded, starting from its type, mode of selection, blocks within the MB, their positional addresses and finally the block pattern. Since MPEG-1 is also a macroblock-based codec, most of these rules are used in MPEG-1. However, because of differences of slice versus GOB, picture type versus a single picture format in H.261, there are bound to be variations in the coding. We first give a general account of these differences, and in the following section, more details are given about the macroblocks in the various picture types.

The first difference is that since a slice has a raster scan structure, macroblocks are addressed in a raster scan order. The top left macroblock in a picture has address 0, the next one on the right has address 1 and so on. If there are M macroblocks in a picture (e.g. $M = 396$), then bottom right macroblock has address $M - 1$. To reduce the address overhead, macroblocks are relatively addressed by transmitting the difference between the current macroblock and the previously coded macroblock. This difference is called *macroblock address increment.* In I-pictures, since all the macroblocks are coded, the macroblock address increment is always 1. The exception is that, for the first coded macroblock at the beginning of each slice, the macroblock address is set to that of the right-hand macroblock of the previous row. This address at the beginning of each picture is set to -1. If a slice does not start at the left edge of the picture (see the slice structure of Figure 7.5), then the macroblock address increment for the first macroblock in the slice will be larger than 1. For example, in the slice structure of Figures 7.4 and 7.5, there are 22 macroblocks/row. For Figure 7.4, at the start of slice 2, the macroblock address is set to 21, which is the address of the macroblock at the right-hand edge of the top row of macroblocks. In Figure 7.5, if the first slice contains 30 macroblocks, 8 of them would be in the second row, so the address of the first macroblock in the second slice would be 30 and the macroblock increment would be 9. For further reduction of address overhead, macroblock address increments are variable length coded.

There is no code to indicate a macroblock address increment of 0. This is why the macroblock address is set to −1 rather than 0 at the top of the picture. The first macroblock will have an increment of 1, making its address equal to 0.

7.3.5 Block

Finally, the smallest part of the picture structure is the *block* of 8 × 8 pixels, for both luminance and chrominance components. DCT coding is applied at this block level. Figure 7.6 illustrates the whole structure of partitioning a video sequence from its GOP level at the top to the smallest unit of block at the bottom.

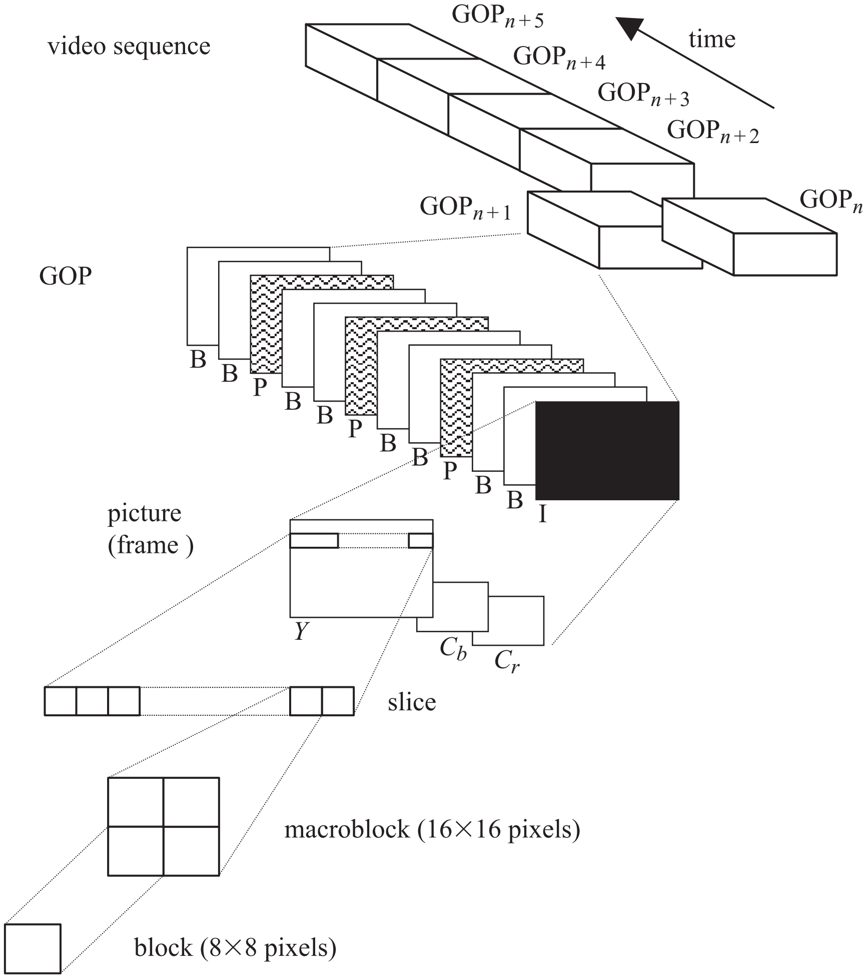

Figure 7.6 MPEG-1-coded video structure

7.4 Encoder

As mentioned, the international standard does not specify the design of the video encoders and decoders. It only specifies the syntax and semantics of the bitstream and signal processing at the encoder/decoder interface. Therefore, options are left open to the video codec manufacturers to trade-off cost, speed, picture quality and coding efficiency. As a guideline, Figure 7.7 shows a block diagram of an MPEG-1 encoder. Again it is similar to the generic codec of Figure 3.19 and the H.261 codec of Chapter 6. For simplicity, the coding flags shown in the H.261 codec are omitted, though they also exist.

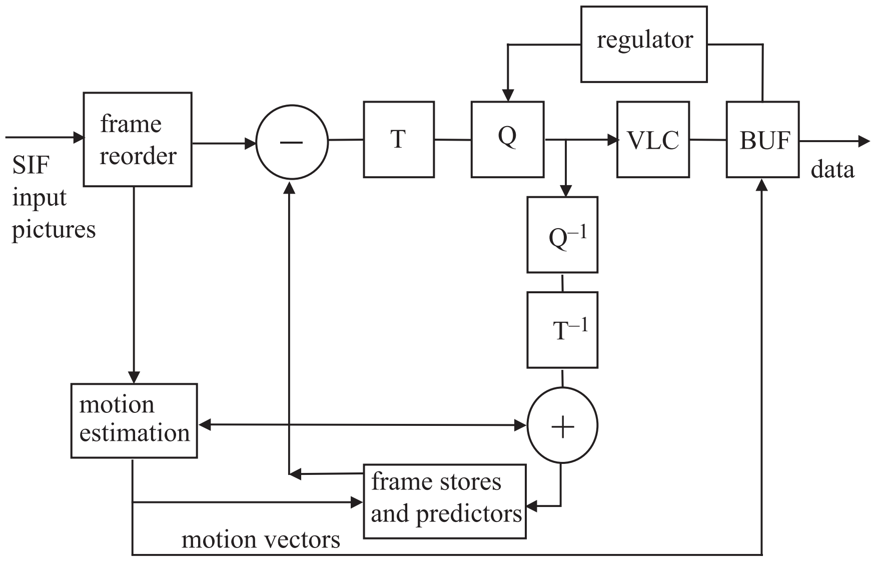

Figure 7.7 A simplified MPEG-1 video encoder

The main differences between this encoder and that defined in H.261 are as follows:

- *Frame reordering*: at the input of the encoder, coding of B-pictures is postponed to be carried out after coding the anchor I- and P-pictures.
- *Quantisation*: intraframe coded macroblocks are subjectively weighted to emulate perceived coding distortions.
- *Motion estimation*: not only is the search range extended but the search precision is increased to half a pixel. B-pictures use bidirectional motion compensation.
- *No loop filter.*
- *Frame store and predictors*: to hold two anchor pictures for prediction of B-pictures.
- *Rate regulator*: here there is more than one type of picture, each generating different bit rates.

Before describing how each picture type is coded, and the main differences between this codec and H.261, we can describe the codec on a macroblock basis, as the basic unit of coding. Within each picture, macroblocks are coded in a sequence from left to right. Since 4:2:0 image format is used, the six blocks of 8×8 pixels, four luminance and one of each chrominance components are coded in turn. Note that the picture area covered by the four luminance blocks is the same as the area covered by each of the chrominance blocks.

First, for a given macroblock, the coding mode is chosen. This depends on the picture type, the effectiveness of motion-compensated prediction in that local region and the nature of the signal within the block. Second, depending on the coding mode, a motion-compensated prediction of the contents of the block based on the past and/or future reference pictures is formed. This prediction is subtracted from the actual data in the current macroblock to form an error signal. Third, this error signal is divided into 8×8 blocks and a DCT is performed on each block. The resulting two-dimensional 8×8 block of DCT coefficients is quantised and is scanned in zigzag order to convert into a one-dimensional string of quantised DCT coefficients. Fourth, the side information for the macroblock, including the type, block pattern, motion vector and address alongside the DCT coefficients are coded. For maximum efficiency, all the data are variable length coded. The DCT coefficients are run length coded with the generation of events, as we discussed in H.261.

A consequence of using different picture types and variable length coding is that the overall bit rate is very variable. In applications that involve a fixed rate channel, a first-in, first-out (FIFO) buffer is used to match the encoder output to the channel. The status of this buffer may be monitored to control the number of bits generated by the encoder. Controlling the quantiser index is the most direct way of controlling the bit rate. The international standard specifies an abstract model of the buffering system (the video buffering verifier) in order to limit the maximum variability in the number of bits that are used for a given picture. This ensures that a bitstream can be decoded with a buffer of known size (see section 7.8).

7.5 Quantisation weighting matrix

The insensitivity of the human visual system to high-frequency distortions can be exploited for further bandwidth compression. In this case, the higher orders of DCT coefficients are quantised with coarser quantisation step sizes than the lower frequency ones. Experience has shown that for SIF pictures, a suitable distortion weighting matrix for the intra-DCT coefficients is the one shown in Figure 7.8. This intra matrix is used as the default quantisation matrix for intraframe coded macroblocks.

If the picture resolution departs significantly from the SIF size, then some other matrix may give perceptively better results. The reason is that this matrix is derived from the vision contrast sensitivity curve, for a nominal viewing distance (e.g. viewing distances of four to six times the picture height) [7]. For higher or lower picture resolutions, or changing the viewing distance, the spatial frequency will change, and hence different weighting will be derived.

It should be noted that different weightings may not be used for interframe coded macroblocks. This is because high-frequency interframe error does not necessarily mean high spatial frequency. It might be due to poor motion compensation or block boundary artefacts. Hence, interframe coded macroblocks use a flat quantisation matrix. This matrix is called the inter or nonintra quantisation weighting matrix.

$$\underset{\text{intra}}{\begin{array}{cccccccc}
8 & 16 & 19 & 22 & 26 & 27 & 29 & 34 \\
16 & 16 & 22 & 24 & 27 & 29 & 34 & 37 \\
19 & 22 & 26 & 27 & 29 & 34 & 34 & 38 \\
22 & 22 & 26 & 27 & 29 & 34 & 37 & 40 \\
22 & 26 & 27 & 29 & 32 & 35 & 40 & 48 \\
26 & 27 & 29 & 32 & 35 & 40 & 48 & 58 \\
26 & 27 & 29 & 34 & 38 & 46 & 56 & 69 \\
27 & 29 & 35 & 38 & 46 & 56 & 69 & 83
\end{array}}
\qquad
\underset{\text{inter}}{\begin{array}{cccccccc}
16 & 16 & 16 & 16 & 16 & 16 & 16 & 16 \\
16 & 16 & 16 & 16 & 16 & 16 & 16 & 16 \\
16 & 16 & 16 & 16 & 16 & 16 & 16 & 16 \\
16 & 16 & 16 & 16 & 16 & 16 & 16 & 16 \\
16 & 16 & 16 & 16 & 16 & 16 & 16 & 16 \\
16 & 16 & 16 & 16 & 16 & 16 & 16 & 16 \\
16 & 16 & 16 & 16 & 16 & 16 & 16 & 16 \\
16 & 16 & 16 & 16 & 16 & 16 & 16 & 16
\end{array}}$$

Figure 7.8 Default intra and inter quantisation weighting matrices

Note that since in H.261 all the pictures are interframe coded and a very few macroblocks might be intra coded, only the nonintra weighting matrix is defined. Little work has been performed to determine the optimum nonintra matrix for MPEG-1, but evidence suggests that the coding performance is more related to the motion and the texture of the scene than the nonintra quantisation matrix. If there is any optimum matrix, it should then be somewhere between the flat default inter matrix and the strongly frequency-dependent values of the default intra matrix.

The DCT coefficients, prior to quantisation, are divided by the weighting matrix. Note that the DCT coefficients prior to weighting have a dynamic range from −2047 to +2047. Weighted coefficients are then quantised by the quantisation step size, and at the decoder, reconstructed quantised coefficients are then multiplied to the weighting matrix to reconstruct the coefficients.

7.6 Motion estimation

In Chapter 3, block matching motion estimation/compensation and its application in standard codecs was discussed in great detail. We even introduced some fast search methods for estimation, which can be used in software-based codecs. As we saw, motion estimation in H.261 was optional. This was mainly due to the assumption that since motion compensation can reduce correlation, DCT coding may not be efficient. Investigations since the publication of H.261 have proved that this is not the case. What is expected from a DCT is to remove the spatial correlation within a small area of 8×8 pixels. Measurement of correlations between the adjacent error pixels has shown that there is still strong correlation between the error pixels, which does not impair the potential of DCT for spatial redundancy reduction. Hence, motion estimation has become an important integral part of all the later video codecs, such as MPEG-1, MPEG-2, H.263, H.264 and MPEG-4. These are explained in the relevant chapters.

Considering MPEG-1, the strategy for motion estimation in this codec is different from the H.261 in four main respects:

1. Motion estimation is an integral part of the codec.
2. Motion search range is much larger.
3. Higher precision of motion compensation is used.
4. B-pictures can benefit from bidirectional motion compensation.

These features are described in the following sections.

7.6.1 Larger search range

In H.261, if motion compensation is used, a search is carried out within every subsequent frame. Also, H.261 is normally used for head-and-shoulders pictures, where the motion speed is normally very small. In contrast, MPEG-1 is used mainly for coding of films with much larger movements and activities. Moreover, in search for motion in P-pictures, since they might be several frames apart, the search range becomes many times larger. For example, in a GOP structure with $M = 3$, where there are two B-pictures between the anchor pictures, the motion speed is three times greater than that for consecutive pictures. Thus, in MPEG-1, we expect a much larger search range. Considering that in full search block matching the number of search positions for a motion speed of w is $(2w + 1)^2$, tripling the search range makes motion estimation prohibitively computationally expensive.

In Chapter 3, we introduced some fast search methods such as logarithmic step searches and hierarchical motion estimation. Although the hierarchical method can be used here, of course needing one or more levels of hierarchy, use of a logarithmic search may not be feasible. This is because these methods are very prone to large search ranges, and at these ranges the final minima can be very far away from the local minima, causing the estimation to fail [8].

One way of alleviating this problem is to use a telescopic search method. This is unique to MPEG with B-pictures. In this method, rather than searching for the motion between the anchor pictures, the search is carried out on all the consecutive pictures, including B-pictures. The final search between the anchor pictures is then the sum of all the intermediate motion vectors, as shown in Figure 7.9. Note that since we are now searching for motion in successive pictures, the search range is smaller, and even fast search methods can be used.

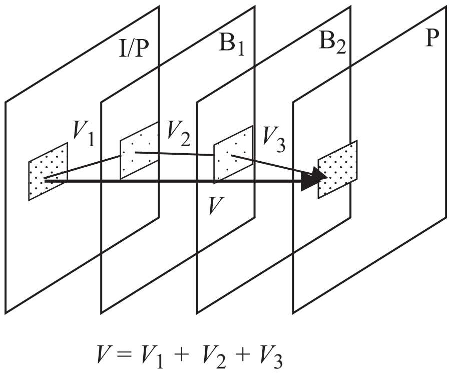

Figure 7.9 Telescopic motion search

7.6.2 Motion estimation with half-pixel precision

In the search process with a half-pixel resolution, normal block matching with integer pixel positions is carried out first. Then eight new positions, with a distance of half a pixel around the final integer pixel, are tested. Figure 7.10 shows a part of the search area, where the coordinate marked A has been found as the best integer pixel position at the first stage.

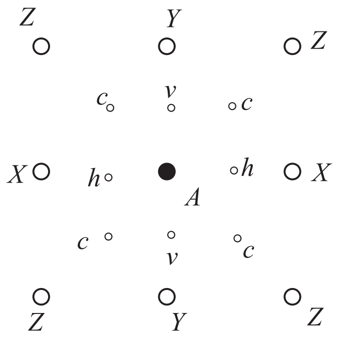

Figure 7.10 Subpixel search positions around pixel coordinate A

In testing the eight subpixel positions, pixels of the macroblock in the previous frame are interpolated, according to the positions to be searched. For subpixel positions, marked with h in the middle of the horizontal pixels, the interpolation is

$$h = \frac{A + X}{2} \tag{7.1}$$

where the division is truncated. For the subpixels in the vertical midpoints, the interpolated values for the pixels are

$$v = \frac{A + Y}{2} \tag{7.2}$$

and for subpixels in the corner (centre of four pixels), the interpolation is

$$c = \frac{A + X + Y + Z}{4} \tag{7.3}$$

Note that in subpixel precision motion estimation, the range of the motion vectors' addresses is increased by 1 bit for each of the horizontal and vertical directions. Thus, the motion vector overhead may be increased by 2 bit/vector (in practice due to variable length coding, this might be less than 2 bits). Despite this increase in motion vector overhead, the efficiency of motion compensation outweighs the extra bits, and the overall bit rate is reduced. Figure 7.11 shows the motion-compensated error, with and without half-pixel precision, for two consecutive frames of the Claire sequence. The motion-compensated error has been magnified by a factor of 4 for better representation. It might be seen that half-pixel precision has fewer blocking artefacts and, in general, motion-compensated errors are smaller.

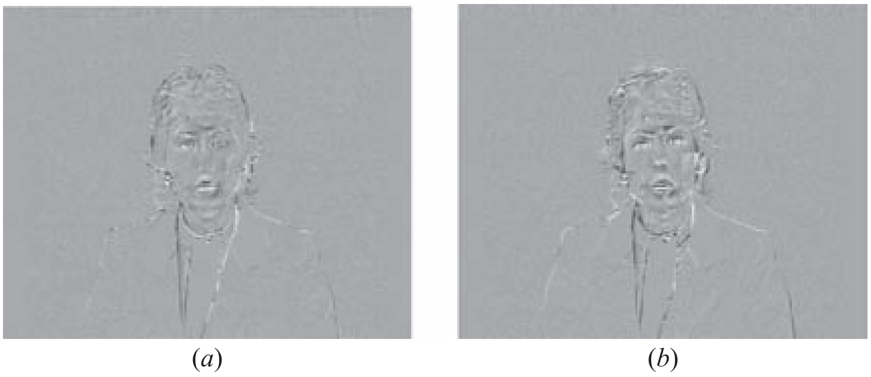

Figure 7.11 Motion-compensated prediction error (a) with and (b) without half-pixel precision

For further reduction on the motion vector overhead, differential coding is used. The prediction vector at the start of each slice and each intra coded macroblock is set to zero. Note that the predictively coded macroblocks with no motion vectors also set the prediction vector to zero. The motion vector prediction errors are then variable length coded.

7.6.3 Bidirectional motion estimation

B-pictures have access to both past and future anchor pictures. They can then use either past frame, called *forward* motion estimation, or the future frame, for *backward* motion estimation, as shown in Figure 7.12.

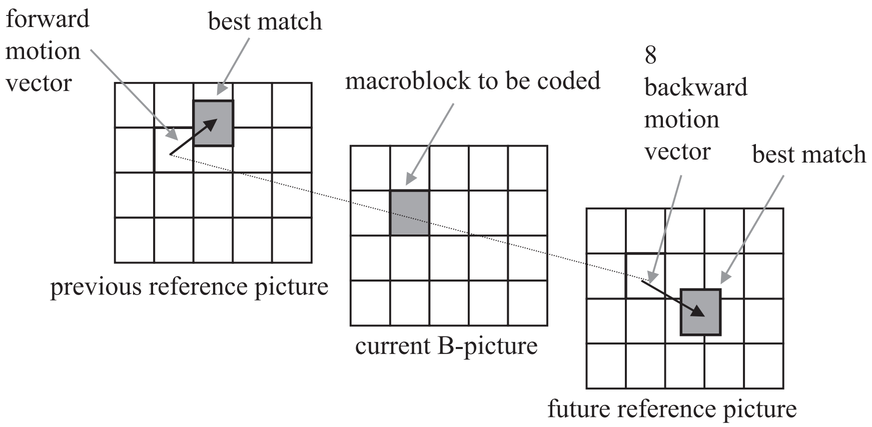

Figure 7.12 Motion estimation in B-pictures

Such an option increases the motion compensation efficiency, particularly when there are occluded objects in the scene. In fact, one of the reasons for the introduction of B-pictures was this fact that the forward motion estimation used in H.261 and P-pictures cannot compensate for the uncovered background of moving objects.

From the two forward and backward motion vectors, the coder has a choice of choosing any of the forward, backward or their combined motion-compensated predictions. In the latter case, a weighted average of the forward and backward motion-compensated pictures is calculated. The weight is inversely proportional to the distance of the B-picture with its anchor pictures. For example, in the GOB structure of I, B_1, B_2, P, the bidirectionally interpolated motion-compensated picture for B_1 would be two-thirds of the forward motion-compensated pixels from the I-picture and one-third from backward motion-compensated pixels of the P-picture. This ratio is reversed for B_2. Note that B-pictures do not use motion compensation from each other, since they are not used as predictors. Also note that the motion vector overhead in B-pictures is much more than in P-pictures. The reason is that, for B-pictures, there are more macroblock types, which increase the macroblock type overhead, and for the bidirectionally motion-compensated macroblocks two motion vectors have to be sent.

7.6.4 Motion range

When B-pictures are present, due to various distances between a picture and its anchor, it is expected that the search range for motion estimation to be different for different picture types. For example, with $M = 3$, P-pictures are three frames apart from their anchor pictures. B_1-pictures are only one frame apart from their past frame and two frames from their future frames, and those of B_2-pictures are in reverse order. Hence, motion range for P-pictures is larger than the backward motion range of B_1-pictures, which is itself larger than the forward motion vector.

For normal scenes, the maximum search range for P-pictures is usually taken as 11 pixels/3 frames, and the forward and backward motion range for B_1-pictures are 3 pixels/frame and 7 pixels/2 frames, respectively. These values for B_2-pictures become 7 and 3.

It should be noted that although motion estimation for B-pictures, due to the calculation of forward and backward motion vectors, is more processing demanding than that of the P-pictures, due to larger motion range for P-pictures, the latter can be costlier than the former. For example, if the full search method is used, the number of search operations for P-pictures will be $(2 \times 11 + 1)^2 = 529$. This value for the forward and backward motion vectors of B_1-pictures will be $(2 \times 3 + 1)^2 = 49$ and $(2 \times 7 + 1)^2 = 225$, respectively. For B_2-pictures, the forward and backward motion estimation cost becomes 225 and 49, respectively. Thus, while motion estimation cost for P-pictures in this example is 529, the cost for a B-picture is about $49 + 225 = 274$, which is less. For motion estimation with half-pixel accuracy, for P- and B-pictures, 8 and 16 more operations have to be added to these values, respectively. For more active pictures, where the search range for both P- and B-pictures is larger, the gap on motion estimation cost becomes wider.

7.7 Coding of pictures

Since the encoder was described in terms of the basic unit of a macroblock, the picture types may be defined in terms of their macroblock types. In the following, each of these picture types is defined.

7.7.1 I-pictures

In I-pictures, all the macroblocks are intra coded. There are two intra macroblock types: one that uses the current quantiser scale, intra-d, and the other that defines a new value for the quantiser scale, intra-q. Intra-d is the default value when the quantiser scale is not changed. Although these two types can be identified with 0 and 1, and no VLC is required, the standard has foreseen some possible extensions to the macroblock types in the future. For this reason, they are variable length coded and intra-d is assigned with 1, and intra-q with 01. Extensions to the VLCs with the start code of 0 are then open. The policy of making the coding tables open in this way was adopted by the MPEG group video committee in developing the international standard. The advantage of future extensions was judged to be worth the slight coding inefficiency.

If the macroblock type is intra-q, then the macroblock overhead should contain an extra 5 bits to define the new quantiser scale between 1 and 31. For intra-d macroblocks, no quantiser scale is transmitted and the decoder uses the previously set value. Therefore, the encoder may prefer to use as many intra-d types as possible. However, when the encoding rate is to be adjusted, which normally causes a new quantiser to be defined, the type is changed to intra-q. Note that since in H.261 the bit rate is controlled at either the start of GOBs or rows of a GOB, if there is any intra-q in a GOB, it must be the first MB in that GOB, or rows of the GOB. In I-pictures of MPEG-1, an intra-q can be any of the macroblocks.

Each block within the MB is DCT coded, and the coefficients are divided by the quantiser step size, rounded to the nearest integer. The quantiser step size is derived from the multiplication of the quantisation weighting matrix and the quantiser index (1–31). Thus, quantiser step size is different for different coefficients and may change from MB to MB. The only exception is the DC coefficients, which are treated differently. This is because the eye is sensitive to large areas of luminance and chrominance errors; then the accuracy of each DC value should be high and fixed. The quantiser step size for the DC coefficient is fixed to eight. Since in the quantisation weighting matrix, the DC weighting element is eight, then the quantiser index for the DC coefficient is always 1, irrespective of the quantisation index used for the remaining AC coefficients.

Because of the strong correlation between the DC values of blocks within a picture, the DC indices are coded losslessly by DPCM. Such a correlation does not exist among the AC coefficients, and hence they are coded independently. The prediction for the DC coefficients of luminance blocks follows the coding order of blocks within a macroblock and the raster scan order. For example, in the macroblocks of 4:2:0 format pictures shown in Figure 7.13, the DC coefficient of block Y_2 is used as a prediction for the DC coefficient of block Y_3. The DC coefficient of block Y_3 is a prediction for the DC coefficient of Y_0 of the next macroblock. For the chrominance, we use the DC coefficients of the corresponding value of the block in the previous macroblock.

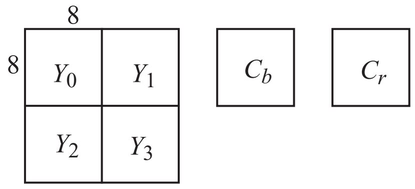

Figure 7.13 Positions of luminance and chrominance blocks within a macroblock in 4:2:0 format

The differentially coded DC coefficient and the remaining AC coefficients are zigzag scanned, in the same manner as was explained for H.261 coefficients in Chapter 6. A copy of the coded picture is stored in the frame store to be used for the prediction of the next P and the past or future B-pictures.

7.7.2 P-pictures

As in I-pictures, each P-picture is divided into slices, which are in turn divided into macroblocks and then blocks for coding. Coding of P-pictures is more complex than for I-pictures, since motion-compensated blocks may be constructed. For inter macroblocks, the difference between the motion-compensated macroblock and the current macroblock is partitioned into blocks, and then DCT transformed and coded.

Decisions on the type of macroblock, or whether motion compensation should be used, are similar to those of H.261 (see Chapter 6). Other H.261 coding tools such as differential encoding of motion vectors, coded block pattern, zigzag scan, and nature of variable length coding are similar. In fact, coding of P-pictures is the same as coding each frame in H.261 with two major differences:

1. Motion estimation has a half-pixel precision, and because of larger distances between the P-frames, the motion estimation range is much larger.
2. In MPEG-1, all intra MBs use the quantisation weighting matrix, whereas in H.261 all MBs use a flat matrix. Also in MPEG-1, the intra MB of P-pictures are predictively coded like those of I-pictures, with the exception that the prediction value is fixed at 128×8 if the previous macroblock is not intra coded.

Locally decoded P-pictures are stored in the frame store for further prediction. Note that if B-pictures are used, two buffer stores are needed to store two prediction pictures.

7.7.3 B-pictures

As in I- and P-pictures, B-pictures are divided into slices, which in turn are divided into macroblocks for coding. Because of the possibility of bidirectional motion compensation, coding is more complex than for P-pictures. Thus, the encoder has more decisions to make than in the case of P-pictures. These are how to divide the picture into slices; determine the best motion vectors to use; decide whether to use forward, backward or interpolated motion compensation or to code intra; and how to set the quantiser scale. These make processing of B-pictures computationally very intensive. Note that motion compensation is the most costly operation in the codecs, and for every macroblock, both forward and backward motion compensations have to be performed.

The encoder does not need to store decoded B-pictures, since they are not used for prediction. Hence, B-pictures can be coded with larger distortions. In this regard to reduce the slice overhead, larger slices (fewer slices in the picture) may be chosen.

In P-pictures, as for H.261, there are eight different types of macroblocks. In B-pictures, because of backward motion compensation and interpolation of forward and backward motion compensation, the number of macroblock types is about 14. Figure 7.14 shows the flow chart for macroblock type decisions in B-pictures.

The decision on the macroblock type starts with the selection of a motion compensation mode based on the minimisation of a cost function. The cost function is the mean-squared/absolute error of the luminance difference between the motion-compensated macroblock and the current macroblock. The encoder first calculates the best forward motion-compensated macroblock from the previous anchor picture for forward motion compensation. It then calculates the best motion-compensated macroblock from the future anchor picture, as the backward motion compensation. Finally, the average of the two motion-compensated errors is calculated to produce the interpolated macroblock. It then selects one that had the smallest error difference with the current macroblock. In the event of a tie, an interpolated mode is chosen.

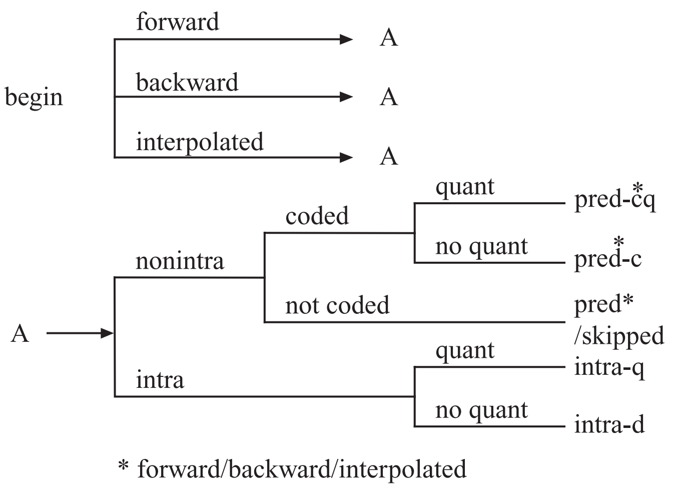

Figure 7.14 Selection of macroblock types in B-pictures

Another difference between macroblock types in B- and P-pictures is in the definition of noncoded and skipped macroblocks. In P-pictures, the skipped MB is the one that none of its blocks has any significant DCT coefficient (coded block pattern, or cbp = 0), and the motion vector is also zero. The first and the last MB in a slice cannot be declared skipped. They are treated as noncoded.

A noncoded MB in P-pictures is the one that none of its blocks has any significant DCT coefficient (cbp = 0), but the motion vector is nonzero. Thus, the first and the last MBs in a slice, which could be skipped, are noncoded with motion vector set to zero! In H.261, the noncoded MB was called motion compensated only (MC).

In B-pictures, the skipped MB has again all zero DCT coefficients, but the motion vector and the type of prediction mode (forward, backward or interpolated) is exactly the same as those of its previous MB. Similar to P-pictures, the first and the last MB in a slice cannot be declared skipped and is, in fact, called noncoded.

The noncoded MB in B-pictures has all of its DCT coefficients zero (cbp = 0), but either its motion vector or its prediction (or both) is different from its previous MB.

7.7.4 D-pictures

D-pictures contain only low-frequency information and are coded as the DC coefficients of the blocks. They are intended to be used for fast visible search modes. A bit is transmitted for the macroblock type, although there is only one type. In addition, there is a bit denoting the end of the macroblock. D-pictures are not part of the constrained bitstream.

7.8 Video buffer verifier

A coded bitstream contains different types of pictures, and each type ideally requires a different number of bits to encode. In addition, the video sequence may vary in complexity with time, and it may be desirable to devote more coding bits to one part of a sequence than to another. For constant bit rate coding, varying the number of bits allocated to each picture requires that the decoder has a buffer to store the bits not needed to decode the immediate picture. The extent to which an encoder can vary the number of bits allocated to each picture depends on the size of this buffer. If the buffer is large, an encoder can use greater variations, increasing the picture quality, but at the cost of increasing the decoding delay. The delay is the time taken to fill the input buffer from empty to its current level. An encoder needs to know the size of the decoder's input buffer in order to determine to what extent it can vary the distribution of coding bits among the pictures in the sequence.

In constant bit rate applications (e.g. decoding a bitstream from a CD-ROM), problems of synchronisation may occur. In these applications, the encoder should generate a bitstream that is perfectly matched to the device. The decoder will display the decoded pictures at their specific rate. If the display clock is not locked to the channel data rate, and this is typically the case, then any mismatch between the encoder and channel clock and the display clock will eventually cause a buffer overflow or underflow. For example, assume that the display clock runs 1 part per million too slow with respect to the channel clock. If the data rate is 1 Mbit/s, then the input buffer will fill at an average rate of 1 bit/s, eventually causing an overflow. If the decoder uses the entire buffer to allocate bits between pictures, the overflow could occur more quickly. For example, suppose the encoder fills the buffer completely except for 1 byte at the start of each picture, then overflow will occur after only 8 s!

The model decoder is defined to resolve three problems: it constrains the variability in the number of bits that may be allocated to different pictures; it allows a decoder to initialise its buffer when the system is started; and it allows the decoder to maintain synchronisation while the stream is played. At the beginning of this chapter, we mentioned multiplexing and synchronisation of audio and video streams. The tools defined in the international standard for the maintenance of synchronisation should be used by decoders when multiplexed streams are being played.

The definition of the parameterised model decoder is known as video buffer verifier (VBV). The parameters used by a particular encoder are defined in the bitstream. This really defines a model decoder that is needed if encoders are to be assured that the coded bitstream they produce will be decodable. The model decoder looks like Figure 7.15.

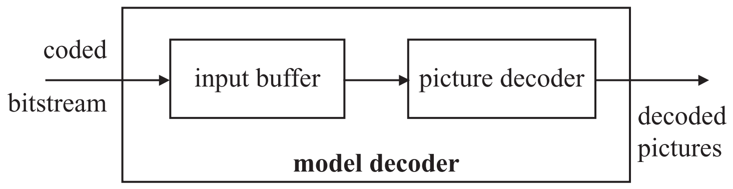

Figure 7.15 Model decoder

A fixed rate channel is assumed to put bits at a constant rate into the buffer, at regular intervals, set by the picture rate. The picture decoder instantaneously removes all the bits pertaining to the next picture from the input buffer. If there are too few bits in the input buffer, that is, all the bits for the next picture have been received, then the input buffer underflows, and there is an underflow error. If during the time between the picture starts, the capacity of the input buffer is exceeded, then there is an overflow error.

Practical decoders may differ from this model in several important ways. They may not remove all the bits required to decode a picture from the input buffer instantaneously. They may not be able to control the start of decoding very precisely as required by the buffer fullness parameters in the picture header, and they take a finite time to decode. They may also be able to delay decoding for a short time to reduce the chance of underflow occurring. But these differences depend in degree and kind on the exact method of implementation. To satisfy the requirements of different implementations, the MPEG video committee chose a very simple model for the decoder. Practical implementations of decoders must ensure that they can decode the bitstream constrained in this model. In many cases, this will be achieved by using an input buffer that is larger than the minimum required and by using a decoding delay that is larger than the value derived from the buffer fullness parameter. The designer must compensate for any differences between the actual design and the model in order to guarantee that the decoder can handle any bitstream that satisfies the model.

Encoders monitor the status of the model to control the encoder so that overflow does not occur. The calculated buffer fullness is transmitted at the start of each picture so that the decoder can maintain synchronisation.

7.8.1 Buffer size and delay

For constant bit rate operation, each picture header contains a variable-delay parameter (*vbv_delay*) to enable decoders to synchronise their decoding correctly. This parameter defines the time needed to fill the input buffer of Figure 7.15 from an empty state to the current level immediately before the picture decoder removes all the bits from the picture. This time thus represents a delay and is measured in units of 1/90 000 s. This number was chosen because it is almost an exact factor of the picture duration in various original video formats: 1/24, 1/25, 1/29.97 and 1/30 s, and because it is comparable in duration to an audio sample.

The delay is given by

$$D = \frac{vbv\_delay}{90\,000}\,\mathrm{s} \tag{7.4}$$

For example, if *vbv_delay* was 9000, then the delay would be 0.1 s. This means that at the start of a picture the input buffer of the model decoder should contain exactly 0.1 s worth of data from the input bitstream.

The bit rate, *R*, is defined in the sequence header. The number of bits in the input buffer at the beginning of the picture is thus given by

$$B = D \times R = \frac{vbv\_delay}{90\,000} \times R\ \mathrm{bits} \tag{7.5}$$

For example, if *vbv_delay* and *R* were 9000 and 1.2 Mbit/s, respectively, then the number of bits in the input buffer would be 120 kbits. The constrained parameter bitstream requires that the input buffers have a capacity of 327 680 bits, and *B* should never exceed this value [3].

7.8.2 Rate control and adaptive quantisation

The encoder must make sure that the input buffer of the model decoder is neither overflowed nor underflowed by the bitstream. Since the model decoder removes all the bits associated with a picture from its input buffer instantaneously, it is necessary to control the total number of bits per picture. In H.261, we saw that the encoder could control the bit rate by simply checking its output buffer content. As the buffer fills up, the quantiser step size is raised to reduce the generated bit rate, and vice versa. The situation in MPEG-1, because of the existence of three different picture types, where each generates a different bit rate, is slightly more complex. First, the encoder should allocate the total number of bits among the various types of picture within a GOP, so that the perceived image quality is suitably balanced. The distribution will vary with the scene content and the particular distribution of I-, P- and B-pictures within a GOP.

Investigations have shown that for most natural scenes, each P-picture might generate as many as two to five times the number of bits of a B-picture, and an I-picture three times those of the P-picture. If there is little motion and high texture, then a greater proportion of the bits should be assigned to I-pictures. Similarly, if there is strong motion, then a proportion of bits assigned to P-pictures should be increased. In both cases, lower quality from the B-pictures is expected to permit the anchor I- and P-pictures to be coded at their best possible quality.

Our investigations with variable bit rate (VBR) video, where the quantiser step size is kept constant (no rate control), show that the ratios of generated bits are 6:3:2, for I-, P- and B-pictures, respectively [9]. Of course, at these ratios, because of the fixed quantiser step size, the image quality is almost constant, not only for each picture (in fact, slightly better for B-pictures due to better motion compensation) but throughout the image. Again, if we lower the expected quality for B-pictures, we can change that ratio in favour of I- and P- pictures.

Although these ratios appear to be very important for a suitable balance in picture quality, one should not worry very much about their exact values. The reason is that it is possible to make the encoder intelligent enough to learn the best ratio. For example, after coding each GOP, one can multiply the average value of the quantiser scale in each picture by the bit rate generated at that picture. Such a quantity can be used as the complexity index, since larger complexity indices should be due to both larger quantiser step sizes and larger bit rates. Therefore, based on the complexity index one can derive a new coding ratio, and the target bit rate for each picture in the next GOP is based on this new ratio.

As an example, let us assume that SIF-625 video is to be coded at 1.2 Mbit/s. Let us also assume that the GOP structure of $N = 12$ and $M = 3$ is used. Therefore, there will be one I-picture, three P-pictures and eight B-pictures in each GOP. First of all, the target bit rate for each GOP is $1200 \times (12/25) = 576$ kbit/GOP. If we assume a coding ratio of 6:3:2, then the target bit rate for each of the I-, P- and B-pictures will be

$$\text{I-picture} \quad \frac{6}{6+3\times 3+2\times 8} \times 576 = \frac{6}{31} \times 576 = 112 \text{ kbits}$$

$$\text{P-picture} \quad \frac{3}{31} \times 576 = 56 \text{ kbits}$$

$$\text{B-picture} \quad \frac{2}{31} \times 576 = 37 \text{ kbits}$$

Therefore, each picture is aiming for its own target bit rate. Similar to H.261, one can control the quantiser step size for that picture, such that the required bit rate is achieved. At the end of the GOP, the complexity index for each picture type is calculated. Note that for P- and B-pictures, the complexity index is the average of three and eight complexity indices, respectively. These ratios are used to define new coding ratios between the picture types for coding of the next GOP. Also, bits generated in that GOP are added together and the extra bit rate, or the deficit, from the GOP target bit rate is transferred to the next GOP.

In practice, the target bit rate for B-pictures compared to that for other picture types is deliberately reduced by a factor of 1.4. This is done for two reasons. First, because of efficient bidirectional motion estimation in B-pictures, their transform coefficients are normally small. Increasing the quantiser step size hardly affects these naturally small value coefficients' distortions, but the overall bit rate can be reduced significantly. Second, since B-pictures are not used in the prediction loop of the encoder, even if they are coarsely coded, the encoding error is not transferred to the subsequent frames. This is not the case with the anchor I- and P-pictures, because through the prediction loop, any saving in one frame due to coarser coding has to be paid back in the following frames.

Experimental results indicate that by reducing the target bit rates of the B-pictures by a factor of 1.4, the average quantiser step size for these pictures rises almost by the same factor, but its quality (PSNR) only slightly deteriorates, which is worth doing it.

Also, note that although in the above example (which is typical) the bits per B-pictures are fewer than those of I- and P-pictures, eight B-pictures in a GOP generate almost $8 \times 37 = 296$ kbits, which is more than 50 per cent of the bits in a GOP. The first implication is that use of a factor 1.4 can have a significant reduction in the overall bit rate. The second implication of this is in the transmission of video over packet networks, where during periods of congestion, if only the B-pictures are discarded, so reducing the network load by 50 per cent, congestion can be eased without significantly affecting the picture quality. Note that B-pictures are not used for predictions, so their loss will result in only a very brief (480 ms) reduction in quality.

7.9 Decoder

The decoder block diagram is based on the same principle as the local decoder associated with the encoder as shown in Figure 7.16.

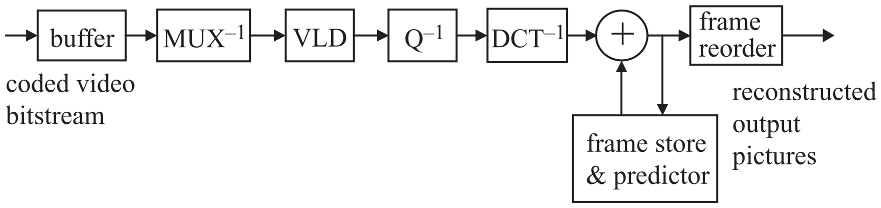

Figure 7.16 A block diagram of an MPEG-1 decoder

The incoming bitstream is stored in the buffer and is demultiplexed into the coding parameters such as DCT coefficients, motion vectors, macroblock types and addresses. They are then variable length decoded using the locally provided tables. The DCT coefficients after inverse quantisation are inverse DCT transformed and added to the motion-compensated prediction (as required) to reconstruct the pictures. The frame stores are updated by the decoded I- and P-pictures. Finally, the decoded pictures are reordered to their original scanned form.

At the beginning of the sequence, the decoder will decode the sequence header, including the sequence parameters. If the bitstream is not constrained and a parameter exceeds the capability of the decoder, then the decoder should be able to detect this. If the decoder determines that it can decode the bitstream, then it will set up its parameters to match those defined in the sequence header. This will include horizontal and vertical resolutions and aspect ratio, the bit rate and the quantisation weighting matrices.

Next the decoder will decode the GOP header field to determine the GOP structure. It will then decode the first picture header in the GOPs and, for constant bit rate operation, determine the buffer fullness. It will then delay decoding the rest of the sequence until the input buffer is filled to the correct level. By doing this, the decoder can be sure that no buffer overflow or underflow will occur during decoding. Normally, the input buffer size will be larger than the minimum required by the bitstream, giving a range of fullness at which the decoder may start to decode.

If it is required to play a recorded sequence from a random point in the bitstream, the decoder should discard all the bits until it finds a sequence start code, a GOP start code or a picture start code that introduces an I-picture. The slices and macroblocks in the picture are decoded and written into a display buffer and perhaps into another buffer. The decoded pictures may be postprocessed and displayed in the order defined by the temporal reference at the picture rate defined in the sequence header. Subsequent pictures are processed at the appropriate times to avoid buffer overflow and underflow.

7.9.1 Decoding for fast play

Fast forward can be supported by D-pictures. It can also be supported by an appropriate spacing of I-pictures in a sequence. For example, if I-pictures were spaced regularly every 12 pictures, then the decoder might be able to play the sequence at 12 times the normal speed by decoding and displaying only the I-pictures. This even simple concept places a considerable burden on the storage media and the decoder. The media must be capable of speeding up and delivering 12 times the data rate. The decoder must be capable of accepting this higher data rate and decoding the I-pictures. Since I-pictures typically require significantly more bits to code than P- and B-pictures, the decoder will have to decode significantly more than the 1/12 of the data rate. In addition, it has to search for picture start codes and discard the data for P- and B-pictures. For example, consider a sequence with $N = 12$ and $M = 3$, such as

I B B P B B P B B P B B I B B

Assume that the average bit rate is C, each B-picture requires $0.6C$, each P-picture requires $1.4C$ and the remaining $3C$ are assigned to the I-picture in the GOP. Then the I-pictures should code $(3/12) \times 100 = 25$ per cent of the total bit rate in just 1/12 of the display time.

Another way to achieve fast forward in a constant bit rate application is for the media itself to sort out the I-pictures and transmit them. This would allow the data rate to remain constant. Since this selection process can be made to produce a valid MPEG-1 video bitstream, the decoder should be able to decode it. If every I-picture of the preceding example were selected, then one I-picture would be transmitted every three-picture periods, and the speed up rate would be $12/3 = 4$ times.

If alternate I-pictures of the preceding example were selected, then one I-picture would again be transmitted every three-picture periods, but the speed up rate would be $24/3 = 8$ times. If one in N I-pictures of the preceding example were selected, then the speed up rate would be $4N$.

7.9.2 Decoding for pause and step mode

Decoding for pause requires the decoder to be able to control the incoming bit-stream and display a decoded picture without decoding any additional pictures. If the decoder has full control over the bitstream, then it can be stopped for pause and resumed when play begins. If the decoder has less control, as in the case of a CD-ROM, there may be a delay before play can be resumed.

7.9.3 Decoding for reverse play

To decode a bitstream and play in reverse, the decoder must decode each GOP in the forward direction, store the entire decoded pictures and then display them in reverse order. This imposes severe storage requirements on the decoder in addition to any problems in gaining access to the decoded bitstream in the correct order.

To reduce decoder memory requirements, groups of pictures should be small. Unfortunately, there is no mechanism in the syntax for the encoder to state what the decoder requirements are in order to play in reverse. The amount of display buffer storage may be reduced by reordering the pictures, either by having the storage unit read and transmit them in another order or by reordering the coded pictures in a decoder buffer. To illustrate this, consider the typical GOP shown in Figure 7.17.

B	B	I	B	B	P	B	B	P	B	B	P	pictures in display order
0	1	2	3	4	5	6	7	8	9	10	11	temporal reference
I	B	B	P	B	B	P	B	B	P	B	B	pictures in decoding order
2	0	1	5	3	4	8	6	7	11	9	10	temporal reference
I	P	P	P	B	B	B	B	B	B	B	B	pictures in new order
2	5	8	11	10	9	7	6	4	3	1	0	temporal reference

Figure 7.17 Example of GOP in the display, decoding and new orders

The decoder would decode pictures in the new order and display them in the reverse of the normal display. Since the B-pictures are not decoded until they are ready to be displayed, the display buffer storage is minimised. The first two B-pictures, 0 and 1, would remain stored in the input buffer until the last P-picture in the previous GOP was decoded.

7.10 Postprocessing

7.10.1 Editing

Editing of a video sequence is best performed before compression, but situations may arise where only the coded bitstream is available. One possible method would be to decode the bitstream, perform the required editing on the pixels and recode the bitstream. This usually leads to a loss in video quality, and it is better, if possible, to edit the coded bitstream itself.

Although editing may take several forms, the following discussion pertains only to editing at the picture level, that is, deletion of the coded video material from a bitstream and insertion of coded video material into a bitstream, or rearrangement of coded video material within a bitstream.

If a requirement for editing is expected (e.g. clip video is provided analogous to clip art for still pictures), then the video can be encoded with well-defined cutting points. These cutting points are places at which the bitstream may be broken apart or joined. Each cutting point should be followed by a closed GOP (e.g. a GOP that starts with an I-picture). This allows smooth play after editing.

To allow the decoder to play the edited video without having to adopt any unusual strategy to avoid overflow and underflow, the encoder should make the buffer fullness take the same value at the first I-picture following every cutting point. This value should be the same as that of the first picture in the sequence. If this suggestion is not followed, then the editor may make an adjustment either by padding (stuffing bits or macroblocks) or by recording a few images to make them smaller.

If the buffer fullness is mismatched and the editor makes no correction, then the decoder will have to make some adjustment when playing over an edited cut. For example, consider a coded sequence consisting of three clips, A, B and C, in order. Assume that clip B is completely removed by editing, so that the edited sequence consists only of clip A followed immediately by clip C, as illustrated in Figure 7.18.

Assume that, in the original sequence, the buffer is three quarters full at the beginning of clip B and one quarter full at the beginning of clip C. A decoder playing the edited sequence will encounter the beginning of clip C with its buffer three quarters full, but the first picture in clip C will contain a buffer fullness value corresponding to a quarter full buffer. To avoid buffer overflow, the decoder may try to pause the input bitstream, or discard pictures without displaying them (preferably B-pictures), or change the decoder timing.

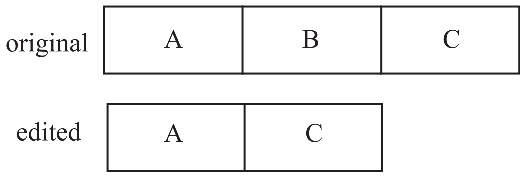

Figure 7.18 Edited sequences

For another example, assume that in the original sequence the buffer is one quarter full at the beginning of clip B and three quarters full at the beginning of clip C. A decoder playing the edited sequence will encounter the beginning of clip C with its buffer one quarter full, but the first picture in clip C will contain a buffer fullness value corresponding to a three quarters full buffer. To avoid buffer underflow, the decoder may display one or more pictures for longer than the normal time.

If provision for editing was not specifically provided in the coded bitstream, or if it must be available at any picture, then the editing task is more complex and places a greater burden on the decoder to manage buffer overflow and underflow problems. The easiest task is to cut at the beginning of a GOP. If the GOP following the cut is open (e.g. GOP stars with two B-pictures), which can be detected by examining the closed GOP flag in the GOP header, then editing must set the broken link bit to 1 to indicate to the decoder that the previous GOP cannot be used for decoding any B-pictures.

7.10.2 Resampling and upconversion

The decoded sequence may not match the picture rate or the spatial resolution of the display device. In such situations (which occur frequently), the decoded video must be resampled or scaled. In Chapter 2, we saw that CCIR-601 video was subsampled into SIF format for coding; hence, for display it is appropriate to upsample them back into their original format. Similarly, they have to be temporally converted for proper display, as was discussed in Chapter 2. This is particularly important for cases where video was converted from film.

7.11 Problems

1. In MPEG-1, with the group of picture structure of $N = 12$ and $M = 3$, the maximum motion speed is assumed to be 15.5 pixels/frame (half-pixel precision), calculate the number of search operations required to estimate the motion in P-pictures with
   a. telescopic method
   b. direct on the P-pictures
2. In an MPEG-1 encoder, for head-and-shoulders type pictures, the maximum motion speed for P-pictures is set to 13 pixels and those of the forward and backward for the first B-picture in the subgroup are set to five pixels and nine pixels, respectively.
   a. Explain why the search range for B-picture is smaller than that of the P-picture.
   b. What would be the forward and backward search ranges for the second B-picture in the subgroup?
   c. Calculate the number of search operations with half-pixel precision for the P- and B-pictures.
3. An I-picture is coded at 50 kbits. If the quantiser step size is linearly distributed between 10 and 16, find the complexity index for this picture.
4. In coding of SIF-625 video at 1.2 Mbit/s, with a GOP structure $N = 12$, $M = 3$, the ratios of complexity indices of I, P and B are 20:10:7, respectively. Calculate the target bit rate for coding of each frame in the next GOP.

5. If in problem 4, the allocated bits to B-pictures were reduced by a factor of 1.4, find the new complexity indices and the target bits to each picture type.

6. In problem 4, if due to scene change the average quantiser step size in the last P-picture of the GOP was doubled, but those of other pictures did not change significantly:
   a. How do the complexity index ratios change?
   b. What is the new target bit rate for each picture type?

7. If in problem 4, the complexity indices ratios were wrongly set to 1:1:1, but after coding the average quantiser step sizes for I, P and B were 60, 20 and 15, respectively, find
   a. the target bit rate for each picture type before coding
   b. the target bit rate for each picture type of the next GOP

References

1. MPEG-1: ‘Coding of moving pictures and associated audio for digital storage media at up to about 1.5 Mbit/s’, ISO/IEC 1117-2: video, November 1991
2. H.261: ‘ITU-T Recommendation H.261, video codec for audiovisual services at p$\times$64 kbit/s’, Geneva, 1990
3. ‘Coding of moving pictures and associated audio for digital storage media at up to about 1.5 Mbit/s’, ISO/IEC 1117-2: systems, November 1991
4. CCIR Recommendation 601: ‘Digital methods of transmitting television information’. Recommendation 601, Encoding parameters of digital television for studios
5. WILSON, D. and GHANBARI, M.: ‘Frame sequence partitioning of video for efficient multiplexing’, *Electron. Lett.*, 1988, **34:15**, pp. 1480–1481
6. GHANBARI, M.: ‘An adapted H.261 two-layer video codec for ATM networks’, *IEEE Trans. Commun.*, **40:9**, 1992, pp. 1481–1490
7. PEARSON, D.E.: *Transmission and Display of Pictorial Information*, Pentech Press, London, 1975
8. SEFERIDIS, V. and GHANBARI, M.: ‘Adaptive motion estimation based on texture analysis’, *IEEE Trans. Commun.*, 1994, **42:2/3/4**, pp. 1277–1287
9. ALDRIDGE, R.P., GHANBARI, M. and PEARSON D.E.: ‘Exploiting the structure of MPEG-2 for statistically multiplexing video’, Proceedings of 1996 International Picture coding symposium, PCS’96, Melbourne, Australia, March 1996, pp. 111–113

Chapter 8
Coding of high-quality moving pictures (MPEG-2)

Following the universal success of H.261 and Motion Picture Experts Group (MPEG)-1 video codecs, there was a growing need for a video codec to address a wide variety of applications. Considering the similarity between H.261 and MPEG-1, ITU-T and ISO/IEC made a joint effort to devise a generic video codec. Joining the study was a special group in ITU-T, Study Group 15 (SG15), who were interested in coding of video for transmission over the future broadband integrated services digital networks (BISDN) using asynchronous transfer mode (ATM) transport. The devised generic codec was finalised in 1995 and takes the name of MPEG-2/H.262, though it is more commonly known as MPEG-2 [1].

At the time of the development, the following applications for the generic codec were foreseen:

•	BSS	broadcasting satellite service (to the home)
•	CATV	cable TV distribution on optical networks, copper, etc.
•	CDAD	cable digital audio distribution
•	DAB	digital audio broadcasting (terrestrial and satellite)
•	DTTB	digital terrestrial television broadcast
•	EC	electronic cinema
•	ENG	electronic news gathering (including satellite news gathering (SNG))
•	FSS	fixed satellite service (e.g. to head ends)
•	HTT	home television theatre
•	IPC	interpersonal communications (videoconferencing, videophone, etc.)
•	ISM	interactive storage media (optical discs, etc.)
•	MMM	multimedia mailing
•	NCA	news and current affairs
•	NDS	networked database services (via ATM, etc.)
•	RVS	remote video surveillance
•	SSM	serial storage media (digital VTR, etc.)

Of particular importance is the application to satellite systems where the limitations of radio spectrum and satellite parking orbit result in pressure to provide acceptable quality TV signals at relatively low bit rates. As we will see at the end of this chapter, today we can accommodate about six to eight high-quality MPEG-2 coded TV programmes into the same satellite channel that used to carry only one analogue TV programme. Numerous new applications have been added to the list. In particular, high definition television (HDTV) and digital versatile disc (DVD) for home storage systems appear to be the main beneficiaries of further MPEG-2 development.

8.1 MPEG-2 systems

The MPEG-1 standard was targeted for coding of audio and video for storage, where the media error rate is negligible [2]. Hence, the MPEG-1 system is not designed to be robust to bit error rates. Also, MPEG-1 was aimed at software-oriented image processing, where large- and variable-length packets could reduce the software overhead [3].

The MPEG-2 standard, on the other hand, is more generic for a variety of audio-visual coding applications. It has to include error resilience for broadcasting, and ATM networks. Moreover, it has to deliver multiple programmes simultaneously without requiring them to have a common time base. These require that the MPEG-2 transport packet length should be short and fixed.

MPEG-2 defines two types of streams: the programme stream and the transport stream. The programme stream is similar to the MPEG-1 systems stream but uses a modified syntax and new functions to support advanced functionalities (e.g. scalability). It also provides compatibility with the MPEG-1 systems stream, that is, MPEG-2 should be capable of decoding an MPEG-1 bitstream. Like the MPEG-1 decoder, programme stream decoders typically employ long- and variable-length packets. Such packets are well suited for software-based processing and error-free transmission environments, such as coding for storage of video on a disc. Here the packet sizes are usually 1–2 kbytes long, chosen to match the disc sector sizes (typically 2 kbytes). However, packet sizes as long as 64 kbytes are also supported.

The programme stream also includes features not supported by MPEG-1 systems. These include scrambling of data, assignment of different priorities to packets, information to assist alignment of elementary stream packets, indication of copyright, indication of fast forward, fast reverse and other trick modes for storage devices. An optional field in the packets is provided for testing the network performance, and optional numbering of a sequence of packets is used to detect lost packets.

In the transport stream, MPEG-2 significantly differs from MPEG-1 [4]. The transport stream offers robustness for noisy channels as well as the ability to assemble multiple programmes into a single stream. The transport stream uses fixed-length packets of size 188 bytes with a new header syntax. This can be segmented into four 47 bytes to be accommodated in the payload of four ATM cells, with the AAL1 adaptation scheme [5]. It is therefore more suitable for hardware processing and for error correction schemes, such as those required in television broadcasting, satellite/cable TV and ATM networks. Furthermore, multiple programmes with independent time bases can be multiplexed in one transport stream. The transport stream also allows synchronous multiplexing of programmes, fast access to the desired programme for channel hopping, multiplexing of programmes with clocks unrelated to transport clock and correct synchronisation of elementary streams for playback. It also allows control of the decoder buffers during start-up and playback for both constant and variable bit rate (VBR) programmes.

A basic data structure that is common to the organisation of both the programme stream and transport stream is called the packetised elementary stream (PES) packet. Packetising the continuous streams of compressed video and audio bitstreams (elementary streams) generates PES packets. Simply stringing together PES packets from the various encoders with other packets containing necessary data to generate a single bitstream generates a programme stream. A transport stream consists of packets of fixed length containing 4 bytes of header followed by 184 bytes of data, where the data are obtained by segmenting the PES packets.

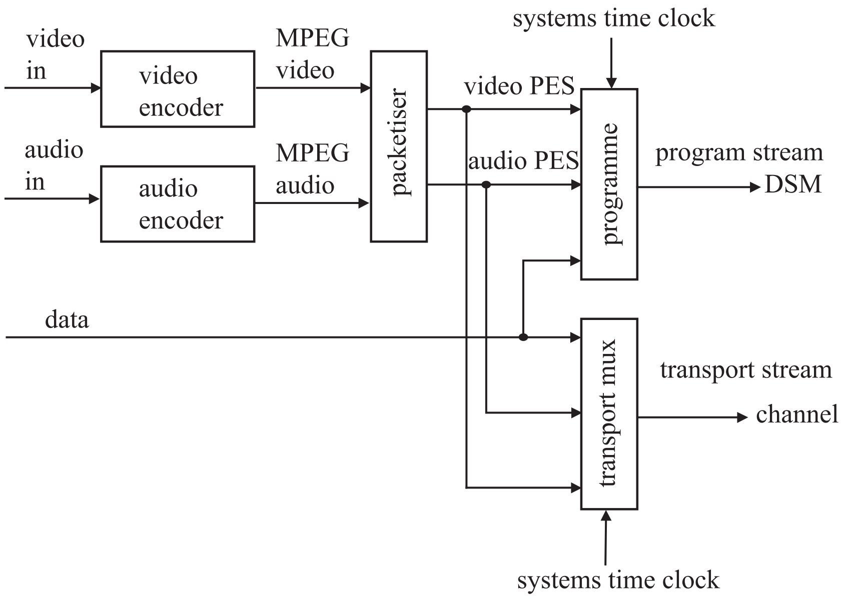

Figure 8.1 MPEG-2 systems multiplex of programme and transport streams

Figure 8.1 illustrates both types of programme and transport stream multiplexes of MPEG-2 systems. Like MPEG-1, the MPEG-2 systems layer is also capable of combining multiple sources of user data along with encoded audio and video. The audio and video streams are packetised to form PES packets, which are sent to either a programme multiplexer or a transport multiplexer, resulting in a programme stream or transport stream, respectively. As mentioned earlier, programme streams are intended for an error-free environment such as digital storage media (DSM).

Transport streams are intended for noisier environments such as terrestrial broadcast channels.

At the receiver, the transport streams are decoded by a transport demultiplexer (which includes a clock extraction mechanism), unpacketised by a de-packetiser and sent to audio and video decoders for decoding, as shown in Figure 8.2.

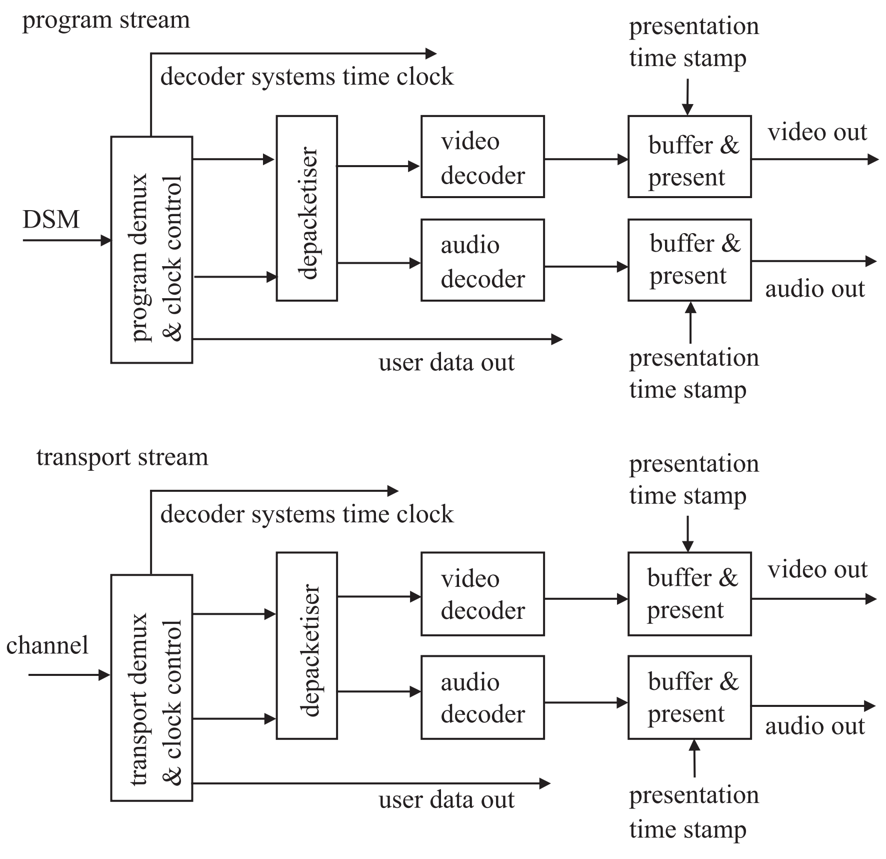

Figure 8.2 MPEG-2 systems demultiplexing of programme and transport streams

The decoded signals are sent to the receiver buffer and presentation unit, which outputs them to a display device and a speaker at the appropriate time. Similarly, if the programme streams are used, they are decoded by the programme stream demultiplexer and depacketiser and sent to the audio and video decoders. The decoded signals are sent to the respective buffer to await presentation. Also similar to MPEG-1 systems, the information about systems timing is carried by the clock reference field in the bitstream that is used to synchronise the decoder systems time clock (STC). Presentation time stamps (PTS), which are also carried by the bitstream, control the presentation of the decoded output.

8.2 Profiles and levels

MPEG-2 is intended to be generic in the sense that it serves a wide range of applications, bit rates, resolutions, qualities and services. Applications should cover, among other things, DSM, television broadcasting and communications. In the course of the development, various requirements from typical applications were considered, and they were integrated into a single syntax. Hence, MPEG-2 is expected to facilitate the interchange of bitstreams among different applications. However, considering the practicality of implementing the full syntax of the bitstream, a limited number of subsets of the syntax are also stipulated by means of profile and level [6].

A profile is a subset of the entire bitstream syntax that is defined by the MPEG-2 specification. Within the bounds imposed by the syntax of a given profile, it is still possible to encompass very large variations in the performance of encoders and decoders depending on the values taken by parameters in the bitstream. For instance, it is possible to specify frame sizes as large as (approximately) 2^{14} samples wide by 2^{14} lines high. It is currently neither practical nor economical to implement a decoder capable of dealing with all possible frame sizes. To deal with this problem, levels are defined within each profile. A level is a defined set of constraints imposed on parameters in the bitstream. These constraints may be simple limits on numbers. Alternatively, they may take the form of constraints on arithmetic combinations of the parameters (e.g. frame width $\times$ frame height $\times$ frame rate). Both profiles and levels have a hierarchical relationship, and the syntax supported by a higher profile or level must also support all the syntactical elements of the lower profiles or levels.

Bitstreams complying with the MPEG-2 specification use a common syntax. To achieve a subset of the complete syntax, flags and parameters are included in the bitstream, which signals the presence or otherwise of syntactic elements that occur later in the bitstream. Then, to specify constraints on the syntax (and hence define a profile), it is only necessary to constrain the values of these flags and parameters that specify the presence of later syntactic elements.

In order to parse the bitstream into specific applications, they are ordered into layers. If there is only one layer, the coded video data are called a nonscalable video bitstream. For two or more layers, the bitstream is called scalable hierarchy. In the scalable mode, the first layer, called the base layer, is always decoded independently. Other layers are called enhancement layers and can only be decoded together with the lower layers.

Before describing how various scalabilities are introduced in MPEG-2, let us see how profiles and levels are defined. MPEG-2 initially defined five hierarchical structure profiles and later on added two profiles that do not fit the hierarchical structure. The profile mainly deals with the supporting tool for coding, such as the group of pictures (GOP) structure, the picture format and scalability. The seven known profiles and their current applications are summarised in Table 8.1.

The level deals with the picture resolutions such as the number of pixels/line, lines/frame, frames/s and bit/s or the bit rate (e.g. Mbit/s). Table 8.2 summarises the levels that are most suitable for each profile.

The main profile main line (MP@ML) is the most widely used pairs for broadcast TV, and the 4:2:2 profile and main line (4:2:2@ML) is for the studio video production and recording.

Table 8.1 Various profiles defined for MPEG-2

Type	**Supporting tools**	**Application**
Simple	I- and P-pictures, 4:2:0 format; nonscalable	Currently not used
Main	Simple profile + B-pictures	Broadcast TV
SNR scalable	Main profile + SNR scalability	Currently not used
Spatial	SNR profile + spatial scalability	Currently not used
High	Spatial profile + 4:2:2 format	Currently not used
4:2:2	IBIBIB... pictures, extension of main profile to high bit rates	Studio postproduction; high-quality video for storage (VTR) and video distribution
Multiview	Main profile + temporal scalability	Several video streams; stereo presentation

Table 8.2 The levels defined for each profile

Level	**Resolutions**	**Simple I, P 4:2:0**	**Main I, P, B 4:2:0**	**SNR I, P, B 4:2:0**	**Spatial I, P, B 4:2:0**	**High I, P, B 4:2:0 4:2:2**	**4:2:2 I, P, B 4:2:0 4:2:2**	**Multiview I, P, B 4:2:0**
Low	pel/line			352	352			352
	line/frame			288	288			288
	frame/s			30/25	30/15			30/25
	Mbit/s			4	4			8
Main	pel/line	720	720	720		720	720	720
	line/frame	576	576	576		576	512/608	576
	frame/s	30/25	30/25	30/25		30/25	30/25	30/25
	Mbit/s	15	15	15		20	50	25
High	pel/line	1440		1440	1440	1440		
1440	line/frame	1152		1152	1152	1152		
	frame/s	60		60	60	60		
	Mbit/s	60		60	80	100		
High	pel/line	1920			1920	1920		1920
	line/frame	1152			1152	1152		1152
	frame/s	60			60	60		60
	Mbit/s	80			100	130		300

8.3 How does the MPEG-2 video encoder differ from MPEG-1?

8.3.1 Major differences

From the profiles and levels, we see that the picture resolutions in MPEG-2 can vary from SIF ($352 \times 288 \times 25$ or 30) to HDTV with $1920 \times 1250 \times 60$. Moreover, most of these pictures are interlaced, whereas in MPEG-1, pictures are non-interlaced (progressive). Coding of interlaced pictures is the first difference between the two coding schemes.

In the MPEG-2 standard, combinations of various picture formats and the interlaced/progressive option create a new range of macroblock (MB) types. While each MB in a progressive mode has 6 blocks in the 4:2:0 format, the number of blocks in the 4:4:4 image format is 12. Also, the dimensions of the unit of blocks used for motion estimation/compensation can change. In the interlaced pictures, since the number of lines per field is half the number of lines per frame, with equal horizontal and vertical resolutions for motion estimation, it might be appropriate to choose blocks of 16×8, that is, 16 pixels over eight lines. These types of sub-MBs have half the number of blocks of the progressive mode.

The second significant difference between the MPEG-1 and the MPEG-2 video encoders is the new function of scalability. The scalable modes of MPEG-2 are intended to offer interoperability among different services or to accommodate the varying capabilities of different receivers and networks upon which a single service may operate. They allow a receiver to decode a subset of the full bitstream in order to display an image sequence at a reduced quality and spatial and temporal resolution.

8.3.2 Minor differences

Apart from the two major distinctions, there are some other minor differences, which have been introduced to increase the coding efficiency of MPEG-2. They are again due to the picture interlacing used in MPEG-2. The first one is the scanning order of discrete cosine transform (DCT) coefficients. In MPEG-1, like H.261, zigzag scanning is used. MPEG-2 has the choice of using alternate scan, as shown in Figure 8.3*b*. For interlaced

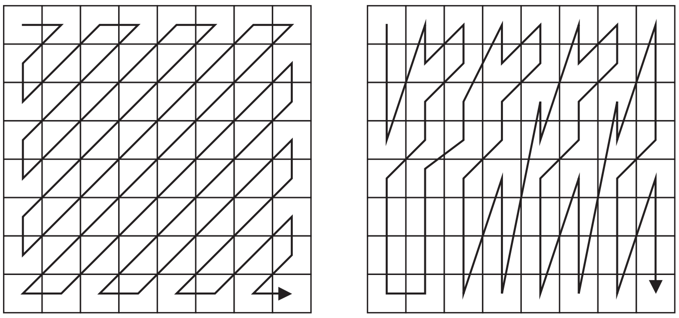
(*a*) (*b*)

Figure 8.3 Two types of scanning method: (a) zigzag scan and (b) alternate scan

pictures, since the vertical correlation in the field pictures is greatly reduced, should the field prediction be used, an alternate scan may perform better than a zigzag scan.

The second minor difference is on the nature of quantisation of the DCT coefficients. MPEG-2 supports both linear and nonlinear quantisation of the DCT coefficients. The nonlinear quantisation increases the precision of quantisation at high bit rates by employing lower quantiser scale values. This improves picture quality at low contrast areas. At lower bit rates, where larger step sizes are needed, again the nonlinear behaviour of the quantiser provides a larger dynamic range for quantisation of the coefficients.

8.3.3 MPEG-1 and MPEG-2 syntax differences

The IDCT mismatch control in MPEG-1 is slightly different from that in MPEG-2. After the inverse quantisation process of the DCT coefficients, the MPEG-1 standard requires that all the nonzero coefficients are added with 1 or –1. In the MPEG-2 standard, only the last coefficient needs to be added with 1 or –1 provided that the sum of all coefficients is even after inverse quantisation. Another significant variance is the run level values. In MPEG-1, those that cannot be coded with a variable length code (VLC) are coded with the escape code, followed by either a 14-bit or a 22-bit fixed-length coding (FLC), whereas for MPEG-2, they are followed by an 18-bit FLC.

The constraint parameter flag mechanism in MPEG-1 has been replaced by the profile and level structures in MPEG-2. The additional chroma formats (4:2:2 and 4:4:4) and the interlaced related operations (field prediction and scalable coding modes) make MPEG-2 bitstream syntax different from that of MPEG-1.

The concept of the GOP layer is slightly different. GOP in MPEG-2 may indicate that certain B-pictures at the beginning of an edited sequence comprise a broken link, which occurs if the forward reference picture needed to predict the current B-pictures is removed from the bitstream by an editing process. It is an optional structure for MPEG-2 but mandatory for MPEG-1. The final point is that slices in MPEG-2 must always start and end on the same horizontal row of MBs. This is to assist the implementations in which the decoding process is split into some parallel operations along horizontal strips within the same pictures.

Although these differences may make direct decoding of the MPEG-1 bitstream by an MPEG-2 decoder infeasible, the fundamentals of video coding in the two codecs remain the same. In fact, as we mentioned, there is a need for backward compatibility so that the MPEG-2 decoder should be able to decode the MPEG-1 encoded bitstream. Thus, MPEG-1 is a subset of MPEG-2. They employ the same concept of a GOP, and the interlaced field pictures now become I-, P- and B-fields, and all the MB types have to be identified as field or frame based. Therefore, in describing the MPEG-2 video codec, we will avoid repeating what has already been said about MPEG-1 in Chapter 7. Instead, we will concentrate on parts that have risen due to interlacing and scalability of MPEG-2. However, for information on the difference between MPEG-1 and MPEG-2 refer to [7].

8.4 MPEG-2 nonscalable coding modes

This simple nonscalable mode of the MPEG-2 standard is the direct extension of the MPEG-1 coding scheme with the additional feature of accommodating interlaced video coding. The impact of the interlaced video on the coding methodology is that interpicture prediction may be carried out between the fields as they are closer to each other. Furthermore, for slow moving objects, vertical pixels in the same frame are closer, making frame prediction more efficient.

As usual, we define the prediction modes on an MB basis. Also, to be in line with the MPEG-2 definitions, we define the odd and the even fields as the top and bottom fields, respectively. A field MB, similar to the frame MB, consists of 16 $\times$ 16 pixels. In the following, five modes of predictions are described [3]. They can be equally applied to P- and B-pictures unless specified otherwise.

Similar to the reference model in H.261, software-based reference codecs for laboratory testing have also been thought for MPEG-1 and MPEG-2. For these codecs, the reference codec is called the test model (TM), and the latest version of the TM is TM5 [8].

8.4.1 Frame prediction for frame pictures

Frame prediction for frame pictures is exactly identical to the predictions used in MPEG-1. Each P-frame can make a prediction from the previous anchor frame, and there is one motion vector for each motion-compensated MB. B-frames may use previous, future or interpolated past and future anchor frames. There will be up to two motion vectors (forward and backward) for each B-frame motion-compensated MB. Frame prediction works well for slow to moderate motion as well as panning over a detailed background.

8.4.2 Field prediction for field pictures

This mode of prediction is similar to the frame prediction except that pixels of the target MB (MB to be coded) belong to the same field. Prediction MBs should also belong to one field, either from the top or the bottom field. Thus, for P-pictures the prediction MB comes from the two most recent fields, as shown in Figure 8.4. For example, the prediction for the target MBs in the top field of a P-frame, T_P, may come either from the top field, T_R, or the bottom field, B_R, of the reference frame.

The prediction for the target MBs in the bottom field, B_P, can be made from its two recent fields, the top field of the same frame, T_P, or the bottom field of the reference frame, B_R.

For B-pictures, the prediction MBs are taken from the two most recent anchor pictures (I/P or P/P). Each target MB can make a forward or a backward prediction from either of the fields.

For example, in Figure 8.5 the forward prediction for the bottom field of a B-picture, B_B, is either T_P or B_P, and the backward prediction is taken from T_F or B_F. There will be one motion vector for each P-field target MB, and two motion vectors for those of B-fields.

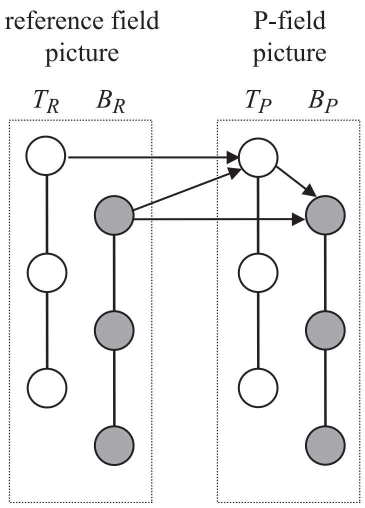

Figure 8.4 Field prediction of field pictures for P-picture MBs

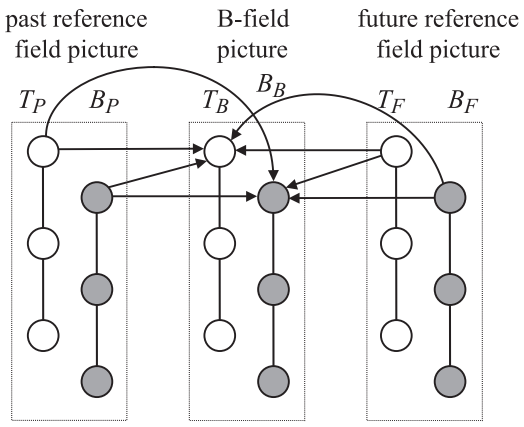

Figure 8.5 Field prediction of field pictures for B-picture MBs

8.4.3 Field prediction for frame pictures

In this case the target MB in a frame picture is split into two top field and bottom field pixels, as shown in Figure 8.6. Field prediction is then carried out independently for each of the 16×8 pixel target MBs.

For P-pictures, two motion vectors are assigned for each 16×16 pixel target MB. The 16×8 predictions may be taken from either of the two most recently decoded anchor pictures. Note that the 16×8 field prediction cannot come from the same frame, as was the case in field prediction for field pictures.

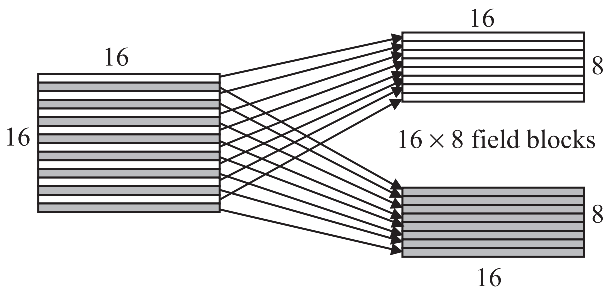

Figure 8.6 A target MB is split into two 16 × 8 field blocks

For B-pictures, because of the forward and the backward motion, there can be two or four motion vectors for each target MB. The 16 × 8 predictions may be taken from either field of the two most recently decoded anchor pictures.

8.4.4 Dual prime for P-pictures

Dual prime is only used in P-pictures, where there are no B-pictures in the GOP. Here only one motion vector is encoded (in its full format) in the bitstream together with a small differential motion vector correction. In the case of the field pictures, two motion vectors are then derived from this information. These are used to form predictions from the two reference fields (one top, one bottom), which are averaged to form the final prediction. In the case of frame pictures, this process is repeated for the two fields so that a total of four field predictions are made.

Figure 8.7 shows an example of dual-prime motion-compensated prediction for the case of frame pictures. The transmitted motion vector has a vertical displacement of three pixels. From the transmitted motion vector, two preliminary predictions are computed, which are then averaged to form the final prediction.

The first preliminary prediction is identical to field prediction except that the reference pixels should come from the previously coded fields of the same parity (top or bottom fields) as the target pixels. The reference pixels, which are obtained from the transmitted motion vector, are taken from two fields (taken from one field for field pictures). In the figure the predictions for target pixels in the top field, T_P, are taken from the top reference field, T_R. Target pixels in the bottom field, B_P, take their predictions from the bottom reference field, B_R.

The second preliminary prediction is derived using a computed motion vector plus a small differential motion vector correction. For this prediction, reference pixels are taken from the parity field opposite to the first parity preliminary prediction. For the target pixels in the top field T_P, pixels are taken from the bottom reference field B_R. Similarly, for the target pixels in the bottom field B_P, prediction pixels are taken from the top reference field T_R.

The computed motion vectors are obtained by a temporal scaling of the transmitted motion vector to match the field in which the reference pixels lie, as shown in Figure 8.7. For example, for the transmitted motion vector of value 3, the

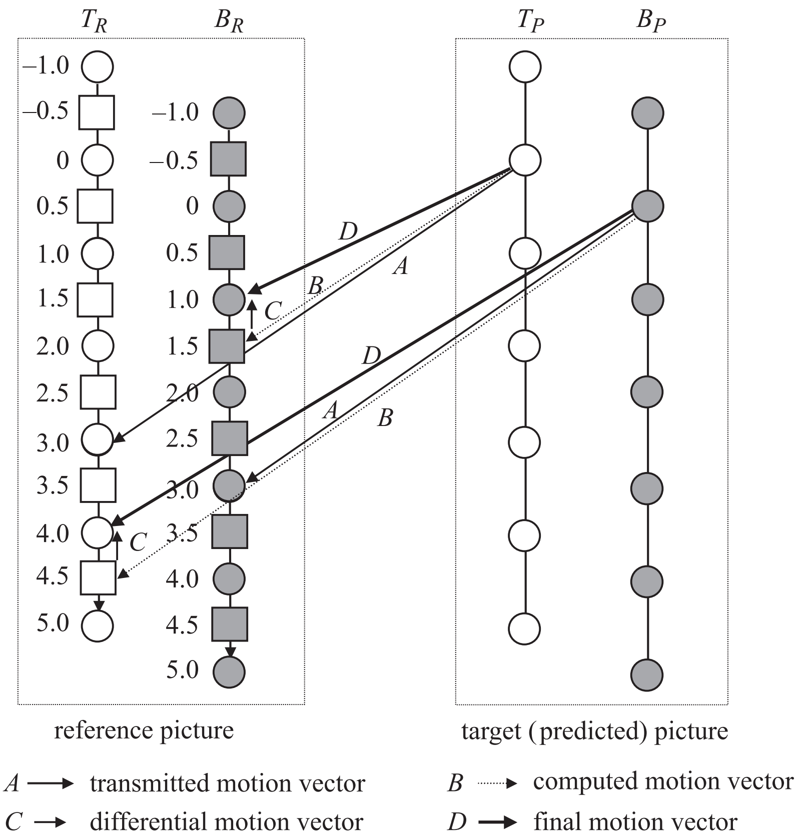

Figure 8.7 Dual-prime motion-compensated prediction for P-pictures

computed motion vector for T_P would be $3 \times 1/2 = 1.5$, since the reference field B_R is midway between the top reference field and the top target field. The computed motion vector for the bottom field is $3 \times 3/2 = 4.5$, as the distance between the reference top field and the bottom target field is three fields (3/2 frames). The differential motion vector correction, which can have up to one-half pixel precision, is then added to the computed motion vector to give the final corrected motion vector.

In the figure, the differential motion vector correction has a vertical displacement of -0.5 pixels. Therefore, the corrected motion vector for the top target field, T_P, would be $1.5 - 0.5 = 1$, and for the bottom target field, it is $4.5 - 0.5 = 4$, as shown with thicker lines in the figure.

For interlaced video, the performance of dual-prime prediction can, under some circumstances, be comparable to that of B-picture prediction and has the advantage of low encoding delay. However, for dual prime, unlike B-pictures, the decoded pixels should be stored to be used as reference pixels.

8.4.5 16 × 8 motion compensation for field pictures

In this mode, a field of 16 × 16 pixel MB is split into upper half and lower half 16 × 8 pixel blocks, and a separate field prediction is carried out for each. Two motion vectors are transmitted for each P-picture MB, and two or four motion vectors for the B-picture MB. This mode of motion compensation may be useful in field pictures that contain irregular motion. Note the difference between this mode and the field prediction for frame pictures in section 8.4.3. Here a field MB is split into two halves, and in the field prediction for frame pictures, a frame MB is split into two top and bottom field blocks.

Thus, the five modes of motion compensation in MPEG-2 in relation to field and frame predictions can be summarised in Table 8.3.

Table 8.3 Five motion compensation modes in MPEG-2

Motion compensation mode	**Use in field pictures**	**Use in frame pictures**
Frame prediction for frame pictures	No	Yes
Frame prediction for field pictures	Yes	No
Field prediction for frame pictures	No	Yes
Dual prime for P-pictures	Yes	Yes
16 × 8 motion compensation for field pictures	Yes	No

8.4.6 Restrictions on field pictures

It should be noted that field pictures have some restrictions on I-, P- and B-picture coding type and motion compensation. Normally, the second field picture of a frame must be of the same coding type as the first field. However, if the first field picture of a frame is an I-picture, then the second field can be either I or P. If it is a P-picture, the prediction MBs must all come from the previous I-picture, and dual prime cannot be used.

8.4.7 Motion vectors for chrominance components

As explained, the motion vectors are estimated on the basis of the luminance pixels; hence, they are used for the compensation of the luminance component. For each of the two chrominance components, the luminance motion vectors are scaled according to the image format as follows:

- 4:2:0: Both the horizontal and vertical components of the motion vector are scaled by dividing by two.
- 4:2:2: The horizontal component of the motion vector is scaled by dividing by two; the vertical component is not altered.
- 4:4:4: The motion vector is unmodified.

8.4.8 Concealment motion vectors

Concealment motion vectors are motion vectors that may be carried by the intra MBs for the purpose of concealing errors, should transmission error result in loss of information. A concealment motion vector is present for all intra MBs if and only if the *concealment_motion_vectors* flag in the picture header is set. In the normal course of events, no prediction is formed for such MBs, since they are of intra type. The specification does not specify how error recovery shall be performed. However, it is a recommendation that concealment motion vectors should be suitable for use by a decoder that is capable of performing the function. If concealment is used in an I-picture, then the decoder should perform prediction in a similar way to a P-picture.

Concealment motion vectors are intended for use in the case that a data error results in information being lost. There is, therefore, little point in encoding the concealment motion vector in the MB for which it is intended to be used. This is because if the data error results in the need for error recovery, it is very likely that the concealment motion vector itself would be lost or corrupted. As a result, the following semantic rules are appropriate:

- For all MBs except those in the bottom row of MBs concealment motion, vectors should be appropriate for use in the MB that lies vertically below the MB in which the motion vector occurs.
- When the motion vector is used with respect to the MB identified in the previous rule, a decoder must assume that the motion vector may refer to samples outside of the slices encoded in the reference frame or reference field.
- For all MBs in the bottom row of MBs, the reconstructed concealment motion vectors will not be used. Therefore, the motion vector (0,0) may be used to reduce unnecessary overhead.

8.5 Scalability

Scalable video coding is often regarded as being synonymous with layered video coding, which was originally proposed by the author to increase robustness of video codecs against packet (cell) loss in ATM networks [9]. At the time (late 1980s), H.261 was under development, and it was clear that purely interframe coded video by this codec was very vulnerable to loss of information. The idea behind layered coding was that the codec should generate two bitstreams, one carrying the most vital video information named as the base layer and the other carrying the residual information to enhance the base layer image quality, named the enhancement layer. In the event of network congestion, only the less important enhancement data should be discarded, and the space made available for the base layer data. Such a methodology had an influence on the formation of ATM cell structure to provide two levels of priority for protecting base layer data [5]. This form of two-layer coding is now known as signal-to-noise ratio (SNR) scalability in the MPEG-2 standard, and currently, a variety of new two-layer coding techniques have been devised. They now form the basic scalability functions of the MPEG-2 standard.

Before describing various forms of scalability in some details, it will be useful to know the similarity and, more importantly, any dissimilarity between these two coding methods. In the next section, this is dealt with in some depth, but since scalability is the commonly adopted name for all the video coding standards, we use scalability throughout the book to address both methods.

The scalability tools defined in the MPEG-2 specifications are designed to support applications beyond that supported by the single-layer video. Among the noteworthy applications areas addressed are video telecommunications, video on ATM networks, interworking of video standards, video service hierarchies with multiple spatial, temporal and quality resolutions, HDTV with embedded TV, systems allowing migration to higher temporal resolution HDTV, etc. Although a simple solution to scalable video is the simulcast technique, which is based on transmission/storage of multiple independently coded reproductions of video, a more efficient alternative is scalable video coding, in which the bandwidth allocated to a given reproduction of video can be partially reutilised in coding of the next reproduction of video. In scalable video coding, it is assumed that given an encoded bitstream, decoders of various complexities can decode and display appropriate reproductions of the coded video. A scalable video encoder is likely to have increased complexity when compared to a single-layer encoder. However, the standard provides several different forms of scalabilities that address nonoverlapping applications with corresponding complexities. The basic scalability tools offered are data partitioning, SNR scalability, spatial scalability and temporal scalability. Moreover, combinations of these basic scalability tools are also supported and are referred to as hybrid scalability. In the case of basic scalability, two layers of video, referred to as the base layer and the enhancement layer, are allowed, whereas in hybrid scalability up to three layers are supported.

8.5.1 Layering versus scalability

Considering the MPEG-1 and MPEG-2 systems functions, defined in section 8.1, we see that MPEG-2 puts special emphasis on the transport of bitstream. This is because MPEG-1 video is mainly for storage and software-based decoding applications in an almost error-free environment, whereas MPEG-2, or known as H.262 in the ITU-T standard, is for transmission and distribution of video in various networks. Depending on the application, the emphasis can be put on either transmission or distribution. In the introduction to MPEG-2/H262, potential applications for this codec were listed. The major part of the application is the transmission of video over networks, such as satellite and terrestrial broadcasting, news gathering, personal communications and video over ATM networks, where, for better quality of service, the bitstream should be protected against channel misbehaviour, which is very common on these environments. One way of protecting data against channel errors is to add some redundancy, like forward error correcting bits into the bitstream. The overhead is a percentage of the bit rate (depending on the amount of protection) and will be minimal if the needed protection part had a small channel rate requirement. Hence, it is logical to design the codec in such a way as to generate more than one bitstream and protect the most vital bitstream against the error to produce a basic quality picture. The remaining bitstreams should be such that their presence enhances the video quality, but their absence or corruptions should not degrade the video quality significantly. Similarly, in ATM networks, partitioning the bitstream into various parts of importance and then providing a guaranteed channel capacity for a small part of the bitstream are much easier than that for the entire bitstream. This is the fundamental concept behind the layered video coding. The most notable point is that the receiver is always expecting to receive the entire bitstream, but if some parts are not received, the picture will not break up or the quality will not degrade significantly. Increasing the number of layers and unequally protecting the layers against errors (cell loss in ATM networks) according to their importance in their contribution to video quality can give a graceful degradation on video quality.

On the other hand, some applications set forth for MPEG-2 are mainly for distribution of digital video to the receivers of various capabilities. For example, in cable TV distribution over optical networks (CATV), the prime importance is to be able to decode various quality pictures from a single bitstream. In this network, there might be receivers with various decoding capability (processing powers) or customers with different requirement for video quality. Then, according to the need, a portion of the bitstream is decoded for that specific service. Here, it is assumed that the error rate in the optical channels is negligible and sufficient channel capacity for the bitstream exists; both the assumptions are plausible.

Thus, in comparing layered coding with scalability, the fundamental difference is that in layered coding the receiver expects to receive the entire bitstream, but occasionally, some parts might be in error or missing, while in scalable coding a receiver expects to decode a portion of the bitstream, but when that is available, it remains so for the entire communication session. Of course, in scalable coding, for efficient compression, generation of the bitstream is made in a hierarchical structure such that the basic portion of the bitstream gives a video of minimum acceptable quality, similar to the base layer video. The subsequent segments of the bitstream enhance the video quality accordingly, similar to the enhancement layers. If the channel requires any protection, then the base layer bitstream should be guarded, or in ATM networks the required channel capacity is to be provided. Now, in this respect, we can say that scalable and layered video coding are the same. This means that scalable coding can be used as a layering technique, but, however, layered coded data may not be scalable. Thus, scalability is a more generic name for layering, and throughout the book we use scalability to address both. Parts in which the video codec acts as a layered encoder but not as a scalable encoder will be particularly identified.

8.5.2 Data partitioning

Data partitioning is a tool intended for use when two channels are available for the transmission and/or storage of a video bitstream, as may be the case in ATM networks, terrestrial broadcasting, magnetic media, etc. Data partitioning, in fact, is not a true scalable coding, but as we will see, it is a layered coding technique. It is a means of dividing the bitstream of a single-layer MPEG-2 into two parts or layers. The first layer comprises the critical parts of the bitstream (such as headers, motion vectors, lower-order DCT coefficients) that are transmitted in the channel with the better error performance. The second layer is made of less critical data (such as higher DCT coefficients) and is transmitted in the channel with poorer error performance. Thus, degradations to channel errors are minimised since the critical parts of a bitstream are better protected. Data from neither channel may be decoded on a decoder that is not intended for decoding data-partitioned bitstreams. Even with the proper decoder, data extracted from the second-layer decoder cannot be used unless the decoded base layer data are available.

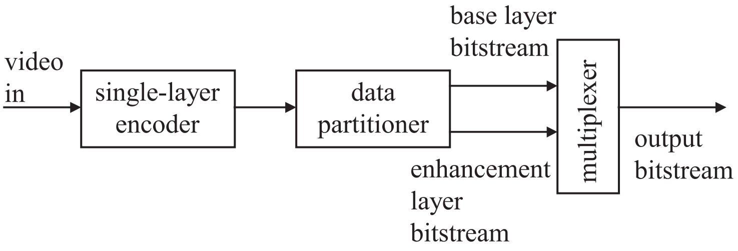

Figure 8.8 Block diagram of a data-partitioning encoder

A block diagram of a data-partitioning encoder is shown in Figure 8.8. The single-layer encoder is, in fact, a nonscalable MPEG-2 video encoder that may or may not include B-pictures. At the encoder, during the quantisation and zigzag scanning of each 8×8 DCT coefficient, the scanning is broken at the priority break point (PBP), as shown in Figure 8.9.

The first part of the scanned quantised coefficients after variable length coding, with the other overhead information such as motion vectors, MB types and addresses, including the PBP, is taken as the base layer bitstream. The remaining scanned and quantised coefficients plus the end of block (EOB) code constitute the enhancement layer bitstream. Figure 8.9 also shows the position of the PBP in the DCT coefficients.

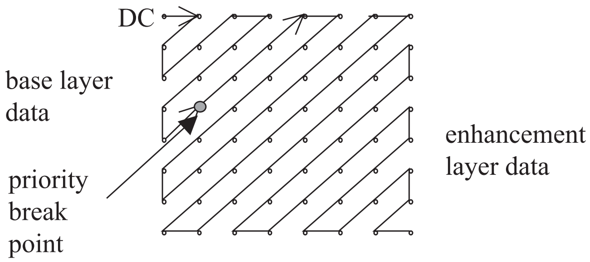

Figure 8.9 Position of the PBP in a block of DCT coefficients

The base and the enhancement layer bitstreams are then multiplexed for transmission into the channel. For prioritised transmission such as ATM networks, each bitstream is first packetised into high- and low-priority cells and the cells are multiplexed. At the decoder, having known the position of PBP, a block of DCT coefficients is reconstructed from the two bitstreams. Note that PBP indicates the last DCT coefficient of the base. Its position at the encoder is determined on the basis of the portion of channel rate from the total bit rate allocated to the base layer.

Figure 8.10 shows single shots of an 8-Mbit/s data-partitioning MPEG-2 coded video and its associated base layer picture. The PBP is adjusted for a base layer bit rate of 2 Mbit/s. At this bit rate, the quality of the base layer is almost acceptable. However, some areas in the base layer show the blocking artefacts, and in others the picture is blurred. Blockiness is due to the reconstruction of some MBs from only the DC and/or from a few AC coefficients. Blurriness is due to loss of high-frequency DCT coefficients.

It should be noted that since the encoder is a single-layer interframe coder, at the encoder both the base and the enhancement layer coefficients are used at the encoding prediction loop. Thus, reconstruction of the picture from only the base layer can result in a mismatch between the encoder and decoder prediction loops. This causes picture drift on the reconstructed picture, that is, a loss of enhancement data at the decoder is accumulated and appears as mosquito-like noise. Picture drift occurs only on P-pictures, but since B-pictures may use P-pictures for prediction, they too suffer from picture drift. Also, I-pictures reset the feedback prediction; hence, they clean up the drift. The more frequent the I-pictures, the less the appearance of picture drift, but at the expense of higher bit rates.

In summary, to have a drift-free video, the receiver should receive the entire bitstream. That is, a receiver that decodes only the base layer portion of the bitstream cannot produce a stable video. Therefore, data-partitioned bitstream is not scalable, but it is layered coded. It is, in fact, the simplest form of layering technique, which has no extra complexity over the single-layer encoder.

Although the base picture suffers from picture drift and may not be usable alone, that of the enhanced (base layer plus the enhancement layer) picture with occasional losses is quite acceptable. This is due to normally low loss rates in most networks (e.g. less than 10^{-4} in ATM networks), such that before the accumulation of loss becomes significant, the loss area is cleaned up by I-pictures.

8.5.3 SNR scalability

SNR scalability is a tool intended for use in video applications involving telecommunications and multiple-quality video services with standard TV and enhanced TV, that is, video systems with the common feature that a minimum of two layers of video quality are necessary. SNR scalability involves generating two video layers of the same spatio-temporal resolution but different video qualities from a single video source such that the base layer is coded by itself to provide the basic video quality and the enhancement layer is coded to enhance the base layer. The enhancement layer, when added back to the base layer, regenerates a higher-quality reproduction of the input video. Since the enhancement layer is said to

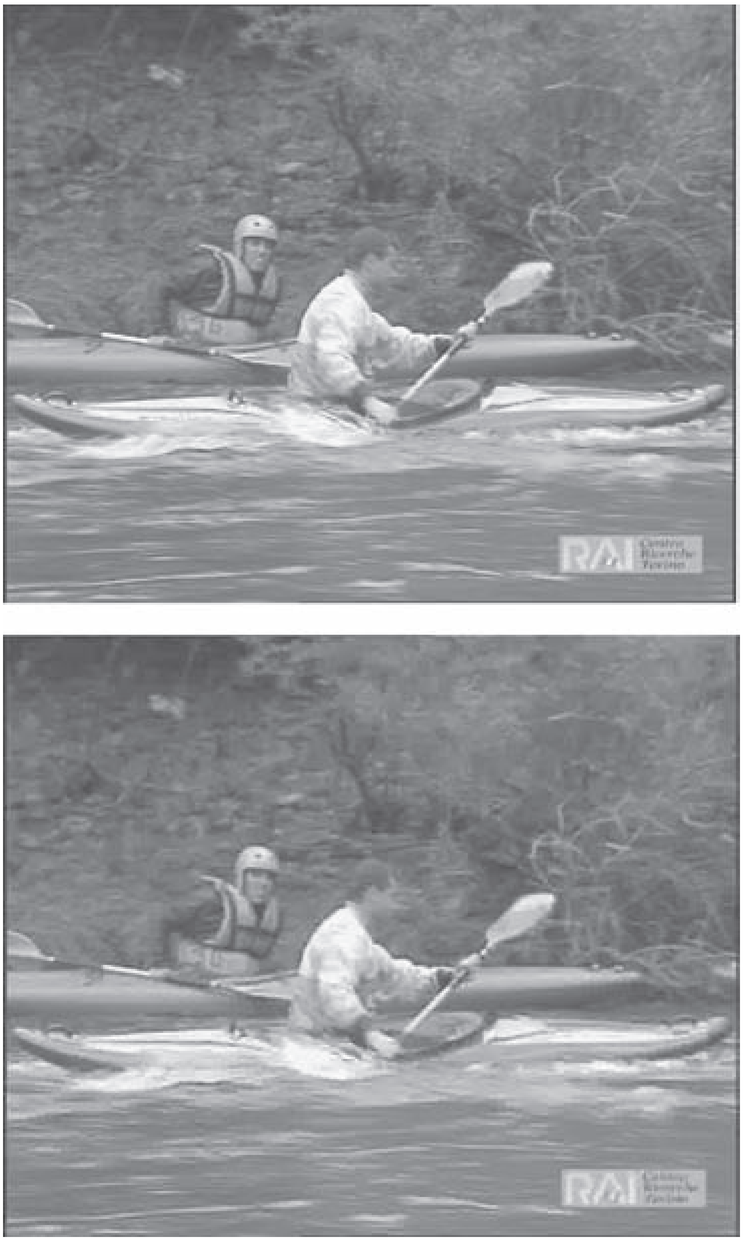

Figure 8.10 Data partitioning: (a) enhanced and (b) base pictures

enhance the SNR of the base layer, this type of scalability is called SNR. Alternatively, as we will see later, SNR scalability could have been called coefficient amplitude scalability or quantisation noise scalability. These types, although a bit wordy, may better describe the nature of this encoder.

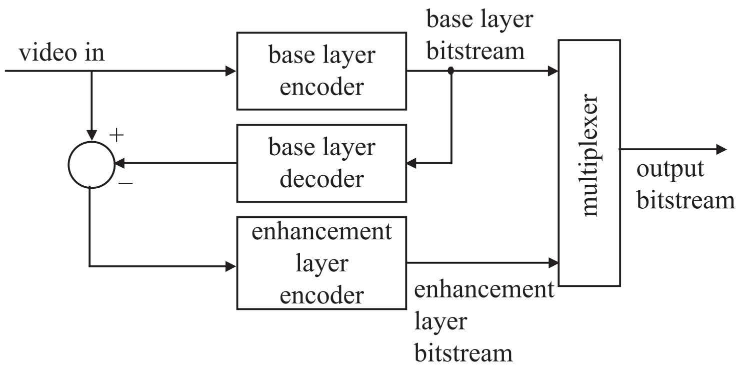

Figure 8.11 Block diagram of a two-layer SNR scalable coder

Figure 8.11 shows a block diagram of a two-layer SNR scalable encoder. First, the input video is coded at a low bit rate (lower image quality) to generate the base layer bitstream. The difference between the input video and the decoded output of the base layer is coded by a second encoder, with a higher precision, to generate the enhancement layer bitstream. These bitstreams are multiplexed for transmission over the channel. At the decoder, decoding of the base layer bitstream results in the base picture. When the decoded enhancement layer bitstream is added to the base layer, the result is an enhanced image. The base and the enhancement layers may either use the MPEG-2 standard encoder or the MPEG-1 standard for the base layer and MPEG-2 for the enhancement layer. That is, in the latter a 4:2:0 format picture is generated at the base layer, but a 4:2:0 or 4:2:2 format picture at the second layer.

It may appear that the SNR scalable encoder is much more complex than is the data-partitioning encoder. The former requires at least two nonscalable encoders, whereas data partitioning is a simple single-layer encoder, and partitioning is just carried out on the bitstream. The fact is that if both layer encoders in the SNR coder are of the same type, for example, both nonscalable MPEG-2 encoders, then the two-layer encoder can be simplified. Consider Figure 8.12, which represents a simplified nonscalable MPEG-2 of the base layer [10].

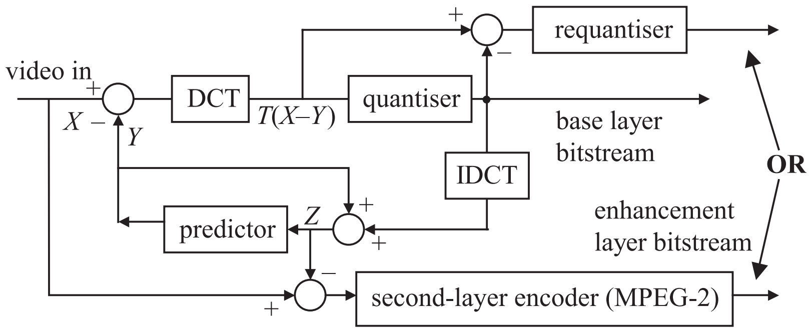

Figure 8.12 A DCT-based base layer encoder

According to the figure, the difference between the input pixels block X and their motion-compensated predictions Y is transformed into coefficients $T(X-Y)$. These coefficients after quantisation can be represented with $T(X-Y)-Q$, where Q is the introduced quantisation distortion. The quantised coefficients, after the inverse DCT (IDCT), reconstruct the prediction error. They are then added to the motion-compensated prediction to reconstruct a locally decoded pixel block Z.

Thus, the interframe error signal $X-Y$, after transform coding, becomes

$$T(X-Y) \tag{8.1}$$

and after quantisation, a quantisation distortion Q is introduced to the transform coefficients. Then eqn. 8.1 becomes

$$T(X-Y)-Q \tag{8.2}$$

After the IDCT, the reconstruction error can be formulated as

$$T^{-1}[T(X-Y)-Q] \tag{8.3}$$

where T^{-1} is the inverse transformation operation. Since transformation is a linear operator, the reconstruction error can be written as

$$T^{-1}T(X-Y)-T^{-1}(Q) \tag{8.4}$$

Also, because of the orthonormality of the transform, where $T^{-1}T=1$, eqn. 8.4 is simplified to

$$X-Y-T^{-1}(Q) \tag{8.5}$$

When this error is added to the motion-compensated prediction Y, the locally decoded block becomes

$$Z=Y+X-Y-T^{-1}(Q)=X-T^{-1}(Q) \tag{8.6}$$

Thus, according to Figure 8.12, what is coded by the second-layer encoder is

$$X-Z=X-X+T^{-1}(Q)=T^{-1}(Q) \tag{8.7}$$

that is, the inverse transform of the base layer quantisation distortion. Since the second-layer encoder is also an MPEG encoder (e.g. a DCT-based encoder), DCT transformation of $X-Z$ in eqn. 8.7 would result in

$$T(X-Z)=TT^{-1}(Q)=Q \tag{8.8}$$

where again the orthonormality of the transform is employed. Thus, the second-layer transform coefficients are, in fact, the quantisation distortions of the base layer transform coefficients, Q. For this reason, the codec can also be called a coefficient amplitude scalability or quantisation noise scalability unit.

Therefore, the second layer of an SNR scalable encoder can be a simple requantiser, as shown in Figure 8.12, without much more complexity than a data-partitioning encoder. The only problem with this method of coding is that since normally the base layer is poor or at least worse than the enhanced image (base plus the second layer), the used prediction is not good. A better prediction would be a picture of the sum of both layers, as shown in Figure 8.13. Note that the second layer is still encoding the quantisation distortion of the base layer.

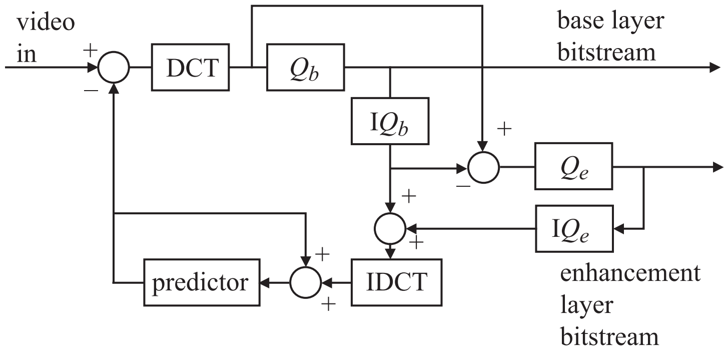

Figure 8.13 A two-layer SNR scalable encoder with drift at the base layer

In this encoder, for simplicity, the motion compensation, variable length coding of both layers and the channel buffer have been omitted. In the figure, Q_b and Q_e are the base and the enhancement layer quantisation step sizes, respectively. The quantisation distortion of the base layer is requantised with a finer precision ($Q_e < Q_b$), and then it is fed back to the prediction loop to represent the coding loop of the enhancement layer. Now, compared with data partitioning, this encoder only requires a second quantiser, and so the complexity is not so great.

Note the tight coupling between the two-layer bitstreams. For freedom from drift in the enhanced picture, both bitstreams should be made available to the decoder. For this reason, this type of encoder is called an SNR scalable encoder with drift at the base layer or no drift in the enhancement layer. If the base layer bitstream is decoded by itself, then because of loss of differential refinement coefficients, the decoded picture in this layer will suffer from picture drift. Thus, this encoder is not a true scalable encoder, but is, in fact, a layered encoder. Again, although the drift should only appear in P-pictures, since B-pictures use P-pictures for predictions, this drift is transferred into B-pictures too. I-pictures reset the distortion, and drift is cleaned up.

For applications with the occasional loss of information in the enhancement layer, parts of the picture have the base layer quality, and other parts that of the enhancement layer. Therefore, picture drift can be noticed in these areas.

If a true SNR scalable encoder with drift-free pictures at both layers is the requirement, then the coupling between the two layers must be loosened. Applications such as simulcasting of video with two different qualities from the same source need such a feature. One way to prevent picture drift is not to feed back the enhancement data into the base layer prediction loop. In this case, the enhancement layer will be intra coded and bit rate will be very high.

To reduce the second-layer bit rate, the difference between the input to and the output of the base layer (see Figure 8.11) can be coded by another MPEG encoder [11]. However, here we need two encoders, and the complexity is much higher than that in data partitioning. To reduce the complexity, we need to code only the quantisation distortion. However, since transformation operator and, most importantly, in SNR scalability, the temporal and spatial resolutions of the base and enhancement layers pictures are identical, the motion estimation and compensation can be shared between them. Following eqns 8.1–8.8, we can also simplify the two independent encoders into one encoder generating two bitstreams, such that each bitstream is drift-free decodable. Figure 8.14 shows a block diagram of a three-layer truly SNR scalable decoder, where the generated picture of each layer is drift free and can be used for simulcasting [12].

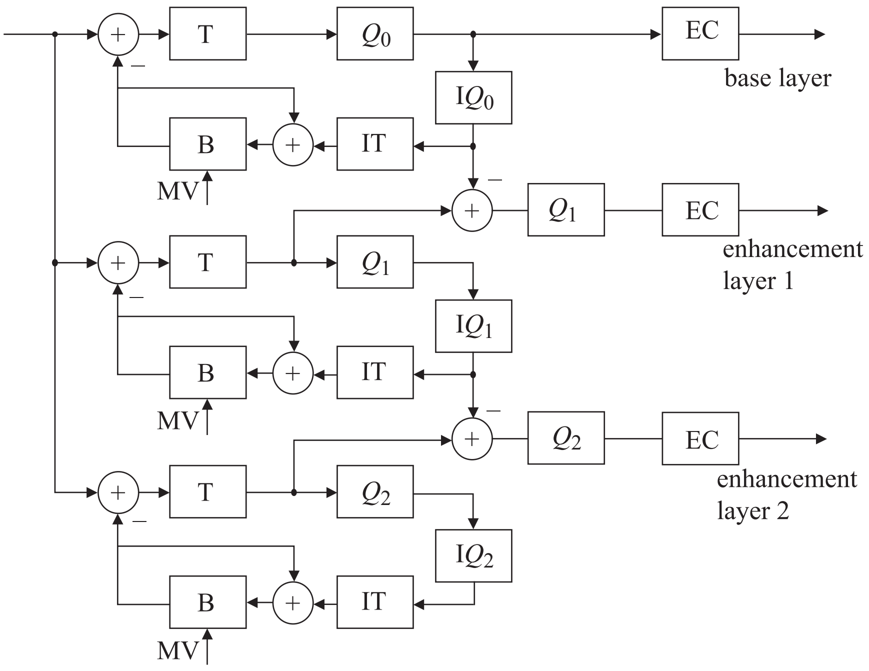

Figure 8.14 A three-layer drift-free SNR scalable encoder

In the figure, T, B, IT and EC represent transformation, prediction buffer, inverse transformation and entropy coding, and Q_i is the *i*th-layer quantiser. A common motion vector is used at all layers. Note that although this encoder looks to be made of several single-layer encoders, but since motion estimation and many coding decisions are common to all the layers and the fact that motion estimation comprises about 55–70 per cent of encoding complexity of an encoder, the increase in complexity is moderate. Figure 8.15 shows the block diagram of the corresponding three-layer SNR decoder.

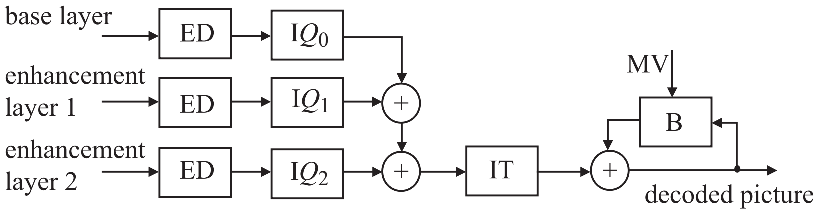

Figure 8.15 A block diagram of a three-layer SNR decoder

Each layer, after entropy decoding (ED), is inverse quantised, and then all are added together to represent the final DCT coefficients. These coefficients are inverse transformed and are added to the motion-compensated previous picture to reconstruct the final picture. Note that there is only one motion vector, which is transmitted at the base layer. Note also that the decoder of Figure 8.13, with drift in the base layer, is also similar to this figure, but with only two layers of decoding.

Figure 8.16 shows the picture quality of the base layer at 2 Mbit/s. That of the base plus the enhancement layer would be similar to those of the data partitioning,

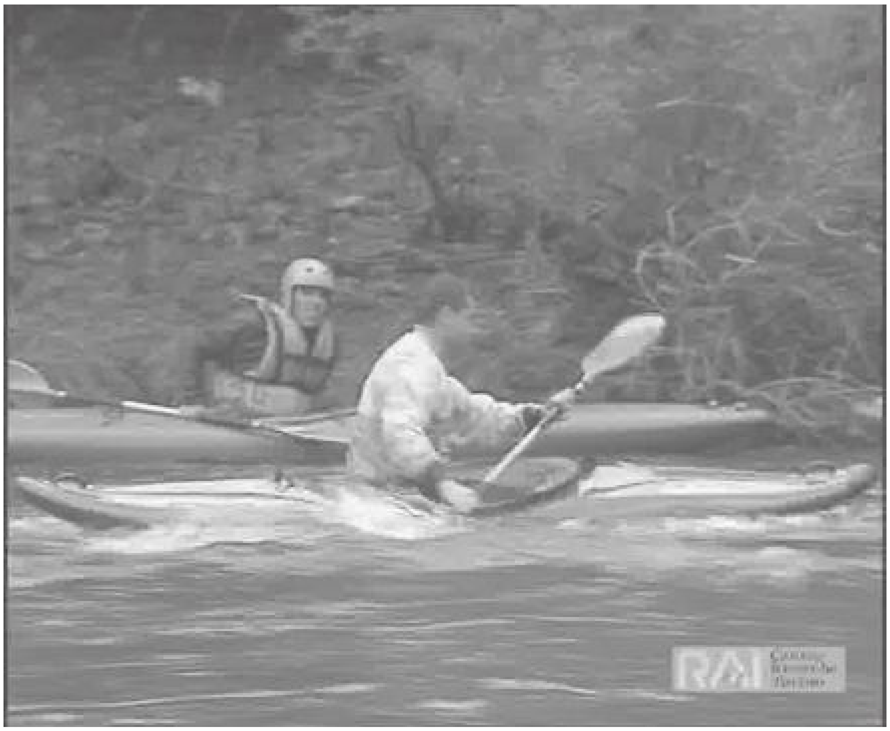

Figure 8.16 Picture quality of the base layer of SNR encoder at 2 Mbit/s

albeit with slightly higher bit rate. At this bit rate, the extra bits would be in the order of 15–20 per cent, due to the overhead of the second-layer data [11] (also see Figure 8.26). Because of coarser quantisation, some parts of the picture are blocky, as was the case in data partitioning. However, since any significant coefficient can be included at the base layer, the base layer picture of this encoder, unlike that of data partitioning, does not suffer from loss of high-frequency information.

Experimental results show that the picture quality of the base layer of SNR scalable coder is much superior to that of data partitioning, especially at lower bit rates [13]. This is because at lower base layer bit rates, data partitioning can only retain DC and possibly one or two AC coefficients. Reconstructed pictures with these few coefficients are very blocky.

8.5.4 Spatial scalability

Spatial scalability involves generating two spatial resolution video streams from a single video source such that the base layer is coded by itself to provide the basic spatial resolution and the enhancement layer employs the spatially interpolated base layer, which carries the full spatial resolution of the input video source [14]. The base and the enhancement layers may either use both the coding tools in the MPEG-2 standard or the MPEG-1 standard for the base layer and MPEG-2 for the enhancement layer or even an H.261 encoder at the base layer and an MPEG-2 encoder at the second layer. Use of MPEG-2 for both layers achieves a further advantage by facilitating interworking between video coding standards. Moreover, spatial scalability offers the flexibility in choice of video formats to be employed in each layer. The base layer can use SIF or even lower-resolution pictures at 4:2:0, 4:2:2 or 4:1:1 formats, while the second layer can be kept at CCIR-601 with 4:2:0 or 4:2:2 format. Like the other two scalable coders, spatial scalability is able to provide resilience to transmission errors as the more important data of the lower layer can be sent over channel with better error performance and the less critical enhancement layer data can be sent over a channel with poorer error performance. Figure 8.17 shows a block diagram of a two-layer spatial scalable encoder.

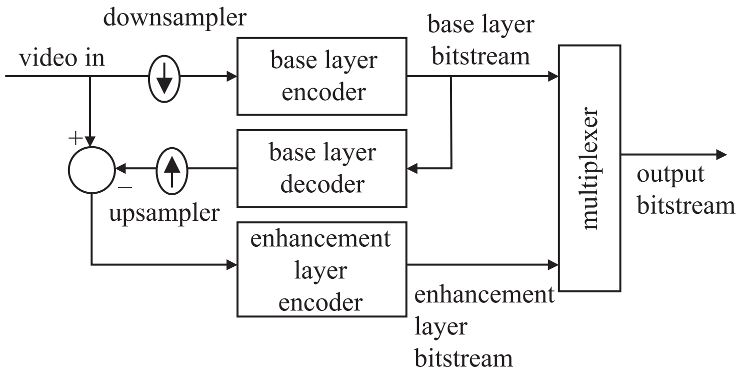

Figure 8.17 Block diagram of a two-layer spatial scalable encoder

An incoming video is first spatially reduced in both the horizontal and vertical directions to produce a reduced picture resolution. For 2:1 reduction, normally a CCIR-601 video is converted into an SIF image format. The filters for the luminance and the chrominance colour components are the seven- and four-tap filters, respectively, described in section 2.3. The SIF image sequence is coded at the base layer by an MPEG-1 or MPEG-2 standard encoder, generating the base layer bitstream. The bitstream is decoded and upsampled to produce an enlarged version of the base layer decoded video at CCIR-601 resolution. The upsampling is carried out by inserting zero-level samples between the luminance and chrominance pixels, and interpolating with the seven- and four-tap filters, similar to those described in section 2.3. An MPEG-2 encoder at the enhancement layer codes the difference between the input video and the interpolated video from the base layer. Finally, the base and enhancement layer bitstreams are multiplexed for transmission into the channel.

If the base and the enhancement layer encoders are of the same type (e.g. both MPEG-2), then the two encoders can interact. This is not only to simplify the two-layer encoder, as was the case for the SNR scalable encoder, but also to make the coding more efficient. Consider an MB at the base layer. Because of 2:1 picture resolution between the enhancement and the base layers, the base layer MB corresponds to four MBs at the enhancement layer. Similarly, an MB at the enhancement layer corresponds to a block of 8 × 8 pixels at the base layer. The interaction would be in the form of upsampling the base layer block of 8 × 8 pixels into an MB of 16 × 16 pixels and using it as a part of the prediction in the enhancement layer coding loop.

Figure 8.18 shows a block of 8 × 8 pixels from the base layer that is upsampled and is combined with the prediction of the enhancement layer to form the final prediction for an MB at the enhancement layer. In the figure, the base layer upsampled MB is weighted by w and that of the enhancement layer by $1 - w$.

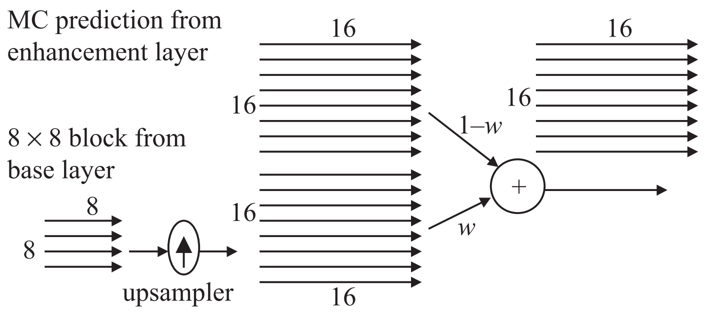
MC prediction from enhancement layer
16
16
16
8 × 8 block from base layer
8
8
upsampler
16
16
16
1−w
w
+

Figure 8.18 Principle of spatio-temporal prediction in the spatial scalable encoder

More details of the spatial scalable encoder are shown in Figure 8.19. The base layer is a nonscalable MPEG-2 encoder, where each block of this encoder is upsampled, interpolated and fed to a weighting table (WT). The coding elements of the enhancement layer are shown without the motion compensation, VLC and the

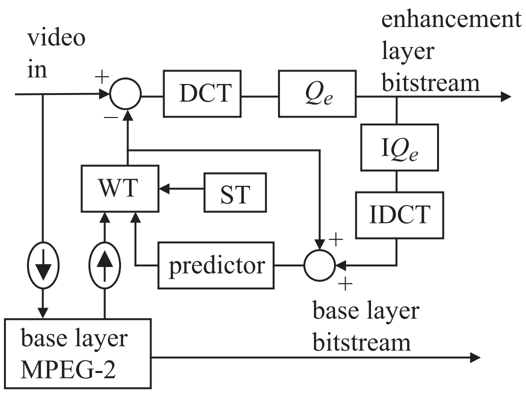

Figure 8.19 Details of spatial scalability encoder

other coding tools of the MPEG-2 standard. A statistical table (ST) sets the WT elements. Note that the weighted base layer MBs are used in the prediction loop, which will be subtracted from the input MBs. This part is similar to taking the difference between the input and the decoded base layer video and coding their differences by a second-layer encoder, as was illustrated in the general block diagram of this encoder in Figure 8.17.

Figure 8.20 shows a single shot of the base layer picture at 2 Mbit/s. The picture produced by the base plus the enhancement layer at 8 Mbit/s would be similar to that resulting for data partitioning, shown in Figure 8.10. Note that since picture size is one-quarter of the original, the 2 Mbit/s allocated to the base layer would be sufficient to code the base layer pictures at almost identical quality to the base plus the enhancement layer at 8 Mbit/s. An upsampled version of the base layer picture to fill the display at the CCIR-601 size is also shown in the figure. Comparing this picture with those of data partitioning and the simple version of the SNR scalable coders, it can be seen that the picture is almost free from blockiness. However, still some very high-frequency information is missing, and the aliasing distortions due to the upsampling will be introduced into the picture. Note that the base layer picture can be used alone without picture drift. This was not the case for data partitioning and the simple SNR scalable encoders. However, the price paid is that this encoder is made up of two MPEG encoders and is more complex than data partitioning and SNR scalable encoders. Note that unlike the true SNR scalable encoder of Figure 8.14, here because of differences in the picture resolutions of the base and enhancement layers, the same motion vector cannot be used for both layers.

8.5.5 Temporal scalability

Temporal scalability is a tool intended for use in a range of diverse video applications from telecommunications to HDTV. In such systems, migration to higher temporal resolution systems from that of lower temporal resolution systems may be necessary. In many cases the lower temporal resolution video systems may be

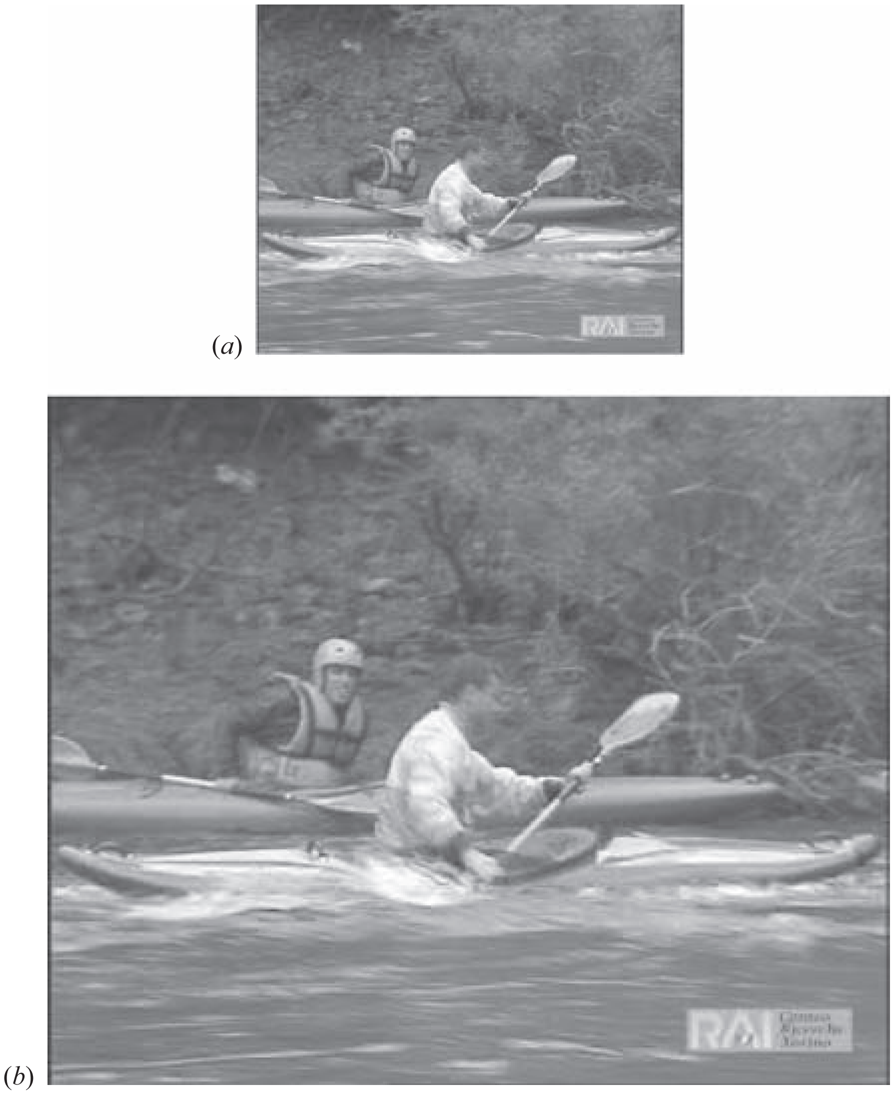

Figure 8.20 (a) Base layer picture of a spatial scalable encoder at 2 Mbit/s and (b) its enlarged version

either the existing systems or the less expensive early-generation systems. The more sophisticated systems may then be introduced gradually.

Temporal scalability involves partitioning of video frames into layers, in which the base layer is coded by itself to provide the basic temporal rate and the enhancement layer is coded with temporal prediction with respect to the base layer. The layers may have either the same or different temporal resolutions, which, when combined, provide full temporal resolution at the decoder. The spatial resolution of frames in each layer is assumed to be identical to that of the input video. The video encoders of the two layers may not be identical. The lower temporal resolution systems may only decode the base layer to provide basic temporal resolution, whereas more sophisticated systems of the future may decode both layers and provide high temporal resolution video while maintaining interworking capability with earlier-generation systems.

Since in temporal scalability the input video frames are simply partitioned between the base and the enhancement layer encoders, the encoder need not be more complex than a single-layer encoder. For example, a single-layer encoder may be switched between the two base and enhancement modes to generate the base and the enhancement bitstreams alternately. Similarly, a decoder can be reconfigured to decode the two bitstreams alternately. In fact, the B-pictures in MPEG-1 and MPEG-2 provide a very simple temporal scalability that is encoded and decoded alongside the anchor I- and P-pictures within a single codec. I- and P-pictures are regarded as the base layer, and the B-pictures become the enhancement layer. Decoding of I- and P-pictures alone will result in the base pictures with low temporal resolution, and when added to the decoded B-pictures, the temporal resolution is enhanced to its full size. Note that since the enhancement data do not affect the base layer prediction loop, both the base and the enhanced pictures are free from picture drift.

Figure 8.21 shows the block diagram of a two-layer temporal scalable encoder. In the figure, a temporal demultiplexer partitions the input video into the base and enhancement layers, input pictures. For a 2:1 temporal scalability shown in the

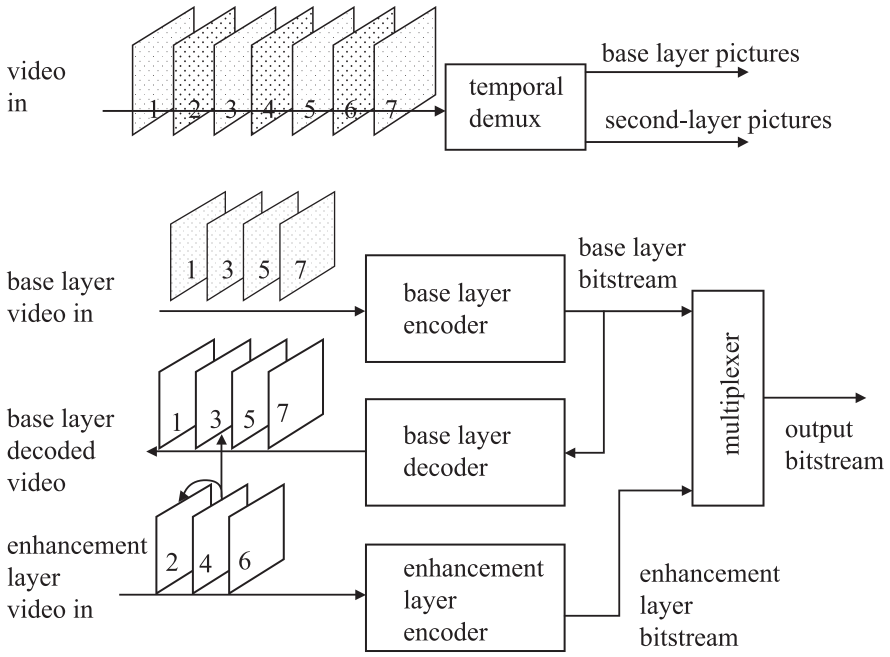

Figure 8.21 A block diagram of a two-layer temporal scalable encoder

figure, the odd-numbered pictures are fed to the base layer encoder and the even-numbered pictures become inputs to the second-layer encoder. The encoder at the base layer is a normal MPEG-1, MPEG-2 or any other encoder. Again, for greater interaction between the two layers, either to make encoding simple or more efficient, both layers may employ the same type of coding scheme.

At the base layer, the lower temporal resolution input pictures are encoded in the normal way. Since these pictures can be decoded independently of the enhancement layer, they do not suffer from picture drift. The second layer may use prediction from the base layer pictures or from its own picture, as shown for frame 4 in the figure. Note that at the base layer, some pictures might be coded as B-pictures, using their own previous, future or their interpolation as prediction, but it is essential that some pictures should be coded as anchor pictures. On the other hand, in the enhancement layer, pictures can be coded at any mode. Of course, for greater compression, at the enhancement layer, most, if not all, of the pictures are coded as B-pictures. These B-pictures have the choice of using past, future and their interpolated values, either from the base or the enhancement layer.

8.5.6 Hybrid scalability

MPEG-2 allows combination of individual scalabilities such as spatial, SNR or temporal scalability to form hybrid scalability for certain applications. If two scalabilities are combined, then three layers are generated, and they are called the base layer, enhancement layer 1 and enhancement layer 2. Here enhancement layer 1 is a lower layer relative to enhancement layer 2, and hence, decoding of enhancement layer 2 requires the availability of enhancement layer 1. In the following sections, some examples of hybrid scalability are shown.

8.5.6.1 Spatial and temporal hybrid scalability

Spatial and temporal scalability is perhaps the most common use of hybrid scalability. In this mode the three-layer bitstreams are formed by using spatial scalability between the base and enhancement layer 1, while temporal scalability is used between enhancement layer 2 and the combined base and enhancement layer 1, as shown in Figure 8.22.

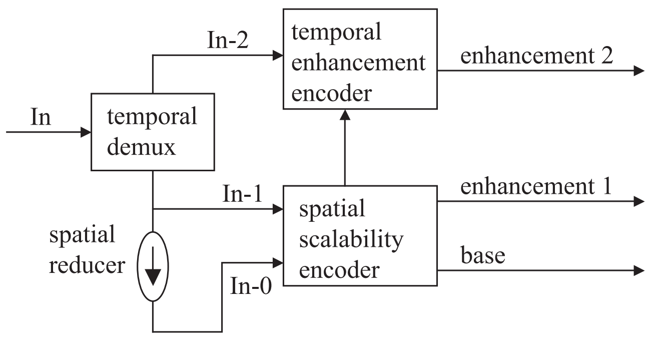

Figure 8.22 Spatial and temporal hybrid scalability encoder

In this figure, the input video is temporally partitioned into two lower temporal resolution image sequences In-1 and In-2. The image sequence In-1 is fed to the spatial scalable encoder, where its reduced version, In-0, is the input to the base layer encoder. The spatial encoder then generates two bitstreams for the base and enhancement layer 1. In-2 image sequence is fed to the temporal enhancement encoder to generate the third bitstream, enhancement layer 2. The temporal enhancement encoder can use the locally decoded pictures of a spatial scalable encoder as predictions, as was explained in section 8.5.4.

8.5.6.2 SNR and spatial hybrid scalability

Figure 8.23 shows a three-layer hybrid encoder employing SNR scalability and spatial scalability. In this coder, the SNR scalability is used between the base and the enhancement layer 1 and the spatial scalability is used between the layer 2 and the combined base and enhancement layer 1. The input video is spatially downsampled (reduced) to lower resolution as In-1 is to be fed to the SNR scalable encoder. The output of this encoder forms the base and enhancement layer 1 bit-streams. The locally decoded pictures from the SNR scalable coder are upsampled to full resolution to form prediction for the spatial enhancement encoder.

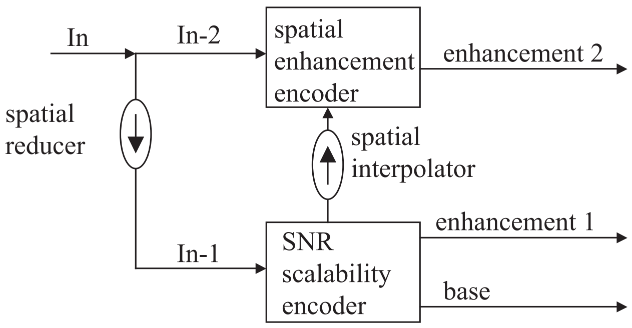

Figure 8.23 SNR and spatial hybrid scalability encoder

8.5.6.3 SNR and temporal hybrid scalability

Figure 8.24 shows an example of an SNR and temporal hybrid scalability encoder. The SNR scalability is performed between the base layer and the first enhancement layer. The temporal scalability is used between the second enhancement layer and the locally decoded picture of the SNR scalable coder. The input image sequence through a temporal demultiplexer is partitioned into two sets of image sequences, and these are fed to each individual encoder.

8.5.6.4 SNR, spatial and temporal hybrid scalability

The three scalable encoders might be combined to form a hybrid coder with a larger number of levels. Figure 8.25 shows an example of four levels of scalability using all the three scalability tools mentioned.

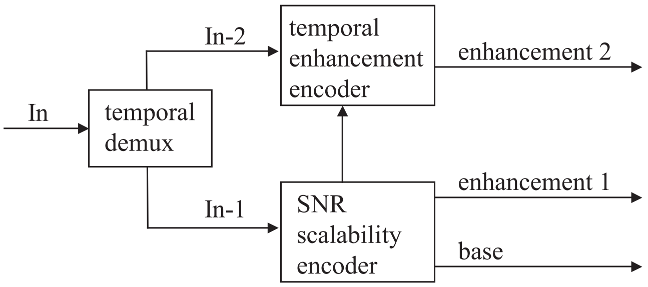

Figure 8.24 SNR and temporal hybrid scalability encoder

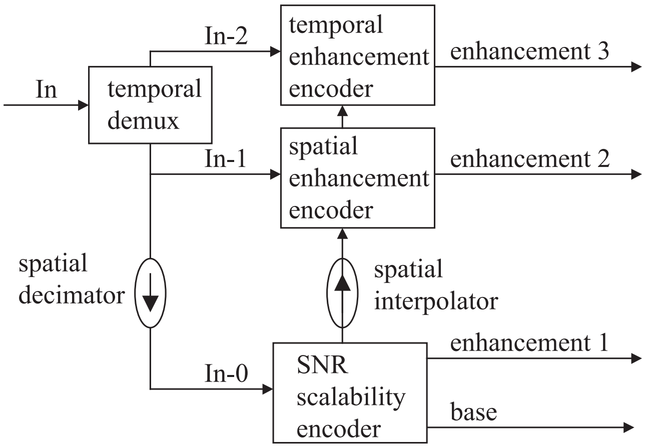

Figure 8.25 SNR, spatial and temporal hybrid scalability encoder

The temporal demultiplexer partitions the input video into image sequences In-1 and In-2. Image sequence In-2 is coded at the highest enhancement layer (enhancement 3), with the prediction from the lower levels. The image sequence In-1 is first downsampled to produce a lower-resolution image sequence, In-0. This sequence is then SNR scalable coded to provide the base and the first enhancement layer bitstreams. An upsampled and interpolated version of the SNR scalable decoded video forms the prediction for the spatial enhancement encoder. The output of this encoder results in the second enhancement layer bitstream (enhancement 2).

Figure 8.25 was just an example of how various scalability tools can be combined to produce bitstreams of various degrees of importance. Of course, depending on the application, formation of the base and the level of the hierarchy of the higher enhancement layers might be defined in a different way to suit the application. For example, when the above scalability methods are applied to each of the I-, P- and B-pictures, since these pictures have different levels of importance, their layered versions can increase the number of layers even further.

8.5.7 Overhead due to scalability

Although scalability or layering techniques provide a means of delivering a better video quality to the receivers than the single-layer encoders, this is done at the expense of higher encoder complexity and higher bit rate. We have seen that data partitioning was the simplest form of layering, and spatial scalability the most complex one. The amount of extra bits generated by these scalability techniques is also different.

Data partitioning is a single-layer encoder, but inclusion of the PBP in the zigzag scanning path and the fact that the zero run of the zigzag scan is now broken into two parts incur some additional bits. These extra bits, along with redundant declaration of the MB addresses at both layers, generate some overhead over the single-layer coder. Our investigations show that the overhead bit is in the order of 3–4 per cent of the single-layer counterpart almost irrespective of the percentage of the bits from the total bit rate assigned to the base layer.

In SNR scalability, the second layer codes the quantisation distortions of the base layer plus the other addressing information. The additional bits over the single layer depend on the relationship between the quantiser step sizes of the base and enhancement layers and, consequently, on the percentage of the total bits allocated to the base layer. At the lower percentages, the quantiser step size of the base layer is large, and hence, the second layer efficiently codes any residual base layer quantisation distortions. This is very similar to successive approximation (two sets of bit planes); hence, the SNR scalable coding efficiency is not expected to be much worse than the single layer.

At the higher percentages of base layer bit rates, the quantiser step sizes of the base and enhancement layers become close to each other. Considering that for a base layer quantiser step size of Q_b, the maximum quantisation distortion of the quantised coefficients is $Q_b/2$ and the nonquantised ones that fall in the dead zone is Q_b, as long as the enhancement quantiser step size $Q_b > Q_e > Q_b/2$, none of the significant base layer coefficients are coded by the enhancement layer except, of course, the ones in the dead zone of the base layer. Thus, again, both layers code the data efficiently, that is, the coefficient is coded at either the base layer or the enhancement layer, and the overall coding efficiency is not worse than that in case of the single layer. Reducing the base layer bit rate from its maximum value means increasing Q_b. As long as $Q_b/2 < Q_e$, none of the base layer quantisation distortions (except the ones on the dead zone) can be coded by the enhancement layer. Hence, the enhancement layer does not improve the picture quality noticeably, and since the base layer is coded at a lower bit rate, the overall quality will be worse than that in case of the single layer. The worst quality occurs when $Q_e = Q_b/2$.

If the aim was to produce the same picture quality, then the bit rate of SNR scalable coder had to be increased, as shown in Figure 8.26. In this figure, the overall bit rate of the SNR scalable coder is increased over the single layer such that the picture quality under both encoders is identical. The percentage of the bits assigned to the base layer from the total bits is varied from its minimum value to its maximum value. As we see, the poorest performance of the SNR scalable

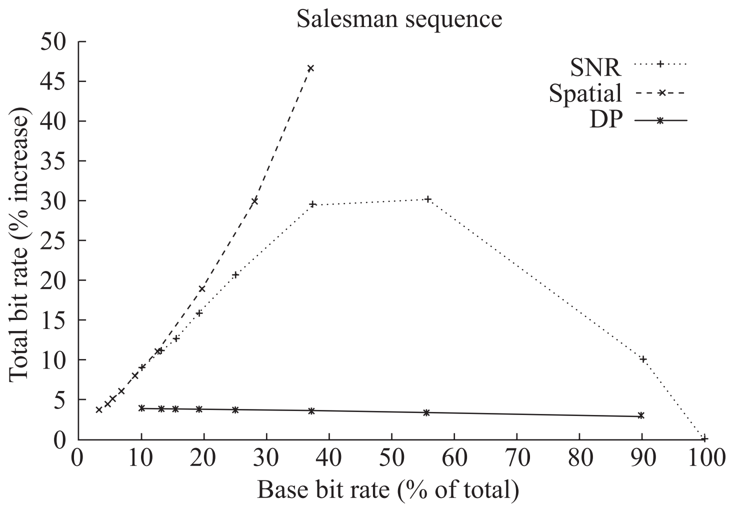

Figure 8.26 Increase in bit rate due to scalability

(the highest overhead) is when the base layer is allocated about 40–60 per cent of the total bit rate. In fact, at this bit rate, the average quantiser step size of the enhancement layer is half of that of the base layer. This maximum overhead is 30 per cent, and that of the data partitioning is also shown, which reads about 3 per cent irrespective of the bits assigned to the base layer.

In spatial scalability, the smaller-size picture of the base layer is upsampled, and its difference with the input picture is coded by the enhancement layer. Hence, the enhancement layer, in addition to the usual redundant addressing, has to code two new items of information. One is the aliasing distortion of the base layer due to upsampling, and the other is the quantisation distortion of the base layer, if there is any.

At the very low percentage of the bits assigned to the base layer, both of these distortions are coded efficiently by the enhancement layer. As the percentage of bits assigned to the base layer increases, similar to SNR scalability, the overhead increases too. At the time where the quantiser step sizes of both layers become equal, $Q_b = Q_e$, any increase in the base layer bit rate (making $Q_b < Q_e$) means that the enhancement layer cannot improve the distortions of the base layer further. Beyond this point, aliasing distortion will be the dominant distortion, and any increase in the base layer bit rate will be wasted. Thus, as the bit rate budget of the base layer increases, the overhead increases too, as shown in Figure 8.26. This differs from the behaviour of the SNR scalability.

In fact, in spatial scalability with a fixed total bit rate, increasing the base layer bit rate beyond the critical point of $Q_b = Q_e$ will reduce the enhancement layer bit rate budget. In this case, increasing the base layer bit rate will increase the aliasing distortion, and hence, as the base layer bit rate increases, the overall quality decreases.

In temporal scalability, in contrast to the other scalability methods, in fact, the bit rate can be less than single-layer encoder. This is because there is no redundant addressing to create overhead. Moreover, since the enhancement layer pictures have more choice for their optimum prediction, from either base or enhancement layers, they are coded more efficiently than the single layer. A good example is the B-pictures in MPEG-2 that can be coded at much lower bit rate than the P-pictures. Thus, temporal scalability can, in fact, be slightly more efficient than for single-layer coding.

8.5.8 Applications of scalability

Considering the nature of the basic scalability of data partitioning, SNR, spatial and temporal scalability and their behaviour with regard to picture drift and the overhead, suitable applications for each method may be summarised as follows:

- *Data partitioning*: This mode is the simplest of all, but since it has a poor base layer quality and is sensitive to picture drift, it can be used in the environment where there is rarely any loss of enhancement data (e.g. loss rate $< 10^{-6}$). Hence, the best application would be video over ATM networks, where, through admission control, the loss ratio can be maintained at low levels [15].
- *SNR scalability*: In this method, two pictures of the same spatio-temporal resolutions are generated, but one has lower picture quality than the other. It generally has a higher bit rate over nonscalable encoders but can have a good base picture quality and can be drift free. Hence, suitable applications can be as follows:
  - transmission of video at different qualities of interest, such as multiquality video, video on demand, broadcasting of TV and enhanced TV
  - video over networks with a high error or packet loss rates, such as Internet or heavily congested ATM networks
- *Spatial scalability*: This is the most complex form of scalability, where each layer requires a complete encoder/decoder. Such a loose dependency between the layers has the advantage that each layer is free to use any codec, with different spatio-temporal and quality resolutions. Hence, there can be numerous applications for this mode, such as the following:
  - interworking between two different standard video codecs (e.g. H.263 and MPEG-2)
  - simulcasting of drift-free good-quality video at two spatial resolutions, such as standard TV and HDTV
  - distribution of video over computer networks
  - video browsing
  - reception of good-quality low spatial resolution pictures over mobile networks
  - similar to other scalable coders, transmission of error resilience video over packet networks

- *Temporal scalability*: This is a moderately complex encoder, where either a single-layer coder encodes both layers, such as coding of B-pictures and the anchor I- and P-pictures in MPEG-1 and MPEG-2 or two separate encoders operating at two different temporal rates. The major applications can then be as follows:
    - migration to progressive (HDTV) from the current interlaced broadcast TV
    - internetworking between lower bit rate mobile and higher bit rate fixed networks
    - video over LANs, Internet and ATM for computer workstations
    - video over packet (Internet/ATM) networks for loss resilience

Tables 8.4, 8.5 and 8.6 summarise a few applications of various scalability techniques that can be applied to broadcast TV. In each application, parameters of the base and enhancement layers are also shown.

Table 8.4 Applications of SNR scalability

Base layer	**Enhancement layer**	**Application**
ITU-R-601	Same resolution and format as lower layer	Two quality service for standard TV
High definition	Same resolution and format as lower layer	Two quality service for HDTV
4:2:0 High definition	4:2:2 Chroma simulcast	Video production/distribution

Table 8.5 Applications of spatial scalability

Base	**Enhancement**	**Application**
Progressive (30 Hz)	Progressive (30 Hz)	CIF/QCIF compatibility or scalability
Interlace (30 Hz)	Interlace (30 Hz)	HDTV/SDTV scalability
Progressive (30 Hz)	Interlace (30 Hz)	ISO/IECE11172-2/compatibility with this specification
Interlace (30 Hz)	Progressive (60 Hz)	Migration to HR progressive HDTV

Table 8.6 Applications of temporal scalability

Base	**Enhancement**	**Higher**	**Application**
Progressive (30 Hz)	Progressive (30 Hz)	Progressive (60 Hz)	Migration to HR progressive HDTV
Interlace (30 Hz)	Interlace (30 Hz)	Progressive (60 Hz)	Migration to HR progressive HDTV

8.6 Video broadcasting

Currently, more than 95 per cent of MPEG-2 coded video is for broadcasting applications, carried via terrestrial, satellite and cable TV networks to homes. In Europe, the standard ITU-R 601 video is encoded in the range of 2–4 Mbit/s depending on the scene content of the video. The lower end of the bit rate is for head-and-shoulders type video such as the video clip of a newsreader, and the higher bit rates are required for the critical scenes such as sports programmes, similar to the snap shot shown in Figure 8.10. Normally, scenes with grass and tree leafs, which have detailed texture and random motion due to wind, if they appear alongside some plain scenes, like lake or stream, are the most difficult scenes to code. Random motions of the detailed area make motion estimation useless, and for a limited bit rate budget, increase in quantiser step size will cause blocking artefacts in the plain areas. For HDTV video, the required bit rate is in the order of 10–15 Mbit/s.

In both terrestrial and satellite TV, for better channel utilisation, several TV programmes may be multiplexed and then digitally modulated on to a carrier. At the destination, the receiver, known as the set-top box, separates the channels and decodes each programme, and the individual analogue signals can be fed to the television set for display. Although the same multiplexing technique can be used, since digital modulation techniques for terrestrial and satellite are different, unfortunately, the same set-top box cannot be used for both.

For multiplexing of TV programmes, the individual bitstreams are first decoded and then reencoded to a new target bit rate. For optimum multiplexing, the target bit rate for each TV channel is made dependent on the content (statistics) of each programme, and hence, it is called statistical multiplexing. Here, more complex video might be assigned higher bit rates, and since video complexity may vary over time, for optimum statistical multiplexing, we need to monitor the video complexity continuously.

One way of calculating the complexity of a scene in a video programme is to define the scene complexity as the sum of the complexity indices of its I-, P- and B-pictures in a GOP [16]. For each picture type, the complexity index is the product of its average quantiser step size and its bit rate in that frame. For example, the video scene complexity index (SCI) of a video with a GOP structure of $N = 12$ and $M = 3$, which has one I-, three P- and eight B-pictures, is

$$\mathrm{SCI} = \frac{1}{12}\left[IQ_I + \sum_{j=1}^{3} P_j Q_{Pj} + \sum_{j=1}^{8} B_j Q_{Bj} \right] \tag{8.9}$$

where I, P and B are the target bit rates for the I-, P- and B-pictures, and Q_I, Q_P and Q_B are their respective average quantiser step sizes. After calculating SCI for each TV programme, the total bit rate is divided between the TV channels in proportion of their SCI. Values of the SCI can be continuously calculated on frame-by-frame basis (within a window of a GOP) to provide an optimum statistical multiplexing.

One of the main attractions of the digital satellite TV is the benefit of broadcasting many TV programmes from a single transponder. In the analogue era, one satellite transponder with a bandwidth of 36 MHz could accommodate only one frequency-modulated (FM) TV programme, whereas currently, about six to eight high-quality digital TV programmes can be multiplexed into 27 Msymbol/s and are accommodated in the same transponder. There are even stations that squeeze about 10–15 digital TV programmes into a transponder, albeit at a slightly lower video quality. In addition to this increase on the TV channels, the required transmitted power for digital can be in the order of 10–20 per cent of analogue, or for the same power, the satellite dishes can be made much smaller (45- to 60-cm diameter dishes compared to 80 cm used in analogue). Digital terrestrial TV also benefits from the low-power transmitters.

In the digital terrestrial TV, normally one programme is digitally modulated into an 8-MHz (European) ultra-high frequency (UHF) channel. The bitstream prior to channel modulation is orthogonal frequency division multiplexed (OFDM) into 1705 carriers (2000 carriers is also an option), and the channel modulation is a 64-QAM. At a higher modulation rate (e.g. 256-QAM), it is even possible to accommodate 18–24 Mbit/s bitstream into the same 8-MHz UHF channel, thus being able to multiplex four to eight digital programmes (or even higher for poorer quality) into one existing analogue UHF terrestrial channel.

Since at the base band, a 2–4 Mbit/s MPEG-2 video is OFDM modulated into almost 2000 carriers, each bit of the video is transmitted at a rate of 1–2 kbit/s. Such a low data rate (large interval) is very robust against interference, similar to a high-frequency burst of noise, and can be cleaned up easily. Thus, OFDM is particularly attractive for ghost-free TV broadcasting in big cities, where multiple reflections from tall buildings can create interference (a common problem with analogue TV). Moreover, it is possible to cover the whole broadcast TV network with a single frequency, since interference is not a problem. This will release a lot of wireless bandwidth for other communication services. Finally, similar to satellite, the transmitter power can be reduced by a factor of 10 (in practice, by a factor of 7).

The price paid for all these benefits of digital TV is the sensitivity of the digital TV to channel errors. During heavy rain or snow, pictures become blocky or, in the more severe cases, there is a complete loss of picture (picture freeze). This is the main disadvantage of digital TV, since in analogue TV weaker reception may cause snowy pictures, which is better than picture break-up or freeze in digital TV. To alleviate this problem, layered video coding with unequal error protection to various layers may be used. Or, one may use a more intelligent technique of distributing the transmitter power among the layers such that the picture quality gradually degrades, closer to quality degradation in analogue TV.

8.7 Digital versatile disc

DVD is a new storage media for MPEG-2 coded high-quality video. DVD discs with 9-Gbyte storage capacity (in two tracks of 4.5 Gbytes) are introduced to replace the 648 (or 700)-Mbyte CD-ROMs. The main reason for the introduction of this new product is that viewers' expectations of video quality have grown over the time. CD-ROMs could only store MPEG-1 compressed video of SIF format at about a target rate of 1.2 Mbyte/s. When SIF pictures are enlarged to the standard size (e.g. 720 pixels by 576 lines) to be displayed on TV sets, for certain scenes the enlarged pictures look blocky. This is usually not sufficient for home movies or HDTV programmes.

In DVD, video of CCIR-601 standard size is MPEG-2 compressed. Considering the double-track DVD discs of total capacity of 9 Gbytes, the nominal movies of 90 min can be coded at an average bit rate of 6–12 Mbit/s, depending on whether one or both tracks are used.

To increase the video quality and, at the same time, to optimise the storage capacity, MPEG-2 encoder is set to encode the video at a VBR. This is done by fixing the quantiser step size at a constant value, producing video of almost constant quality over the entire programme, irrespective of scene complexity. Because of constant quantiser step size, during high picture activity, the instantaneous bit rate of the encoder can be very high (e.g. 30 Mbit/s). However, these events only occur for a short period, and there are occasions when the scenes might be very quiet, producing lower bit rates (e.g. 2 Mbit/s). Depending on the proportions of the scene activities in the video, its peak-to-mean bit rate ratio, even smoothed over a GOP, can be in the order of 3–5 (peak-to-mean ratio smoothed over one frame can easily rise above 10). Thus, had the video been coded at a constant bit rate (CBR), then for the same picture quality as VBR, the target bit rate would have to be set to the peak bit rate. Hence, at the quiet scenes, the storage capacity of the disc can be wasted. In fact, the advantage of VBR over CBR is the saving in storage capacity by the ratio of the peak bit rate to the mean bit rate, which can be considerable.

The main problem with VBR is that the chunk of compressed data read from the disc decodes a variable number of pictures per given time unit (e.g. seconds). For a uniform and smooth display (e.g. 25 pictures/s), the read data from the disc has to be smoothed. This is done by writing them into a random access memory (RAM) and reading it at the desired rate of the decoder. Considering that today the electronic notebooks are equipped with 1–2 Gbytes RAM, they are not too expensive to be included in the DVD decoders. These are sufficient to store about 5–10 min of the programme, well over what is needed to produce pictures without interruptions.

8.8 Video over ATM networks

MPEG-2 and in particular layered video coding and the ATM networks have a very strong link. They were introduced at about the same time (early 1990) and influenced each other's development. The cell loss priority in ATM is the direct product of the success of layered two-layer video coding in delivering a minimum acceptable picture quality [9]. Selection of 188-byte packet size for the MPEG-2 transport stream was influenced by the ATM cell size. An ATM cell (packet) is 53 bytes long, with a 5-byte header and a 48-byte payload. One of the AAL (where the data to be transported are interfaced to the channel) called AAL1 accepts 47-byte raw data and adds 1-byte synchronisation and other information to the payload [15]. Hence, each MPEG-2 packet can be transported with four ATM cells.

ATM is a slotted channel, where each 53-byte cell is seized by the server to insert its data for transmission. If the server has nothing to send, the cell is left empty. Hence, the source can send its data at a variable rate. VBR video transmission is particularly attractive since compressed video is variable in rate by nature. With a constant quantiser step size, the video is coded at almost constant quality. At low picture activity (low motion and low texture), less bits are generated, and at high picture activity, more bits are generated. Such VBR transmission makes statistical multiplexing even more effective than the one used with the fixed bit rate broadcast TV. It is easy to show that more VBR services can be accommodated in a given channel than the fixed bit rate services.

The main problem with VBR transmission is that if bursts of data from various services occur at the same time, there will be more traffic than the network can handle, and it will be congested. In this case, cells carrying visual information might be excessively delayed. There is a maximum tolerable delay beyond which late arrival cells will be of no use. Either the switching nodes or the receiver can discard these cells. In the former case, the cell discard is due to the limited capacity of the switching multiplex buffer, and in the latter the received information is too late to be of any use by the decoder. In both cases, loss of cells leads to degradation in picture quality.

The cell loss priority bit in ATM cells coupled with two-layer video coding can enhance the video quality significantly. Here the base layer video is assigned high priority, and the enhancement layer the lower priority. In the event of network congestion, low-priority cells (enhancement data) can be discarded and room made available to the high-priority cells (base layer). For example, even in the normal MPEG-2 with a GOP structure of $N = 12$ and $M = 3$, which can be regarded as temporal scalability, during the network congestion, all the B-pictures can be temporarily discarded to make room for the I- and P-pictures.

In ATM network, in addition to layering, the packetisation strategy also plays an important role on the video quality. One form of packetisation may confine the effect of a lost packet to a small area of the picture, while other methods may spread degradation to a larger area. With AAL1 packetisation [15], where every 47 bytes of the bitstream are packed into the ATM cell payload without any further processing, if a cell is lost, the following cells may not be recoverable until the next slice or GOB. Thus, a large part of a picture slice may be degraded depending on the location of the lost MB. This problem can be overcome by making the first MB of each cell absolutely addressed; hence, the loss can be confined to a smaller area of the picture [17]. Let us call this method of packing AAL*x*, as shown in Figure 8.27.

In AAL*x*, where the first MB in each ATM cell is absolutely addressed, the lost area could be confined to the area covered by the lost cell. All following cells could then be decodable. For the decoder to be able to recognise the absolute address, an

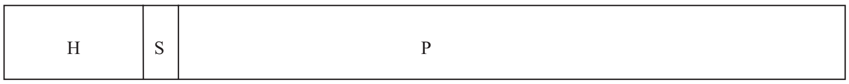

AAL1: H: header, 5 bytes
S: cell sequency number, 1 byte
P: payload, 47 bytes

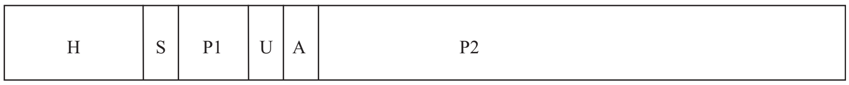

AAL*x*: H: header, 5 bytes
S: cell sequency number, 1 byte
U: unique pattern, 11 bits
A: absolute address, 9 bits
P1 and P2: payload, 45.5 bytes

*Figure 8.27 Structure of ALL1 and AAL*x *cells*

additional 11-bit header (absolute address header) must be inserted before the address. Also, the average length of the relative addressing is normally 2 bits, whereas the length of the absolute address can be 9 bits, resulting in an additional 7 bits [17]. Thus, AAL*x* has an almost 5 per cent extra overhead compared to AAL1. Referring to the multiplex cell discard graphs, this can result in five to ten times more cell loss depending on the network load and the number of channels in the multiplex [18].

In an experiment, 90 frames of the Salesman image sequence were MPEG-2 coded with the first frame being intra (I-frame) coded and the remaining frames predictively (P-frame) coded ($N = \infty$, $M = 1$). Two types of packetisation methods, AAL*x* and AAL1, were used. The AAL*x* type cells were discarded with the ITU-T cell loss model with a cell loss rate of 10^{-2} and a mean burst length of 1 (see Appendix E) [19]. Those of AAL1 were discarded at cell loss rates of 10^{-3} (10 times lower) and 10^{-4} (100 times lower) with the same mean burst length. From Figure 8.28, it can be seen that AAL*x* outperforms AAL1 at ten times lower cell loss rate, but is inferior to AAL1 with a cell loss rate of 100 times lower. Considering that in the experiment AAL*x* is likely to experience five to ten times more loss than AAL1, AAL*x* is a better packetisation scheme for this type of image format (e.g. H.261 or H.263).

In another experiment the same 90 frames of the Salesman image sequence were MPEG-2 coded with a GOP structure of $N = 12$ and $M = 1$. The packetisation techniques were similar to that in the previous experiment. In this case, shown in Figure 8.29, AAL*x* does not show the same improvement over AAL1, as was the case for Figure 8.28. In fact, its performance, because of higher overhead, is worse than AAL1, with ten times lower cell loss rate.

The implications of these two experiments are that with MPEG-1 and MPEG-2 structures, where there are regular I-pictures every *N* frames, AAL1 outperforms AAL*x*. But for very large *N* (e.g. in H.261), AAL*x* is better than AAL1.

It should be noted that the video quality can be improved by concealing the effect of packet loss or channel errors. In MPEG-2, there is an option that additional

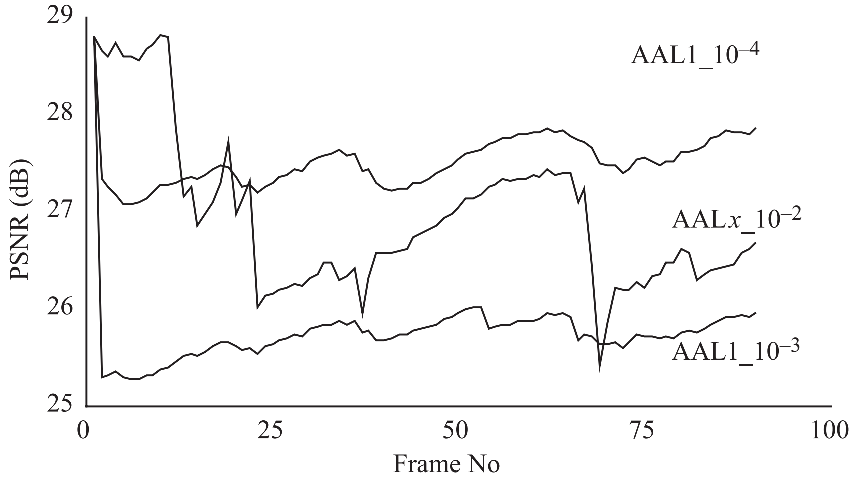

Figure 8.28 PSNR of MPEG-2 coded video sequence GOP (IPPPPPP...): AALx with error rate of 10^{-2}, AAL1 with error rate of 10^{-3} and AAL1 with error rate of 10^{-4}

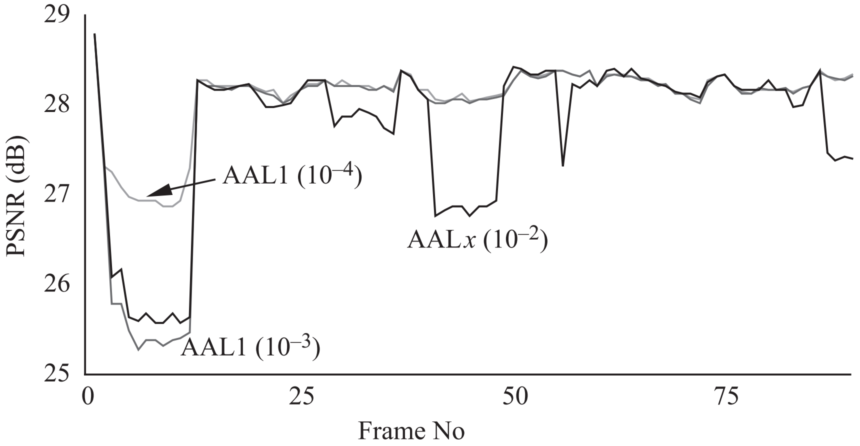

Figure 8.29 PSNR of MPEG-2 coded video sequence with 12 frames per GOP (IPP...IPPP...IP...): AALx with error rate of 10^{-2}, AAL1 with error rate of 10^{-3} and AAL1 with error rate of 10^{-4}

motion vectors for I-pictures are derived and they are transmitted in the following slice. In case some of the MBs are damaged, these motion vectors are used to copy pixels from the previous frame, displaced by the amount of motion vectors to replace the damaged MBs. In the next chapter, more general forms of concealing side effects of packet losses and channel errors are discussed in greater depth.

8.9 Problems

1. Why are the systems in MPEG-2 different from those in MPEG-1?

2. Which of the following represents level and profile?
   a. 1.5 Mbit/s
   b. SIF
   c. SNR scalability
   d. 720 × 576 pixels

3. The DCT coefficients of a motion-compensated picture block are given as follows:

33	−10	−41	3	17	2	7	−13
61	−5	23	12	−11	5	6	−9
−3	11	3	9	−15	6	3	−1
2	−34	6	4	0	1	3	1
−21	−3	0	5	12	3	0	1
−7	−5	9	3	2	7	−1	−2
6	3	2	5	7	−2	−3	1
−5	4	−2	6	3	1	2	1

   They are linearly quantised with $th = q$ and zigzag scanned and the assigned bits are calculated from Figure 6.12. For $q = 8$, identify the two-dimensional events of (run, index) and the number of bits required to code the block.

4. The block of problem 3 is partitioned into two, and the PBP is set at coefficient (2,2). Assuming that PBP can be identified with 6 bits and the quantiser step size is $q = 8$, calculate the number of bits generated in each layer and the total number of bits. (Note that the first DCT coefficient is defined at (0,0).)

5. The block in problem 3 is SNR scalable coded with the base and enhancement quantiser step sizes of 14 and 8, respectively. What are the number of generated bits in each layer and the total number of bits (assume in each layer $th = q$)?

6. An MPEG-2 coded video with its associated audio and forward error correcting codes comprises 8 Mbit/s. With a 64-QAM modulation, determine how many such videos can be accommodated in a UHF channel of 8-MHz bandwidth with 2-MHz guard band. Assume that each modulated symbol occupies 1.25 Hz of the channel.

7. Draw a two-state channel error model and determine the transition probabilities for each of the following conditions:
   a. bit error rate of $P = 10^{-5}$ and burst length of $B = 5$
   b. bit error rate of $P = 10^{-5}$ and burst length of $B = 1$

8. Table 8.7 shows the duration of various parts of a 90-min VBR-MPEG-2 coded video stored on a DVD. The given bit rate is smoothed over a GOP but is presented in Mbit/s.
   a. Calculate the required storage capacity.
   b. Calculate the peak-to-mean bit rate ratio.

Table 8.7 Duration of various picture activities in a DVD programme

Duration (min)	0.5	5	10	20	30	24.5
Bit rate (Mbit/s)	20	15	10	7.5	5	4

c. Calculate the storage required if the video was coded in CBR at a quality not poorer than that of the VBR.

9. The ATM cells with AAL1 adaptation layer have a 5-byte header and a 48-byte payload, of which 47 bytes are used for packing the video data. If the channel bit error rate is 10^{-7}, calculate the probability that
   a. video is decoded erroneously
   b. the cell is lost

10. The stored DVD video in problem 8 is to be streamed via an ATM network, with a maximum channel capacity of 50 Mbit/s. Because of the other users on the link, on the average, only 30 per cent of the link capacity can be used by the DVD server. With an AAL1 packetisation, calculate the time required to download the entire DVD video stream over the link.

11. The cell loss rate of an ATM link can be modelled with $P = 10^{-10(1-\rho^2)}$, where $0 \le \rho \le 1$ is the load of the link. Twenty-five video sources, each coded at an average bit rate of 4 Mbit/s, are streamed via a 155-Mbit/s ATM link, with AAL1 adaptation layer.
    a. Calculate the network load, ρ.
    b. Calculate the loss rate that each ATM cell may experience.

12. The video sources in problem 11 were two-layer coded with SNR scalability, but the overall video quality was assumed to remain the same. If in each source, 50 per cent of its data are assigned to the base layer and the base layer cells are always served in preference to the enhancement layer cells, calculate the cell loss probability at the
    a. base layer
    b. enhancement layer

    (Hint: use Figure 8.26 for the additional overhead due to scalability)

13. Repeat problem 12 for data partitioning.

14. Repeat problem 12 for spatial scalability.

References

1. MPEG-2: ‘Generic coding of moving pictures and associated audio information’, ISO/IEC 13818-2: video, Draft International Standard, November 1994

2. MPEG-1: 'Coding of moving pictures and associated audio for digital storage media at up to about 1.5 Mbit/s', ISO/IEC 1117-2: video, November 1991
3. HASKEL, B.G., PURI, A. and NETRAVALI, A.N.: *Digital Video: An Introduction to MPEG-2*, Chapman and Hall, New York, 1997
4. 'Generic coding of moving pictures and associated audio information', ISO/IEC 13818-1 Systems, Draft International Standard, November 1994
5. ITU-T recommendation I.363: 'B-ISDN ATM adaptation layer (AAL) specification', June 1992
6. OKUBA, S., MCCANN, K. and LIPPMAN, A.: 'MPEG-2 requirements, profile and performance verification', *Signal Process., Image Commun.*, 1995, **7:3**, pp. 201–209
7. SAVATIER, T.: 'Difference between MPEG-1 and MPEG-2 video'. ISO/IEC JTC1/SC29/WG11 MPEG94/37, March 1994
8. Test model editing committee, 'MPEG-2 video test model 5', ISO/IEC JTC1/SC29/WG11 Doc. N0400, April 1993
9. GHANBARI, M.: 'Two-layer coding of video signals for VBR networks', *IEEE J. Sel. Areas Commun.*, 1989, **7:5**, pp. 771–781
10. GHANBARI, M.: 'An adapted H.261 two-layer video codec for ATM networks', *IEEE Trans. Commun.*, 1992, **40:9**, pp. 1481–1490
11. GHANBARI, M. and SEFERIDIS, V.: 'Efficient H.261 based two-layer video codecs for ATM networks', *IEEE Trans. Circuits Syst. Video Technol.*, 1995, **5:2**, pp. 171–175
12. ITU-T study group XVI: 'Efficient coding of synchronised H.26L streams', Document VCG-N35, September 2001
13. HERPEL, C.: 'SNR scalability vs data partitioning for high error rate channels', ISO/IEC JTC1/SC29/WG11 doc. MPEG 93/658, July 1993
14. MORRISON, G. and PARKE, I.: 'A spatially layered hierarchical approach to video coding', *Signal Process. Image Commun.*, 1995, **5:5-6**, pp. 445–462
15. ITU-T Draft Recommendation I.371: 'Traffic control and congestion control in B-ISDN', Geneva, 1992
16. ROSDIANA, E. and GHANBARI, M.: 'Picture complexity based rate allocation algorithm for transcoded video over ABR networks', *Electron. Lett.*, 2000, **36:6**, pp. 521–522
17. GHANBARI, M. and HUGHES, C.J.: 'Packing coded video signals into ATM cells', *IEEE ACM Trans. Networking*, 1993, **1:5**, pp. 505–509
18. HUGHES, C.J., GHANBARI, M., PEARSON, D.E., SEFERIDIS, V. and XIONG, J.: 'Modelling and subjective assessment of cell discard in ATM video', *IEEE Trans. Image Process.*, 1993, **2:2**, pp. 212–222
19. ITU SGXV working party XV/I, Experts Group for ATM video coding, working document AVC-205, January 1992

Chapter 9

Video coding for low bit rate communications (H.263)

The H.263 recommendation specifies a coded representation that can be used for compressing the moving picture components of audio-visual services at low bit rates. Detailed specifications of the first generation of this codec under the test model (TM) to verify the performance and compliance of this codec were finalised in 1995 [1]. The basic configuration of the video source algorithm in this codec is based on the ITU-T recommendation H.261, which is a hybrid of interpicture prediction to utilise temporal redundancy and transform coding of the residual signal to reduce spatial redundancy. However, during the course of the development of H.261 and the subsequent advances on video coding in MPEG-1 and -2 video codecs, substantial experience was gained, which has been exploited to make H.263 an efficient encoder [2–4]. In this chapter, those parts of the H.263 standard that make this codec more efficient than its predecessors are explained.

It should be noted that the primary goal in the H.263 standard codec was coding of video at low or very low bit rates for applications such as mobile networks, public switched telephone network (PSTN) and the narrowband Integrated Services Digital Network (ISDN). This goal could only be achieved with small image sizes such as sub-quarter of common intermediate format (sub-QCIF) and QCIF, at low frame rates. Later on, the codec was found so attractive that higher-resolution pictures could also be coded at relatively low bit rates. The standard recommends operation on five standard pictures of the CIF family, known as sub-QCIF, QCIF, CIF, 4CIF and 16CIF.

Soon after the finalisation of the H.263 in 1995, work began to improve the coding performance of this codec further. The H.263+ was the first set of extensions to this family, which was intended for near-term standardisation of enhancements of H.263 video coding algorithms for real-time telecommunications [5]. Work on improving the encoding performance was an ongoing process under H.263++, and every now and then a new extension called annex was added to the family [6]. The codec for long-term standardisation was called H.26L [7]. The H.26L project had the mandate from ITU-T to develop a very low bit rate (less than 64 kbit/s with emphasis on less than 24 kbit/s) video coding recommendation achieving better video quality, lower delay, lower complexity and better error resilience than were available at the time. In 2001, MPEG-4 committee joined the project in investigating new video coding techniques and technologies as candidates for recommendation.

The joint team eventually recommended the joint video team (JVT) codec which is informally known as advanced video coding (AVC). The standard is formally known as H.264 by the ITU-T and MPEG-4 part 10 by the International Standards Organisation (ISO)/International Electrotechnical Commission (IEC) [8]. Details of this codec are given in Chapter 11, but since H.264/AVC is an evolution of H.263, most of the materials given in the current chapter will be the foundations to follow H.264/AVC. Hence, readers are recommended to read this chapter before Chapter 11. In explaining the current chapter, any part or its improved version that leads to a recommendation in the H.264/AVC standard will be reminded.

9.1 How does H.263 differ from H.261 and MPEG-1?

The source encoder of H.263 follows the general structure of the generic discrete cosine transform (DCT)-based interframe coding technique used in the H.261 and MPEG-1 codecs (see Figure 3.19). The core H.263 employs a hybrid inter picture prediction to utilise temporal redundancy and transform coding of the residual signal to reduce spatial redundancy. The decoder has motion compensation capability, allowing optional incorporation of this technique at the encoder. Half-pixel precision is used for the motion compensation, as opposed to the optional full-pixel precision and loop filter used in the recommendation H.261. In the improved versions of H.263, use of a quarter of pixel precision for luminance and one-eighth for chrominance is recommended [6].

Perhaps the most significant differences between the core H.263 and H.261/MPEG-1 are in the coding of the transform coefficients and motion vectors. In the following sections, these and some other notable differences such as the additional optional modes are explained.

9.1.1 Coding of H.263 coefficients

In H.261 and MPEG-1, we saw that the transform coefficients are converted via a zigzag scanning process into two-dimensional run and index events (see section 6.4). In H.263, these coefficients are represented as a three-dimensional event of (last, run, level). Similar to the two-dimensional event, the run indicates the number of zero-valued coefficients preceding a nonzero coefficient in the zigzag scan, and level is the normalised magnitude of the nonzero coefficient which is sometimes called index. A new variable, last, replaces the end of block (EOB) code of H.261 and MPEG-1. It takes only two values, 0 and 1; last 0 means that there are more nonzero coefficients in the block, and 1 means that this is the last nonzero coefficient in the block.

The most likely events of (last, run, level) are then variable length coded. The remaining combinations of (last, run, level) are coded with a fixed 22-bit word consisting of 7 bits escape, 1 bit last, 6 bits run and 8 bits level.

9.1.2 Coding of motion vectors

The motion compensation in the core H.263 is based on one motion vector per macroblock of 16 $\times$ 16 pixels, with half-pixel precision. The macroblock motion vector is then differentially coded with predictions taken from three surrounding macroblocks, as indicated in Figure 9.1. The predictors are calculated separately for the horizontal and vertical components of the motion vectors, *MV*1, *MV*2 and *MV*3. For each component, the predictor is the median* value of the three candidate predictors for this component:

$$\begin{aligned}\text{pred}_x &= \text{median}(MV1_x, MV2_x, MV3_x)\\ \text{pred}_y &= \text{median}(MV1_y, MV2_y, MV3_y)\end{aligned} \tag{9.1}$$

The difference between the components of the current motion vector and their predictions is variable length coded. The vector differences are defined by

$$\begin{aligned}\text{MVD}_x &= MV_x - \text{pred}_x\\ \text{MVD}_y &= MV_y - \text{pred}_y\end{aligned} \tag{9.2}$$

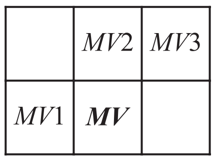

MV: current motion vector
*MV*1: previous motion vector
*MV*2: above motion vector
*MV*3: above right motion vector

Figure 9.1 Motion vector prediction

In the special cases, at the borders of the current group of blocks (GOB) or picture, the following decision rules are applied in order:

1. The candidate predictor *MV*1 is set to zero if the corresponding macroblock is outside the picture at the left side (Figure 9.2*a*).
2. The candidate predictors *MV*2 and *MV*3 are set to *MV*1 if the corresponding macroblocks are outside the picture at the top, or if the GOB header of the current GOB is nonempty (Figure 9.2*b*).
3. The candidate predictor *MV*3 is set to zero if the corresponding macroblock is outside the picture at the right side (Figure 9.2*c*).
4. When the corresponding macroblock is intra coded or was not coded, the candidate predictor is set to zero.

The values of the difference components are limited to the range $-$ 16 to 15.5. Since in H.263 the source images are of the CIF family with the 4:2:0 format, each macroblock comprises four luminance and two chrominance components, C_b and C_r. Hence, the motion vector of the macroblock is used for all four luminance blocks in the macroblock. Motion vectors for both chrominance blocks are derived

* To find the median value, the components are rank ordered and the middle value is chosen.

by dividing the component values of the macroblock vector by 2, due to the lower chrominance resolution. The resulting values of the quarter pixel resolution vectors are modified towards the nearest half-pixel position. (*Note*: The macroblock motion vector has half-pixel resolution.)

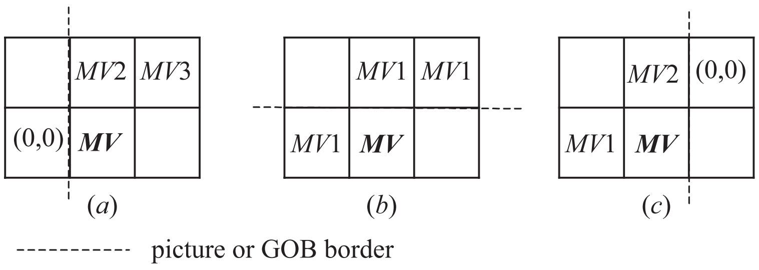

Figure 9.2 (a–c) Motion vector prediction for the border macroblocks

9.1.3 Source pictures

The source encoder operates on noninterlaced pictures at approximately 29.97 frames/s. These pictures can be one of the following five standard picture formats of the CIF family: sub-QCIF, QCIF, CIF, 4CIF and 16CIF. Since in CIF the luminance and chrominance sampling format is 4:2:0, for either of these pictures the horizontal and vertical resolutions of the chrominance components are half the luminance. Table 9.1 summarises pixel resolutions of the CIF family used in H.263.

Table 9.1 Number of pixels per line and number of lines per picture for each of the H.263 picture formats

Picture format	**Number of pixels for luminance per line**	**Number of lines for luminance per picture**	**Number of pixels for chrominance per line**	**Number of lines for chrominance per picture**
Sub-QCIF	128	96	64	48
QCIF	176	144	88	72
CIF	352	288	176	144
4CIF	704	576	352	288
16CIF	1408	1152	704	576

Each picture is divided into a GOB. A GOB comprises $k \times 16$ lines depending on the picture format ($k = 1$ for sub-QCIF, QCIF and CIF; $k = 2$ for 4CIF; $k = 4$ for 16CIF). The number of GOBs per picture is 6 for sub-QCIF, 9 for QCIF and 18 for CIF, 4CIF and 16CIF. Each GOB is divided into 16×16 pixel macroblocks, of which there are four luminance blocks and one each of chrominance blocks of 8×8 pixels.

9.1.4 Picture layer

The picture layer contains the picture header, the GOB header together with various coding decisions on macroblocks in a GOB and finally the coded transform coefficients, which are also used in H.261 and MPEG-1 and -2. The most notable difference in the header information for H.263 is in the type information, called PTYPE. For the first generation of H.263, this is a 13-bit code that gives information about the complete picture, in the form of [1]:

bit 1:	always 1, in order to avoid start code emulation
bit 2:	always 0, for distinction with H.261
bit 3:	split screen indicator – 0, off; 1, on
bit 4:	document camera indicator – 0, off; 1, on
bit 5:	freeze picture release – 0, off; 1, on
bits 6–8:	source format – 000, forbidden; 001, sub-QCIF; 010, QCIF; 011, CIF; 100, 4CIF; 101, 16CIF; 110, reserved; 111, extended PTYPE
bit 9:	picture coding type – 0, intra; 1, inter
bit 10:	optional unrestricted motion vector mode – 0, off; 1, on
bit 11:	optional syntax-based arithmetic coding mode – 0, off; 1, on
bit 12:	optional advanced prediction mode – 0, off; 1, on
bit 13:	optional PB frames mode – 0, normal picture; 1, PB frame

The split screen indicator is a signal that indicates the upper and lower halves of the decoded picture could be displayed side by side. This has no direct effect on the encoding and decoding of the picture.

The freeze picture release is a signal from an encoder which responds to a request for packet retransmission (if not acknowledged) or fast update request, and allows a decoder to exit from its freeze picture mode and display decoded picture in the normal manner.

Bits 10–13 refer to the early four optional modes of H.263. Since 1995, more options as annexes have been added to the extensions of this codec. These optional modes are activated when the bits 6–8 of the PTYPE header are in the extended mode of 111, and necessarily some additional bits define the new options. Hence, extensions of H.263 have a longer PTYPE header and also a different picture layer than the above 13 bits. All these optional modes are only used after negotiation between the encoder and the decoder via the control protocol recommendation H.245 [9].

Also, for further reduction in the overhead, the code for macroblock type and coded block pattern are combined. For example, the combined code of macroblock type and coded block pattern is called MCBPC. MCBPC is always present for each macroblock, irrespective of its type and the options used. Note that in H.261, MPEG-1 and -2, the coded block pattern is defined separately from the macroblock type.

9.2 Switched multipoint

One of the initial aims in the design of a new low bit rate video codec was to replace H.261 with a more efficient one, which took the name of H.263. Hence, the functionalities of H.261, but with some improvements, need to be included in this codec; they appear in Annex C of the H.263 specification that can be activated or disabled as desired [22-C]. Since this annex was introduced prior to all the other annexes, which later on were called optionalities, we introduce this annex prior to all the other options.

In H.263, the decoder can be instructed to alter its normal decoding mode and provide some extra display functions. Instructions for the alterations may be issued by an external device such as recommendation H.245, which is a control protocol for multimedia communications [9]. Some of the commands and the actions are given in the following sections.

9.2.1 Freeze picture request

This signal causes the decoder to freeze its displayed picture until a freeze release signal is received or a time-out period of at least 6 s has expired. A frozen picture is much better perceived by the viewer than say a broken picture due to channel errors, or if the encoder cannot deliver the compressed bitstream on time for a continuous display.

9.2.2 Fast update request

This command causes the encoder to encode its next picture in intra mode, with coding parameters to avoid buffer overflow. This mode in conjunction with the back channel reduces the probability of error propagation into the subsequent pictures. This mode improves the resilience of the codec to channel errors.

9.2.3 Freeze picture release

Freeze picture release is a signal from the encoder, which has responded to a fast update request, and allows a decoder to exit from its freeze mode and display decoded pictures in the normal manner. This signal is transmitted by the PTYPE in the picture header of the first picture coded in response to the fast update request.

9.2.4 Continuous presence multipoint

In a multipoint connection, a multipoint control unit (MCU) can assemble two to four video bitstreams into one video bitstream, so that up to four different video signals can be displayed simultaneously at the receiver. In H.261, this can be done on a quad screen by only editing the GOB header, but in H.263 it is more complex due to a different GOB structure, overlap motion estimation, multiple motion vectors, etc. Therefore, in H.263, a special continuous presence multipoint mode is provided in which four independent video bitstreams are transmitted in the four logical channels of a single H.263 video bitstream.

9.3 Extensions of H.263

In the late 1990s, the Video Coding Experts Group (VCEG) of the ITU-telecommunications standardisation sector set up two activities. The aim was to develop very low bit rate video coding at bit rates less than 64 kbit/s and more specifically at less than 24 kbit/s. One activity was looking at the video coding for very low bit rates, under the name of H.263+ [5]. Later on, work of this activity continued under the name of H.263++, indicating further improvements on H.263+ [6]. The other activity, which had more in common with MPEG-4, is work on advanced low bit rate video coding, under the name of H.26L [7].

The H.263+/H.263++ development effort was intended for short-term standardisation of enhancements of the H.263 video coding algorithm for real-time telecommunication and related nonconversational services. The H.26L development effort was aimed at identifying new video coding technology beyond the capabilities of enhancements to H.263 by the H.263+/H.263++ coding algorithms.

These two subgroups also had a close cooperation in the development of their codecs, since the core codec is still H.263. They also worked closely with the other bodies of ITU. For example, the collaboration between the H.263+ and the mobile group has led to the consideration for greater video error resilience capability. The back channel error resilience in H.263+ is especially designed to address the needs of mobile video and other such unreliable bitstream transport environments. The H.26L group worked very closely with the MPEG-4 group, as this group had the mandate of developing advanced video coding for storage and broadcasting applications [7]. The team work was proven very fruitful and led to the recommendation H.264/AVC that is explained in detail in Chapter 11.

One of the key features of the H.263+, H.263++ and H.26L is the real-time audio-visual conversational services. In a real-time application, information is simultaneously acquired, processed and transmitted and is usually used immediately at the receiver. This feature implies critical delay and complexity constraints on the codec algorithm.

An important component in any application is the transmission media over which it will need to operate. The transmission media for H.263+/H.26L applications include PSTN, ISDN (1B), dial-up switched 56/64 kbit/s service, local area networks (LANs), mobile networks (including GSM, DECT, UMTS, FLMPTS, NADC, PCS, etc.), microwave and satellite networks, digital storage media (i.e. for immediate recording) and concatenation of the above media. Because of the large number of likely transmission media and the wide variations in the media error and channel characteristics, error resiliency and recovery are critical requirements for this application class.

9.3.1 Scope and goals of H.263+

The expected enhancements of H.263+ over H.263 fall into two basic categories:

- enhancing quality within existing applications;
- broadening the current range of applications.

A few examples of the enhancements are as follows:

- improving perceptual compression efficiency;
- reducing video coding delay;
- providing greater resilience to bit errors and data losses.

Note that H.263+ has all the features of H.263, and further tools are added to this codec to increase its coding efficiency and its robustness to errors. This was an ongoing process, and more tools were added every year. In 2000, this codec was upgraded to H.263++, to emphasise the ongoing improvement in the coding efficiency [6].

9.3.2 Scopes and goals of H.26L

The long-term objective of the ITU-U video experts group, under the AVC project, was to provide a video coding recommendation which at very low bit rates can perform substantially better than that achievable with the existing standards of that time (e.g. H.263+). The adopted technology should provide for:

- enhanced visual quality at very low bit rates and particularly at PSTN rates (e.g. at rates below 24 kbit/s);
- enhanced error robustness in order to accommodate the higher error rates experienced when operating, for example, over mobile links;
- low complexity appropriate for small, relatively inexpensive, audio-visual terminals;
- low end-to-end delay as required in bidirectional personal communications.

In addition, the group was closely working with the MPEG-4 experts group, to include new coding methods and promote interoperability. This work was formally ratified in 2003 and named H.264 in ITU-T and MPEG-4 part 10 in ISO/IEC. Details of this codec are covered in Chapter 11.

9.3.3 Optional modes of H.263

In the course of development of H.263, numerous optional modes have been added as annexes to the main specifications to improve the visual communication efficiency of this codec. Some of the annexes were introduced along with the introduction of the core H.263, and many more were added gradually under the H.263+ and H.263++. The intention is neither to introduce all these annexes nor to specify which annex belongs to which generation of the codec. Instead, we try to classify them into groups, without specifying in which generation they were introduced, to give a better appreciation of these optional modes in improving the coding efficiency. As we will see, since H.263 video codec is primarily aimed for mobile video communications, and UHF channels are particularly prone to channel errors, the majority of the annexes deal with the protection of visual data against channel errors. It is worth noting that improved versions of most of these annexes or options are taken as the core parts of H.264/AVC (depending on the profile). Thus, their study here will help readers to better appreciate the fundamentals behind the compression efficiency and error resiliency of H.264/AVC.

9.4 Advanced motion estimation/compensation

Motion estimation/compensation is probably the most evolutionary coding tool in the history of video coding. For every previous generation of video codecs, motion estimation has been considered as a means of improving coding efficiency. In the first video codec (H.120) under COST211, which was a differential pulse code modulation (DPCM)-based codec, working on pixel-by-pixel, motion estimation for each pixel would have been costly, and hence it was never used. Motion estimation was made optional for the H.261 block-based codec, on the grounds that the DCT of this codec is to decorrelate interframe pixels, and since motion compensation reduces this correlation, nothing is left for DCT! Motion compensation in MPEG-1 was considered seriously, since for B-pictures, which refer to both past and future, the motion of objects, even those hidden in the background, can be compensated. It was so efficient that it was also recommended for the P-pictures, and even with a half-pixel precision. In MPEG-2, due to interlacing, a larger variety of motion estimation/compensation between fields and frames or their combinations was introduced. The improvement in coding efficiency was at the cost of additional overhead for delivering the motion vectors to the receiver. However, for MPEG-1 and -2, coding at a rate of 1–5 Mbit/s, this overhead is negligible, but the question is: how this overhead can be justified for H.263 at a rate of 24 kbit/s or less? In fact, as we will see below, some extensions of H.263 recommend using smaller block sizes, which imply more motion vectors per picture, and they even suggest motion estimation precision should be at quarter of a pixel. All these increase the motion vector overhead, which is very significant at a very low bit rate of 24 kbit/s.

The fact is that if motion compensation is efficient, the motion-compensated pictures may not need to be coded by the DCT, that is, these blocks are only represented by their motion vectors. In H.261 and MPEG-1, we have seen a form of macroblock that was coded only by the motion vector, without coding the motion-compensated error. However, if the expected video quality is low and the motion estimation is efficient, then we can see more of these macroblocks in a codec. This is in fact what is happening with motion compensation in H.263. In the following sections, some improvements to motion estimation/compensation, in addition to those introduced for H.261, MPEG-1 and -2, are discussed. At the end of this section, a form of motion estimation that warps the picture for better compensation of complex motion is introduced. Although this method is neither a part of any form of H.263 nor recommended for other video coding standards, there is no reason why we cannot have this form of motion estimation and compensation in the future video codecs.

9.4.1 Unrestricted motion vector

In the default prediction mode of H.263, motion vectors are restricted so that all pixels referenced by them are within the coded picture area. In the optional unrestricted motion vector mode, this restriction is removed and therefore motion vectors are allowed to point outside the picture [22-D]. When a pixel referenced by a motion vector is outside the coded picture area, an edge pixel is used instead. This edge pixel is found by limiting the motion vector to the last full-pixel position inside the coded picture area. Limitation of the motion vector is performed on a pixel-by-pixel basis and separately for each component of the motion vector.

9.4.2 Advanced prediction

The optional advanced prediction mode of H.263 employs overlapped block matching motion compensation and may have four motion vectors per macroblock [22-F]. The use of this mode is indicated in the macroblock type header. This mode is only used in combination with the unrestricted motion vector mode [22-D], described in the previous subsection.

9.4.2.1 Four motion vectors per macroblock

In H.263, one motion vector per macroblock is used except in the advanced prediction mode, where either one or four motion vectors per macroblock are employed. In this mode, the motion vectors are defined for each 8 × 8 pixel block. If only one motion vector for a certain macroblock is transmitted, this is represented as four vectors with the same value. When there are four motion vectors, the information for the first motion vector is transmitted as the code word motion vector data (MVD), and the information for the three additional vectors in the macroblock is transmitted as the code word $MVD_{2–4}$.

The vectors are obtained by adding predictors to the vector differences indicated by MVD and $MVD_{2–4}$, as was the case when only one motion vector per macroblock was present (see section 9.1.2). Again the predictors are calculated separately for the horizontal and vertical components. However, the candidate predictors *MV*1, *MV*2 and *MV*3 are redefined as indicated in Figure 9.3.

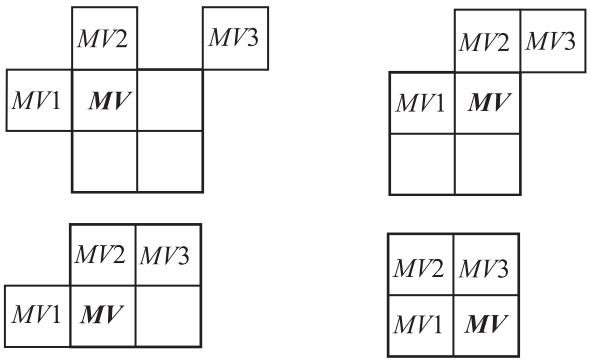

Figure 9.3 Redefinition of the candidate predictors MV1, MV2 and MV3 for each luminance block in a macroblock

As Figure 9.3 shows, the neighbouring 8 × 8 blocks that form the candidates for the prediction of the motion vector *MV* take different forms depending on the position of the block in the macroblock. Note that if only one motion vector in the neighbouring macroblocks is used, then *MV*1, *MV*2 and *MV*3 are defined as 8 × 8 block motion vectors, which possess the same motion vector of the macroblock. It is worth noting that this option now is a core element in H.264 with even smaller block size of 4 × 4 pixels and quarter of a pixel precision. There even the motion vectors of the subblocks are also predictively addressed, similar to Figure 9.3.

9.4.2.2 Overlapped motion compensation

Overlapped motion compensation is only used for the 8 × 8 luminance blocks. Each pixel in an 8 × 8 luminance prediction block is the weighted sum of three prediction values, divided by 8 (with rounding). To obtain the prediction values, three motion vectors are used. They are the motion vector of the current luminance block and two out of four remote vectors, as follows:

- the motion vector of the block at the left or right side of the current luminance block;
- the motion vector of the block above or below the current luminance block.

The remote motion vectors from other GOBs are treated in the same way as the remote motion vectors inside the GOB.

For each pixel, the remote motion vectors of the block at the two nearest block borders are used. This means that for the upper half of the block, the motion vector corresponding to the block above the current block is used, while for the lower half of the block, the motion vector corresponding to the block below the current block is used, as shown in Figure 9.4. In this figure, the neighbouring pixels closer to the pixels in the current block take greater weights.

2	2	2	2	2	2	2	2	bottom of the current block
1	2	2	2	2	2	2	1	
1	1	1	1	1	1	1	1	
1	1	1	1	1	1	1	1	
1	1	1	1	1	1	1	1	
1	1	1	1	1	1	1	1	top of the current block
1	2	2	2	2	2	2	1	
2	2	2	2	2	2	2	2	

Figure 9.4 Weighting values for prediction with motion vectors of the luminance blocks on top or bottom of the current luminance block, $H_1(i, j)$

Similarly, for the left half of the block, the motion vector corresponding to the block at the left side of the current block is used, and for the right half of the block the motion vector corresponding to the block at the right side of the current block is used, as shown in Figure 9.5.

right of the current block

2	1	1	1	1	1	1	2
2	2	1	1	1	1	2	2
2	2	1	1	1	1	2	2
2	2	1	1	1	1	2	2
2	2	1	1	1	1	2	2
2	2	1	1	1	1	2	2
2	2	1	1	1	1	1	2
2	1	1	1	1	1	1	2

left of the current block

Figure 9.5 Weighting values for prediction with motion vectors of luminance blocks to the left or right of current luminance block, $H_2(i, j)$

The creation of each interpolated (overlapped) pixel, $p(i, j)$, in an 8×8 reference luminance block is governed by

$$p(i,j) = [q(i,j) \times H_0(i,j) + r(i,j) \times H_1(i,j) + s(i,j) \times H_2(i,j) + 4]//8 \quad (9.3)$$

where $q(i, j)$, $r(i, j)$ and $s(i, j)$ are the motion-compensated pixels from the reference picture with the three motion vectors defined by

$$\begin{aligned} q(i,j) &= p(i + MV_x^0, j + MV_y^0) \\ r(i,j) &= p(i + MV_x^1, j + MV_y^1) \\ s(i,j) &= p(i + MV_x^2, j + MV_y^2) \end{aligned}$$

where (MV_x^0, MV_y^0) denotes the motion vector for the current block, (MV_x^1, MV_y^1) denotes the motion vector of the block either above or below and (MV_x^2, MV_y^2) denotes the motion vector of the block to either the left or right of the current block. The matrices $H_0(i, j)$, $H_1(i, j)$ and $H_2(i, j)$ are the current, top–bottom and left–right weighting matrices, respectively. Weighting matrices of $H_1(i, j)$ and $H_2(i, j)$ are shown in Figures 9.4 and 9.5, respectively, and the weighting matrix for prediction with the motion vector of the current block, $H_0(i, j)$, is shown in Figure 9.6.

If one of the surrounding blocks was not coded or was in intra mode, the corresponding remote motion vector is set to zero. However, in PB frames mode (see section 9.5), a candidate motion vector predictor is not set to zero if the corresponding macroblock is intra mode.

If the current block is at the border of the picture and therefore a surrounding block is not present, the corresponding remote motion vector is replaced by the current motion vector. In addition, if the current block is at the bottom of the macroblock, the remote motion vector corresponding with an 8×8 luminance block in the macroblock below the current macroblock is replaced by the motion vector for the current block.

4	5	5	5	5	5	5	4
5	5	5	5	5	5	5	5
5	5	6	6	6	6	5	5
5	5	6	6	6	6	5	5
5	5	6	6	6	6	5	5
5	5	6	6	6	6	5	5
5	5	5	5	5	5	5	5
4	5	5	5	5	5	5	4

Figure 9.6 Weighting values for prediction with motion vector of current block, $H_0(i, j)$

9.4.3 *Importance of motion estimation*

To demonstrate the importance of motion compensation and to some extent the compression superiority of H.263 over H.261 and MPEG-1 in an experiment, the CIF Claire test image sequence was coded at 256 kbit/s (30 frames/s) with the following encoders:

- H.261;
- MPEG-1, with a group of pictures (GOP) length of 12 frames and two B-frames between the anchor pictures, that is, $N = 12$ and $M = 3$ (MPEG-GOP);
- MPEG-1, with only P-pictures, that is, $N = \infty$ and $M = 1$ (MPEG-IPPPP...);
- H.263 with advanced mode (H.263-ADV).

Figure 9.7 illustrates the peak-to-peak signal-to-noise ratio (PSNR) of the coded sequence. At this bit rate, the worst performance is that of MPEG-1, with a GOP structure of 12 frames/GOP, and two B-frames between the anchor pictures (IBBPBBPBBPBBIBB...). The main reason for the poor performance of this codec at this bit rate is that I-pictures consume most of the bits, and compared to the other coding modes, relatively lower bits are assigned to the P- and B-pictures.

The second poorest is the H.261, where all the consecutive pictures are inter-frame coded with an integer pixel precision motion compensation. The second best performance is the MPEG-1 with only P-pictures. It is interesting to note that this mode is similar to H.261 (every frame is predictively coded), except that motion compensation is carried out with half-pixel precision. Hence, this mode shows the advantage of using half-pixel precision motion estimation. The amount of improvement for the used sequence at 256 kbit/s is almost 2 dB.

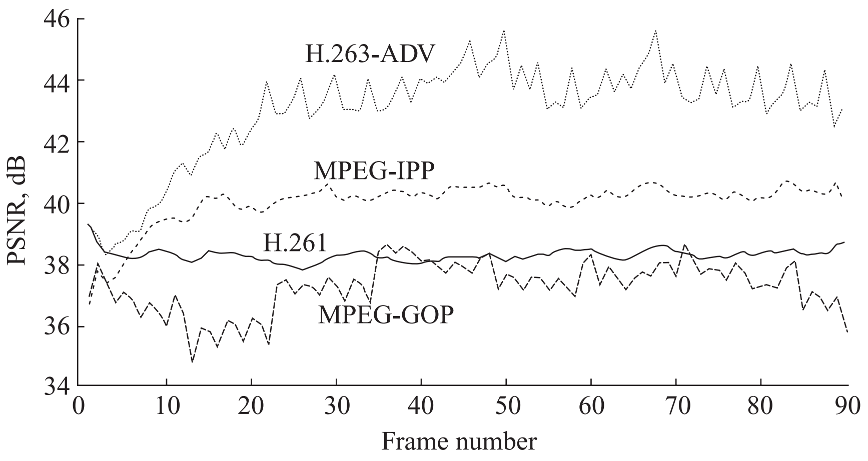

Figure 9.7 PSNR of Claire sequence coded at 256 kbit/s, with MPEG-1, H.261 and H.263

Finally, the best performance comes from the advanced mode of H.263, which results in an almost 4-dB improvement over the best of MPEG-1 and 6 dB over H.261. The following are some of the factors that may have contributed to such a good performance:

- motion compensation on smaller block sizes of 8×8 pixels results in smaller error signals than for the macroblock compensation used in the other codecs;
- overlapped motion compensation; by removing the blocking artefacts on the block boundaries, the prediction picture has a better quality, thus reducing the error signal, and hence the number of significant DCT coefficients;
- efficient coding of DCT coefficients through three-dimensional events of (last, run, level);
- efficient representation of the combined macroblock type and block pattern.

Note that, in this experiment, other options such as PB frames mode and arithmetic coding were not used. Had the arithmetic coding been used, it is expected that the picture quality would be further improved by 1–2 dB. Experimental results have confirmed that arithmetic coding has approximately 5–10 per cent better compression efficiency over the Huffman coding [10].

It is worth mentioning that overlapped motion compensation removes blockiness artefacts of block-based motion compensation. Such an artefact can also be reduced by the deblocking filter, to be explained below. It appears that if deblocking filter is used, there is no need for overlapped motion compensation. Hence, H.264 has adopted deblocking filter tool and does not use overlapped motion compensation.

9.4.4 Deblocking filter

At very low bit rates, the block of pixels is mainly made of low-frequency DCT coefficients. In these areas, when there is a significant difference between the DC levels of the adjacent blocks, they appear as block borders. At the extreme case, pictures break into blocks, and the blocking artefacts can be very annoying.

The overlapped block matching motion compensation to some extent reduces these blocking artefacts. For further reduction in the blockiness, the H.263 specification recommends deblocking of the picture through the block edge filter [22-J]. The filtering is performed on 8×8 block edges and assumes that 8×8 DCT is used and the motion vectors may have either 8×8 or 16×16 resolution. Filtering is equally applied to both luminance and chrominance data, and no filtering is permitted on the frame and slice edges.

Consider four pixels A, B, C and D on a line (horizontal or vertical) of the reconstructed picture, where A and B belong to block 1 and C and D belong to a neighbouring block 2, which is either to the right of or below block 1, as shown in Figure 9.8.

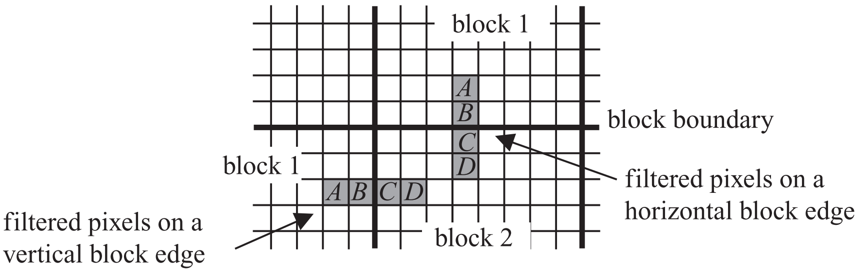
block 1
block boundary
block 1
filtered pixels on a horizontal block edge
filtered pixels on a vertical block edge
block 2
A
B
C
D
A B C D

Figure 9.8 Filtering of pixels at the block boundaries

To turn the filter on for a particular edge, either block 1 or block 2 should be an intra or a coded macroblock with the code COD = 0. In this case, B_1 and C_1 replace values of the boundary pixels B and C, respectively, where

$$\begin{aligned} B_1 &= B + d_1 \\ C_1 &= C - d_1 \\ d_1 &= \text{sign}(d) \times (\text{Max}(0, |d|) - \text{Max}(0, 2 \times |d| - QP)) \\ d &= \frac{3A - 8B + 8C - 3D}{16} \end{aligned} \tag{9.4}$$

QP : quantisation parameter of block 2

The amount of alteration of pixels, $\pm d_1$, is related to a function of pixel differences across the block boundary, d, and the quantiser parameter QP, as shown in (9.4). The sign of d_1 is the same as the sign of d.

Figure 9.9 shows how the value of d_1 changes with d and the quantiser parameter QP, to make sure that only block edges which may suffer from blocking artefacts are filtered and not the natural edges. As a result of this modification, only the pixels on the edge are filtered so that their luminance changes are less than the quantisation parameter, QP.

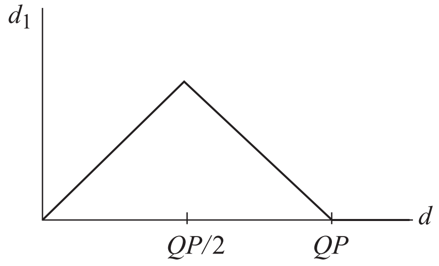

Figure 9.9 d_1 *as a function of d*

This optional tool of H.263 improves both objective (PSNR) and subjective quality of video. Hence, it is made a core element of H.264/AVC, but is implemented in a more efficient way. Since H.264 does not use overlapped motion compensation, the decision for filtering a border pixel is also made depending on the motion of adjacent blocks. Details of this filter in H.264/AVC codec are given in Chapter 11.

9.4.5 *Motion estimation/compensation with spatial transforms*

The motion estimation we have seen so far is based on matching a block of pixels in the current frame against a similar size block of pixels in the previous frame, the so-called block matching algorithm (BMA). It relies on the assumptions that the motion of objects is purely translational and the illumination is uniform, which of course are not realistic. In practice, motion has a complex nature that can be decomposed into translation, rotation, shear, expansion and other deformation components, and the illumination changes are nonuniform. To compensate for these nonuniform changes between the frames, a block of pixels in the current frame can be matched against a deformed block in the previous frame. The deformation should be such that all the components of the complex motion and illumination changes are included.

A practical method for deformation is to transform a square block of $N \times N$ pixels into a quadrilateral of irregular shape, as shown in Figure 9.10.

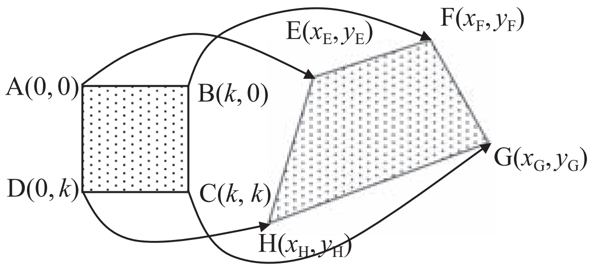

Figure 9.10 Mapping of a block to a quadrilateral

One of the methods for this purpose is the bilinear transform, defined as [11]

$$\begin{aligned} x &= \alpha_0 u + \alpha_1 v + \alpha_2 uv + \alpha_3 \\ y &= \alpha_4 u + \alpha_5 v + \alpha_6 uv + \alpha_7 \end{aligned} \tag{9.5}$$

where a pixel at a spatial coordinate (u, v) is mapped into a pixel at coordinate (x, y). To determine the eight unknown mapping parameters α_0–α_7, eight simultaneous equations relating the coordinates of vertices A, B, C and D into E, F, G and H of Figure 9.10 must be solved. To ease computational load, all the coordinates are offset to the position of coordinates at $u = 0$ and $v = 0$, as shown in the figure. Referring to the figure, the eight mapping parameters are derived as

$$\begin{aligned} &\alpha_0 = \frac{x_F - x_E}{k}; \quad \alpha_4 = \frac{y_F - y_E}{k}; \quad \alpha_1 = \frac{x_H - x_E}{k}; \quad \alpha_5 = \frac{y_H - y_E}{k} \\ &\alpha_2 = \frac{x_E - x_F + x_G - x_H}{k}; \quad \alpha_6 = \frac{y_E - y_F + y_G - y_H}{k}; \quad \alpha_3 = x_E; \\ &\alpha_7 = y_E \end{aligned} \tag{9.6}$$

where $k = N - 1$ and N is the block size, for example, for $N = 16$, $k = 15$.

To use this kind of spatial transformation as a motion estimator, the four corners E, F, G and H in the previous frame are chosen among the pixels within a vertex search window. Using the offset coordinates of these pixels in (9.6), the motion parameters that transform all the pixels in the current square macroblock of ABCD into a quadrilateral are derived. The positions of E, F, G and H that result in the lowest difference between the pixels in the quadrilateral and the pixels in the transformed block of ABCD are regarded as the best match. Then α_0–α_7 of the best match are taken as the parameters of the transform that define the motion estimation by spatial transformation.

It is obvious that in general the number of pixels in the quadrilateral is not equal to the N^2 pixels in the square block. To match these two unequal size blocks, the corresponding pixel locations of the square block in the quadrilateral must be determined. Since these in general do not coincide with the pixel grid, their values should be interpolated from the intensity of their four surrounding neighbours, I_0, I_1, I_2 and I_3, as shown in Figure 9.11.

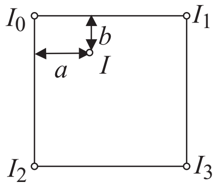

Figure 9.11 Intensity interpolation of a nongrid pixel

The interpolated intensity of the mapped pixels, I, from its four immediate neighbours, is inversely proportional to their distances and is given by

$$I = (1-a)(1-b)I_0 + a(1-b)I_1 + (1-a)bI_2 + abI_3 \tag{9.7}$$

which is simplified to

$$I = (I_1 - I_0)a + (I_2 - I_0)b + (I_0 + I_3 - I_1 - I_2)ab + I_0$$

where a and b are the horizontal and vertical distances of the mapped pixel from the pixel with intensity I_0.

Note that this type of motion estimation/compensation is much more complex than the simple block matching. First, in block matching for a maximum motion speed of ω pixels/frame, there are $(2\omega + 1)^2$ matching operations, while in the spatial transforms, since each vertex is free to move in any direction, the number of matching operations becomes $(2\omega + 1)^8$. Still each operation is more complex than BMA, since for each match the transformation parameters α_0–α_7 have to be calculated, and all the mapped pixels should be interpolated.

There are numerous methods of simplifying the operations [11]. For example, a fast matching algorithm, such as the orthogonal search algorithm (OSA) introduced in section 3.3, can be used. Since for a motion speed of 8 pixels/frame, OSA needs only 13 operations, then the total search operations become $13^4 = 28\,561$, which is practical and is much less than using the full-search method of $(2 \times 8 + 1)^8 = 7 \times 10^9$, which is not practical! Also, the use of simplified interpolation reduces the interpolation complexity to some extent [12].

To appreciate the motion compensation capability of this method, a head-and-shoulders video sequence was recorded, at a speed of almost 12 frames/s, where the head moves from one side to another in 3 s. Assuming that the first frame is available at the decoder, the remaining 35 frames were reconstructed by the motion vectors only, and no motion-compensated error was coded. Figure 9.12 shows frames 5, 15, 25 and 35 of the reconstructed pictures by the bilinear transform, called here block matching with spatial transform (BMST) and the conventional BMA. At frame 5, where the eye should be closed, the BMA cannot track it, as this method only translates the initial eye position of frame 1, where it was open, but BMST tracks it well. Also, throughout the sequence, the BMST tracks all the eye's and head's movements (plus opening and closing the mouth) and produces almost good-quality picture, while that of BMA performs a noisy image.

To explain why the BMST can produce such a remarkable performance, consider Figure 9.13, where the reconstructed pictures around frame 30, that is, frames 28–32, are shown. Looking at the back of the ear, we see that from frame to frame the hair grows, such that at frame 32 it looks quite natural. This is because if, for example, the quadrilateral is only made up of a single black dot and it is then interpolated over 16×16 pixels to be matched to the current block of the same size in hair, then the current block can be made from a single pixel.

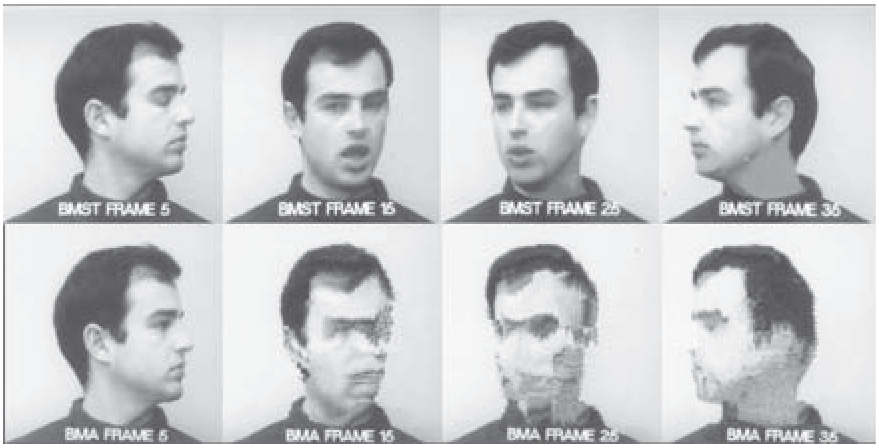

Figure 9.12 Reconstructed pictures with operating individually the BMST and BMA motion vectors

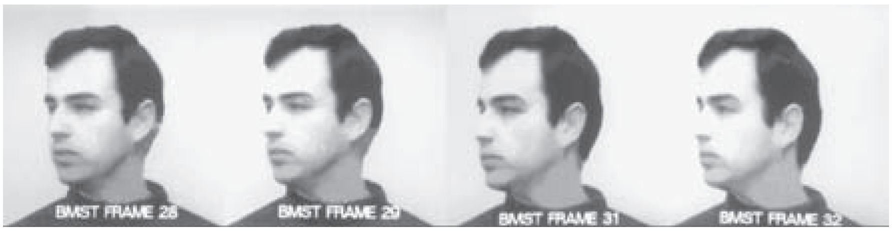

Figure 9.13 Frame-by-frame reconstruction of the pictures by BMST

Note that in BMST, each block requires eight transformation parameters equal to four motion displacements at the four vertices of the quadrilateral. Either the eight parameters a_0–a_7 or four displacement vectors at the four vertices of the quadrilateral as four motion vectors should be sent. The second method is preferred, since a_0–a_7 are in general noninteger values and need more bits than the four motion vectors. Hence, the motion vector overhead of this method is four times that of BMA of the same block size. However, if BMA of 8×8 pixels is used as in the advanced prediction mode [22-F], then we have the same overhead. Again this is irrespective of the block size, since BMA compensates for translational motion only and cannot produce any better results than those above.

One way of reducing the motion vector overhead is to force the vertices of the four adjacent quadrilaterals to a common vertex. This generates a net-like structure or *mesh*, as shown in Figure 9.14*a*. As can be seen, the motion-compensated picture (Figure 9.14*b*) is smooth and free from blocking artefacts.

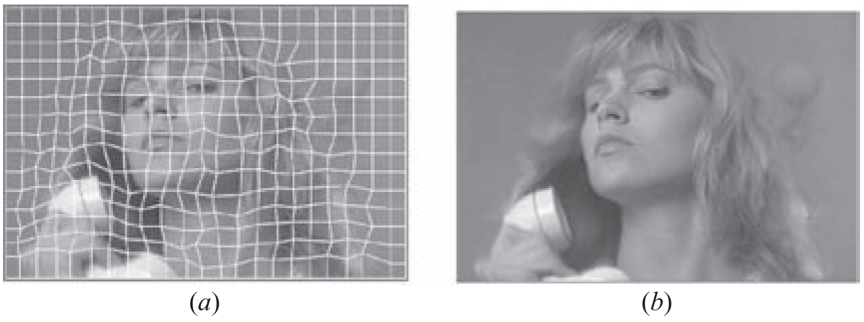

Figure 9.14 Mesh-based motion compensation: (a) mesh and (b) motion-compensated picture

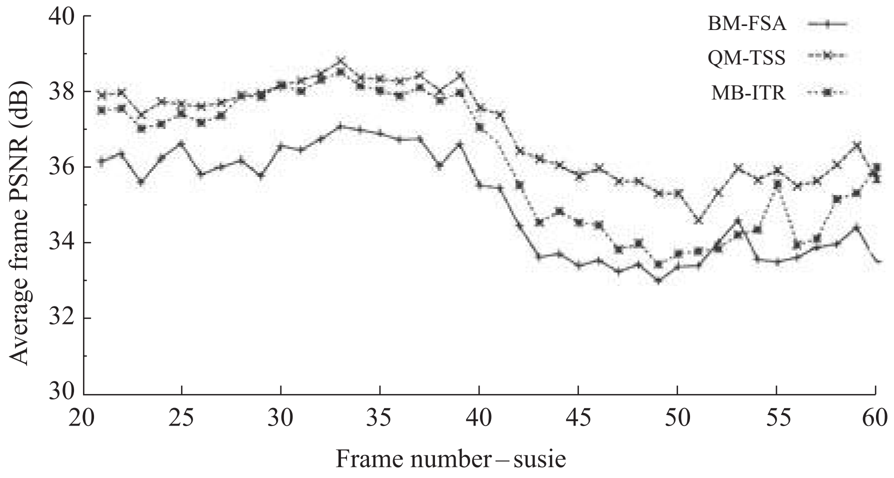

Figure 9.15 Performance of spatial transform motion compensation

To generate such a mesh, the three vertices of a quadrilateral are fixed to their immediate neighbours and only one (bottom right vertex) is free to move. This constrains the efficiency of the motion estimation, and for better performance, motion estimation for the whole frame has to be iterated several times. Thus, it is not expected to perform as well as the unconstrained movement of the vertices applied to Figure 9.12. Despite this, since mesh-based motion estimation creates a smooth boundary between the quadrilaterals, the motion-compensated picture will be free from blockiness. Also, it needs only one motion vector per quadrilateral, similar to BMA. Thus, this mesh-based motion estimation is expected to be better than the BMA with the same motion vector overhead, but of course with increased computational complexity. Figure 9.15 compares the motion compensation efficiency of the full-search block matching algorithm (BM-FSA) with the quadrilateral matching, using three-step search (QM-TSS) and the mesh-based iterative algorithm (MB-ITR). The motion compensation is applied between the incoming pictures to eliminate accumulation of errors. Also, since QM requires four motion vectors per block, in order to reduce motion vector overhead, each macroblock is first tested with BMA, and if the MBA motion-compensated error is larger than a given threshold, QM is used; otherwise, BMA is used. Hence, MQ overhead is less than four times of BMA. Our investigations show that for head-and-shoulders type pictures, about 20–30 per cent of the macroblocks need QM and the rest can be faithfully compensated by the BMA method. In this figure, QM also used overlap motion compensation [13]. However, the mesh-based (MB) method requires the same overhead as BMA (slightly less, no need at the picture borders).

As the figure shows, mesh-based motion compensation is superior to the conventional block matching technique, with the same motion vector overhead. Considering the smooth motion-compensated picture of mesh-based method (Figure 9.14) and its superiority over the block matching, it is a good candidate to be used in the future standard codecs.

More information on motion estimation with the spatial transforms is given in [11], [14] and [15]. In these papers some other spatial transforms such as affine and perspective are also tested. Methods for their use in a video codec to generate equal overhead to those used in H.263 are also explained.

9.5 Treatment of B-pictures

B-pictures play an important role in low bit rate applications. If they are coded at lower quality, the quantisation distortion is not accumulated (since they are not used for prediction; see section 7.6). This is not the case for P-pictures, where any gain in reducing the bits in one frame may have to be returned at a higher cost later, when the distortion accumulates in a noise-like signal, which is difficult to code. For very low bit rate video, such as video for mobile networks, normally the frame rate is low (e.g. 5–10 frames/s), and hence the number of B-pictures between the anchor P- and I-pictures cannot be large. Apparently only one B-picture is an ideal choice. Also, in these applications I-pictures are hardly used, or if they are used, the GOP length is normally very large. Hence, it is plausible to assume, if there is any B-picture in a video, that it is accompanied by a neighbouring P-picture. Thus, one can nearly always code B-pictures in relation to the P-picture counterpart, and interrelate their addressing. Two of these are used as annexes in the H.263 family, and are discussed in the following.

9.5.1 PB frames mode

A PB frame consists of two P- and B-pictures coded as one unit [22-G]. The P-picture is predicted from the last decoded P-picture, and the B-picture is predicted from both the last decoded P-picture and the P-picture currently being decoded. The prediction process is illustrated in Figure 9.16.

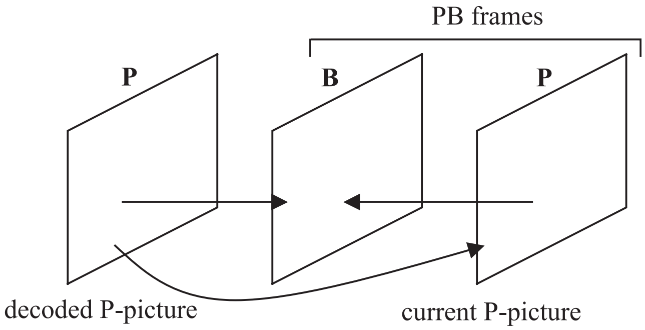

Figure 9.16 Prediction in PB frames mode

9.5.1.1 Macroblock type

Since in the PB frames mode a unit of coding is a combined macroblock from P- and B-pictures, the composite macroblock comprises 12 blocks. First the data for the six P-blocks are transmitted as the default H.263 mode, and then the data for the six B-blocks. The composite macroblock may have various combinations of coding status for the P- and B-blocks, which are dictated by the MCBPC. One of the modes of the MCBPC is the intra macroblock type that has the following meaning:

- the P-blocks are intra coded;
- the B-blocks are inter coded with prediction as for an intra block.

The MVD is also included for intra blocks in pictures for which the type information PTYPE indicates inter. In this case, the vector is used for the B-block only. The code words $\mathrm{MVD}_{2\text{–}4}$ are never used for intra. The candidate motion vector predictor is not set to zero if the corresponding macroblock was coded in intra mode.

9.5.1.2 Motion vectors for B-pictures in PB frames

In the PB frames mode, the motion vectors for the B-pictures are calculated as follows. Assume that we have a motion vector component MV in half-pixel units to be used in the P-pictures. This MV represents a vector component for an 8×8 luminance block. If only one motion vector per macroblock is transmitted, then MV has the same value for each of the 8×8 luminance blocks.

For prediction of the B-picture, we need both forward and backward vector components MV_F and MV_B. Assume also that MV_D is the delta vector component given by the motion vector data of a B-picture (MVDB) and corresponds to the vector component MV. Now MV_F and MV_B are given in half-pixel units by the following formulae:

$$\begin{aligned} MV_F &= \frac{TR_B \times MV}{TR_D} + MV_D \\ MV_B &= \frac{(TR_B - TR_D) \times MV}{TR_D}, \quad \text{if} \quad MV_{\mathrm{D}} = 0 \\ MV_B &= MV_F - MV, \qquad \text{if} \quad MV_{\mathrm{D}} \neq 0 \end{aligned} \tag{9.8}$$

Here TR_D is the increment of temporal reference (*TR*) from the last picture header. In the optional PB frames mode, *TR* only addresses P-pictures. TR_B is the TR for the B-pictures, which indicates the number of nontransmitted pictures since the last P- or I-picture and before the B-picture.

Division is done by truncation, and it is assumed that scaling reflects the actual position in time of P- and B-pictures. Care is also taken that the range of MV_F should be constrained. Each variable length code (VLC) for MVDB represents a pair of difference values. Only one of the pairs will yield a value for MV_F falling within the permitted range of -16 to $+15.5$. The above relations between MV_F, MV_B and *MV* are also used in the case of intra blocks, where the vector is used for predicting B-blocks.

For chrominance blocks, the forward and backward motion vectors, MV_F and MV_B, are derived by calculating the sum of the four corresponding luminance vectors and dividing this sum by 8. The resulting one-sixteenth pixel resolution vectors are modified towards the nearest half-pixel position.

9.5.1.3 Prediction for a B-block in PB frames

In PB frames mode, predictions for the 8×8 pixel B-blocks are related to the blocks in the corresponding P-macroblock. First, it is assumed that the forward and backward motion vectors MV_F and MV_B are calculated. Second, it is assumed that the luminance and chrominance blocks of the corresponding P-macroblock are decoded and reconstructed. This macroblock is called P_{REC}. On the basis of P_{REC} and its prediction, the prediction for the B-block is calculated.

The prediction of the B-block has two modes that are used for different parts of the block:

- For pixels where the backward motion vector MV_B points to inside P_{REC}, use bidirectional prediction. This is obtained as the average of the forward prediction using MV_F relative to the previously decoded P-picture, and the backward prediction using MV_B relative to P_{REC}. The average is calculated by dividing the sum of the two predictions by 2 with truncation.
- For all other pixels, forward prediction using MV_F relative to the previously decoded P-picture is used.

Figure 9.17 shows forward and bidirectionally predicted B-blocks. Part of the block that is predicted bidirectionally is shaded, and the part that uses forward prediction only is shown unshaded.

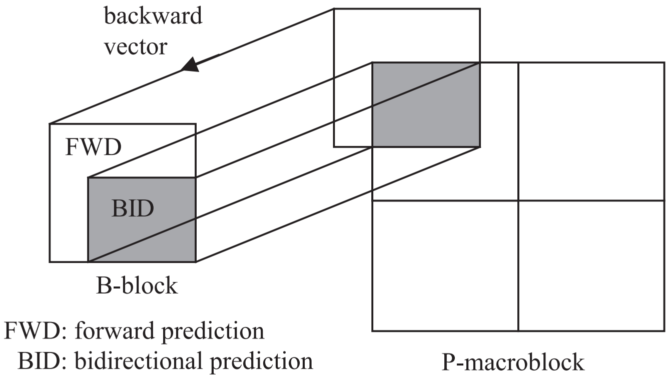

Figure 9.17 Forward and bidirectional prediction for a B-block

9.5.2 Improved PB frames

This mode is an improved version of the optional PB frames mode of H.263 [22-M]. Most parts of this mode are similar to the PB frames mode, the main difference being that in the improved PB frames mode, the B part of the composite PB-macroblock, known as B_{PB}-macroblock, may have a separate motion vector for forward and backward prediction. This is in addition to the bidirectional prediction mode that is also used in the normal PB frames mode.

Hence, there are three different ways of coding a B_{PB}-macroblock, and the coding type is signalled by the MVDB parameter. The B_{PB}-macroblock coding modes are as follows:

1. *Bidirectional prediction*: In the bidirectional prediction mode, prediction uses the reference pictures before and after the B_{PB}-picture. These references are the P-picture part of the temporally previous improved PB frames and the P-picture part of the current improved PB frames. This prediction is equivalent to the prediction in normal PB frames mode when $MV_D = 0$. Note that in this mode the MVD of the PB-macroblock must be included if the P-macroblock is intra coded.
2. *Forward prediction*: In the forward prediction mode the vector data contained in MVDB are used for forward prediction from the previous reference picture (an intra or inter picture, or the P-picture part of PB or improved PB frames). This means that there is always only one 16×16 vector for the B_{PB}-macroblock in this prediction mode. A simple prediction is used for coding of the forward motion vector. The rule for this predictor is that if the current macroblock is not at the far left edge of the current picture or slice and the macroblock to the left has a forward motion vector, then the predictor of the forward motion vector for the current macroblock is set to the value of the forward motion vector of the lock to the left; otherwise, the predictor is set to zero. The difference between the predictor and the desired motion vector is

then variable length coded in the same way as vector data to be used for the P-picture (MVD).

3. *Backward prediction*: In the backward prediction mode the prediction of B_{PB}-macroblock is identical to B_{REC} of normal PB frames mode. No MVD is used for the backward prediction.

9.5.3 Quantisation of B-pictures

In normal mode the quantisation parameter quant is used for each macroblock of P- and B-pictures. In PB frames mode, quant is used for P-blocks only, while for the B-blocks a different quantisation parameter bquant is used. In the header information a relative quantisation parameter known as dbquant is sent which indicates the relation between quant and bquant, as defined in Table 9.2.

Table 9.2 dbquant codes and relation between quant and bquant

dbquant	**bquant**
00	$(5 \times \text{quant})/4$
01	$(6 \times \text{quant})/4$
10	$(7 \times \text{quant})/4$
11	$(8 \times \text{quant})/4$

Division is done by truncation, and bquant ranges from 1 to 31. If the range exceeds these values, they are clipped to their limits. Note that since dbquant is a 2-bit code word, whereas quantisation information, such as quant, is a 5-bit word (indicating quantisation indices in the range of 1–31), such a strategy significantly reduces the overhead information.

Despite the good results of PB frames mode and its improved version, later on it was discovered that if B-pictures are allowed to be used as references, there is no need to have only one B-picture to be combined with a P-picture. When B-pictures can refer to each other, their consecutive numbers can be increased to improve compression gain. This is a strategy implemented in H.264 and called hierarchical B-pictures, which is explained in Chapter 11.

9.6 Advanced variable length coding

H.263 pays special attention to the VLC for two different reasons. First, since H.263 is a low bit rate codec, it uses any means as well as arithmetic coding as an efficient VLC to enhance the compression efficiency. On the other hand, since H.263 is intended for mobile applications, where the channel error can be very severe and variable length coded data are very prone to the effects of errors, it uses a less compression-efficient VLC to localise the side effect of channel errors. These two contradictory requirements are of course for two different applications, and both are optional. In the normal mode, H.263 like the other standard video codecs uses the conventional VLC.

9.6.1 Syntax-based arithmetic coding

The video syntax is arranged in a hierarchical order of picture, slice/GOB, macroblock and block. In the normal VLC mode of H.263, each element of syntax (e.g. vector data) as a symbol is variable length coded. There are several Huffman-designed VLC tables, each specifically designed for a syntax. A symbol is variable length encoded using one of these tables, based on the syntax of the encoder. The symbol is first mapped to an entry of the table in a look-up operation, and the output is a binary code word.

In the optional arithmetic coding of H.263 [22-E], all the Huffman VLC operations are replaced by arithmetic coding, and instead of each table, a cumulative frequency function defines the probability model for each symbol. This is called syntax-based arithmetic coding (SAC). There are as many probability models as are syntaxes. Both encoder and decoder have the same cumulative frequency SAC model stored in their buffer, similar (but not the same) to the one given in Appendix D. In section 3.4.2.5, we have shown how a symbol with a given probability model is arithmetic coded. It is shown that use of arithmetic coding improves the compression efficiency by approximately 5–10 per cent depending on the type of data to be coded [10]. The use of this mode is indicated by the type information, PTYPE.

Arithmetic coding is another successful optional coding tool of H.263, and its refined version is implemented in H.264. The main refinement is on adapting the probability model to the context of the symbols. However, since context adaptation in binary symbols is easier, context adaptive binary arithmetic coding (CABAC) is the type adopted in H.264. More details of CABAC are given in Chapter 11.

9.6.2 Reversible variable length coding

To decode variable length coded data, decoders need to find the beginning of the code word that starts after the resynchronisation marker. The marker has a unique pattern which is known to the decoder. Variable length coded data are decoded 1 bit at a time, and each time the found bits are compared against a set of code words in a look-up table. If a valid code word is found, the symbol is decoded; otherwise, another bit from the bitstream is appended to the code and tested again. In the event of any error in the bitstream, either a wrong symbol is decoded or the result is declared invalid. In the former, it is more likely that the decoded symbols that follow will all be wrong, and/or eventually an invalid code word is detected. In the case of an invalid code word, decoding is halted, and the decoder waits for the next resynchronisation marker to start decoding. Thus, a single-bit error may cause a large part of the picture, from the occurrence of the error to the next resynchronisation marker, to be corrupted.

One way of reducing the damaged area is to be able to decode the bitstream backward as well as forward. This is called reversible variable length code (RVLC). The decoder normally decodes in the forward mode, but when an invalid code word is detected, it stops decoding, and stores the remaining data, up to the next resynchronisation marker. It then decodes backward from the marker, to find an invalid code word, as shown in Figure 9.18. The area between the forward and reverse nondecodable part becomes the erroneous part.

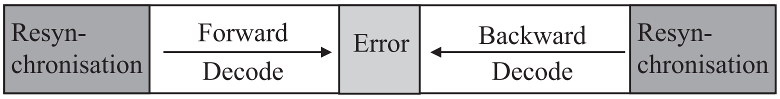

Figure 9.18 A reversible VLC

RVLC to work as a variable length code on both ways is required to be symmetric, and its success very much depends on finding an invalid code word arising from the error. If this is not found, then there is no way of identifying the erroneous area unless by postprocessing, which is discussed in section 9.7.4. Fortunately, due to symmetry of RVLCs, any error will most likely destroy the symmetry and will cause a nonvalid code word.

9.6.3 Resynchronisation markers

The resynchronisation markers play an important role in the performance of H.263 video codec. If used too often, they limit the damaged area more tightly, thus improving the error resilience of the codec. On the other hand, they incur some overheads, which can be costly for low bit rate video. In secure communication environments, they might be used only along with the picture header, where a single-bit error can damage the whole picture. In this case, the overhead is minimised and the error-free picture quality is at its best. In normal transmission media, the resynchronisation markers are preferred to be used at each GOB to give a balance between the compression efficiency (nonerroneous picture quality) and resilience to errors.

For an optimum balance between the resilience and the coding efficiency, the resynchronisation markers may be inserted where they are needed the most. For example, if a GOB does not produce enough bits or if it belongs to a B-picture, then markers may be inserted between several GOBs. Similarly, if a part of a picture is very active, such as the intraframe coded macroblocks, then within a GOB several markers can be inserted.

This optional mode of H.263 is defined under Annex K and is called slice structure mode [22-K]. Two slicing formats are defined. One type is called rectangular slice (RS) submode that occupies a rectangular region of width specified at the slice header. It contains integer number of MBs in the scanning order within the rectangular region. The other type is called arbitrary slice ordering (ASO) submode, where slices may appear in any order within the bitstream. Slices are treated independent of each other to prevent error propagation within the picture. Slice headers such as GOB headers also act as the resynchronisation markers for bit error and packet loss recovery. However, a slice header has more information than a GOB header (e.g. repeating picture header), such that out-of-order decoding of slices within a picture is possible. This is particularly useful for packetised transmission of H.263 coded data, where out-of-sequence decoding of packets reduces the decoding delay. Note that there is no complete independence between the slices, since some processing tools such as deblocking filter mode interrelate adjacent slices [22-J].

To ensure that slice boundary locations can act as resynchronisation points and that slices can be sent out of order without causing additional decoding delays, the following rules are adopted in the slice structure mode:

- The prediction of motion values is the same as if a GOB header was present (see section 9.1.2), preventing the use of motion vectors of blocks outside the current slice for the prediction of the values of motion vectors within the slice.
- The advanced intra coding mode [22-I] treats the slice boundary as if it was a picture boundary with respect to the prediction of intra block DCT coefficient values.
- The assignment of remote motion vectors for use in overlapped block motion compensation within the advanced prediction mode [22-F] also prevents the use of motion vectors of blocks outside the current slice for use as remote motion vectors.

For complete independency between slices, the recommendation describes the optional independent segment decoding mode [22-R]. When this mode is used, the slice boundaries are treated like the picture boundaries, including the treatment of motion vectors which cross those boundaries. If need be, the boundary pixels are extrapolated to be able to use other optional modes such as unrestricted motion vector, advanced prediction mode, deblocking filter and scalability [22-R].

This slicing structure option of H.263 is another fruitful feature of this codec that has been taken into the H.264 standard. Its error resiliency feature has been so impressive that in H.264 not only the concept of GOB is abandoned but the picture type is also abolished and all encoding conditions are defined for slices. Moreover, flexible ordering of macroblocks within the slice and grouping of slices have improved the error robustness of the H.264 codec. This part is extensively addressed in Chapter 11.

9.6.4 Advanced intra/inter VLC

For further improvement to compression efficiency, H.263 specifies some optional modes that can use the normal Huffman-designed VLCs differently from the other standard video codecs. The following two optional modes describe situations where proper use of VLC improves the encoding efficiency.

9.6.4.1 Advanced intra coding

In this optional mode [22-I], intra blocks are predictively coded using nearby blocks in the image to predict values in each intra block. A separate VLC is used for the intra VLC coefficients, and also quantisation of the DC coefficient for intra is different. This is all done to improve the coding efficiency of the intra macroblocks.

The prediction may be made from the block above or the block to the left of the current block being decoded. An exception occurs in the special case of an isolated intra coded macroblock in an inter coded frame with the macroblock neither above nor to the left being intra coded. In this case, no prediction is made. In prediction, DC coefficients are always predicted in some manner, although either the first row or column of AC coefficients may or may not be predicted as signalled on a macroblock-by-macroblock basis. Inverse quantisation of the intra DC coefficient is identical to the inverse quantisation of AC coefficients for predicted blocks, unlike the core H.263 or other standards that use a fixed quantiser of 8 bits for intra DC coefficients.

Also, in addition to zigzag scanning, two more scans are employed, alternate horizontal and alternate vertical scans, as shown in Figure 9.19. Alternate vertical is similar to the alternate scan mode of MPEG-2. For intra predicted blocks, if the prediction mode is set to zero, a zigzag scan is selected for all blocks in a macro-block; otherwise, the prediction direction is used to select a scan on a block basis. For instance, if the prediction refers to the horizontally adjacent block, an alternate vertical scan is selected for the current block; otherwise (for DC prediction referring to vertically adjacent block), alternate horizontal scan is used for the current block.

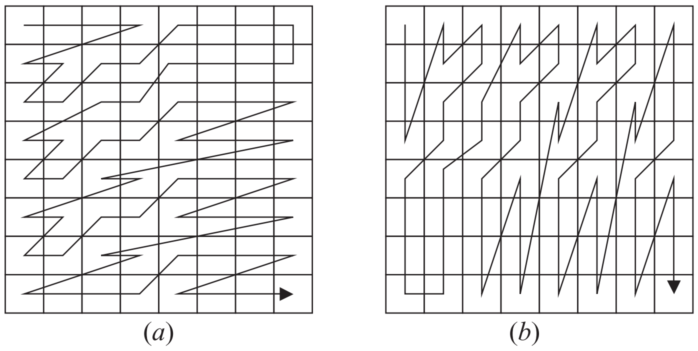

Figure 9.19 Alternate scans: (a) horizontal and (b) vertical

For nonintra blocks, the 8 × 8 blocks of transform coefficients are always scanned with zigzag scanning, similar to all the other standard codecs. A separate VLC table is used for all intra DC and AC coefficients.

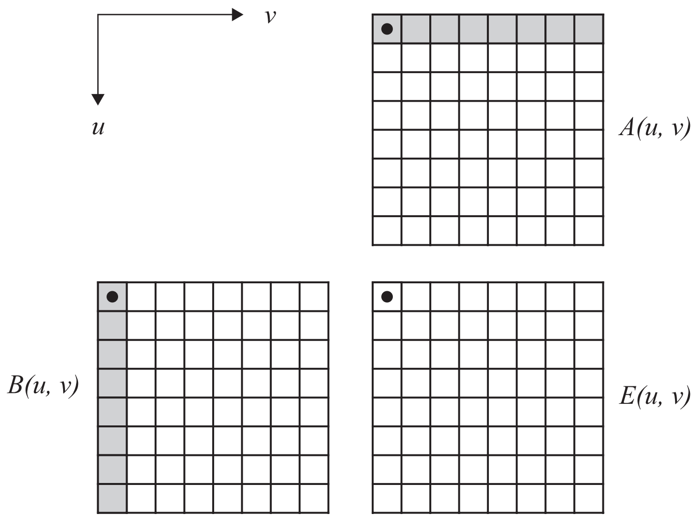

Figure 9.20 Three neighbouring blocks in the DCT domain

Depending on the value of intra mode, either one or eight coefficients are the prediction residuals that must be added to a predictor. Figure 9.20 shows three 8 × 8 blocks of quantised DC levels and prediction residuals labelled $A(u, v)$, $B(u, v)$ and $E(u, v)$, where u and v are row and column indices, respectively.

$E(u, v)$ denotes the current block that is being decoded. $A(u, v)$ denotes the block immediately above $E(u, v)$, and $B(u, v)$ denotes the block immediately to the left of $E(u, v)$. Define $C(u, v)$ to be the actual quantised DCT coefficient. The quantised level $C(u, v)$ is recovered by adding $E(u, v)$ to the appropriate prediction as signalled in the intra mode field.

The reconstruction for each coding mode is given by

Mode 0: DC prediction only

$$\begin{aligned} C(0,0) &= E(0,0) + \frac{1}{2}\left(\frac{A(0,0)\times QP_A}{QP_C} + \frac{B(0,0)\times QP_B}{QP_C}\right) \\ C(u,v) &= E(u,v), \quad u \neq 0;\ v \neq 0;\ u = 0,\ldots,7;\ v = 0,\ldots,7 \end{aligned} \tag{9.9}$$

Mode 1: DC and AC prediction from the block above

$$\begin{aligned} C(0,v) &= E(0,v) + \frac{A(0,v)\times QP_A}{QP_C},\ v = 0,\ldots,7 \\ C(u,v) &= E(u,v), \quad u = 1,\ldots,7;\ v = 0,\ldots,7 \end{aligned} \tag{9.10}$$

Mode 2: DC and AC prediction from the block to the left

$$\begin{aligned} C(u,0) &= E(u,0) + \frac{B(u,0)\times QP_B}{QP_C},\ u = 0,\ldots,7 \\ C(u,v) &= E(u,v), \quad u = 0,\ldots,7;\ v = 1,\ldots,7 \end{aligned} \tag{9.11}$$

where QP_A, QP_B and QP_C denote the quantisation parameters (taking values between 1 and 31) used for $A(u, v)$, $B(u, v)$ and $C(u, v)$, respectively.

The outcome of this option has also influenced the way intra blocks in H.264 are coded. First, as this annex shows, predictions are carried out in the transform domain and only applied to the 2D transform coefficients at the block borders. In H.264, prediction is carried out in the pixel domain and applied to all pixels within the block. However, it should be borne in mind that these transform coefficients mainly carry the block energy and if prediction is to be carried out in the transform domain, they are the more appropriate candidates. However, in textured areas all transform coefficients become important, and for efficient compression they are better to be predicted. Hence, pixel domain prediction is superior to the transform domain, which is observed in H.264. Second, in this annex only three types of predictions (DC, horizontal and vertical) are used, but in H.264 either four or nine directional predictions are used. These predictors can significantly reduce the transform coefficient residues in detailed areas, and hence intra MBs in H.264 are very efficiently coded. Details of various directional predictions for intra blocks are discussed in Chapter 11.

9.6.4.2 Advanced inter coding with switching between two VLC tables

At low frame rates (very common for low bit rate applications), the DCT coefficients of interframe coded macroblocks are normally large. Also, in general, the VLC tables designed for intraframe coded macroblocks suit larger value coefficients better. Hence, to improve the compression efficiency of the H.263 codec, the inter coded macroblocks are allowed to use the VLC tables that are primarily designed for intra macroblocks, but with a different interpretation of level and run. This is made optional and is called alternative inter VLC mode [22-S]. It is activated when significant changes are evident in the picture.

The intra VLC is constructed so that code words have the same value for last (0 or 1) in both the inter and intra tables. The intra table is therefore produced by reshuffling the meaning of the code words with the same value of last. Furthermore, for events with large level, the intra table uses a code word which in the inter table has large run.

Encoder action

The encoder uses the intra VLC table for coding an inter block if the following two criteria are satisfied:

- The intra VLC results in fewer bits than inter VLC.
- If the coefficients are coded with the intra VLC table but the decoder assumes that the inter VLC is used, coefficients outside the 64 coefficients of an 8×8 block are addressed.

With many large coefficients, this will easily happen due to the way the intra VLC is used.

Decoder action

At the decoder the following actions are taken:

- The decoder first receives all coefficient codes of a block.

- The code words are then interpreted assuming that inter VLC is used; if the addressing of coefficients stays inside the 64 coefficients of a block, the decoding is ended.
- If coefficients outside the block are addressed, the code words are interpreted according to the intra VLC.

The outcome of this annex [22-S] in a different form is also used in H.264. In H.264, rather than switching between 2 VLC tables, selection is made among 11 VLC tables. Decision for selection of the most suitable table is based on the context of data to be coded. This is called context adaptive VLC (CAVLC), explained in great detail in Chapter 11.

9.7 Protection against error

H.263 provides error protection, robustness and resilience to allow accessing of video information over a wide range of transmission media. In particular, due to the rapid growth of mobile communications, it is extremely important that access is available to video information via wireless networks. This implies a need for useful operation of video compression algorithms in a very error-prone environment at low bit rates (i.e. less than 64 kbit/s).

In the previous sections, we studied the two important coding tools of VLC and resynchronisation markers in the H.263 codec. The former spreads the errors, and the latter tries to confine them into a small area. In this section, we introduce some more useful tools that can enhance the video quality beyond what we have seen so far. Some of these are recommended as options (or annexes) and some as postprocessing tools that can be implemented at the decoder without the help of the encoder. They can be used either together or individually to improve video quality.

9.7.1 Forward error correction

Forward error correction is the simplest and most effective means of improving video quality in the event of channel errors. It is based on adding some redundancy bits, known as parity bits, to a group of data bits, according to some rules. At the receiver, the decoder, invoking the same rule, can detect if any error has occurred, and in certain cases even correct it. However, for video data, error correction is not as important as is error detection.

The forward error correction for H.263 is the same as for H.261, and is optional [22-H]. However, since the main usage of H.263 will be in a mobile environment with poor error characteristics, forward error correction is particularly important. In most cases (e.g. the GSM system), the error correction will be an integral part of the transmission channel. If it is not, or if additional protection is required, then it should be built into the H.263 system.

To allow the video data and error correction parity information to be identified by the decoder, an error correction framing pattern is included. This pattern consists of multiframes of eight frames, each frame comprising 1-bit framing, 1-bit fill indicator (FI), 492 bits of coded data and 18-bit parity. One bit from each one of the eight frames provides the frame alignment pattern of $(S_1S_2S_3S_4S_5S_6S_7S_8) =$ (00011011) that will help the decoder to resynchronise itself after the occurrence of errors.

The error detection/correction code is a BCH (511, 493) [16]. The parity is calculated against a code of 493 bits, comprising 1-bit FI and 492 bits of coded video data. The generator polynomial is given by

$$g(x) = (x^9 + x^4 + 1)(x^9 + x^6 + x^4 + x^3 + 1) \tag{9.12}$$

The parity bits are calculated by dividing the 493 bits (left shifted by 18 bits) of the video data (including the fill bit) to this generating function. Since the generating function is a 19-bit polynomial, the remainder will be an 18-bit binary number (that is why data bits had to be shifted by 18 bits to the left), to be used as the parity bits. For example, for the input data of 01111 . . . 11 (493 bits), the resulting correction parity bits are 011011010100011011 (18 bits). The encoder appends these 18 bits to the 493 data bits, and the whole 511 bits are sent to the receiver as a block of data. Now these 511-bit data are exactly divisible to the generating function, and the remainder will be zero. Thus, the receiver can perform a similar division, and if there is any remainder, it is an indication of channel error. This is a very robust form of error detection, since burst of errors can also be detected.

9.7.2 Back channel

The impact of error on interframe coded pictures becomes objectionable when error propagates through the picture sequence. Errors affecting only one video frame are easily tolerated by the viewers, especially at high frame rates. To improve quality of video services, propagation of errors through the picture frames must be prevented. A simple method for this task is that when the decoder detects errors in the bitstream (e.g. section 9.7.1), it may ask the encoder to code that part of the picture in the next frame in intra mode. This is called forced updating, and of course requires a back channel from the decoder to the encoder.

Since intraframe coded macroblocks generate more bits than interframe coded ones, forced updating may not be too impressive. In particular, in normal interframe coding, only a small number of MBs in a GOB are coded. Forced updating will encode all the MBs in the GOB (including the noncoded MBs) in intra mode, which increases the bit rate significantly. This can have a side effect of impairing video quality in the subsequent frames. Moreover, if errors occur in more than one GOB, the situation becomes much worse, since the encoder can exceed its bit rate budget, dropping some picture frames. This results in picture jerkiness, which is equally annoying.

A better way of preventing propagation of errors is to ask the encoder to change its prediction to an error-free picture. For example, if error occurs in frame

N, then in coding of the next frame (frame $N + 1$), the encoder uses frame $N - 1$, which is free of error at the decoder. This of course requires some additional picture buffers at both the encoder and the decoder.

The optional reference picture selection mode of H.263 uses additional picture memory at the encoder to perform such a task [22-N]. The amount of additional picture memory accommodated in the decoder may be signalled by external means to help memory management at the encoder. The source encoder for this mode is similar to the generic interframe coder, but several picture memories are provided in order that the encoder may keep a copy of several past pictures, as shown in Figure 9.21.

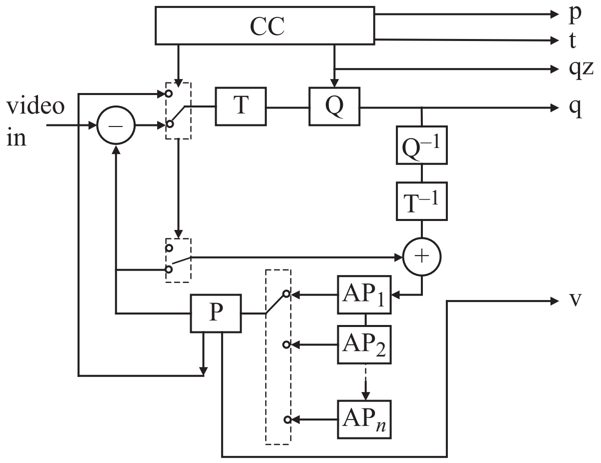

Figure 9.21 An encoder with multiple reference pictures (T, transform; Q, quantiser; CC, coding control; P, picture memory with motion-compensated variable delay; AP, additional picture memory, v, motion vector; p, flag for intra/inter; t, flag for transmitted or not; qz, quantisation indication; q, quantisation index for DCT coefficients)

The source encoder selects one of the picture memories according to the backward channel message GOB-by-GOB to suppress the temporal error propagation due to the interframe coding. The information to signal which picture is selected for prediction is included in the encoded bitstream. The decoder of this mode also has an additional plural number of picture memories to store the correctly decoded video signals with its temporal reference (TR) information. The decoder uses the stored picture whose TR is TRP as the reference picture for interframe decoding, instead of the last decoded picture, if the TRP field exists in the forward message. When the picture whose TR is TRP is not available at the decoder, the decoder may send the forced intra update signal to the encoder.

A positive acknowledgment (ACK) or a negative acknowledgment (NACK) is returned depending on whether the decoder successfully decodes a GOB.

An improved version of this annex [22-N] is used in H.264, under the concept of multiple reference frames. It is used to improve both compression efficiency, by searching for better motion vectors among several frames, and error robustness as discussed here. Multiple reference motion compensation and error-free selection of reference frame are studied in some detail in Chapter 11.

9.7.3 Data partitioning

Although the individual bits of the variable length coded symbols in a bitstream are equally susceptible to channel errors, the impact of the error on the symbols is unequal. Between the two resynchronisation markers, symbols that appear earlier in the bitstream suffer less from the errors than those which come later. This is due to the cumulative impact of VLC on decoding of the subsequent data. To illustrate the extent of difference on the unequal susceptibility to errors, consider a segment of variable length coded video data between two resynchronisation markers. Also, assume that the segment has N symbols with an average VLC length of L bit/symbol and a channel with a bit error rate of P. If any of the first L bits of the bitstream (those immediately after the first marker) are in error, then the symbol would be in error with a probability of LP. The probability that the second symbol in the bitstream is in error now becomes $2LP$, since any error in the first L bits also affects the second symbol. Hence, the probability that the last symbol in the bitstream is in error will be NLP, since every error ahead of this symbol can change the value of this symbol. Thus, the last symbol is N times more likely to be in error than the first symbol in the bitstream.

In applications where some video data are more important than the others, such as the macroblock addresses (as distinct from interframe DCT coefficients), by sending the important data ahead of the nonimportant data, one can significantly reduce the channel error side effects. This form of partitioning the variable length coded data into segments of various importance is called data partitioning, which is one of the optional modes of H.263 [22-V]. Note that this form of data partitioning is different from the data partitioning used as a layering technique, described in section 8.5.2. There, through the priority break point the DCT coefficients were divided into two parts, and the lower frequency coefficients along with the other data comprised the base layer and the high-frequency DCT coefficients were the second layer. Inclusion of the priority break points and other overheads increase the bit rate by about 3–4 per cent (see Figure 8.25). But here, the entire set of data in a GOB is partitioned, and the data are ordered according to the importance of their contributions in video quality, without any additional overhead. For example, within a GOB, the order of importance of data can be as follows: coding status of MBs, motion vectors, block pattern, quantiser parameter, DC coefficients and AC coefficients. Thus, it is also possible to extract all the DC coefficients of the blocks in a GOB, and send them ahead of all the AC coefficients.

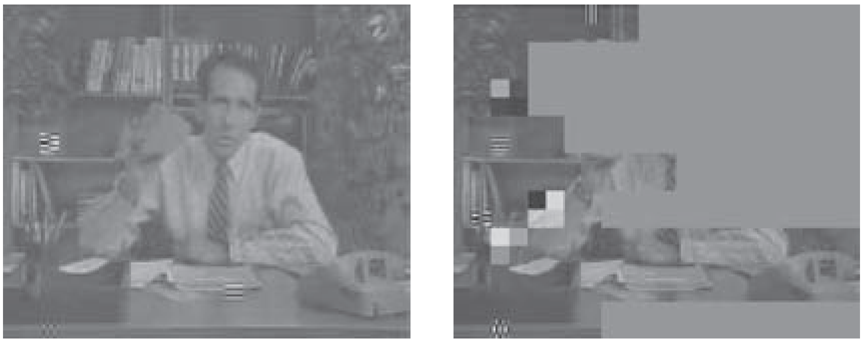
(*a*) (*b*)

Figure 9.22 Effects of errors (a) with and (b) without data partitioning

To appreciate the importance of data partitioning in protecting video against channel errors, Figure 9.22 shows two snap shots of a video sequence with and without data partitioning. It was assumed that in data partitioning, only the DCT coefficients were subjected to errors, but for the normal mode, the bit error could affect any bit of the data. This is a plausible assumption, since normally the important data comprise a small fraction of the bitstream and they can be heavily protected against error. The important data can also use an RVLC, such that some of the corrupted data can be retrieved. In fact, Annex V of data partitioning recommends RVLC for slice header (including the macroblock type) and motion vectors [22-V]. The DCT coefficients according to this recommendation use normal VLC. The good picture quality with data partitioning over the normal as shown in Figure 9.22 justifies such a decision. This also shows the insignificance of the DCT coefficients, as their loss hardly affects the picture quality. It should be noted that in this picture, all the macroblocks were interframe coded. Had there been any intraframe coded macroblock, then its loss would have been noticeable.

Table 9.3 compares the normal VLC and RVLC for the MCBPC for I-pictures. Note that RVLC is symmetric, and it has more bits than the normal VLC. Hence, its use should be avoided, unless it is vital to prevent drastic image degradation.

Table 9.3 VLC and RVLC bits of MCBPC (for I-pictures)

Index	MB type	CBPC	Normal VLC	RVLC
0	3 (intra)	00	1	1
1	3	01	001	010
2	3	10	010	0110
3	3	11	011	01110
4	4 (intra+Q)	00	0001	00100
5	4	01	000001	011110
6	4	10	000010	001100
7	4	11	000011	0111110

Table 9.4 shows the average number of bits used in an experiment for each slice of a QCIF size *salesman* image test sequence (picture in Figure 9.22). The last column is the average bit/slice in normal coding of the sequence, for the whole nine slices. For data partitioning, the second column is the slice overhead (including the macroblock type, resynchronisation markers), the third column is the motion vector overhead and the fourth column is the number of bits used for the DCT coefficients. The sum of all the bits in data partitioning is given in the fifth column.

Table 9.4 Number of bits per slice for data partitioning

	Data partitioning				
Slice no.	**Slice header**	***MV***	**Coefficient**	**Sum**	**Normal**
1	52	30	211	293	269
2	63	34	506	603	571
3	45	42	748	835	803
4	48	42	1025	1115	1083
5	45	71	959	1075	1043
6	41	46	844	931	899
7	48	34	425	507	475
8	51	32	408	491	459
9	38	24	221	283	251

First, since the sum of slice header and motion vectors is only 8–28 per cent of the data, less for more active slices, they can be easily protected without significantly increasing the total bit rate. Second, comparing the total number of bits in data partitioning with normal coding (columns 5 and 6), we see that data partitioning uses about 3–12 per cent more bits than does normal coding. Considering that this increase is due to the use of RVLC for only the header and the motion vectors and some more resynchronisation markers at the end of the important data, had we used RVLC for the entire bits, the increase in bit rate would have been much higher. Hence, the fact that DCT coefficients do not contribute too much to image quality and RVLC needs more bits than VLC; it is very wise not to use RVLC for the DCT coefficients, as Annex V recommends [22-V]. It should be noted that the main cause for the unpleasant appearance of the picture without data partitioning (Figure 9.22*b*) is the error on the important data of the bitstream, such as MB address and motion vectors. When the coding status of an MB is wrongly addressed to the decoder, visual information is misplaced. Also, in the non-data-partitioning mode, since the data, MB and motion vectors variable length coded are mixed, any bit error easily causes nonvalid code words, and a large area of the picture will be in error, as shown in Figure 9.22*b*.

Note that data partitioning is only used for P- and B-pictures, because for I-pictures, DCT coefficients are all important and their absence degrades picture quality significantly.

Data partitioning is one of the most efficient error resilience tools with the least overhead. A more comprehensive way of partitioning data is implemented in H.264. In H.264, the coded data are partitioned into three groups, in the order of sensitivity to errors, as: data part A, part B and part C. Part A contains the most important information such as headers, addresses, coding modes and MVD. Part B contains the intra coded transform coefficients, and those of inter coded are carried into part C. Since part A can be heavily protected against errors, H.264 does not need RVLC that incurs high overhead. Like H.263, I-pictures in H.264 (in fact, I-slices) are not data partitioned. These are discussed in greater depth in Chapter 11.

9.7.4 *Error detection by postprocessing*

In the error correction/detection section of 9.7.1, we saw that with the help of parity bits the decoder can detect an erroneous bitstream. In data communications, the decoder normally ignores the entire segment of the bits and requests for retransmission. Because of the delay-sensitive nature of visual services, in video communication retransmission is never used. Moreover, the decoder can decode a part of the bitstream, up to the point where it finds an invalid code word. Hence, a part of the corrupted bitstream can be recovered, limiting the damaged area.

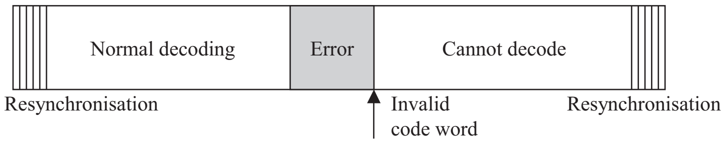

Figure 9.23 Error in a bitstream

However, the decoder still cannot identify the exact location of the error (if this was possible, it could have corrected it!). What is certain is that the bits after the invalid code word up to the next resynchronisation marker are not decodable, as shown in Figure 9.23.

It is to be expected that several symbols are wrongly decoded before the decoder finds an invalid code word. In some cases, the entire data may be decodable without encountering an invalid code word, although this rarely happens. For example, the grey parts of the slices in Figure 9.22*b* are due to the invalid code words that the decoder has given up decoding. Figure 9.22*b* also shows wrongly decoded blocks of pixels, where the decoder can still carry on decoding beyond these blocks. Hence, in those parts that are decodable, the correctly decoded data cannot be separated from the wrongly decoded ones, unless some form of processing on the decoded pixels is carried out.

A simple and efficient method of separating correctly decoded blocks from the wrongly decoded ones is to test for pixel continuity at the macroblock (MB) boundaries. For nonerroneous pictures, due to high interpixel correlation pixel, differences at the MB borders are normally small, and those due to errors create large differences. As shown in Figure 9.24*a*, for every decoded MB, the average of upper and lower pixel differences at the MB boundaries is calculated as

$$\mathrm{BD} = \frac{1}{N}\sum_{i=1}^{N} |P_i^{\mathrm{in}} - P_i^{\mathrm{out}}| \tag{9.13}$$

where N is the total number of pixels at the upper and lower borders of the MB.

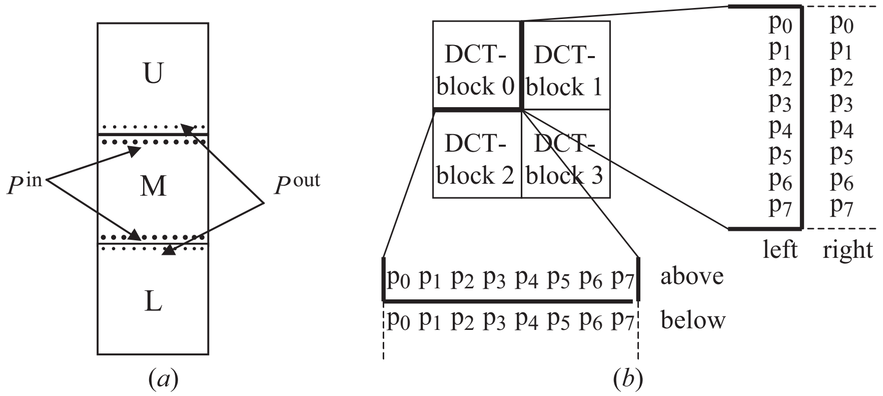

Figure 9.24 Pixels at the boundary of (a) a macroblock and (b) four blocks

The boundary difference (BD) of each MB is then compared against a threshold, and for those MBs which are larger, the implication is that they are most likely to be erroneously decoded. Since due to texture or edges in the image, there might be some inherent discontinuity at the MB boundaries, the boundary threshold can be made dependent on the local image statistics. For example, the mean value of the BDs of all the MB in the slice, or the slice above, with some tolerance (a few times the standard deviation of the mean differences) can be used as the threshold. Our experiments show that mean plus four times the standard deviation is a good value for the threshold [17]. The BD can be calculated separately for luminance and each of the colour differences. A macroblock might have been erroneously decoded if any of these BDs so indicated.

Another method is to calculate the BDs around the 8×8 pixel block boundaries, as shown in Figure 9.24*b*. In 4:2:0 image format, each MB has four luminance blocks and one of each chrominance block, and hence the BD is applied only to the luminance blocks.

In a similar fashion to the BD of (9.13), the block boundary is calculated on the inner and outer pixels of the blocks, as shown in Figure 9.24*b*. Again, if any of the four block boundary values, BD, indicates a discontinuity, the macroblock is most likely to be erroneously decoded. Combining BDs of macroblock (Figure 9.24*a*) and the block (Figure 9.24*b*) increases the reliability of detection [17].

Assuming that these methods can detect an erroneously decoded MB, if the first erroneous MB in a slice is found and provided that the error had only occurred in the bits of this MB, then in general it is possible to retrieve the remaining data. Here, after identifying the first erroneous MB, some of the bits are skipped and decoding is performed on the remaining bits. The process is continued, such that the remaining bits up to the next resynchronisation marker are completely decodable (no invalid code word is encountered). In doing so, even parts of the slice/GOB that were not decodable before are now decoded and the erroneous part of the GOB can be confined to one MB.

If errors occur in more than one MB, then it may not be possible to have perfect decoding (no invalid code word) up to the next resynchronisation marker. Thus, in general, when decoding proceeds up to the next resynchronisation marker, the number of erroneous MBs is counted. This number should be less than the number of erroneous MB in the previous run. The process ends when any further skips in bits and decoding do not further reduce the number of erroneous macroblocks in a GOB.

Figure 9.25 shows the decoded pictures at each stage of this step-by-step skipping and decoding of the bits. For the purpose of demonstration, only 1 bit was introduced in the bitstream between the resynchronisation markers of some of the slices. The first picture shows the erroneous picture without any postprocessing. The second picture shows the reconstructed picture after the first round of bit skipping in each slice, and so on. As we see in each stage the erroneous area (number of erroneous MBs) is reduced, and further processing does not reduce the number of erroneous MBs (not much differences between pictures *d* and *e*). There is only one erroneous MB in each slice of the final picture (Figure 9.25*e*), which can easily be concealed.

In the above example, it was assumed that a single-bit error affected one MB, or a burst of errors affected only one MB. If errors affect more than one MB, then at the end more than one MB will be in error and of course it will take more time to

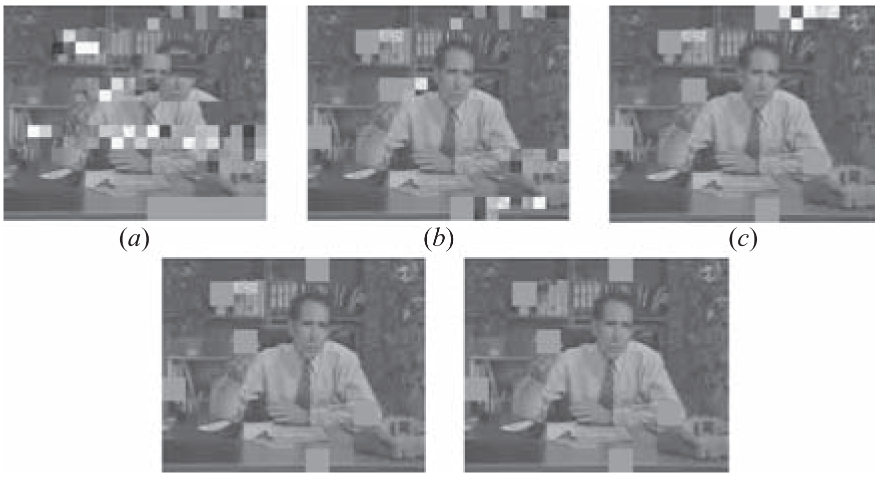

Figure 9.25 (a–e) Step-by-step decoding and skipping of bits in the bitstream

find these erroneous MBs in the decoding. This is because, after finding the first erroneous MB, since there are some erroneous MBs to follow, perfect decoding (not to find invalid code word) is not possible. Our experiments show that in most cases, all the macroblocks between the first and the last erroneous MBs in a slice will be in error. However, it is still possible to recover some of the macroblocks, which without this sort of processing was not possible.

9.7.5 Error concealment

If any of the error resilience methods mentioned so far or their combinations is not sufficient to produce satisfactory picture quality, then one may try to hide the image degradation from the viewer. This is called error concealment.

The main idea behind error concealment is to replace the damaged pixels with pixels from some parts of the video that have maximum resemblance. In general, pixel substitution may come from the same frame or from the previous frame. These are called intraframe and interframe error concealment, respectively [18].

9.7.5.1 Intraframe error concealment

In intraframe error concealment, pixels of an erroneous MB are replaced by those of a neighbouring MB with some form of interpolation. For example, pixels at the macroblock boundary may be directly replaced by the pixels from the other side of the border, and for the other pixels, the average of the neighbouring pixels inversely weighted by their distances may be substituted.

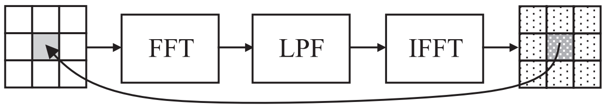

Figure 9.26 An example of intraframe error concealment

An efficient method of intraframe error concealment is shown in block diagram of Figure 9.26. A block of pixels, larger than the size of a macroblock (preferably 48 × 48 pixels, equivalent to 3 × 3 MBs), encompassing the MB to be concealed is fast Fourier transformed (FFT). Pixels of the MB to be concealed initially are filled with grey-level values. The FFT coefficients are two-dimensionally low-pass filtered (LPF) to remove the discontinuity due to these inserted pixels. The resultant low-pass filtered coefficients are then inverse fast Fourier transformed (IFFT) to reconstruct a replica of the input pixels. Because of low pass filtering, the reconstructed pixels are similar but not exactly the same as the input pixels. The extent of dissimilarity depends on the cut-off frequency of the low-pass filter. The lower the cut-off frequency, the stronger is the influence of the neighbouring pixels into the concealed MB. The centre MB at the output now replaces the centre MB at the input, and the whole process of FFT, LPF and IFFT repeats again. The process is repeated several times, and at each time the cut-off frequency of the LPF is gradually increased. To improve the quality of error concealment, the low-pass filter can be made directional, based on the characteristics of the surrounding pixels. The process is terminated when the difference between the pixels of the concealed MB at the input and output is less than a threshold.

This form of error concealment assumes an isolated erroneous MB surrounded by eight immediate nonerroneous neighbours. This is suitable for JPEG or motion JPEG coded pictures, where error is localised (see Figure 5.17), or for interframe coded pictures, if by means of postprocessing error is confined to an MB (e.g. Figure 9.25*e*). For video, where there is a danger of error at the same slice/GOB, pixels of the top and bottom slices should be used, and the two right and left MBs are treated as they are in error. This impairs the performance of the concealment, and may not be suitable. For video, a more suitable error concealment is interframe error concealment, which is explained in the following.

9.7.5.2 Interframe error concealment

In interframe error concealment, pixels from the previous frame are substituted for the pixels of the MB to be concealed, as shown in Figure 9.27. This could be either by direct substitution or by their motion-compensated version, using an estimated motion vector. Obviously, due to movement, motion-compensated substitution is better. The performance of this method depends on how accurately the motion vector for concealment is estimated. In the following sections, several methods of estimating this motion vector are explained, and their error concealment fidelities are compared against each other.

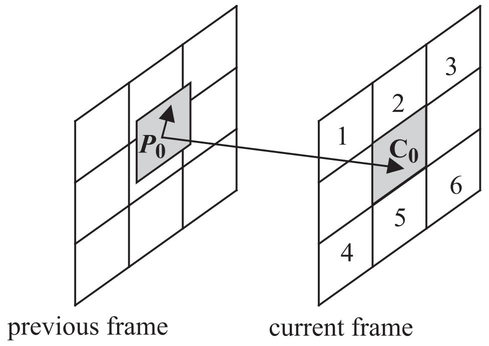

Figure 9.27 A grid of 3 × 3 macroblocks in the current and previous frames

Zero MV

Direct substitution of pixels from the MB of the previous frame at the same spatial position of the MB to be concealed (zero motion vector). This is the simplest method of substitution, and is effective in the picture background, or in the foreground with slow motion.

Previous MV

The estimated motion vector is the same as the motion vector of the spatially similar MB in the previous frame. This method, which assumes a uniform motion of objects, performs well most of the time, but however it is eventually bound to fail.

Top MV
The estimated motion vector is the same as the motion vector of MB at the top of the wanted MB (e.g. MB number 2 of Figure 9.27). Similarly, the motion vector of the bottom MB (e.g. MB number 5) may be used. Since these two MBs are closest to the current MB, it is expected that their *MV* will have the highest similarity. However, this method is as simple as the direct substitution (zero *MV*) and previous *MV*.

Mean MV
The average of the motion vectors of the six immediate neighbours represents the estimated *MV*. The mean values for horizontal displacement, x_0, and vertical displacement, y_0, are taken separately:

$$x_0 = \frac{1}{6}\sum_{i=1}^{6} x_i; \quad y_0 = \frac{1}{6}\sum_{i=1}^{6} y_i \tag{9.14}$$

where x_i and y_i are the horizontal and vertical components of the motion vector i, $MV_i(x_i, y_i)$. Note that due to averaging, any small perturbations in the neighbouring motion vector components will cancel each other. Thus, the estimated motion vector will be different from the motion vector of the neighbouring MB, creating discontinuity at the macroblock borders. This method of error concealment may not produce a smooth picture. The discontinuity at the MB boundaries produces a blocking artefact that appears very annoying. Hence, this method is not good for parts of the picture with motion in various directions, such as the movement of lips and eyes of a talking head.

Majority MV
The majority of the motion vectors are grouped together, and their mean or other representative value is taken as the estimated motion vector:

$$x_0 = \frac{1}{N}\sum_{i=1}^{N} x_i; \quad y_0 = \frac{1}{N}\sum_{i=1}^{N} y_i, \quad N \le 6 \tag{9.15}$$

where N out of six motion vectors are almost at the same direction. Since in general all motion vectors can differ from each other, to find the majority, the motion vectors should be vector quantised, and the majority is found among their original values. This method works well for rigid body movement, where the neighbouring motion vectors normally move at the same direction. However, since there are only six neighbouring motion vectors, a definite majority among them cannot be found reliably. Hence, for nonrigid movement, such as lips and eyes, this method may not work well.

Vector median MV
The median of a group of vectors is one of the vectors in the group that has the smallest Euclidean distance from all. Thus, among the six neighbouring motion vectors MV_1–MV_6 of Figure 9.27, the jth motion vector, MV_j, is the median if

$$dist_j = \frac{1}{5}\sum_{i=1}^{6}\sqrt{(x_i - x_j)^2 + (y_i - y_j)^2}, \quad i \neq j \tag{9.16}$$

such that for all motion vectors MV_k, $1 \leq k$ 6, distance of vector j, $dist_j$, is less than the distance of vector k, $dist_k$ [19].

This method is expected to produce a good result, because since the median of vectors has the least distance from all, it has the largest correlation with them. Also, since the macroblock to be concealed is at the centre of all and has the highest correlation with them, it has the same property as the median vector. This good performance is achieved at a higher computational cost. Here, a Euclidean distance of each vector from all the other five vectors should be calculated first, which requires $(1/2)(6 \times 5) = 15$ vector distance calculations. Then for each vector, the five distances should be averaged to represent the average distance of a vector from the others. Finally, they should be rank ordered to find the minimum distance.

To compare the relative error concealment performance of each method, four sets of head-and-shoulders type image sequences at QCIF resolutions were subjected to channel errors. In the event of error, the whole GOB was concealed by the above-mentioned methods. This is because, due to VLC, a single-bit error may cause the remaining bits up to the next GOB nondecodable, as shown on the erroneous picture of Figure 9.22. Tables 9.5 and 9.6 summarise the quality of these error concealment methods for QCIF video at 5 and 12.5 frames/s, respectively. To show just the impact of error concealment, measurements were carried out only on the concealed areas.

As the tables show, the vector median method gives the best result at both high and low frame rates. That of the majority method is the second best. In all cases, the performance of the average method is as poor as the simple method of top and, in some cases it is even poorer (seq-1 and seq-4 of Table 9.5). The poor performance of the previous *MV* means that motion is not uniform. This is particularly evident at the low frame rate of 5 frames/s. However, all the methods are superior to zero

Table 9.5 PSNR (dB) of various error concealment methods at 5 frames/s

Type	**Sequence**[a]			
	Seq-1	**Seq-2**	**Seq-3**	**Seq-4**
Zero	17.04	18.15	14.54	13.08
Previous	17.28	18.34	14.53	13.48
Top	19.27	21.08	17.04	16.25
Average	19.18	21.74	17.51	16.18
Majority	19.35	21.83	17.89	16.61
Median	19.87	22.52	18.29	16.89
No errors	22.57	26.94	20.85	19.88

[a]64 kbps, 5 fps, QCIF.

Table 9.6 PSNR (dB) of the various error concealment methods at 12.5 frames/s

Type	**Sequence**[a]			
	Seq-1	**Seq-2**	**Seq-3**	**Seq-4**
Zero	20.62	22.11	18.64	16.62
Previous	22.49	22.19	18.19	16.53
Top	22.97	25.16	20.97	20.04
Average	22.92	25.99	21.24	20.08
Majority	23.33	26.32	21.57	20.36
Median	24.36	26.72	22.16	20.81
No errors	26.12	29.69	23.93	23.04

[a]64 kbps, 12.5 fps, QCIF.

motion, implying that loss concealment by an estimated motion vector improves picture quality.

Also, note that since quality measurements were carried out at the error-concealed areas, the performance at a lower frame rate is poorer than the higher frame rate, that is, as the frame rate is reduced, the estimated motion vector is less similar to the actual motion vector. Despite this, estimating motion vectors by all the methods gives better performance than not estimating them (zero *MV*). Figure 9.28 shows an accumulated erroneous picture of seq-3 at 5 frames/s and its concealed one with the median vector method [19].

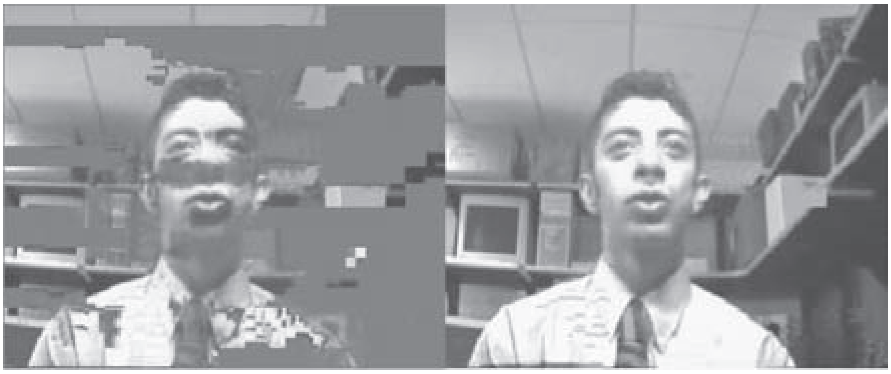

Figure 9.28 An erroneous picture along with its error-concealed one

Bidirectional MV

If B-pictures are present in the GOP, then due to stronger relation between the motion vector of a B-picture and its anchor P- or I-picture, a better estimation of the motion vector can be made. As an example, consider a GOP of $N = \infty$ and $M = 2$, that is, the image sequence is made of alternate P- and B-pictures, as shown in Figure 9.29.

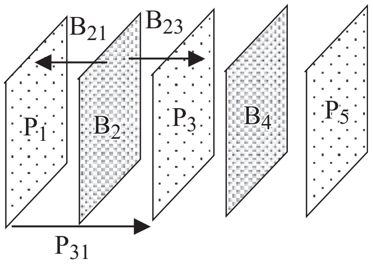

Figure 9.29 A group of alternate P- and B-pictures

To estimate a missing motion vector for a P-picture, say P_{31}, the available motion vectors of the same spatial coordinates of the B-pictures can be used, with the following substitutions:

If only B_{23} is available, then $P_{31} = 2 \times B_{23}$.
If only B_{21} is available, then $P_{31} = -2 \times B_{21}$.
If both B_{23} and B_{21} are available, then $P_{31} = B_{23} - B_{21}$.
If none of them are available, then set $P_{31} = 0$.

To estimate a missing motion vector of a B-picture, simply divide that of the P-picture by 2; $B_{23} = (1/2)P_{31}$ or $B_{21} = -(1/2)P_{31}$.

Here we have used a simple previous *MV* estimation method, explained earlier. Although in the tests of Tables 9.5 and 9.6 (image sequences made of P-pictures only), this method did not perform well, but since the relation here between P- and B-pictures is strong, the method works well. For example, using MPEG-1 video we have achieved about 3- to 4-dB improvement over the majority method [20]. The amount of improvement is picture dependent, and it appears for QCIF images coded with H.263; at least 1-dB improvement over the majority can be achieved. Interested readers should consult [20] for further detailed information.

9.7.5.3 Loss concealment

In transmission of video over packet networks such as IP, ATM or wireless packet networks, the video data are packed into the payload of the packets. In this transmission mode, two types of distortion may occur. One is the error in the payload, which results in erroneous reception of the bitstream, similar to the effect of channel errors. The second one is either error in the packet header, which results in a packet loss, or the loss of a packet if it is queued in a congested network. Excessively delayed packets will be of no use, and hence they will be discarded either by the switching nodes (routers) or by the receiver itself.

Detection, correction and concealment of the error in the packet payload are similar to those of the previous methods mentioned. For packet loss the methods can be slightly different. First, the decoder by examining the packet sequence number discovers that a packet is missing. Second, when a packet is lost, unlike channel errors, no part of the video data is decodable. Hence, loss concealment is more vital to video over packet networks than the error concealment in nonpacket transporting environment.

Considering that in coding of video, in particular at low bit rates, not all parts of the picture are coded, the best concealment for noncoded macroblocks is the direct copy of the previous macroblock without any motion compensation (i.e. zero *MV*). For those which are coded, as Tables 9.5 and 9.6 show, a motion-compensated macroblock gives a better result. However, the information as to which macroblock was or was not coded is not available at the decoder. It is obvious that any attempt to replace the noncoded area by the motion-compensated macroblock will degrade the image quality rather than improve it. Our simulations show that replacing a noncoded MB with an estimated motion-compensated MB would degrade the quality of the pixels in that MB by 7–10 dB [21]. One solution is to build a probability model for an MB to be concealed or not. More information can be found in [21].

9.7.5.4 Selection of best-estimated motion vector

Although Tables 9.5 and 9.6 show that one method of estimating a lost motion vector is better than the other, nevertheless they represent the average quality over the entire video sequence. Had we compared these methods on macroblock-by-macroblock basis, there can be situations in which an overall best method will not perform well. The reason is that the quality of such error/loss concealment depends on the directions and values of the surrounding motion vectors of that macroblock. What makes poor error/loss concealment is that the motion-compensated replacement macroblock shows some pixel discontinuity. This makes the reconstructed picture to look blocky, which is very disturbing.

To improve the error/loss-concealed image quality, one may apply all the above motion estimation methods, and test for image discontinuity around the reconstructed macroblock. The method that gives the least discontinuity is then chosen. Methods introduced in section 9.7.4 can be used as a discontinuity measure.

Both intraframe and interframe error/loss concealment have been used in H.264. In this codec, the intraframe error concealment is simple bilinear interpolation of boundary pixels. The interframe error concealment is based on block edge discontinuity with a similar method shown in Figure 9.24, which is looked at some detail in Chapter 11.

9.8 Scalability

Although we have extensively described the scalability under JPEG2000 and MPEG-2, but since in H.263 it is used with a different terminology, we visit this subject again. It might be useful to know that scalability in H.263 is not used for distribution purposes, but more as a layering technique. Hence, by unequal error protection on the base layer, this method in conjunction with the other error resilience methods, explained in section 9.7, further improves the robustness of this codec.

Extensions of H.263 also support temporal, SNR and spatial scalability as optional modes [22-O]. This mode is normally used in conjunction with the error control scheme. The capability of this mode and the extent to which its features are supported are signalled by external means such as H.245 [9].

There are three types of enhancement picture in the H.263+ codec that are known as B-, EI- and EP-pictures [5]. Each of these has an enhancement layer number, ELNUM, that indicates to which layer it belongs to, and a reference layer number, RLNUM, that indicates which layer is used for its prediction. The encoder may use either of its basic scalability modes of temporal, SNR, spatial or their combinations in a multilayer scalability mode. Details of the basic and multilayer scalabilities are given in section 8.5. However, due to the different nature and application of H.263 compared to that of MPEG-2, there are some differences.

9.8.1 Temporal scalability

Temporal scalability is achieved using bidirectionally predicted pictures or B-pictures. As usual, B-pictures use prediction from either or both of a previous and subsequent reconstructed picture in the reference layer. These B-pictures differ from the B-picture part of PB or improved PB frames in that they are separate entities in the bitstream. They are not syntactically intermixed with a subsequent P or its enhancement part EP.

B-pictures and the B part of PB or improved PB frames are not used as reference pictures for the prediction of any other pictures. This property allows for B-pictures to be discarded if necessary without adversely affecting any subsequent pictures, thus providing temporal scalability. There is no limit to the number of B-pictures that might be inserted between the pairs of the reference pictures in the base layer. A maximum number of such pictures may be signalled by external means (e.g. H.245). However, since H.263 is normally used for low frame rate applications (low bit rates, e.g. mobile), due to larger separation between the base layer I- and P-pictures, there is normally one B-picture between them. Figure 9.30 shows the position of base layer I- and P-pictures and the B-pictures of the enhancement layer for most applications.

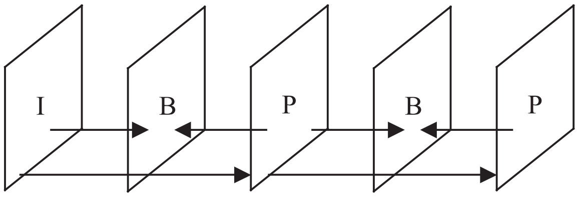

Figure 9.30 B-picture prediction dependency in the temporal scalability

9.8.2 SNR scalability

In SNR scalability, the difference between the input picture and lower quality base layer picture is coded. The picture in the base layer which is used for the prediction of the enhancement layer pictures may be an I-picture, a P-picture, or the P part of PB or improved PB frames, but should not be a B-picture or the B part of a PB or its improved version.

In the enhancement layer two types of picture are identified, EI and EP. If prediction is only formed from the base layer, then the enhancement layer picture is referred to as EI-picture. In this case, the base layer picture can be an I- or a P-picture (or the P part of PB frames). It is possible, however, to create a modified bidirectionally predicted picture using both a prior enhancement layer picture and temporally simultaneous base layer reference picture. This type of picture is referred to as an EP-picture or enhancement P-picture. Figure 9.31 shows the positions of the base and enhancement layer pictures in an SNR scalable coder. The figure also shows the prediction flow for the EI and EP enhancement pictures.

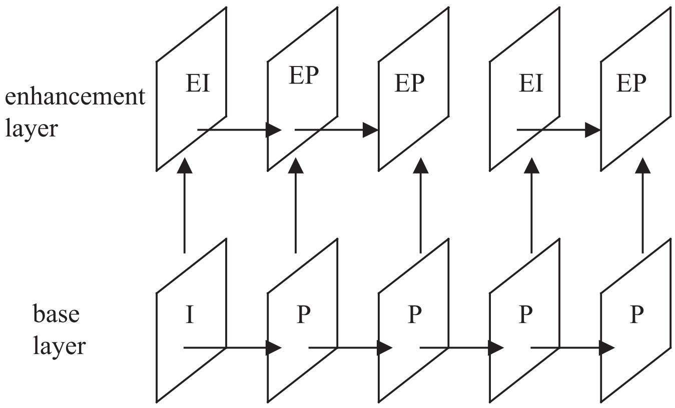

Figure 9.31 Prediction flow in SNR scalability

For both EI- and EP-pictures, prediction from the reference layer uses no motion vectors. However, EP may be predictively coded with respect to its previous reconstructed picture at the same layer, called forward prediction. It might be just the difference between the enhancement and base layer, called upward prediction, or the average of the two predictions, called bidirectional prediction. Decisions are made based on the one that gives the least prediction error.

9.8.3 Spatial scalability

The arrangement of the enhancement layer pictures in the spatial scalability is similar to that of SNR scalability. The only difference is that before the picture in the reference layer is used to predict the picture in the spatial enhancement layer, it is downsampled by a factor of 2 either horizontally or vertically (one-dimensional spatial scalability), or both horizontally and vertically (two-dimensional spatial scalability). Figure 9.32 shows the flow of the prediction in the base and enhancement layer pictures of a spatial scalable encoder.

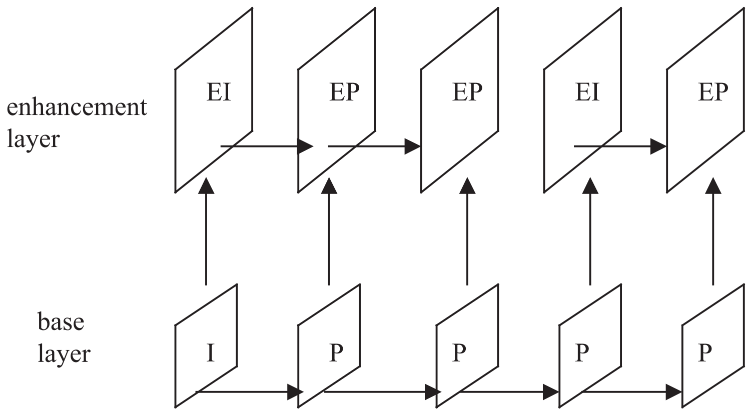

Figure 9.32 Prediction flow in spatial scalability

9.8.4 Multilayer scalability

Undoubtedly multilayer scalability will increase the robustness of H.263 against the channel errors. In the multilayer scalable mode, it is possible for B-pictures to be temporally inserted not only between the base layer pictures of type I, P, PB and improved PB, but also between the enhancement picture types of EI and EP, whether these consist of SNR or spatial enhancement pictures. It is also possible to have more than one SNR or spatial enhancement layer in conjunction with the base layer. Thus, a multilayer scalable bitstream can be a combination of SNR layers, spatial layers and B-pictures. The size of a picture cannot be decreased by increasing the layer number. Figure 9.33 illustrates the prediction flow in a multilayer scalable encoder.

As with the two-layer case, B-pictures may occur in any layer. However, any picture in an enhancement layer which is temporally simultaneous with a B-picture in its reference layer must be a B-picture or the B-picture part of PB or improved PB frames. This is to preserve the disposable nature of B-pictures. Note, however, that B-pictures may occur in any layers that have no corresponding picture in the lower layers. This allows an encoder to send enhancement video with a higher picture rate than the lower layers.

The enhancement layer number and the reference layer number of each enhancement picture (B, EI or EP) are indicated in the ELNUM and RLNUM fields, respectively, of the picture header (when present). If a B-picture appears in an enhancement layer in which temporally surrounding SNR or spatial pictures also appear, the reference layer number (RLNUM) of the B-picture is the same as the enhancement layer number (ELNUM). The picture height, width and pixel aspect ratio of a B-picture are always equal to those of its temporally subsequent reference layer picture.

9.8.5 Transmission order of pictures

Pictures, which are dependent on other pictures, are located in the bitstream after the pictures on which they depend. The bitstream syntax order is specified such that

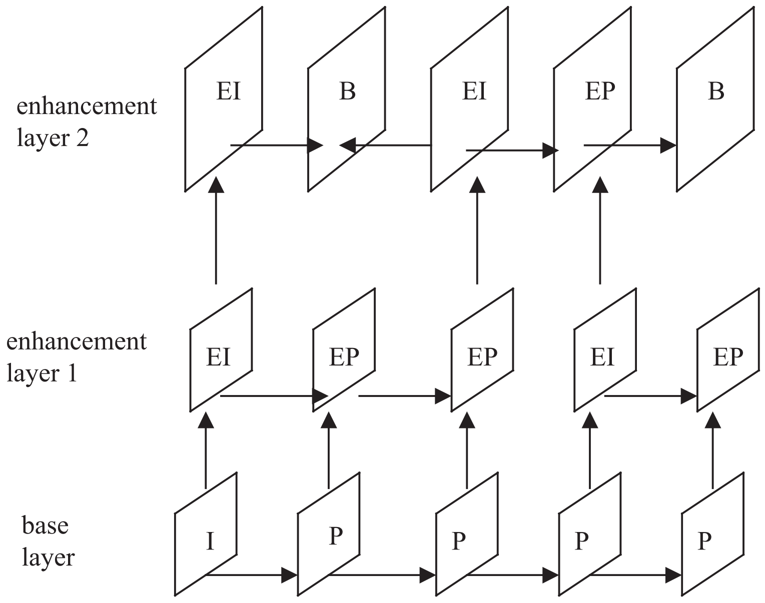

Figure 9.33 Positions of the base and enhancement layer pictures in a multilayer scalable bitstream

for reference pictures (i.e. pictures having types I, P, EI, EP or the P part of PB or improved PB) the following two rules shall be obeyed:

1. All reference pictures with the same temporal reference appear in the bitstream in increasing enhancement layer order. This is because each lower layer reference picture is needed to decode the next higher layer reference picture.
2. All temporally simultaneous reference pictures as discussed in item 1 appear in the bitstream prior to any B-pictures for which any of these reference pictures is the first temporally subsequent reference picture in the reference layer of the B-picture. This is done to reduce the delay of decoding all reference pictures, which may be needed as references for B-pictures.

Then, the B-pictures with earlier temporal references follow (temporally ordered within each enhancement layer). The bitstream location of each B-picture complies with the following rules:

- Be after that of its first temporally subsequent reference pictures in the reference layer. This is because the decoding of the B-pictures generally depends on the prior decoding of that reference picture.
- Be after that of all reference pictures that are temporally simultaneous with the first temporally subsequent reference picture in the reference layer. This is to reduce the delay of decoding all reference pictures, which may be needed as references for B-pictures.

- Precede the location of any additional temporally subsequent pictures other than B-pictures in its reference layer. Otherwise, it would increase picture storage memory requirement for the reference layer pictures.
- Be after that of all EI- and EP-pictures that are temporally simultaneous with the first temporally subsequent reference picture.
- Precede the location of all temporally subsequent pictures within the same enhancement layer. Otherwise, it would introduce needless delay and increase picture storage memory requirements for the enhancement layer.

Figure 9.34 shows two allowable picture transmission orders given by the rules above for the layering structure shown as an example. Numbers next to each picture indicate the bitstream order, separated by commas for the two alternatives.

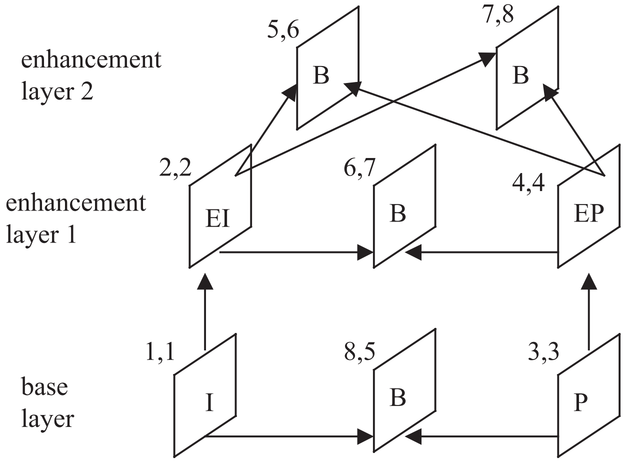

Figure 9.34 Example of picture transmission order

Scalability is also introduced in H.264, under the name of scalable extension of H.264 video coding (H.264/SVC), as well as in the reference model known as joint scalable video model (JSVM). H.264/SVC has improved the compression deficiency of scalable coding (discussed in section 8.5.7), by better inter layer prediction, as well as by introducing a large number of B-pictures in the form of hierarchical B-pictures. More on SVC is given in Chapter 11.

9.9 Buffer regulation

Regulation of output bit rates for better distribution of the target bit rate among the encoding parameters is an important part of any video encoder. This is particularly vital in the H.263 encoder, at least for the following reasons:

- Better bit rate regulation requires larger buffer sizes, hence longer delays.
- H.263 is intended for visual telephony, and the encoding delay should be limited; hence, smaller buffer sizes are preferred.

- The target bit rate is in the order of 24 kbit/s, and even small-size buffers can introduce long delays.

There is no best known method for buffer regulation, and the recommendation H.263 does not standardise any method (neither do other standard encoders). However, at least for the laboratory simulations, one can use those methods designed for the test models. The following is a method that can be used in the simulations [5]. The bit rate is controlled at a macroblock level by changing the quantiser parameter, *QP*, depending on the bit rate, the source and target frame rates.

For the first picture, which is intraframe coded, the quantisation parameter is set to its mid range $QP = 16$ (*QP* varies from 1 to 31). After the first picture, the buffer content is set to

$$\frac{R}{f_{target}} + 3 \times \frac{R}{FR} \quad \text{and} \quad B_{i-1} = \overline{B} \tag{9.17}$$

For the following pictures the quantiser parameter is updated at the beginning of each new macroblock line. The formula for calculating the new quantiser parameter is

$$\begin{aligned} QP_{new} &= \overline{QP_{i-1}}\left(1 + \frac{\Delta_1 B}{2\overline{B}} + \frac{12\Delta_2 B}{R}\right) \\ \Delta_1 B &= B_{i-1} - \overline{B} \end{aligned} \tag{9.18}$$

and

$$\Delta_2 B = B_{i,mb} - \frac{mb}{MB} \times \overline{B}$$

where

$\overline{QP_{i-1}}$ = mean quantiser parameter for the previous picture
$B_i{-}1$ = number of bits spent for the previous picture
$\overline{B}$ = target number of bits per picture
mb = present macroblock number
MB = number of macroblocks in a picture
$B_{i,mb}$ = number of bits spent until now for the picture
R = bit rate
FR = frame rate of the source picture (typically 25 or 30 Hz)
f_{target} = target frame rate

The first two terms of the above formula are fixed for macroblocks within a picture. The third term adjusts the quantiser parameter during coding of the picture.

The calculated new quantisation parameter, QP_{new}, must be adjusted so that the difference fits within the definition of dquant. The buffer content is updated after each complete picture by using the following C program:

```
buffer_content=buffer_content+Bi,99;
while(buffer_content>(3R/FR)){
  buffer_content=buffer_content (R/FR);
frame_incr++;
}
```

The variable `frame_incr` indicates how many times the last coded picture must be displayed. It also indicates which picture from source is coded next and how many pictures are skipped.

To regulate the frame rate, f_{target}, a new $\overline{B}$ is calculated at the start of each frame:

$$f_{target} = 10 - \frac{\overline{QP_{i-1}}}{4}, \quad 4 < f_{target} < 10$$

$$\overline{B} = \frac{R}{f_{target}} \tag{9.19}$$

For this buffer regulation, it is assumed that the process of encoding is temporarily stopped when the physical transmission buffer is nearly full, preventing buffer overflow. However, this means that no minimum frame rate and delay can be guaranteed.

9.10 Problems

1. Assume the DCT coefficients of problem 3 of Chapter 8 are generated by an H.263 encoder. After zigzag scanning, and quantisation with $th = q = 8$, they are converted into three-dimensional events of (last, run, level). Identify these events.

2. The neighbouring motion vectors of the motion vector MV are shown in Figure 9.35.
   a. Find the median of the neighbouring motion vectors.
   b. Find the MVD, if the motion vector MV is (2, 1).

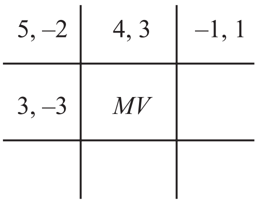

Figure 9.35

3. The intensity of four pixels A, B, C and D of the borders of two macroblocks is given in Figure 9.36.

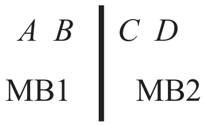

Figure 9.36

Using the deblocking filter of (9.4), find the interpolated pixels B_1 and C_1 at the macroblock boundary for each of:

a. $A = 100$, $B = 150$, $C = 115$ and $D = 50$
b. $A = B = 150$ and $C = D = 50$

Assume the quantiser parameter of macroblock 2 is $QP = 16$.

4. Figure 9.37 shows the six neighbouring macroblocks of a lost motion vector. The values of these motion vectors are also given. Calculate the estimated motion vector for this macroblock for each of the following loss concealment methods:
   a. top
   b. bottom
   c. mean
   d. majority
   e. vector median

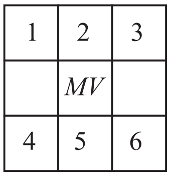

$MV_1=(2, 3)$; $MV_2=(3, 4)$; $MV_3=(-2, -1)$
$MV_4=(4, 1)$; $MV_5=(0, -3)$; $MV_6=(-1, -1)$

Figure 9.37

References

1. Draft ITU-T Recommendation H.263: 'Video coding for low bit rate communication', July 1995
2. H.261: 'ITU-T Recommendation H.261, video codec for audiovisual services at p$\times$64 kbit/s', Geneva, 1990
3. MPEG-1: 'Coding of moving pictures and associated audio for digital storage media at up to about 1.5 Mbit/s', ISO/IEC 1117-2: video, November 1991
4. MPEG-2: 'Generic coding of moving pictures and associated audio information', ISO/IEC 13818-2: video, Draft International Standard, November 1994
5. Draft ITU-T Recommendation H.263+: 'Video coding for very low bit rate communication', September 1997
6. ITU-T recommendation H.263++: 'Video coding for low bit rate communication', ITU-T SG16, February 2000
7. WIEGAND, T.: 'H.26L test model long-term number 9 (TML-9) draft0', VCEG-N83 d1, Germany, December 2001
8. WIEGAND, T. and SULLIVAN, G.: 'Draft ITU-T recommendation and final draft international standard of joint video specification (ITU-T Rec. H.264 | ISO/IEC 14496-10 AVC)', March 2003

9. ITU-T Recommendation H.245, 'Control protocol for multimedia communication', September 1998
10. WALLACE, G.K.: 'The JPEG still picture compression standard', *Commun. ACM*, 1991, **34**, pp. 30–44
11. GHANBARI, M., DE FARIA, S., GOH, I.N. and TAN, K.T.: 'Motion compensation for very low bit rate video', *Signal Process. Image Commun.*, 1994, **7**, pp. 567–580
12. NETRAVALI, A.N. and ROBBINS, J.B.: 'Motion-compensated television coding: Part I', *Bell Syst. Tech. J.*, 1979, **58**, pp. 631–670
13. LOPES, F.J.P. and GHANBARI, M.: 'Analysis of spatial transform motion estimation with overlapped compensation and fractional-pixel accuracy', *IEE Proc. Vis. Image Signal Process.*, 1999, **146**, pp. 339–344
14. SEFERIDIS, V. and GHANBARI, M.: 'General approach to block matching motion estimation', *Opt. Eng.*, 1993, **32**, pp. 1464–1474
15. NAKAYA, Y. and HARASHIMA, H.: 'Motion compensation based on spatial transformation', *IEEE Trans. Circuits Syst. Video Technol.*, 1994, **4**, pp. 339–356
16. BLAHUT, R.E.: *Theory and Practice of Error Control Codes*, Addison-Wesley, Boston, NJ, 1983
17. KHAN, E., LEHMANN, S., GUNJI, H., and GHANBARI, M.: 'Error detection and step-by-step correction of H.263 coded video over wireless networks', *IEEE Trans. Circuits Syst. Video Technol.,* 2004, **14:12**, pp. 1294–1307
18. GHANBARI, M. and SEFERIDIS, V.: 'Cell loss concealment in ATM video codecs', *IEEE Trans. Circuits and Syst. Video Technol.*, special issue on packet video, 1993, **3:3**, pp. 238–247
19. GHANBARI, S. and BOBER, M.Z.: 'A cluster-based method for the recovery of lost motion vectors in video coding', The 4th IEEE Conference on Mobile and Wireless Communications Networks, MWCN'2002, 9–11 September, 2002, Stockholm, Sweden
20. SHANABLEH, T. and GHANBARI, M.: 'Loss concealment using B-pictures motion information', *IEEE Trans. Multimedia*, 2003, **5:2**, pp. 257–266
21. LIM, C.P., TAN, E.A.W., GHANBARI, M. and GHANBARI, S.: 'Cell loss concealment and packetisation in packet video', *Int. J. of Imaging Syst., Technol.*, 1999, **10**, pp. 54–58
22. Some of the H.263 Annexes used in this chapter:
Annex C 'Considerations for Multipoint'
Annex D 'Unrestricted Motion Vector Mode'
Annex E 'Syntax-Based Arithmetic Coding Mode'
Annex F 'Advanced Prediction Mode'
Annex G 'PB-Frames Mode'
Annex H 'Forward Error Correction for Coded Video Signal'
Annex I 'Advanced INTRA Coding Mode'
Annex J 'Deblocking Filter Mode'

Annex K ‘Slice Structured Mode’
Annex M ‘Improved PB-Frames Mode’
Annex N ‘Reference Picture Selection Mode’
Annex O ‘Temporal, SNR, and Spatial Scalability Mode’
Annex R ‘Independent Segment Decoding Mode’
Annex S ‘Alternative INTER VLC mode’
Annex V ‘Data Partitioning’

Chapter 10
Content-based video coding (MPEG-4 visual)

MPEG-4 is another ISO/IEC standard developed by Moving Picture Experts Group (MPEG), the committee that also developed the Emmy Award winning standards of MPEG-1 and MPEG-2. While MPEG-1 and MPEG-2 video aimed at devising coding tools for CD-ROM and digital television, respectively, MPEG-4 video aims at providing tools and algorithms for efficient storage, transmission and manipulation of video data in multimedia environments [1,2]. The main motivations behind such a task are the proven success of digital video in three fields of digital television, interactive graphics applications (synthetic image content) and the interactive multimedia (World Wide Web, distribution and access to image content). The MPEG-4 group believe these can be achieved by emphasising the functionalities of the proposed codec, which include efficient compression, object scalability, spatial and temporal scalability, error resilience, etc.

The approach taken by the experts group in coding of video for multimedia applications relies on a content-based visual data representation of scenes. In content-based coding, in contrast to conventional video coding techniques, a scene is viewed as a composition of video objects (VO) with intrinsic properties such as shape, motion and texture. It is believed that such a content-based representation is a key to facilitating interactivity with objects for a variety of multimedia applications. In such applications, the user can access arbitrarily shaped objects in the scene and manipulate these objects.

The MPEG-4 group has defined the specifications of their intended video codec in the form of verification models (VMs) [3]. The verification model in MPEG-4 has the same role as the reference and test models defined for H.261 and MPEG-2, respectively. The verification model has evolved over time by means of core experiments in various laboratories round the world. It is regarded as a common platform with a precise definition of the encoding and decoding algorithms that can be represented as tools addressing specific functionalities of MPEG-4. New algorithms/tools are added to the VM and old algorithms/tools are replaced in the VM by successful core experiments.

So far, the verification model has been gradually evolved from version 1.0 to version 11.0, and during each evolution new functionalities have been added. In this chapter, we do not intend to review all of them but instead to address those functionalities that have made MPEG-4 video coding radically different from its predecessors. Hence, it is intended to look at the fundamentals of new coding algorithms that have been introduced in MPEG-4.

It is worth noting that if the whole video frame is coded as a single object, then the object-based video coding becomes similar to the other frame-based video coding. To distinguish this codec from MPEG-4 part 10, which is another name for H.264, object-based MPEG-4 is commonly known as MPEG-4 visual. MPEG-4 visual for frame-based coding is very similar to H.263 with almost equal compression performance. At the end of this chapter, this codec is contrasted against the H.263 codec. Before going into details of object-based video coding, let us examine the functionalities of this codec.

10.1 Profiles and levels

MPEG-4, as with MPEG-2, has so many functionalities that the users may only be interested in a subset of them. These are defined as profiles. For each profile, a number of resolution states such as bit rate, frame rate, pixel resolutions can be defined as levels. Since MPEG-4 is a very versatile video coding tool, it has several profiles and levels, and every now and then many more are added to them. Profile in MPEG-4 is also synonymous to the support of a set of annexes in H.263. Some well-known profiles with the associated commonly used levels are as follows:

- *Simple profile*: this profile provides the simplest tool for low-cost applications, such as video over mobile and Internet. It supports up to four rectangular objects in a scene within quarter of common intermediate format (QCIF) pictures. There are three levels in this profile to define bit rates from 64 to 384 kbit/s (64, 128 and 384 kbit/s for level 1, level 2 and level 3, respectively). The simple profile also supports most of the optionalities (annexes in H.263) that are mainly useful for error resilience transmission. In addition to I- and P-VOPs (video object planes (VOPs) defined in section 10.2), they include AC/DC prediction, four motion vectors, unrestricted motion vectors, quarter-pixel spatial accuracy, slice synchronisation, data partitioning and reversible variable length code (RVLC). This profile can decode a bitstream generated by the core H.263.
- *Simple scalable profile*: this adds the support for B-VOPs and temporal and spatial scalability to the simple profile. It provides services to the receivers requiring more than one level of quality of service, such as video over Internet.
- *Advanced real-time simple profile*: this adds the error protection to the simple profile through the introduction of the back channel. In response to a negative acknowledgement from the decoder, the encoder encodes the affected parts of the picture in intra mode. This profile improves the robustness of real-time visual services over error-prone channels such as videophone.
- *Advanced simple profile*: this improves the compression efficiency of the simple profile by supporting quarter-pixel resolution and global motion estimation in addition to B-VOPs.
- *Fine granular scalability profile*: this is similar to SNR scalability, but the enhancement layers are represented in bit planes to offer up to eight scalable

layers. It is mainly used with the simple or advanced simple profile as the base layer.

- *Core profile*: this adds scalability to still textures, B-VOPs, binary shape coding, and temporal scalability of rectangular as well as binary shape objects to the simple profile. Its maximum bit rate for level 1 is 384 kbit/s and for level 2 is 1 Mbit/s. This profile is useful for high-quality interactive services as well as mobile broadcast services.
- *Core scalable visual profile*: this adds object-based SNR, spatial and temporal scalability to the core profile.
- *Main profile*: this supports for interlaced video, greyscale alpha maps and sprites. This profile is intended for broadcast services that can handle both progressive and interlaced video. It can handle up to 32 objects with a maximum bit rate of 38 Mbit/s.
- *Advanced coding efficiency*: this profile is an extension of the main profile, but for bit rates less than 1 Mbit/s. It adds quarter pixel and global motion estimation to the main profile to improve the encoding efficiency. However, it does not support sprites.
- *Simple studio profile*: this only supports I-VOP pictures coded at very high quality up to 1200 Mbit/s. As the name implies, it is designed for studio applications and can support high-resolution video for HDTV and digital cinema. Each I-VOP may have an arbitrary shape and have several alpha planes.
- *Core studio profile*: this adds P-VOPs to the simple studio profile to reduce the bit rate for very high quality video.

10.2 Video object plane

In object-based coding, the video frames are defined in terms of layers of video object planes (VOP). Each VOP is then a video frame of a specific object of interest to be coded, or to be interacted with. Figure 10.1*a* shows a video frame that is made of three VOPs. In this figure, the two objects of interest are the balloon and the aeroplane. They are represented by their video object planes of VOP_1 and VOP_2. The remaining part of the video frame is regarded as a background, represented with VOP_0. For coding applications, the background is coded only once, and the other object planes are encoded through the time. At the receiver, the reconstructed background is repeatedly added to the other decoded object planes. Since in each frame the encoder only codes the objects of interest (e.g. VOP_1 and/or VOP_2), and usually these objects represent a small portion of the video frame, the bit rate of the encoded video stream can be extremely low. Note that had the video frame of Figure 10.1*a* been coded with a conventional codec such as H.263, since clouds in the background move, the H.263 encoder would have inevitably encoded most parts of the picture with a much higher bit rate than that generated from the two objects.

The VOP can be a semantic object in the scene, such as the balloon and aeroplane in Figure 10.1. It is made of *Y*, *U* and *V* components plus theirs shapes. The shapes are used to mask the background and help to identify object boarders.

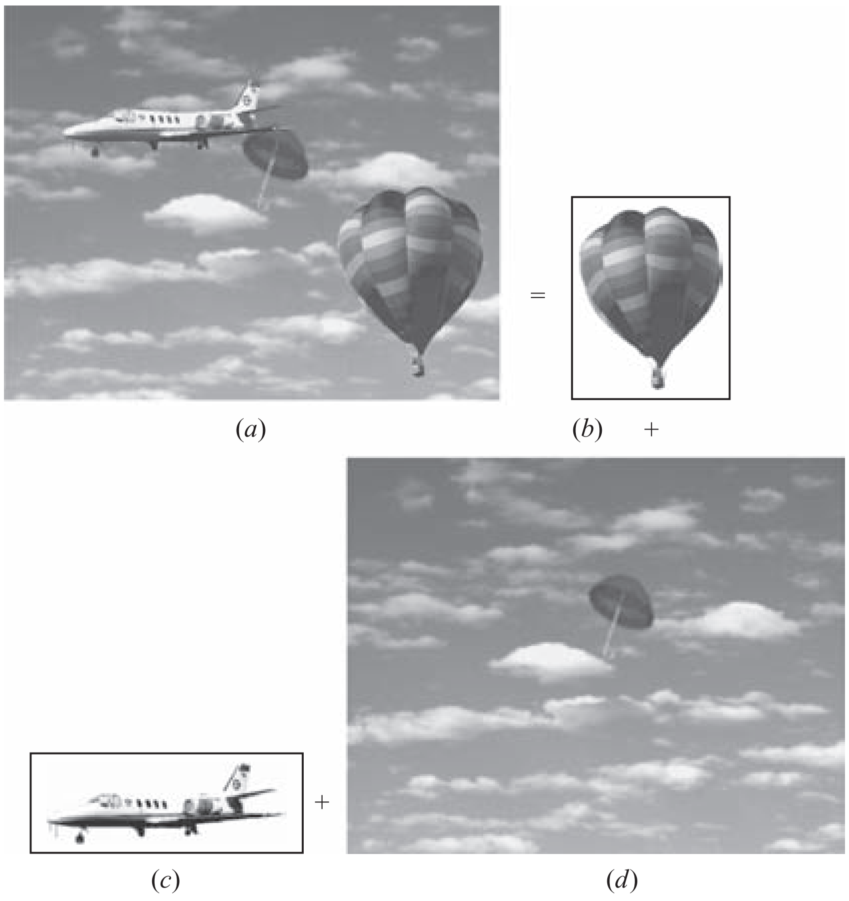

Figure 10.1 (a) A video frame composed of (b) balloon VOP_1, (c) aeroplane VOP_2 and (d) the background VOP_0

In MPEG-4 video, the VOPs are either known by construction of the video sequence (hybrid sequence based on blue screen composition or synthetic sequences) or are defined by semiautomatic segmentation. In the former, the shape information is represented by 8 bits, known as greyscale alpha plane. This plane is used to blend several video object planes to form the video frame of interest. Thus, with 8 bits, up to 256 objects can be identified within a video frame. In the second case, the shape is a binary mask to identify individual object borders and their positions in the video frames.

Figure 10.2 shows the binary shapes of the balloon and aeroplane in the above example. Both cases are currently considered in the encoding process. The VOP can have an arbitrary shape. When the sequence has only one rectangular VOP of fixed size displayed at a fixed interval, it corresponds to the frame-based coding, and is mostly known as MPEG-4 visual to distinguish it from MPEG-4 v10 (H.264/AVC). MPEG-4 visual is similar to H.263, with some minor differences, which will be discussed in section 10.12.

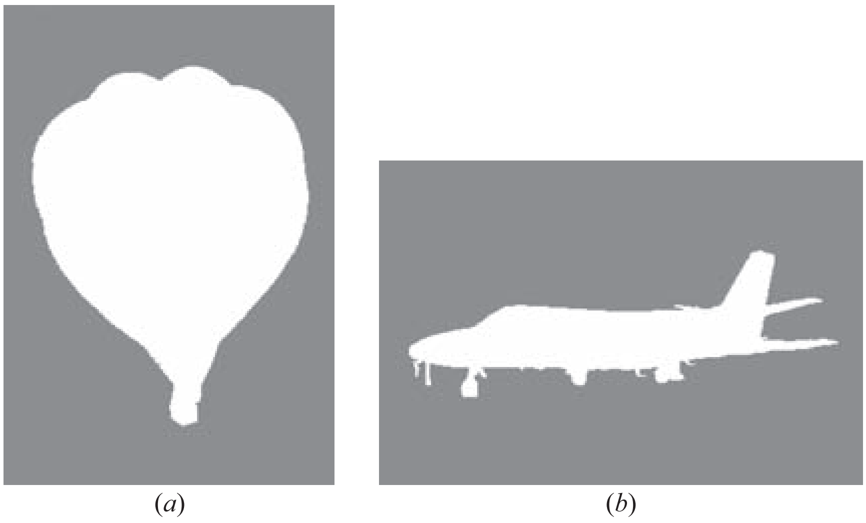

Figure 10.2 Shape of objects (a) balloon and (b) aeroplane

10.2.1 Coding of objects

Each video object plane corresponds to an entity that after being coded is added to the bitstream. The encoder sends, together with the VOP, composition information to indicate where and when each VOP is to be displayed. Users are allowed to trace objects of interest from the bitstream. They are also allowed to change the composition of the entire scene displayed by interacting with the composition information.

Figure 10.3 illustrates a block diagram of an object-based coding verification model. After defining the video object planes, each VOP is encoded, and the encoded bitstreams are multiplexed to a single bitstream. At the decoder, the chosen object planes are extracted from the bitstream and then are composed into an output video to be displayed.

10.2.2 Encoding of VOPs

Figure 10.4 shows a general overview of the encoder structure for each of the video object planes (VOPs). The encoder is mainly composed of two parts: the shape encoder and the traditional motion and texture encoder (e.g. H.263) applied to the same VOP.

Before explaining how the shape and the texture of the objects are coded, in the following, we first explain how a VOP should be represented for efficient coding.

10.2.3 Formation of VOP

The shape information is used to form a VOP. For maximum coding efficiency, the arbitrary shape VOP is encapsulated in a bounding rectangle such that the object

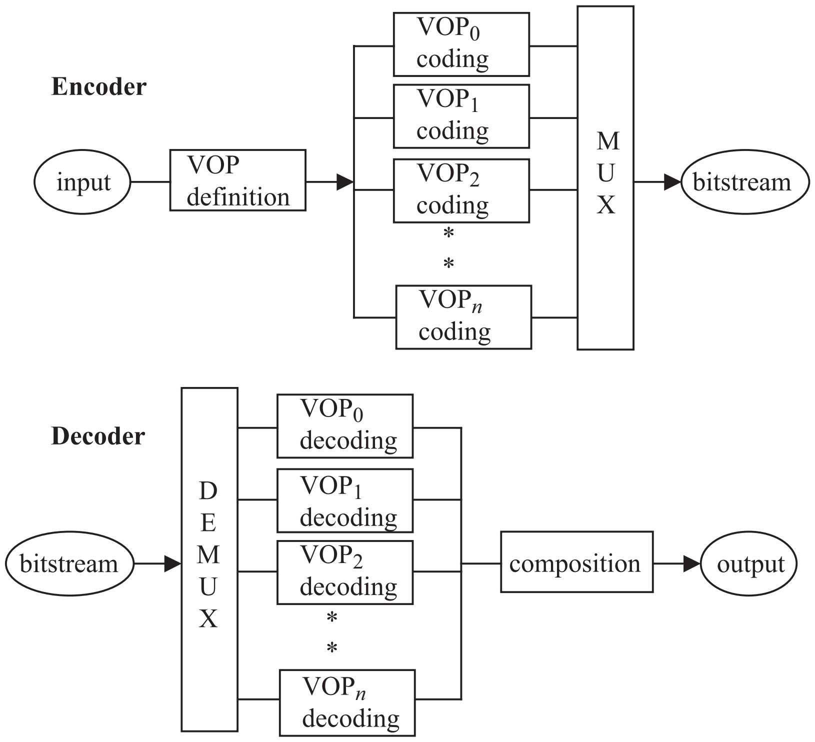

Figure 10.3 An object-based video encoder/decoder

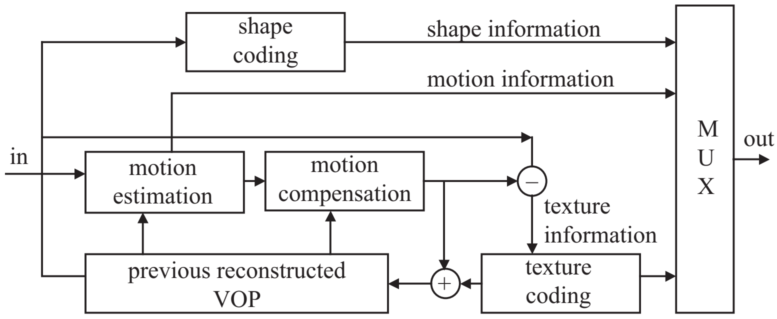

Figure 10.4 VOP encoder structure

contains the minimum number of macroblocks. To generate the bounding rectangle, the following steps are followed:

1. Generate the tightest rectangle around the object, as shown in Figure 10.5. Since the dimensions of the chrominance VOP are half of the luminance VOP (4:2:0), the top left position of the rectangle should be an even-numbered pixel.

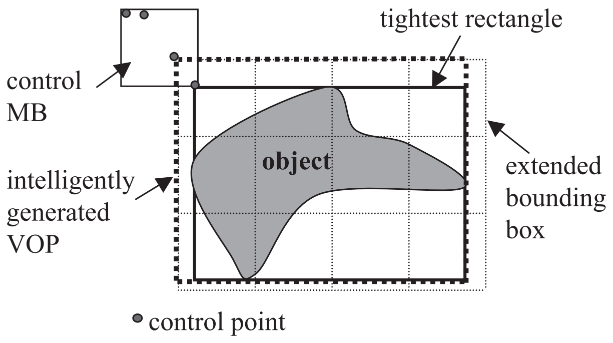

Figure 10.5 Intelligent VOP formation

2. If the top left position of this rectangle is the origin of the frame, skip the formation procedure.
3. Form a control macroblock at the top left corner of the tightest rectangle, as shown in Figure 10.5.
4. Count the number of macroblocks that completely contain the object, starting at each even-numbered point of the control macroblock. Details are as follows:
   (i) Generate a bounding rectangle from the control point to the right bottom side of the object that consists of multiples of 16 × 16 pixel macroblocks.
   (ii) Count the number of macroblocks in this rectangle that contain at least one object pixel.
5. Select that control point which results in the smallest number of macroblocks for the given object.
6. Extend the top left coordinate of the tightest rectangle to the selected control coordinate.

This will create a rectangle that completely contains the object but with the minimum number of macroblocks in it. The VOP horizontal and vertical spatial references are taken directly from the modified top left coordinate.

10.3 Image segmentation

If VOPs are not available, then video frames need to be segmented into objects and a VOP derived for each one. In general, segmentation consists of extracting image regions of similar properties such as brightness, colour or texture. These regions are then used as masks to extract the objects of interest from the image [4]. However, video segmentation is by no means a trivial task and requires the use of a combination of techniques that were developed for image processing, machine vision and video coding. Segmentation can be performed either automatically or semiautomatically.

10.3.1 Semiautomatic segmentation

In semiautomatic video segmentation, the first frame is segmented by manually tracing a contour around the object of interest. This contour is then tracked through the video sequence by dynamically adapting it to the object's movements. The use of this deformable contour for extracting regions of interest was first introduced by Kass *et al.* [5], and it is commonly known as active contour or active snakes.

In the active snakes method, the contour defined in the first frame is modelled as a polynomial of an arbitrary degree, the most common being a cubic polynomial. The coefficients of the polynomial are adapted to fit the object boundary by minimising a set of constraints. This process is often referred to as the minimisation of the contour energy. The contour stretches or shrinks dynamically while trying to seek a minimal energy state that best fits the boundary of the object. The total energy of a snake is defined as the weighted sum of its internal and external energy, given by

$$E_{total} = \alpha E_{internal} + \beta E_{external} \tag{10.1}$$

In this equation, the constants α and β give the relative weightings of the internal and the external energy. The internal energy ($E_{internal}$) of the snake constrains the shape of the contour and the amount it is allowed to grow or shrink. External energy ($E_{external}$) can be defined from the image property, such as the local image gradient. By suitable use of the gradient-based external constrain, the snake can be made to wrap itself around the object boundary. Once the boundary of the object is located in the first frame, the shape and positions of the contours can be adapted automatically in the subsequent frames by repeated applications of the energy minimisation process.

10.3.2 Automatic segmentation

Automatic video segmentation aims to minimise user intervention during the segmentation process and is a significantly harder problem than the semiautomatic segmentation. Foreground objects or regions of interest in the sequence have to be determined automatically with minimal input from the user. To achieve this, spatial segmentation is first performed on the first frame of the sequence by partitioning it into regions of homogeneous colour or grey level. Following this, motion estimation is used to identify moving regions in the image and to classify them as foreground objects.

Motion information is estimated for each of the homogenous region using a future reference frame. Regions that are nonstationary are classified as belonging to the foreground object and are merged to form a single object mask. This works well in simple sequences that contain a single object with coherent motion. For more complex scenes with multiple objects of motion disparity, a number of object masks have to be generated. Once the contours of the foreground objects have been identified, they can be tracked through the video sequence using techniques such as active snakes. In the following sections, each element of the video segmentation is explained.

10.3.3 Image gradient

The first step of the segmentation process is the partitioning of the first video frame into regions of homogenous colour or grey level. A technique that is commonly used for this purpose is the watershed transform algorithm [6]. This algorithm partitions the image into regions that correspond closely to the actual object boundaries, but direct application of the algorithm on the image often leads to over-segmentation. This is because, in addition to the object borders in the image, texture and noise may also create artificial contours. To alleviate this problem, the image gradient is used as input to the watershed transform instead of the actual image itself.

10.3.3.1 Nonlinear diffusion

To eliminate the false contours, the image has to be smoothed in such a way that edges are not affected. This can be done by diffusing the image iteratively without allowing the diffusion process to cross the object borders. One of the best-known filters for this purpose is nonlinear diffusion, where the diffusion is prohibited across edges but unconstrained in regions of almost uniform texture.

Nonlinear diffusion can be realized by space variant filtering, which adapts the Gaussian kernel dynamically to the local gradient estimate [7]. The Gaussian kernel is centred at each pixel, and its coefficients are weighted by a function of the gradient magnitude between the centre pixel and its neighbours. The weighted coefficients a_{ij} are given by

$$a_{ij} = \frac{w_{ij}c_{ij}}{\sum_{i,j=1} w_{ij}c_{ij}} \qquad w_{ij} = g(||\nabla I_{ij}||) \tag{10.2}$$

where c_{ij} is the initial filter coefficient, w_{ij} is the weight assigned to each coefficient based on the local gradient magnitude∇I_{ij}, and g is the diffusion function [8]. If $w_{ij} = 1$, then the diffusion is linear. The local gradient is computed for all pixels within the kernel by taking the difference between the centre and the corresponding pixels. More precisely, $\nabla I_{ij} = I_{ij} - I_c$, where I_c is the value of the centre pixel and I_{ij} are the pixels within the filter kernel.

Figure 10.6 shows the diffusion function and the corresponding adapted Gaussian kernel to inhibit diffusion across a step edge. The figure shows that for large gradient magnitudes, the filter coefficient is reduced in order not to diffuse across edges. Similarly at the lower gradient magnitudes (well away from the edges) within the area of almost uniform texture, the diffusion is unconstrained, so as to have maximum smoothness. The gradient image generated in this form is suitable to be segmented at its object borders by the watershed transform.

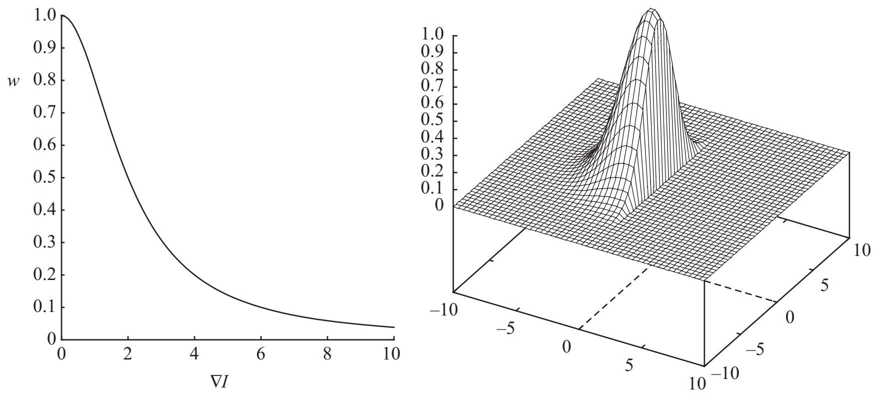

Figure 10.6 Weighting function (left), adapted Gaussian kernel (right)

10.3.3.2 Colour edge detection

Colour often gives more information about the object boundaries than the luminance. However, while gradient detection in greyscale images is to some extent easy, deriving the gradient of colour images is less straightforward because of separation of the image into several colour components. Each pixel in the RGB colour space can be represented by a position vector in the three-dimensional RGB colour cube.

$$\vec{p} = R\vec{i} + G\vec{j} + B\vec{k} \tag{10.3}$$

Likewise, pixels in other colour spaces can be represented in a similar manner. Hence, the problem of detecting edges in a colour image can be redefined as the problem of computing the gradient between vectors in the three-dimensional colour space. Various methods have been proposed for solving the problem of colour image gradient detection, and they include component-wise gradient detection and vector gradient.

Component-wise gradient

In this approach, gradient detection is performed separately for each colour channel, followed by the merging of the results. The simplest way is to apply the Prewitt or the Sobel operator separately on each channel and then combine the gradient magnitude using some linear or nonlinear function [10]. For example,

$$\nabla I = \frac{\nabla I_R + \nabla I_G + \nabla I_B}{3} \text{ or } \nabla I = \max(\nabla I_R; \nabla I_G; \nabla I_B) \tag{10.4}$$

where ∇I_R, ∇I_G, ∇I_B represent the gradient magnitude computed for each of the colour channels.

Vector gradient

This approach requires the definition of a suitable colour difference metric in the three-dimensional colour space. This metric should be based on human perception of colour difference, such that a large value indicates significant perceived difference and a small value indicates colour similarity. A metric that is commonly used is the Euclidean distance between two colour vectors. For the n-dimensional colour space, the Euclidean distance between two colour pixels, A and B, is defined as follows:

$$euclid(A, B) = \sqrt{\sum_{i=1}^{n} (A_i - B_i)^2} \tag{10.5}$$

The gradient of the image is then derived on the basis of the sum of the colour differences between each pixel and its neighbours. This approximates the Prewitt kernel and is given by the following equations:

$$\begin{aligned} \frac{\partial I}{\partial x} &= \sum_{a=y-1}^{y+1} euclid[I(x+1, a), I(x-1, a)] \\ \text{and} \quad \frac{\partial I}{\partial y} &= \sum_{a=x-1}^{x+1} euclid[I(a, y+1), I(a, y-1)] \end{aligned} \tag{10.6}$$

The gradient magnitude is then defined as,

$$\| \nabla I \| = \sqrt{\left(\frac{\partial I}{\partial x}\right)^2 + \left(\frac{\partial I}{\partial y}\right)^2}$$

The use of Euclidean distance in the RGB colour space does not give good indication of the perceived colour differences. Hence, in [9], it was proposed that the vector gradient should be computed in the CIELUV colour space. CIELUV is an approximation of a perceptually uniform colour space, which is designed so that the Euclidean distance could be used to quantify colour similarity or difference [10].

10.3.4 Watershed transform

The watershed transform algorithm can be visualized by adopting a topological view of the image, where high-intensity values represent peaks and low-intensity values represent valleys. Water is flooded into the valleys, and the lines where the waters from different valleys meet are called the watershed lines, as shown in Figure 10.7. The watershed lines separate one region (catchment basin) from another. In actual implementation, all pixels in an image are initially classified as unlabelled and they are examined starting from the lowest-intensity value. If the pixel that is currently being examined has no labelled neighbours, it is classified as a new region or a new catchment basin. On the other hand, if the pixel was a neighbour to exactly one labelled region, it would be classified as belonging to that region. However, if the pixel separates two or more regions, it would be labelled as part of the watershed line.

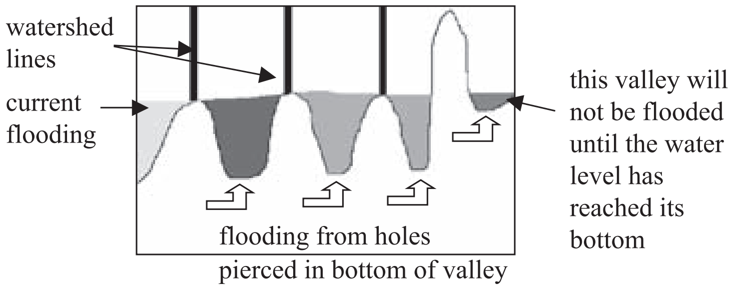
watershed lines
current flooding
this valley will not be flooded until the water level has reached its bottom
flooding from holes pierced in bottom of valley

Figure 10.7 Immersion-based watershed flooding

The algorithm can be seeded with a series of markers (seed regions), which represent the lowest point in the image from where water is allowed to start flooding. In other words, these markers form the basic catchment basins for the flooding. In some implementations, new basins are not allowed to form, and hence, the number of regions in the final segmented image will be equal to the number of markers. In other implementations, new regions are allowed to be formed if they are at a higher (intensity) level as compared to the markers. In the absence of markers, the lowest point (lowest-intensity value) in the valley is usually chosen as the default markers.

There are two basic approaches to the implementation of watershed transform and they are the immersion method [11] and the topological distance method [5]. Results obtained using different implementations are usually not identical.

10.3.4.1 Immersion watershed flooding

Efficient implementations of immersion-based watershed flooding are largely based on Vincent and Soille's algorithm [11]. Immersion flooding can be visualized by imagining that holes are pierced at the bottom of the lowest point in each valley. The image is then immersed in water, which flows into the valley from the holes. Obviously, the lowest-intensity valley will get flooded first before valleys that have a higher minimum point, as shown in Figure 10.7.

Vincent and Soille's algorithm uses a sorted queue in which pixels in the image are sorted on the basis of their intensity level. In this way, pixels of low intensity (lowest points in valleys) could be examined first before the higher-intensity pixels. This algorithm achieves fast performance since the image is scanned in its entirety only once during the queue set-up phase.

10.3.4.2 Topological distance watershed

In the topological distance approach, a drop of water that falls on the topology will flow to the lowest point via the slope of the steepest descent. The slope of the steepest descent is loosely defined as the shortest distance from the current position to the local minima. If a certain point in the image has more than one possible steepest descent, then that point would be a potential watershed line that separates two or more regions. A more rigorous mathematical definition of this approach can be found in [5].

10.3.5 Colour similarity merging

Despite the use of nonlinear diffusion and the colour gradient, the watershed transformation algorithm still produces an excessive number of regions. For this reason, the regions must be merged based on colour similarity in a suitable colour space. The CIELUV uniform colour space is a plausible candidate due to the simplicity of quantifying colour similarity based on Euclidean distances. The mean luminance L and colour differences $u*$ and $v*$ values are computed for each region of the watershed-transformed image. The regions are examined in the increasing order of size and merged with their neighbours if the colour difference between them is less than a threshold (T_h). More precisely, the regions A and B are merged *iff*,

$$euclid(A_{L,u^*,v^*}, B_{L,u^*,v^*}) < T_h \tag{10.7}$$

where $A_{L,u*,v*}$ and $B_{L,u*,v*}$ are the mean CIELUV values of the respective regions. Since it is likely that each region would have multiple neighbours, the neighbour that minimizes the Euclidean distance is chosen as the target for merging. After each merging, the mean L, $u*$ and $v*$ values of the merged region are updated accordingly.

10.3.6 Region motion estimation

Spatial segmentation alone cannot discriminate the foreground objects in a video sequence. Motion information between the current frame and a future reference frame must be utilized to identify the moving regions of the image. These moving regions can then be classified as foreground objects or as regions of interest.

Motion estimation is performed for each of the regions after the merging process. Since regions can have any arbitrary shapes, the boundary of each region is extended to its tightest fitting rectangle. Using the conventional block matching motion estimation algorithm, the motion of the fitted rectangular is estimated.

Figure10.8 gives a pictorial summary of the whole video segmentation process. The first frame of the video after filtering and gradient operator generates the gradient of the diffused image. This image is then watershed transformed into various regions, some of whom might be similar in colour and intensity. In the above example, the watershed-transformed image has about 2660 regions, but many regions are identical in colour. Through the colour similarity process, identical colour regions are merged into about 60 regions (in this picture). Finally, homogeneous neighbouring regions are grouped together and are separated from the static background, resulting in two objects: the ball and the hand and the table tennis racket.

10.3.7 Object mask creation

The final step of the segmentation process is the creation of the object mask. Object mask is synonymous with object segmentation, since it is used to extract the object

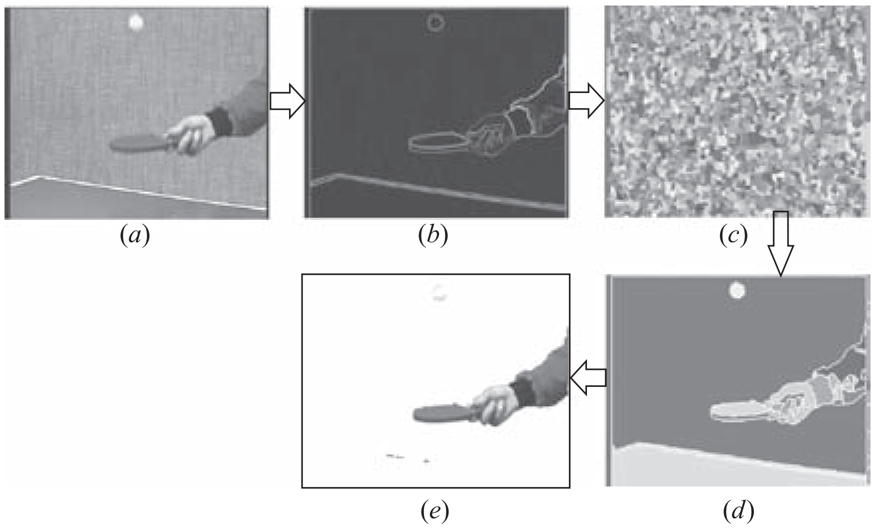

Figure 10.8 A pictorial representation of video segmentation (a) original, (b) gradient, (c) watershed transformed, (d) colour merged and (e) segmented image

from the image. The mask can be created from the union of all regions that have nonzero motion vectors. This works well for sequences that have a stationary background with a single moving object. For more complex scenes with nonstationary background and multiple moving objects, nine object masks are created for the image. Each mask is the union of all regions with coherent motion. Mask 0 corresponds to regions of zero motion, and the other 8 masks are regions with motion in the N, NE, E, SE, S, SW, W and NW directions, respectively. These object masks are then used to extract the foreground objects from the video frame.

Figure 10.9 shows two examples of creating the object mask and extracting the object for two video sequences. The mother and daughter sequence has a fairly stationary background, and hence, the motion information, in particular motion over several frames, can easily separate foreground from the background.

For the BBC car, due to the camera following the car, the background is not static. Here before estimating the motion of the car, the global motion of the background needs to be compensated. In section 10.7, we will discuss global motion estimation.

The contour or shape information for each object can also be derived from the object masks and used for tracking the object through the video sequence. Once the object is extracted and its shape is defined, the shape information has to be coded and sent along with the other visual information to the decoder. In the following section, several methods for coding of shapes are presented.

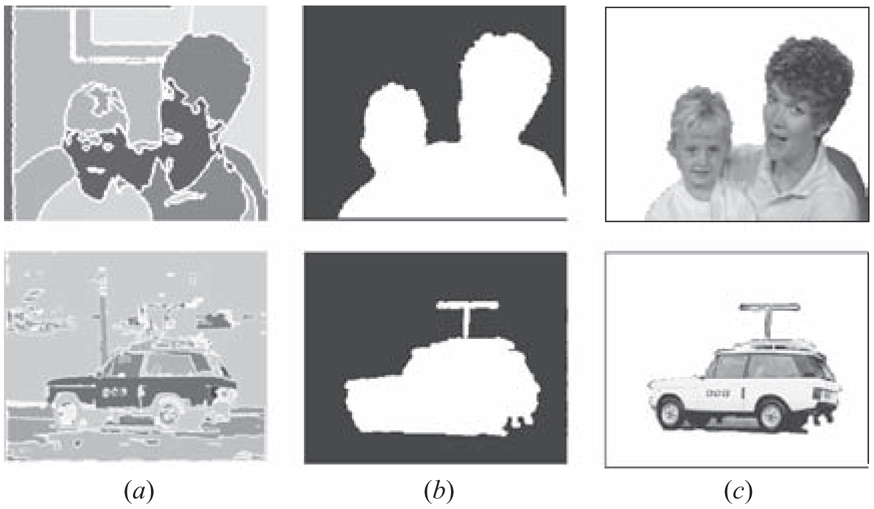

Figure 10.9 (a) Gradient image, (b) object mask and (c) segmented object

10.4 Shape coding

The binary and greyscale shapes are normally referred to binary and greyscale alpha planes. Binary alpha planes are encoded with one of the binary shape-coding methods (to be explained later), while the greyscale alpha planes are encoded by motion-compensated discrete cosine transform (DCT) similar to texture coding (e.g. H.263). An alpha plane is bounded by a rectangle that includes the shape of the VOP, as described in the formation of VOP in section 10.2.3. The bounding rectangle of the VOP is then extended on the right bottom side to multiples of 16×16 pixel macroblocks. The extended alpha samples are set to zero. Now the extended alpha plane can be partitioned into exact multiples of 16×16 pixel macroblocks. Hereafter, these macroblocks are referred to alpha blocks, and the encoding and decoding process for block-based shape coding is carried out per alpha block.

If the pixels in an alpha block are all transparent (all zero), the block is skipped before motion and/or texture coding. No overhead is required to indicate this mode since this transparency information can be obtained from shape coding. This skipping applies to all I-, P- and B-VOPs. Since shape coding is unique to MPEG-4 (no other standard codecs use it), in the following sections we pay special attention to various shape-coding methods.

10.4.1 Coding of binary alpha planes

A binary alpha plane is encoded in the intra mode for I-VOPs and the inter mode for P-VOPs and B-VOPs. During the development of MPEG-4, several methods for coding of the binary alpha planes have been considered. These include chain coding of the object contours, quad tree coding, modified modified reed (MMR) and context-based arithmetic encoding (CAE) [3,12]. It appears that CAE, recommended in the latest version of the verification model (VM-11) [3], is the best. Hence, in the introduction of these methods, more details are given on the CAE.

10.4.2 Chain code

In the chain code method, the object boundaries are represented by a closed contour, as shown in Figure 10.10, and the chain codes are then applied to the contour. Derivation of the contour from the binary alpha plane is similar to detection of the edge, as discussed in section 10.3. For coding, it involves moving on the contour in one of eight directions, as shown in the figure, and coding the direction. The chain code terminates when the starting point is revisited.

Each chain code contains a start point data followed by the first chain code and the subsequent differential chain codes. If VOP contains several closed contours, then plural chain codes are coded following the data for the number of regions.

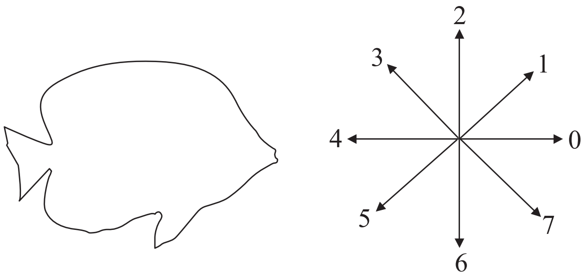

Figure 10.10 Object boundaries for chain coding and the eight directions of the chain around the object

Since a chain code has a cyclic property, a differential chain code in eight directions can be expressed in the range from -3 to 4 by the following definition:

$$d = \begin{cases} c_n - c_{n-1} + 8, & \text{if } c_n - c_{n-1} < -3 \\ c_n - c_{n-1} - 8, & \text{if } c_n - c_{n-1} > 4 \\ c_n - c_{n-1}, & \text{otherwise} \end{cases} \tag{10.8}$$

where d is the differential chain code, c_n is the current chain code and c_{n-1} is the previous chain code. Huffman code is used to encode the differential chain code d. The Huffman table is shown in Table 10.1.

At the receiver, after the variable length decoding of d, the current chain code, c_n, is then reconstructed as follows:

$$c_n = (c_{n-1} + d + 8) \quad \text{mode } 8 \tag{10.9}$$

Table 10.1 Huffman table for the differential chain code

d	Code
0	1
1	00
−1	011
2	0100
−2	01011
3	010100
−3	0101011
4	0101010

10.4.3 Quad tree coding

Each binary alpha block (BAB) of 16 × 16 pixels, represented by binary data (white 255 and black 0), is first quad tree segmented. The indices of the segments, according to the rules to be explained, are calculated and then Huffman coded. Figure 10.11 shows the quad tree structure employed for coding of a binary alpha block.

At the bottom level (level 3) of the quad tree, a 16 × 16 alpha block is partitioned into 64 subblocks of 2 × 2 samples. Each higher level as shown also contains 16 × 16 pixels, but in groups of 4 × 4, 8 × 8 and 16 × 16 subblocks.

The calculation of the indices is as follows:

- The indexing of subblocks starts at level 3, where an index is assigned to each 2 × 2 subblock pixel.
- For the four pixels of the subblock $b[0]$ to $b[3]$ of Figure 10.12, the index is calculated as

$$\text{index} = (27 \times b[0]) + (9 \times b[1]) + (3 \times b[2]) + b[3] \tag{10.10}$$

where $b[i] = 2$ if the sample value is 255 (white) and $b[i] = 0$ if it is black. Hence, there are 16 different index values with a minimum of 0 and a maximum of 80.

Step 1. Indexing of subblocks at level 3

These indices then become inputs to level 2 for the generation of a new set of indices at this level. However, to increase inter block correlation, the subblocks are swapped in decreasing order of indices. The swapping also causes the distribution of index values to be predominantly low and hence this nonuniform distribution is more efficiently variable length coded. Arrangement for the swap of the four subblocks is carried out according to the relationship of the neighbouring indices in the following order. The upper and left neighbouring indices are shown in Figure 10.13.

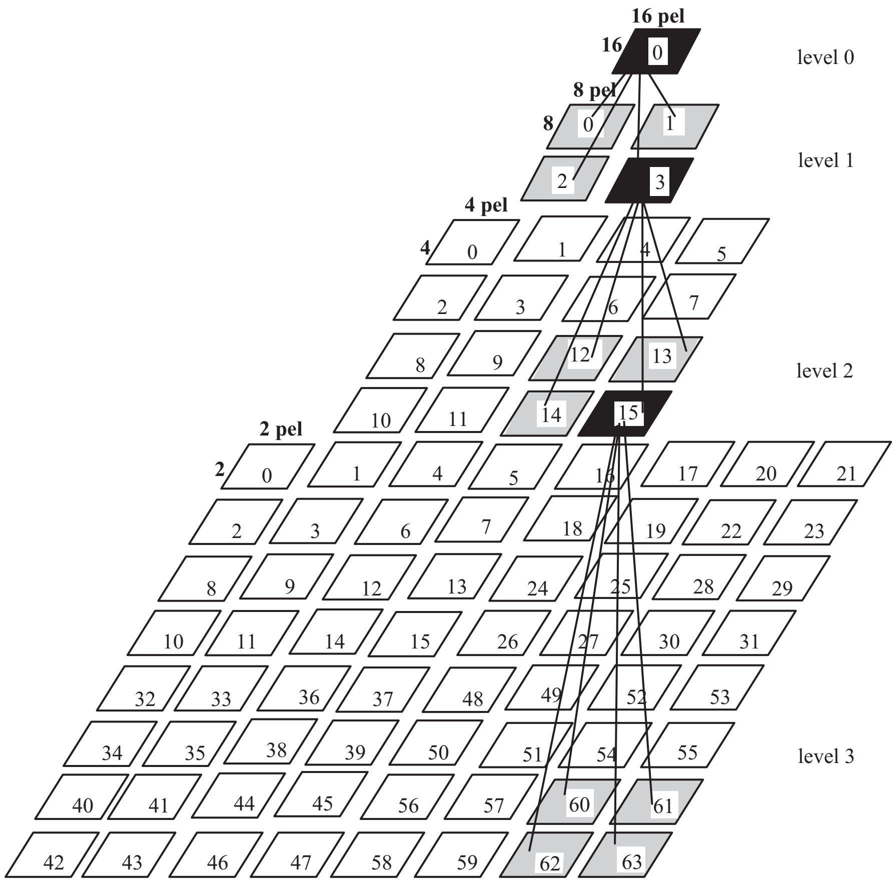

Figure 10.11 Quad tree representation of a shape block

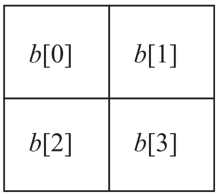

Figure 10.12 A subblock of 2 × 2 pixels

- If upper_index[0] is less than upper_index[1], then swap index[0] with index[1] and index[2] with index[3], except for subblocks numbered 0, 1, 4, 5, 16, 17, 20 and 21.
- If left_index[0] is less than left_index[1], then swap index[0] with index[2] and index[1] with index[3], except for subblocks numbered 0, 2, 8, 10, 32, 34, 40 and 42.

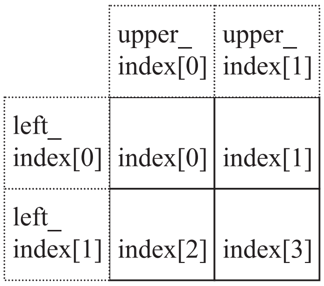

Figure 10.13 Upper and left level indices of a subblock

- If upper_index[0] + upper_index[1] is less than left_index[0] + left_index[1], then swap index[1] with index[2], except for subblocks numbered 0, 1, 2, 4, 5, 8, 10, 16, 17, 20, 21, 32, 34, 40 and 42.
- The index of level 2 is computed from index[0], index[1], index[2] and index[3] after swapping according to:

  $$\text{index\_level\_2} = 27 \times f(\text{index}[0]) + 9 \times f(\text{index}[1]) + 3 \times f(\text{index}[2]) + f(\text{index}[3])$$

  where

  $$\begin{aligned} f(x) &= 0 \quad \text{if } x = 0 \\ f(x) &= 2 \quad \text{if } x = 80 \\ f(x) &= 1 \quad \text{otherwise} \end{aligned} \tag{10.11}$$

  The current subblock is then reconstructed and used as a reference when processing subsequent subblocks.

Step 2. Grouping process for higher levels
The grouping process of blocks at the higher level first starts at level 2 where four subblocks from level 3 are grouped to form a new subblock. The grouping process involves swapping and indexing similarly to that discussed for level 3, except that in this level a 4 × 4 pixel block is represented by a 2 × 2 subblock whose elements are indices rather than pixels. The current subblock is then reconstructed and used as a reference when processing subsequent subblocks. At the decoder, swapping is done following a reverse sequence of steps as at the encoder.

The grouping process is also performed similarly for level 1 where four subblocks from level 2 are grouped to form a new subblock. The swapping, indexing and reconstruction of a subblock follow grouping, the same as that for other levels.

Now arrangement of subblocks in decreasing order of their indices at level 2, to utilise inter block correlation, is done as follows:

- If f(upper_index[0]) is less than f(upper_index[1]), then swap index[0] with index[1] and index[2] with index[3], except for subblocks numbered 0, 1, 4 and 5.

- If f(left_index[0]) is less than f(left_index[1]), then swap index[0] with index[2] and index[1] with index[3] except for subblocks numbered 0, 2, 8 and 10.
- If f(upper_index[0]) + f(upper_index[1]) is less than f(left_index[0]) + f(left_index[1]), then swap index[1] with index[2] except for subblocks numbered 0, 1, 2, 4, 5, 8 and 10.
- The index of level 1 is computed from index[0], index[1], index[2] and index[3] after swapping, according to (10.11).

At level 1 no swapping is required.

Step 3. Encoding process
The encoding process involves use of results from the grouping process that produces a total of 85 (= 1 + 4 + 16 + 64) indices for a 16 × 16 alpha block. Each index is encoded from the topmost level (level 0). At each level, the order for encoding and transmission of indices is shown by numbers in Figure 10.11. Indices are Huffman coded. Note that indices at level 3 can take only 16 different values, but at the other levels they take 80 different values. Hence, for efficient variable length coding, two different Huffman tables are used, one with 16 symbols at level 3 and the other with 80 symbols at levels 0–2. These tables are shown in Appendix C.

10.4.4 Modified modified reed

During the course of MPEG-4 development, another shape-coding method named modified modified reed (MMR) was also investigated [12]. The basic idea in this method is to detect the pixel intensity changes (from opaque to transparent and vice versa) within a block and to code the positions of the changing pixels. The changing pixels are defined by pixels whose colour changes while scanning an alpha block in raster scan order. Figure 10.14 illustrates the changing pixels in an intra and motion-compensated inter alpha block. Also in the figure are the top and left reference row and column of pixels, respectively.

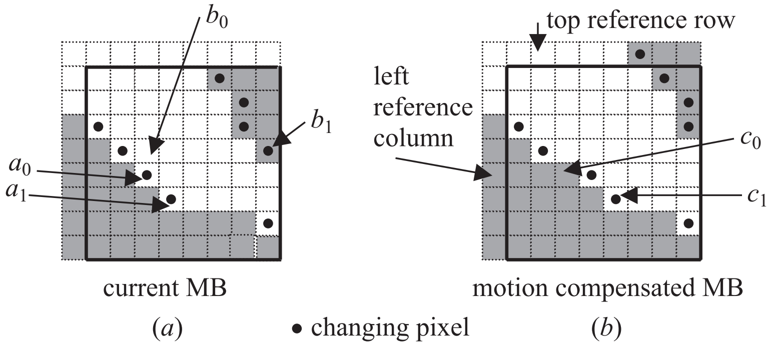

Figure 10.14 Changing pixels of (a) intra and (b) inter alpha block

To code the position of the changing pixels, the following parameters, as shown in Figure 10.14, are defined.

For each length, the starting pixel is denoted by a_0. Initially a_0 is positioned at the right end in the top reference and addressed as abs_$a_0 = -1$. The first changing pixel appearing after a_0 is called a_1. For intra blocks, the pixel located above a_0 is called b_0. The area from the next pixel to b_0 down to a_0 is called the reference area in intra-MMR. In this case, the reference-changing pixel is called b_1. This pixel is found in reference area r_1 or r_2, shown in Figure 10.15*a*. Searching in r_1, the first changing pixel whose colour is the opposite of a_0 is named b_1; if not found, the first changing pixel in r_2 is named b_1. Thus b_1 might become identical to a_0. Exceptionally b_1 may not be found when abs_$a_0 = -1$.

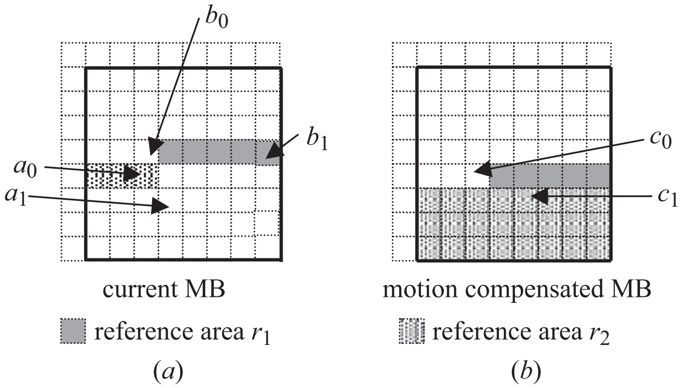

Figure 10.15 Reference area for detecting reference-changing pixel (a) b_1 and (b) c_1

For inter-MMR, the pixel at the corresponding position to a_0 is called c_0. The area from the next pixel to c_0 down to the end of alpha block is called reference area in inter-MMR. The reference-changing pixel in this mode is called c_1. This pixel is found in the reference area r_1 or r_2, shown in Figure 10.15*b*. Searching in r_1, the first changing pixel whose colour is opposite of a_0 is named c_1; if not found, the first changing pixel in r_2 is named c_1.

Given a_0, the eventual task is to identify a_1 by referring to either b_1 or c_1, depending on the intra-MMR or inter-MMR mode, respectively. This is achieved in three different modes as vertical, horizontal and vertical pass modes. The vertical mode is the first option that is considered and if it is decided not to be applicable, the horizontal mode or the vertical pass mode is employed in turn.

In the vertical mode, the position of a_1 is identified relative to that of b_1. It is invoked only when the absolute value of the relative distance defined by the relative address DIST $= r\_a_1 - r\_b_1$ is equal to or less than a predefined threshold [12]. The DIST is then variable length coded using the appropriate intra-MMR and inter-MMR VLC tables.

If the vertical mode is not used (DIST $>$ threshold), then the horizontal mode is considered for coding. In this mode, the position of a_1 is identified on the basis of the absolute distance from a_0. If this distance is less than the width of the alpha block, then it is used; otherwise, the vertical pass mode is used, which implies that one row of the pixels in the alpha block is passed (not coded).

Finally, the decision to use intra-MMR or inter-MMR is to first scan the alpha block in the horizontal and vertical scanning directions. The one requiring the least of bits is chosen. In the case of a tie, the horizontal scanning is chosen. For the final decision between intra-MMR and inter-MMR, again the one that gives the least coding bits is selected.

10.4.5 Context-based arithmetic coding

Each intra coded binary alpha block (BAB) and the inter coded one, after being motion compensated by block-based motion compensation, is context-based arithmetic encoded (CAE). In general each binary alpha block is coded according to one of the following seven modes (in C terminology):

1. MVDs == 0 && No_Update
2. MVDs ! = 0 && No_Update
3. All_0
4. All_255
5. Intra-CAE
6. MVDs == 0 && Inter-CAE
7. MVDs ! = 0 && Inter-CAE

The first and second modes indicate that the shape will not be updated, and the All_0 and All_255 indicate that the BAB contains only black and white pixels, respectively. None of these modes are required to be arithmetic coded. Also in the quad tree and MMR methods, All_0 and All_255 are not coded further.

Intra-CAE is the mode for context-based arithmetic coding of BABs that contains a mixture of black and white pixels. In modes 6 and 7, the interframe BABs (mixed black and white pixels) with and without motion compensation, respectively, are arithmetic coded.

The motion vector data of shape (MVDS) is the difference between the shape motion vector and its predictor, MVP. The prediction procedure is similar to that of the motion vector data for texture, described in section 9.1.2. However, there are differences, such as

- the prediction motion vectors can be derived from the candidate motion vectors of shape MVS1, MVS2, MVS3 or the candidate motion vectors of the texture, MV1, MV2 and MV3, similar to those of H.263 illustrated in Figure 9.2; the prediction motion vector is determined by taking the first encountered motion vector that is valid; if no candidate is valid, the prediction is set to zero;
- overlapped, half-pixel precision and 8×8 motion compensation is not carried out;

- in the case that the region outside the VOP is referred to, the value for that is set to zero;
- for B-VOPs, only forward motion compensation is used and neither backward nor interpolated motion compensation is allowed.

It should be noted that when the shape prediction motion vector (MVPS) is determined, the difference between the motion-compensated BAB indicated with MVPS and the current BAB is calculated. If the motion-compensated error is less than a certain threshold (AlphaTH) for any 4×4 subblock of the BAB, the MVPS is directly employed as the best prediction. If this condition is not met, MV is searched around the prediction vector MVPS by comparing the BAB indicated by the MV and the current BAB. The MV that minimises the error is taken as the best motion vector for shape (MVS), and the motion vector data for shape (MVDS) is given by MVDS = MVS − MVPS.

10.4.5.1 Size conversion

Rate control and rate reduction in MPEG-4 is realised through size conversion of the binary alpha information. This method is also applicable to quad tree and MMR. It is implemented in two successive steps.

In the first step, if required, the size of the VOP can be reduced by half in each of the horizontal and vertical directions. This is indicated in the VOP header, as the video object plane conversion ratio (VOP_CR), which takes a value of either 1 or ½. When VOP_CR is ½, the size conversion is carried out on the original bounding box of Figure 10.5.

In the case that the value of VOP_CR is ½, the locally decoded shape that is size converted at the VOP level is stored in the frame memory of the shape frame. For the shape motion estimation and compensation, if VOP_CR of the reference shape VOP is not equal to that of the current shape VOP, the reference shape frame (not VOP) is size converted corresponding to the current shape VOP.

For P-VOPs, if the VOP_CR is ½, the components of the shape motion information vector are measured on the downsampled shape frame. The predicted motion vector for the shape, MVPS, is calculated only using the shape motion vectors MVS1, MVS2 and MVS3.

In the second step, when required, the size conversion is carried out for every binary alpha block, BAB, except for All_0, All_255 and No_Update. At the block level, the conversion ratio can be one of ¼, ½ and 1 (the original size).

For CR = ½, if the average of pixel values in a 2×2 pixel block is equal to or larger than 128, the pixel value of the downsampled block is set to 255, otherwise it is set to zero. For CR = ¼, if the average of pixels in a 4×4 pixel block is equal to or larger than 128, the pixel value of the downsampled block is set to 255, otherwise it is set to zero. In either of these cases, upsampling is carried out for the BAB. The values of the interpolated pixels are calculated from their neighbouring pixels according to their Euclidean distances.

Selection of a suitable value for the conversion ratio is done based on the conversion error between the original BAB and the BAB that is once downsampled and then reconstructed by upsampling. The conversion error is computed for each 4×4 subblock by taking the absolute difference of pixels in the corresponding subblocks of the original and reconstructed BABs. If this difference is greater than a certain threshold, this subblock is called an error pixel block (Error_PB). Size conversion at a certain conversion ratio is accepted if there is no Error_PB at that ratio. Figure 10.16 summarises determination of the conversion ratio, CR.

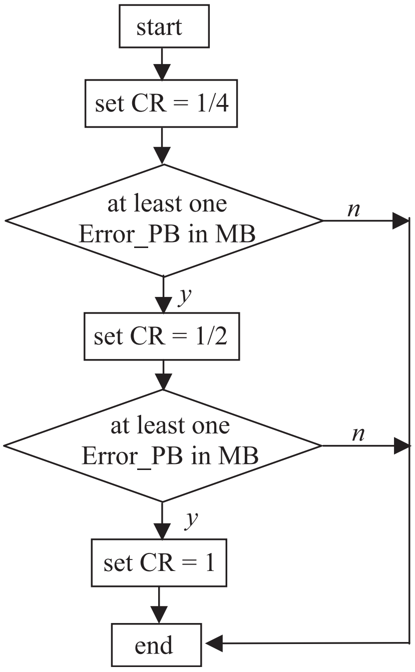

Figure 10.16 CR determination algorithm

If a downsampled BAB turns out to be all transparent or all opaque and the conversion error in any 4×4 subblocks in the BAB is equal to or lower than the threshold, the shape information is coded as shape_mode = All_0 or All_255. Unless this is the case, the BAB is coded with a context-based arithmetic coding at the size determined by the algorithm for the rate control.

10.4.5.2 Generation of context index

The pixels in the binary alpha block (BABs) are context-based arithmetic coded for both intra and inter modes. The number of pixels in the BAB is determined by the conversion ratio (CR), which is either 16×16, 8×8 or 4×4 pixels for CR values of 1, ½ and ¼, respectively.

The context based arithmetic encoding (CAE) is a binary arithmetic coding, where the symbol probability is determined from the context of the neighbouring pixels. Such a coding is applied to each pixel of the BAB in the following manner.

First, prior to encoding of each BAB, the arithmetic encoder is initialised. Each binary pixel is then encoded in the raster scan order. The process for coding a given pixel is carried out using the following steps:

1. compute the context number
2. index a probability table using the context number
3. use the indexed probability to derive an arithmetic encoder

When the final pixel has been encoded, the arithmetic code is terminated.

Figure 10.17 shows the template of the neighbouring pixels that contribute to the creation of the context number for intra and inter shape pixels.

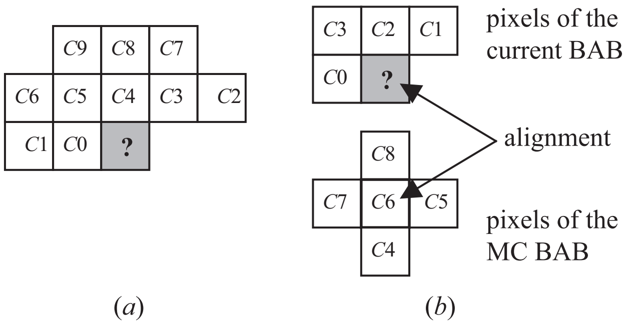

Figure 10.17 Template for the construction of the pixels of (a) the intra and (b) inter BABs. The pixel to be coded is marked with '?'

For intra coded BABs, a 10-bit context $C = \sum_{k=0}^{9} c_k 2^k$ is calculated for each pixel, as shown in Figure 10.17*a*. In this figure, the pixel to be encoded is represented by **?**, and the 10 neighbouring pixels are ordered as shown. For inter coded BABs, in addition to spatial redundancy, temporal redundancy is exploited by using pixels from the bordered motion-compensated BAB, to make up part of the context, as shown in Figure 10.17*b*. In this mode, only 9 bits are required to calculate the context number, for example, $C = \sum_{k=0}^{8} c_k 2^k$.

In both modes, there are some special cases to note:

- In building contexts, any pixel outside the bounding box of the current VOP to the left and above are assumed to be zero.
- The template may cover pixels from BABs that are not known at the decoding time. The values of these unknown pixels are estimated by template padding in the following manner:
  - When constructing the intra context, the following steps are taken in sequence:
    – If ($C7$ is unknown) $C7 = C8$.
    – If ($C3$ is unknown) $C3 = C4$.
    – If ($C2$ is unknown) $C2 = C3$.

- When constructing the inter context, the following conditional assignment is performed:
  – If ($C1$ is unknown) $C1 = C2$.

Once the context number is calculated, it is used to derive a probability table for binary arithmetic coding. Two probability tables, a 10-bit for intra and a 9-bit for inter BABs, are given in Appendix D. These tables contain the probabilities for a binary alpha pixel being equal to 0 for intra and inter shape coding using the context-based arithmetic coding. All probabilities are normalised to the range of [1, 65 535].

As an example, let us assume the neighbouring pixels for an intra BAB template has a black and white pattern as shown in Figure 10.18.

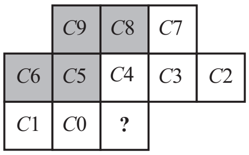

Figure 10.18 An example of an intra BAB template

In this figure, $C0 = C1 = C2 = C3 = C4 = C7 = 1$, and $C5 = C6 = C8 = C9 = 0$. Hence, the context number for coding of pixel **?** is $C = 2^0 + 2^1 + 2^2 + 2^3 + 2^4 + 2^7 = 159$.

If pixel **?** was a black pixel it would have been coded with an Intra_prob[159]. This value according to Appendix D is 74 out of 65 535. If it was a white pixel, its probability would have been 65 535 – 74 = 65 461 out of 65 535. Such a high probability for a white pixel in this example is expected, since this pixel is surrounded by many white pixels. Note also, although the given probability table is fixed, as the pattern of neighbouring pixels changes, the calculated context number changes such that the assigned probability to the pixel is better suited for that pattern. This is a form of adaptive arithmetic coding that only looks at the limited number of past coded symbols. It has been shown that adaptive arithmetic coding with limited past history has more efficient compression over fixed rate arithmetic coding [13].

10.4.6 Greyscale shape coding

The grey level alpha plane is encoded as its support function and the alpha values on the support. The support is obtained by thresholding the grey level alpha plane by 0, and the remaining parts constitute the alpha values, as shown in Figure 10.19.

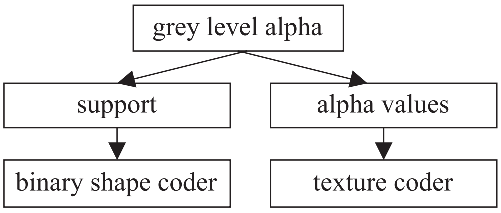

Figure 10.19 Greyscale shape coding

The support function is encoded by binary shape coding, as described in section 10.4.5. The alpha values are partitioned into 16×16 blocks and encoded the same way as the luminance of texture is coded.

10.5 Motion estimation and compensation

The texture of each VOP is motion compensated prior to coding. The motion estimation and compensation is similar to that of H.263 with the exception that the blocks on the VOP borders have to be modified to cater for the arbitrary shapes of the VOPs. These modified macroblocks are referred to as polygons, and the motion estimation is called polygon-based matching. Furthermore, since shapes change from time to time, some conversion is necessary to ensure the consistency of the motion compensation.

A macroblock that lies on the VOP boundary, called a boundary macroblock, is padded by replicating the boundary samples of the VOP towards the exterior. This process is carried out by repetitive padding in the horizontal and vertical directions. In case there are macroblocks completely outside the VOP, they are padded by extended padding.

In horizontal padding, each sample at the boundary of a VOP is replicated horizontally in the left or right direction in order to fill the transparent region outside the VOP of a boundary macroblock. If there are two boundary sample values for filling a sample outside a VOP, the two boundary samples are averaged. A similar method is used for vertical padding of the boundary macroblocks in the vertical direction.

Exterior macroblocks immediately next to boundary macroblocks are filled by replicating the samples at the border of the boundary macroblocks. The boundary macroblocks are numbered in a prioritised order according to Figure 10.20.

The exterior macroblock is then padded by replicating upwards, downwards, leftwards or rightwards the rows of sampling from the horizontal, vertical border of the boundary macroblock having the largest priority number. Note that the boundary macroblocks have already been padded by horizontal and vertical

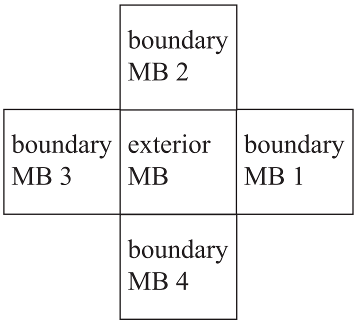

Figure 10.20 Priority of boundary macroblocks surrounding an exterior macroblock

repetitive padding. The remaining macroblocks that is; those which are not located next to any boundary macroblock are filled with 128. The original alpha plane for the VOP is used to exclude the pixels of the macroblocks that are outside the VOP.

The reference VOP is padded based on its own shape information. For example, when the reference VOP is smaller than the current VOP, the reference is not padded up to the size of the current VOP.

The motion estimation and compensation with the padded VOPs can be carried out in several different forms, such as integer pixel motion estimation, half and quarter sample search, unrestricted motion estimation/compensation, overlapped motion compensation and advanced mode prediction. Motion vectors are then differentially encoded, similar to H.263.

10.6 Texture coding

The intra VOPs and motion-compensated inter VOPs are coded with 8×8 block DCT. The DCT is performed separately for each of the luminance and chrominance planes.

For an arbitrarily shaped VOP, the macroblocks that completely reside inside the VOP shape are coded with a technique identical to H.263. For the boundary macroblocks, if it is of intra type, it is padded with horizontal and vertical repetition. For inter macroblocks, not only is the macroblock repeatedly padded, but also the region outside the VOP within the block is padded with zeros. Transparent blocks are skipped and therefore are not coded. These blocks are then coded in a manner identical to the interior blocks. Blocks that lie outside the original shape are padded with 128, 128 and 128 for the luminance and the two chrominances in the case of intra, and 0, 128 and 128 for inter macroblocks. Blocks that belong neither to the original nor to the coded arbitrary shape but to the inside of the bounding box of the VOP are not coded at all.

10.6.1 Shape-adaptive DCT

At the boundary macroblocks, the horizontally/vertically padded blocks can be coded with a standard 8×8 block DCT. This padding removes any abrupt transitions within a block, and hence reduces the number of significant DCT coefficients. At the decoder, the added pixels are removed by the help of shape parameters from the decoded BABs.

Since the number of opaque pixels in the 8×8 blocks of some of the boundary macroblocks is usually less than 64 pixels, it would have been more efficient if these opaque pixels could have been DCT coded without padding. This method of DCT coding is called shape-adaptive DCT (SA-DCT). The internal processing of SA-DCT is controlled by the shape information that has to be derived from the decoded BAB. Hence, only opaque pixels within the boundary blocks are actually coded. As a consequence, in contrast to standard DCT, the number of DCT coefficients in an SA-DCT is equal to the number of opaque pixels.

There are two types of SA-DCT, one used for inter blocks, known as SA-DCT, and the other for intra blocks, known as ΔSA-DCT, which is an extension of

SA-DCT. For both cases, a two-dimensional separable DCT with a varying length of basis vectors is used.

The basic concept of SA-DCT is shown in Figure 10.21. Segments of the opaque pixels are encapsulated in the picture grids of 8 × 8 pixel blocks as shown in Figure 10.21*a*. Each row of the pixels is then shifted and aligned to the left, as shown in Figure 10.21*b*. The aligned pixels are then one-dimensionally DCT coded in the horizontal direction with variable basis functions, where the lengths of the basis functions are determined by the number of pixels in each line. For example, the first pixel of the segment is represented by itself as a DC coefficient.

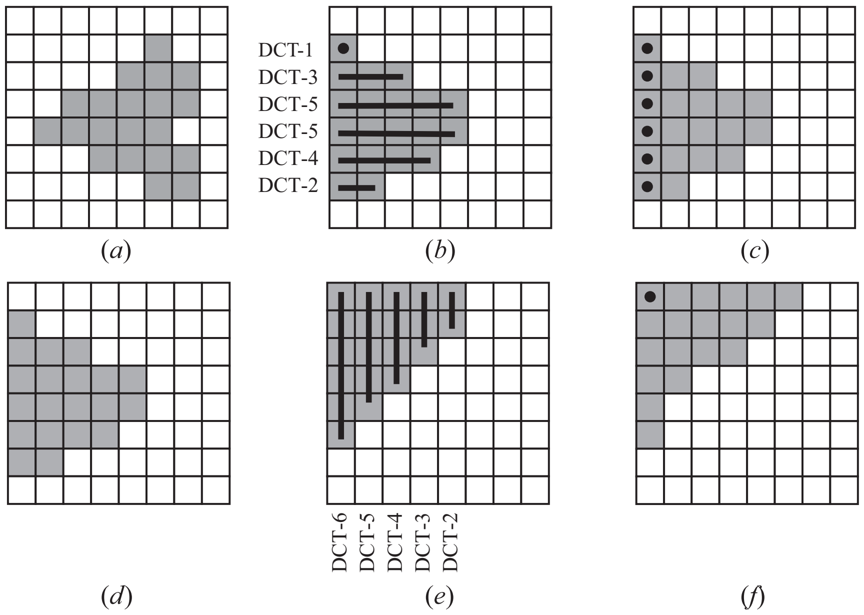

Figure 10.21 An example of SA-DCT (a) original segment, (b) ordering of pixels and horizontal SA-DCT, (c) location of 1D coefficients, (d) location of samples prior to vertical SA-DCT, (e) ordering of 1D samples and vertical (f) location of 2D SA-DCT coefficients

The second line of the pixels is DCT coded with a three-point transform, and the third line with a five-point transform, and so on. The coefficients of the N-point DCT, c_j, are defined by

$$c_j = \sqrt{\frac{2}{N}}\, c_0 \cos\left[p(k+0.5)\frac{\pi}{N}\right]$$
$$\text{and}\quad c_0 = \frac{\sqrt{2}}{2} \quad \text{if } p = 0; \qquad c_0 = 1 \text{ otherwise} \tag{10.12}$$

Figure 10.21*c* illustrates the horizontal DCT coefficients, where the DC values are represented with a dot. These coefficients now become the input to the second-stage one-dimensional DCT in the vertical direction. Again they are shifted upwards and aligned to the upper border, and the *N*-point DCT is applied to each vertical column, as shown in Figure 10.21*e*. The final two-dimensional DCT coefficients are shown in Figure 10.21*f*. Note that since the shape information from the decoded BABs is known, these processes of shifting and alignments in the horizontal and vertical directions are reversible.

The ΔSA-DCT algorithm that is used for intra coded macroblocks is similar to SA-DCT but with extra processing. This additional processing is simply calculating the mean of the opaque pixels in the block, and subtracting the mean from each individual pixel. The resultant zero mean opaque pixels are then SA-DCT coded. The mean value is separately transmitted as the DC coefficient.

Zigzag scanning, quantisation and the variable length coding of the SA-DCT coefficients operations are similar to those of standard DCT used in H.263.

10.7 Coding of the background

An important advantage of the content-based coding approach in MPEG-4 is that the compression efficiency can be significantly improved by not coding the video background. If the background is completely static, all the other noncontent-based codecs would not code the background either. However, because of noise, camera shaking, or deliberate camera movement, such as panning, zooming, and tilt, the background cannot be entirely static. One of the attractive features of the content-based or object-based coding is that the background movement does not need to be represented at its exact form. Viewers normally do not pay attention to the accuracy of the background video, unless it is badly coded, such that the coding distortion distracts the viewer from the main scene.

An efficient way of coding the background is to represent the background movement with a global motion model. In section 9.4.5, we saw that motion compensation with the spatial transform was capable of dealing with complex motions such as translation, sheering, and zooming. The same concept can be used to compensate for the global motion of the background. Here the whole background VOP is transformed to match against the VOP of the previous frame. The transformation parameters then represent the amount of information required to code the background VOP, which corresponds to an extremely low bit rate.

In MPEG-4, the global motion is represented either by six motion parameters (three motion vectors) through the affine transform, defined as

$$x = a_0 u + a_1 v + a_2 \quad \text{and} \quad y = a_3 u + a_4 v + a_5 \tag{10.13}$$

or by eight parameters (four motion vectors), using the perspective transform, defined by

$$x = \frac{a_0 u + a_1 v + a_2}{a_6 u + a_7 v + 1} \quad \text{and} \quad y = \frac{a_3 u + a_4 v + a_5}{a_6 u + a_7 v + 1} \tag{10.14}$$

In both cases, similar to the bilinear transform of section 9.4.5, the coordinates (u, v) in the current frame are matched against the coordinates (x, y) in the previous frame. The best matching parameters then define the motion of the object (in this case, the background VOP).

In MPEG-4, global motion compensation is based on the transmission of a static sprite. A static sprite is a (possibly large) still image, describing panoramic background. For each consecutive image in a sequence, only eight global motion parameters describing camera motion are coded to reconstruct the object. These parameters represent the appropriate perspective transform of the sprite transmitted in the first frame.

Figure 10.22 depicts the basic concept for coding an MPEG-4 video sequence using a sprite panorama image. It is assumed that the foreground object (tennis player, top right image) can be segmented from the background and that the sprite panorama image can be extracted from the sequence prior to coding. (A sprite panorama is a still image that describes the content of the background over all frames in the sequence.) The large panorama sprite image is transmitted to the receiver only once as the first frame of the sequence to describe the background. The sprite is stored in a sprite buffer. In each consecutive frame, only the camera parameters relevant for the background are transmitted to the receiver. This allows the receiver to reconstruct the background image for each frame in the sequence based on the sprite. The moving foreground object is transmitted separately as an arbitrary shape VO. The receiver composes both the foreground and background images to reconstruct each frame (bottom picture in Figure 10.22). For low-delay applications, it is possible to transmit the sprite in multiple smaller pieces over consecutive frames or to build up progressively the sprite at the decoder.

The global motion compensation can also be applied to the foreground objects. Here for each VOP, a spatial transform, like the perspective transform, is used to

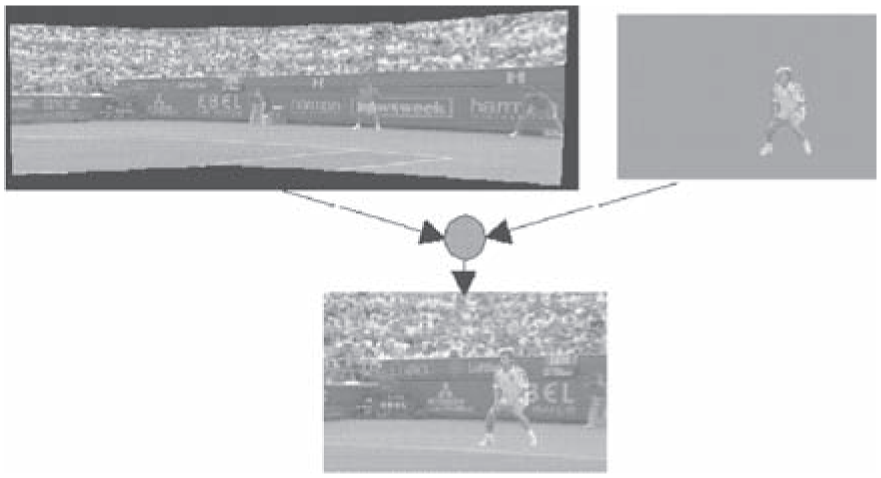

Figure 10.22 Static sprite of Stefan (Courtesy of MPEG-4)

estimate the transformation parameters. These are regarded as the global motion parameters that are used to compensate for the global motion of the foreground object. Globally, motion-compensated VOP is then coded by the motion-compensated texture coding, where it is motion compensated once more, but this time with a conventional block matching technique.

10.8 Coding of synthetic objects

Synthetic images form a subset of computer graphics, which can be supported by MPEG-4. Of particular interest in synthetic images is the animation of head-and-shoulders or cartoon-like images. Animation of synthetic faces was studied in the first phase of MPEG-4, and the three-dimensional body animation was addressed in the second phase of MPEG-4 development [2].

The animation parameters are derived from a two-dimensional mesh, which is a tessellation of a two-dimensional region into polygonal patches. The vertices of the polygonal patches are referred to as the node points or vertices of the mesh. In coding of the objects, these points are moved according to the movement of the body, head, eyes, lips and changes in the facial expressions. A two-dimensional mesh matched to the Claire image is shown in Figure 10.23*a*. Since the number of nodes representing the movement can be very small, this method of coding, known as model-based coding, requires a very low bit rate, possibly in the range of 10–100 bit/s [14].

To make synthetic images look more natural, the texture of the objects is mapped into the two-dimensional mesh, as shown in Figure 10.23*b*. For coding of the animated images, triangular patches in the current frame are deformed by the movement of the node points to be matched into the triangular patches or facets in the reference frame. The texture inside each patch in the reference frame is thus warped onto the current frame, using a parametric mapping, defined as a function of the node point motion vectors.

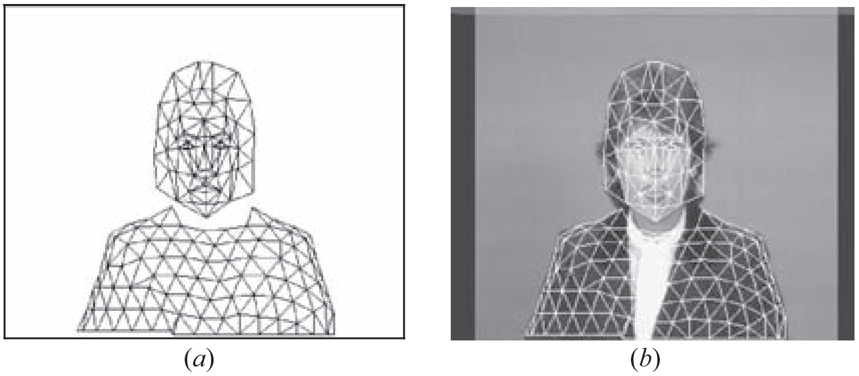
(*a*) (*b*)

Figure 10.23 (a) A two-dimensional mesh and (b) the mapped texture

For triangular meshes, the affine mapping with six parameters (three node points or vertices) is a common choice [15]. Its linear form implies that texture mapping can be accomplished with a low computational complexity. This mapping can model a general form of motion including translation, rotation, scaling, reflection and shear, and preserves straight lines. This implies that the original two-dimensional motion field can be compactly represented by the motion of the node points, from which a continuous, piecewise affine motion field can be reconstructed. At the same time, the mesh structure constrains movements of adjacent image patches. Therefore, meshes are well suited to represent mildly deformable but spatially continuous motion fields.

However, if the movement is more complex, like the motion of lips, then affine modelling may fail. For example, Figure 10.24 shows the reconstructed picture of Claire after nine frames of affine modelling. The accumulated error due to model failure around the lips is very evident.

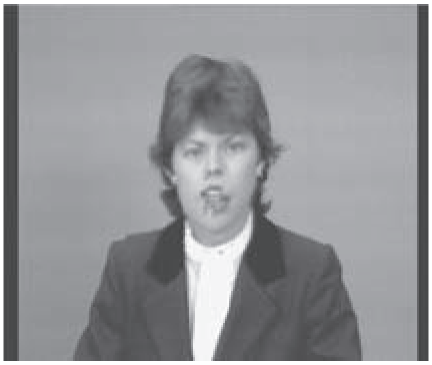

Figure 10.24 Reconstructed model-based image with the affine transform

For a larger complex motion, requiring a more severe patch deformation, one can use quadrilateral mappings with eight degrees of freedom. Bilinear and perspective mappings are these kinds of mappings, which have a better deformation capability over the affine mapping [16,17].

10.9 Coding of still images

MPEG-4 also supports coding of still images with a high coding efficiency as well as spatial and SNR scalability. The coding principle is based on the discrete wavelet transform, which was described in some length in Chapter 4. The lowest subband after quantisation is coded with a differential pulse code modulation (DPCM) and the higher bands with a variant of embedded zero tree wavelet (EZW) [18]. The quantised DPCM and zero tree data are then entropy coded with an arithmetic encoder. Figure 10.25 shows a block diagram of the still image encoder.

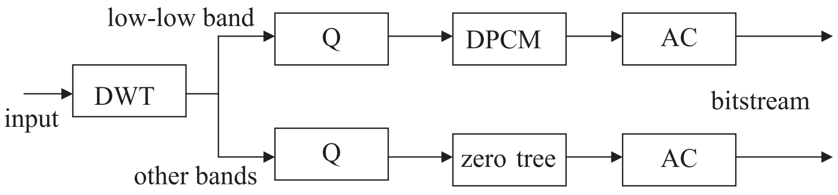

Figure 10.25 Block diagram of a wavelet-based still image encoder

In the following sections, each part of the encoder is described.

10.9.1 Coding of the lowest band

The wavelet coefficients of the lowest band are coded independently from the other bands. These coefficients are DPCM coded with a uniform quantiser. The prediction for coding a wavelet coefficient w_x is taken from its neighbouring coefficients w_A or w_C, according to

$$\begin{aligned} &\text{if } |w_A - w_B| < |w_A - w_C| \quad w_{prd} = w_C \\ &\text{otherwise} \quad w_{prd} = w_A, \end{aligned} \tag{10.15}$$

The difference between the actual wavelet coefficient w_x and its predicted value w_{prd} is coded. The positions of the neighbouring pixels are shown in Figure 10.26.

The coefficients after DPCM coding are encoded with an adaptive arithmetic coder. First the minimum value of the coefficient in the band is found. This value, known as *band_offset*, is subtracted from all the coefficients to limit their lower bound to zero. The maximum value of the coefficients as *band_max_value* is also calculated. These two values are included in the bitstream.

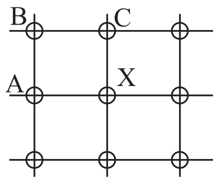

Figure 10.26 Prediction for coding the lowest band coefficients

For adaptive arithmetic coding [19], the arithmetic coder model is initialised at the start of coding with a uniform distribution in the range of 0 to *band_max_value*. Each quantised and DPCM-coded coefficient after arithmetic coding is added to the distribution. Hence, as the encoding progresses, the distribution of the model adapts itself to the distribution of the coded coefficients (adaptive arithmetic coding).

10.9.2 Coding of higher bands

For efficient compression of higher bands as well as for a wide range of scalability, the higher order wavelet coefficients are coded with the embedded zero tree

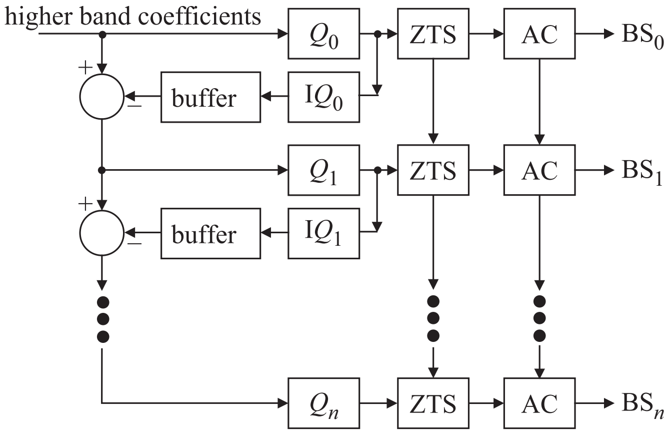

Figure 10.27 A multiscale encoder of higher bands

wavelet (EZW) algorithm first introduced by Shapiro [18]. Details of this coding technique are given in Chapter 4. Here we show how it is used within the MPEG-4 still image coding algorithm.

Figure 10.27 shows a multiscale zero tree coding algorithm, based on EZW, for coding of higher bands. The wavelet coefficients are first quantised with a quantiser Q_0. The quantised coefficients are scanned with the zero tree concept (exploiting similarities among the bands of the same orientation), and then entropy coded with an arithmetic coder (AC). The generated bits comprise the first portion of the bitstream, as the base layer data, BS_0. The quantised coefficients of the base layer after inverse quantisation are subtracted from the input wavelet coefficients, and the residual quantisation distortions are requantised by another quantiser, Q_1. These are then zero tree scanned (ZTS) entropy coded to represent the second portion of the bitstream, BS_1. The procedure is repeated for the all the quantisers, Q_0 to Q_N, to generate $N + 1$ layers of bitstream.

The quantisers used in each layer are uniform with a dead band zone of twice the quantiser step size of that layer. The quantiser step size in each layer is specified by the encoder in the bitstream. As we are already aware, each quantiser is multilayer, and the quantiser step size of a lower layer is several times that of its immediate upper layer. This is because, for a linear quantiser Q_i, with a quantiser step size of q_i, the maximum residual quantisation distortion is q_i (for those that fall in the dead zone of Q_i) and $q_i/2$ (for those that are quantised). Hence, for a higher-layer quantiser Q_{i+1}, with a quantiser step size of q_{i+1} to be efficient, the q_{i+1} should be several times smaller than q_i. If $q_{i+1} = \frac{1}{2}q_i$, then it becomes a bilevel quantiser.

The number of quantisers indicates the number of SNR-scalable layers, and the quantiser step size in each layer determines the granularity of SNR scalability at that layer. For finest granularity of SNR scalability, all the layers can use a bilevel (1 bit) quantiser. In this case, for optimum encoding efficiency, the quantiser step size of each layer is exactly twice that of its immediate upper layer. Multistage quantisation in this mode now becomes quantisation by successive approximation or the bit plane encoding, described in Chapter 4. Here, the number of quantisers is equal to the number of bit planes required to represent the wavelet transform coefficients. In this bilevel quantisation, instead of quantiser step sizes, the maximum number of bit planes is specified in the bitstream.

As the figure shows, the quantised coefficients are zero tree scanned (ZTS) to exploit similarities among the bands of the same orientation. The zero tree takes advantage of the principle that if a wavelet coefficient at a lower frequency band is insignificant, then all the wavelet coefficients of the same orientation at the same spatial location are also likely to be insignificant. A zero tree exists at any node when a coefficient is zero and all the node's children are zero trees. The wavelet trees are efficiently represented and coded by scanning each tree from the root at the lowest band through the children and assigning symbols to each state of the tree.

If multilevel quantiser is used, then each node encounters three symbols: zero tree root, value zero tree root (VZ) and value (V). A zero tree root symbol denotes a coefficient that is the root of a zero tree. When such a symbol is coded, the zero tree does not need to be scanned further, because it is known that all the coefficients in such a tree have zero values. A value zero tree root symbol is a node where the coefficient has a nonzero value, and all its four children are zero tree roots. The scan of this tree can stop at this symbol. A value symbol identifies a coefficient with value either zero or nonzero, but some of the descendents are nonzero. The symbols and the quantised coefficients are then entropy coded with an adaptive arithmetic coder.

When a bilevel quantiser is used, then the values of each coefficient is either 0 or 1. Hence, depending on the implementation procedure, different types of symbols can be defined. Since multilayer bilevel quantisation is, in fact, quantisation by successive approximation, this mode is exactly the same as coding the symbols at EZW. There we defined four symbols of +, −, ZT and Z, where ZT is a zero tree root symbol, Z is an isolated zero within a tree, and + and − are the values for refinement (see section 4.5 for details).

To achieve both spatial and SNR scalability, two different scanning methods are employed in this scheme. For spatial scalability, the wavelet coefficients are scanned from subband to subband, starting from the lowest frequency band to the highest frequency band. For SNR scalability, the wavelet coefficients are scanned quantiser to quantiser. The scanning method is defined in the bitstream.

10.9.3 Shape-adaptive wavelet transform

Shape-adaptive wavelet (SA-wavelet) coding is used for compression of arbitrary shaped textures. SA-wavelet coding is different from the regular wavelet coding mainly in its treatment of the boundaries of arbitrary shaped texture. The coding ensures that the number of wavelet coefficients to be coded is exactly the same as the number of pixels in the arbitrary shaped region, and coding efficiency at the object boundaries is the same as for the middle of the region. When the object boundary is rectangular, SA-wavelet coding becomes the same as the regular wavelet coding.

The shape information of an arbitrary shaped region is used in performing the SA-wavelet transform in the following manner. Within each region, the first row of pixels belonging to that region and the first segment of the consecutive pixels in the row are identified. Depending on whether the starting point in the region has odd or even coordinates, and the number of pixels in the row of the segment is odd or even, the proper arrangements for 2:1 downsampling and use of symmetric extensions are made [3].

Coding of the SA-wavelet coefficients is the same as coding of regular wavelet coefficients, except that a modification is needed to handle partial wavelet trees that have wavelet coefficients corresponding to pixels outside the shape boundary. Such wavelet coefficients are called out nodes of the wavelet trees. Coding of the lowest band is the same as that of the regular wavelet, but the out nodes are not coded. For the higher bands, for any wavelet trees without out nodes, the regular zero tree is applied. For a partial tree, a minor modification to the regular zero tree coding is needed to deal with the out nodes. That is, if the entire branch of a partial tree has out nodes only, no coding is needed for this branch, because the shape information is available to the decoder to indicate this case. If a parent node is not an out node, all the children out nodes are set to zero, so that the out nodes do not affect the status of the parent node as the zero tree root or isolated zero. At the decoder, the shape information is used to identify such zero values as out nodes. If the parent node is an out node and not all of its children are out nodes, there are two possible cases. The first case is that some of its children are out nodes, but they are all zeros. This case is treated as a zero tree root and there is no need to go down the tree. The shape information indicates which children are zeros and which are out nodes. The second case is that some of its children are not out nodes and at least one of such nodes is nonzero. In this case, the out node parent is set to zero, and the shape information helps the decoder to know that this is an out node, and coding continues further down the tree. There is no need to use a separate symbol for any out nodes.

10.10 Video coding with the wavelet transform

The success of the zero tree in efficient coding of wavelet transform coefficients has encouraged researchers to use it for video coding. Although wavelet-based video coding is not part of the standard, there is no reason why wavelet-based video coding cannot be used in the future. This, of course, depends on the encoding efficiency of wavelet-based coding and its functionalities. For this reason, in this section, we look at some video coding scenarios and examine the encoding efficiency.

One way of wavelet-based video coding is to use the generic video encoder of Figure 3.19, but replacing the DCT with the DWT, as shown in Figure 10.28. Here, variable length coding of the quantised coefficients is replaced by the zero tree coding of either EZW or set partitioning in hierarchical tree (SPIHT) [18,21]. Also, overlapped motion compensation has been found to be very effective with the wavelet transform, as it prevents the motion compensation blocking artefacts from creating spurious vertical and horizontal edges.

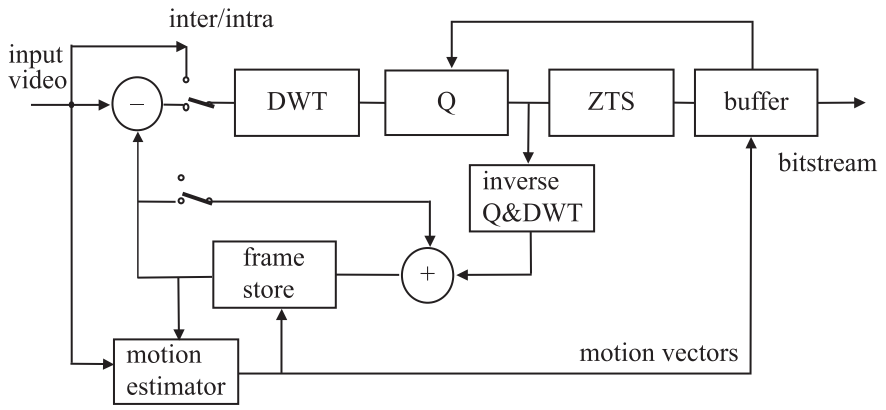

Figure 10.28 Block diagram of a wavelet video codec

Another method that might be used with the wavelet transform is shown in Figure 10.29.

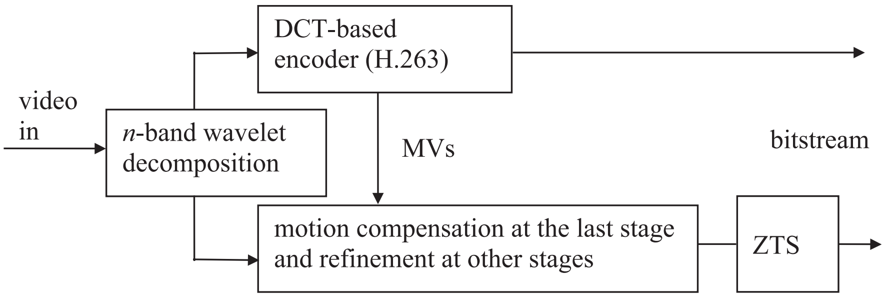
DCT-based encoder (H.263)
video in
n-band wavelet decomposition
MVs
bitstream
motion compensation at the last stage and refinement at other stages
ZTS

Figure 10.29 A hybrid H.263/wavelet video coding scheme

Each frame of the input video is transformed into *n*-band wavelet subbands. The lowest LL band is fed into a DCT-based video encoder, such as MPEG-1 or H.263. The other bands undergo a hierarchical motion compensation. First, the three high-frequency bands of the last stage are motion compensated using the motion vectors from MPEG-1/H.263. The reconstructed picture from these four bands (LL, LH, HL and HH), which is the next level LL band, only requires a ± 1 pixel refinement [20]. The other three bands at this stage are also motion compensated by the same amount. This process is continued for all the bands. Hence, at the end all the bands are motion compensated. Now these motion-compensated bands are coded with a zero tree-based coding method (EZW or SPIHT).

10.10.1 Virtual zero tree algorithm

The lowest band of the wavelet, LL, is a reduced size replica of the original video and hence can be encoded with an efficient encoder, such as H.263. When a zero tree-based coding such as EZW/SPIHT is used along with the standard codecs (e.g. Figure 10.29), it meets some problems. First, the subband decomposition stops when the top level LL band reaches a size of SIF/QSIF or sub-QSIF. At these levels there will be too many clustered zero tree roots. This is very common for either static parts of the pictures or when motion compensation is very efficient. Even for still images or I-pictures, a large part of the picture may contain only low spatial frequency information. As a result, at the early stages of the quantisation by successive approximation, where the yardstick is large, a vast majority of the wavelet coefficients fall below the yardstick. Second, even if the subband decomposition is taken to more stages, such that the top stage LL is a small picture of 16 × 16 pixels (e.g. Figure 10.28), it is unlikely that many zero trees can be generated. In other words, with a higher level of wavelet decomposition, the tree structure is bound to break and hence the efficiency of EZW/SPIHT is greatly reduced.

To improve the efficiency of zero tree-based coding, we have devised a version of it called virtual zero tree (VZT) [22]. The idea is to build trees outside the image boundary, hence the word virtual, as an extension to the existing trees that have roots in the top stage, so that the significant map can be represented in a more efficient way. It can be imagined as replacing the top level LL band with zero value coefficients. These coefficients represent the roots of wavelet trees of several virtual subimages in normal EZW/SPIHT coding, although no decomposition and decimation actually take place, as demonstrated in Figure 10.30.

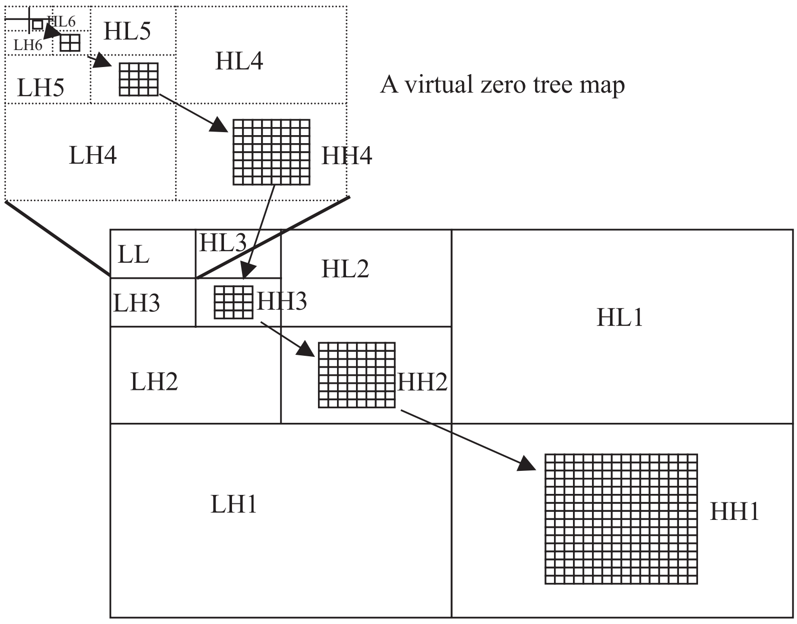

Figure 10.30 A virtual zero tree

In this figure, virtual trees, or a virtual map, are built in the virtual subbands on the high-frequency bands of the highest stage. Several wavelet coefficients of the highest stage form a virtual node at the bottom level of the virtual map. Then in the virtual map, four nodes of a lower level are represented by one node of a higher level in the same way a zero tree is formed in EZW/SPIHT coding. The virtual map has only two symbols: VZT root or non-VZT root. If four nodes of a 2×2 block on any level of a virtual tree are all VZT roots, the corresponding node on the higher level will also be a VZT root. Otherwise this one node of the higher level will be a non-VZT node. This effectively constructs a long-rooted tree of clustered real zero trees. One node on the bottom level of the virtual map is a VZT root only when the four luminance coefficients of a 2×2 block and their two corresponding chrominance coefficients on the top stage wavelet band are all zero tree roots. Chrominance pictures are also wavelet decomposed and, for a 4:2:0 image format, four zero tree roots of the luminance and one from each chrominance can be made a composite ZT root [22].

10.10.2 Coding of high-resolution video

A wavelet transform can be an ideal tool for coding of high-resolution pictures or video. This is because the high correlation among the dense pixels of high-resolution pictures are better exploited if a larger area for decorrelation of pixels are used. Unfortunately, in the standard video codecs, the DCT block sizes are fixed at 8×8, and hence pixel correlation beyond eight-pixel distances cannot be exploited. On the other hand, in the wavelet transform, increasing the number of decomposition levels means decorrelating the pixels at larger distances if so desired.

We have tested the encoding efficiency of the wavelet transform (for Figure 10.29) for high definition video (HDTV) as well as super HDTV (SHD). For HDTV, we have used the test sequence Gaynor (courtesy of BBC). For this image sequence, a two-stage (seven-band) wavelet transform is used, and the LL band of the SIF size was MPEG-1 coded. Motion-compensated higher bands were coded with VZT and EZW. For the SHD video, the park sequence with 2048×2048 pixels at 60 Hz (courtesy of NHK Japan [21]) was used. The SHD images after three-stage subband decomposition result in ten bands. The LL band, with picture resolutions of 256×256 pixels, is MPEG-1 coded; the remaining nine bands are VZT and EZW coded in two separate experiments.

It appears at first that by creating virtual nodes, we have increased the number of symbols to be coded, and hence the bit rate tends to increase rather than to decrease. However, these virtual roots will cluster the zero tree roots into a bigger zero tree root, such that instead of coding these roots one by one, at the expense of a large overhead by a simple EZW, we can code the whole cluster by a single VZT with only a few bits. VZT is more powerful at the early stages of encoding, where the vast majority of top stage coefficients are zero tree roots. This can be seen from Table 10.2, where a complete breakdown of the total bit rate required to code a P-picture of the park sequence by both methods is given.

Table 10.2 Breakdown bit rate in coding of a P-picture with VZT and EZW

	VZT (kbits)					**EZW (kbits)**		
	Virtual pass	**Real pass**	**Dominanat pass**	**Sub-ordinate pass**	**Sum**	**Dominanat pass**	**Sub-ordinate pass**	**Sum**
MPEG	–	–	–	–	171	–	–	171
MV	–	–	–	–	15	–	–	15
Pass-1	1.5	3.2	4.4	0.16	4.9	25	0.16	25
Pass-2	7.7	31	39	1.7	41	153	1.7	156
Pass-3	18	146	164	11	175	465	11	476
Pass-4	29	371	400	41	441	835	41	896
Pass-5	42	880	992	128	1050	1397	128	1326
Grand total					1898			3265

The first row of the table shows that 171 kbits are used to code the LL band by MPEG-1. The second row shows that 15 kbits is used for the additional ± 1 pixel refinement in all bands. For the higher bands, the image is scanned in five passes, where the bits used in the dominant and subordinate passes of VZT and EZW are shown. In VZT, the dominant pass is made up of two parts: one used in coding of the virtual nodes and the other parts for real data in the actual nine bands. Note that although some bits are used to code the virtual nodes (are not used in EZW), the total bits of the dominant pass in VZT are much less than for EZW. The number of bits in the subordinate passes, which code the real subordinate data, is the same for both methods. In the table, the grand total is the total number of bits used to code the P-frame under the two coding schemes. It can be seen that VZT requires two-thirds of the bit rate required by EZW.

For HDTV, our results show that although a good quality video at 18 Mbit/s can be achieved under EZW, the VZT only needs 11 Mbit/s [22].

10.10.3 Coding of low-resolution video

Although coding of low spatial resolution (e.g. QCIF, sub-QCIF) video may not benefit from the wavelet decomposition to the extent that higher-resolution video does, nevertheless zero tree coding is efficient enough to produce good results. In fact, the multiresolution property of the wavelet-based coding is a bonus that the DCT-based coding most suffer from. In section 8.5.7, we saw that two-layer spatial and SNR scalability of the standard codecs (MPEG-2, H.263) reduces the compression efficiency by as much as 30 per cent. That is spatial/SNR coders are required to generate about 30 per cent more bits to be able to produce the same video quality as a single-layer coder does. Undoubtedly, increasing the number of layers, or combining them in a hybrid form, will widen this deficiency gap.

On the other hand, with the wavelet transform, as the number of decomposition levels increases, the encoding efficiency increases too. Moreover, with the concept of virtual zero tree, a large area of static parts of the picture can be grouped together for efficient coding, as we have seen from the results of higher-resolution pictures of the previous section.

To compare the quality of wavelet-coded video (purely wavelet-based video codec of Figure 10.28) against the best of the standard codec, we have coded 10 Hz QCIF size of Akio and Carphone standard video test sequences at various bit rates, as shown in Figure 10.31, for Akio and Figure 10.32 for Carphone.

For the wavelet coder, we have used three levels of wavelet decomposition (ten bands) and two levels of virtual nodes, with an SPIHT-type zero tree coding, called virtual SPHIT [23]. Unlike Figure 10.29, where the lowest subband was coded by a standard DCT codec, here we have coded all the bands, including the LL band, with the virtual SPIHT (Figure 10.28). This is because after three-level wavelet decomposition, the lowest LL band has a dimension of 22×18 pixels, which is neither viable nor practical to be coded with codecs using 16×16 pixel macroblocks. On the motion compensation, the whole QCIF image was motion compensated with an overlapped block matching algorithm, with half a pixel precision. Motion-compensated wavelet coefficients after the zero tree scan were arithmetic coded.

For comparison we have also coded these sequences with a single- and two-layer SNR-scalable H.263 codecs, at various bit rates from 20 up to 60 kbit/s. For the two-layer H.263, 50 per cent of the total bits were assigned to the base layer. As the PSNR Figures 10.31 and 10.32 show, single-layer H.263 is consistently better than the wavelet that itself is better than the two-layer H.263. However, subjectively wavelet-coded video appears better than single-layer H.263, despite being 1–2 dB poorer on the PSNR.

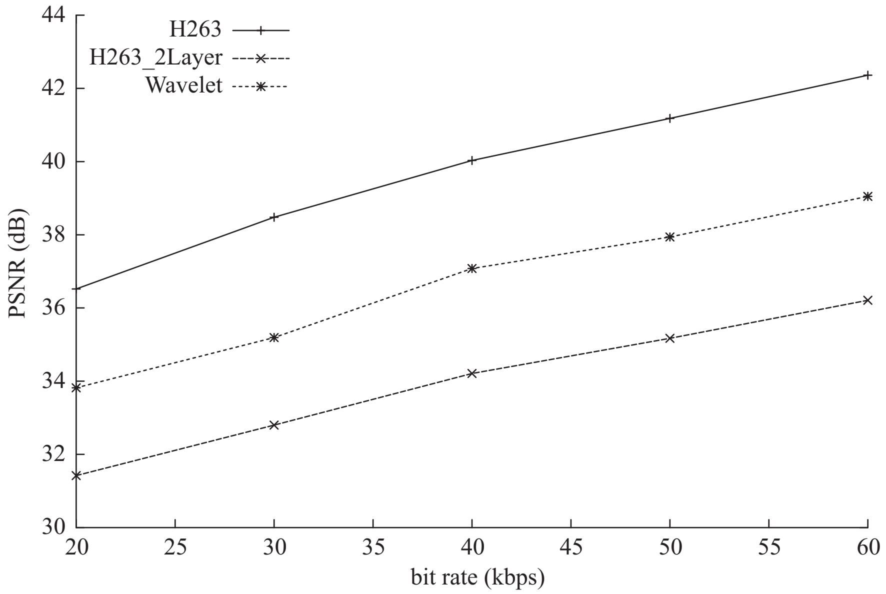

Figure 10.31 Quality of QCIF size Akio sequence coded at various bit rates

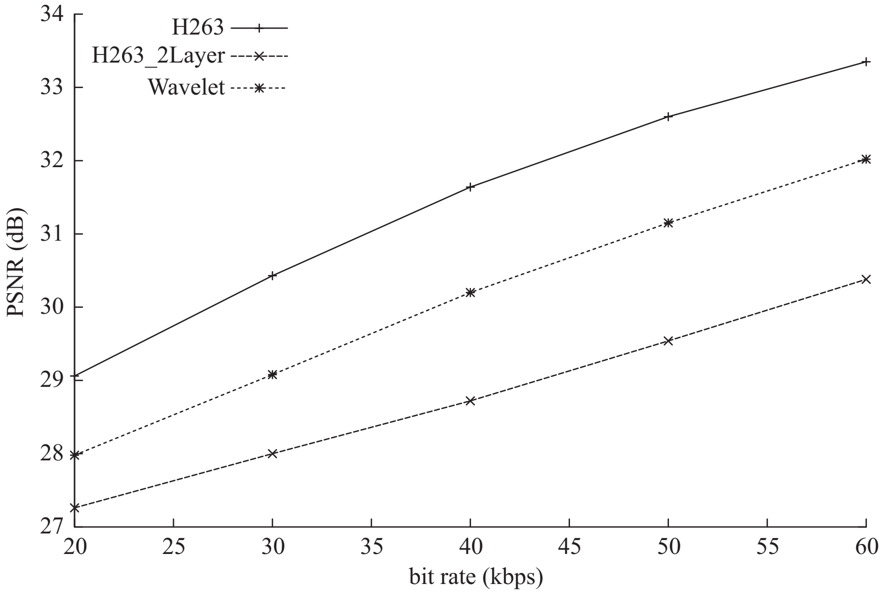

Figure 10.32 Quality of QCIF size Carphone sequence coded at various bit rates

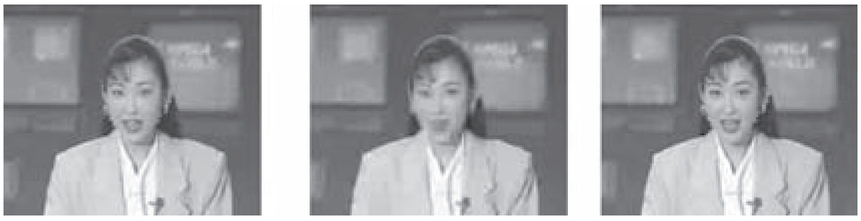

(*a*) (*b*) (*c*)

Figure 10.33 A snap shot of Akio coded at 20 kbit/s, 10 Hz, (a) H.263, (b) SNR-scalable H.263 and (c) wavelet SPIHT

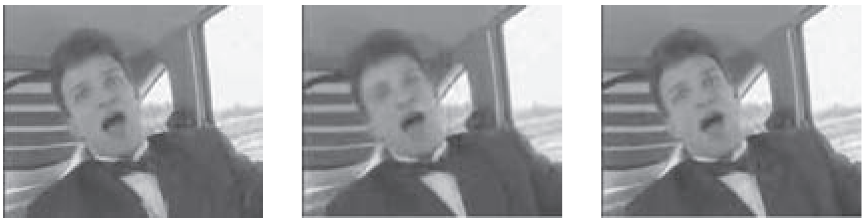

(*a*) (*b*) (*c*)

Figure 10.34 A snap shot of Carphone coded at 40 kbit/s, 10 Hz, (a) H.263, (b) SNR-scalable H.263 and (c) wavelet SPIHT

Figures 10.33 and 10.34 show snap shots of the Akio and Carphone, coded at 20 and 40 kbit/s, respectively. Although these small pictures may not show the subjective quality differences between the two codecs, the fact is that the H.263 picture is blocky while that of wavelet is not. In the Carphone picture, wavelet-coded picture is smeared but it is still much sharper than the two-layer H.263. Some nonexperts prefer smeared picture to the blocky one, but expert viewers have a different opinion. Comparing wavelet with the two-layer H.263, both subjective and objective results are in favour of wavelet.

Considering that the above three-level decomposition wavelet transform can be regarded as an *N*-layer video without impairing its compression efficiency, it implies that the wavelet has a high potential for multilayer coding of video. Although this video codec is not a part of any standard, there is no doubt that its high potential for multilayer coding makes it very attractive.

10.11 Scalability

We have covered scalability in the standard codecs several times, but because of the nature of content-based coding, scalability in MPEG-4 can be different from the other standard codecs. However, since MPEG-4 is also used as a frame-based video codec, the scalability methods we have discussed so far can also be used in this codec. Thus, we introduce two new methods of scalability that are only defined for MPEG-4.

10.11.1 Fine granularity scalability

The scalability methods we have seen so far, SNR, spatial and temporal, are normally carried out in two or a number of layers. These create coarse levels of representing various quality, spatial and temporal resolutions. A few spatial and temporal resolutions are quite acceptable for the natural scenes, as it is of no practical use to have more resolution levels of these kinds. Hence, for the frame-based video, MPEG-4 also recommends the spatial and temporal scalabilities as we have discussed so far.

On the other hand, the existing SNR scalability has the potential to be represented in more quality levels. The increment in quality is both practical and appreciated by the human observer. Thus, in MPEG-4, instead of SNR scalability, a synonymous method named fine granularity scalability (FGS) is recommended. In this method, the base layer is coded similar to the base layer of an SNR-scalable coder, namely, coding of video at a given frame rate and a relatively large quantiser step size. Then the difference between the original DCT coefficients and the quantised coefficients in the base layer (base layer quantisation distortion) rather than being quantised with a finer quantiser step size, as is done in the SNR-scalable coder, are represented in bit planes. Starting from the highest bit plane that contains nonzero bits, each bit plane is successively coded using run length coding, on block-by-block basis. The code words for the run lengths can be derived from either

Huffman or arithmetic coding. Typically, different codebooks are used for different bit planes, because the run length distributions across the bit planes are different.

10.11.2 Object-based scalability

In the various scalability methods described so far, including the FGS, the scalability operation is applied to the entire frame. In object-based scalability, the scalability operations are applied to the individual objects. Of particular interest to MPEG-4 is the object-based temporal scalability (OTS), where the frame rate of a selected object is enhanced, such that it has a smoother motion than the remaining area. That is, the temporal scalability is applied to some objects to increase their frame rates against the other objects in the frames.

MPEG-4 defines two types of OTS. In type-1, the VO layer 0 (VOL0) comprises the background and the object of interest. Higher frame rates of the object of interest are coded at VOL1, as shown in Figure 10.35, where it is predictively coded, or Figure 10.36, if the enhancement layer is bidirectionally coded.

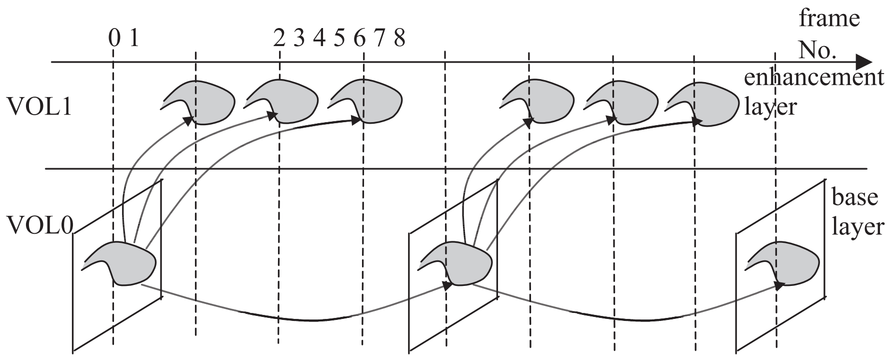

Figure 10.35 OTS enhancement structure of type-1, with predictive coding of VOP

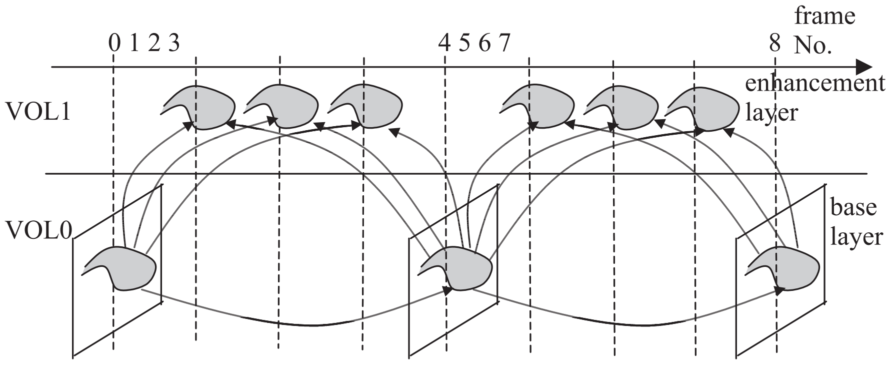

Figure 10.36 OTS enhancement structure of type-1, with bidirectional coding of VOP

On type-2 OTS, the background is separated from the object of interest, as shown in Figure 10.37. The background VO0 is sent at low frame rate without scalability. The object of interest is coded at two frame rates of base and enhancement layers of VOL0 and VOL1, respectively, as shown in the figure.

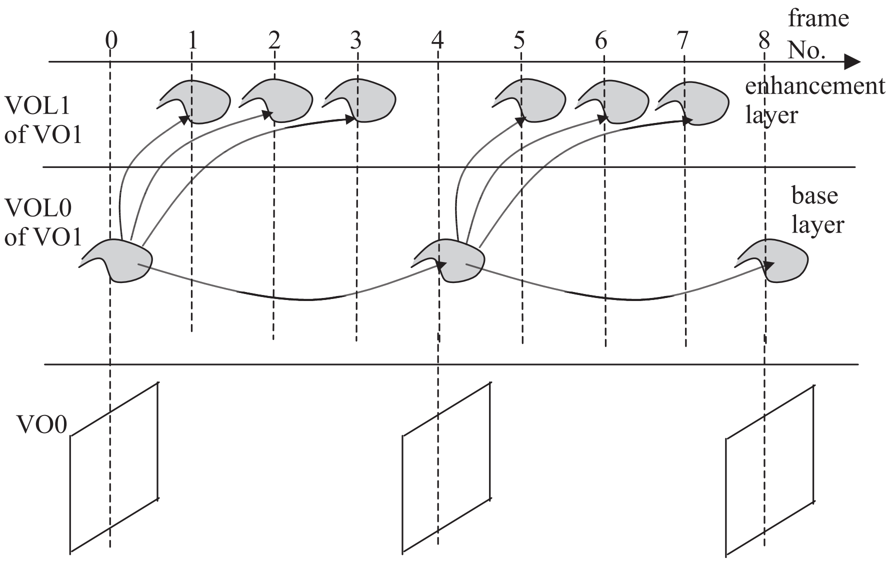

Figure 10.37 OTS enhancement structure of type-2

10.12 MPEG-4 versus H.263

There is a strong similarity between the simple profile MPEG-4 and H.263, such that a simple profile MPEG-4 can decode a bitstream generated by the core H.263. In fact, most of the annexes introduced into H.263 after the year 2000 were parts of the profiles designed for MPEG-4 in mid-1990s. However, there is no absolute reverse compatibility between the simplest profile of MPEG-4 and the H.263.

The main source of incompatibility is concerned with the systems function of MPEG-4. Like its predecessor, MPEG-4 uses a packet structure form of transporting compressed audio-visual data. In MPEG-2, we saw that packetised elementary streams (PES) of audio, video and data are multiplexed into a transport packet stream. In MPEG-4, because of the existence of many objects (up to 256 visual objects plus audio and data), the transport stream becomes significantly important. Even if one object is coded (frame-based mode), the same transport stream should be used. In particular, for transmission of MPEG-4 video over mobile networks, the packetised system has to add extra error resilience to the MPEG-4 bitstream. It is this packetised format of MPEG-4 that makes it non-decodable by an H.263 codec.

In MPEG-4, the elementary objects of the audio-visual media are fed to the synchronisation layer (SL) to generate SL-packets. An SL-packet has a resynchronisation marker, similar to the GOB and slice resynchronisation markers in H.263. However, in MPEG-4, the resynchronisation marker is inserted after certain number of bits are coded, but in H.263 they are added after several macroblocks. Since the number of bits generated per macroblock is variable, while distances between the resynchronisation markers in H.263 are variable, those of MPEG-4 are fixed. This helps to reduce the effect of channel errors in MPEG-4, hence making it more error resilient.

A copy of picture header is repeated in every SL-packet to make them independent of each other. Each media may generate more than one SL-packet. For example, if scalability is used, several interrelated packets are generated. Packets are then multiplexed into the output stream. This layer is unaware of the transport or delivery layer. The sync layer is interfaced to the delivery layer through the delivery multimedia integration framework (DMIF) application interface (DAI). The DAI is network independent but demands for session set-up and stream control functions. It also enables setting up quality of service for each stream.

The transport or delivery layer is delivery aware but unaware of media. MPEG-4 does not define any specific delivery layer. It relies mainly on the existing transport layers, such as Real-time Transport Protocol (RTP) for Internet, MPEG-2 transport stream for wired and wireless or ATM for B-ISDN networks.

There are also some small differences on the employment of the coding tools in the two codecs. For example, RVLC used in the simple profile of MPEG-4 is not exactly the same as the RVLC used in data partitioning of Annex V of H.263. In the former, RVLC is also used for DCT coefficients, while in the latter it is used for the non-DCT coefficients, for example, motion vectors and macroblock addresses. Although in Chapter 9 we showed that RVLC because of its higher overhead over the conventional VLC is not viable for the DCT coefficients, nevertheless in the experiments of Chapter 9, macroblocks of the P-pictures were all interframe coded. Had any macroblock been intraframe coded, its retrieval through RVLC would have improved the picture quality.

These differences are significant enough to ask which one of the H.263 or MPEG-4 might be suitable for video over mobile networks. In late 1990s, an international collaboration under the project 3gpp (third-generation partnership project) set up extensive investigation to compare the performance of these two codecs [24]. The outcome of one of the experiments is shown in Figure 10.38.

In this experiment, wireless channels of 64 kbit/s were used, of which 7.6 kbit/s were assigned to speech signal. The remaining bits were the target video bit rates for coding of the overtime video test sequence for the two codecs, including the overheads. The channel errors were set to 10^{-6}, 2×10^{-4} and 10^{-3} for both fixed and mobile sets, identified by F and M in the figure, respectively. The H.263 codec is equipped with annexes D, F, I, J and N (see list of H.263 annexes in Chapter 9 [22]) and that of MPEG-4 was the simple profile (see section 10.1). The performance of the reconstructed pictures after error concealment was subjectively evaluated. The average of the viewers' scores (see section 2.4) as the mean opinion score (MOS) is plotted in Figure 10.38 against the tested error rates.

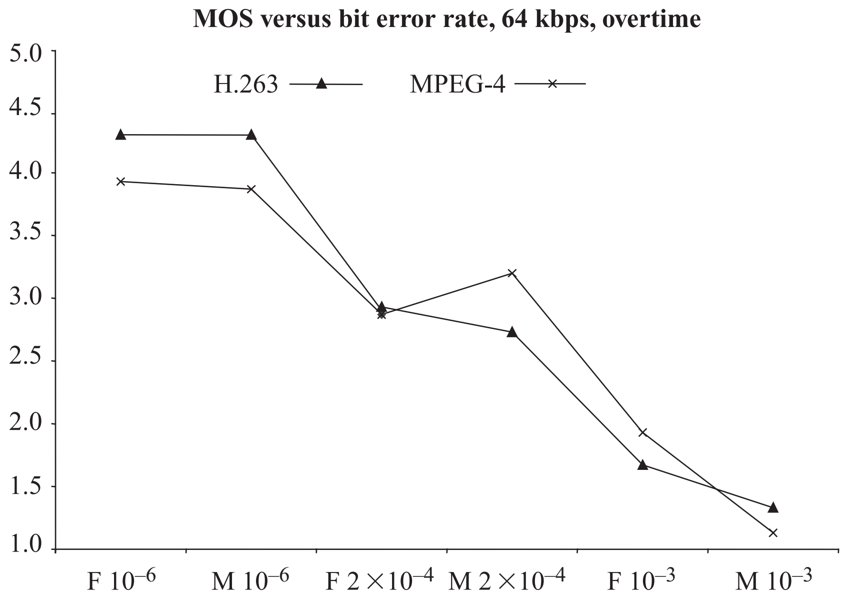

Figure 10.38 Comparison between MPEG-4 and H.263

At the low error rate of 10^{-6}, H.263 outperforms MPEG-4 for both mobile and fixed environments. Thus, it can be concluded that H.263 is a more compression efficient encoder than the MPEG-4. Much of this is due to the use of RVLC in the MPEG-4, as we have seen in Table 9.3, RVLC is less compression efficient than MPEG-4. Other overheads, such as packet header, more frequent resynchronisation markers add to this overhead. On the other hand, at high error rates, the superior error resilience of MPEG-4 over H.263 compensates for compression inefficiency and in some cases the decoded video under MPEG-4 is perceived better than H.263.

Considering the above analysis, one cannot for sure say whether H.263 is better or worse than MPEG-4. In fact, what makes bigger impact on the experimental results is not the basic H.263 or MPEG-4 definitions, but the annexes or optionalities of these two codecs that make all the differences. For example, had data partitioning (Annex V) been used in H.263, it would have performed as well at high error rate as MPEG-4 would have. Unfortunately, data partitioning in H.263 was introduced in 2001, while this study was carried out in 1997. Hence, the 3ggp project fails to show the true difference between the H.263 and MPEG-4.

10.13 Problems

1. Figure 10.39 shows a part of a binary alpha plane, where shaded pixels are represented by 1 and blank pixels by 0:
   a. calculate the context number for pixels A, B and C
   b. use the intra table of Appendix D to calculate the probability for coding of alpha pixels A, B and C

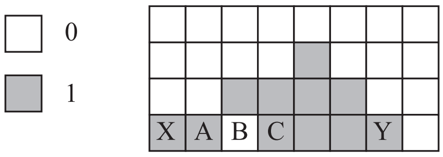

Figure 10.39

2. Draw a part of the contour of the shape of Figure 10.39 starting from point X and ending at point Y. Use the Huffman Table 10.1 to calculate the number of bits required to differentially chain code the part of the contour from X to Y.
3. Figure 10.40 shows a part of quad tree binary alpha block (BAB). Assume shaded pixels at level 3 are binary 1 and blank ones binary 0:
   a. calculate the index of each pixel at level 2
   b. calculate the index of pixel at level 1

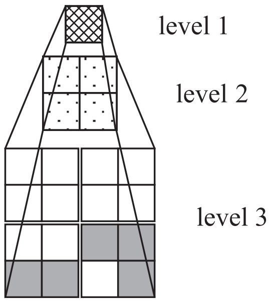

Figure 10.40

4. A part of a foreground texture within an 8×8 pixel block is shown in Figure 10.41. The background pixels are shown in blank. The block is DCT coded and the quantised coefficients with a step size of $th = q = 8$ are zigzag scanned. Compare the efficiency of the following two coding methods:
   a. use an SA-DCT to code the block, assume that the shape of this object is available to the decoder
   b. use normal DCT, but assume the background pixels are zero

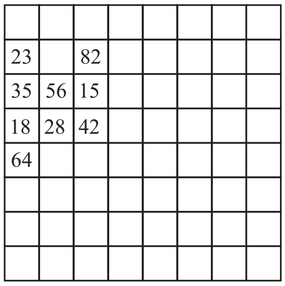

23		82					
35	56	15					
18	28	42					
64							

Figure 10.41

References

1. KOENEN, R., PEREIRA, F. and CHIARIGLIONE, L.: 'MPEG-4: context and objectives', *Image Commun. J.*, 1997, **9:4**, pp. 295–304
2. MPEG-4: 'Generic coding of audio-visual objects: Part 2 - visual', ISO/IEC JTC1/SC29/WG11 N1902, FDIS of ISO/IEC 14496-2, Atlantic City, November 1998
3. MPEG-4 video verification model version-11, ISO/IEC JTC1/SC29/WG11, N2171, Tokyo, March 1998
4. Special issue on segmentation, *IEEE Trans. Circuits Syst. Video Technol.*, 1998, **8:5**
5. KASS, M., WITKIN, A. and TERZOPOULOS, D.: 'Snakes: active contour models', *Inter. J. Comput. Vis.*, 1987, **1**, pp. 321–331
6. ROERDINK, J.B.T.M. and MEIJSTER, A.: 'The watershed transform: definitions, algorithms, and parallellization strategies', *Fundamental Informatics*, 2000, **41**, pp. 187–228
7. IZQUIERDO, E. and GHANBARIM, M.: 'Key components for an advanced segmentation systems', *IEEE Trans. Multimedia*, 2002, **4:1**, pp. 97–113
8. PERONA, P. and MALIK, J.: 'Scale-space and edge detection using anisotropic diffusion', *IEEE Trans. Pattern Anal. Mach. Intell.* 1990, **12:7**, pp. 629–639
9. SHAFARENKO, L., PETROU, M. and KITTLER, J.: 'Automatic watershed segmentation of randomly textured color images', *IEEE Trans. Image Process.*, 1997, **6:11**, pp. 1530–1544
10. WYSZCKI, G. and STILES, W.S.: *Color Science: Concepts and Methods, Quantitative Data and Formulae*, 2nd edn, Wiley, Hoboken, NJ, 1982
11. VINCENT, L., and SOILLE, P.: 'Watersheds in digital spaces: an efficient algorithm based on immersion simulations', *IEEE Trans. Pattern Anal. Mach. Intell.*, 1991, **13:6**, pp. 583–589
12. MPEG-4: 'Video shape coding'. ISO/IEC JTC1/SC29/WG11, N1584, March 1997
13. GHANBARI, M.: 'Arithmetic coding with limited past history', *Electron. Lett.*, 1991, **27:13**, pp. 1157–1159
14. PEARSON, D.E.: 'Developments in model-based video coding', *Proc. IEEE*, 1995, **83:6**, pp. 892–906
15. WOLBERG, G.: 'Digital Image Warping', IEEE Computer Society Press, Los Alamitos, CA, 1990
16. SEFERIDIS, V. and GHANBARI, M.: 'General approach to block matching motion estimation', *J. Opt. Engineering*, 1993, **37:7**, pp. 1464–1474
17. GHANBARI, M., De FARIA, S., GOH, I.J. and TAN, K.T.: 'Motion compensation for very low bit-rate video', *Signal Process. Image Commun.*, special issue on very low bit-rate video, 1995, **7:(4–6)**, pp. 567–580
18. SHAPIRO, J.M.: 'Embedded image coding using zero-trees of wavelet coefficients', *IEEE Trans. Signal Process.*, 1993, **4:12**, pp. 3445–3462

19. WITTEN, I.H., NEAL, R.M. and CLEARY, J.G.: 'Arithmetic coding for data compression', *Commun. ACM*, 1987, **30:6**, pp. 520–540
20. WANG, Q. and GHANBARI, M.: 'Motion-compensation for super high definition video', Proceedings of IS&T/SPIE Symposium, on Electronic imaging, science and technology, very high resolution and quality imaging, San Jose, CA, 27 January–2 February, 1996
21. SAID, A. and PEARLMAN, W.A.: 'A new, fast and efficient image codec based on set partitioning in hierarchical trees', *IEEE Trans. Circuits Syst. Video Technol.*, 1996, **6:3**, pp. 243–250
22. WANG, Q. and GHANBARI, M.: 'Scalable coding of very high resolution video using the virtual zero-tree', *IEEE Trans. Circuits Syst. Video Technol.*, special issue on multimedia, 1997, **7:5**, pp. 719–729
23. KHAN, E. and GHANBARI, M.: 'Very low bit rate video coding using virtual SPIHT', *Electron. Lett.,* 2001, **37:1**, pp. 40–42
24. 3rd Generation Partnership Project (3gpp): TSG-SA codec working group, release 1999, technical report TR 26.912 V 3.0.0

Chapter 11
Advanced video coding (H.264)

The ITU-T video coding experts group, after successful completion of their H.263 video codec in 1995, started to work on the advanced video coding (AVC) project. Their long-term objective was to recommend a video codec to be at least twice better than the existing video codec, such as H.263. The project was initially called H.26L, with L standing for long-term objectives [1]. However, H.263 was under constant improvement. Its improved version under H.263+ was finalised in 1997, and in 2000, the H.263++ specification was ratified, where each + is an indication of major improvement. Most of the innovations in H.263+ in the forms of options or annexes were also fed to H.26L. ITU-T submitted H.26L to MPEG call for proposals in 2001. MPEG-4 experts group of ISO/IEC, who were not very happy with their content-based video codec (due to high complexity the codec could not be marketed), and its frame-based counterpart had a similar performance to H.263, showed an interest in this new codec. They joined the AVC project and worked closely with the ITU-T team. The project's name was then changed to joint video team (JVT).

The final work of H.264 was recommended by ITU-T as H.264 in 2003. This codec in ISO is known as 14496-10 or MPEG-4 part 10. Since the project started as AVC, it is informally known as AVC. Finally, due to the joint team work of ITU-T and ISO, it is also known as JVT. However, eliminating any confusion with all these names as well as the MPEG-4 content-based (visual) codec of Chapter 10, in this chapter, we refer to this codec mainly as H.264/AVC, or simply H.264.

The H.264 codec, since its formal introduction in 2003, has proven to be a universally accepted video codec for all kinds of applications. Now in 2010, it is the codec for all new video services. For telecommunications, it has replaced H.263 and is the de facto video compressor for both terrestrial and satellite broadcast of digital high definition (HD) TV. Although terrestrial and satellite broadcast of digital TV in Europe is on MPEG-2, because when these services were launched in 1998, H.264 was not available, now countries who want to start broadcasting digital SD TV are seriously thinking of using H.264. This is mainly due to at least twice better compression performance of H.264 over MPEG-2, which makes it possible to double the number of TV programmes in the satellite transponders and the terrestrial UHF channels. Such a trend is also seen in storage of high-quality video on Blu-ray, for increased quality and storage efficiency. Finally, for new video services launched by telcos, such as IPTV, video over Internet, catch-up TV and video streaming in general, H.264 family are the only codecs. A variant of this codec, such as Microsoft VC1, Chinese AVS, X.264, DivX+ and Sorenson, which are based on H.264, are becoming a household tool kit. Like other standards, there is a laboratory software model for this codec, called joint mode (JM), and its latest version is given in [4]. Now in 2010, we can only say that H.264 is a codec for all video communication, distribution, storage and networking applications.

Towards the end of this chapter, we will compare H.264 compression efficiency over the other standard codecs. However, early simulations with the nuclei of this codec, H.26L, had shown substantial superiority over most optimised H.263 and frame-based MPEG-4 (visual or part 2) codecs. Most notable features of this new codec are as follows:

- **Up to 50 per cent in bit rate saving**: Compared to H.263+ (H.263V2) or MPEG-4 simple profile (MPEG-4 visual or part 2, see Chapter 10), the new codec achieved an average reduction in bit rate by up to 50 per cent for a similar degree of encoder optimisation at most bit rates. This means that H.264 offers consistently higher quality at all bit rates including low bit rates over the previous standards.
- **Adaptation to delay constraints**: H.264/AVC can operate in a low-delay mode to adapt telecommunication applications (e.g. H.264 for videoconferencing), while allowing higher processing delay in applications with no delay constraints such as video storage and server-based video streaming applications (MPEG-4 part 10).
- **Error resilience**: H.264 provides the tools necessary to deal with packet loss in packet networks and bit errors in error-prone wireless networks.
- **Network friendliness**: The codec has a feature that conceptually separates the video coding layer (VCL) from the network abstraction layer (NAL). The former provides the core high-compression representation of the video picture content, and the latter supports delivery over various types of network. This facilitates easier packetisation and better information priority control. The NAL can provide compressed video data in two formats, for the stream-based protocols like H.320, H.324 or MPEG-2 and for the packet-based protocols like RTP/IP and TCP/IP. For the stream-based protocols, the data are provided with start codes such that the transport layers and the decoder can easily identify the structure of the bitstream. For the packet-based protocol, the bit structure is identified by the packet headers [5].

Before going into details of how this codec works, let us look at some of its features, which are different from that of its predecessors.

- Two entropy coding schemes, context-adaptive variable length coding (CAVLC) and context-adaptive binary arithmetic coding (CABAC).
- Multiple reference pictures motion compensation as well as allowing B-slices to be used as references, even for P-slices.
- Variable block size motion estimation from 4×4 to 16×16 pixels.

- Quarter-pixel precision motion compensation with improved prediction accuracy and lower interpolation complexity.
- Directional spatial prediction in intra coded macroblocks (MBs) for efficient compression.
- The discrete cosine transform (DCT) is replaced by a reversible integer transform avoiding inverse transform mismatch.
- Variable block size integer transforms of 8×8 and 4×4.
- Deblocking filter to remove artefacts caused by motion compensation and quantisation.
- Parameter sets are used between the encoder and decoder for syntax synchronisation.
- More error resiliency through flexible arrangement of MBs and slices.
- Data partitioning (DP) and packetisation of video slices into three priority levels to provide transmission protection.
- Redundant transmission of some regions to enhance robustness to data loss.
- Synchronisation/switching pictures for robust video streaming.

Despite the above mentioned differences, H.264 has its roots in the other standard codecs, especially in the H.263 standard. Hence, in describing the codec with the aim of addressing these specific changes, it is assumed that the reader is not only familiarised with the principles of video compression, given in the previous chapters, but has also read Chapter 9 on H.263. However, to make this chapter self-contained, some important concepts of previous standards are revisited.

11.1 Picture format

The H.264 standard supports both interlaced and progressive video. Since its main function is video distribution, the picture format is 4:2:0, though for contribution where higher-quality colour is required, 4:2:2 format may also be used, as well as the 4:4:4 format for the high 4:4:4 profile. Like other standard codecs, an MB of 16×16 pixels is the basic unit of compression, which, when coding 4:2:0 sampled video, is comprised of 16×16 luminance (luma) pixels and 8×8 pixels for each of C_b and C_r chrominance colour components (chroma). Each MB can optionally be further subdivided into smaller blocks, called sub-MBs, to provide the possibility of better compression gain. Further partitioning is a result of trade-off between efficient motion compensation with smaller blocks and the amount of data required to represent the motion vector (MV) overhead. Various MB partitions are discussed in the motion estimation section (section 11.3.1).

11.1.1 Slicing

A group of MBs represent a picture slice, or simply a slice. In this standard, slice structure is of arbitrary shape, which is different from the other standards, as shown in Figure 11.1*a*. For interlaced video, when MB-adaptive frame/field (MB-AFF) decoding is used, the picture is partitioned into slices containing an integer number of MB pairs, as shown in Figure 11.1*b*.

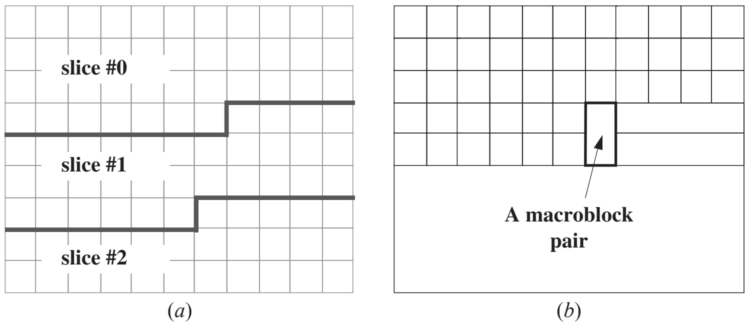

Figure 11.1 (a) Subdivision of a picture into slices and MB. (b) Slices with MB pairs

Different numbers of MBs are normally raster scanned from left to right and top to bottom to form a slice. Other forms of slice structure, like flexible macroblock ordering (FMO), are also available, which are discussed in the error resilience section (section 11.8.2). There is no constraint on the size of a slice; its size ranges from one MB per slice to an entire picture per slice.

As usual, slices are a self-contained group of MBs, where they can be encoded and decoded independent of each other. Hence, the syntax elements of each slice can be parsed from the bitstream, and the portion of picture can be decoded independent of other slices. This of course reduces the compression gain of the encoder, but it prevents error propagation, which is important for video transmission. However, at the slice boundaries, information from adjacent slices is used in the deblocking filter.

Each slice has a header that defines the slice type and the picture to which the slice belongs. The slice data consist of a series of coded and/or information about the non-coded (skipped) blocks. Slicing involves overhead depending on the bit rate, image content, motion activity, interlacing, redundant slices, etc. The maximum overhead per slice can be as high as 54 bytes, which is a very significant figure for low bit rate applications. Various forms of slices in terms of number of MBs are as follows:

- One slice per picture: It is the simplest picture slice in which the whole picture is coded as one slice. This may lead to larger packet size than what the communication protocol (e.g. IP layer) can handle, and hence, data can be fragmented during transmission.
- Fixed number of MBs per slice: The picture is subdivided into slices, with the same number of MBs per slice. This results in packets with different lengths in bytes.
- Fixed number of bytes per slice: The picture is subdivided into slices having almost the same byte length but different number of MBs per slice. In this case, normally, a maximum packet size is specified, and if the slice is bigger than the maximum packet size defined, the remaining bytes go into a smaller packet.

Slices can be grouped for more error resilience coding. This is discussed in the error resilience section (section 11.8.2).

11.1.2 Slice types

Unlike other standards in which the coding tools are defined for picture types, in H.264 they are defined for slice types. H.264 defines five types of slice, which are as follows:

- I-slice: A slice where all the MBs are intra coded.
- P-slice: In addition to intra coded MBs, some MBs can be inter predicted with at most one motion-compensated prediction signal per block.
- B-slice: In addition to coding available to a P-slice, some MBs can be inter predicted with two motion-compensated predictions.
- Switching predictive (SP)-slice: A switching slice/picture used for efficient switching between two references to prevent picture drift.
- Switching intra (SI)-slice: Used for random access to a bitstream as well as for error recovery.

In the following sections, we explain how I-, P- and B-slices are coded, and in section 11.8.7 on robust video coding, SP- and SI-slices are explained.

It is worth emphasising that in H.264, there is no traditional picture header, though there is an optional picture delimiter. It is optionally inserted between the coded pictures to indicate the start of a new picture and to indicate the types of slices it contains. All slices representing a picture do not need to be of the same type, so a picture could be made up of a mixture of I-, P- and B-slices. Moreover, slice structure can be different from one picture to another. Despite this, for simplicity of description, and in line with most implementations, one may consider that all slice types of a picture are the same and, hence, define a picture of a specific type. Hence, one may also define group of pictures (GOP) for H.264 to highlight the existence of anchor (key) pictures. This is dealt with in section 11.12 on scalable video coding.

11.1.3 An overview of the encoder

Before explaining how these slices are coded, it is worth noting that H.264 uses the generic encoder of Figure 3.19, described in Chapter 3. That is, MBs are divided into smaller blocks (here 4×4), and they are then either intra or inter coded. The residual pixels resulting from the prediction (intra or inter) are transformed, zigzag scanned and quantised, and, along with other coding parameters, such as addressing, *MV*s are entropy coded for further bit rate reduction. A copy of the compressed MB is reconstructed to be used for prediction of the forthcoming MBs. The decoding loop of the encoder also contains a deblocking filter as well as several picture stores for multiple reference picture prediction, which are discussed in details later. Such a structure is similar to the H.263 codec of Figure 9.21.

There is no single element in this encoder that can claim the overall improvement in coding efficiency, but it is the combination of smaller improvements that add up for the entire gain in compression. In the remaining sections, each of these elements is described in details.

11.1.4 Progressive and interlaced coding

In coding of interlaced video, for higher compression efficiency, the H.264 design allows encoders to code a picture either in a frame or in a field mode. In the frame mode, every MB comprising of 16×16 luma pixels of the two fields is coded together. In the field mode, the picture is first divided into two fields, and then 16×16 luma pixels of each field represent an MB. This choice is signalled at the picture parameter set (PPS) and is called picture-adaptive frame/field (PAFF) mode. A field MB is coded similar to a frame MB, but reference *MV* should come from a field picture, and zigzag scanning is different. Also, strong deblocking filter should not be used in horizontal edges for field blocks, because the field rows are spatially twice as far apart as frame rows and the length of the filter thus covers a larger spatial area. Figure 11.2 shows the frame and field zigzag scans.

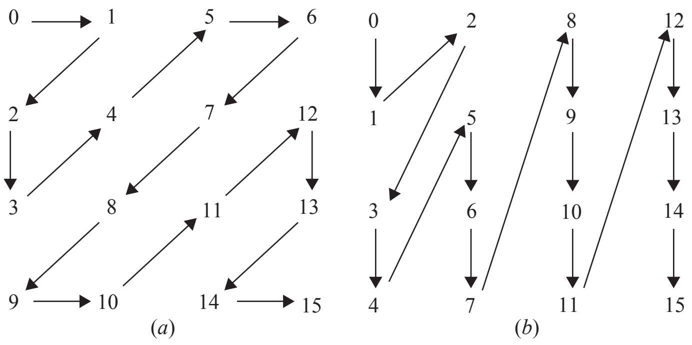

Figure 11.2 Zigzag scans: (a) frame scan and (b) field scan

Frame coding is better for progressive content as well as detailed slow-moving interlaced content. On the other hand, field coding is better for fast-moving content. However, if content is a mixture of both types, it is best coded if localised frame/field adaptation can be made. For this reason, H.264 defines a new block type made up of vertically adjacent pairs of MBs (Figure 11.1). When this mode is chosen, these MB pairs are then split into two 16×16 MBs of either frame or field, as shown in Figure 11.3. This mode of block-by-block adaptation is called macroblock adaptive frame/field MB-AFF mode. Presence of MB-AFF can be signalled at the sequence parameter set (SPS), as it is normally applied to the whole pictures in a sequence and does not change from picture to picture. The frame and field MBs are coded similar to the respective MBs of PAFF, as discussed above. It should be noted that throughout the chapter, picture is used as a general term for both frame and field, and if frame or field is specifically meant, they are explicitly mentioned.

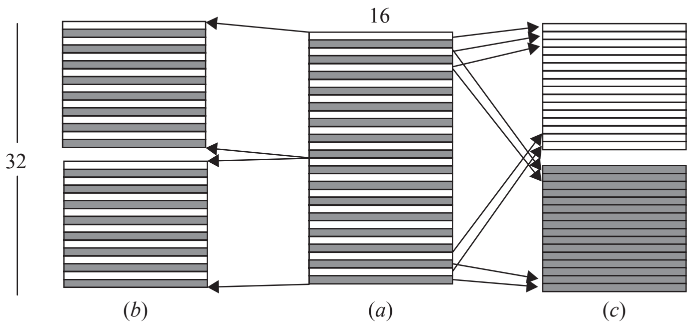

Figure 11.3 MB-adaptive frame/field mode: (a) a 16 × 32 block pair, (b) two frame pair MB and (c) two field pair MB

11.1.5 Macroblock syntax elements

Since MB is the basic encoding unit of any standard video codec, for proper decoding of pictures, the decoder needs to know how an MB was coded. This information is known as the MB syntax, and its elements include MB type (*mb_type*), which determines its intra-, inter- and bidirectional prediction nature (I, P and B), the mode, where for intra- and inter-MB what predictions they have used as well as the list (see section 11.3). *MV*s are differentially addressed, and *sub_mb* prediction defines how the partitions of an MB are predicted. *mb_qd* delta indicates the changes in the quantiser parameter (*QP*), and its offset indicates the relative *QP* of chroma to luma. Coded block pattern (CBP), like other standards, defines which blocks of an MB are not coded, how they are addressed and, finally, where the transform coefficients are.

11.2 Intra prediction

Intra coded MBs are used in all types of slice, and for efficient compression, they are spatially predictive coded. The spatial predictions are made from the decoded pixel blocks to the left and/or above the current block from the same picture. This is a major difference in intra coding between H.264 and the previous standards, such as H.263+ and MPEG-4 visual, which use prediction in the transform domain (see section 9.6.4).

Spatial prediction is based on the idea that adjacent MBs tend to have similar textures, improving the predicted signal quality. Since adjacent blocks may be inter coded, to prevent error propagation, a constraint on intra prediction can be imposed such that prediction should only come from the intra coded areas.

There are three types of intra coding modes for the luma known as intra 4 × 4, intra 16 × 16 and I_PCM, though intra 8 × 8 does also exist, which uses similar prediction pattern to intra 4 × 4 (see later in this section). In the intra 4 × 4 mode, an MB is divided into 16 blocks of size 4 × 4 pixels and each has an independently specified prediction mode; this is best suited for the picture areas with significant details. In the intra 16 × 16 mode, all pixels of an MB use the same prediction mode. In I_PCM, the prediction and transformation are bypassed, and the raw values of the pixels (PCM) are sent without performing any prediction and transform coding; this mode is primarily intended to prevent data expansion when encoding at very high quality.

11.2.1 Intra 4 × 4

In the intra 4 × 4 mode, each 4 × 4 block is predicted spatially from the neighbouring encoded and reconstructed blocks. There are a total of nine prediction modes in which eight are directional and one is DC. In Figure 11.4*a*, the pixels of a 4 × 4 block to be predicted are labelled a–p. The prediction pixels are the border pixels A–H in the upper horizontal row and M–L in the left vertical row of the current block that come from the past reconstructed blocks as reference blocks. The eight directional predictions are shown in Figure 11.4*b* labelled from 0 to 8 and are known as mode 0 (vertical), mode 1 (horizontal), mode 3 (diagonal down left), mode 4 (diagonal down right), mode 5 (vertical right), mode 6 (horizontal down), mode 7 (vertical left), mode 8 (horizontal up) and a nondirectional DC mode 2. Figure 11.5 shows the directions of various modes applied to the pixels of the current block. Predictions for modes 0 and 1 are, respectively, the top and left border pixels. In mode 2, the prediction is the average of four top and four left border pixels. For the other six modes, various combinations of border pixels, even within the mode, are used. For example, in mode 3 (diagonal down left), predictions for samples are

$$
\begin{aligned}
&a\text{: } (A + 2B + C + 2) \gg 2\\
&b \text{ and } c\text{: } (B + 2C + D + 2) \gg 2\\
&c, f \text{ and } i\text{: } (C + 2D + E + 2) \gg 2\\
&\text{but prediction for sample } p\text{: } (G + 3H + 2) \gg 2
\end{aligned} \tag{11.1}
$$

Readers should consult draft recommendation for details [3], as for some modes, due to the availability of the border pixels and prediction direction, a complex mixture of border pixels are used.

It is obvious that if the block texture is in any of these directions, the prediction error would be minimal, resulting in bit rate reduction. DC mode does the same if block is plain with no significant details. Note that every 4 × 4 block may use a different prediction mode.

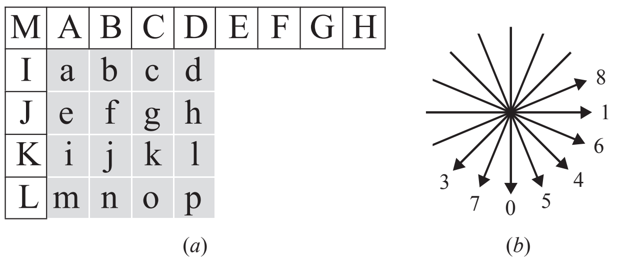

Figure 11.4 Intra 4 × 4 prediction: (a) prediction samples and (b) prediction directions

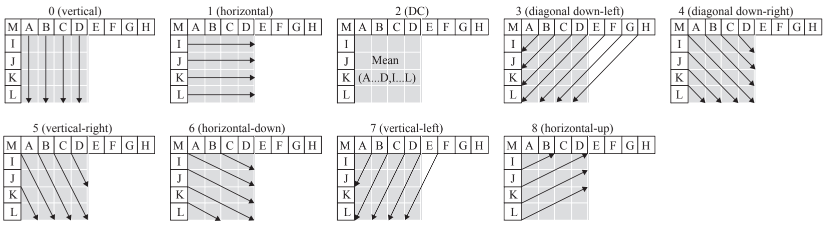

Figure 11.5 Intra 4 × 4 prediction modes

In case the prediction samples E–H are not available for modes 3 and 7, they are replaced by sample D.

11.2.2 Intra 16 × 16

In intra 16 × 16, the MB is treated in its entirety but with only four prediction modes. They are mode 0 (vertical), mode 1 (horizontal), mode 2 (DC) and mode 3 (plane) as shown in Figure 11.6. These modes are similar to the corresponding modes in intra 4 × 4, with difference in the block size. The plane prediction uses a linear prediction between the neighbouring pixels to the left and top to predict the current pixel.

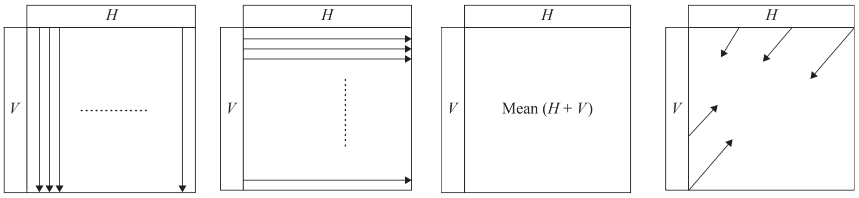

Figure 11.6 Intra 16 × 16 prediction modes

Intra 16 × 16 is efficient in smooth and low detailed areas, as it has much lower overhead than intra 4 × 4. The entropy of overhead per MB for the former is 2 bits (4 modes), and for the latter, this value is $16 \times \log_2(9) \approx 51$ bits! On the other hand, intra 4 × 4 with nine directional predictors and small block size (pixels are very close to the predictions) result in small residue, reducing the transform coefficient bits. To reduce the overhead and, at the same time, to have a good predictor, the standard also defines intra 8 × 8. In this mode, each 8 × 8 block also uses nine directional predictors, similar to intra 4 × 4, and hence, the overhead is only $4 \times \log_2(9) \approx 13$ bits. However, since pixels in blocks of 8 × 8 are farther away from their predictors than those of 4 × 4 blocks, the residues are larger, reducing the compression gain.

11.2.3 Chroma prediction

Since chroma is usually smooth over large areas, its intra predictions are similar to the luma samples of intra 16 × 16. However, mode numbering is different, and predictions are carried out on 8×8 samples of each chroma MB. In intra chroma, the prediction modes are defined as mode 0 (DC), mode 1 (horizontal), mode 2 (vertical) and mode 3 (plane).

11.2.4 I_PCM

Finally, I_PCM is another intra coding mode, but as stated before, the encoder bypasses the prediction and transformation and the data are sent in the raw PCM format. The I_PCM mode helps in accurately representing the values of the anomalous picture contents without significant data expansion. It also places a hard limit on the number of bits per MB a decoder must handle without compromising the coding efficiency.

11.3 Inter prediction

Interframe predictive coding refers to encoding the difference between pixels of the current picture and the predicted ones from reference pictures. The reference pictures are the previously encoded pictures, and both the encoder and decoder maintain a list of these pictures in the decoded picture buffer (DPB). Pictures used for prediction of blocks in P-slices are referred to in list 0, and for B-slices, the reference pictures are divided into two lists: list 0 and list 1. Both lists can contain previous and future pictures, and hence, in H.264, blocks in P-slices can also be predicted from the future pictures.

In multipicture prediction, during encoding, it is determined whether a previously decoded picture is to be used as a future reference picture and, if it is a reference picture, whether it should belong to a short term of references or a long term. A short-term reference picture is normally the most recent one, and a long-term reference picture is the one that is most likely to be used for prediction of many forthcoming pictures. This decision is carried out by the reference picture management system. The system also uses a sliding window, with a size determining the maximum number of short- and long-term reference pictures, such that when a recent reference picture is added to the list, an old picture is deleted from the list. The system also decides whether a reference picture of either short or long term for B-slices should belong to list 0 or list 1.

Since interframe coding involves motion-compensated prediction, in terms of motion estimation, interframe coding in H.264 has three distinct differences from the previous standards, which are

1. variable block size motion estimation,
2. quarter-pixel precision of *MV*s and
3. multiple reference picture motion compensation.

11.3.1 Variable block size motion estimation

In the previous standards, motion estimation/compensation is performed on fixed size blocks of 16×16 pixels (8×8 also in H.263). Large blocks are not suitable for motion estimation when the block size is comparable or bigger than the size of the moving object. This mostly happens for QCIF images, where a large block may contain motions at several directions. Surely, motion compensation of such a block is not plausible. Also, for larger-size picture formats, like SD and HD, motion of objects at their borders can be better compensated with smaller block sizes. On the other hand, smaller block sizes require a large overhead. To overcome this problem, H.264 has introduced variable block size motion compensation, which allows an MB to be partitioned into seven different size blocks as illustrated in Figure 11.7.

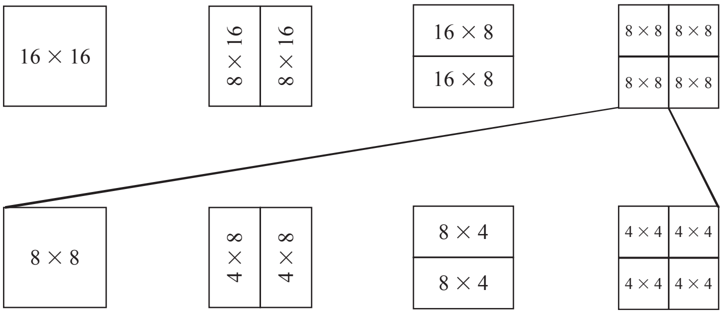

Figure 11.7 Block partition types

In the figure, a luma MB 16 × 16 can be partitioned into 16 × 8, 8 × 16 and 8 × 8 pixel sub-MBs. If an 8 × 8 sub-MB is selected, then it can be further divided into smaller blocks of 8 × 4, 4 × 8 and 4 × 4 pixels. This partitioning of MBs into motion-compensated sub-MBs is sometimes called tree-structured motion compensation.

Partitioning of the MB into smaller blocks is carried out such that cost of coding of the MB is minimised. In plain areas, larger block sizes have less *MV* overheads. On the other hand, smaller block sizes in detailed areas, despite having larger *MV* overhead, have much reduced motion-compensated error, and the overall bit rate is reduced. Some well motion-compensated blocks need not be transform coded and are just represented by their *MV*s (e.g. skipped MBs), where the *MV*s themselves need not be sent at all.

It may appear that multiple block size motion estimation increases motion estimation complexity by a factor of seven. Of course, by proper implementation, this huge volume of complexity can be simplified. In practice, for every MB, motion is only estimated for the sixteen 4 × 4 block sizes, and for each search position, the motion-compensated error (MCE) in the form of sum absolute difference (SAD) is stored in an auxiliary buffer. To derive *MV*s for 4 × 8 blocks, first, for any position (*x*,*y*), the SAD of the two 4 × 4 constituent blocks is retrieved from the buffer. If the estimated bits associated with the sum of the two SADs plus the entropy of the new *MV* are less than the sum of two individual 4 × 4 block bits (their estimated SAD bits plus their *MV* bits), then 4 × 8 (or 8 × 4) can replace the two 4 × 4 blocks. Note that in order a block of two 4 × 8 (or 8 × 4) to replace four subblocks of 4×4, the other 4×8 (or 8×4) part of the block is also required to have lower estimated bits than its corresponding two 4×4 subblocks. If this is not satisfied, the four 4×4 subblocks cannot be replaced by two 4×8 (or 8×4), since a block of only one part with 4×8 and two parts with 4×4 is not allowed.

Also, how to search for the best position of (x,y) in the auxiliary buffer is a matter of implementation issue (standard has no recommendation for any parts of the encoder as well as for motion estimation), but common sense says that the search position (x,y) should be at the vicinity of the *MV*s of the two participating 4×4 subblocks.

With a similar procedure, it can be tested if the four 4×4 subblocks can be represented by one 8×8 block, as well as merging 8×8 blocks to bigger 8×16, 16×8 and 16×16 blocks. Hence, the extra complexity over the individual 16 motion searches of the 4×4 subblocks includes an auxiliary buffer, small motion refinement plus a set of rate distortion (RD) optimisations. The latter part is dealt with in some details in section 11.7. Throughout this chapter, we see that RD optimisation is involved in almost all the decision-making parts of the H.264 encoder.

The positions of the derived *MV*s are predictively coded, with the median of left, top and top-right *MV*s, similar to those used in H.263 (section 9.1.2). The predictions for the *MV*s of subblocks come from the neighbouring *MV*s of the subblocks within the MB.

11.3.2 Motion estimation

11.3.2.1 Fast motion estimation in H.264

Throughout the book, the importance of motion compensation for bit rate reduction has been reiterated several times. We have seen that there was no new codec and that its motion estimation strategy had not been improved. Moreover, since motion estimation consumes the major processing power of the encoder (could be as high as 70 per cent, especially with multiple reference pictures), attempts to reduce the motion estimation complexity have long lived with the developments of the codecs. In section 3.3, several fast motion estimation algorithms were introduced, where, through a logarithmic step search, the local minima is located. Unfortunately, these methods work well when the search area is small, and they fail when the dynamic range of the motion is large. The bad news is that when multiple reference picture motion compensation is used, the search range is multiplied by the furthest picture distance, which could be as high as 16 pictures (could be longer – depends on how the DPB is managed). In such a large range, direct use of previous fast motion estimation algorithms like TSS, TDA, CSA and OSA all fail.

Considering that standard does not recommend any specific method for motion estimation and as long as the derived *MV* syntax complies with the decoder requirement, encoders are free to estimate it as best as they can. From the several proposals for fast motion estimation in the past decade, the methods that exploit the spatio-temporal correlations among the adjacent spatial and temporal *MV*s appear to perform best. Zonal search algorithms like predictive *MV* field adaptive search technique (PMVFAST) and enhanced predictive zonal search (EPZS) belong to these families that have almost equal RD performance to the full search method (FSM), and it is claimed to have 1/200 of its computational complexity [6].

The zonal search methods are based on three principles: predicting a starting point for search, early termination of search if the resultant motion-compensated error is less than a threshold and, finally, refinement of search if the motion-compensated error is still not satisfactory. In the following sections, these methods are briefly explained.

11.3.2.2 Prediction selection

The cost of search is significantly reduced if the search starting point is as close to the final displacement position as possible. EPZS suggests four subsets of predictors for the starting point. These predictors are selected in the following order of their priority:

Subset 1: The median of left, top and top-right (or top-left) *MV*s of the current block is the first choice for the starting point. This is an ideal position, because if the final *MV* is found at the vicinity of this point, since the *MV*s are predicatively coded with prediction from that median value, then the *MV* overhead is minimised.

Subset 2: The *MV* of the colocated block in the previous picture, along with the four *MV*s of left, top-left, top and top-right of the current block as well the (0,0) *MV* (total of six), is tested. The one that gives the least motion-compensated error is chosen.

Subset 3: Use of adjacent or colocated *MV*s in subsets 1 and 2 is useful if motion is respectively homogeneous or constant. When motion between the pictures varies, adding acceleration/deceleration to the previous pictures *MV*s improves prediction reliability. In this case, for instance, the *MV* difference between pictures $n-2$ and $n-3$, $MV_{n-2} - MV_{n-3}$ can be added to the colocated *MV* at picture $n-1$, MV_{n-1} to make a prediction for the current block. At this stage, the eight surrounding *MV*s of the colocated block can also be offset with this accelerator/decelerator and used as candidates. It appears that among these eight candidates, the diagonal blocks are not very useful, and to save computational cost, they can be ignored, and the *MV*s of the colocated block plus the four left, right, top and bottom blocks, after being offset, become the five candidates in subset 3.

Subset 4: Although predictions of the previous subsets give almost good results, there are times when motion is not predictable, and in this case, prearranged fixed search positions might be preferred. These positions can be spaced either equally or logarithmically around the main centre (0,0) or even around the best predictor of any subset. The density and the number of these positions define the complexity and quality of search, as tightly spaced positions are equal to full search. Figure 11.8 shows a grid of equally spaced positions for a search range of 16 pixels.

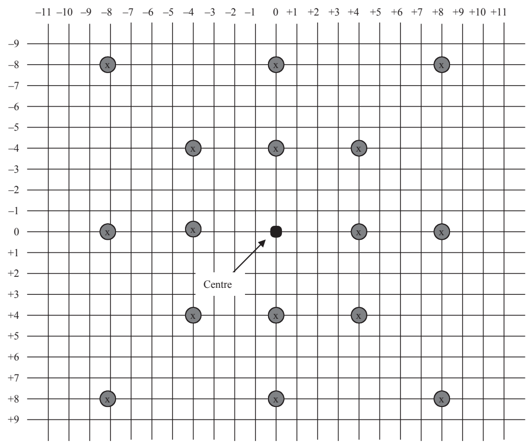

Figure 11.8 Additional fixed predictor grid for search range 16

11.3.2.3 Early termination

In search for a good predictor in any subset, if the resultant motion-compensated error is satisfactory, that is, it is less than a threshold, the search can be terminated. To find a proper threshold level, one may consider that motion-compensated errors of adjacent blocks, similar to the *MV*s themselves, tend to be highly correlated. Hence, a measure of past motion-compensated errors might be used as the threshold. Threshold values may vary from subset to subset and can depend on the block type as well as the temporal distance of the reference picture to the current picture. Although setting a suitable threshold level looks simple, it should be carried out with great care. Too small values of a threshold may not lead to any early termination, and hence, the search for the best predictor is wasted. Too large values can lead to early termination, producing a false *MV*, impairing motion compensation efficiency.

11.3.2.4 Motion vector refinement

With proper threshold values, if the early termination does not occur, it means that the estimated *MV*, so far, is not desirable and further refinement is required. The additional search around the best predicted *MV* of the four subsets may have various patterns and ranges. Figure 11.9 shows some of the patterns, like small diamond, square and large diamond patterns [6].

Any of these may be iteratively used to refine the *MV*. Iteration means that at the end of the search of all the points, the position with the least distortion becomes a new centre and the search is repeated, as shown in Figure 11.10. The search can be terminated at either meeting a threshold value or reaching a maximum search range.

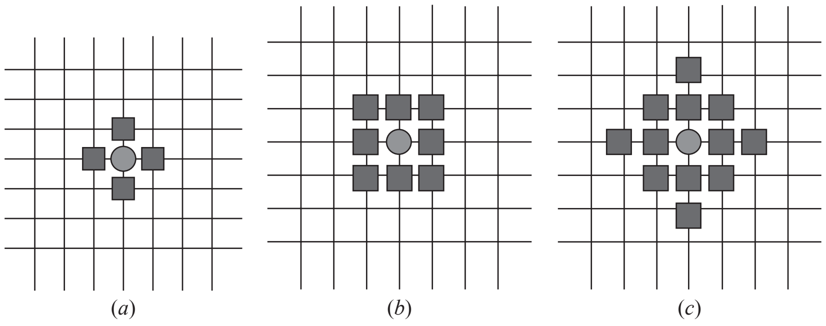

Figure 11.9 Search patterns: (a) small diamond, (b) square and (c) large diamond

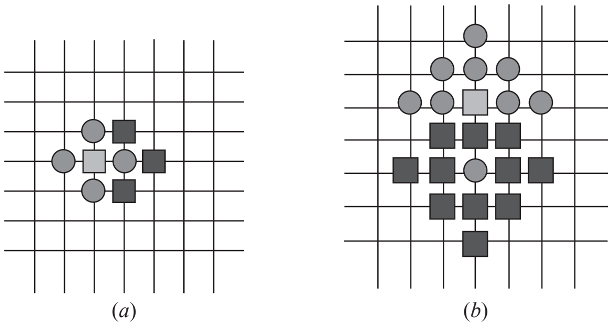

Figure 11.10 Iteration of search for (a) small diamond and (b) large diamond

11.3.3 Fractional precision of motion vectors

Equally important to variable block size motion compensation is the fractional bit representation of the *MV*s. In section 9.4.3, it was shown that half-pixel precision motion compensation can improve the compression gain of an encoder by almost 2 dB. In H.264, the precision of estimated motion for luma and chroma samples can be up to one-quarter and one-eighths of pixel, respectively, in both horizontal and vertical directions. To estimate motion with fractional-pixel precision, the estimated *MV*s pointing to an integer sample location of the previous section undergo another round of refinement. In this round, the current block is contrasted against the interpolated pixels of the reference block from the integer positions. For half-sample precision, the interpolation is carried out by a six-tap FIR filter vertically and horizontally. For the quarter-pixel motion compensation, interpolation is done by averaging samples at already found half-pixel positions or their integer positions, as need be [7].

Figure 11.11 shows the interpolation at fractional sample positions for the luma samples *a–s* inside the box. In the figure, integer samples found at the first round of search are shown in shaded blocks with upper case letters. The interpolated samples

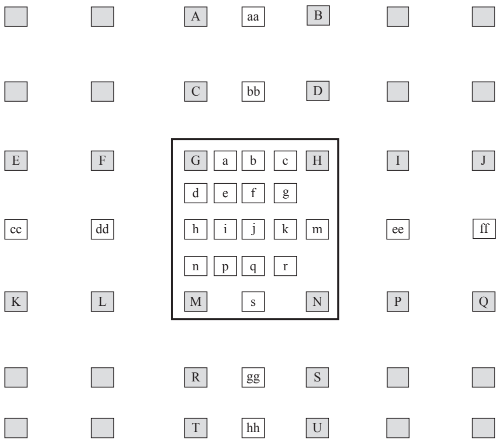

Figure 11.11 Integer half- and quarter-pixel positions

with quarter-sample precision are shown in unshaded blocks with lower case letters. For a half-sample interpolation like that at position b and h, a six-tap filter with coefficients of (1, −5, 20, 20, −5, 1) is used in a two-step operation. First, the intermediate values b_1 and h_1 are derived by applying the filter horizontally and vertically, respectively, on the integer positions A, C, E, ... of the figure as

$$b_1 = (E - 5 \times F + 20 \times G + 20 \times H - 5 \times I + j) \tag{11.2}$$

$$h_1 = (A - 5 \times C + 20 \times G + 20 \times M - 5 \times R + T)$$

The final values of b and h are calculated by rounding and clipping the above values in the range 0–255:

$$\begin{aligned} b &= clip(b_1 + 16) \gg 5 \\ h &= clip(h_1 + 16) \gg 5 \end{aligned} \tag{11.3}$$

The half-sample value at the centre, j, is derived in a similar manner and can be done in two ways:

$$j_1 = cc - 5 \times dd + 20 \times h_1 + 20 \times m_1 - 5 \times ee + ff$$

or

$$j_1 = aa - 5 \times bb + 20 \times b_1 + 20 \times s_1 - 5 \times gg + hh \tag{11.4}$$

and is rounded and clipped in the range 0–255.

$$j = clip(j_1 + 512) \gg 10$$

The remaining half-sample values s and m are calculated similar to b and h, with the final values of

$$s = clip((s_1 + 16) \gg 5)$$
$$m = clip((m_1 + 16) \gg 5) \qquad (11.5)$$

These half-sample values are used to derive the quarter-sample luma values a, c, d, n, f, i, k and q. They are derived by averaging and rounding up to the nearest sample at integer and half-sample positions. For example, the interpolated value for a in Figure 11.11 is

$$a = clip(G + b + 1) \gg 1 \qquad (11.6)$$

The remaining quarter-sample positions labelled, for example, p and r, are derived by averaging and rounding up the nearest half samples at diagonal positions. For instance, interpolated value for e in Figure 11.11 is

$$e = clip(b + h + 1) \gg 1 \qquad (11.7)$$

11.3.3.1 Chroma interpolation

As the human visual system is more sensitive to brightness than colour, motion estimation is usually carried out on the luma. For 4:2:0 image format, the estimated *MV*s are scaled down by a factor of 2 and used to compensate for chroma. Both the chroma samples (C_b and C_r) are partitioned similar to the luma MB, with the difference that the horizontal and vertical resolutions are halved and their *MV*s have a maximum of one-eighth-pixel precision. The chroma MB partitions (see Figure 11.12) are similar to the luma partitions of Figure 11.7, with the exception that the largest block size is 8 × 8 and the smallest size 2 × 2.

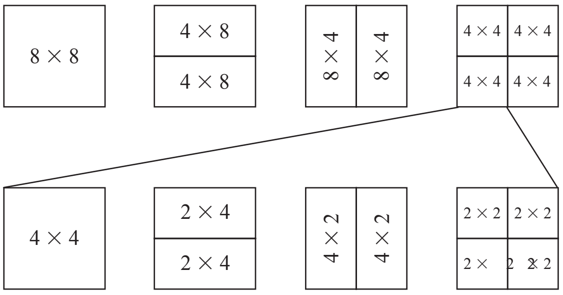

Figure 11.12 Chroma partitions

The prediction of the chroma components at one-eighth sample position is obtained by bilinear interpolation of integer positions as shown in Figure 11.13, without any additional filtering. These integer chroma positions are neighbours to the truncated half-luminance *MV* lengths, and the remainder of division defines the one-eighth position of the sample to be interpolated. For example, the sample labelled a is interpolated as

$$a = round\left(\frac{[(8-d_x)(8-d_y)A + d_x(8-d_y)B + (8-d_x)d_yC + d_xd_yD]}{64}\right)$$

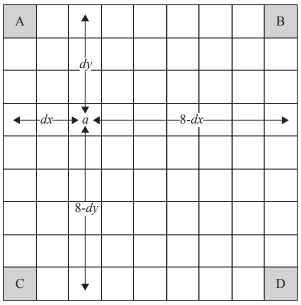

Figure 11.13 Interpolation of chroma with one-eighth sample position

With the given values of $d_x = 2$ and $d_y = 3$ in Figure 11.13, the interpolated value of a becomes

$$a = round\left[\frac{(30A + 10B + 18C + 6D)}{64}\right] \tag{11.8}$$

11.3.4 Motion compensation and slice type

11.3.4.1 P-skip

Picture areas with no changes and efficient motion compensation result in small interframe error signals with almost no significant transform coefficients (residuals). If these areas also contain constant motion like slow panning, then differential *MV* may also be zero. In the case when all residues are zero, the differential *MV* is zero, and the reference picture has index 0 in list 0, no additional information about the residuals or the *MV*s and reference picture index are required to be transmitted. Such a block in P-slices is called P-skip, and the block is reconstructed from the reference picture with index 0 in the buffer. The method applies equally to all block lengths, 4×4 to 16×16.

11.3.4.2 Motion compensation in B-slices

In H.264, the concept of B-pictures is generalised and is different from that in the previous standards. In this new codec, B-slices are allowed to be used as references for another B-slice, whereas in the previous standard, a B-picture cannot be used as a reference. This creates a hierarchy of B-pictures, and it is also known with this name. Since in this hierarchy, B-pictures can be close to their references (another B-picture), their number can be very long, improving the compression efficiency.

Note that in the other standards that do not use B-pictures for prediction, increasing the number of B-pictures beyond a few pictures reduces the compression efficiency, rather than improving it. More details of hierarchical B-pictures are given in the temporal scalability section 11.12.

In H.264, B-pictures support two lists of reference pictures, list 0 and list 1, and use four types of prediction:

1. list 0 prediction
2. list 1 prediction
3. biprediction
4. direct prediction

In which list to include a reference picture is a decision taken by the multireference picture buffer control. Usually, reference pictures in list 0 and list 1 are arranged as follows:

> List 0: Index starts from the temporally closest past picture, followed by the rest of the past pictures and then the future pictures.
> List 1: It is numbered starting from the temporally closest future picture, followed by the remaining future and then past pictures.

In the biprediction mode, weighted average of the motion-compensated prediction signals from list 0 and list 1 is taken as:

$$P(i,j) = (P_0(i,j) + P_1(i,j) + 1) \gg 1 \tag{11.9}$$

where $P(i,j)$ is the bipredictive sample and $P_0(i,j)$ and $P_1(i,j)$ are the prediction signals derived from list 0 and list 1. This prediction is then subtracted from the MB signals of the current picture at the locations.

In the direct mode, no *MV* is transmitted, and at the decoder, they are inferred from list 0 and list 1 *MV*s, knowing the previously coded vectors. Generally, despite not having *MV*, the block may contain transform coefficients. If the transform coefficients are also zero, then, like P-skip mode, these blocks are called B-skip. However, B-skip is defined at the MB level, but direct mode is generally defined at the sub-MB level. Thus, in addition to block size differences, the main element discriminating direct mode from the skip mode is that the former contains some transform coefficients, but the latter has none.

11.3.4.3 Multiple reference picture motion compensation

Syntax of H.264 supports multiple reference picture motion compensation in contrast to the previous standards, where only one reference picture is used in P-pictures and at the most two reference pictures in B-pictures. Multiple reference picture motion compensation improves compression efficiency by allowing the encoder to select from a number of reference pictures. Both the encoder and the decoder must have the same decoded pictures in the buffer. Each part of a sub-MB may refer to a different picture, but subpartitions of 8×8 blocks use the same reference picture (index) for all the subblocks in the 8×8 region. A reference index for each used reference picture is transmitted. Figure 11.14 shows how various partitions of a current MB of a B-slice use their motion-compensated predictions from various references. In this figure, as an example, the top-left 8×8 block in picture n uses two reference pictures, one from picture $n+1$ and the other from picture $n-3$ (bidirectional prediction). The four 4×4 blocks of the top-right 8×8 partitions use the same reference picture $n-2$. The two 4×8 blocks of the bottom-left 8×8 also use the same reference picture $n-1$. Finally, the bottom right block 8×8 uses a prediction from picture $n+1$. Note that two different parts of an MB can point to the same reference picture, albeit at different locations.

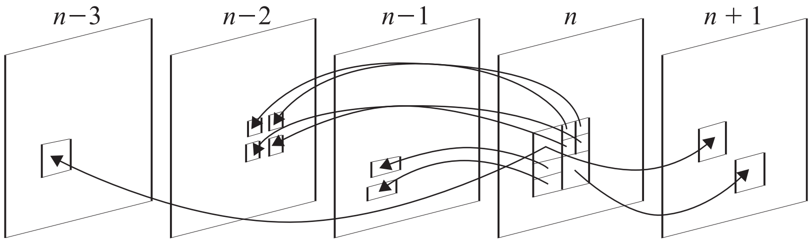

Figure 11.14 Multipicture motion compensation prediction

Using a larger number of reference pictures can potentially increase the motion compensation efficiency due to the use of a more diversified and temporally distant list of pictures. The H.264 standard allows up to 16 reference pictures for motion estimation. These pictures are organised in two different lists. Depending on the MB type, P or B, each block can be predicted using one or two lists of reference pictures. For P MBs, each partition chooses its prediction from a single picture in list 0, but B MB partitions can use two predictions, one from list 0 and another from list 1.

11.3.4.4 Multiple reference picture weighted prediction

Weighted prediction is used to scale the relative effect of the *MV*s from different reference pictures. In the previous standards, the weighted prediction was not used in the P MBs, and in the B MBs, it was a simple averaging of the two prediction signals, that is, $(P_0 + P_1)/2$. In H.264, the concept of weighted prediction is not only extended to P MBs but also with a different weighting factor.

Figure 11.14 can also be used to illustrate the concept of multiple reference picture weighted prediction, where the selected predictions from various references are properly weighted and used as the final interframe prediction for the current block. There are two modes for weighting the motion compensations of the pictures. In the explicit mode, the weighting factor for each used prediction for both P- and B-slices is sent to the decoder. In the implicit mode, which is applied to B-slices, weighting factor is determined by the temporal distance of the reference picture from the current picture. Closer the reference picture to the current picture, the larger is the weighting factor and vice versa.

11.4 Transformation and quantisation

11.4.1 Transformation

Similar to previous standards, the pixel residues (intra or inter) are transform coded to condense spatial detail residues into a few transform coefficients. The transform coefficients are then quantised for redundancy reduction and entropy coded for bit rate reduction. However, H.264 uses smaller block size of 4×4 integer transform instead of 8×8 DCT. This includes all the 16 luma and 4 of each chroma blocks in an MB. The transformation matrix approximates a 4×4 DCT with integer values, given by

$$H_1 \begin{bmatrix} 1 & 1 & 1 & 1 \\ 2 & 1 & -1 & -2 \\ 1 & -1 & -1 & 1 \\ 1 & -2 & 2 & -1 \end{bmatrix} \tag{11.10}$$

This transform, in addition to its simplicity, which can be realised through shift and add operations on 16-bit integers, has an exact inverse transform, and hence, there is no transformation mismatch. This is very useful for lossless video coding that the conventional DCT cannot provide.

In order for the approximated transformation matrix to be orthonormal, the two-dimensional transform coefficients (after horizontal and then vertical transformation) are postmultiplied by a forward-scaling matrix E_f:

$$E_f = \begin{bmatrix} a^2 & \frac{ab}{2} & a^2 & \frac{ab}{2} \\ \frac{ab}{2} & \frac{b^2}{4} & \frac{ab}{2} & \frac{b^2}{4} \\ a^2 & \frac{ab}{2} & a^2 & \frac{ab}{2} \\ \frac{ab}{2} & \frac{b^2}{4} & \frac{ab}{2} & \frac{b^2}{4} \end{bmatrix} \tag{11.11}$$

That is, the two-dimensional transform coefficients T_C of a block of pixels P are given by

$$T_C = (H_1 P H_1^T) \otimes E_f \tag{11.12}$$

where T stands for transpose of the matrix and $\otimes$ is element-by-element (Kronecker) product. Thus, the final two-dimensional transform coefficients become

$$T_C = \left\{ \begin{bmatrix} 1 & 1 & 1 & 1 \\ 2 & 1 & -1 & -2 \\ 1 & -1 & -1 & 1 \\ 1 & -2 & 2 & -1 \end{bmatrix} [P] \begin{bmatrix} 1 & 2 & 1 & 1 \\ 1 & 1 & -1 & -2 \\ 1 & -1 & -1 & 2 \\ 1 & -2 & 1 & -1 \end{bmatrix} \right\} \otimes \begin{bmatrix} a^2 & \dfrac{ab}{2} & a^2 & \dfrac{ab}{2} \\ \dfrac{ab}{2} & \dfrac{b^2}{4} & \dfrac{ab}{2} & \dfrac{b^2}{4} \\ a^2 & \dfrac{ab}{2} & a^2 & \dfrac{ab}{2} \\ \dfrac{ab}{2} & \dfrac{b^2}{4} & \dfrac{ab}{2} & \dfrac{b^2}{4} \end{bmatrix} \tag{11.13}$$

Also, the inverse transformation matrix is defined as

$$H_1^{-1} = \begin{bmatrix} 1 & 1 & 1 & 1 \\ 1 & \frac{1}{2} & -\frac{1}{2} & -1 \\ 1 & -1 & -1 & 1 \\ \frac{1}{2} & -1 & 1 & -\frac{1}{2} \end{bmatrix} \tag{11.14}$$

Because of orthonormality, the two-dimensional transform coefficients before the inverse transform are weighted with an inverse scaling matrix of E_i:

$$E_i = \begin{bmatrix} a^2 & ab & a^2 & ab \\ ab & b^2 & ab & b^2 \\ a^2 & ab & a^2 & ab \\ ab & b^2 & ab & b^2 \end{bmatrix} \tag{11.15}$$

And hence, the reconstructed pixel block P of transform coefficients T_C becomes

$$P = H_{-1}^T (T_C \otimes E_i) H_{-1}$$

$$P = \begin{bmatrix} 1 & 1 & 1 & \frac{1}{2} \\ 1 & \frac{1}{2} & -1 & -1 \\ 1 & -\frac{1}{2} & -1 & -1 \\ 1 & -1 & 1 & -\frac{1}{2} \end{bmatrix} \left\{ [T_C] \otimes \begin{bmatrix} a^2 & ab & a^2 & ab \\ ab & b^2 & ab & b^2 \\ a^2 & ab & a^2 & ab \\ ab & b^2 & ab & b^2 \end{bmatrix} \right\} \begin{bmatrix} 1 & 1 & 1 & 1 \\ 1 & \frac{1}{2} & -\frac{1}{2} & -1 \\ 1 & -1 & -1 & 1 \\ \frac{1}{2} & -1 & 1 & -\frac{1}{2} \end{bmatrix} \tag{11.16}$$

where $a = 1/2$ and $b = \sqrt{2/5}$. Note the positions of the transposed matrices in the forward and inverse transforms, as well as the positions of Kronecker products.

For intra 16×16, since the four spatial predictions cannot completely remove all the spatial redundancies, the DC values of all the sixteen 4×4 blocks do show high correlation. To reduce it, the standard defines a second transform, of type 4×4 Hadamard, as

$$H_2 = \begin{bmatrix} 1 & 1 & 1 & 1 \\ 1 & 1 & -1 & -1 \\ 1 & -1 & -1 & 1 \\ 1 & -1 & 1 & -1 \end{bmatrix} \tag{11.17}$$

to be applied on the DC values of 4×4 integer transform coefficients.

Similarly, the chroma DC values, due to poorer directional prediction, undergo a 2 × 2 Hadamard transform of

$$H_a = \begin{bmatrix} 1 & 1 \\ 1 & -1 \end{bmatrix} \tag{11.18}$$

This creates a hierarchy of intra coded transform coefficients, and their transmission order is shown in Figure 11.15. If the MB is of type intra 16 × 16, the block with label −1 is transmitted. This block contains all the DC coefficients of the luma 4 × 4 blocks. It is followed by coefficients in blocks 0–25, where blocks 0–15 contain the luma AC coefficients and blocks 16 and 17 contain the DC coefficients of the chroma. Their AC coefficients are in blocks 18–25. Note that for nonintra 16 × 16, there is no block label −1, and blocks 0–15 contain all the luma coefficients, including the DC ones.

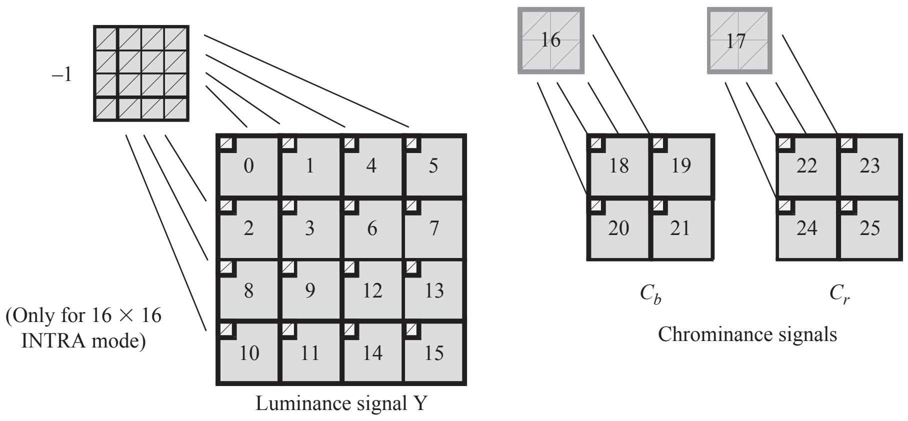

Figure 11.15 Transmission order of the coefficients of MB

For high profiles of H.264, transformation matrix in the horizontal and vertical directions can be an 8 × 8 integer transform. It is an approximation of 8 × 8 DCT and is defined as

$$H = \frac{1}{8}\begin{bmatrix} 8 & 8 & 8 & 8 & 8 & 8 & 8 & 8 \\ 12 & 10 & 6 & 3 & -3 & -6 & -10 & -12 \\ 8 & 4 & -4 & -8 & -8 & -4 & 4 & 8 \\ 10 & -3 & -12 & -6 & 6 & 12 & 3 & 10 \\ 8 & -8 & -8 & 8 & 8 & -8 & -8 & 8 \\ 6 & -12 & 3 & 10 & -10 & -3 & 12 & -6 \\ 4 & -8 & 8 & -4 & -4 & 8 & 8 & 4 \\ 3 & -6 & 10 & -12 & 12 & -10 & 6 & -3 \end{bmatrix} \tag{11.19}$$

Thus, with H.264, blocks of 4 × 8, 8 × 4 and 8 × 8 can also be coded, but the standard recommends only 4 × 4 or 8 × 8. When 8 × 8 transform is used, the transform coefficients are scanned in two forms, known as frame and field scan, as shown in Figure 11.16.

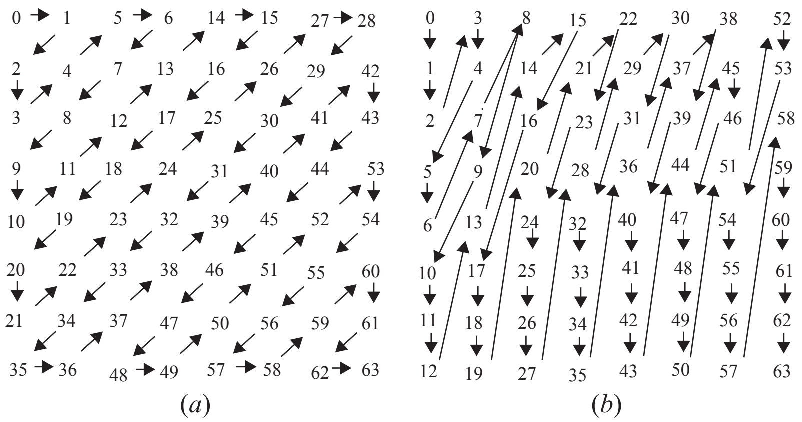

Figure 11.16 8 × 8 transform coefficients scan: (a) frame scan and (b) field scan

11.4.2 Quantisation

Transform coefficients are quantised with a semilogarithmic step size quantiser. The lowest step size Q_{step} is 0.625 and the largest step size is 224. These step sizes are addressed with the QP ranging from 0 to 51. Relation between QP and Q_{step} is shown in Table 11.1. As seen, Q_{step} is doubled with every six increments in QP. Thus, a single-unit increase in QP results in approximately 12.5 per cent increase in the Q_{step}. The exact relation between Q_{step} and QP can be derived from the first six QP and their step sizes, given by

$$Q_{step}(QP) = Q_{step}(QP\%6)2^{floor(QP/6)} \tag{11.20}$$

where $QP\%6$ and $floor(QP/6)$, respectively, represent the remainder and smallest integer ratio of QP to 6. For example, the quantiser step size for a $QP = 16$ is $16\%6 = 4$ and $floor(16/6) = 2$. From the table, $Q_{step}(4) = 1$, and hence, $Q_{step}(16) = 1 \times 2^2 = 4$.

Table 11.1 Table of Q_{step} in terms of QP

QP	0	1	2	3	4	5	6	7	8
Q_{step}	0.625	0.6875	0.8125	0.875	1	1.125	1.25	1.375	1.625
QP	9	10	11	12	13	14	15	16	17
Q_{step}	1.75	2	2.25	2.5	2.75	3.25	3.5	4	4.5
QP	18	–	24	–	30	–	36	–	51
Q_{step}	5		10		20		40		224

The postmultiplied transform coefficients of eqn. 11.13 T_C are then divided by the quantiser step size, Q_{step}, to give the quantised transform index Q_c.

$$Q_c = round\left(\frac{T_c}{Q_{step}}\right) \tag{11.21}$$

The quantised transform indices are scanned in frame or field scan order, and the 2×2 transform coefficients of the chroma components are scanned in raster (the same as zigzag) order and are then entropy coded.

Quantised transform indices prior to inverse transform are multiplied by the quantisation step size to regain their approximated values.

$$T_c = Q_c \times Q_{step} \tag{11.22}$$

The final reconstructed pixel residues are then obtained by the inverse transformation matrix of eqn. 11.16 and clipping the values within the range 0–255.

It is worth noting that at larger QP (e.g. $QP > 30$), the quantiser step sizes become very large. These are suitable for the luma transform coefficients but are too big for the chroma transform coefficients, which normally have lower spatial resolutions (details) than luma, resulting in lower values of chroma residues. The standard recommends that the chroma quantiser step sizes for $QP > 30$ should be less than those of luma step size. A user-defined offset between $Q_{step}Y$ and $Q_{step}C$ may be signalled in the picture parameter set (PPS). Table 11.2 shows the nominal relation between the chroma and luma quantiser parameters QPC and QP, respectively. In this table, for $QP < 30$, the same quantiser step size of luma is used for the chroma, but at higher QP, the quantiser step size of chroma is derived from a lower QP than that used for luma.

Table 11.2 Specification of QPC as a function of QP

$QP < 30$	30	31	32	33/34	35	36/37	38/39	40/41	42–44	45–47	48–51
$QPC = QP$	29	30	31	32	33	34	35	36	37	38	39

It is also worth noting that for high profiles where 10 and 12 bit/ pixel are used, the QP for every bit is incremented by 6. For instance, in 10 bit/pixel input pictures, the QP range is 0–63.

11.5 Deblocking filter

Principles of deblocking filter in the block-based codecs such as H.263 were studied in section 9.4.4, but since this filter is a core element of the H.264 codec, the test model has some recommendations for its characteristics and use. Note that since deblocking filter is used at the decoder as well as in the decoder loop of the encoder, following the recommendation for decoding compatibility is essential. It is recommended that filtering should be applied at MB level to each of 4×4 subpartitions first in the horizontal and then in the vertical direction. Both the filtering operations are completed before moving to the next MB in a raster scan order. The same procedure is applied to the chroma samples. The filtering procedure is adaptively changed on slice, block edge and sample levels [8]. The overall filtering operation is determined in three steps.

1. filter strength
2. filtering decision
3. filter implementation

11.5.1 Boundary strength

The filter strength, or most commonly, the boundary strength (BS), is the amount of filtering exerted to the pixels. The BS is made dependent on the inter/intra prediction decision, motion and reference picture differences and the presence of residues in the two participating blocks. Table 11.3 summarises BS values in the range 0–4, derived from every two 4×4 subpartitions of luma pixels. Value 0 means no filtering, and 4 corresponds to the heaviest filtering operation.

Table 11.3 Boundary strength (BS)

If either of blocks is intra coded and the block boundary coincides with the block edge	BS = 4 (heaviest filtering)
Otherwise	BS = 3
If both blocks are inter coded and at least one of the luma blocks has non-zero transform coefficients	BS = 2
Otherwise if they have different reference pictures or different motion vectors	BS = 1
Otherwise	BS = 0 (no filtering)

Thus, at areas where there are more distortions, higher values of BS are selected, such as the boundary of an intra coded MB or a boundary between blocks that contain coded coefficients (residues).

11.5.2 Filtering decision

One of the most important decisions on the filtering operation is to distinguish between the artificial edges created by picture blockiness and the natural contextual edges of the image, as filtering of natural edges may lead to picture blurriness. One way of discriminating contextual edges from the artificial block boundaries is to analyse relations between the pixels of the two participating blocks. Let us name the participant blocks p and q, and their four samples along a line, either in the horizontal or vertical direction, by p_3, p_2, p_1 and p_0, and q_0, q_1, q_2 and q_3 on either side of a boundary line, as shown in Figure 11.17. The gradient of the pixels at the block boundary, $|p_0 - q_0|$ can be an indication of block edge. Pixel differences at either side of the edge, like $|p_2 - p_0|$ for block p, can be used as an indication of texture (details) in that block. Hence, comparing them, one might be able to determine if the gradient $|p_0 - q_0|$ is due to a natural or an artificial edge. However, since blockiness is due to coarse quantisation, the gradients should be contrasted against some thresholds, α and β, whose values change with the quantisation parameters QP.

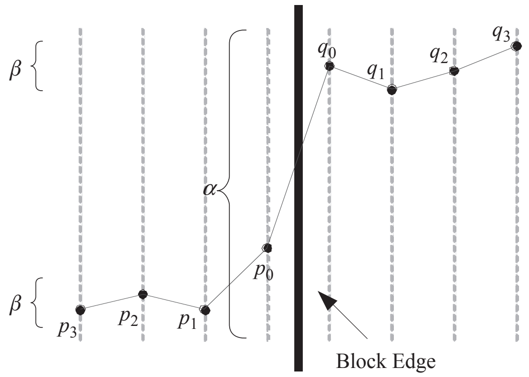

Figure 11.17 One-dimensional representation of pixels of two adjacent blocks

α and β increase and decrease with the average QP of the two blocks p and q. The idea is that if the difference between the samples near the block edge is so large that it cannot be explained by the coarseness of QP, it can be taken as a true edge in the picture. Otherwise, it is taken as blocking artefact and is required to be smoothed. The values of $\alpha(QP)$ and $\beta(QP)$ are given by [8]

$$\begin{aligned} \alpha(x) &= 0.8(2^{(x/6)} - 1) \\ \beta(x) &= 0.5x - 7 \end{aligned} \tag{11.23}$$

The actual values can vary based on empirical tests to produce visually pleasing results for a variety of content.

11.5.3 Filter implementation

Knowing the boundary strength (BS) and the various pixel gradients, one can decide either not to filter a pixel or to filter it with various degrees, indicated by the filter length. Table 11.4 summarises the conditions set on the pixel gradients along with the BS to filter the boundary pixels. Under the conditions set in this table, pixels along each side and each line (vertical, horizontal) are filtered with three to five tap filters as well as not being filtered at all. In the table, values of the filtered pixels are identified by ($'$) and the remaining pixels are not filtered.

Experiments indicate that deblocking filter can reduce the blocking artefacts without notably harming the sharpness of the true edges. For moderate picture details, it can reduce the bit rate by 6–9 per cent for the same objective quality, and subjective quality improvement is even better [9].

Table 11.4 Conditions set for deblocking filters

BS value	Conditions	Filtered sample
0	NA	No
1, 2, 3	NA	$p_0' = p_0 + clip(4(q_0 - p_0) + p_1 - q_1 + 4)/8$ $q_0' = q_0 + clip(4(p_0 - q_0) + q_1 - p_1 + 4)/8$
	$\|p_2 - p_0\| < \beta$	$p_1' = p_1 + clip(p_2 + 0.5(p_0 + q_0 + 1) - 2p_1)$ else $p_1' = p_1$
	$\|q_2 - q_0\| < \beta$	$q_1' = q_1 + clip(q_2 + 0.5(q_0 + p_0 + 1) - 2q_1)$ else $q_1' = q_1$
4	$\|p_2 - p_0\| < \beta$ and $\|p_0 - q_0\| < \alpha/4$ and luma sample	$p_0' = \frac{p_2 + 2p_1 + 2p_0 + 2q_0 + q_1 + 4}{8}$ $p_1' = \frac{p_2 + p_1 + p_0 + q_0 + 2}{4}$ $p_2' = \frac{2p_3 + 3p_2 + p_1 + p_0 + q_0 + 4}{8}$
	else	$p_0' = \frac{2p_1 + p_0 + q_1 + 2}{4}$
	$\|q_2 - q_0\| < \beta$ and $\|p_0 - q_0\| < \alpha/4$ and luma sample	$q_0' = \frac{q_2 + 2q_1 + 2q_0 + 2p_0 + p_1 + 4}{8}$ $q_1' = \frac{q_2 + q_1 + q_0 + p_0 + 2}{4}$ $q_2' = \frac{2q_3 + 3q_2 + q_1 + q_0 + p_0 + 4}{8}$
	else	$q_0' = \frac{2q_1 + q_0 + p_1 + 2}{4}$

11.6 Entropy coding

Entropy coding is the last step in redundancy reduction. In Annex E of H.263, arithmetic coding was introduced to improve the coding efficiency. The results were not as promising as expected for some reasons. First, the arithmetic coding was equally applied to all symbols, addresses, block type, *MV*s and transform residual coefficients alike, but these coding syntaxes have their own characteristics. Second, the model was not adaptive, and third, it was an m-ary arithmetic coding, which not only makes it complex but its adaptation is also almost impossible. In H.264, it was thought that through binarisation and adaptation of the symbol model, one can improve the compression efficiency. This, of course, increases coding complexity, as there are numerous symbols each requiring its own model. For this reason, H.264 has adopted two methods of entropy coding. One is called context adaptive variable length code (CAVLC), where, based on the context of past symbols, a set of Huffman tables are adaptively selected. The other is called context adaptive arithmetic coding (CABAC), where the probability model of the arithmetic coder is adapted to the context. However, most elements of a codec, such as MB type, *MV*s and their addresses, do not need adaptation. To make entropy coding simple, both CAVLC and CABAC use a single infinite extent code word, called exponential-Golomb (Exp-Golomb), to generate the required code for these kinds of data. In the following, the fundamental elements of the entropy coding methods defined in H.264 are presented, and for more detailed information and implementation issues, one should refer to [10].

11.6.1 Exp-Golomb

Exp-Golomb code is a universal code with a regular construction structure that can be tailored for any symbol without the need for look-up tables [11]. Their generated code words are also known as universal variable-length code (UVLC). The code word can be constructed by concatenation of a prefix and a suffix, as

$$\text{code word} = [M]1[\mathit{info}] \tag{11.24}$$

where M zeros represent the prefix followed by a 1 and then a suffix called *info*, which is the binary representation of the source symbol. Values of M, *info* and the length of the code word of a symbol x for a kth-order Exp-Golomb (EGK) are given by

$$M = \mathit{floor}\left(\log_2\left[\frac{x}{2^k} + 1\right]\right)$$

$$\mathit{info} = x + 2^k(1 - 2^M) \tag{11.25}$$

The *info* is the binary representation of the above expression within $k + M$ significant bits. Hence, the length of the code word becomes

$$\text{length of code word} = k + 2M + 1 \tag{11.26}$$

The EGK is used in CABAC, but its zero-order version, EG0, is used in CAVLC for coding of all symbols except the transform coefficients. EG0 code word then has a length of only $2M + 1$ bits, and its prefix M and suffix *info* become

$$M = \mathit{floor}(\log_2[x + 1])$$

$$\mathit{info} = x + 1 - 2^M \tag{11.27}$$

Table 11.5 lists the Exp-Golomb code for nine positive integers, generated from the above equation.

Table 11.5 Exp-Golomb code for nine positive integers

Symbol (x)	0	1	2	3	4	5	6	7	8	.....
Code word	1	010	011	00100	00101	00110	00111	0001000	0001001	...

Any encoding parameter (except transform coefficients) is first mapped to a symbol, and the symbol is then Exp-Golomb coded. Depending on the syntax of the parameter, mapping is done by one of the following three methods:

1. Unsigned direct mapping: The symbol x is taken as the parameter itself. Examples of this kind include MB type and reference picture index.
2. Signed direct mapping: Parameters that can be either positive or negative, like the *MV* differences or *QP* differences, are mapped to symbol x by

$$\begin{aligned} &x = 2\ |parameter| \quad \text{if} \quad parameter \le 0 \\ &x = 2\ |parameter| - 1 \quad \text{if} \quad parameter > 0 \end{aligned} \tag{11.28}$$

3. Mapped symbols: Parameters other than the above two are mapped to a symbol through some tables for mapping provided by the standard. The tables are designed such that the most frequent occurring parameters have shorter symbol lengths x to generate shorter code words. Coded block pattern (CBP) is one of the examples.

11.6.2 CAVLC encoding for residual data

CAVLC is used as a lesser complex entropy coder of the transform coefficients in the baseline profile of H.264. As mentioned, all the coding parameters except the transform coefficients are Exp-Golomb coded. The transform coefficients are Huffman-derived variable length coded, and based on some context adaptation an appropriate VLC table is selected from a set of 11. To make VLC efficient, each table is designed for a particular distribution of transform coefficient value. Selection of one of these tables is based on the value of some of the previously coded coefficients.

Transform coefficients after quantisation and zigzag scanning have some properties that can be taken advantage of for more efficient coding. These are as follows:

- They are typically sparse, containing a large number of zero coefficients. These trains of zeroes can be easily run length coded.
- Most of the nonzero coefficients are sequences of ± 1s with equal probabilities. These sequences should be represented in a compact manner.
- The nonzero coefficients of the adjacent blocks are highly correlated. Hence, the number of nonzero coefficients of the neighbouring blocks can be used as a context for adaptive selection of the look-up tables.
- The magnitudes of the nonzero coefficients tend to decrease from the start of the scanning towards the end. This can be exploited for the choice of magnitude (level) parameter.

With the above properties of the quantised transform coefficients, their CAVLC coding (after zigzag scanning) is as follows.

11.6.2.1 Encode number of coefficients and trailing 1s (*T*1s)

First, the number of nonzero coefficients and the number of trailing ± 1s are coded. For blocks of 4×4 pixels, the number of coefficients can be anything from 0 to 16, but the number of trailing ±1s is assumed to be between 0 and 3. If the number of ±1s is greater than three, then the remaining ±1s are treated as normal coefficients.

Both the number of nonzero coefficients and the number of trailing ±1s are variable length coded from a choice of four look-up tables. Three of these tables are variable-length code tables, and one is a fixed-length code table. The choice of table depends on the number of nonzero coefficients in the blocks above and to the left of the current block. For example, if the number of nonzero coefficients is less than two, the first VLC table, known as num-VLC0, is chosen.

11.6.2.2 Encode sign of each *T*1

The trailing 1s need only sign information as their values are known to be 1. A single bit 1 or 0 represents the negative and positive signs, respectively. They are encoded in the reverse order from the highest frequency of *T*1s towards the lowest.

11.6.2.3 Encode levels of nonzero coefficients

The magnitude (level) of each nonzero coefficient is encoded with a look-up table. There are seven look-up tables to choose from, and the selection is done adaptively depending on the encoding of each prior level. The level of each nonzero coefficient is encoded in the reverse order of frequent occurrence of coefficient values, that is, the highest frequency first and then moving back towards the DC coefficient. The tables are such that table 0 is biased towards lower magnitudes and table 1 is biased towards slightly higher magnitudes and so on. Adaptive selection of the look-up tables is achieved through the following:

- The table is initialised to the lowest look-up table 0. Another look-up table is chosen only if there are more than ten nonzero coefficients and less than three *T*1s, in which case, the starting table is look-up table 1.
- The highest-frequency nonzero coefficient is encoded first.
- If the magnitude of the current coefficient is greater than a predefined threshold, then the look-up table number is incremented by 1.

11.6.2.4 Encode each run of zeros

The number of zeros preceding each nonzero coefficient is encoded in reverse order. This value is not encoded if the following two conditions are encountered:

1. If there are no more zeros to be encoded.
2. It is not required to encode the number of zeros before the last nonzero coefficient.

The number of zeros encoded before a nonzero coefficient depends on the number of zeros left to be encoded.

11.6.3 CABAC: Context-adaptive binary arithmetic coding

In the CAVLC of the baseline coder, although the tables are adaptively selected, each code itself is in fact a Huffman code, with a minimum of 1 bit. This is not efficient for symbols with probability of occurrences greater than 0.5, and we have seen in the earlier chapters that arithmetic coding of these symbols is more efficient. To make arithmetic coding practical and, at the same time, context adaptive, H.264 has chosen the context adaptive binary arithmetic coding (CABAC) strategy. A block diagram of this encoder is shown in Figure 11.18, with three main building blocks.

1. binarisation
2. context modelling
3. binary arithmetic coding

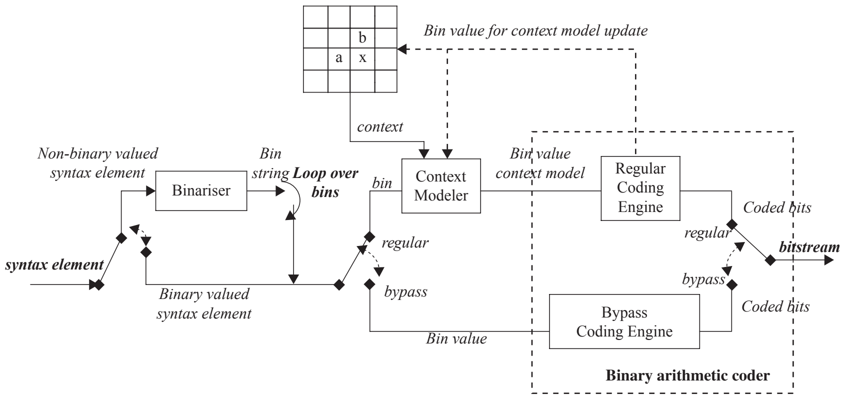

Figure 11.18 A block diagram of CABAC

In the figure, an incoming symbol, called syntax element, is uniquely mapped to a binary sequence, the so-called bin string. In the regular mode, prior to arithmetic coding, a probability model is assigned either to a bin or to the syntax element. The selected probability model depends on the previously encoded bins or elements. After assigning the context model, the bin value and its associated model are passed to a regular arithmetic coding engine. Alternatively, the bypass coding engine may be chosen, where bins are arithmetic coded without any specific model. This mode is suitable for symbols with nearly uniform distribution.

In the following, these three fundamental building blocks are explained in general, and for more detailed information, one should refer to [10].

11.6.3.1 Binarisation

Prior to arithmetic coding and context modelling, the syntax elements are converted from an m-ary code to a binary string. The reason for binarisation is that binary arithmetic coding is much simpler than m-ary arithmetic coding to implement, and context adaptation can be even carried out at the bin level. For the latter reason, binarisation is not a simple binary representation of an m-ary, but it is a kind of Huffman coding. In the Huffman tree, the last level of the child nodes would represent the binary code word for a syntax element, and the probability of a bin at each node can be related to all the probabilities of the bins in the tree to the root. This is an interesting property that can be used for estimating and adapting the probability model based on the context.

For binarisation, CABAC does not use Huffman-designed VLC tables, as this requires several tables to be stored. Instead, four coding methods are used, which are simpler to compute on the fly:

1. unary code
2. truncated unary code
3. EGK codes
4. fixed-length codes

Unary and truncated unary binarisation

In unary binarisation, each unsigned integer value symbol x 0 is represented by x number of 1 bits followed by a terminating 0 bit. In the truncated unary, where the value of x is truncated to a maximum of S, $0 \leq x \leq S$, for $x < S$, unary code is used, but for $x = S$, the code word consists of only x number of 1s without the terminating 0 bit.

EGK codes

This is similar to the EG0 coding scheme used in CAVLC, which consists of a prefix M zeros and a suffix *info*, as was explained in section 11.6.1. In the kth order of EGK, the code length is given by $K + 2M + 1$.

Fixed-length binarisation

In this coding scheme, a symbol x within a finite size of S is represented by its bit representation of a fixed length (FL), with a length $l = \lfloor \log_2 S \rfloor$ bits. This kind of binarisation is typically applied to syntax elements with fairly uniform distribution, where each bit in the *FL* binary representation represents a specific coding decision. Examples include a part of coded block-pattern symbol related to the luma residual data.

In addition to the above four binarisation schemes, three additional schemes are defined by their concatenation. One is a concatenation of fixed length and truncated unary, which is used for binarisation of coded block pattern. The other two are derived from the concatenation of truncated unary and EGK, which are used for the *MV* differences and the absolute values of the transform coefficients levels. For example, for *MV* difference with one-quarter-pixel precision, ± 2 extra samples are needed, which is catered for by EGK of $k = 3$ [10].

11.6.3.2 Context modelling

Context modelling is the process of selecting a probability model for one or more bins of a binary symbol. The choice of model depends on the statistics of the recently coded syntax elements or bins. Thus, through context adaptation, an appropriate probability model is assigned to a binary value 0 and 1. The compression achieved by the arithmetic coder is highly dependant on the good fit of the used model. Ideally, a model should explore maximum statistical dependencies to achieve maximum compression. Considering that training the model for adaptation is costly and the cost increases exponentially with the number of probabilities to be modelled, one might think that not all symbols need context modelling. Only symbols with high frequency of occurrence that have major contributions to the generated bit rate should be modelled, hence decreasing modelling cost.

CABAC uses four different types of context models [10]. The first model is applied on the syntax element based on the modelling of the related bin values of the neighbouring elements, which lie to the top and left of the current syntax element. Thus, context adaptation is carried out at syntax element level.

The second model is used for modelling of MB type (mbtype) and sub-MB type (sub_mbtype). In this type of model, the values of the previously coded bins are used as the choice of a model for the current bin with an index i. Thus, the context adaptation is done at the bin level.

The third and the fourth types are used for coding of residual transform coefficients only. In the third type, coding is based on the position of the bin in the scanning path. This position is provided by a significance map. The fourth type is based on the level information of prior encoded (decoded) bins to fix the level information of the current bin to be encoded (decoded).

The reason for these two types of context modelling for the residual data is the way the transform coefficients in CABAC are coded. The idea has been borrowed from wavelet image coding, where the significance of coefficients are noted and, knowing the characteristics of the coefficients (listed in section 11.6.2), their presence and values are coded. Here, for each block with at least one nonzero quantised transform coefficient, a sequence of binary significance flags, indicating the positions of the significant (i.e. nonzero) coefficients within the scanning path, is generated. These significance flags are interleaved with another sequence of so-called last flags (one for each significant coefficient level) for signalling the position of the last significant level within the scanning path. This so-called significance information is transmitted as a preamble of the regarded transform block followed by the magnitude and sign information of nonzero levels in the reverse scanning order. The context modelling of binarised-level magnitudes is based on the number of previously transmitted level magnitudes greater or equal to 1 within the reverse scanning path, which is motivated by the observation that levels with magnitude equal to 1 are statistically dominant at the end of the scanning path. For context-based coding of the significance information, each significance/last flag is conditioned on its position within the scanning path, which can be interpreted as a frequency-dependent context modelling. Furthermore, for each of the different transforms (integer, 4×4 and 2×2 Hadamard) in H.264 as well as for luma and chroma components, a different set of contexts denoted as context category is employed. This allows the discrimination of statistically different sources, with the result of a significantly better adaptation to the individual statistical characteristics.

The context models are accessed through an index parameter γ, which is determined by two values: one is a 6-bit probability state (64 probability states) index a and another is the most probable symbol (MPS) b. The context index ranges from 0 to 398. The indices from 0 to 72 are related to syntax elements of MB type, sub-MB type, prediction modes of spatial and temporal type and slice- and

MB-based control information [10]. The remaining context indices are all used to represent residual transform coefficients.

The context index in the range 0–72 is given by

$$\gamma = \Gamma_s + \chi_s \tag{11.29}$$

where Γ_s is the context index offset and χ_s is the context index increment for a given syntax element *S*. Its value for the range 73–398 is given by

$$\gamma = \Gamma_s + \Delta_s(ctx_c at) + \chi_s \tag{11.30}$$

where $ctx_c at$ is the context category dependant offset. An important factor about context modelling is that only the past coded values of the current slice are considered for the coding of a current syntax element.

11.6.3.3 Binary arithmetic coding

In the previous chapters, binary arithmetic coding was described in detail. Now that the model adaptation for CABAC is known, its binary arithmetic coding is easy to follow. As we had seen, binary arithmetic coding is carried out by recursively subdividing an interval according to the probability of symbols. If the least probable binary symbol (LPS) 0 or 1 has a probability $\rho_{LPS} < 0.5$, and the interval has a lower bound *L* and its width or range is *R*, then the interval is divided into two subintervals with

$$R_{LPS} = R \times \rho_{LPS} \tag{11.31}$$

associated to the LPS, and its dual interval $R_{MPS} = R - R_{LPS}$, assigned to the most probable binary symbol (MPS), having the complementary probability of $1 - \rho_{LPS}$. Depending on whether LPS or MPS was encoded, the new range *R* is set to either R_{MPS} or R_{LPS}. A binary value pointing into that interval represents the sequence of binary decisions processed so far, and the range of that interval corresponds to the products of the probabilities of those binary symbols [11].

For adaptation, it remains to estimate the probability of least probable symbol, ρ_{LPS}. CABAC defines 64 representative probability values, ρ_{LPS}, in the range 0.01875–0.5 for LPS, by the following recursive equations:

$$\begin{aligned} &\rho_\sigma = \alpha \times \rho_{\sigma-1} \quad \textit{for all } \sigma = 1, ..., 63 \\ &\text{with } \alpha = (0.01875/0.5)^{1/62} \text{ and } \rho_0 = 0.5 \end{aligned} \tag{11.32}$$

Both the scaling factor $\alpha \approx 0.95$ and the cardinality $N = 64$ are chosen to represent a good compromise for fast adaptation and accurate estimation. Thus, each context model in CABAC can be completely determined by two parameters: its current estimate of LS probability, which in turn is characterised by an index σ between 0 and 63 and its value of MPS being either 0 or 1.

Another interesting feature adopted by the CABAC scheme is the use of a simplified bypass coding mode as shown in Figure 11.18. If the syntax elements are found to be uniformly distributed, then the computationally intensive process of context modelling can be skipped, and the syntax elements are directly arithmetically coded with a fixed probability.

11.7 Rate distortion optimisation

In H.264, similar to the other standards, only the bitstream syntax and the decoding procedure are specified, and the encoder is flexible to have any implementations. This means that the encoder is free to encode an MB in any way it prefers and hence to spend its bit rate budget as long as the generated bitstream is decodable. The idea behind rate distortion (RD) optimisation is to distribute bits among the parts of MB encoding elements, like coding modes, predictions, *MV*s, *QP* and the residual data out of several choices such that larger reduction in distortion is achieved for minimum spent bits. For a good and efficient RD optimiser, selection of these huge ranges of choices can only be achieved through an exhaustive search. To simplify the search, one may assume an analytical model relating the rate and distortion and through Lagrangian optimisation to achieve RD efficiency.

11.7.1 Lagrangian optimisation technique

Lagrangian techniques are based on converting a constraint optimisation problem to an unconstrained one [12]. In eqn. 11.33, the task is to minimise the distortion, D, with a constraint that the rate R should be less than a target value R_c:

$$\text{minimize } D \quad \text{subject to } R \leq R_c \tag{11.33}$$

The constrained eqn. 11.33 can be solved by converting it to a nonconstrained equation, through the Lagrangian cost function J, with parameter λ. In this case, the task becomes to minimise the cost function J, which has a well-defined equation, given by

$$J = D + \lambda \times R \tag{11.34}$$

Encoding of every MB in a picture generates a rate of r and distortion d, and the sum of these values over a slice or picture results in R and D. Assuming that r and d of an MB are only dependant on the MB's own coding parameters and not the others, the optimisation of eqn. 11.34 is simplified to minimising the cost of coding each MB separately:

$$j = d + \lambda \times r \tag{11.35}$$

11.7.2 Optimisation process

An MB can be coded in a variety of forms, like SKIP, inter 16 × 16, inter 16 × 8, inter 8 × 16, inter 8 × 8 as well as intra 16 × 16 and intra 4 × 4. Inter 8 × 8 itself can be divided into inter 8 × 4, inter 4 × 8 or inter 4 × 4. Since interframe coding is more common than the other modes, its cost is first estimated. The Lagrangian optimiser starts by finding the optimal *MV*s of inter coded MB and the optimal mode for any block. Here through Lagrangian optimisation, the cost of coding the *MV*s in bits, and their motion-compensated distortions in the form of sum of absolute distortion (SAD_{MV}) of motion-compensated pixels in the MB is derived.

$$j_{MV} = SAD_{MV} + \lambda_{MV} \times r_{MV} \tag{11.36}$$

where λ_{MV} is the Lagrangian parameter of the *MV*. After determining the optimum *MV*s for inter modes, the Lagrangian optimisation is used again to choose the optimal mode by minimising the overall Lagrangian cost of each (intra and inter) and the skip mode (j_{mode}).

$$j_{mode} = SSD_{mode} + \lambda_{mode} \times r_{mode} \tag{11.37}$$

where r_{mode} includes all the required bits to code an MB and SSD_{mode} is the sum of squared differences (SSD) between the original and the reconstructed pixels. The mode that has the least j_{mode} among all others is selected as the optimum mode. Note that in intra slices, only the intra modes are allowed and searched, but in inter slices, both types are examined.

11.7.3 Selection of λ

In the above optimisations, the values of λ are empirically found to be [13]

$$\begin{aligned} \lambda_{mode} &= 0.85 \times 2^{(QP-12)/3} \\ \lambda_{MV} &= \sqrt{\lambda_{mode}} \end{aligned} \tag{11.38}$$

These relationships between the parameters can be verified experimentally. For each MB, by varying λ, the *QP* that yields the least bit rate is recorded. The average values of *QP* for the given λ establish this relation. For instance, Figure 11.19 shows the results of the experiment for the foreman test sequence. The encoder examines various values of *QP* as well as MB modes and selects a *QP* that has the least Lagrangian cost. The figure indicates that values of *QP* that have λ given according to eqn. 11.38 on the average are the most frequently selected *QP* for an optimum bit rate [14]. Hence, relation between λ and *QP* given in eqn. 11.38 looks very plausible.

It is worth mentioning that for higher compression, normally B-slices are quantised coarser than I- and P-slices. In MPEG-1, we saw that the quantiser step size of B-pictures was 1.4 times larger than that of I- and P-pictures. In some versions of the JM software of H.264, it is noted that the λ_{mode} of B-slices are set at four times that of I- and P-slices. This ratio, according to eqn. 11.38, means that $QP_B = QP_P + 6$. Since a six-level increment in the *QP* doubles its step size, the quantiser step size of B-slices will be twice that of I- and Q-slices, that is, $Q_{stepB} = 2Q_{stepP}$. Such a very high quantise step size for B-slices is mainly due to very efficient motion compensation of these slices, such that larger quantiser step size forces many of their MBs to be skipped, reducing the bit rate significantly without noticeable picture degradations.

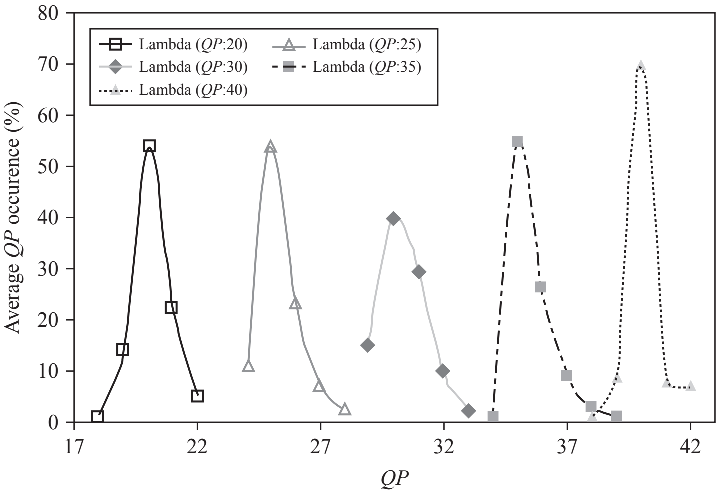

Figure 11.19 Average occurrence of QP for various values of λ

The above discussions imply that the optimisation outcome is heavily dependent on the *QP*, as both λ_{mode} and λ_{MV} are *QP* dependent. This creates the chicken and egg dilemma, as the main goal of optimisation is to find the most suitable *QP*, but we see that the outcome of optimisation is *QP* dependent. In practice, selection of *QP* comes first. In variable bit rate (VBR) coding, for a given video quality, a fixed *QP* is chosen. In the constant bit rate (CBR) coding, for a given bit rate budget, through a rate control strategy, an appropriate *QP* is determined, though it may change from slice to slice. Thus, although we start with a given *QP*, the outcome of optimisation may indicate that a better *QP* should have been selected. Hence, new *QP* can be chosen, but it should be ensured for CBR that the bit rate budget is not exceeded.

RD optimisation is extensively used in various parts of the H.264 encoder, and it comprises a significant portion of the encoding complexity, perhaps comparable to motion estimation (see section 11.11.1). Even a small part of motion estimation complexity is due to its use of RD optimisation, as merging inter 4×4 *MV*s to larger blocks is carried out through RD decision, as discussed in section 11.3.1. The spatial prediction modes of intra 4×4/intra 16×16 are also determined through RD, and the one with the least cost is selected. In fact, in the encoder, no decision, such as the intra/inter/skip decisions, is made without referring to RD optimisation, and this is why RD optimisation consumes a major portion of the encoder complexity.

11.8 Error resilient encoding

Although the H.264 standard through the network abstraction layer (NAL) tries to protect the video coding layer (VCL) bitstream against the underlying transport channel uncertainties, some degree of error resiliency within the VCL stream itself has also been envisaged. Most of these techniques like data partitioning, error concealment, reference picture selection are either borrowed from the previous standards or their improved versions are adopted. The new standard also has some of its own, like flexible macroblock ordering (FMO), redundant slices, parameter setting and switching pictures, which have been developed specifically for this codec. In the following, some of the most important error resiliency techniques used in H.264 are explained.

11.8.1 Error detection

The syntax elements for a standard decoder, like addresses, picture number, *MV*s and transform coefficients are all defined within a format and range. They have to be received in proper order and form to be decodable. Any violation in the syntax elements due to channel errors can lead to illegal value of these elements, and hence, the decoder can abandon decoding till the next synchronisation is received. Because of predictive coding nature of the codec, a single error may cause all elements within a slice not to be decodable. The syntax errors may include [3]

- illegal value of syntax elements
- illegal synch header
- more than 16 transform coefficients
- incorrect number of stuffing bits

When a part of a slice is not decodable, it may be copied from the same positions from the previous picture. This is informally known as frame copy. Alternately, the lost area can be concealed by copying correlated pixels from other parts of the picture itself or previous pictures. The standard defines two intra- and interframe error concealment techniques, which is explained in details in section 11.9. Inter-frame error concealment is colloquially known as motion copy.

11.8.2 Flexible macroblock ordering (FMO)

Although picture slicing can prevent error propagation beyond a slice, proper arrangement of MBs in forming a slice can improve the degraded slice quality. For example, if MBs are arranged in a checkerboard pattern, error concealment can perform better on the lost slice, where each lost MB is surrounded by several safely received ones. The final outcome of course very much depends on how efficiently the error concealment algorithm is implemented.

For robust transmission, the standard allows the MBs of various parts of the picture to be grouped in a flexible manner, the so-called flexible macroblock ordering (FMO). In this technique, MBs are grouped together according to a user-defined shape known as slice grouping. Each slice group is a set of MBs defined by an MB to slice group map, specified in the picture parameter set (PPS) and some information in the slice header. This map consists of a slice group identification number for each MB in the picture, which specifies to which slice group it belongs to. To reduce addressing information, as well as preventing data fragmentation, each slice group is partitioned into one or more slices, such that a slice is a sequence of MBs within the same slice group, which are processed in the raster scan order [3].

The slice grouping and ordering of MBs within slices depend on applications. Figure 11.20*a* shows two foreground slice groups #0 and #1 and a background slice group #2, and in Figure 11.20*b*, two slice groups #0 and #1 are interleaved in a checkerboard pattern. While the first method can be used for coding of region of interest (or importance), in the second method, when a slice is lost, it can be easily concealed from the neighbouring MBs of the other slice. Hence, this method is useful for multiple descriptions coding, where each slice can be sent through a different channel, such that one covers for the loss of other.

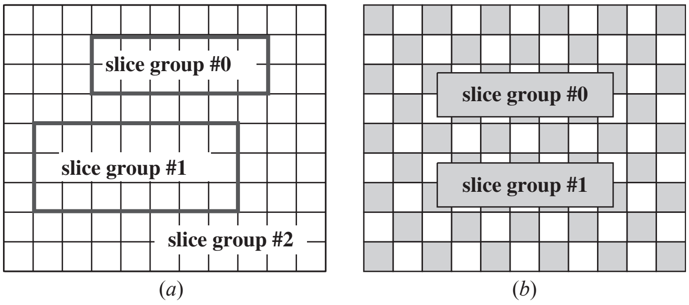

Figure 11.20 Subdivision of a QCIF picture into slice groups: (a) foreground/ background and (b) checkerboard pattern

H.264 defines six implicit types of MB classification pattern, known from type 0 to type 5, plus an explicit pattern, in which the MB map is user defined (a total of seven patterns). Figure 11.21 shows the six implicit patterns of FMO for two slice groups #0 and #1. These types are defined as: type 0 is interleaved, type 1 is checkerboard (or dispersed), type 2 is foreground and background, type 3 is box

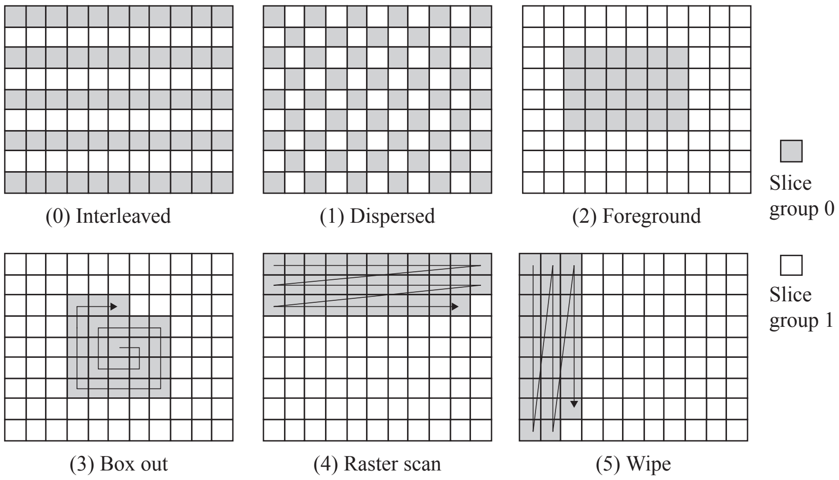

Figure 11.21 Various types of FMO

out, type 4 is raster scan and type 5 is wipe. In the explicit case, the parameter slice_group_id is transmitted for each MB in the picture specifying the slice group to which it belongs to.

Proper arrangement of MBs in multiple slice groups increases error resiliency of the bitstream. For example, MBs with high texture and motion, which normally create strong transform coefficients residues, can be grouped and better protected against the channel errors. Moreover, by spreading MBs in different groups in the form of interleaved or checkerboard (dispersed), one can conceal the loss of MBs in the missing slice by the safely received ones. Experiments show that for video-conferencing applications (low activity), without unequal error protection, a loss rate of 10 per cent can be easily concealed without showing any annoying artefacts. If slice groups containing important MBs are strongly protected against the channel errors, the bitstream can even stand much higher error rates than the 10 per cent.

However, reordering MB positions reduces the correlations between the neighbouring MB, impairing the compression efficiency of the encoder. The largest penalty is that of the checkerboard (dispersed) pattern, where predictions from the neighbouring blocks are abandoned to prevent error propagation. This is followed by the interleaving of slices, especially when they are line by line interleaved. The penalty in bit rate in error-free environment is both content and bit rate (*QP*) dependent, and can vary from 5 to even 20 per cent of the no-error resilience bit rate [3]. But in an error-prone environment, where forward error correcting (FEC) code is required, the compression deficiency of the FMO mode can be offset with the required FEC overhead.

Figure 11.22 shows the error resilience of six forms of implicit FMO without any external FEC. Here the side effects of lost MBs at the decoder are concealed, and hence, the superiority of one method over the other indicates how an FMO pattern has a better loss concealment property. The ultimate video quality depends on how efficiently the error concealment algorithm is implemented. In this figure, the foreman test sequence with QCIF@15 frame/s was coded at 64 kbyte/s for all modes, and each picture was divided into two slices. The erroneous pictures were then decoded by a JM decoder with the motion copy facility for loss concealment. As seen, the checkerboard (dispersed) followed by the interleave modes produces better quality than the other modes.

It is also worth noting that as the slices can be decoded independently, this gives rise to the concept of the arbitrary slice ordering (ASO). In this case, the slices of a picture can be in any order in the bitstream, and this can reduce the decoding delay in case of out-of-order delivery of the NAL units.

11.8.3 Data partitioning

The importance of data partitioning (DP) in making video stream more robust to errors was addressed in section 9.7.3. There it was discussed that if the more important encoding parameters like addressing and *MV*s are sent before the less important data, like the residual transform coefficients, then the impact of errors on the video quality is minimised. However, one can still improve the perceived video

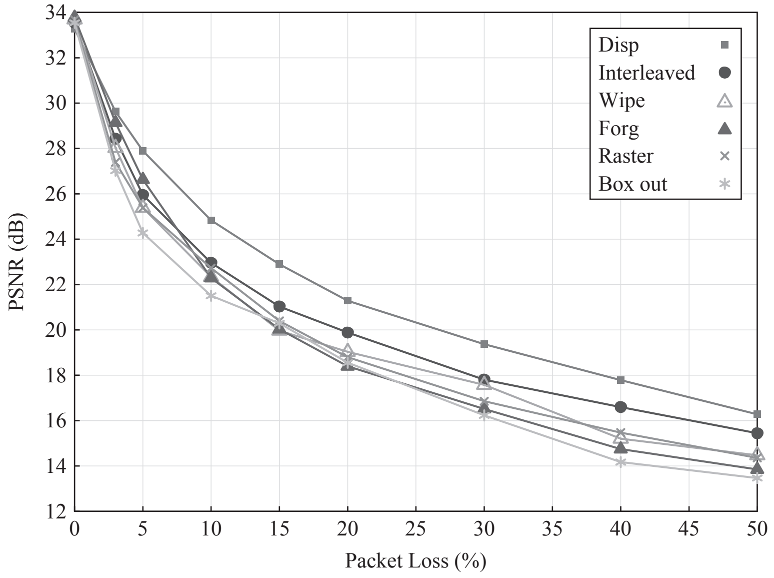

Figure 11.22 Error resilience performance of various FMO modes

quality by discriminating and better protecting the important encoding parameters over the nonimportant ones. Such a strategy called unequal error protection was an option for H.263, but now, due to its importance, has become an important part of H.264. H.264 has even some recommendations for better protection of bitstream against the error. This standard partitions the bitstream into three different classes called DP_A, DP_B and DP_C in the descending order of importance. Each part is encapsulated into a separate unit of the NAL for transmission, described in section 11.13. The partitioned data in H.264 are defined as follows:

- Data partition A (DP_A) contains header information, MB types, addresses, quantisation parameters and *MV*s. These are the most important information, and if this data is missing, the other partitions cannot be decoded.
- Data partition B (DP_B) is the second-most important partition, consisting of intra coefficients and intra-CBP. Because of the importance of intra coded information in preventing error propagation, the loss of this partition severely degrades the quality of the forthcoming pictures and may result in synchronisation loss. To decode partition B, partition A of the same slice needs to be available.
- Data partition C (DP_C) is the least important data and it contains only inter-CBP and inter coded residues. It usually comprises the largest portion of a coded slice. Its loss may lead to some picture artefacts, but it does not disturb the encoder/decoder synchronisation.

Since parts A and B are important, they can be more heavily protected with forward error correcting code (FEC) code than data from part C. For normal pictures at nominal bit rates, this does not impose significant increase in the bit rate. Despite this protection, some of these partitions may not be available at the decoder. It can be due to severe channel condition such that the used FEC is not sufficient for their correct decoding, or in a packet network environment, due to network congestion, they are lost. However, to decode a picture completely, all the partitions should be available; if some partitions are missing, the others can still be used to conceal the ill effects of the lost partition in the following order:

1. If partition C is missing, it can be concealed with the *MV*s from partition A and texture from partition B using intraframe concealment.
2. If only partition B is missing, it can be concealed with *MV*s from partition A and inter information from partition C.
3. If partitions B and C are missing, *MV*s of partition A are used for concealment.
4. If partition A is missing and B and/or C are available, *MV*s spatially above the MB row for each lost MB are used.

11.8.4 Intra-MB/IDR

Intra pictures or intra slices are used to confine the picture drifting errors and prevent their propagation into the following pictures/slices. H.264 supports two types of intra slices, the instantaneous decoding refresh (IDR) slice and the intra slice. Furthermore, some of the MBs inside inter coded slices can be intra coded to prevent error propagation, or they are chosen because their bit rates might be less than that of inter coded ones (e.g. when motion is unpredictable).

Both the intra and the IDR are intra coded slices/pictures without reference to any other pictures. The difference between the two is that the IDR picture invalidates all the reference pictures in the buffer prior to itself and thus can completely confine the drifting errors induced by the previous pictures. The intra slices, on the other hand, do not invalidate the reference pictures in the buffer and thus can confine drift error at that picture position only. If the future pictures refer to any picture older than the intra picture, the drift error can occur again.

Decision for inter/intra coding is done according to the RD optimisation such that an appropriate coding mode is selected minimising the Lagrangian cost function. In the RD optimisation, the rate of intra coded blocks is that of block coefficients, but in inter coded block, the rate is a sum of block coefficients and the *MV*s rates.

To prevent picture drift due to error/loss, some of the MBs in each slice might be forced to be intra coded. Arrangement for intra coding is such that the whole picture is updated after several frames. For this reason, this method is also called forced intra update. Forced intra updating can be done either randomly or within a certain update pattern. For example, a row of MBs in each frame in turn is intra coded.

Figure 11.22 compares the error resiliency of FMO (checkerboard/dispersed), data partition (DP), intra update and intra update combined with FMO against no-error resilience coding. For this test, the foreman sequence at CIF@30 Hz with IPPP... Group of Pictures (GOP) was coded with JM software at a target bit rate of

1 Mbit/s under all encoding conditions. Compressed bitstream of each method was packetised into 1-kbyte packets, and packets were randomly dropped. Each point in the figure is the average video quality over 20 runs. For intra update, at each picture, a row of MBs (22 MBs in CIF) in turn were forcibly intra coded. For DP, partitions B and C of each slice were subject to loss, but not partition A. For FMO plus intra update, first of all, one row of MBs in each picture was intra coded, and then the MBs of the whole picture were grouped into two sets and reordered in checkerboard pattern. In fact, in this case, forced intra coded MBs are spread into more rows of MBs, which should create better condition for loss concealment.

The intra update due to inefficient coding of intra over inter coding has lower video quality at no or very low loss rate. Increasing the loss rate intra update due to its ability to prevent error propagation yields the best result of all the error resilient schemes (see Figure 11.23). When this is combined with FMO, the better-quality images of intra updates with the better loss concealment environment provided by FMO give the best result.

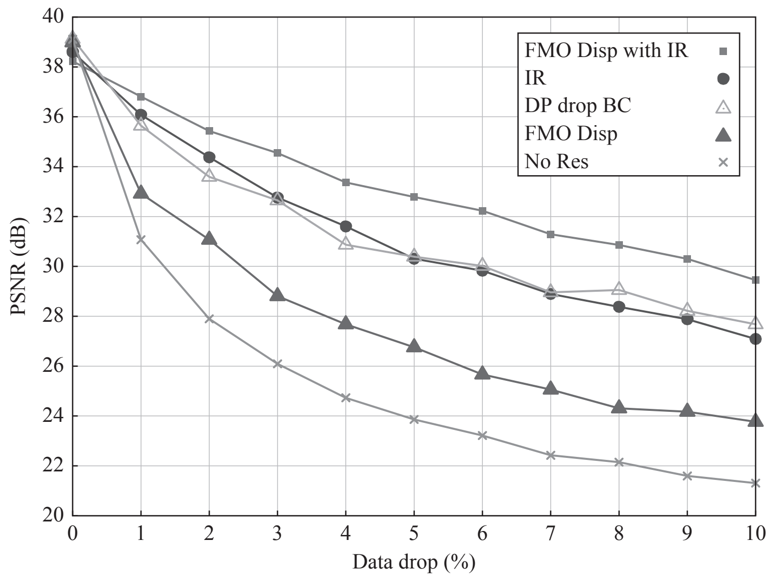

Figure 11.23 Performance of various error resilient modes

Data-partitioned video quality at no loss is better than intra update (IR in the Figure), but as the loss rate increases, accumulated loss of residual transform coefficients of parts B and C makes it poorer than intra update (DP drop BC, in the figure). However, at high loss rates, due to its better loss concealment, it overtakes intra update. Note that in DP with protected part A, loss concealment is carried out with the exact *MV*s, producing better image quality than interframe loss concealment, which estimates the lost *MV*s. Nevertheless, it is still inferior to intra plus FMO. It should be noted that adding FMO to DP may not improve its performance as done with intra update; this is because, as stated above, its loss concealment is done with its exact *MV*s and does not need a good estimate. However, FMO due to isolation of neighbouring MBs prevents spatial propagation of errors, improving image quality in any case.

Finally, FMO gives the poorest performance, as it has to just rely on the loss concealment. This, of course, depends on how well the loss concealment has been implemented, and it can be improved with better loss concealment strategy. Nevertheless, it is always worse than DP, which uses exact *MV*s; one should note that in DP, protection of part A exerts extra overheads. All methods outperform no-error resilience coding (No Res in the figure).

11.8.5 Multiple reference pictures

Multiple reference pictures, in addition to efficient motion compensation for improving the compression gain of the encoder, can also be used in a different form for error robustness in error-prone environments. In section 9.7.2, we discussed that if one of the error-free references is selected, then error propagation can be prevented. In H.263, this was an option for the encoder, but in H.264, it plays an important role, and the standard recommends some guidelines for its better use, to be defined shortly. This procedure can be used with and without a back channel. In systems with a back channel like bidirectional conversational application, the decoder can initiate the selection of reference pictures using one of the following modes [15]:

- ACK mode: The decoder acknowledges safe reception of the message, and the encoder marks the correctly received slices for future references.
- NACK mode: The decoder sends a negative acknowledgement for every lost/corrupted slice (e.g. through checking slice reference time or receiving an erroneous slice). When the encoder receives a NACK message, that picture is not used for future reference, and the reference picture is selected from the pictures before the NACK picture.
- ACK+NACK mode: In this case, the encoder switches between the above two modes according to the message from the decoder.

The ACK mode incurs too much overhead on the back channel, but the encoder is ensured that the used reference picture is error free and error propagation is limited. The other side effect is in the long routes, where a large gap between the current picture to be coded and the error-free reference picture reduces the compression gain. On the other hand, the NACK mode has no significant back channel load for good-quality communication link, but if for any reason the NACK signal is not received by the encoder, the error will be persistent and propagates through the pictures. Even future reception of NACK cannot prevent this error propagation. However, the NACK mode has high coding gain, since any chosen picture can be used as a reference, unless it was not acknowledged.

The combination of ACK+NACK is perhaps the best solution for compression efficiency and robustness to channel errors. To minimise the back channel signalling load, the encoder initiates communication with the NACK mode. After receiving *N* consecutive NACK signals, which is an indication of a bad channel, the encoder switches to ACK mode. The encoder can switch back to NACK mode, when *M* consecutive ACK signals are received. Thus, ACK+NACK has a source channel optimisation property, such that in good channel conditions, it uses NACK mode, and hence, closer reference pictures are used for higher compression, and in bad channels, through ACK, it is ensured that the used reference pictures are error free and the error is not propagated. In erroneous environment, error robustness is more desired than higher error-free compression gain.

In the systems without a back channel, such as multicasting, video redundancy coding (VRC) technique is used instead [16]. In VRC, the input video is separated into two or more threads, and pictures in each thread use their own predictions. For example, odd pictures can go into one thread and the even pictures into the other. The bitstream in each thread starts and ends with a sync picture, and the sync pictures can also be inserted at specific intervals. The sync picture may be an I-picture or an SI-picture. A simple example is shown in Figure 11.24, with two streams having odd- and even-numbered pictures in different threads. When a picture is lost from one stream, the other stream is decoded intact, and the temporal resolution of decoded pictures is temporally reduced. If display of higher frame rate is desired, the decoded pictures of the safe route can be repeated. Alternately, the corrupted/lost picture of the erroneous route is reconstructed from the pictures of the other stream having shorter temporal distances (i.e. loss concealment), and the remaining pictures are decoded following the lost concealed reference picture (picture quality can be slightly degraded).

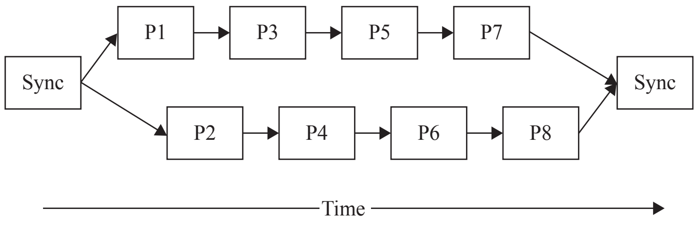

Figure 11.24 VRC scheme with two threads and four pictures per thread

This technique is also called multiple description coding, and in wireless communications, it can be combined with space diversity technique to make sure that at least one of the channels is not affected by fading. The missing data are then interpolated from the safely received channel data. For better loss concealment, slice and MB ordering, ASO and FMO may be used in each of the odd and even pictures.

11.8.6 Redundant slices

To enhance error robustness in H.264, the encoder can send duplicate copies of some or all slices of a picture. To minimise the extra bits of redundant transmission, these slices are coded with coarser *QP* than the main slice. If both representations of the same slice are received by the decoder, then the redundant slice is discarded and the main slice is decoded. In case the main slice is lost, then the redundant representation is decoded. Redundant slices have been introduced for mobile applications but can be efficiently used in IP-based communication.

11.8.7 Stream switching

In H.264, two new types of slice called switching predictive (SP)- and switching intra (SI)-slices have been defined. Since pictures containing these slices have specific applications such as stream switching, splicing, random access, fast forward, fast backward and error resilience/recovery, all slices in a picture are of the same type, and hereafter, we refer to them as SP/SI-pictures [18]. For error resiliency, the idea behind the switching pictures is to regain loss of synchronisation between the encoder and decoder, which may arise due to channel errors. In this case, the encoder sends a switching picture referenced to a correctly received picture, and the decoder can follow drift-free decoding with reference to this switching picture.

There are numerous other applications for the switching pictures. For example, in channel capacity varying environment, a video may be coded at two different rates. At low channel rate, users stream low-quality video, and when channel capacity increases, they may switch to a higher-quality video. Or, in a fixed-capacity channel, lower-rate video can be better protected by heavier FEC code than the higher-rate (quality) video. When channel condition is poor, lower-quality video is streamed, and when the condition improves, it is switched to higher-quality stream. Forward/backward switching may occur as many times as required.

Switching pictures are either predictive coded (SP) or intra coded (SI). The predictive pictures (SP) themselves are of two types: primary (PSP) and secondary (SSP) switching pictures, which are explained in the following sections.

11.8.7.1 PSP-picture

The primary switching pictures (PSP) are motion-compensated predictive pictures and are coded like the P-pictures. Their main difference is the extra quantisation imposed on the PSP-picture to make sure that its quality is the same as that of the secondary pictures, SSP (see below). Thus, PSP-pictures generate slightly more bits than the normal P-pictures. They are inserted into the bitstream to mark the positions where the switching can take place. When switching occurs, a secondary switching picture is used instead. Although the bit rate of the secondary switching picture might be high, since they are used only once and the frequently transmitted PSP-pictures have much lower rate than the I-pictures, switching pictures are used in video streaming instead of I-pictures.

11.8.7.2 SSP-picture

A secondary switching picture (SSP) is, in fact, the picture used for switching purposes. The decoder can decode the bitstream with reference to this picture irrespective of what its encoded reference picture was. These pictures are only sent at the switching instants or for regaining synchronisation between the encoder and decoder, which may arise due to channel errors.

11.8.7.3 SI-picture

SI-pictures are the intra coded representation of the SSP-pictures. Although these pictures can be used for switching, they are normally used for accessing a bit-stream, as they act like an I-picture, as shown in Figure 11.25.

11.8.7.4 Switching between two streams

To see how switching pictures act and how they should be coded, let us look at switching between two streams, as shown in Figure 11.24. Each stream is populated with PSP-pictures at specific locations to mark a possible location for switching. Every PSP-picture has an SSP counterpart stored in the server, but SSP is only transmitted when switching becomes necessary. In the figure, two bitstreams, switched-from and switched-to, are shown with periodically inserted PSP-pictures. The solid arrows in the figure indicate the transmission path. As an example, it starts by sending all the pictures from the switched-from stream up to a PSP-picture, which demands switching. In this case, an SSP-picture is transmitted instead of a PSP and followed by pictures from the switched-to stream. The SSP-picture is the counterpart of the PSP-picture of the switched-to bitstream (second PSP in the figure) coded with reference to the previous picture of the switched-from bitstream. The dotted arrows show the pictures that are coded but not transmitted. The PSP-picture can be inserted at any place, but currently, only periodic implementation is available in the JM software encoder.

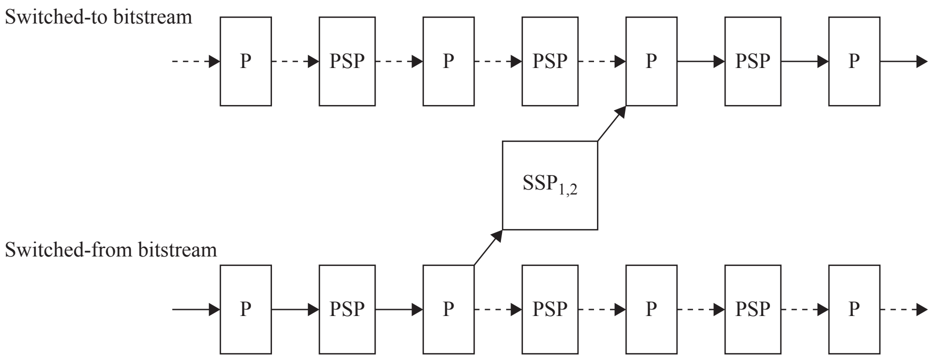

Figure 11.25 Bitstream switching with SSP-picture

Switching with SI-picture is shown in Figure 11.26. The only difference is that the SI-picture is the intra representation of the SSP-picture without reference to any previous picture. Although SI-pictures can also be used instead of SSP-pictures, but since they generate higher bit rates than the SSP-pictures, the latter is preferred (note: if switching occurs infrequently, the added bits are negligible). However, the main use of SI-pictures will be random access of the stream.

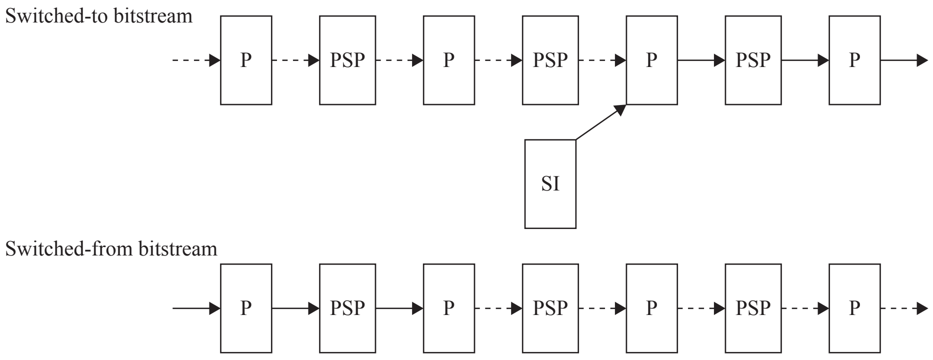

Figure 11.26 Bitstream switching with SI-picture

11.8.7.5 Error recovery

As another example, Figure 11.27 shows switching pictures used for error recovery. In this figure, SSP-picture is coded with reference to a picture that ensures that the receiver has an error-free copy of it. When error occurs, the client signals a picture loss, to which the server responds by sending an SSP-picture in place of the next PSP-picture. The picture immediately after the PSP-picture switches its prediction to the SSP-picture, and decoding continues, as shown in the figure. It is worth noting that the longer the communication link, the farther away is the SSP-picture from its prediction, increasing its bit rate.

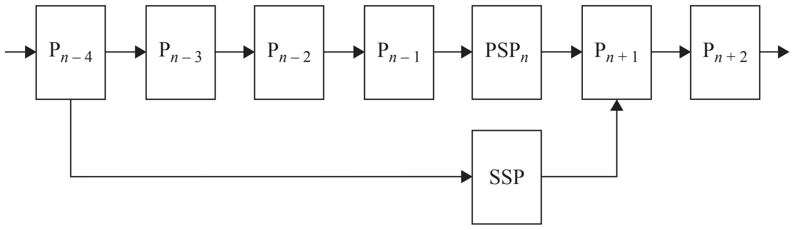

Figure 11.27 Switching picture in error recovery

11.8.7.6 Encoding of switching pictures

Encoding of PSP-picture

The primary switching picture, PSP, is predictive coded like a P-picture, with the main difference that it is doubly quantised. That is, it is first motion compensated, transform coded and quantised with its own stream quantiser parameter *QSP*, as shown in Figure 11.28. It is then dequantised and requantised with the quantiser parameter of the secondary switching picture, QSSP of the other stream. The reconstructed picture with the second quantiser is a predictor for coding the next P-picture. Quantisation of the predicted picture before residue calculation is optional, but it improves the switched picture quality by almost 0.4 dB [19].

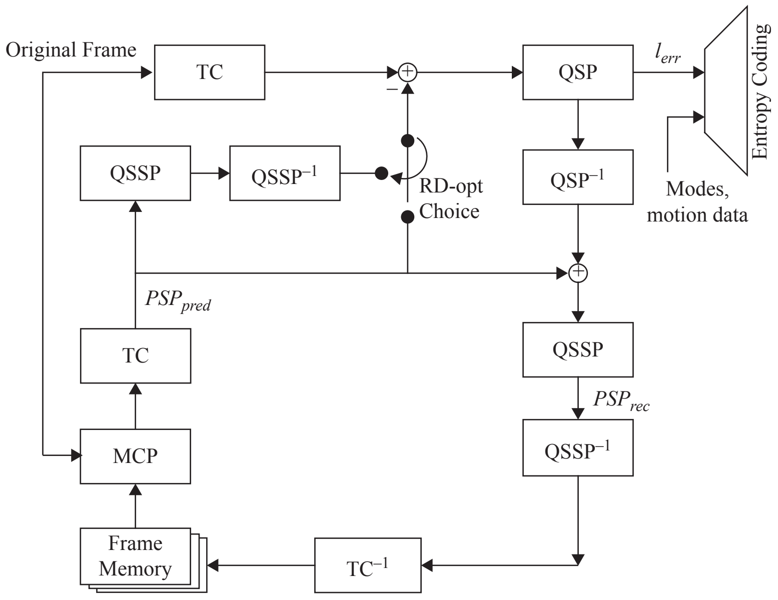

Figure 11.28 PSP-picture encoder

Encoding of SSP-picture

Figure 11.29 shows encoding of an SSP-picture with the quantiser parameter QSSP. Since after switching, the first predictive picture of the switched-to stream, P_{st}, will be predicted from the SSP, rather than from its own PSP-picture, SSP is required to have the same quality as the PSP_{st}. However, according to Figure 11.25, SSP was coded with reference to a P-picture from the switched-from stream, P_{sf}. Thus, to generate an SSP-picture, first the primary switching picture of switched-to stream PSP_{st} is motion compensated with the reference to P_{sf}, transform coded and quantised with QSSP. This generates the mismatch between the PSP_{st} and the picture stored from the previous stream at the receiver buffer. The mismatch residues are then subtracted from the transform coefficients of the PSP_{st}, shown as

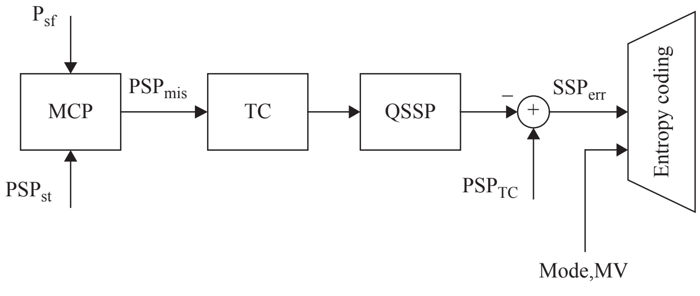

Figure 11.29 SSP-picture encoder

PSP_{TC} in the figure to generate an error signal for SSP. The resulting error signal is the SSP residue, SSP_{err}, to be entropy coded and transmitted. The overall operation is summarised by

$$SSP_{err} = VLC(PSP_{TC} - (QSSP(MCP(f_{sf}, PSP_{st})))) \tag{11.39}$$

Encoding of SI-picture
SI-picture is an intra coded picture with the quality of the PSP-picture. Thus, the PSP-picture is reencoded as intraframe, and any difference between the intra- and interframe is added to the predictive coded PSP-picture.

11.9 Error concealment

Despite all the error robustness procedures envisaged for the codec, some parts of the bitstream either may not be received by the decoder (lost data) or are severely damaged, which are not decodable and are inevitably discarded by the decoder. The best a decoder does is to conceal or hide the ill effect of lost data. In section 9.7.5, the general idea for loss/error concealment was introduced. However, loss/error concealment is not a part of any standard, and hence, it is not a normative feature to be within the scope of the H.264 standard. Despite this, the test model of the standard provides a basic level of error concealment for the decoder [4]. Two error concealment algorithms are defined in the H.264 test mode:

1. weighted pixel value averaging for intraframe concealment
2. boundary matching based *MV*s for interframe concealment

11.9.1 Weighted pixel value averaging

Weighted pixel value averaging is used for intraframe concealment, in which pixels of a lost MB are interpolated from the weighted average values of the border pixels of the intra neighbouring MBs. If a lost MB has only two correctly decoded MBs, they are used in the interpolation process; otherwise, previously concealed MBs are used. The procedure is pictorially shown in Figure 11.30, and the interpolated value of a lost pixel p_0 is given by

$$p_0 = \frac{\sum_{i=1}^{4} d_i p_i}{\sum_{i=1}^{4} d_i} \tag{11.40}$$

where p_i are the values of the four pixels at the left, right, top and bottom border pixels of the surrounding blocks to the lost pixel and d_i are the distances of the pixels p_i from pixel p_0.

11.9.2 Boundary matching based motion vectors

In the interframe error concealment, pixels from the reference picture but motion compensated with an estimated *MV* are used to reconstruct missing pixels. In the proposed loss concealment method of the reference model, MBs of the whole

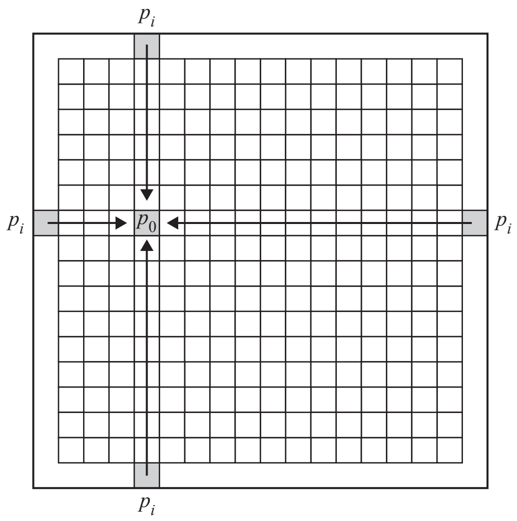

Figure 11.30 Spatial concealment 16 × 16 block

picture are considered together in two steps. The motion activities of the correctly received slices are considered first. If the average length of the *MV*s in the slice is less than a threshold (e.g. quarter or half a pixel), all the lost slices are copied from the colocated reference pictures (frame copy). Otherwise, motion-compensated error concealment with estimated *MV*s for the lost MBs is used (motion copy). For better estimation of *MV*s, the whole picture is scanned MBs column wise from left and right edges towards the picture centre. Consecutive lost MBs in a column are concealed starting from top and bottom of the area towards the centre.

Each 8 × 8 block luminance of the MB is handled separately. Only the *MV*s and reference pictures of the spatially adjacent correctly received blocks are used for concealment. If all the *MV*s of the neighbouring block are missing, their concealed *MV*s are used instead. In addition, the colocated block from the previous picture is always one of the candidates.

In section 9.7.5, we showed how among the several candidate *MV*s, the one that gives the least block boundary discontinuity can be selected. As an example, this is shown in Figure 11.31, where a lost 8 × 8 block has two 4 × 4 blocks MV^{top1} and MV^{top2} at the top and three 8 × 8 blocks MV^{left}, MV^{right} and MV^{bot} at the left, right and bottom, respectively. The difference between the border pixels of a missing block, shown as outer pixels in the figure and the motion compensated inner pixels by the motion vectors of the neighbouring top, bottom, left, right and co-located blocks in turn are tested according to eqn. 11.41

$$\min\arg_{\{colocated,top,bot,left,right\}} d_{sm} = \left\{ \sum_{j=1}^{N} |\hat{Y}(MV)_j^{IN} - Y_j^{OUT}|/N \right\} \tag{11.41}$$

where $\hat{Y}$ and Y represent the pixel values of the motion-compensated and the neighbouring blocks at the border, respectively. The one that results in the least border difference (discontinuity) is chosen.

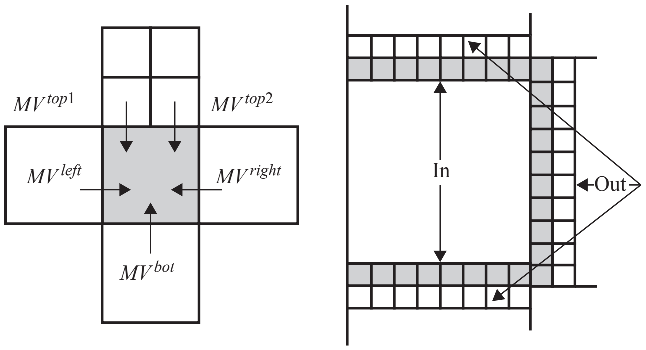

Figure 11.31 Estimating MVs for prediction

11.10 Profiles and levels

As discussed in earlier chapters, due to the heterogeneity of the communication systems and video services, the standard codecs are required to support interoperability between various scenarios. This is even more stringent for H.264 that has to cover a wide range of video services from telcos, IPTV and storage to broadcast. To cope with this diverse range of application conditions, the H.264 standard defines several profiles and levels to tailor the codec for a specific application. Otherwise, the codec would be extremely complex and expensive. Conforming to the codec for a specific application is determined with profiles and levels.

Profiles and levels specify restrictions on bitstreams and hence the capabilities needed to decode them. Profile defines a subset of coding tools in the bitstream specified by the standard, for instance, if the encoder supports B-slices, error resiliency and DP. Within the capabilities defined for a given profile, it is still possible to have a variety of performances, like bit rates, picture resolutions and frame rates. These are the constraints imposed on the values of the syntax elements in the bitstream and are defined under the level.

The first version of the standard specifies three profiles: the baseline, main and extended profiles, all with 4:2:0 picture format at 8-bit depth. Major applications of the baseline profile include video telephony, videoconferencing and wireless communication. The main profile is for television broadcasting and video storage. The extended profile is mainly defined for streaming media applications. The features of H.264 that each profile can support are summarised in Figure 11.32.

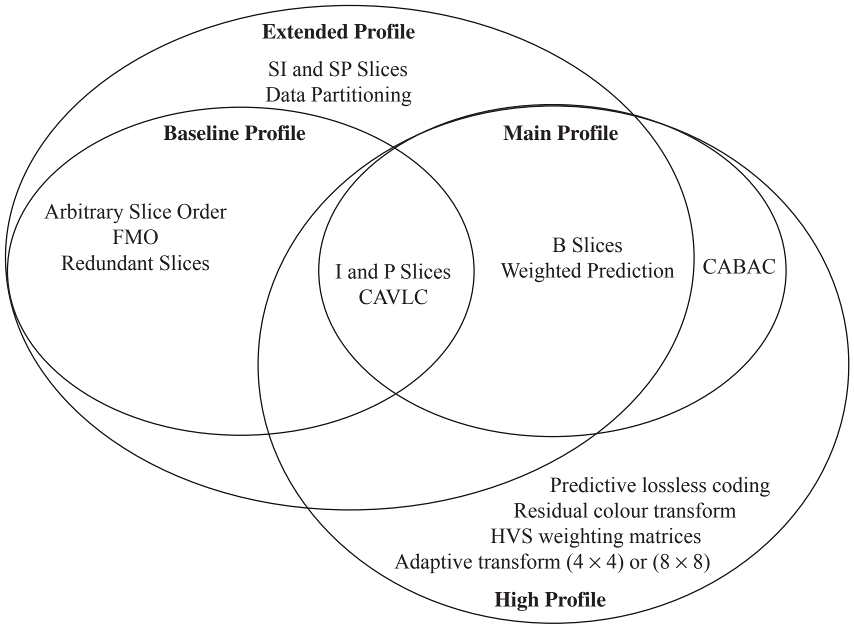

Figure 11.32 Profiles for H.264

The baseline profile is the simplest profile of H.264 and is defined for progressive video. It supports most of the features of the standard except for B-slices, weighted prediction, CABAC, interlaced video, SP/SI-slices and DP. It emphasises on coding efficiency and robustness with low computational complexity.

The main profile contains all the features of the standard with the exception of error resilience tools of FMO, ASO, redundant slices, data partition and SP/SI-slice. Thus, only a subset of the coded video sequences that are decodable by a baseline profile decoder can be decoded by a main profile decoder. This is a major departure from the earlier profiles defined in the previous standards. In those standards, profiles are normally subset of each other, and a higher-layer profile can decode the lower-layer one.

The extended profile emphasises on robustness and flexibility with high coding efficiency and supports all the features of H.264 including switching pictures and DP, except CABAC.

The standard later on introduced professional or fidelity range extensions (FREx) profile for very high quality applications, mainly known as high profile. It is a superset of the main profile with enhanced bit depths and chroma resolutions. The fidelity range extensions (high) profile has two added optional tools of 8×8 transform of motion-compensated residual blocks and perceptual-based scaling quantisation matrices to the main profile. The scaling factors are derived based on the spatial frequency response of the human visual system. That is, higher transform coefficients that represent higher spatial frequency are quantised coarser than lower ones, as discussed in section 7.5. These profiles are themselves defined in terms of four high profiles.

High profile = 4:2:0, 8 bits
High 10 profile = 4:2:0, 8–10 bits
High 4:2:2 profile = 4:2:2, 8–10 bits
High 4:4:4 profile = 4:4:4, 8–12 bits

The high profile is the simplest superset of the main profile, having the same chroma bit depth and resolution for the same application. Hence, it is expected to replace the main profile in the future applications that were expected to be used. Higher-order profiles increase either the chroma bit depth or the resolution or both. At the extreme of the high profiles, stands the high 4:4:4 profile with 8- to 12-bit resolution. In this profile, colour has the same resolution of luminance, and transformation and quantisation of the encoder are bypassed, and the residual data are directly entropy coded. Differences between the encoding tools supported by various profiles are tabulated in Table 11.6. The remaining encoding tools, such as deblocking filters, CAVLC, I/P-slices, variable block size and quarter-sample motion estimation, and intra prediction, which are not listed in this table, are common to all.

Various applications of these profiles, compared to the MPEG-4 visual profiles, are summarised in Table 11.7.

The standard also defines 16 levels by setting constraints on the encoding parameters of picture size, bit rates, buffer, etc. Table 11.8 summarises the level parameters defined for various picture resolutions and bit rates from QCIF to 4K video of digital cinema.

Table 11.6 Coding tools supported by various profiles

Feature	**Base**	**Ext.**	**Main**	**High**	**High 10**	**High 4:2:2**	**High 4:4:4**
B-slice	No	Yes	Yes	Yes	Yes	Yes	Yes
SI/SP	No	Yes	No	No	No	No	No
FMO	Yes	Yes	No	No	No	No	No
ASO	Yes	Yes	No	No	No	No	No
Redundant slice	Yes	Yes	No	No	No	No	No
DP	No	Yes	No	No	No	No	No
PAFF/MB-AFF	No	Yes	Yes	Yes	Yes	Yes	Yes
CABAC	No	No	Yes	Yes	Yes	Yes	Yes
Adaptive $4 \times 4/8 \times 8$ transform	No	No	No	Yes	Yes	Yes	Yes
Quantisation scaling matrix	No	No	No	Yes	Yes	Yes	Yes
Separate chroma *QP*	No	No	No	Yes	Yes	Yes	Yes
Monochrome (4:0:0)	No	No	No	Yes	Yes	Yes	Yes
Lossless coding	No	No	No	No	No	No	Yes
Bit depth	8	8	8	8	8–10	8–10	8–12
Chroma format	4:2:0	4:2:0	4:2:0	4:2:0	4:2:0	4:2:0/ 4:2:2	4:2:0/ 4:2:2/ 4:4:4

Table 11.7 Applications of various profiles

Application	Requirements	H.264 profile	MPEG-4 profile
Broadcast TV	Coding efficiency, reliability, interlace, low-complexity decoder	Main	ASP (advanced simple profile)
Video streaming	Coding efficiency, reliability, scalability	Extended	ARTS (advanced real time simple or FGS)
Video storage and playback	Coding efficiency, interlace, low-complexity encoder and decoder	Main	ASP
Videoconferencing	Coding efficiency, reliability, low latency, low-complexity encoder and decoder	Baseline	SP (simple profile)
Mobile video	Coding efficiency, reliability, low latency, low-complexity encoder and decoder, low power consumption	Baseline	SP
Studio distribution	Lossless or near lossless, interlace, efficiency transcoding	main	Studio profile

Table 11.8 Levels defined for H.264

Level	Constraints	Level	Constraints
Level 1	15 Hz QCIF@64 kbit/s	Level 3	25 Hz 625SD@10 Mbit/s
Level 1b	15 Hz QCIF@128 kbit/s	Level 3.1	30 Hz 720p@20 Mbit/s
Level 1.1	30 Hz QCIF@192 kbit/s	Level 3.2	60 Hz 720p@20 Mbit/s
Level 1.2	15 Hz CIF@384 kbit/s	Level 4	30 Hz 1080@20 Mbit/s
Level 1.3	30 Hz QCIF@768 kbit/s	Level 4.1	30 Hz 1080@50 Mbit/s
Level 2	30 Hz QCIF@2 Mbit/s	Level 4.2	60 Hz 16VGA@135 Mbit/s
Level 2.1	25 Hz 625HHR@4 Mbit/s	Level 5	30 Hz 16VGA@135 Mbit/s
Level 2.2	12.5 Hz 625SD@4 Mbit/s	Level 5.1	30 Hz 4k $\times$ 2k@240 Mbit/s

11.11 Compression gain and complexity of H.264

11.11.1 Compression gain

The changes introduced to the H.264 encoder throughout sections 11.3 to 11.7 can each improve the compression gain of H.264 over its predecessors. It is difficult to specify exactly how much each part contributes to the overall coding gain, as the amount of improvement is picture content (texture) dependent, can vary with the nature of motion and also depends on the bit and frame rates. Moreover, very often a combination of encoding tools makes them more efficient.

For example, spatial predictions of intra-MB or the variable block length motion estimation without RD optimisation may not show their true benefits, since performance depends on how wisely a mode is selected. Finally, manipulation of compressed elements, or the so-called coding tricks, can have a significant role in reducing the bit rate. Proper addressing of *MV*s, MB modes, skipped MB, *QP* change, selected look-up table, etc. all affect the bit rate. Although the amount of contribution from each coding trick might be small, their collective impact can be significant.

Despite these arguments, through experience and experiments, one can roughly estimate the contributions that each part can make to the overall coding gain. For instance, in normal video at nominal bit rates, the average contributions to the coding gains are [20]: variable block size motion estimation of 4×4 to 16×16, can give about 15 per cent improvement over the two block sizes of 8×8 and 16×16 of H.263, where this itself gives 5–8 per cent improvement over the fixed block size of 16×16 of MPEG-2. The quarter-pixel resolution of *MV*s gives 10–20 per cent improvement over the half-pixel resolution, and that itself gives the same degree of improvement over the integer pixel resolution. The coding gain due to multiple reference picture motion compensation is about 10–15 per cent depending on the motion model and the number of reference pictures. The CABAC entropy coder is about 5–15 per cent more efficient than CAVLC, and CAVLC itself is 10–20 per cent more efficient than the conventional nonadaptive Huffman coding, used in the earlier standards. The deblocking filter can contribute about 5–8 per cent in the objective (PSNR) quality of video, and its subjective quality improvement is even more impressive. Finally, the RD optimiser adds another 5–8 per cent in bit rate reduction, though its true benefit through decision making in the other coding parts is much greater. In fact, no new coding element as much as RD optimiser is involved in numerous coding activities, and for that reason, it is one of the more costly operations of the encoder.

These all easily add up to about 100 per cent, making the codec to be twice better than say H.263 and far better than MPEG-2. It appears that H.264 has achieved its goal set out at the beginning of this chapter. However, it should be borne in mind that during the development of H.264, the learnt lessons have also been exploited in the older standards, improving their compression performance over time, since encoders are free to code MBs the way they want, of course, to the extent the coding syntax is not violated. For instance, RD optimisation can be easily used in any codec without affecting its standard syntax.

Figure 11.33 compares the compression performance of four codecs, MPEG-2, H.263, MPEG-4 visual and H.264, for various bit rates of foreman standard test sequence of CIF@10 Hz resolution. The quality improvement is very noticeable.

The above relative coding gain of the codecs is just for one sequence, and the relative performance can vary with video content. Considering that H.264 has already replaced H.263/MPEG-4 visual, it is of vital importance to know its relative superiority over MPEG-2. This is because currently, several broadcasting organisations throughout the world who are in the process of moving towards digital terrestrial TV want to know how much real benefit one can get from H.264 over MPEG-2. Does the compression gain justify its extra complexity?

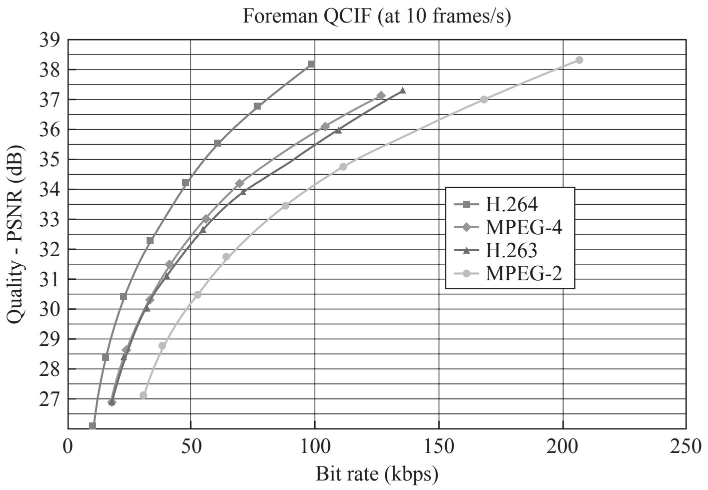

Figure 11.33 Comparisons of MPEG-2, MPEG-4, H.263 and H.264

To answer this question, let us look at the relative performance of H.264 over MPEG-2 derived from the hardware codecs of a manufacturer for a very wide range of video contents at various bit rates, shown in Figure 11.34 [21]. Each point on the scatter diagram shows the coding outcome of one video content. Each video is coded with an MPEG-2 encoder at a certain bit rate, and it was also coded with H.264, targeting for the same subjective quality produced under MPEG-2. The reduction in bits of H.264 is calculated as the amount of saved bits over the MPEG-2 at that quality and bit rate.

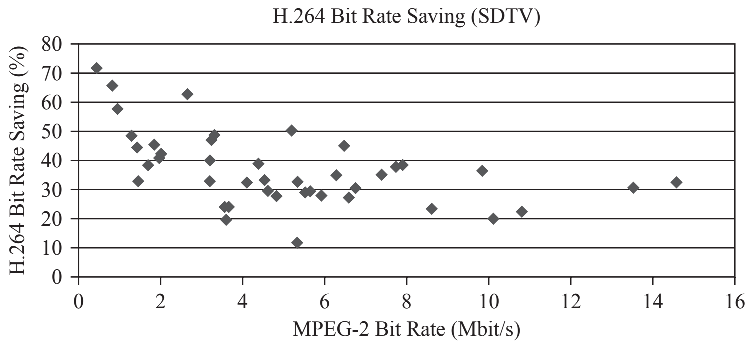

Figure 11.34 Bit rate saving of H.264 over MPEG-2 at equal bit rates (Source: [21])

The figure shows that saving in bits is video content dependent and also varies with the bit rate. For some video, the bit saving is more than 70 per cent, meaning that H.264 requires less than 30 per cent of MPEG-2 bit rate or that it is more than three times compression efficient than MPEG-2. On the other side, one can find a video that saves almost 10 per cent in bit rates, or requires 90 per cent of MPEG-2 bit rate. For broadcast entertainment TV, where programme quality is expected to be at its best and video content is unpredictable, perhaps one has to be conservative and look for the minimum saved bit rates. In this case, as seen, it is not too much.

However, if there are several videos to be accommodated in a given channel and saving bits on each is achieved according to this figure, then through statistical multiplexing, on the average, saving in bits can be significant. The larger the number of channels, the more likely is the average of these values to be achieved. This is more likely to be realised in satellite than terrestrial broadcast, as the former with a bandwidth of 36 MHz can accommodate more TV channels than the latter with 8 MHz.

11.11.2 Complexity

The compression gain of H.264 over its predecessors is achieved at the cost of extra encoding and decoding complexity. Similar to compression gain, it is difficult to give a complexity figure to any encoding function. Moreover, the hardware complexity of one element over the other does not match its software complexity ratio. For example, in terms of hardware, CABAC is far more complex than motion estimation, especially full search motion estimation is simple in hardware, but in terms of software, motion estimation requires too many CPU operations and cycles. If we resort to software complexity, which is easier to measure on the CPU time, our tests with numerous videos at various bit rates indicate that the two most costly encoding operations are motion estimation and RD optimisation. The motion estimation complexity is mainly influenced by the search window size. With EPZS and a maximum search of 16 pixels, it comprises about 65 per cent of the encoding time, down to 25 per cent for a search area of four pixels. These values each becomes about 8 per cent lower for smaller *QP*. The reason is that at larger *QP*, due to early termination and more of the MBs to be skipped, other encoding operations are seized and the major portion of CPU time goes to motion estimation. On the other hand, RD optimisation time is more image content dependent and varies with the quantisation parameter (encoding bit rate). In textured images with lower *QP*, RD execution time is significantly higher than that in softer images, and motion estimation range does not affect this complexity too much. However, in terms of portion of encoding time, when motion estimator uses less time, RD portion is increased. For example, at high-quality detailed image with a search of four pixels, where motion estimation is only 17 per cent of the encoding time, this portion for RD is about 70 per cent! When *QP* is increased, the RD portion is about 60 per cent, and that of motion estimation increases to 27 per cent. Though the actual motion estimation time does not increase, it is just the proportion that changes. On the other side of complexity, for a large motion search of 16 pixels, at high bit rate (low *QP*) coding, the RD portion of CPU time is about 27 per cent and that of motion estimation is 57 per cent, but at lower quality, these values become, respectively, 28 and 66 per cent. These arguments imply that if motion estimation has a proper starting point in the search window such that only small search window is sufficient, the cost of RD would be higher than that in motion estimation.

Thus, one may conclude that sum of motion estimation and RD optimisation complexities can contribute to more than 85 per cent of encoding time, and hence, the other encoding parts contribute to less than 15 per cent. Now, if we compare encoder and decoder complexities, there are numerous operations in the encoder that are not needed at the decoder. These include motion estimation, RD optimisation, entropy coding, transformation and various MB encoding decisions. Thus, it can be seen that the decoder complexity can be less than 10 per cent of the encoder, or that an encoder is ten times more complex than a decoder. Within the decoder itself, the most costly operation will be the deblocking filter, followed by the inverse transform, though these comprise a tiny portion of encoding complexity.

11.12 Scalable video coding

The three forms of scalability, temporal, spatial and quality, for the MPEG-2, H.263 and MPEG-4 visual were studied in details in the relevant chapters. H.264, which is an extension to H.263, very strongly supports this feature. This is mainly due to its wide range of applications, ranging from video distribution at various qualities and resolutions (scalabilities) to protection of video against transmission loss and errors (layering).

At the early stage of design, to perform temporal scalability, the ITU/ISO group were thinking to use short kernel wavelet filters in the temporal direction. This is called motion-compensated temporal filtering (MCTF), where through motion compensation, pictures are aligned temporally, and through dyadic filter (Haar transform), a hierarchy of temporally filtered pictures are generated [22]. However, experiments have shown that hierarchical B-pictures already supported in H.264 are more compression efficient than the MCTF pictures. Hence, the group opted for hierarchical B-pictures instead. These pictures are so efficiently coded that they even reshaped the structure of spatial and SNR scalability, which is defined in the following [23]. That is, spatial and SNR scalabilities do always include temporal scalability to offset their compression deficiency due to layering. The laboratory software model for this coder is called joint scalable video model (JSVM) [24].

11.12.1 Temporal scalability

In the standard codecs, temporal scalability is realised in the form of B-pictures. Since AVC allows B-pictures to be used as references for themselves, increasing the number of B-pictures in the hierarchy (up to 32 frames) can increase the compression gain, of course at the expense of longer coding delay. Note that in the other standards, B-pictures only refer to the anchor pictures of I and P, and hence, too many consecutive B-pictures are not efficiently coded. Some pictures are very far away from their references, and those which are close are inclined to get their predictions from only one reference (see Figure 11.35), nullifying the concept of bidirectional prediction. Hence, on the whole, the compression efficiency that one expects from bidirectional prediction does not materialise.

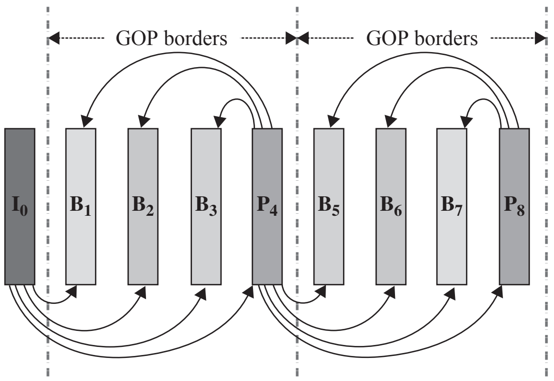

Figure 11.35 Classical B-picture prediction

Figure 11.36 illustrates the concept of hierarchical B-pictures, where the dyadic temporal enhancement layers, due to their proximity to their reference pictures, can be efficiently coded. Here the reference picture in lists 0 and 1 are restricted to be temporally preceding and succeeding reference pictures, respectively. In the figure, the base layer picture, normally a P- or an I-picture, is identified by the temporal layer identifier T_0, called key picture. Distance between the two key pictures defines the length of the GOP. The identifiers of the temporal enhancement layers in the order of their importance in the level of hierarchy are also shown. Each set of temporal layers $\{T_0, T_1, \ldots, T_k\}$ can be extracted and decoded independently of all the layers with a temporal identifier $T > K$. The transmission/decoding order of the pictures in the GOP follows their temporal layer order T_i.

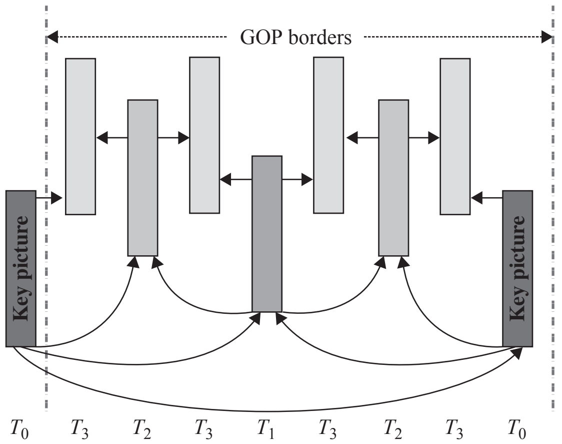

Figure 11.36 Hierarchical B-pictures with four dyadic levels (GOP of 8)

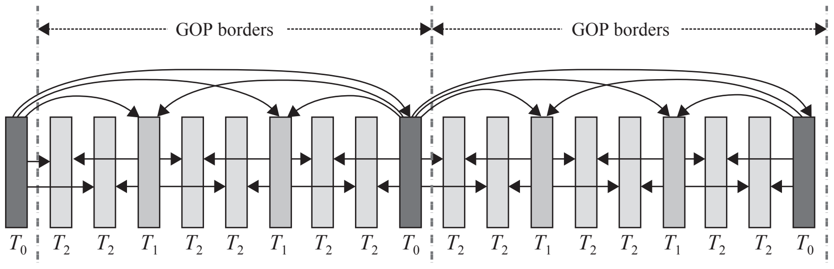
GOP borders
GOP borders
T_0 T_2 T_2 T_1 T_2 T_2 T_1 T_2 T_2 T_0 T_2 T_2 T_1 T_2 T_2 T_1 T_2 T_2 T_0

Figure 11.37 Nondyadic hierarchical B-pictures

Considering that multiple reference pictures can also be used in H.264, the reference picture lists can be reconstructed from more than one reference picture, and these pictures can be of the same temporal level of the predicted ones. Furthermore, prediction hierarchy may not be dyadic, and various sets of pictures may be decoded. For example, in Figure 11.37, two independent subsequences of one-ninth and one-third of the full frame rate can be decoded. Hence, by changing the prediction structure and the number of reference pictures, a variety of temporal scalabilities can be generated. These all affect the compression efficiency of temporal scalability and, at the same time, the dependability of the decoded pictures.

Finally, the relation between the quantiser step sizes of the layers affects the compression efficiency. In MPEG-2, we saw that B-pictures, due to better prediction, could be coded coarser than the P-pictures. Here too, we can make quantiser step sizes of closely predicted pictures to be coarser than those further away from their references. The JSVM recommends that for a quantiser parameter QP_0 at the base layer, the QP at a given temporal layer T is [24]

$$QP_T = QP_0 + 3 + T \tag{11.42}$$

Although this strategy makes picture quality in terms of PSNR to fluctuate, nevertheless, reconstructed pictures appear smooth, and the impact to overall bit rate reduction is very significant, especially at high GOP sizes.

11.12.2 Spatial scalability

Spatial scalability in H.264/scalable video coding (SVC) follows the same principles used in the other standard codecs of MPEG-2, H.263 and MPEG-4 visual. That is, video is coded in such a way that pictures of various spatial resolutions from a single bitstream can be extracted. The main difference between H.264/SVC and the previous scalable codecs is the way the interlayer information is exploited. In the earlier standards, the prediction signal for the enhancement layer is formed by motion-compensated pixels of the same layer, upsampled reconstructed reference layer or averaging both. The main problem with this strategy is that in a highly textured area, the upsampled pictures are contaminated by heavy aliasing noise and are not good predictors for the enhancement layer. In such a condition, the encoder prefers to use motion-compensated prediction of its own layer, and the reference layer data will not be of any use. Thus, for a two-layer scalability, there are two independent encoders, and compared with a single-layer encoder, it has to code, first of all, 25 per cent more pixels (base layer). Second, since these pixels are less correlated than the single-layer pixels, the overall bit rate will be much higher. Thus, it is of no surprise, if we see in section 8.5.7 that spatial scalability generates more than 30 per cent bits over the single layer.

To solve this problem, H.264/SVC tries to use interlayer information more efficiently than the previous standards. First of all, through analysing the local signal characteristics, the encoder decides to use either interlayer or intralayer prediction. Switching between the two can occur on MB by MB basis. In the intralayer prediction, the enhancement layer is independently coded from the base layer, and its MBs are either intra coded or motion compensated inter coded from the enhancement layer pictures. For interlayer coding, a new MB type is defined, which is signalled by setting the base flag mode [23]. When this mode is set, two types of predictions are made. These are defined in the following sections.

11.12.2.1 Prediction of macroblock modes

When the base mode flag is set, information from every 8×8 pixels of lower layer, such as mode, reference indices and *MV*s, are transferred to the colocated MB at the upper layer. In this case, if the reference layer is inter coded, then the enhancement layer is also interceded. Here, MB partitioning of the base layer in the area of 8×8 of the reference layer is upsampled and carried into the enhancement layer (each four blocks in the enhancement layer use one reference layer mode). The associated *MV*s are then derived by upscaling the reference layer *MV*s by a factor of 2. Now, the enhancement layer uses all these data to code its motion-compensated residue, without any overhead.

In addition to this new MB type, *MV*s of the reference layer can also be used as a predictor for efficient coding of the enhancement layer *MV*s. Thus, here the enhancement layer sends a refinement to the reference layer *MV*s. This is used if the cost of additional *MV* at the enhancement layer justifies the reduced motion-compensated error at this layer.

11.12.2.2 Prediction of residuals

Information from the reference layer can also be used as predictions for coding the enhancement layer residues. This equally applies to whether the enhancement layer MB is a new type (i.e. the base mode flag is set) or of a conventional type. This is signalled by the residual prediction flag. In this case, the residual signal of the corresponding 8×8 subblock in the reference layer is block-wise upsampled and used as a predictor to code the residuals of the enhancement layer. Thus, only the corresponding difference signal needs to be coded at the enhancement layer. The upsampling of the reference layer residuals is better to be carried out in the transform domain. This ensures no filtering will be carried out by the deblocking filter at the block boundaries.

If the colocated 8 × 8 subblock in the reference layer is intra coded, then the prediction will be the upsampled reconstructed reference layer subblock. This is similar to the interlayer coding used in the other standard.

In the above interlayer prediction, the enhancement layer uses the reference layer information without any significant overhead, reducing the bit rate. In addition to this, the standard also employs temporal scalability in all the layers, as shown in Figure 11.38. Now as it is claimed, the additional bits over the single layer are about 10 per cent [23]. When spatial scalability is combined with temporal scalability, the main anchor base layer picture (P or I) is called the key picture, and it defines the GOP size. Also, note that in spatio-temporal scalability, the number of pictures in the base and enhancement layer GOP can be different. As shown in Figure 11.38, some of the enhancement layer pictures do not have a temporally corresponding base layer picture and do not use any interlayer prediction. They use only intralayer bidirectional motion compensation, which can be equally efficient.

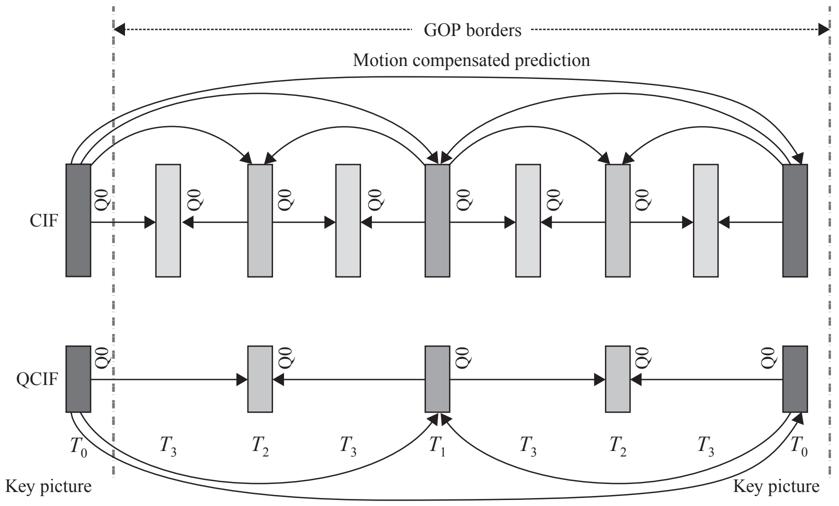

Figure 11.38 Two spatio-temporal scalability layers with GOP sizes of 4 for QCIF and 8 for CIF

11.12.3 Quality (SNR) scalability

In quality (SNR) scalability, pictures of the same size but different quality are coded. As was discussed in MPEG-2 and H.263, in this form of scalability, the enhancement layer codes the residual quantisation distortion of the base layer. There, we also noted that this kind of scalability, like spatial one, generates more bits than the single layer (about 30 per cent). To combat against the excessive bits, the standard also combines this scalability with the temporal one to gain from bidirectional predictions. However, temporal prediction can be applied in a variety of ways, where some of the base or enhancement layers are better to use their predictions from each other for more compression efficiency. Of course, this increases their inter dependency and might create picture drift. In MPEG-2, we discussed the role of including the enhancement pictures at the base layer prediction loop for increased compression, but at the expense of picture drift. It is claimed that this kind of scalability has about 10 per cent more bits over the single layer [23].

H.264/SVC defines two types of quality scalability, coarse grain scalability (CGS) and medium grain scalability (MGS). These are defined with the same purpose of the fine granular scalability defined for MPEG-4 visual. The CGS is similar to the SNR scalability of H.263 defined in section 9.8.2. In CGS, the quantiser parameter of the enhancement layer is less than that of the base layer, Q1 < Q0, to code its residual quantisation distortion. Figure 11.39 shows CGS for a group of four pictures. As all CGS layers are of identical sizes, interlayer upsampling prediction is not used. CGS allows a limited number of rate points equal to the number of layers, that is, a set of base and enhancement layer pictures that give the target bit rate.

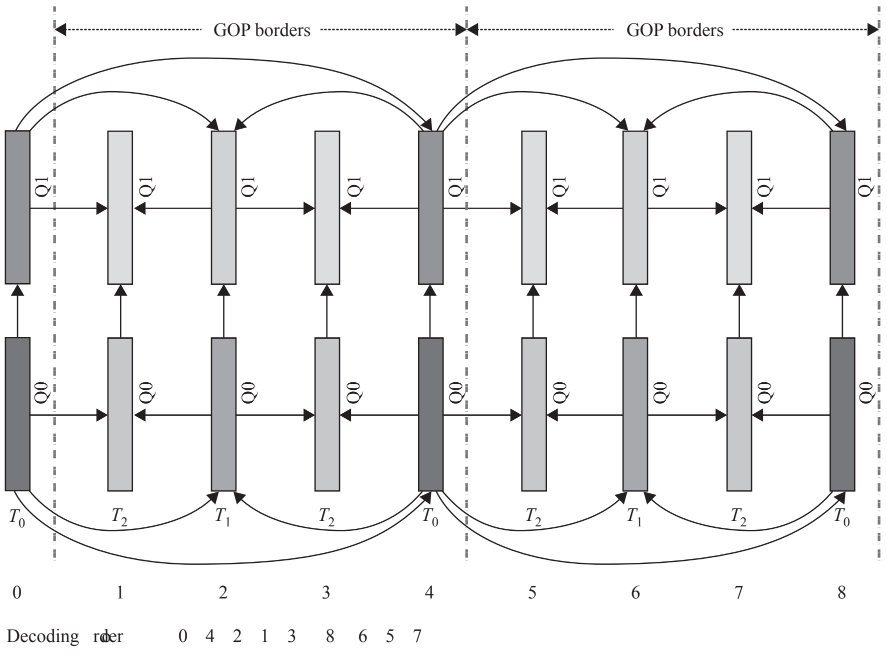

Figure 11.39 SNR with CGS scalability

To increase the coding efficiency and the supported number of rate points, MGS is defined. In MGS, the enhancement block transform coefficients can be partitioned into several layers, similar to the layering technique with frequency selective data partitioning introduced in MPEG-2 (see section 8.5.2). The break points in the zigzag scan define the picture quality at various layers. Since block size is 4 × 4, theoretically, up to 16 MGS layers can be defined. Thus, MGS can provide graceful degradation between quality layers by switching between different MGS layers in any access unit. To limit drift propagation, key pictures are used as synchronisation points between the encoder and the decoder. MGS provides flexibility for bitstream adaptation and error robustness. Bitstream adaptation is provided at the packet level (NAL unit).

Figure 11.40 shows an MGS layer with transform coefficients partitioned over three MGS quality layers.

Figure 11.41 shows an example of how the enhancement block transform coefficients can be partitioned into three sets of coefficients that can provide the enhancement pictures in Figure 11.40, identified by quality layers Q1–Q3.

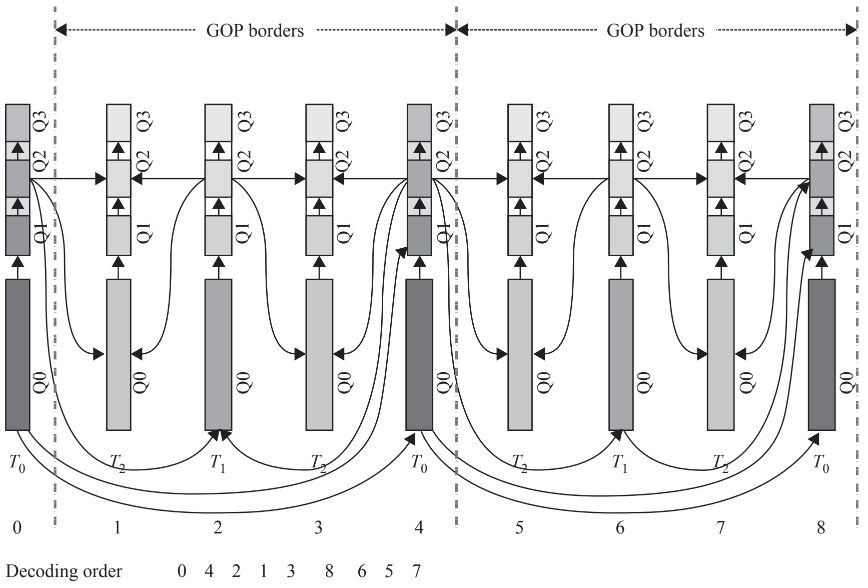
GOP borders
GOP borders
Q3
Q2
Q1
Q0
T_0 T_2 T_1 T_2 T_0 T_2 T_1 T_2 T_0
0 1 2 3 4 5 6 7 8
Decoding order 0 4 2 1 3 8 6 5 7

Figure 11.40 SNR with MGS scalability

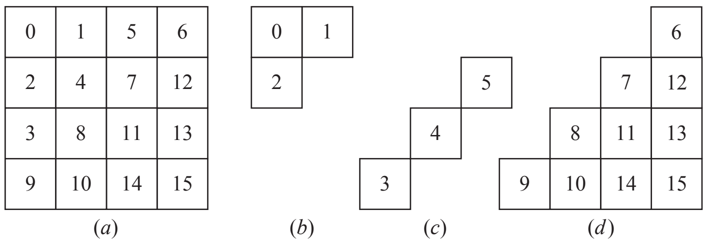

Figure 11.41 (a) Original block, and parts of the block for quality layers (b) Q1, (c) Q2 and (d) Q3

This scalability technique thus generates more layers of quality, and hence, quality differences between the layers are softer than in case of CGS. Note that the prediction loops in CGS (Figure 11.39) are different from those of MGS (Figure 11.40). Thus, even if in the MGS, the enhancement block is not partitioned and it has only one quality layer like CGS, due to different prediction directions, the resultant pictures have different quality and errors resiliency.

The key pictures (P or I), at temporal reference T_0, are the main base layer reference pictures that feed the others. The direction of the prediction of the remaining base and all of the enhancement layers, as shown, are very interdependent. Therefore, this kind of scalability can have a strong picture drift within the GOP boundaries, unless for the wanted application, the prediction loop for certain pictures may be disconnected, which inevitably reduces the compression gain.

11.12.4 Combined scalability

It is possible to combine the concepts of spatial, SNR and temporal scalabilities to generate a bitstream that supports a variety of spatial, quality and temporal rate points. Figure 11.42 shows an example of spatio-SNR-temporal scalability with a GOP of four pictures. In this figure, the enhancement layer of a spatial scalable

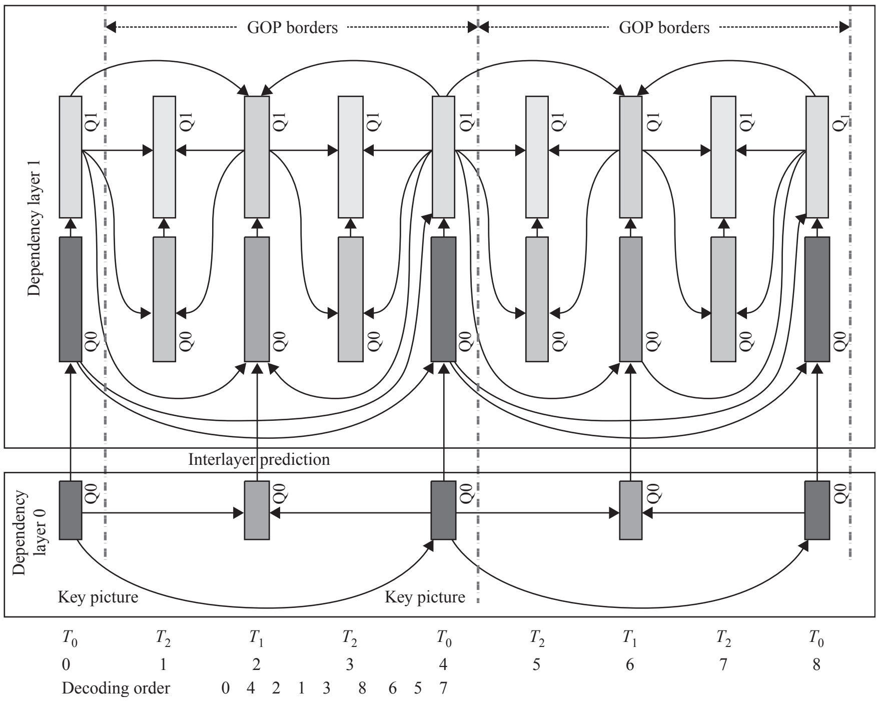

Figure 11.42 Combined spatial, SNR and temporal scalability with a GOP size of 4 (2 for the base layer)

coder is coded at two quality layers, Q0 and Q1 (SNR scalability), generating enhance 1 and enhance 2 bitstreams. Temporal scalability, as usual, is present, where the base layer, with low spatio-temporal resolution pictures, has lower picture rate and smaller pictures than the enhancement layers, generating the base layer bitstream. In this figure, the spatial scalability uses the base enhancement interlayer prediction, but in the SNR scalability, prediction between enhance 1 and enhance 2 is both interlayer and intralayer.

The spatio-temporal quality resolution at various points is better visualised on a three-dimensional plot, as shown in Figure 11.43. This figure shows various extraction points of the corresponding combined scalable video of Figure 11.42. For a CIF@30 Hz input video sequence, a CIF@30 Hz and Q1 is the highest rate point, and a QCIF@7.5 Hz, Q0 is the lowest extractable rate point.

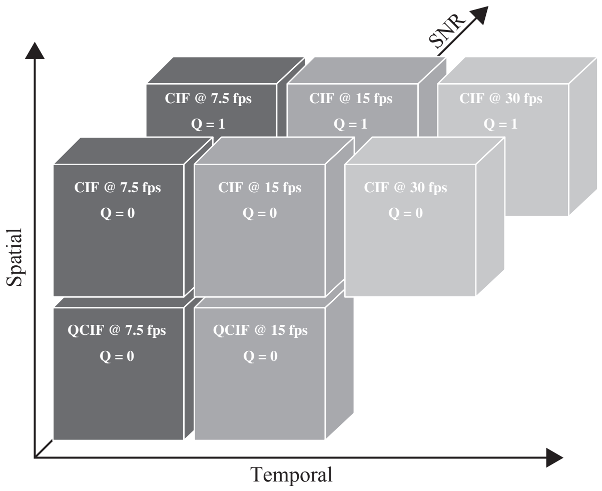

Figure 11.43 Three-dimensional representation of spatio-temporal quality at various points

11.12.5 SVC profiles

For the SVC extension of H.264, the standard specifies three profiles, known under H.264/SVC as scalable baseline profile, scalable high profile and scalable high intra profile.

11.12.5.1 Scalable baseline profile

This profile is primarily targeted for videoconferencing, mobile broadcasting and surveillance applications with limited processing capabilities. The profile builds on top of a constrained version of the H.264 baseline profile to which the base layer of the scalable stream must conform. In this profile, the resolution ratio between successive spatial layers is limited to 1.5 and 2 in both horizontal and vertical directions. Furthermore, interlaced coding is not included in this profile. The profile supports B-slices in the enhancement layers.

11.12.5.2 Scalable high profile

This profile is built on top of the H.264 high profile and is primarily designed for broadcast, streaming and storage applications. The scalable baseline profile limitations are not present. The base layer of scalable high-profile bitstream should conform to the H.264 high profile.

11.12.5.3 Scalable high intra profile

This profile mainly targets professional applications. All pictures of bitstreams conforming to this profile are IDR pictures. All the tools for the scalable high profile are supported in this profile.

11.13 Network abstraction layer

One of the distinct departures of H.264 from its predecessors is its two-layer architecture for separating video compression methodology from its transport over the network. The first layer called video coding layer (VCL), like other standard codecs, defines the methodologies used for compression of video that we have described so far. The second layer, called network abstraction layer (NAL), facilitates the delivery of the VCL data as well as the auxiliary data (non-VCL) to the underlying protocols such as RTP/UDP/IP, H.32X or MPEG-2 transport stream.

VCL NAL units contain data that represent video pictures in the form of a slice or data partition, while the non-VCL NAL units contain other additional information such as parameter sets, timing information and other supplemental data.

Figure 11.44 shows the basic view of interfacing VCL and non-VCL data into the network transport layer via the NAL. Each NAL unit could be considered as a packet that contains an integer number of bytes including a header and a payload. The header specifies the NAL unit type, and the payload contains the related data.

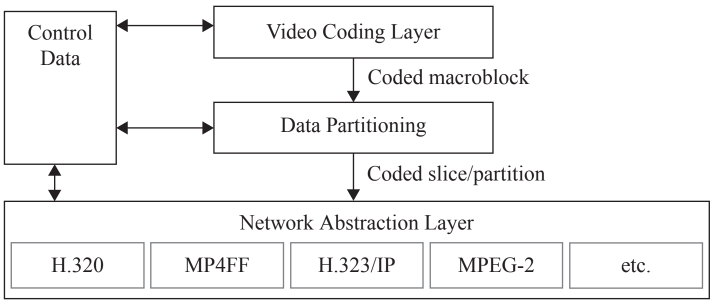

Figure 11.44 H.264 in transport environment

Ideally, the VCL should never generate NAL units larger than the medium transfer unit (MTU) size to avoid IP-layer fragmentation. This can easily be achieved by packing data of each slice into one NAL unit. However, as long as the NAL units are smaller than 64 kbytes, IP performs the fragmentation and the recombination of fragmented packets. Hence, even by simple packetisation, most prerecorded NAL unit streams can be conveyed.

11.13.1 NAL header format

The NAL unit specifies a generic format for sending video data over both packet oriented (e.g. Internet protocol/RTP systems) and bitstream-oriented transport systems (e.g. H.320 and MPEG-2/H.222.0 systems). In the latter, the data are transmitted in packets with the identification of the boundaries of NAL units for the systems that require delivery of the entire or partial NAL unit stream as ordered streams of bytes or bits.

Each NAL unit consists of a 1-byte header and a payload of variable number of bytes containing the coded symbols. The header indicates the type of the NAL unit and whether a VCL NAL unit is a part of a reference or nonreference. Furthermore, it can also signal the relative importance of the NAL unit and any syntax violation. Format of the NAL header is shown in Figure 11.45.

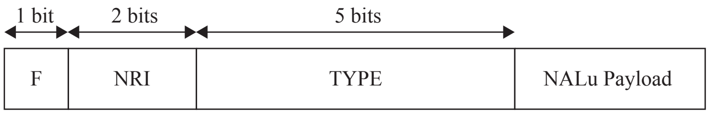

Figure 11.45 NAL unit

The first bit *F* is the forbidden bit, usually set to zero at the source. The network elements can use it for indication of errors and set it to 1 in the presence of errors in the NAL unit. It can also be used in heterogeneous network environments, like combined wired line and wireless environments, where some decoders may be prepared to operate on NAL units containing bit errors and others do not.

The two bit field *NRI* (*nal_ref_idc*) can be used to indicate the importance of a NAL unit for the reconstruction process. The higher this value is, the more the importance of the NAL unit. For instance, a zero indicates that the NAL unit is not used as a reference by other units and hence can be discarded by the decoder or by network elements without risking picture drift.

The *TYPE* is a 5-bit field, which characterises the NAL unit as one of 32 different types, out of which the first 12 are currently defined by H.264. Types 24–31 are made available for uses outside of H.264. The RTP payload specifies some of these values for signalling, aggregation and fragmentation of packets. All other values are reserved for future use by H.264.

In byte stream format, the NAL unit is prefixed with a 3-byte start code prefix. The boundaries of the NAL unit can then be identified by searching the coded data for the unique start code prefix pattern. To prevent accidental generation of start code prefix inside the payload data, the payload is interleaved with the 'emulation prevention' bytes.

11.13.2 Parameter sets

For correct decoding of bitstream, the decoder should synchronise itself with the encoder, as well as with the syntax. The decoder needs to know how slices are coded. Some information that may change from slice to slice, like slice type, can be sent in the slice header. There are other coding parameters, such as picture format, picture size, the type of entropy encoder, bit rate and *MV* resolution, that do not change very often during a video session, and hence, they are not required to be repeatedly transmitted. Various combinations of these parameters, called parameter sets, can be stored in tables by both the encoder and the decoder [17]. When needed, the encoder sends an index of the table and the receiver gets all the used parameters from its twin table.

There are two parameter sets of the VCL data. One set is called the picture parameter set (PPS) that contains information about the all slices of one or more pictures. The other set, called the sequence parameter set (SPS), contains information about the sequence. Each VCL NAL unit contains an identifier for the PPS, and the PPS has an identifier for the relevant SPS.

Parameter set is not an error resilience tool, but since it decouples the transmission of frequently changing encoded video samples from infrequently changing information, its proper usage can improve both error robustness and compression efficiency. It must be ensured that the PPS and SPS arrive at the decoder in time. Therefore, they can be transmitted out-of-band using reliable control protocol or can be sent in-band with appropriate application layer protection. Figure 11.46 illustrates an example of communication on the parameter set. In the figure, the

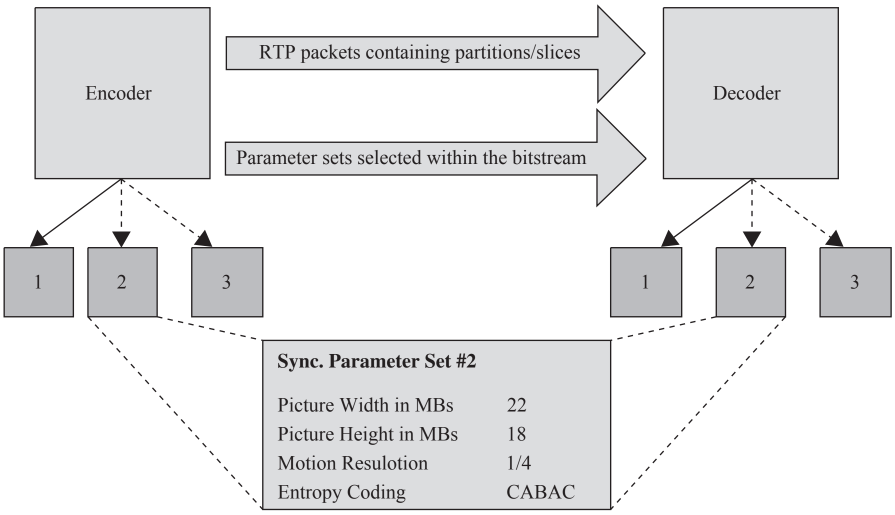

Figure 11.46 Parameter set concept of H.264

encoder only sends table index #2 to inform the decoder about the picture dimensions, *MV* and entropy coding type, and the decoder fetches these data from its own table at index #2. The bits required to send an index are much less then sending all those parameter sets one by one, improving compression efficiency. They can be sent as frequently as required to improve the error robustness.

Up to 32 SPS can be defined, but only one set is sent until the next IDR. These sets define profile and level, picture size, chroma format and bit depth, scaling matrix, picture order count, etc. The PPS can be up to 256, but only one set is used for each picture. They define entropy coder (CAVLC or CABAC), slice group parameters, number of reference pictures in list 0 and list 1, scaling matrix, initial *QP*, etc.

In addition to the parameter sets of the video coding layer (VCL), some non-VCL supplemental enhancement information (SEI) that helps the decoding and display process is also sent. SEI contains a number of features that can enhance the utility of decoded video data without requiring alteration of the decoding process. For example, parameters for gradual decoder refresh can be signalled within SEI. Similarly, decoding and presentation time stamps for pictures are transmitted as SEI. Other supported functionalities of SEI include buffering parameters and timing information, which do not affect the pixel values and can be discarded by the decoder.

11.13.3 Access unit

A set of NAL units containing exactly one complete decoded picture is called an access unit. In addition, the access unit may contain one or more redundant coded slices/pictures or other NAL units of auxiliary information. For example, it can contain SEI to indicate the type of slices present in the main coded picture and to specify detection of the boundary between access units.

All NAL units within an access unit have the same temporal identifier *T*. The first access unit of each video sequence is an IDR access unit, and the subsequent units are of type non-IDR. The access unit that is associated with the buffering period of SEI message that initialises the coded picture buffer (CPB) is referred to access unit 0. The value of the identifier is incremented by 1 for each subsequent access unit in decoding order.

In SVC, similar to the temporal identifier in AVC, one can define layer identifier. This identifier, in addition to time identifier *T*, also defines a layer dependency identifier *D*, indicating how construction of pictures at each layer depends on each other. Each dependency layer contains one or more quality layers identified by a quality identifier *Q*. Thus, the SVC layers are identified by three IDs: the temporal ID (*T*), dependency ID (*D*) and quality (i.e. SNR) ID (*Q*), which are written as triplet (*D*,*T*,*Q*). For example, the base layer NAL unit of the lowest temporal resolution and SNR scalability is identified as (0,0,0).

In each access unit, layers are encoded in increasing order of their layer identifier. For coding of a layer, already transmitted data of another layer with a small layer identifier can be employed. The layer to predict from can be selected on an access unit basis and is referred to as the reference layer. Base layer has a layer identifier equal to zero and is coded in conformance with one of the H.264 profiles.

Temporal scalability is achieved by partitioning the access units into a temporal base and one or more temporal enhancement layers. Thus, layers are separated by their temporal ID, as we have seen in, for example, Figure 11.36, and decoded in the order of their temporal ID, T_i.

At any time defined by temporal ID, access units of spatial and SNR scalability are defined based on their dependency and quality IDs. For spatial scalability, normally base and enhancement layers have the same quality ID, but their dependency IDs are different. For SNR scalability, especially the MGS, there are numerous quality and dependency layers. Switching between quality refinement layers is possible in any access unit, while switching between different dependency layers is only possible at IDR access units. Using quality refinement layers within the same dependency layer, it is possible to define packet-based scalability as the decoder cannot detect if a packet is dropped or has been intentionally discarded.

11.13.4 NAL type

Table 11.9 summarises a list of 32 NAL unit types, identified within the 5-bit NAL header. NAL units 1–5 contain different VCL data, which are described later. NAL units 6–12 are non-VCL units containing additional information such as parameter sets and supplemental information. Parameter sets are header data that are unchanged in a number of NAL units and are then sent to prevent their repetition. Supplemental information is timing or other addressing data that enhances the decoder usability but is not essential in decoding the pictures. NAL units 12–23 are reserved for future use of H.264 extensions, and the types 24–31 are available for use by different applications.

Of the five NAL unit types carrying VCL data, the slices of an IDR or I-picture (i.e. a picture with all intra slices) are located in the type 5 NAL unit, while those belonging to a non-IDR or non-I-picture (P- or B-pictures) are packed in NAL units of type 1, and in types 2–4 when DP is used.

However, in H.264, when DP is enabled, every slice is divided into three separate partitions and each partition is located in type 2, type 3 or type 4 NAL unit.

Table 11.9 NAL unit types

NAL unit type	Class	Content of NAL unit
0		Unspecified
1	VCL	Coded slice data
2	VCL	Coded slice data partition A
3	VCL	Coded slice data partition B
4	VCL	Coded slice data partition C
5	VCL	Coded slice of an IDR picture
6–12	Non-VCL	Supplemental information, parameter sets, etc.
12–23		Reserved
23–31		Unspecified

A NAL unit of type 2, also known as partition A, comprises the most important information of the compressed video bitstream for P- and B-slices, including the MBs addresses, *MV*s and essential headers. If any MBs in these slices are intra coded, their coded block pattern and transform coefficients are packed into a type 3 NAL unit, also known as partition B. Type 4 NAL, also known as partition C, carries transform coefficients of the motion-compensated inter picture and the inter coded block-pattern MBs.

11.13.4.1 NAL for SVC

Although full specifications of SVC have not been finalised yet, there are suggestions for their packetisation. The proposal put forward to the Internet engineering task force (IETF) suggests a 3-byte extended header to the 1-byte NAL unit header [25]. This new NAL unit for SVC stream is shown in Figure 11.47 with some brief description of each flag.

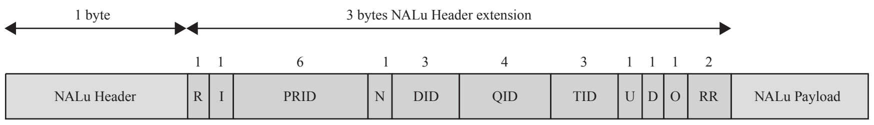

Figure 11.47 Extended NAL unit header for SVC

R: 1-bit reserved_one_bit. Reserved bit for future extension. R must be equal to 1.
I: 1-bit idr_flag. This component specifies whether the represented layer is an (IDR) information.
PRID: 6-bit priority_id. This flag specifies a priority identifier for the NAL unit. A lower value of prid indicates a higher priority.
N: 1-bit no_inter_layer_pred_flag. This flag specifies whether interlayer prediction may be used for decoding the coded slice.
DID: 3-bit dependency_id. This component indicates the interlayer coding dependency level of a layer. At any access unit, a layer representation with a given dependency_id may be used for interlayer prediction of a layer with a higher dependency_id but cannot not be used for interlayer prediction of a lower dependency_id.
QID: 4-bit quality_id. This component indicates the quality level of an MGS layer representation. At any access unit and for identical dependency_id values, a layer with quality_id equal to Qi uses a layer of quality_id $= Qi - 1$ for interlayer prediction.
TID: 3-bit temporal_id. This component indicates the temporal level of a layer representation. The temporal_id is associated with the frame rate, with lower values of temporal_id corresponding to lower frame rates. A layer representation at a given temporal_id typically depends on layer representations with lower temporal_id values, but it never depends on layer representations with higher temporal_id values.
U: 1-bit use_ref_base_pic_flag. A value of 1 indicates that only reference base pictures are used during the inter prediction process, and a value of 0 means that they are not used.
D: 1-bit discardable_flag. A value of 1 indicates that the current NAL unit is not used for decoding NAL units with values of dependency_id higher than the one of the current NAL unit in the current and all subsequent access units. Such NAL units can be discarded without risking the integrity of layers with higher dependency_id values. discardable_flag equal to 0 indicates that the decoding of the NAL unit is required to maintain the integrity of layers with higher dependency_id.
O: 1-bit output_flag. Affects the decoded picture output process.
RR: 2-bit reserved_three_2bits. Reserved bits for future extension. RR must be equal to ‘11’ (in binary form).

11.14 Problems

1. Pixels *a–d* of Figure 11.48 belong to a 4 × 4 block with the given neighbouring border pixels as shown. Find their prediction values if they are intra 4 × 4 coded with the following modes:
   a. 0
   b. 1
   c. 2

100	70	110	150	190
80	a			
60		b		
40			c	
20				d

Figure 11.48

2. Show that for the integer transforms of length 4 to be orthonormal, the DC and the second AC coefficients should be divided by 2, but the first and the third AC coefficients should be divided by $\sqrt{10}$. Determine the inverse transformation matrix, and show that it is an orthonormal matrix.

3. A block of 4 × 4 pixels given by

$$[x] = \begin{bmatrix} 100 & 120 & 85 & 10 \\ 80 & 70 & 60 & 50 \\ 110 & 90 & 100 & 120 \\ 180 & 200 & 150 & 200 \end{bmatrix}$$

   are two-dimensionally transformed by 4 × 4 integer transform of problem 2. Show that the resultant two-dimensional transform coefficients would be the same as used in eqn. 11.13.

4. In problem 3, find the reconstructed pixel block for the following QP:
   a. $QP = 4$
   b. $QP = 36$

5. Find the quantiser step sizes for the following luma QP:
   a. $QP = 8$
   b. $QP = 26$
   c. $QP = 48$
   d. $QP = 51$

6. Find the quantiser step size for chroma of problem 5.

7. Find the zero-order Exp-Golomb of parameter p with signed direct mapping if
   a. $p = 5$
   b. $p = -5$

8. Find the mode and motion Lagrangian parameters for $QP = 36$.

References

1. WIEGAND, T.: 'H.26L Test Model Long-Term Number 9 (TML-9) draft0', VCEG-N83 d1, Germany, December 2001
2. ITU-T recommendation H.264: 'Advanced video coding for generic audio visual services', March 2005
3. WIEGAND, T. and SULLIVAN, G.: 'Draft ITU-T recommendation and final draft international standard of joint video specification (ITU-T Rec. H.264 | ISO/IEC 14496-10 AVC)', March 2003
4. TOURAPIS, A.M., LEONTARIS, A., SUHRING, K. and SULLIVAN, G.: 'H.264/14496-10AVC reference software manual', Joint Video Team (JVT) of ISO/IEC MPEG&ITU-T VCEG, 31st meeting, London, UK, 28 June–3 July 2009
5. KUMAR, S., XU, L., MANDAL, M.K. and PANCHANATHAN, S.: 'Error resiliency schemes in H.264/AVC standard', *J. Vis. Commun. Image Representation*, special issue on emerging H.264/AVC video coding standard, **17:2**, April 2006, pp. 425–450
6. TOURAPIS, H.Y.C., TOURAPIS, A.M. and TOPIWALA, P.: 'Fast motion estimation within the JVT codec', Joint Video Team (JVT) of ISO/IEC MPEG&ITU VCEG, 9–17 October 2002, Document JVT-E023
7. WIEGAND, T., SULLIVAN, G.J., BJONTEGARD, G. and LUTHRA, A.: 'Overview of the H.264/AVC video coding standard', *IEEE Trans. Circuits Syst. Video Technol.*, 2003, **13:7**, pp. 560–576
8. LISM, P., JOCH, A., LAINEMA, J., BJONTEGRAD, G. and KARCZEWICZ, M.: 'Adaptive deblocking filter', *IEEE Trans. Circuits Syst. Video Technol.*, 2003, **13:7**, pp. 614–619
9. OSTERMAN, J., BORMANS, J., LIST, P., MARPE, D., NORROSCHKE, M., PEREIRA, F., STOCKHAMMER, T. and WIEGAND, T.: 'Video coding with H.264/AVC: tools, performance and complexity', *IEEE Trans. Circuits Syst. Magazine*, 2004, pp. 7–28
10. MARPE, D., SCHWARZ, H. and WIEGAND, T.: 'Context-based adaptive binary arithmetic coding in the H.264/AVC video compression standard', *IEEE Trans. Circuits Syst. Video Technol.*, 2003, **13:7**, pp. 620–636
11. DESAI, D.: 'Study and evaluation of the H.264 coding standard', March 2008
12. ORTEGA, A. and RAMCHANDRAN, K.: 'Rate-distortion methods for image and video compression', *IEEE Signal Process. Mag.*, 1998, **15**, pp. 23–50
13. WIEGAND, T., SCHWARZ, H., JOCH, A., KOSSENTINI, F. and SULLIVAN, G.J.: 'Rate-constrained coder control and comparison of video coding standards', *IEEE Trans. Circuits Syst. Video Technol.* 2003, **13:7**, pp. 688–703
14. GHANDI, M.M. and GHANBARI, M.: 'A Lagrangian optimised rate control algorithm for the H.264/AVC encoder', *Proc. IEEE Int. Conf. on Image Process. (ICIP04)*, 24–27 October 2004, Singapore

15. STOCKHAMMER, T., HANNUKSELA, M.M. and WIEGAND, T.: 'H.264/AVC in wireless environment', *IEEE Trans. Circuits Syst. Video Technol.*, 2003, **13:7**, pp. 657–673
16. WENGER, S., KNORR, G.D., OTT, J. and KOSSENTINIS, F.: 'Error resilience support in H.263+', *IEEE Trans. Circuits Syst. Video Technol.*, 1998, **8**, pp. 867–877
17. WENGER, S.: 'H.264/AVC over IP', *IEEE Trans. Circuits Syst. Video Technol.*, 2003, **13:7**, pp. 645–656
18. KARCZEWICZ, M. and KURCEREN, R.: 'The SP- and SI-frames design for H.264/AVC', *IEEE Trans. Circuits Syst. Video Technol.*, 2003, **13:7**, pp. 637–644
19. SETTON, E. and GIROD, B.: 'Rate-distortion analysis and streaming of SP and SI frames', *IEEE Trans. Circuits Syst. Video Technol.,* 2006, **16:6**, pp. 733–743
20. GHANBARI, M., CRAWFORD, D., FLEURY, M., KHAN, E., WOODS, J., LU, H., *et al.*: 'Future performance of video codecs', Research report for Office of Communications (Ofcom), London, November, 2006
21. MITCHINSON, D.: 'Tandberg television SMPTE presentation', http://www.atlanta-smpte.org
22. OHM, J.: 'Three-dimensional subband coding with motion compensation', *IEEE Trans. Image Process.*, 1994, **3:5**, pp. 559–571
23. SCHWARZ, H., MARPE, D. and WIEGAND, T.: 'Overview of the scalable extension of the H.264/MPEG-4 AVC video coding standard', *IEEE Trans. Circuits Syst. Video Technol.*, September 2007
24. REICHEL, J., SCHWARZ, H. and WEIN, M.: 'Joint scalable video model 11 (JSVM 11)', Joint Video Team, Doc. JVT-X202, 2007
25. WANG, Y.K. and SCHIERL, T.: 'RTP payload format for SVC video', draft-ietf-avt-rtp-svc-21.txt, 26 April 2010

Chapter 12

Content description, search and delivery (MPEG-7 and MPEG-21)

As more and more audio-visual information becomes available in digital form, there is an increasing pressure to make use of it. However, before one can use any information, it has to be located. Unfortunately, widespread availability of interesting material makes this search extremely difficult.

For textual information, currently, many 'text-based' search engines, such as Google, Yahoo and AltaVista, are available on the World Wide Web (www), and they are among the most visited sites. This is an indication of real demand for searching information on the public domain. However, identifying information for audio-visual content is not so trivial, and no generally recognised description of these materials exists. In the meantime, there is no efficient way of searching the www for say a piece of video concert by Pavarotti or improving the user friendliness of interconnected computers via Internet by rich-spoken queries, hand-drawn sketches and image-based queries.

The question of finding contents is not restricted to database retrieval applications. For example, producers of TV programmes may want to search and retrieve famous events stored among the thousands hours of audio-visual records in order to collect material for a programme. This will reduce programme time and increase the quality of its content. Another example is the selection of a favourite TV programme from a vast number of available satellite television channels. Currently, 10 to 15 MPEG-2 coded TV programmes can be accommodated in a satellite transponder. Considering that each satellite can have up to 12 transponders, each in horizontal and vertical polarisation mode, and satellites can be stationed within 2 degrees guard band, it is not unrealistic that users may have access to thousands of TV channels. Certainly, the current method of printing weekly TV programmes will not be practical (tens of thousands of pages per week!), and more intelligent computerised way of choosing a TV programme is needed. MPEG-7, under the name of 'multimedia content-based description standard', aims to address these issues and define how humans expect to interact with computers [1].

The increasing demand for searching multimedia contents in the Web has opened up new opportunities for creation and delivery of these contents on the Internet. Today, many elements exist to build an infrastructure for the delivery and consumption of multimedia content. There is, however, no standard way of describing these elements or relating to each other. It is hoped that such a standard will be devised by the International Standards Organisation/International Electrotechnical Commission (ISO/IEC) MPEG committee under the name of MPEG-21 [2].

The main aim of this standard is to specify how various elements for content creation fit together, and when a gap exists, MPEG-21 will recommend which new standards are required. The MPEG standard will then develop new standards as appropriate, while other bodies may develop other relevant standards. These specifications will be integrated into the 'multimedia framework' through collaboration between MPEG and these bodies. The result is an open framework for multimedia delivery and consumption, with both the content creators and content consumers as the main beneficiaries. The open framework aims to provide content creators and service providers with equal opportunities in the MPEG-21 enabled market. It will also be to the benefit of the content users, providing them access to a large variety of data in an interoperable manner.

In summary, MPEG-7 is about describing and finding contents, and MPEG-21 deals with the delivery and consumption of these contents. As we see, none of these standards are about the video compression, which is the main subject of this book. However, for the completeness of the book on the standard codecs, we briefly describe these two new standards that are incidentally developed by the ISO/IEC MPEG standard bodies.

12.1 MPEG-7: multimedia content description interface

The main goal of MPEG-7 is to specify a standard set of descriptors that can be used to describe various types of multimedia information coded with the standard codecs, as well as other databases and even analogue audio-visual information. This will be in the form of defining descriptor schemes or structures and the relationship between various descriptors. The combination of the descriptors and description schemes will be associated with the content itself to allow a fast and efficient searching method for the material of user's interest. The audio-visual material that has MPEG-7 data associated with it can be indexed and searched for. This material may include still pictures, graphics, three-dimensional models, audio, speech, video and information about how these elements are combined in a multimedia presentation.

Figure 12.1 shows a highly abstract block diagram of the MPEG-7 mission. In this figure, object features are extracted and are described in a manner meaningful

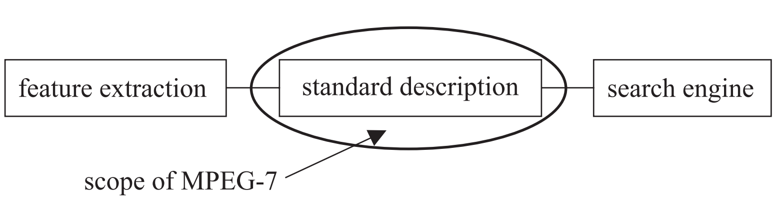

Figure 12.1 Scope of MPEG-7

to the search engine. As usual, MPEG-7 neither specifies how features should be extracted nor how they should be searched for, but specifies only the order in which features should be described.

12.1.1 Description levels

Since the description features must be meaningful in the context of the application, they may be defined in different ways for different applications. Hence, a specific audio-visual event might be described with different sets of features if their applications are different. To describe 'visual' events, they are first described by their lower abstraction level, such as shape, size, texture, colour, movement and their positions inside the picture frame. At this level, the 'audio' material may be defined as key, mood, tempo, tempo changes and position in the sound space.

The high level of the abstraction is then a description of the semantic relation between the above lower-level abstractions. For the earlier example of 'a piece of Pavarotti's concert', the lower level of abstraction for the picture would be Pavarotti's portrait, a picture of a band of music, shapes of musical instruments, etc. For the audio, this level of abstraction could be, of course, his song, as well as other background music. All these descriptions are, of course, coded in a way to be searched as efficiently as possible.

The level of abstraction is related to the way the required features are extracted. Many low-level features can be extracted in a fully automatic manner. High-level features, however, need more human interactions to define the semantic relations between the lower-level features.

In addition to the description of contents, it may also be required to include other types of information about the multimedia data. For example:

- *The form*: An example of the form is the coding scheme used (e.g. JPEG, MPEG-2) or the overall data size.
- *Conditions for accessing material*: This would include copyright information, price, etc.
- *Classification*: This could include parental rating and content classification into a number of predefined categories.
- *Links to other relevant material*: This information will help the users to speed up the search operation.
- *The context*: For some recorded events, it is very important to know the occasion of recording (e.g. World Cup 2002, final between Brazil and Germany).

In many cases, addition of textual information to the descriptors may be useful. Care must be taken such that the usefulness of the descriptors is as independent as possible from the language. An example of this is giving names of authors, films and places. However, providing text-only documents will not be among the goals of MPEG-7.

The MPEG group has also defined a laboratory reference model for MPEG-7. This time it is called eXperimental Model (XM), which has the same role as RM, TM, JM, and VM in the H.261, MPEG-2, H.264, and MPEG-4, respectively.

12.1.2 Application area

The elements that MPEG-7 standardises will support a broad range of applications. MPEG-7 will also make the Web as searchable for multimedia content as it is for text today. This would apply especially to large content archives as well as to multimedia catalogues, enabling people to identify content for purchase. The information used for content retrieval may also be used by agents for the selection and filtering of broadcasted material or for personalised advertising.

All application domains making use of multimedia will benefit from MPEG-7. Some of these domains that might find MPEG-7 useful are as follows:

- architecture, real estate and interior design (e.g. searching for idea);
- broadcast multimedia selection (e.g. radio and TV channels);
- cultural service (e.g. history museums, art galleries);
- digital libraries (e.g. image catalogue, musical dictionary, biomedical imaging catalogues, film, video and radio archives);
- e-commerce (e.g. personalised advertising, online catalogues, directories of electronic shops);
- education (e.g. repositories of multimedia courses, multimedia search for support material);
- home entertainment (e.g. systems for the management of personal multimedia collections, including manipulation of content, such as home video editing, searching a game);
- investigation services (e.g. human characteristics recognition, forensics);
- journalism (e.g. searching speeches of a certain politician using his/her name, voice or face);
- multimedia directory services (e.g. yellow pages, tourist information, geographical information systems);
- multimedia editing (e.g. personalised electronic news services, media authoring);
- remote sensing (e.g. cartography, ecology, natural resources management);
- shopping (e.g. searching for cloths that you like);
- surveillance (e.g. traffic control, surface transportation, nondestructive testing in hostile environment); and many more.

The way MPEG-7 data will be used to answer user queries is outside the scope of the standard. In principle, any type of audio-visual material may be retrieved by means of any type of query material. For example, video material may be queried using video, music and speech. It is for the search engine to match the query data and the MPEG-7 audio-visual description. A few query examples are as follows:

- Play a few notes on a keyboard and retrieve a list of musical pieces similar to the required tune.
- Draw a few lines on a screen and find a set of images containing similar graphics, logos and ideograms.
- Sketch objects, including colour patches or textures, and retrieve examples among which you select the interesting objects to compose your design.

- On a given set of multimedia objects, describe movements and relations between the objects and search for animations fulfilling the described temporal and spatial relations.
- Describe actions and get a list of scenarios containing such actions.
- Use an excerpt of Pavarotti's voice and obtain a list of his records, video clips where he is singing and photographic material portraying him.

12.1.3 Indexing and query

The current status of research at this stage of MPEG-7 development is concentrated into two interrelated areas, 'indexing' and 'query'. In the former, significant events of video shots are indexed, and in the latter, given a description of an event, the video shot for that event is searched for. Figure 12.2 shows how the indices for a video clip can be generated.

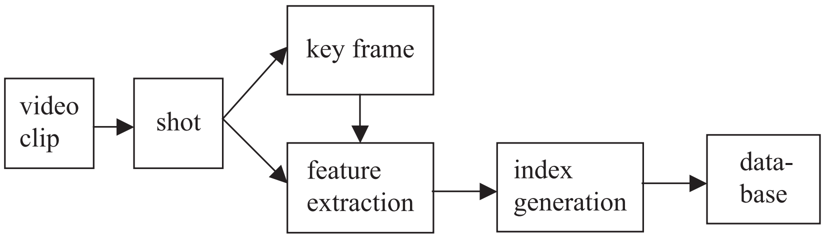

Figure 12.2 Index generation for a video clip

In this figure, a video programme (normally 30–90 min) is temporally segmented into video 'shots'. A shot is a piece of video clip where the picture content from one frame to the other does not change significantly, and in general there is no scene cut within a shot. Therefore, a single frame in a shot has a high correlation to all the pictures within the shot. One of these frames is chosen as the 'key frame'. Selection of the key frame is an interesting research issue. An ideal key frame is the one that has maximum similarity with all the pictures within its own shot but minimum similarity with those of the other shots. The key frame is then spatially segmented into objects with meaningful features. These may include colour, shape and texture, where a semantic relation between these individual features defines an object of interest. As mentioned, depending on the type of application, the same features might be described in a different order. Also, in extracting the features, other information like motion of the objects, background sound or sometimes text might be useful. Here, features are then indexed, and the indexed data along with the key frames are stored in the database, sometimes called 'metadata'.

The query process is the opposite of indexing. In this process, the database is searched for a specific visual content. Depending on how the query is defined to the search engine, the process can be very complex. For instance, in our earlier example of 'Pavarotti's singing', the simplest form of the query is that a single frame (picture) of him or a piece of his song is available. This picture (or song) is then matched against all the key frames in the database. If such a picture is found, then, due to its index relation with the actual shot and video clip, that piece of video is located. Matching of the query picture with the key frames is under active research, since this is very different from the conventional pixel-to-pixel matching of the pictures. For example, due to motion, obstruction of the objects, shading and shearing, the physical dimensions of the objects of interest might change, such that pixel-to-pixel matching does not necessarily find the right object. For instance, with the pixel-to-pixel matching, a circle can be more similar to a hexagon of almost the same number of pixels and intensity than to a smaller or larger circle, which is not a desired match.

The extreme complexity in the query is when the event is defined verbally or in a text, like the text of 'Pavarotti's song'. Here, these data have to be converted into audio-visual objects to be matched with the key frames. There is no doubt that most of the future MPEG-7 activity will be focused in this extremely complex audio and image processing task.

In the following sections, some of the description tools used for indexing and retrieval are described. To be consistent, we have ignored speech and audio, and considered only the visual description tools. Currently, there are five visual description tools that can be used for indexing. During the search, either of them or their combination, as well as other data, say from audio description tools, might be used for retrieval.

12.1.4 Colour descriptors

Colour is the most important descriptor of an object. MPEG-7 defines seven colour descriptors to be used in combinations for describing an object. These are defined in the following sections.

12.1.4.1 Colour space

Colour space is the feature that defines how the colour components are used in other colour descriptors. For example, R, G, B (red, green, blue), Y, C_r, C_b (luminance and chrominance), HSV (hue, saturation, value) components or monochrome are the types describing the colour space.

12.1.4.2 Colour quantisation

Once the colour space is defined, the colour components of each pixel are quantised to represent them with a small (manageable) number of levels or 'bins'. These bins can then be used to represent the 'colour histogram' of the object, that is, the distribution of the colour components at various levels.

12.1.4.3 Dominant colour(s)

This colour descriptor is most suitable for representing local (object or image region) features where a small number of colours are enough to characterise the colour information in the region of interest. Dominant colour can also be defined for the whole image. To define the dominant colour, colour quantisation is used to extract a small number of representing colours in each region or image. The percentage of each quantised colour in the region then shows the degree of the dominance of that colour. A spatial coherency on the entire descriptor is also defined and is used in similarity retrieval (objects having similar dominant colours).

12.1.4.4 Scalable colour

The scalable colour descriptor is a colour histogram in HSV colour space, which is encoded by a Haar transform. Its binary representation is scalable in terms of bin numbers and bit representation accuracy over a wide range of data rates. The scalable colour descriptor is useful for image-to-image matching and retrieval based on colour feature. Retrieval accuracy increases with the number of bits used in the representation.

12.1.4.5 Colour structure

The colour structure descriptor is a colour feature that captures both colour content (similar to colour histogram) and information about the structure of this content (e.g. colour of the neighbouring regions). The extraction method embeds the colour structure information into the descriptor by taking into account the colours in a local neighbourhood of pixels instead of considering each pixel separately. Its main usage is image-to-image matching and is intended for still-image retrieval. The colour structure descriptor provides additional functionality and improved similarity-based image retrieval performance for natural images compared to the ordinary histogram.

12.1.4.6 Colour layout

This descriptor specifies the spatial distribution of colours for high-speed retrieval and browsing. It can be used not only for image-to-image matching and video-to-video clip matching but also in layout-based retrieval for colour, such as sketch-to-image matching, which is not supported by other colour descriptors. For example, to find an object, one may sketch the object and paint it with the colour of interest. This descriptor can be applied either to a whole image or to any part of it. This descriptor can be applied to arbitrary shaped regions.

12.1.4.7 GOP colour

The group of pictures (GOP) colour descriptor extends the scalable colour descriptor that is defined for still images to a video segment or a collection of still images. Before applying the Haar transform, the way colour histogram is derived should be defined. MPEG-7 considers three ways of defining the colour histogram for GOP colour descriptor, namely ‘average’, ‘median’ and ‘intersection’ histogram methods.

The average histogram refers to averaging the counter value of each bin across all pictures, which is equivalent to computing the aggregate colour histogram of all pictures with proper normalisation. The median histogram refers to computing the median of the counter value of each bin across all pictures. It is more robust to round off errors and the presence of the outliers in image intensity values compared to the average histogram. The intersection histogram refers to computing the minimum of the counter value of each bin across all pictures to capture the least common colour traits of a group of images. The same similarity/distance measures that are used to compare scalable colour descriptions can be employed to compare GOP colour descriptors.

12.1.5 Texture descriptors

Texture is an important structural descriptor of objects. MPEG-7 defines three texture-based descriptors, which are explained in the following sections.

12.1.5.1 Homogeneous texture

Homogeneous texture has emerged as an important primitive for searching and browsing through large collections of similar looking patterns. In this descriptor, the texture features associated with the regions of an image can be used to index the image. Extraction of texture features is done by filtering the image at various scales and orientations. For example, using the wavelet transform with Gabor filters in say 6 orientations and 4 levels of decompositions, one can create 24 subimages. Each subimage reflects a particular image pattern at certain frequency and resolution. The mean and the variance of each subimage are then calculated. Finally, the image is indexed with a 48-dimensional vector (24 mean and 24 standard deviations). In image retrieval, the minimum distance between this 48-dimensional vector of the query image and those in the database is calculated. The one that gives the minimum distance is retrieved. The homogeneous texture descriptor provides a precise and quantitative description of a texture that can be used for accurate search and retrieval in this respect.

12.1.5.2 Texture browsing

This descriptor is useful for representation of homogeneous texture for browsing-type applications, and is defined by at most 12 bits. It provides a perceptual characterisation of texture, similar to a human characterisation, in terms of regularity, coarseness and directionality. Derivation of this descriptor is done in a similar way to the homogeneous texture descriptor of section 12.1.5.1; that is, the image is filtered with a bank of orientation and scale-tuned filters using Gabor functions. From the filtered image, the two dominant texture orientations are selected. Three bits are needed to represent each of the dominant orientations (out of say 6). This is followed by analysing the filtered image projections along the dominant orientations to determine the regularity (quantified by 2 bits) and coarseness (2 bits $\times$ 2). The second dominant orientation and second scale feature are optional. This descriptor, combined with the homogeneous texture descriptor, provides a scalable solution to representing homogeneous texture regions in images.

12.1.5.3 Edge histogram

This descriptor represents the spatial distribution of five types of edges, namely four directional edges and one nondirectional edge. It consists of the distribution of pixel values in each of these directions. Since edges are important in image perception, they can be used to retrieve images with similar semantic meaning. The primary use of this descriptor is image-to-image matching, especially for natural edges with nonuniform edge distribution. The retrieval reliability of this descriptor is increased when it is combined with other descriptors, such as the colour histogram descriptor.

12.1.6 Shape descriptors

Humans normally describe objects by their shapes, and hence shape descriptors are very instrumental in finding similar shapes. One important property of shape is its invariance to rotation, scaling and displacement. MPEG-7 identifies three shape descriptors, which are defined in the following sections.

12.1.6.1 Region-based shapes

The shape of an object may consist of either a single region or a set of regions. Since a region-based shape descriptor makes use of all pixels constituting the shape within a picture frame, it can describe shapes of any complexity.

The shape is described as a binary plane, with the black pixel within the object corresponding to 1 and the white background corresponding to 0. To reduce the data required to represent the shape, its size is reduced. MPEG-7 recommends shapes to be described at a fixed size of 17.5 bytes. The feature extraction and matching processes are straightforward to have low order of computational complexities so as to be suitable for tracking shapes in the video data processing.

12.1.6.2 Contour-based shape

The contour-based shape descriptor captures the characteristics of the shapes more similar to the human notion of understanding shapes. It is the most popular method for shape-based image retrieval. Section 12.2 demonstrates some of its practical applications in image retrieval.

The contour-based shape descriptor is based on the so-called curvature scale space (CSS) representation of the contour. That is, by filtering the shape at various scales (various degrees of smoothness of the filter), a contour is smoothed at various levels. The smoothed contours are then used for matching. This method has several important properties:

- It captures important characteristics of the shapes, enabling similarity-based retrieval.
- It reflects properties of the perception of human visual system.
- It is robust to nonrigid motion or partial occlusion of the shape.
- It is robust to various transformations on shapes, such as rotation, scaling and zooming.

12.1.6.3 Three-dimensional shape

Advances in multimedia technology have brought three-dimensional contents into today's information systems in the forms of virtual worlds and augmented reality. The three-dimensional objects are normally represented as polygonal meshes, such as those used in MPEG-4 for synthetic images and image rendering. Within the MPEG-7 framework, tools for intelligent content-based access to three-dimensional information are needed. The main applications for the three-dimensional shape description are search, retrieval and browsing of three-dimensional model databases.

12.1.7 Motion descriptors

Motion is a feature that discriminates video from still images. It can be used as a descriptor for video segments, and MPEG-7 standard recognises four motion-based descriptors.

12.1.7.1 Camera motion

Camera motion is a descriptor that characterises the three-dimensional camera motion parameters. These parameters can be automatically extracted or generated by the capturing devices.

The camera motion descriptor supports the following well-known basic camera motion:

- fixed: camera is static
- panning: horizontal rotation
- tracking: horizontal traverse movement, also known as travelling in the film industry
- tilting: vertical rotation
- booming: vertical traverse movement
- zooming: change of the focal length
- dollying: translation along the optical axis
- rolling: rotation around the optical axis

The subshots for which all frames are characterised by a particular camera motion, which can be single or mixed, determine the building blocks for the camera motion descriptor. Each building block is described by its start time, duration, speed of the induced image motion, fraction of time of its duration compared with a given temporal window size and focus of expansion or focus of contraction.

12.1.7.2 Motion trajectory

The motion trajectory of an object is a simple high-level feature defined as the localisation in time and space of one representative point of this object. This descriptor can be useful for content-based retrieval in object-oriented visual databases. If a priori knowledge is available, the trajectory motion can be very useful. For example, in surveillance, alarms can be triggered if an object has a trajectory that looks unusual (e.g. passing through a forbidden area).

The descriptor is essentially a list of key points along with a set of optional interpolating functions that describe the path of the object between the key points in terms of acceleration. The key points are specified by their time instant and either two- or three-dimensional Cartesian coordinates, depending on the intended application.

12.1.7.3 Parametric motion

Parametric motion models of affine, perspective, etc. have been extensively used in image processing, including motion-based segmentation and estimation, global motion estimation. We have seen some of these in Chapter 9 for motion estimation and in Chapter 10 for global motion estimation used in the sprite of MPEG-4. Within MPEG-7 framework, motion is a highly relevant feature, related to the spatio-temporal structure of a video and concerning several MPEG-7 specific applications, such as storage and retrieval of video databases and hyperlinking purposes.

The basic underlying principle consists of describing the motion of objects in video sequences in terms of its model parameters. Specifically, affine model includes translations, rotations, scaling and a combination of them. Planar perspective models can take into account global deformations associated with perspective projections. More complex movements can be described with the quadratic motion model. Such an approach leads to a very efficient description of several types of motions, including simple translations, rotations and zooming or more complex motions such as combinations of the above-mentioned motions.

12.1.7.4 Motion activity

Video scenes are usually classified in terms of their motion activity. For example, sports programmes are highly active and newsreader video shots represent low activity. Therefore, motion can be used as a descriptor to express the activity of a given video segment.

Activity descriptor can be useful for applications such as surveillance, fast browsing, dynamic video summarisation and movement-based query. For example, if the activity descriptor shows a high activity, then during the playback, the frame rate can be slowed down to make highly active scenes viewable. Another example of an application is finding all the high-action shots in a news video programme.

12.1.8 Localisation

This descriptor specifies the position of a query object within the image, and it is defined with two types of descriptions.

12.1.8.1 Region locator

The region locator is a descriptor that enables localisation of regions within images by specifying them with a brief and scalable representation of a ‘box’ or a ‘polygon’.

12.1.8.2 Spatio-temporal locator

This descriptor defines the spatio-temporal locations of the regions in a video sequence, such as moving object regions, and provides localisation functionality. The main application of it is hypermedia, which displays the related information when the designated point is inside the object. Another major application is object retrieval by checking whether the object has passed through particular points, which can be used in surveillance. The spatio-temporal locator can describe both spatially connected and nonconnected regions.

12.1.9 Others

MPEG-7 is an ongoing process, and in the future, other descriptors will be added to the above list. In this category, the most notable descriptor is 'face recognition'.

12.1.9.1 Face recognition

The face recognition descriptor can be used to retrieve face images. The descriptor represents the projection of a face vector onto a set of basis vectors, which are representative of possible face vectors. The face recognition feature set is extracted from a normalised face image. This normalised face image contains 56 lines, each line with 46 intensity values. At the 24th row, the centres of the two eyes in each face image are located at the 16th and 31st column for the right and left eye, respectively. This normalised image is then used to extract the one-dimensional face vector that consists of the luminance pixel values from the normalised face image arranged into a one-dimensional vector in the scanning direction. The face recognition feature set is then calculated by projecting the one-dimensional face vector onto the space defined by a set of basis vectors.

12.2 Practical examples of image retrieval

In this section, some of the methods described in the previous sections are used to demonstrate the practical application of these methods in retrieving visual information from image databases. I have chosen the texture- and shape-based retrievals for demonstration purposes, since those of colour- and motion-based methods are not feasible to be demonstrated in black and white pictures and within the limited space of the book.

12.2.1 Texture-based image retrieval

Spatial frequency analysis of textures provides an excellent way of classifying them. The complex Gabor wavelet, which is a modulated Gaussian function to a complex exponential, is ideal for this purpose [3]. A two-dimensional complex Gabor wavelet is defined as

$$g(x,y) = \frac{1}{2\pi\sigma_x\sigma_y} e^{1/2((x^2+y^2)/(\sigma_x^2+\sigma_y^2))} \times e^{j2\pi f_0 x} \tag{12.1}$$

where σ_x and σ_y are the horizontal and vertical standard deviations of the Gaussian and f_0 is the filter bandwidth. Thus, its frequency domain representation (Fourier transform) is given by

$$G(u,v) = e^{1/2(((u-f_0)^2+v^2)/(\sigma_u{}^2+\sigma_v{}^2))} \tag{12.2}$$

where u and v are the horizontal and vertical spatial frequencies and σ_u and σ_v are their respected standard deviations.

The $g(x, y)$ of eqn. 12.1 can be used as the mother wavelet to decompose a signal into various levels and orientations. In Chapter 4, we showed how mother wavelets could be used in the design of discrete wavelet transform filters. The same procedure can be applied to the mother Gabor wavelet.

Figure 12.3 shows the spectrum of the Gabor filter at four levels and six orientations. It is derived by setting the lowest and highest horizontal spatial frequencies to $u_l = 0.05$ and $u_h = 0.4$, respectively. The intermediate frequencies are derived by constraining the bands to touch each other.

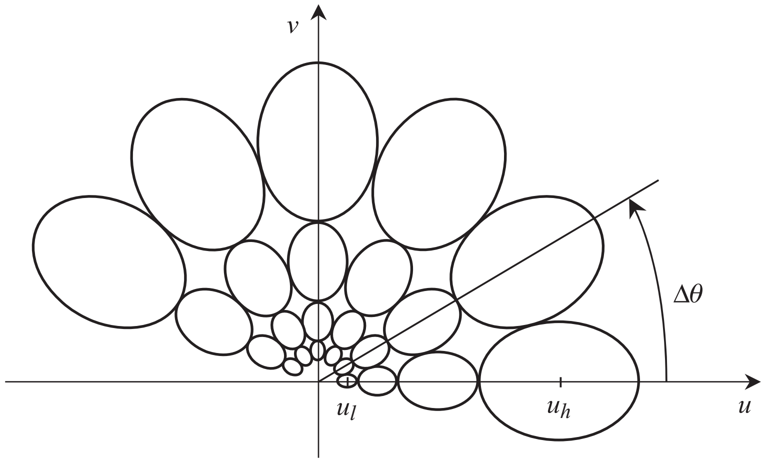

Figure 12.3 Gabor filter spectrum; the contours indicate the half-peak magnitude of the filter responses in the Gabor filter dictionary. The filter parameters used are $u_h = 0.4$, $u_l = 0.05$, $M = 4$ and $L = 6$

The above set of filters can decompose an image into $4 \times 6 = 24$ subimages. As we had seen in Chapter 4, each subimage reflects characteristics of the image at a specific direction and spatial resolution. Hence, it can analyse textures of images and describe them at these orientations and resolutions. For the example given above, one can calculate the mean and standard deviation of each subimage, and use it as a 48-dimensional vector to describe it. This is called the 'feature vector', which can be used for indexing the texture of an image, and is given by

$$\text{Feature vector} = [\mu_{00}\mu_{01}\mu_{02}\mu_{03}\mu_{04}\mu_{05}\mu_{10}\mu_{11}\ldots \mu_{35}\sigma_{00}\sigma_{01}\sigma_{02}\sigma_{03}\sigma_{04}\sigma_{05}\sigma_{10}\sigma_{11}\ldots\sigma_{35}]_{1\times 48} \quad (12.3)$$

To retrieve a query texture, its feature vector is compared with the feature vectors of the textures in the database. The similarity measure is the Euclidean distance between the feature vectors, and the one that gives the least distance is the most similar texture.

Figure 12.4 demonstrates retrieving of a texture from a texture database of 112 images. In this database, images are identified as D1 to D112. The query image,

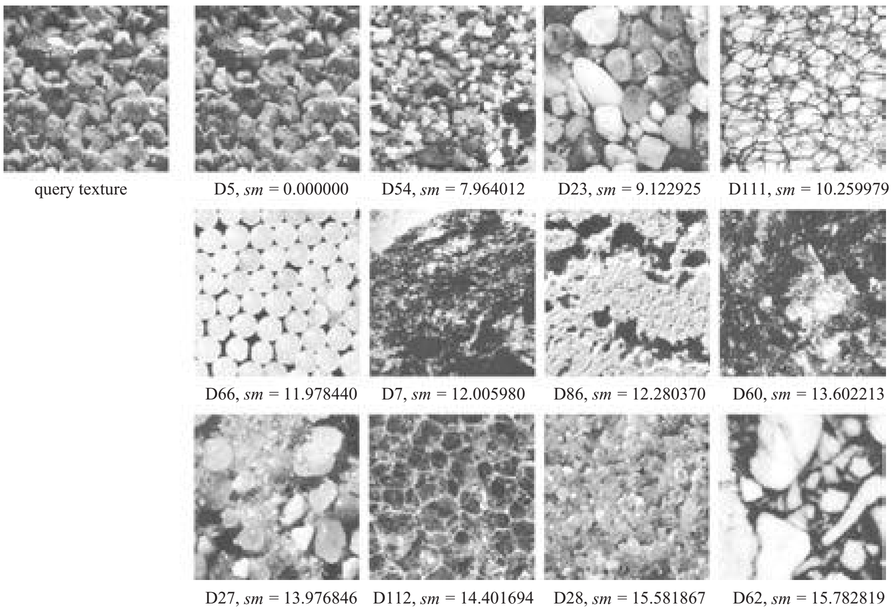

Figure 12.4 An example of texture-based image retrieval; query texture: D5

D5, is shown at the top left, along with 12 most similar retrieved images, in the order of their similarity measure. As we see, the query texture itself, D5, is found as the closest match, followed by a visually similar texture, D54, and so on. In the figure, the similarity distance, *sm*, of each retrieved candidate texture is also given.

12.2.2 Shape-based retrieval

Shapes are best described by the strength of their curvatures along their contours. A useful way of describing this strength is the 'curvature function', $k(s, \theta)$, defined as the instantaneous rate of change of the angle of the curve (tangent) θ over its arc length s:

$$k(s, \theta) = \frac{d\theta}{ds} \tag{12.4}$$

At sharp edges, where the rate of change of the angle is fast, the curvature function, $k(s, \theta)$, has large values. Hence, contours can be described by some values of their curvature functions as feature points. For example, feature points can be defined as the positions of large curvature points or their zero crossings. However, since contours are normally noisy, direct derivation of the curvature function from the contour can lead to false feature points.

To eliminate these unwanted feature points, contours should be denoised through smoothing filters. Care should be taken on the degree of filter smoothness, since heavily filtered contours loose the feature points and lightly filtered ones cannot get rid of the false feature points. Large number of feature points also demand more storage and heavy processing for retrieval.

Filtering a contour with a set of Gaussian filters of varying degrees of smoothness is the answer to this question, the so-called scale space representation of curves [4]. Figure 12.5 shows four smoothed contours of a shape at scaling (smoothing) factors of 16, 64, 256 and 1024. The positions of the curvature extremes on the contour at each scale are also shown. These points very well exhibit the most important structure of each contour.

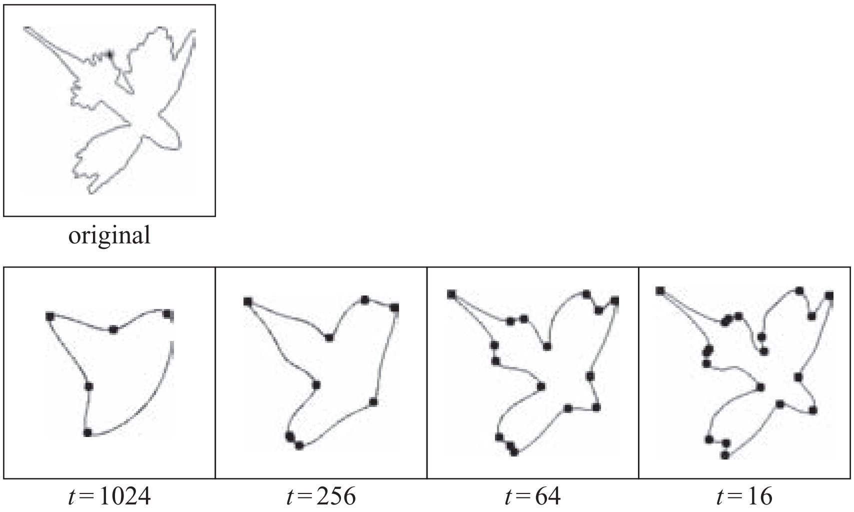

Figure 12.5 A contour and the positions of its curvature extremes at four different scales

For indexing and retrieval applications, these feature points can be joined together to approximate each smoothed contour with a polygon [5]. Moving round the contour, the angle of every polygon line with horizontal is recorded, and this set of angles is called 'turning function'. The turning function is the index of the shape that can be used for retrieval.

The similarity measure is based on the minimisation of the Euclidean distance between the query turning function and the turning functions of the shapes in the database. That is,

$$sm = \min \sum_{i=1}^{N} \|\theta_q^i - \theta_j^i\| \tag{12.5}$$

where θ_q^i is the ith angle of the query turning function, θ_j^i is the ith angle of jth shape turning function in the database and N is the number of angles in the turning function (e.g. number of vertices of the polygons or feature points on the contours). Calculation of the Euclidean distance necessitates that all the indices should have equal number of turning angles in their turning functions. This is done by inserting additional feature points on the contours such that polygons have *N* vertices.

Insertion of new feature points on the contour should be such that they should also represent important curvature extremes. This is done by inserting points on the contour, one at a time, where the contour has its largest distance from the polygon. Figure 12.6 shows the polygons of Figure 12.5 with the added new vertices. The number of total vertices is chosen such that approximation distortion of the original contour with a polygon is less than an acceptable value.

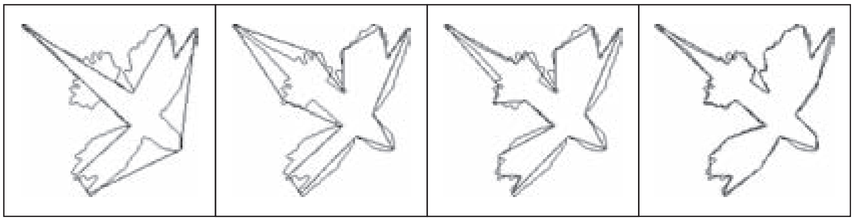

Figure 12.6 New polygons of Figure 12.5 with some added vertices

To show the retrieval efficiency of this method of shape description, Figure 12.7*a* shows a query shape to be searched in a database of almost 1100 marine creatures. The query marine is found as the closest shape, followed by three next closest marine shapes in the order of their closeness as shown in Figure 12.7.

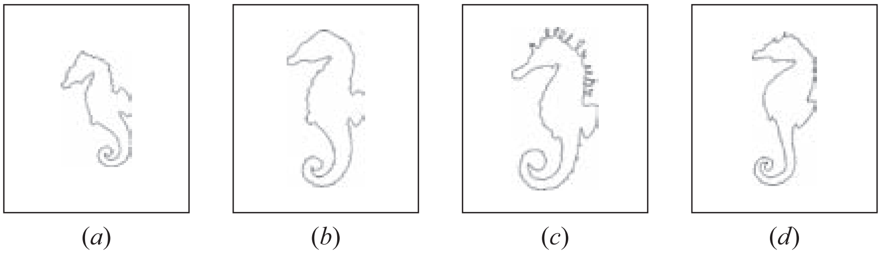

Figure 12.7 (a) The query shape; (b, c and d) the three closest shapes in order

12.2.3 Sketch-based retrieval

In the above two examples of image retrieval, it was assumed that the query image (texture or shape) is available to the user. However, there are occasions where these query images may not be available. What users might have could be a verbal description of the objects of interest, or have in their minds images of some visual objects.

One way of searching for visual objects without the query images is to sketch the object of interest and submit it to the search engine. Then, based on a set of retrieved objects, the user may iteratively modify his sketch till he finds the desired object. Assume that the fish in Figure 12.8*c1* is the desired shape in a database. The user first draws a rough sketch of this fish, as he imagines, like the one shown in Figure 12.8*a0*. On the basis of shape similarity, the three best similar shapes in the order of their similarity to the drawn shape are shown in Figure 12.8*a1*, 12.8*a2* and 12.8*a3*.

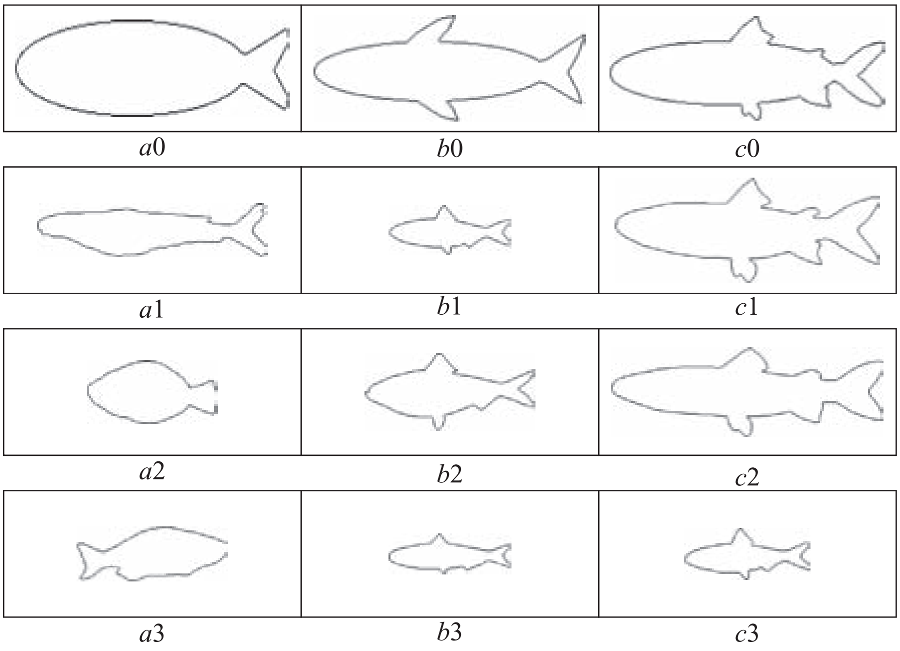

Figure 12.8 Sketch-based shape retrieval

By inspecting these outputs, the user then realises that none of the matched fish has any fins. Adding a dorsal and a ventral fin to the sketched fish, the new query fish of Figure 12.8*b0* is created. With this new query shape, the new set of best-matched shapes in the order of their similarity to the refined sketch becomes Figure 12.8*b1*, 12.8*b2* and 12.8*b3*.

Finally, adding an anal fin and a small adipose fin to the refined sketch, a further refined query shape of Figure 12.8*c0* is created. The new set of retrieved shapes, in the order of their similarity to the refined sketch, now becomes Figure 12.8*c1*, 12.8*c2* and 12.8*c3*. This is the last iteration step, as the desired shape in Figure 12.8*c1* comes as the best-matched shape.

This technique can also be extended to other retrieval methods. For example, one might paint or add some texture to the above drawings. This would certainly improve the reliability of the retrieval system.

12.3 MPEG-21: multimedia framework

Today multimedia technology is so advanced that access to the vast amount of information and services from almost anywhere at any time, through ubiquitous terminals and networks, is possible. However, no complete picture exists of how different communities can best interact with each other in a complex infrastructure. Examples of these communities are the content, financial, communication, computer and consumer electronics sectors and their customers. Developing a common multimedia framework will facilitate cooperation between these sectors and support a more efficient implementation and integration of different models, rules, interests and content formats. This is the task given to the multimedia framework project under the name of MPEG-21. The name is chosen to signify the coincidence of the start of the project with the twenty-first century.

The chain of multimedia content delivery encompasses content creation, production, delivery and consumption. To support this, the content has to be identified, described, managed and protected. The transport and delivery of content will undoubtedly be over a heterogeneous set of terminals and networks. Reliable delivery of contents, management of personal data, financial transaction and user privacy are some of the issues that the multimedia framework should take into account. In the following sections, the ‘seven architectural key elements’ that the multimedia framework considers instrumental in the realisation of the task are explained.

12.3.1 Digital item declaration

In multimedia communication to facilitate a wide range of actions involving ‘digital items’, there is a strong need for concrete description of defining exactly what constitutes such an ‘item’. Clearly, there are many kinds of content and possibly as many possible ways of describing it. This presents a strong challenge to lay out a powerful and flexible model for digital item, from which the content can be described more accurately. Such a model is only useful if it yields a format that can be used to represent any digital items defined within the model unambiguously and communicate them successfully.

Consider a simple Web page as a digital item. This Web page typically consists of an HTML (hypertext markup language) document with embedded links or dependencies to various image files (e.g. JPEG images) and possibly some layout information (e.g. style sheet). In this simple case, it is a straightforward exercise to inspect the HTML document and deduce that this digital item consists of the HTML document itself plus all the other resources upon which it depends.

Now let us constrain the above example such that the Web page should be viewed with the JavaScript language. The presence of the language logic now raises the question of what constitutes this digital item and how it can be unambiguously determined. The first problem is that addition of the scripting code changes the declaration of the links, since the links can be determined only by running the embedded script on the specific platform. This could still work as a method of deducing the structure of digital item, assuming the author intended each translated version of the Web page to be a separate and distinct digital item. This assumption creates a second problem, as it is ambiguous whether the author actually intends for each translation of the page to be a stand-alone digital item or whether the intention is for the digital item to consist of the page with the language choice left unresolved. If the latter is the case, it makes it impossible to deduce the exact set of resources that this digital item consists of, which leads back to the first problem. In the course of standardisation, MPEG-21 aims to come up with a standard way of defining and declaring digital items.

12.3.2 Digital item identification and description

Currently, the majority of content lacks identification and description. Moreover, there is no mechanism to ensure that this identity and description is persistently associated with the content, which hinders any kind of efficient content storage.

However, in the meantime, some identifiers have been successfully implemented and commonly used for several years, but they are defined in a single media type. ISBN (International Standard Book Number) and URN (Universal Resource Name) are two examples of digital identifiers. This is just the beginning, and in the future we will see more of these.

There are many examples of business that have requirements for the deployment of a unique identification system on a global scale. Proprietary solutions such as labelling and watermarking for insertion, modification and extractions of IDs have emerged in the past. However, no international standard is available today for the deployment of such technologies, and it is the second task of MPEG-21 to identify and describe them.

12.3.3 Content handling and usage

The availability and access of content within networks is exponentially increasing over time. With the goal of MPEG-21 to enable transparent use of this content over a variety of networks and devices, it becomes extremely important that standards should exist to facilitate searching, locating, caching, archiving, routing, distributing and using content. In addition, the content has to be relevant to the customer needs and a better return of money for the business.

Thus, the goal of MPEG-21 multimedia framework is to provide interfaces and protocols that enable creation, manipulation, search, access, storage, delivery and use of content across the content creation and consumption chain. The emphasis should be given to improve interaction model for users with personalisation and content handling.

12.3.4 Intellectual property and management

MPEG-21 should provide a uniform framework that enables users to express their rights and interests in, and agreements related to, digital items. They should be assured that those rights, interests and agreements will be persistently and reliably managed and protected across a wide range of networks and devices.

12.3.5 Terminal and networks

Accessibility of heterogeneous content is becoming widespread to many network devices. Today, we receive a variety of information through set-top boxes for terrestrial/cable/satellite networks, personal digital assistants, mobile phones, etc. Additionally, these access devices are used in different locations and environments. This makes it difficult for service providers to ensure that content is available anywhere and anytime, and can be used and rendered in a meaningful way.

The goal of MPEG-21 is to enable transparent use of multimedia resources across a wide range of networked devices. This inevitably has an impact on the way network and terminal resources themselves are being dealt with.

Users accessing content should be offered services with a known subjective quality, perhaps at a known or agreed price. They should be shielded from network and terminal installation, management and implementation issues.

From the network point of view, it is desirable that the application serving the user translates the user requirements into a network Quality of Service (QoS) contract. This contract, containing a summary of negotiated network parameters, is handled between the user or their agents and the network. This guarantees the delivery of service over the network for a given QoS. However, the actual implementation of network QoS does not fall within the scope of MPEG-21. The intent is to make use of these mechanisms and propose requirements to network QoS functionality extensions to fulfil the overall MPEG-21 QoS demands.

12.3.6 Content representation

Content is the most important element of a multimedia framework. Within the framework, content is coded, identified, described, stored, delivered, protected, transacted, consumed, etc.

Although MPEG-21 assumes content is available in digital form, it should be represented in a form to fulfil some requirements. For example, digital video, as a digital item, needs to be compressed and converted into a format to be stored more economically. Although there are several standards for efficient compression (representation) of image and video, they have been devised for specific purposes. Throughout the book, we have seen that JPEG and JPEG-2000 are some of the standards for coding of still images. For video, H.261, H.263, H.26L, MPEG-1 and MPEG-2 are used for frame-based video and MPEG-4 is for coding of arbitrary shaped objects; but this is not enough for unique and unambiguous representation of digital video item. The same is true for audio.

In fact, users are becoming more mobile and have a need to access information on multiple devices in different context at different locations. Currently, content providers and authors have to create multiple formats of content and deploy them in a multitude of networks. Also, no satisfactory automated configurable way of delivering and consuming content that scales automatically to different network characteristics and device profiles exists. This is despite the introduction of various scalable coding of video to alleviate some of these problems.

Content representation element of the framework intends to address the technology needed so that the content is represented in a way adequate to pursue the general objectives of MPEG-21. In this regard, MPEG-21 assumes that content consists of one or a combination of the following:

1. content represented by MPEG standards (e.g. MPEG-4 video)
2. content used by MPEG but not covered by MPEG standards, for example, plain text and HTML.
3. content that can be represented by (1) and (2) but is represented by different standards or proprietary specifications
4. future standards for other sensory media

12.3.7 Event reporting

Every interaction is an 'event', and there is a necessity that events should be reported. However, there are a number of difficulties in providing an accurate report about the event. Different observers of the event may have different perspectives, needs and focuses. Currently, there exists no standardised means of event reporting.

In multimedia environment, there are many events that need reporting. For example, accurate product cost, consumer cost, channel costs or their profitability information need to be reported. This allows users to understand operational processes and simulate dynamics in order to optimise efficiencies and outputs.

However, every industry reports information about its performance to other users. A number of issues make this difficult for the receiving users to process this information. For example, different reporting formats, different standards from country to country, different currencies and languages make event processing difficult. As the last key architectural element, MPEG-21 intends to standardise event reporting to eliminate these shortfalls.

References

1. ISO/IEC JTC1/SC29/WG11/N4031: 'Overview of the MPEG-7 standard', Singapore, March 2001
2. ISO/IEC JTC1/SC29/WG11/N4040: 'Study on MPEG-21 (digital audiovisual framework) Part 1', Singapore, March 2001
3. LEE, T.S.: 'Image representation using 2D Gabor wavelets', *IEEE Trans. Pattern Anal. Mach. Intell.*, 1996, **18:10**, pp. 959–971
4. IZQUIERDO, E. and GHANBARI, M.: 'Nonlinear Gaussian filtering approach for object segmentation', *IEE Proc. Vis. Image Signal Proc.*, 1999, **146:3**, pp. 137–143
5. ARKIN, E., CHEW, L., HUTTENLOCHER, D. and MITCHELL, J.: 'An efficiently computable metric for comparing polygonal shapes', *IEEE Trans. Pattern Anal. Mach. Intell*, 1991, **PAMI-13**, pp. 209–216

Appendix A

A 'C' program for the fast discrete cosine transform

```
/*ffdct.c*/
/*fast forward discrete cosine transform in the
current frame */

#include "config.h"
#include "global.h"

#define W1 2841     /* sqrt(2)cos(π/16) << 11 */
#define W2 2676     /* sqrt(2)cos(2π/16) << 11 */
#define W3 2408     /* sqrt(2)cos(3π/16) << 11 */
#define W5 1609     /* sqrt(2)cos(5π/16) << 11 */
#define W6 1108     /* sqrt(2)cos(6π/16) << 11 */
#define W7 565      /* sqrt(2)cos(7π/16) << 11 */
#define W10 2276    /* W1 - W7 */
#define W11 3406    /* W1 + W7 */
#define W12 4017    /* W3 + W5 */
#define W13 799     /* W3 - W5 */
#define W14 1568    /* W2 - W6 */
#define W15 3784    /* W2 + W6 */

/* global declarations */
void ffdct _ANSI_ARGS_((int *block));

void ffdct(block)
int *block;
{
int s[10],t[10],r[10];
int *p;
int j, temp;
```

```
/*forward transformation in "H" direction*/
p = block;
for(j=0; j<64; j +=8 )
    {
    /* first stage transformation */
    s[0]= (*(p) + *(p+7));
    s[1]= (*(p+1) + *(p+6));
    s[2]= (*(p+2) + *(p+5));
    s[3]= (*(p+3) + *(p+4));
    s[4]= (*(p+3) - *(p+4));
    s[5]= (*(p+2) - *(p+5));
    s[6]= (*(p+1) - *(p+6));
    s[7]= (*(p)- *(p+7));

    /* second stage transformation */
    t[0]= s[0] + s[3];
    t[1]= s[1] + s[2];
    t[2]= s[1] - s[2];
    t[3]= s[0] - s[3];
    t[5]= ((s[6] - s[5]) * 181) >> 8;
    t[6]= ((s[6] + s[5]) * 181) >> 8;

    /* third stage transformation */
    r[4]= s[4] + t[5];
    r[5]= s[4] - t[5];
    r[6]= s[7] - t[6];
    r[7]= s[7] + t[6];

    /* fourth stage transformation */
    block[0+j]= (t[0] + t[1]);
    block[4+j]= (t[0] - t[1]);
    temp = (r[4] + r[7]) * W1;
    block[1+j]= (temp - r[4] * W10) >> 11;
    block[7+j]= (r[7] * W11 - temp) >> 11;
    temp = ( r[5] + r[6]) * W3;
    block[3+j]= (temp - r[5] * W12) >> 11;
    block[5+j]= (temp - r[6] * W13) >> 11;
    temp = (t[2] + t[3]) * W6;
    block[2+j]= (temp + t[3] * W14) >> 11;
    block[6+j]= (temp - t[2] * W15) >> 11;
    p += 8;
    }
```

```
/* forward transformation in 'V' direction */
for(j=0; j<8; j++)
    {
    /* first stage transformation */
    s[0] = block[j ] + block[j+ 56];
    s[1] = block[j+8] + block[j+ 48];
    s[2] = block[j+16] + block[j+ 40];
    s[3] = block[j+24] + block[j+ 32];
    s[4] = block[j+24] - block[j+ 32];
    s[5] = block[j+16] - block[j+ 40];
    s[6] = block[j+8] - block[j+ 48];
    s[7] = block[j ] - block[j+ 56];

    /* second stage transformation */
    t[0] = s[0] + s[3];
    t[1] = s[1] + s[2];
    t[2] = s[1] - s[2];
    t[3] = s[0] - s[3];
    t[5] = ((s[6] - s[5]) * 181) >> 8;
    t[6] = ((s[6] + s[5]) * 181) >> 8;

    /* third stage transformation */
    r[4] = s[4] + t[5];
    r[5] = s[4] - t[5];
    r[6] = s[7] - t[6];
    r[7] = s[7] + t[6];

    /* fourth stage transformation */
    /* transform coefficients */
    /* coefficients are divided by 8 and rounded */
    block[0+j]= ((t[0] + t[1]) + 4 ) >> 3;
    block[32+j]= ((t[0] - t[1]) + 4 ) >> 3;
    temp = ( r[4] + r[7] ) * W1;
    block[8+j]= ((temp - r[4] * W10) + 8192) >> 14;
    block[56+j]=(((r[7]*W11)-temp)+8192)>>14;
    temp = ( r[5] + r[6] ) * W3;
    block[24+j]=((temp - r[5] * W12) + 8192) >> 14;
    block[40+j]=((temp - r[6] * W13) + 8192) >> 14;
    temp = ( t[2] + t[3] ) * W6;
    block[16+j]=((temp + t[3] * W14) + 8192) >> 14;
    block[48+j]=((temp - t[2] * W15) + 8192) >> 14;
    }
```

Appendix B

Huffman tables for the DC and AC coefficients of the JPEG baseline encoder

Table B.1 DC Huffman coefficients of luminance

Category (CAT)	Code word
0	00
1	010
2	011
3	100
4	101
5	110
6	1110
7	11110
8	111110
9	1111110
10	11111110
11	111111110

Table B.2 AC Huffman coefficients of luminance

(RUN,CAT)	Code word	(RUN,CAT)	Code word
0,0 (**EOB**)	1010		
0,1	00	4,1	111011
0,2	01	4,2	1111111000
0,3	100	4,3	1111111110010110
0,4	1011	4,4	1111111110010111
0,5	11010	4,5	1111111110011000
0,6	1111000	4,6	1111111110011001
0,7	11111000	4,7	1111111110011010
0,8	1111110110	4,8	1111111110011011
0,9	1111111110000010	4.9	1111111110011100
0,10	1111111110000011	4,10	1111111110011101
1,1	1100	5,1	1111010
1,2	11011	5,2	11111110111
1,3	1111001	5,3	1111111110011110
1,4	111110110	5,4	1111111110011111
1,5	11111110110	5,5	1111111110100000

(*Continues*)

Table B.2 (*Continued*)

(RUN,CAT)	**Code word**	**(RUN,CAT)**	**Code word**
1,6	1111111110000100	5,6	1111111110100001
1,7	1111111110000101	5,7	1111111110100010
1,8	1111111110000110	5,8	1111111110100011
1,9	1111111110000111	5,9	1111111110100100
1,10	1111111110001000	5,10	1111111110100101
2,1	11100	6,1	1111011
2,2	11111001	6,2	11111110110
2,3	1111110111	6,3	1111111110100110
2,4	111111110100	6,4	1111111110100111
2,5	1111111110001001	6,5	1111111110101000
2,6	1111111110001010	6,6	1111111110101001
2,7	1111111110001011	6,7	1111111110101010
2,8	1111111110001100	6,8	1111111110101011
2,9	1111111110001101	6,9	1111111110101100
2,10	1111111110001110	6,10	1111111110101101
3,1	111010	7,1	11111010
3,2	111110111	7,2	11111110111
3,3	111111110101	7,3	1111111110101110
3,4	1111111110001111	7,4	1111111110101111
3,5	1111111110010000	7,5	1111111110110000
3,6	1111111110010001	7,6	1111111110110001
3,7	1111111110010010	7,7	1111111110110010
3,8	1111111110010011	7,8	1111111110110011
3,9	1111111110010100	7,9	1111111110110100
3,10	1111111110010101	7,10	1111111110110101
8,1	111111000	12,1	1111111010
8,2	111111111000000	12,2	1111111111011001
8,3	1111111110110110	12,3	1111111111011010
8,4	1111111110110111	12,4	1111111111011011
8,5	1111111110111000	12,5	1111111111011100
8,6	1111111110111001	12,6	1111111111011101
8,7	1111111110111010	12,7	1111111111011110
8,8	1111111110111011	12,8	1111111111011111
8,9	1111111110111100	12,9	1111111111100000
8,10	1111111110111101	12,10	1111111111100001
9,1	111111001	13,1	11111111000
9,2	1111111110111110	13,2	1111111111100010
9,3	1111111110111111	13,3	1111111111100011
9,4	1111111111000000	13,4	1111111111100100
9,5	1111111111000001	13,5	1111111111100101
9,6	1111111111000010	13,6	1111111111100110
9,7	1111111111000011	13,7	1111111111100111
9,8	1111111111000100	13,8	1111111111101000
9,9	1111111111000101	13,9	1111111111101001
9,10	1111111111000110	13,10	1111111111101010
10,1	111111010	14,1	1111111111101011
10,2	1111111111000111	14,2	1111111111101100
10,3	1111111111001000	14,3	1111111111101101
10,4	1111111111001001	14,4	1111111111101110

10,5	1111111111001010	14,5	1111111111101111
10,6	1111111111001011	14,6	1111111111110000
10,7	1111111111001100	14,7	1111111111110001
10,8	1111111111001101	14,8	1111111111110010
10,9	1111111111001110	14,9	1111111111110011
10,10	1111111111001111	14,10	1111111111110100
11,1	1111111001	15,1	1111111111110101
11,2	1111111111010000	15,2	1111111111110110
11,3	1111111111010001	15,3	1111111111110111
11,4	1111111111010010	15,4	1111111111111000
11,5	1111111111010011	15,5	1111111111111001
11,6	1111111111010100	15,6	1111111111111010
11,7	1111111111010101	15,7	1111111111111011
11,8	1111111111010110	15,8	1111111111111100
11,9	1111111111010111	15,9	1111111111111101
11,10	1111111111011000	15,10	1111111111111110
The special symbol representing 16 zero		15,0 (**ZRL**)	11111111001

Appendix C

Huffman tables for quad tree shape coding

Huffman tables for quad tree shape coding: table_012.dat is used at levels 0,1 and 2 and table_3.dat is used at level 3.

Table C.1 table_012.dat

Index	Code	Index	Code
0	–	41	11110011
1	10011	42	11111111010
2	11110101	43	11110010
3	101101	44	0101
4	0010	45	1110011
5	1110110	46	1101111
6	111111011	47	11110111
7	1100110	48	111111111100
8	01110	49	11101111
9	101111	50	101110
10	10010	51	111111111111101
11	11110100	52	111111111001
12	1111111111100	53	110001
13	11110000	54	11110001
14	1110100	55	1111111111101
15	1111111111111111	56	111111111111110
16	111111111010	57	110000
17	1101110	58	1111111001
18	11111011	59	1111111111110
19	11111000	60	0100
20	110010	61	1101010
21	111111111111100	62	11111010
22	1111111000	63	10000
23	11111001	64	1111111011
24	1111111111111110	65	111111111000
25	11111111001	66	1101000
26	111111010	67	11110000
27	10001	68	11111111011
28	1111111010	69	11101110
29	111111111101	70	01101
30	01111	71	101100
31	1110101	72	0000

(*Continues*)

Table C.1 (*Continued*)

Index	Code	Index	Code
32	11111111000	73	1100111
33	1101011	74	1101101
34	1110010	75	1101001
35	11111100	76	0011
36	0001	77	10100
37	1110001	78	1101100
38	111111111011	79	01100
39	11110110	80	–
40	10101		

Table C.2 *table_3.dat*

Index	Code
0	–
2	1101
6	1111110
8	1011
18	11101
20	100
24	11111111
26	111110
54	1100
56	11111110
60	01
62	11110
72	00
74	1010
78	11100
80	–

Appendix D

Frequency tables for the CAE encoding of binary shapes

Frequency tables for intra and inter blocks, used in the context-based arithmetic encoding (CAE) method of binary shapes.

```
Intra_prob[1024] = {
65267,16468,65003,17912,64573,8556,64252,5653,40174,3932,29789,277,45152,1140,32768,2043,
4499,80,6554,1144,21065,465,32768,799,5482,183,7282,264,5336,99,6554,563,
54784,30201,58254,9879,54613,3069,32768,58495,32768,32768,32768,2849,58982,54613,32768,12892,
31006,1332,49152,3287,60075,350,32768,712,39322,760,32768,354,52659,432,61854,150,
64999,28362,65323,42521,63572,32768,63677,18319,4910,32768,64238,434,53248,32768,61865,13590,
16384,32768,13107,333,32768,32768,32768,32768,32768,32768,1074,780,25058,5461,6697,233,
62949,30247,63702,24638,59578,32768,32768,42257,32768,32768,49152,546,62557,32768,54613,19258,
62405,32569,64600,865,60495,10923,32768,898,34193,24576,64111,341,47492,5231,55474,591,
65114,60075,64080,5334,65448,61882,64543,13209,54906,16384,35289,4933,48645,9614,55351,7318,
49807,54613,32768,32768,50972,32768,32768,32768,15159,1928,2048,171,3093,8,6096,74,
32768,60855,32768,32768,32768,32768,32768,32768,32768,32768,32768,32768,32768,55454,32768,57672,
32768,16384,32768,21845,32768,32768,32768,32768,32768,32768,32768,5041,28440,91,32768,45,
65124,10923,64874,5041,65429,57344,63435,48060,61440,32768,63488,24887,59688,3277,63918,14021,
32768,32768,32768,32768,32768,32768,32768,32768,690,32768,32768,1456,32768,32768,8192,728,
32768,32768,58982,17944,65237,54613,32768,2242,32768,32768,32768,42130,49152,57344,58254,16740,
32768,10923,54613,182,32768,32768,32768,7282,49152,32768,32768,5041,63295,1394,55188,77,
63672,6554,54613,49152,64558,32768,32768,5461,64142,32768,32768,32768,62415,32768,32768,16384,
1481,438,19661,840,33654,3121,64425,6554,4178,2048,32768,2260,5226,1680,32768,565,
60075,32768,32768,32768,32768,32768,32768,32768,32768,32768,32768,32768,32768,32768,32768,32768,
16384,261,32768,412,16384,636,32768,4369,23406,4328,32768,524,15604,560,32768,676,
49152,32768,49152,32768,32768,32768,64572,32768,32768,32768,54613,32768,32768,32768,32768,32768,
4681,32768,5617,851,32768,32768,59578,32768,32768,32768,3121,3121,49152,32768,6554,10923,
32768,32768,54613,14043,32768,32768,32768,3449,32768,32768,32768,32768,32768,32768,32768,32768,
57344,32768,57344,3449,32768,32768,32768,3855,58982,10923,32768,239,62259,32768,49152,85,
58778,23831,62888,20922,64311,8192,60075,575,59714,32768,57344,40960,62107,4096,61943,3921,
39862,15338,32768,1524,45123,5958,32768,58982,6669,930,1170,1043,7385,44,8813,5011,
59578,29789,54613,32768,32768,32768,32768,32768,32768,32768,32768,32768,58254,56174,32768,32768,
64080,25891,49152,22528,32768,2731,32768,10923,10923,3283,32768,1748,17827,77,32768,108,
62805,32768,62013,42612,32768,32768,61681,16384,58982,60075,62313,58982,65279,58982,62694,62174,
32768,32768,10923,950,32768,32768,32768,32768,5958,32768,38551,1092,11012,39322,13705,2072,
54613,32768,32768,11398,32768,32768,32768,145,32768,32768,32768,29789,60855,32768,61681,54792,
32768,32768,32768,17348,32768,32768,32768,8192,57344,16384,32768,3582,52581,580,24030,303,
62673,37266,65374,6197,62017,32768,49152,299,54613,32768,32768,32768,35234,119,32768,3855,
31949,32768,32768,49152,16384,32768,32768,32768,24576,32768,49152,32768,17476,32768,32768,57445,
51200,50864,54613,27949,60075,20480,32768,57344,32768,32768,32768,32768,32768,45875,32768,32768,
11498,3244,24576,482,16384,1150,32768,16384,7992,215,32768,1150,23593,927,32768,993,
65353,32768,65465,46741,41870,32768,64596,59578,62087,32768,12619,23406,11833,32768,47720,17476,
32768,32768,2621,6554,32768,32768,32768,32768,32768,32768,5041,32768,16384,32768,4096,2731,
63212,43526,65442,47124,65410,35747,60304,55858,60855,58982,60075,19859,35747,63015,64470,25432,
58689,1118,64717,1339,24576,32768,32768,1257,53297,1928,32768,33,52067,3511,62861,453,
64613,32768,32768,32768,64558,32768,32768,2731,49152,32768,32768,32768,61534,32768,32768,35747,
32768,32768,32768,32768,13107,32768,32768,32768,32768,32768,32768,32768,20480,32768,32768,32768,
32768,32768,32768,54613,40960,5041,32768,32768,32768,32768,32768,3277,64263,57592,32768,3121,
32768,32768,32768,32768,32768,10923,32768,32768,32768,8192,32768,32768,5461,6899,32768,1725,
63351,3855,63608,29127,62415,7282,64626,60855,32768,32768,60075,5958,44961,32768,61866,53718,
32768,32768,32768,32768,32768,32768,6554,32768,32768,32768,32768,32768,2521,978,32768,1489,
58254,32768,58982,61745,21845,32768,54613,58655,60075,32768,49152,16274,50412,64344,61643,43987,
32768,32768,32768,1638,32768,32768,32768,24966,54613,32768,32768,2427,46951,32768,17970,654,
65385,27307,60075,26472,64479,32768,32768,4681,61895,32768,32768,16384,58254,32768,32768,6554,
37630,3277,54613,6554,4965,5958,4681,32768,42765,16384,32768,21845,22827,16384,32768,6554,
65297,64769,60855,12743,63195,16384,32768,37942,32768,32768,32768,32768,60075,32768,62087,54613,
41764,2161,21845,1836,17284,5424,10923,1680,11019,555,32768,431,39819,907,32768,171,
65480,32768,64435,33803,2595,32768,57041,32768,61167,32768,32768,32768,32768,32768,32768,1796,
60855,32768,17246,978,32768,32768,8192,32768,32768,32768,14043,2849,32768,2979,6554,6554,
65507,62415,65384,61891,65273,58982,65461,55097,32768,32768,32768,55606,32768,2979,3745,16913,
61885,13827,60893,12196,60855,53248,51493,11243,56656,783,55563,143,63432,7106,52429,445,
65485,1031,65020,1380,65180,57344,65162,36536,61154,6554,26569,2341,63593,3449,65102,533,
47827,2913,57344,3449,35688,1337,32768,22938,25012,910,7944,1008,29319,607,64466,4202,
64549,57301,49152,20025,63351,61167,32768,45542,58982,14564,32768,9362,61895,44840,32768,26385,
59664,17135,60855,13291,40050,12252,32768,7816,25798,1850,60495,2662,18707,122,52538,231,
65332,32768,65210,21693,65113,6554,65141,39667,62259,32768,22258,1337,63636,32768,64255,52429,
60362,32768,6780,819,16384,32768,16384,4681,49152,32768,8985,2521,24410,683,21535,16585,
65416,46091,65292,58328,64626,32768,65016,39897,62687,47332,62805,28948,64284,53620,52870,49567,
65032,31174,63022,28312,64299,46811,48009,31453,61207,7077,50299,1514,60047,2634,46488,235
};

Inter_prob[512] = {
65532,62970,65148,54613,62470,8192,62577,8937,65480,64335,65195,53248,65322,62518,62891,38312,
65075,53405,63980,58982,32768,32768,54613,32768,65238,60009,60075,32768,59294,19661,61203,13107,
63000,9830,62566,58982,11565,32768,25215,3277,53620,50972,63109,43691,54613,32768,39671,17129,
59788,6068,43336,27913,6554,32768,12178,1771,56174,49152,60075,43691,58254,16384,49152,9930,
23130,7282,40960,32768,10923,32768,32768,32768,27307,32768,32768,32768,32768,32768,32768,32768,
36285,12511,10923,32768,45875,16384,32768,32768,16384,23831,4369,32768,8192,10923,32768,32768,
10175,2979,18978,10923,54613,32768,6242,6554,1820,10923,32768,32768,32768,32768,32768,5461,
28459,593,11886,2030,3121,4681,1292,112,42130,23831,49152,29127,32768,6554,5461,2048,
65331,64600,63811,63314,42130,19661,49152,32768,65417,64609,62415,64617,64276,44256,61068,36713,
64887,57525,53620,61375,32768,8192,57344,6554,63608,49809,49152,62623,32768,15851,58982,34162,
55454,51739,64406,64047,32768,32768,7282,32768,49152,58756,62805,64990,32768,14895,16384,19418,
57929,24966,58689,31832,32768,16384,10923,6554,54613,42882,57344,64238,58982,10082,20165,20339,
62687,15061,32768,10923,32768,10923,32768,16384,59578,34427,32768,16384,32768,7825,32768,7282,
58052,23400,32768,5041,32768,2849,32768,32768,47663,15073,57344,4096,32768,1176,32768,1320,
24858,410,24576,923,32768,16384,16384,5461,16384,1365,32768,5461,32768,5699,8192,13107,
46884,2361,23559,424,19661,712,655,182,58637,2094,49152,9362,8192,85,32768,1228,
65486,49152,65186,49152,61320,32768,57088,25206,65352,63047,62623,49152,64641,62165,58986,18304,
64171,16384,60855,54613,42130,32768,61335,32768,58254,58982,49152,32768,60985,35289,64520,31554,
51067,32768,64074,32768,40330,32768,34526,4096,60855,32768,63109,58254,57672,16384,31009,2567,
23406,32768,44620,10923,32768,32768,32099,10923,49152,49152,54613,60075,63422,54613,46388,39719,
58982,32768,54613,32768,14247,32768,22938,5041,32768,49152,32768,32768,25321,6144,29127,10999,
41263,32768,46811,32768,267,4096,426,16384,32768,19275,49152,32768,1008,1437,5767,11275,
5595,5461,37493,6554,4681,32768,6147,1560,38229,10923,32768,40960,35747,2521,5999,312,
17052,2521,18808,3641,213,2427,574,32,51493,42130,42130,53053,11155,312,2069,106,
64406,45197,58982,32768,32768,16384,40960,36864,65336,64244,60075,61681,65269,50748,60340,20515,
58982,23406,57344,32768,6554,16384,19661,61564,60855,47480,32768,54613,46811,21701,54909,37826,
32768,58982,60855,60855,32768,32768,39322,49152,57344,45875,60855,55706,32768,24576,62313,25038,
54613,8192,49152,10923,32768,32768,32768,32768,32768,19661,16384,51493,32768,14043,40050,44651,
59578,5174,32768,6554,32768,5461,23593,5461,63608,51825,32768,23831,58887,24032,57170,3298,
39322,12971,16384,49152,1872,618,13107,2114,58982,25705,32768,60075,28913,949,18312,1815,
48188,114,51493,1542,5461,3855,11360,1163,58982,7215,54613,21487,49152,4590,48430,1421,
28944,1319,6868,324,1456,232,820,7,61681,1864,60855,9922,4369,315,6589,14
};
```

Appendix E
Channel error/packet loss model

Digital channels and packet networks can be modelled as a discrete two-state Elliot–Gilbert model, as shown in Figure E.1.

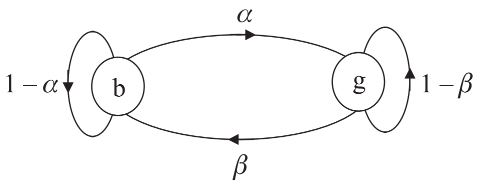

Figure E.1 An Elliot–Gilbert two-level error model

When the model is at the bad state, b, a bit is corrupted or a packet is received erroneously, and can be regarded as lost. The model is run for every bit (or packet) to be transmitted, and the average number of times that the model stays at the bad position is the average bit error rate, or packet loss rate, P. Consequently, the average number of times it stays at the good state is $1 - P$. In the following, we show how the average bit error or packet loss rate is related to the transition probabilities α and β. We analyse on packet loss rate, and the same procedure can be used for bit error rate. The model has also been accepted by the ITU-T for the evaluation of ATM networks.*

Calculation of mean packet loss rate

At each run of the model, a packet is lost in two ways. First, before the run it was at the bad state, but after the run it is also at the bad state. Second, it was in a good state, but after the run it is at the bad state. Thus, the probability of being at bad state (loss), P, is

$$P = P(1 - \alpha) + (1 - P)\beta$$

* ITU SGXV working party XV/I, Experts Group for ATM video coding, working document AVC-205, January 1992.

and rearranging the equation, the average packet loss rate P is

$$P = \frac{\beta}{\alpha + \beta} \tag{E.1}$$

Calculation of mean burst length

A burst of lost packets is defined as a sequence of consecutive packets, all of which are marked as lost. The burst starts when a packet is lost after one or more packets have not been lost. Thus, the probability of a burst length of 1 is just being at the bad state and then going to the good state. This probability is α. Similarly, the probability of burst length of 2 is the probability of being at the bad state but coming to this state at the next run. This probability is $(1 - \alpha)\alpha$. Thus, in general, the probability of a burst length of k packets is to be at the bad state for $k - 1$ times and the next run to go to the good state, which is $(1 - \alpha)^{(k-1)}\alpha$

The mean burst length B is then

$$B = \alpha + 2(1-\alpha)\alpha + 3(1-\alpha)^2\alpha + 4(1-\alpha)^3\alpha + \cdots + k(1-\alpha)^{k-1}\alpha + \cdots$$

Summing this series leads to

$$B = \frac{1}{\alpha} \tag{E.2}$$

Rearranging eqn. E.2 gives

$$\alpha = \frac{1}{B} \tag{E.3}$$

and rearranging eqn. E.1 and substituting for α from eqn. E.3 gives

$$\beta = \frac{P}{B(1-P)} \tag{E.4}$$

Simulation of packet loss

For a given mean packet loss rate P and average burst length B, the transition probabilities α and β can be calculated from eqns E.3 and E.4. The model is run for as many packets as are to be served, and at each run it is decided whether the packet should be marked as lost or not. To do this, each run is equivalent to running a random number between 0 and 1, and if it is less than the relevant transition probabilities, the packet is marked lost, otherwise it is received safely.

A pseudo code to perform packet loss is given below.

```
PreviousPacketLost=FALSE;
Readln(P,B);
α =(1/B);
β =P/(B×(1-P));
```

```
FOR (number of packets to be transmitted)
   BEGIN
   CASE PreviousPacketLoss OF
      TRUE: IF random <1-α THEN PacketLoss=TRUE;
                            ELSE Packetloss=FALSE;
      FALSE: IF random <β THEN PacketLoss=TRUE;
                            ELSE Packetloss=FALSE;
   END
```

Appendix F
Solutions to the problems

Chapter 2

1.

	r	g	b	y	c	m	w
R	1	0	0	1	0	1	1
G	0	1	0	1	1	0	1
B	0	0	1	0	1	1	1

2.

	r	g	b	y	c	m	w
Y	82	145	41	210	170	107	235
C_b	90	54	240	16	166	202	128
C_r	240	34	110	146	16	222	128

3. $T = \dfrac{1}{25 \times 625} = 64\,\mu\text{s}$ and $T = \dfrac{1}{30 \times 525} = 63.5\,\mu\text{s}$

4. $\dfrac{13.5 \times 10^6}{25 \times 625} = 864$ pixels; $864 - 720 = 144$ pixels; $\dfrac{144}{13.5 \times 10^6} = 10.67\,\mu\text{s}$

5. 857 pixels; $857 - 720 = 137$ pixels; 10 μs

6. a. $720 \times 576 \times 25 \times 2 \times 8 = 166$ Mbit/s
   b. $720 \times 525 \times 30 \times 2 \times 8 = 166$ Mbit/s
   c. $360 \times 288 \times 25 \times 1.5 \times 8 = 31$ Mbit/s
   d. $360 \times 240 \times 30 \times 1.5 \times 8 = 31$ Mbit/s
   e. 37 Mbit/s
   f. 31 Mbit/s
   g. 31 Mbit/s
   h. 4.7 Mbit/s
   i. 1.4 Mbit/s

7. 94 73 194 184 50 204 207

8. 94 82 73 132 194 201 184 109 50 121 204 222 207
   PSNR = 20.2 dB

9. a. A sinusoid with amplitude A has a peak-to-peak $2A = 2^n\,\Delta \Rightarrow \Delta = A\,2^{1-n}$

$$\text{SNR} = 10\,\log_{10}\left(\frac{A^2/2}{\Delta^2/12}\right) = 10\,\log(3 \times 2^{2n-1}) = 1.78 + 6n \text{ dB}$$

   b. Peak-to-peak power of the sinusoid is $10\,\log_{10}\left(\frac{(2A)^2}{A^2/2}\right) = 9$ dB higher than its mean power $\Rightarrow$ PSNR $= 10.78 + 6n$
   c. $10.78 + 6n \geq 58 \Rightarrow n \geq 8$ bits

Chapter 3

1. a. $|x| \le 16;\ y = 0 \quad 16 < |x| \le 32; y = \pm 24 \quad 32 < |x| \le 48; y = \pm 40,$ etc.
   b. $|x| \le 16;\ y = \pm 8 \quad 16 < |x| \le 32; y = \pm 24 \quad 32 < |x| \le 48; y = \pm 40,$ etc.
2. 12 16 28 240 196 32 PSNR = 43.4 dB
3. 6 12 27 77 127 77 PSNR = 10.7 dB
4. $\underbrace{15\ \ 21\ \ 19\ \ 21\ \ 19}_{\text{G-noise}}\ \underbrace{69\ \ 119\ \ 169\ \ 219\ \ 234}_{\text{Slope overload}}\ \underbrace{232\ \ 230\ \ 232\ \ 230}_{\text{G-noise}}$
5.

$$T = \frac{1}{2}\begin{vmatrix} 0.71 & 0.71 & 0.71 & 0.71 & 0.71 & 0.71 & 0.71 & 0.71 \\ 0.98 & 0.83 & 0.56 & 0.2 & -0.2 & -0.56 & -0.83 & -0.98 \\ 0.92 & 0.38 & -0.38 & -0.92 & -0.92 & -0.38 & 0.38 & 0.92 \\ 0.83 & -0.2 & -0.98 & -0.56 & 0.56 & 0.98 & 0.2 & -0.83 \\ 0.71 & -0.71 & -0.71 & 0.71 & 0.71 & -0.71 & -0.71 & 0.71 \\ 0.56 & -0.98 & 0.2 & 0.83 & -0.83 & -0.2 & 0.98 & -0.56 \\ 0.38 & -0.92 & 0.92 & -0.38 & -0.38 & 0.92 & -0.92 & 0.38 \\ 0.2 & -0.56 & 0.83 & -0.98 & 0.98 & -0.83 & 0.56 & -0.2 \end{vmatrix}$$

$$T^{-1} = T^{T} = \frac{1}{2}\begin{vmatrix} 0.71 & 0.98 & 0.92 & 0.83 & 0.71 & 0.56 & 0.38 & 0.2 \\ 0.71 & 0.83 & 0.38 & -0.2 & -0.71 & -0.98 & -0.92 & -0.56 \\ 0.71 & 0.56 & -0.38 & -0.98 & -0.71 & 0.2 & 0.92 & 0.83 \\ 0.71 & 0.2 & -0.92 & -0.56 & 0.71 & 0.83 & -0.38 & -0.98 \\ 0.71 & -0.2 & -0.92 & 0.56 & 0.71 & -0.83 & -0.38 & 0.98 \\ 0.71 & -0.56 & -0.38 & 0.98 & -0.71 & -0.2 & 0.92 & -0.83 \\ 0.71 & -0.83 & 0.38 & 0.2 & -0.71 & 0.98 & -0.92 & 0.56 \\ 0.71 & -0.98 & 0.92 & -0.83 & 0.71 & -0.56 & 0.38 & -0.2 \end{vmatrix}$$

6. a. 364 15 −211 −26 −5 38 −2 −1
   b. The basis vector of the second AC coefficient matches the input pixels
   c. 35 82 190 250 200 150 101 23. Because of the mismatch (approximating the cosine elements) some of the input pixels cannot be reconstructed, for example, 81/82 and 100/101.
7. quantised coefficients: 360 0 –216 –24 0 40 0 0
   reconstructed pixels: 30 70 185 250 204 153 104 27
   PSNR = 30 dB
8. a. reconstructed pixels: 128 128 128 128 128 128 128 128
   PSNR = 10.4 dB
   b. reconstructed pixels: 28 87 169 227 227 169 87 28
   PSNR = 23.4 dB
9. a. $MV\,(-1, -1)$
   b. $MV\,(-1, -1)$
10. a. 169
    b. (i) multiplications = 256 × 169, additions = 511 × 169
    (ii) multiplications = 0, additions = 510 × 169
11.

type	*operation*	*multiplication*	*addition*
TDL	23	23 × 256	23 × 511
TSS	25	25 × 256	25 × 511
CSA	17	17 × 256	17 × 511
OSA	13	13 × 256	13 × 511

12. **a** = 010, **b** = 1, **c** = 00, **d** = 011 Av bits = 1.8 entropy = 1.72
13. a. **cbdad** = 001011010011
    b. (i) first bit in error, decoded string = **babbad**
    (ii) third bit in error, decoded string = **ccbbad**
    (iii) fifth bit in error, decoded string = **cbcbad**
14. lower value = 0.83875, upper value = 0.841875
15. a. the first three symbols = **cbc**
    b. the first five symbols = **cbcab**
16. Same as 15
17. 11010110111
18. Same as 17
19. a. First bit in error = 0.01010110111 = $2^{-2} + 2^{-4} + 2^{-6} + 2^{-7} + 2^{-9} + 2^{-10} + 2^{-11}$ = 0.33935546875, which is decoded to string **bbacb**
    b. Similarly, with the third bit in error the decimal number would be 0.96435546875, decoded to **dbacb**
    c. With the fifth bit in error, the decimal number is 0.87060546875 and it is decoded to string **cbacb**

Chapter 4

1. $P(z) = H_0(z)H_1(-z)$ should be factorised into two terms. The given $P(z)$ is zero at $z^{-1} = -1$; hence it is divisible by $1 + z^{-1}$. Divide as many times as possible that gives:

   a. $\frac{1}{16}(1+z^{-1})(-1+z^{-1}+8z^{-2}+8z^{-3}+z^{-4}-z^{-5})$
   b. $\frac{1}{16}(1+z^{-1})^2(-1+2z^{-1}+6z^{-2}+2z^{-3}-z^{-4})$
   c. $\frac{1}{16}(1+z^{-1})^{-3}(-1+3z^{-1}+3z^{-2}-z^{-3})$
   d. $\frac{1}{16}(1+z^{-1})^{-4}(-1+4z^{-1}-z^{-2})$

   Thus, in (a) the low-pass analysis filter will be $H_0(z) = \frac{1}{16}(-1+z^{-1}+8z^{-2}+8z^{-3}+z^{-4}-z^{-5})$ and the high-pass analysis filter is $H_1(z) = 1 - z^{-1}$.
   In (b) $H_0(z) = \frac{1}{8}(-1+2z^{-1}+6z^{-2}+2z^{-3}-z^{-4})$ and the high pass is $H_1(z) = \frac{1}{2}(1-z^{-1})^2 = \frac{1}{2}(1-2z^{-1}+z^{-2})$, which are the (5,3) subband filter pairs.
   In (c) $H_0(z) = \frac{1}{4}(-1+3z^{-1}+3z^{-2}-z^{-3})$ and the high pass is $H_1(z) = \frac{1}{4}(1-z^{-1})^{-3} = \frac{1}{4}(1-3z^{-1}+3z^{-2}-z^{-3})$, which gives the second set of (4,4) subband filters.
   In (d) $H_0(z) = \frac{1}{2}(-1+4z^{-1}-z^{-2})$ and $H_1(z) = \frac{1}{8}(1-z^{-1})^4 = \frac{1}{2}(1-4z^{-1}+6z^{-2}-4z^{-3}+z^{-4})$
   Any other combinations may be used, as desired.

2. a. $P(z) = H_0(z) \times H_1(-z) = \frac{1}{2}(1+z^{-1})^2 = \frac{1}{2} + z^{-1} + \frac{1}{2}z^{-2}$. Thus, with $P(z) - P(-z) = 2z^{-1}$ results in one sample delay.
   b. $G_0(z) = H_1(-z) = \frac{1}{\sqrt{2}}(1+z^{-1})$

   $G_1(z) = -H_0(-z) = -\frac{1}{\sqrt{2}}(1-z^{-1})$

3. a. With a weighting factor of k, $P(z) = k(1 + z^{-1})^{-4}(-1 + 4z^{-1} - z^{-2})$, and using $P(z) - P(-z) = 2z^{-m}$ gives $k = 1/16$ and $m = 3$.
   b. The factor for the other set will be $k = 3/256$ and $m = 5$ samples delay.
4. In problem 3, $P(z)$ is in fact the type (d) of problem 1. Hence, it leads not only to the two sets of (5,3) and (4,4) filter pairs but also to two new types of filters, given in (a) and (d) of problem 1.
5. With $P(z) = \frac{3}{256}(1 + z^{-1})^6(1 - 6z^{-1} + \frac{38}{3} - 6z^{-3} + z^{-4})$, retaining $H_1(-z) = (1 + z^{-1})^2 = 1 + 2z^{-1} + z^{-2}$, which gives the three-tap high-pass filter of $H_1(z) = 1 - 2z^{-1} + z^{-2}$ and the remaining parts give the nine-tap low-pass filter.

$$H_0(z) = \frac{3}{256}(1 + z^{-1})^4(1 - 6z^{-1} + \frac{38}{3}z^{-2} - 6z^{-3} + z^{-4})$$

or

$$H_0(z) = \frac{1}{25}[3 - 6z^{-1} - 16z^{-2} + 38z^{-3} + 90z^{-4} + 38z^{-5} - 16z^{-6} - 6z^{-7} - 3^{-8}].$$

Had we divided the high-pass filter coefficients, $H_1(z)$, by $2\sqrt{2}$, and hence multiplying those of low-pass $H_0(z)$ by this amount, we get the (9,3) tap filter coefficients of Table 4.2.
6. Use $G_0(z) = H_1(-z)$ and $G_1(z) = -H_0(-z)$ to derive the synthesis filters
7. See pages 82 to 86
8. 33 bits
9. 29 bits

Chapter 5

1. a. Multiply all the luminance matrix elements by $\alpha = 50/25 = 2$
   b. $\alpha = 2 - \frac{2\times 99}{100} = 0.02$, and small elements of the matrix will be 1 and larger ones become 2.
   c. $\alpha = 0$, hence all the matrix elements will be 1
2. Same as problem 1.
3. a.

$$\begin{matrix} 62 & 0 & 3 & 1 & 0 & 0 & 1 & 0 \\ 0 & 1 & -1 & 0 & 1 & 0 & 0 & 0 \\ 0 & 0 & 0 & 0 & 1 & 0 & 0 & 0 \\ -1 & 0 & 0 & 0 & 0 & 0 & 0 & 0 \\ 0 & 0 & 1 & 0 & 0 & 0 & 0 & 0 \\ 0 & 0 & 0 & 0 & 0 & 0 & 0 & 0 \\ 0 & 0 & 0 & 0 & 0 & 0 & 0 & 0 \\ 0 & 0 & 0 & 0 & 0 & 0 & 0 & 3 \end{matrix}$$

   b.

$$\begin{matrix} 31 & 0 & 1 & 0 & 0 & 0 & 0 & 0 \\ 0 & 0 & 0 & 0 & 0 & 0 & 0 & 0 \\ 0 & 0 & 0 & 0 & 0 & 0 & 0 & 0 \\ 0 & 0 & 0 & 0 & 0 & 0 & 0 & 0 \\ 0 & 0 & 0 & 0 & 0 & 0 & 0 & 0 \\ 0 & 0 & 0 & 0 & 0 & 0 & 0 & 0 \\ 0 & 0 & 0 & 0 & 0 & 0 & 0 & 0 \\ 0 & 0 & 0 & 0 & 0 & 0 & 0 & 1 \end{matrix}$$

4. For 50% quality: DIFF = 62 − 50 = 12, symbol_1 = 4, symbol_2 = 12
   scanned pairs: (3,1)(0,3)(0,1)(0,−1)(1,−1)(6,1)(6,1)(1,1)(1,1)(35,3) and the resultant events: (3,1)(0,2)(0,1)(0,1)(1,1)(6,1)(6,1)(1,1)(1,1)(15,0)(15,0)(3,3)
   For 25% quality: DIFF = 31 − 50 = −19, symbol_1 = 5, symbol_2 = −19 − 1 = −20
   scanned pairs: (4,1)(57,1)
   events: (4,1)(15,0)(15,0)(15,0)(9,1)
5. For DC: DIFF = −19 ⇒ CAT = 5; DIFF − 1 = −20
   VLC for CAT = 5 is **110** and –20 in binary is 111**01100**; hence, the VLC for the DC coefficient is 11001100
   For AC, using the AC VCLC tables:
   for each (15,0) the VLC is 11111111001
   and for (9,1) the VLC is 111111001
   total number of bits: 8 + (3 × 11) + 9 = 50 bits.
6. At bit plane 6 coefficient 65 at clean-up pass. At bit plane 5 coefficient 65 at all passes and coefficient 50 at clean-up pass.

Chapter 6

1. a. 33, 198
   b. 396, 2376
2. CIF : $\frac{1}{30\times396} = 84.2\ \mu\text{s}$ QCIF : $\frac{1}{10\times99} = 1\text{ms}$
3. a. MC
   b. NO_MC
   c. NO_MC
4. Due to motion vector overhead
5. a. inter
   b. intra
   c. inter
6. For small values in intra mode DC still needs 8 bits, while in inter mode it is less.
7. a. 63
   b. 60
   c. 3
8. $$\begin{array}{cccccccc} 83 & 0 & 2 & 1 & 0 & 0 & 4 & 0 \\ 0 & 0 & -1 & 0 & 3 & 0 & 0 & 0 \\ 0 & 0 & 0 & 0 & 3 & -1 & 0 & 0 \\ -1 & 1 & 0 & 0 & 0 & 0 & 0 & 0 \\ 0 & 0 & 3 & 0 & 2 & 0 & 0 & 0 \\ 0 & 0 & 0 & 0 & 0 & 0 & 0 & 1 \\ -1 & 4 & 0 & 0 & 0 & 0 & 0 & 0 \\ 2 & 0 & 0 & 0 & 0 & 0 & 0 & 31 \end{array}$$
   events: (0,83)(4,2)(0,1)(0,−1)(1,−1)(1,1)(4,3)(4,−1)(1,3)(1,3)(1,4)(2,−1)(3,4)(0,2)(3,2)(20,1)(2,31)
   number of bits (including the sign bit): 20 + 10 + 5 + 5 + 6 + 6 + 11 + 8 + 8 + 8 + 9 + 7 + 11 + 5 + 8 + 20 + 20 = 167
   no EOB is used, as the last coefficient is coded

9. 159 149 170
   105 113 133
10. @384 kbit/s $P = 6$ and with $q = 62$ and $P = 6$, the buffer content is 36 kbits, leftover capacity $= 5000 \times 8 - 36000 = 4000$ bits

Chapter 7

1. a. each operation $= (2 \times 15 + 1)^2 + 8 = 969$, total operations $= 3 \times 969 = 2907$
   b. $\omega = 3 \times 15 = 45$, total no of operations $= (2 \times 45 + 1)^2 + 8 = 8289$
2. a. The first B-picture is closer to its forward prediction than its backward prediction picture.
   b. for the second B-picture, FWD = 9 and BWD = 5
   c. for P-picture $(2 \times 13 + 1)^2 + 8 = 737$
      and for each B-picture $(2 \times 5 + 1)^2 + 8 + (2 \times 9 + 1)^2 + 8 = 498$
3. Average $Q = \frac{10+16}{2} = 13$ and the complexity index is $50 \times 1000 \times 13 = 65 \times 10^4$.
4. $(8 \times 7) + (3 \times 10) + 20 = 106$

   for I-pictures:

   $$\frac{1.2 \times 10^6 \times 12 \times 20}{25 \times 106} = 108.7$$

   for P = 54.3 kbits and for B = 38 kbits
5. The new index ratio for B becomes 7/1.4 = 5
   $(8 \times 5) + (3 \times 10) + 20 = 90$, and bits for I = 128 kbits, for P = 64 and for B = 32 kbits
6. $20 + 10 + 10 + 20 + 8 \times 7 = 116$
   for P, the average index of $(10 + 10 + 20)/3 = 13.3$ should be used, hence the target bit rates for I = 99.3 kbits, for P = 66.2 kbits and for B = 34.75 kbits.
7. a. all equal to 48 kbit/s
   b. $60 + 3 \times 20 + 8 \times 15 = 240$

      For I $= \frac{1.2 \times 10^6 \times 12 \times 60}{25 \times 240} = 144$ kbits, for P = 48 kbits and for B = 36 kbits

Chapter 8

2. a. L
   b. L
   c. P
   d. L

3.
$$\begin{array}{rrrrrrrr}
4 & -1 & -5 & 0 & 2 & 0 & 0 & -1 \\
7 & 0 & 2 & 1 & -1 & 0 & 0 & -1 \\
0 & 1 & 0 & 1 & -1 & 0 & 0 & 0 \\
0 & -4 & 0 & 0 & 0 & 0 & 0 & 0 \\
-2 & 0 & 0 & 0 & 1 & 0 & 0 & 0 \\
0 & 0 & 1 & 0 & 0 & 0 & 0 & 0 \\
0 & 0 & 0 & 0 & 0 & 0 & 0 & 0 \\
0 & 0 & 0 & 0 & 0 & 0 & 0 & 0
\end{array}$$

2D-events: (0,4)(0,−1)(0,7)(2,−5)(1,2)(0,1)(1,−2)(0,−4)(1,1)(0,2)(1,−1) (0,1) (7,−1)(2,−1)(4,1)(5,1)(2,−1)EOB (using Figure 6.12 the bits including the sign bit)
$8 + 5 + 11 + 20 + 7 + 5 + 7 + 8 + 6 + 5 + 6 + 5 + 9 + 6 + 8 + 8 + 6 + 2 =$ 132 bits

4. The base layer events: (0,4)(0,−1)(0,7)(2,−5)(1,2)(0,1)(1,−2)(0,4) + PBP
the bits: $8 + 5 + 11 + 20 + 7 + 5 + 7 + 8 + 6 = 77$ bits
The enhancement layer events: (1,1)(0,2)(1,−1)(0,1)(7,−1)(2,−1)(4,1) (5,1)(2,−1) + EOB the bits: $6 + 5 + 6 + 5 + 9 + 6 + 8 + 8 + 6 + 2 = 61$
Total bits $77 + 61 = 138$ bits, about 4.5 per cent extra over one-layer coding

5.
$$\begin{array}{lrrrrrrrr}
\text{base} & 2 & 0 & 2 & 0 & 1 & 0 & 0 & 0 \\
 & 4 & 0 & 1 & 0 & 0 & 0 & 0 & 0 \\
 & 0 & 0 & 0 & 0 & -1 & 0 & 0 & 0 \\
 & 0 & -2 & 0 & 0 & 0 & 0 & 0 & 0 \\
 & -1 & 0 & 0 & 0 & 0 & 0 & 0 & 0 \\
 & 0 & 0 & 0 & 0 & 0 & 0 & 0 & 0 \\
 & 0 & 0 & 0 & 0 & 0 & 0 & 0 & 0 \\
 & 0 & 0 & 0 & 0 & 0 & 0 & 0 & 0
\end{array}$$

$$\begin{array}{lrrrrrrrr}
\text{enhancement} & 0 & -1 & 0 & 0 & 0 & 0 & 0 & -1 \\
 & 0 & 0 & 0 & 1 & -1 & 0 & 0 & -1 \\
 & 0 & 1 & 0 & 1 & 0 & 0 & 0 & 0 \\
 & 0 & 0 & 0 & 0 & 0 & 0 & 0 & 0 \\
 & 0 & 0 & 0 & 0 & 1 & 0 & 0 & 0 \\
 & 0 & 0 & 0 & 0 & 0 & 0 & 0 & 0 \\
 & 0 & 0 & 0 & 0 & 0 & 0 & 0 & 0 \\
 & 0 & 0 & 0 & 0 & 0 & 0 & 0 & 0
\end{array}$$

Base layer events: (0,2)(1,4)(2,−2)(1,1)(2,−1)(0,−2)(2,1)(10,−1)EOB
Bits: $5 + 9 + 7 + 6 + 6 + 5 + 6 + 10 + 2 = 56$ bits
Enhancement layer events: (1,−1)(6,1)(4,1)(2,−1)(0,1)(10,−1)(10,1)(2,−1) EOB
Bits: $6 + 9 + 8 + 6 + 5 + 10 + 10 + 6 + 2 = 62$ bits
Total bits $= 56 + 62 = 118$
Note: the overall bit rate is less than the one layer, but the distortion will be larger.

6. $\frac{8-2}{1.25}\log_2 64 = 28.8$ Mbit/s, $28.8/8 = 3.5$; thus, three TV programmes
7. a. for $B = 1$, $\alpha = 1$ and $\beta = 10^{-5}$
   b. for $B = 5$, $\alpha = 0.2$ and $\beta = 2 \times 10^{-6}$
8. a. 34 980 Mbits = 4.3725 Gbytes
   b. mean bit rate $= 34\,980/(90 \times 60) = 6.478$ Mbit/s
   c. CBR $= 90 \times 60 \times 20/8 = 13.5$ Gbytes, peak-to-mean $= 3.09$
9. a. if error in any video bits, packet is in error; $P = 47 \times 8 \times 10^{-7} = 3.76 \times 10^{-7}$
   b. if error in the header, packet is lost $P = 5 \times 8 \times 10^{-7} = 4 \times 10^{-6}$

10. available link rate $= 50 \times 30 \times 10^2 = 15$ Mbit/s
    total data to be sent $= 34\,980 \times 53/47 = 39\,445.5$ Mbits
    time required $= 39\,445.5/15$ Mbit/s $= 43$ min 50 s
11. $25 \times 4 = 100$ Mbit/s, load $\rho = \frac{100\times53}{155\times47} = 0.7275$
    and the error rate is $P = 10^{-10(1-0.7275^2)} = 2 \times 10^{-6}$
12. With SNR scalability, assume 30% more load, then total load $= 100 \times 1.3 =$ 130 Mbit/s, of which 65 Mbit/s is assigned to the base layer. Since the base layer has an absolute priority, then network load for the base layer $\rho = \frac{65\times53}{155\times47} = 0.4729$ and at this load $P = 1.72 \times 10^{-8}$
    For the enhancement layer, it sees the whole load, of 130 Mbit/s, thus load will be $\rho = \frac{130\times53}{155\times47} = 0.9457$ and the error rate will be $P = 0.088$
13. In data partitioning, with 4 per cent extra bits over one layer and 50 per cent to the base layer, the base layer load will be $\rho = \frac{1}{2} \times 0.7275 \times 1.04 = 0.3783$ and the error rate $P = 2.7 \times 10^{-9}$. The enhancement layer has a load of $2 \times 3.783 =$ 0.7566 that leads to an error rate of $P = 5.3 \times 10^{-5}$.
14. With spatial scalability, assuming 50 per cent more bits over one layer and 50 per cent assigned to the base layer, then the allocated bits to the base layer will be 75 Mbit/s. Base layer load is $\rho = \frac{75\times53}{155\times47} = 0.5456$, leading to $P =$ 9.5×10^{-8}. For the enhancement layer, the load will be more than 100 per cent and the loss probability will be $P = 1$!

Chapter 9

1. Prepend 0 to all events of problem 3 of Chapter 8, except the last event, where 1 should be appended, and no need for EOB, for example, first event (0,4,0) and the last event (2,−1,1)
2. For x, the median of (3,4,−1) is 3 and for y, the median of (−3,3,1) is 1. Hence, the prediction vector is (3,1) and MVD $= (2 - 3 = -1;\ 1 - 1 = 0) = (-1,0)$
3. a. $d = \frac{300-1200+920-150}{16} = -8.125$, $d_1 = -(\max(0, 8.125 - \max(0, 2 \times 8.125 - 16))) = 8$
      Thus, $B_1 = 150 - 8 = 142$ and $C_1 = 115 + 8 = 123$
   b. $d = -31.25$, and $d_1 = 0$, hence B and C do not change
4. a. (3,4)
   b. (0,−3),
   c. (1,0.5)
   d. (3,2.6)
   e. (−1,−1)

Chapter 10

1. For A: $c_0 = c_2 = c_3 = 1$, index $= 1 + 4 + 8 = 13$, the given frequency table in Appendix D is for prob(0); hence prob(0) $= 29789$, but since A is a 1 pixel, then its probability prob(1) $= 1 - 29789 = 35746$ out of 65 535
   For B: $c_0 = c_1 = c_2 = c_3 = c_4 = 1$, and index $= 1 + 2 + 4 + 8 + 16 = 31$, prob (0) $= 6554$. As we see this odd pixel of 0 among the 1s has a lower probability.

For C: $c_1 = c_2 = c_3 = c_4 = c_5 = c_7 = 1$, and the index becomes 190. Like pixel A the prob(0) = 91, but its prob(1) = 65 535 − 91 = 65 444 out of 65 535, which is as expected.

2. The chain code is 0, 1, 0, 1, 7, 7. The differential chain code will be: 0,1,−1,1, −2,0 with bits 1 + 2 + 3 + 2 + 5 + 1 = 14 bits
3. At level 2 the indices (without swapping) will be 0 for the two blank blocks and index = 27 × 2 + 9 × 2 + 0 + 2 = 74 and index = 0 + 0 + 3 × 2 + 2 = 8 for the two blocks.
   At the upper level the index is: index = 0 + 0 + 3 × 0 + 1 = 4
4. The coefficients of the shape adaptive DCT will be

$$\begin{array}{rrr} 127 & -40 & 1 \\ 10 & -15 & \\ 23 & -7 & \\ -6 & & \end{array}$$

confined to the top left corner, while that of the normal DCT with padded zeros, the significant coefficients are scattered all over the 8 × 8 area.

Chapter 11

1. a. a: 70, b: 110, c: 150, d: 190
   b. a: 80, b: 60, c: 40, d: 20
   c. a:b:c:d:90
2. In order for a matrix to be orthonormal, multiplying each row by itself should be 1. Hence, in rows 1 and 3 (basis vectors 0 and 2), their values are 4, hence they should be divided by $\sqrt{4} = 2$. In rows 2 and 4 their products give: 4 + 1 + 1 = 2 = 10, hence their values should be divided by $\sqrt{10}$.

   Thus, the forward 4 × 4 integer transform becomes

$$T = \begin{array}{c} 0.5 \\ \sqrt{10} \\ 0.5 \\ \sqrt{10} \end{array} \begin{bmatrix} 1 & 1 & 1 & 1 \\ 2 & 1 & -1 & -2 \\ 1 & -1 & -1 & 1 \\ 1 & -2 & 2 & -1 \end{bmatrix}$$

And the inverse transform is its transpose.

$$T^{-1} = T^T = \begin{bmatrix} \frac{1}{2} & \frac{2}{\sqrt{10}} & \frac{1}{2} & \frac{1}{\sqrt{10}} \\ \frac{1}{2} & \frac{1}{\sqrt{10}} & -\frac{1}{2} & -\frac{2}{\sqrt{10}} \\ \frac{1}{2} & -\frac{1}{\sqrt{10}} & -\frac{1}{2} & \frac{2}{\sqrt{10}} \\ \frac{1}{2} & -\frac{2}{\sqrt{10}} & \frac{1}{2} & -\frac{1}{\sqrt{10}} \end{bmatrix}$$

As can be tested, this inverse transform is orthonormal, for example, $\left(\frac{1}{2}\right)^2 + \left(\frac{2}{\sqrt{10}}\right)^2 + \left(\frac{1}{2}\right)^2 + \left(\frac{1}{\sqrt{10}}\right)^2 = \frac{1}{4} + \frac{4}{10} + \frac{1}{4} + \frac{1}{10} = 1$

3. With the integer transform of problem 2, the 2D transform coefficients (rounded to the nearest integer) will be

$$\begin{matrix} 431 & 42 & -6 & -13 \\ -157 & 51 & -46 & 28 \\ 91 & 29 & -26 & -19 \\ -15 & 0 & -7 & 14 \end{matrix}$$

Exactly similar values are obtained through eqn. 11.13

4. a. With $QP = 4$, $Q_{\text{step}} = 1$, and the resultant coefficients in problem 3 can be used in eqn. 11.16, resulting the pixel values of

$$\begin{matrix} 100 & 120 & 85 & 10 \\ 80 & 70 & 60 & 50 \\ 110 & 90 & 100 & 120 \\ 180 & 200 & 150 & 200 \end{matrix}$$

which are exact values of the input pixels.

b. With $QP = 36$, the quantiser step size $Q_{\text{step}} = 40$. Rounding the transform coefficients of problem 3 to 40 results in the quantised transform indices of

$$\begin{matrix} 11 & 1 & 0 & 0 \\ -4 & 1 & -1 & 1 \\ 2 & 1 & -1 & 0 \\ 0 & 0 & 0 & 0 \end{matrix}$$

and the inverse quantised coefficients become

$$\begin{matrix} 440 & 40 & 0 & 0 \\ -160 & 40 & -40 & 40 \\ 80 & 40 & -40 & 0 \\ 0 & 0 & 0 & 0 \end{matrix}$$

and the reconstructed pixels with eqn. 11.16 become

$$\begin{matrix} 107 & 125 & 117 & 70 \\ 87 & 70 & 89 & 81 \\ 113 & 91 & 89 & 119 \\ 158 & 167 & 151 & 145 \end{matrix}$$

5. For $N = 10$ with reference to the six quantiser step sizes of Table 11.1
$8\%6 = 2$ and $floor(8/6) = 1$; $Q_{\text{step}}(8) = 0.8125 \times 2^1 = 1.65$
$26\%6 = 2$ and $floor(26/6) = 4$; $Q_{\text{step}}(26) = 0.8125 \times 2^4 = 13$
$48\%6 = 0$ and $floor(48/6) = 8$; $Q_{\text{step}}(48) = 0.625 \times 2^8 = 160$
$51\%6 = 3$ and $floor(51/6) = 8$; $Q_{\text{step}}(51) = 0.875 \times 2^8 = 224$

6. According to Table 11.2, the corresponding quantiser parameters for the chroma will be
   $QP = 8$, hence $Q_{\text{step}}(8) = 1.65$
   $QP = 26$, hence $Q_{\text{step}}(26) = 1.65$
   $QP = 39$, $39\%6 = 3$ and $floor(39/6) = 6$; $Q_{\text{step}}(39) = 0.875 \times 2^6 = 56$
   $QP = 39$, $Q_{\text{step}}(39) = 56$
7. a. parameter $= 5 > 0$; $x = 2 \times 5 - 1 = 9$; $M = floor(\log_2[9 + 1]) = 3$ and $info = 9 + 1 - 2^3 = 2$, which should be defined in binary at 3 bits; thus code word $= 0001010$
   b. parameter $= -5 < 0$; $x = 2 \times 5 = 10$; $M = floor(\log_2[10 + 1]) = 3$ and $info = 10 + 1 - 2^3 = 3$; thus, code word $= 0001011$
8. $\lambda_{mode} = 0.85 \times 2^{\frac{36-12}{3}} = 0.85 \times 2^8 = 217.6$

   $\lambda_{MV} = \sqrt{217.6} = 14.76$

Appendix G

Glossary of acronyms

2D-VLC	two-dimensional variable length code
3D-VLC	three-dimensional variable length code
AAL	ATM adaptation layer
ABT	adaptive block transform
ACK	acknowledgement
ASO	adaptive slice ordering
ATM	asynchronous transfer mode
AVC	advanced video coding
BD	boundary difference
BISDN	broadband ISDN
BMA	block matching algorithm
BS	boundary strength
CABAC	context-adaptive binary arithmetic coding
CAVLC	context-adaptive variable length coding
CAT	category
CBP	coded block pattern
CBR	constant bit rate
C_b, C_r (u,v)	chrominance components
CCF	cross-correlation function
CCIR	International Radio Consultative Committee (now called ITU)
CGS	coarse grain scalability
CIF	common intermediate format
CPU	central processing unit
CSA	cross-search algorithm
DCT	discrete cosine transform
DIFF	difference between DC coefficients
DP	data partition
DPCM	differential pulse code modulation
DSCQS	double stimulus continuous quality score
DSIS	double stimulus impairment scale
DSM	digital storage media
DTS	decoding time stamp
DVD	digital versatile (video) disc
DWT	discrete wavelet transform

EBCOT	embedded block coding with optimised truncation
EG0	zero-order Exp-Golomb code
EGK	*k*th-order Exp-Golomb code
ELNUM	enhancement layer number
EOB	end of block
EPZS	enhanced predictive zonal search
EZW	embedded zero tree
FEC	forward error correcting
FFT	fast Fourier transform
FGS	fine granular scalability
FIR	finite impulse response
FLC	fixed-length code
FMO	flexible macroblock ordering
FR-TV	full reference TV
FSM	full search method
GOB	group of blocks
GOP	group of pictures
HBMA	hierarchical block matching algorithm
HDTV	high definition television
HVS	human visual system
ICT	irreversible colour transform
IEC	International Electrotechnical Commission
INTER	interframe
INTRA	intraframe
IDCT	inverse DCT
IDR	instantaneous decoding refresh
IP	Internet Protocol
IQ, Q^{-1}	inverse quantiser
ISDN	integrated services digital network
ISO	International Standards Organisation
ITC, TC^{-1}	inverse transform
ITU-T	International Telecommunication Union (telegraphy section)
JPEG	Joint Photographic Experts Group
JM	joint model
JSVM	joint scalable video model
L (Y)	luminance component
LAN	local area network
LIP	list of insignificant pixels
LIS	list of insignificant set
LPF	low-pass filter
LPS	least probable symbol
LSB	least significant bit
LSP	list of significant pixels
MAE	mean absolute error

MB	macroblock
MB-AFF	macroblock adaptive frame/field
MC	motion compensation
MCBPC	macroblock type and coded block pattern
MCU	multipoint control unit
MCTF	motion-compensated temporal filtering
ME	motion estimation
MGS	medium grain scalability
MOS	mean opinion score
MPEG	Motion Picture Experts Group
MPS	most probable symbol
MSB	most significant bit
MSE	mean-squared error
MTU	medium transfer unit
MV	motion vector
MVD	motion vector data
MVDB	motion vector data for B-pictures
MVDS	motion vector data for shape
NACK	negative acknowledgement
NAL	network abstraction layer
NR-TV	no reference TV
NTSC	National Television System Committee
OFDM	orthogonal frequency division multiplex
OSA	orthogonal search algorithm
PAFF	picture-adaptive frame/field
PAL	phase alternate line
PBP	priority break point
PCRD	post compression rate distortion
PES	packetised elementary stream
PMVFAST	predictive motion vector field adaptive search technique
PPS	picture parameter set
PSNR	peak signal-to-noise ratio
PSTN	public switched telephone network
PTS	presentation time stamp
Q	quantiser
QCIF	quarter of CIF
QP	quantiser parameter
RCT	reversible colour transform
RGB	red, green and blue colour primaries
RD	rate distortion
RLNUM	reference layer number
RM	reference model
ROI	region of interest
RR-TV	reduced reference TV

PSP	primary switching predictive
RTP	real-time transport protocol
RVLC	reversible variable length code
SAC	syntax-based arithmetic coding
SAD	sum absolute difference
SCR	systems clock reference
SD TV	standard television
SECAM	sequential couleur avec memoire
SEI	supplemental enhancement information
SI-slice	switching intra slice
SIF	source input format
SOT	special orientation tree
SP-slice	switching predictive slice
SPIHT	set partitioning in hierarchical tree
SPS	sequence parameter set
SSCQE	single stimulus continuous quality evaluation
SSP	secondary switching picture
ST	statistical table
STC	systems time clock
STD	system target decoder
sub-QCIF	one-ninth of CIF
SVC	scalable video coding
TC	transform coding
TM	test model
TTS	three-step search
UBR	unspecified bit rate
UDP	user datagram protocol
UTQ	uniform threshold quantiser
UTQ-DZ	uniform threshold quantiser with dead zone
VBR	variable bit rate
VCL	video coding layer
VCR	video cassette recorder
VLC	variable length code
VLD	variable length decode
VQEG	Video Quality Experts Group
VRC	video redundancy coding
WT	weighting table
ZT	zero tree

Index

Standard Codecs

Image compression to advanced video coding

3rd Edition

A substantially updated edition of *Video Coding: An introduction to standard codecs* (IEE 1999, winner of IEE Rayleigh Award as the best book of 2000), this book discusses the growth of digital television technology, from image compression to advanced video coding. This third edition also includes the latest developments on H.264/MPEG-4 video coding and the scalability defined for this codec, which were not available at the time of the previous edition (IEE 2003). The book highlights the need for standardisation in processing static and moving images and extensively exploits the ITU and ISO/IEC standards defined in this field. The book gives an authoritative explanation of pictures and video coding algorithms, working from basic principles through to the advanced video compression systems now being developed. It discusses the reasons behind the introduction of a standard codec for a specific application and its chosen parameters. Each chapter is devoted to a standard video codec, and chapters are introduced in an evolutionary manner complementing the earlier chapters. This book will enable readers to appreciate the fundamentals needed to design a video codec for any given application and should prove a valuable resource for managers, engineers and researchers working in this field.

Mohammed Ghanbari is Professor of Video Networking at the University of Essex, UK. He is best known for pioneering work on two-layered video coding for ATM networks, now known as SNR scalability in standard video codecs. Prior to his academic career, Professor Ghanbari worked for 10 years in broadcasting. He has published more than 550 technical papers, registered for 11 patents and authored/co-authored five books on video networking, many of which have had a fundamental influence in this field. He has been Associate Editor to *IEEE Transactions on Multimedia*, is on the advisory board of *Journal of Image Communication* and has been guest editor of numerous special issues on video coding. He is a Fellow of both IEEE and IET, as well as a Chartered Engineer.

ISBN 978-0-86341-964-5

9 780863 419645

The Institution of Engineering and Technology
www.theiet.org
978-0-86341-964-5